REVISS

REVISS Services
Technical and Manufacturing Group

Test Report No. RTR 245

3981/01
1.0m Punch Test – Angled Inverted

Author:		**Reviewer:**	
Name	P J G Robbins	Name	D W Rogers
Signature		Signature	
Date	02/07/09	Date	03/07/09

1. PURPOSE AND SCOPE

The purpose of this document is to record the performance of the R7021 specimen, 3981/01, in an IAEA drop test for Type B radioactive materials package designs. The full test programme is discussed, justified and detailed in the test plan, RTM 118.

2. DESCRIPTION

2.1 DESIGN

The outer components of the R7021, a cylindrical, insulated jacket, a top shield (with energy absorbing structures and insulation), and a pallet, are constructed predominantly from carbon steel. There is also a stainless steel grill around the top of the jacket to restrict access to hot surfaces. The flask is a stainless steel, lead shielded, upright, finned cylinder with a conventional plug type closure in the top and thermal insulation built into its top and bottom corners. The closure has a vent point and the cavity has a drain tube to allow the flask to be operated in ponds as well as in cells. The cylindrical cavity holds encapsulated radioactive material (solid cobalt metal) in a basket. Although primarily intended to carry Special Form capsules, the flask has a containment system as it may also be used to carry non-Special Form encapsulated cobalt. The closure and the vent and drain plugs are therefore equipped with testable O-ring seals. In addition, to prevent the migration of coarse solids outside the shielded volume, the top of the drain tube is fitted with a mesh filter and a spring gasket is used to seal the gap under the closure around the top of the cavity.

2.2 TEST

1.0 m Punch Test – Angled Inverted (Drop 11, RTM 118). Drop II test for Type B packages (paras. 656 & 727(b), TS-R-1).

2.3 TEST INTENT

To generate the maximum damage to the lowermost top shield cone prior to the 9.0m angled inverted drop test.

2.4 PASS/FAIL CRITERIA

The pallet, top shield and jacket shall be secure in order for the specimen to continue to the next test. For internal inspection see IR 0675.

2.5 TARGET

The R8085 target (Drg. No. R8085/001) consists of a 50mm thick steel plate bonded to reinforced concrete of dimensions 4m square x 3m deep set flush with the ground. The total mass, 113000 kg, exceeds the RTM 118 minimum requirement of 45000 kg by 150%.

The punch (Drg. No. R8099/002) met RTM 118 requirements and was securely fastened to the target with four M24 screws.

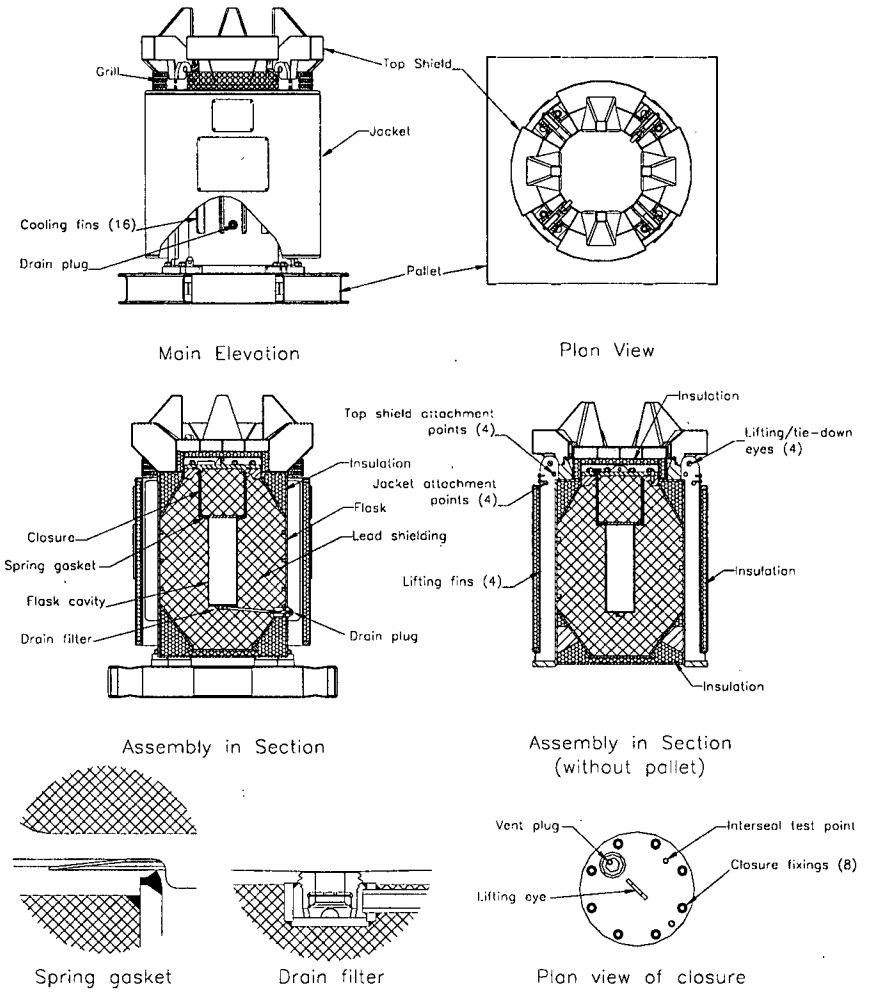

Figure 1: R7021 Constructional Details

2.6 SPECIMEN DETAILS (SEE ALSO IR 0674)

- Identity: 3981/01.
- Contents: A basket containing 48 stainless steel rods.
- Assembly:
  - The specimen was re-assembled in accordance with the test plan, RTM 118, (closure, vent plug and drain plug remaining undisturbed from previous test) with pallet 3981/01, top shield 3981/02 and new jacket and top shield shoulder bolts (Figures 2, 4 & 5). All components fitted cleanly, although there was initially a small gap under one of the flask feet indicating it had been deformed upwards (Figure 3).
  - The flask-to-pallet fixings were tightened to a torque of 150 N.m. The slight gap under the flask foot closed up.
  - The jacket and top shield fixings were tightened to a torque of 80 N.m. The jacket was orientated with the vertical seam weld next to the drain plug in readiness for

punch testing later.

  - The grill fixings were tightened to a torque of 20 N.m.

- Weight: 4374 kg.
- Existing Damage: See IR 0674 & RTR 244.

2.7 TEST PROCEDURE

As the weight of the container assembly was less than the design maximum gross weight (4500kg), the drop height was increased pro rata to compensate. The test height was therefore (4500/4374) x 1.0 = 1.030m.

The test was conducted in accordance with OP 225. The specified angle was 17° ± 2° from the vertical. All key actions were recorded on the test record sheet (attached).

3. RESULTS

- The test was executed correctly (Figures 6-9). The angle measured for the drop was 73.8° from the horizontal, i.e. 16.2° from the vertical (Figure 10).
- The pallet, jacket, top shield and grill remained securely attached (Figure 11).
- The impact cone crushed to a height of 180mm above inner surface of top shield (Figures 12, 13 & 17).
- There was minor damage to the supporting segment, inner surface and edge of the pallet from secondary impacts (Figures 14-16).
- The punch showed good impact location and no significant deformation (Figure 18).
- There was no other externally visible damage.

See Illustrations for photographic record.

4. CONCLUSIONS

The R7021 test specimen, 3981/01, was fit to continue to the next test.

5. REFERENCES

- IR 0674: 3981/01 Assembly Prior to Accident Conditions Drop Testing, REVISS Services (UK) Ltd.
- IR 0675: 3981/01 Inspection After Accident Conditions Drop Testing, REVISS Services (UK) Ltd.
- OP 225: Drop Testing Procedure, REVISS Services (UK) Ltd.
- R8085/001 issue B: Drop Test Target, REVISS Services (UK) Ltd.
- R8099/002 issue A: Drop Test Punch, REVISS Services (UK) Ltd.
- RTR 244: 1.0m Punch Test – Angled Inverted, REVISS Services (UK) Ltd.
- TS-R-1: Safety Standards Series, Regulations for the Safe Transport of Radioactive Material 1996 Edition (As amended 2003), IAEA, Vienna.

6. ATTACHMENTS

RTR 245: Drop Test Checklist, REVISS Services (UK) Ltd.

7. ILLUSTRATIONS

page
Figure 2: Assembly of flask onto pallet 3981/01 6
Figure 3: Initial gap under foot 6
Figure 4: Replacement jacket and top shield fasteners 7
Figure 5: Assembly of the jacket on to flask 7
Figure 6: Test action sequence – Angle 1 8
Figure 7: Test action sequence – Angle 2 9
Figure 8: Above target 10
Figure 9: 1.030m above target 10
Figure 10: Inclinometer readings (2 planes) 11
Figure 11: After drop 11
Figure 12: Damage to top shield 12
Figure 13: Damage to top shield cone 12
Figure 14: Damage to top shield (secondary impact) 13
Figure 15: Damage to top shield (secondary impact) 13
Figure 16: Damage to pallet (secondary impact) 14
Figure 17: Damage to cone 14
Figure 18: Condition of punch 15

Figure 2: Assembly of flask onto pallet 3981/01

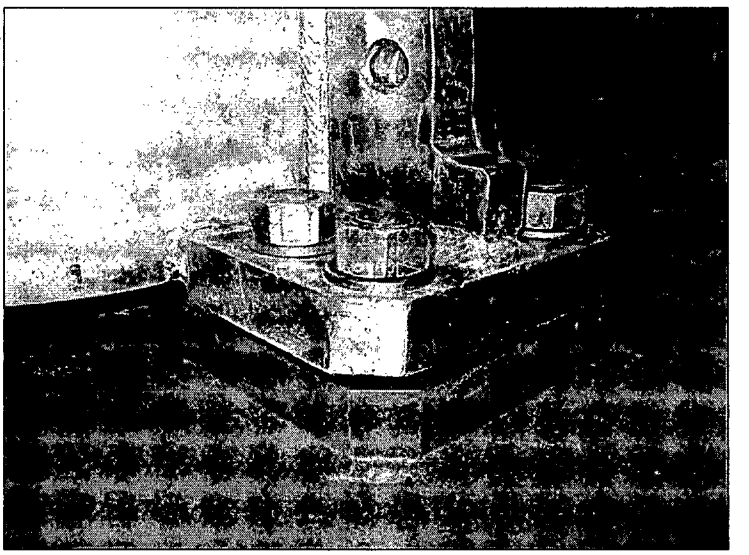

Figure 3: Initial gap under foot

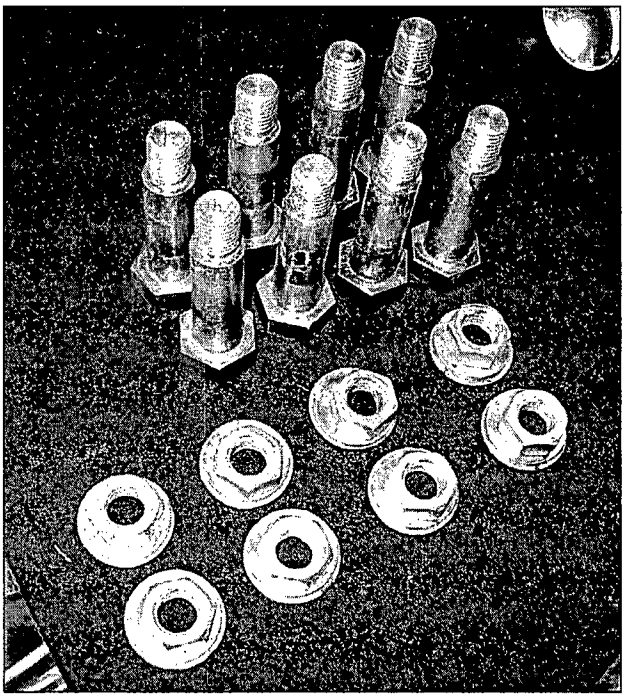

Figure 4: Replacement jacket and top shield fasteners

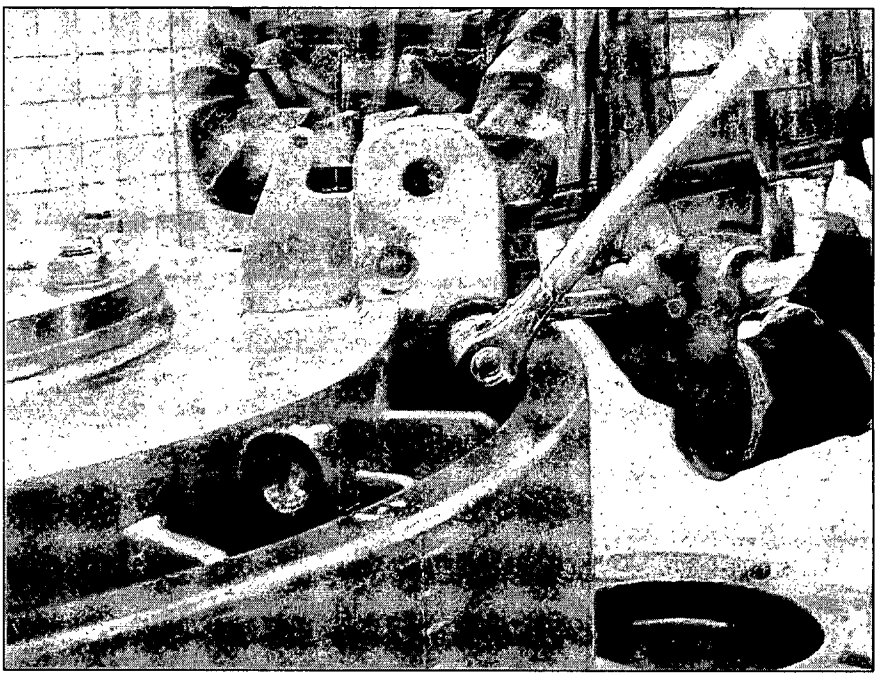

Figure 5: Assembly of the jacket on to flask

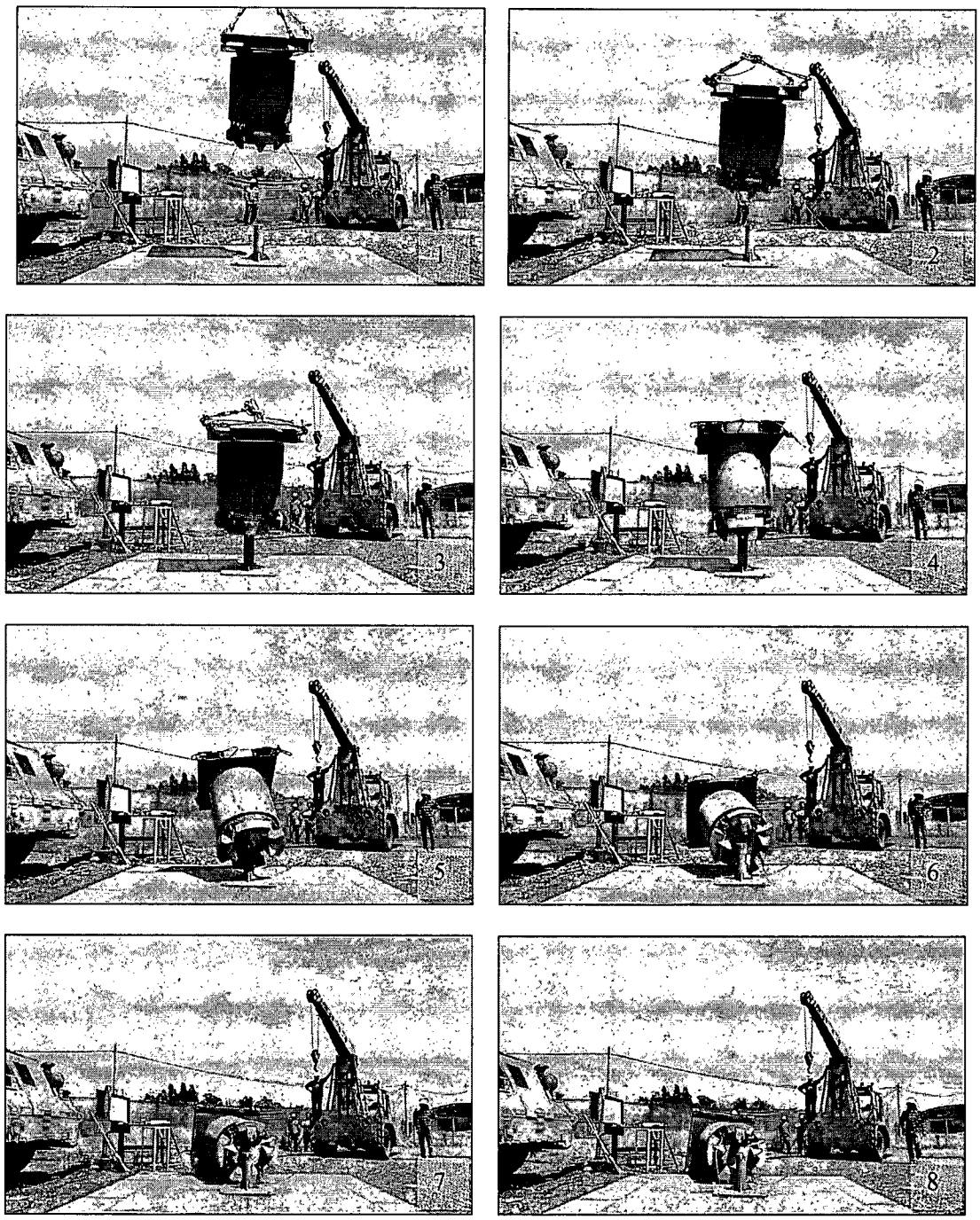

Figure 6: Test action sequence – Angle 1

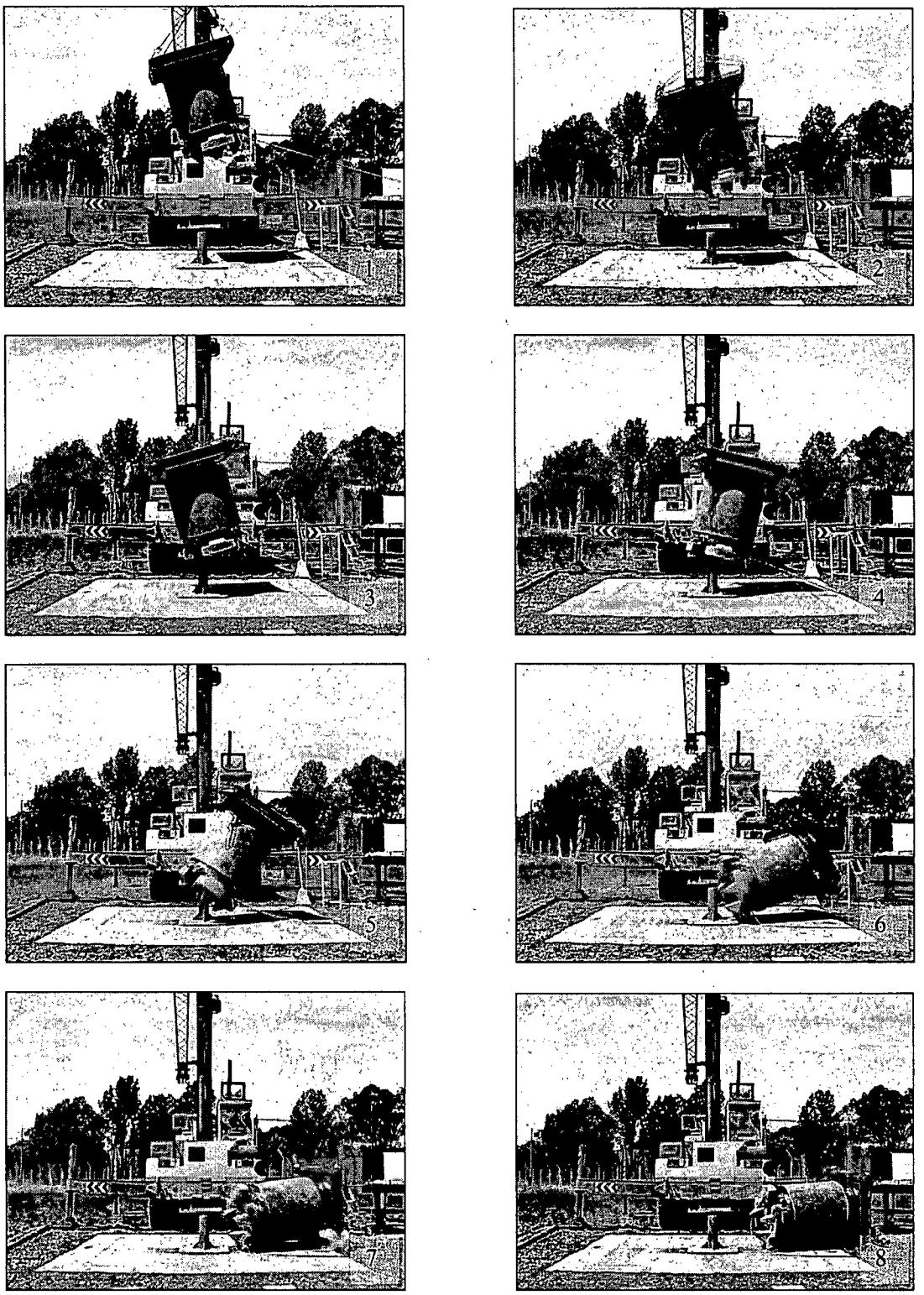

Figure 7: Test action sequence – Angle 2

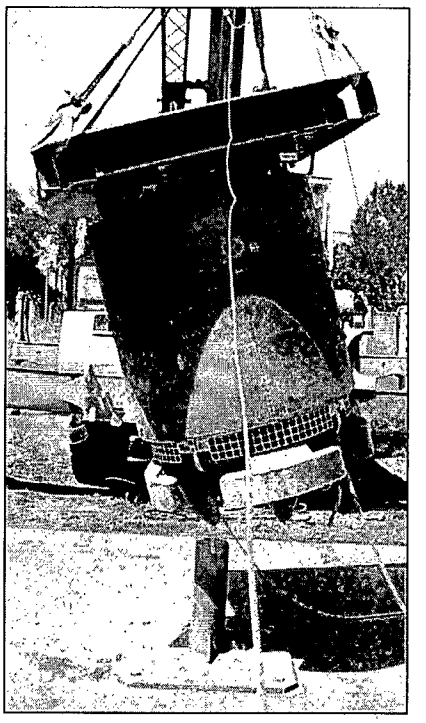

Figure 8: Above target

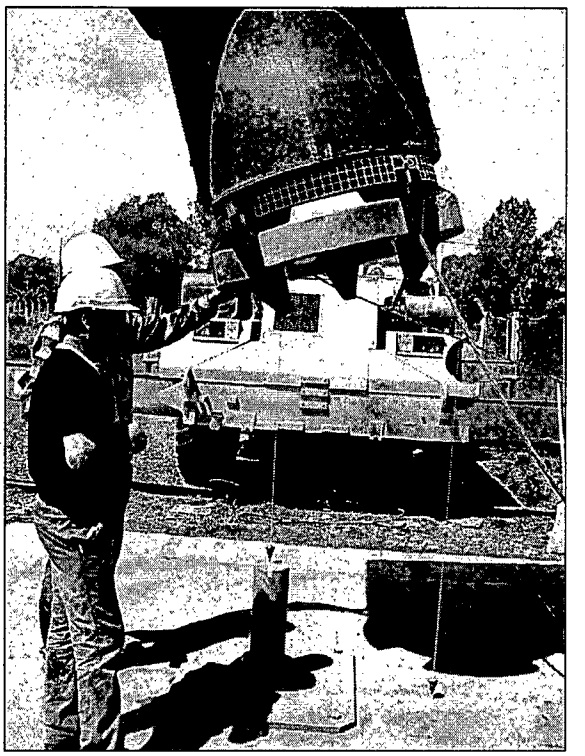

Figure 9: 1.030m above target

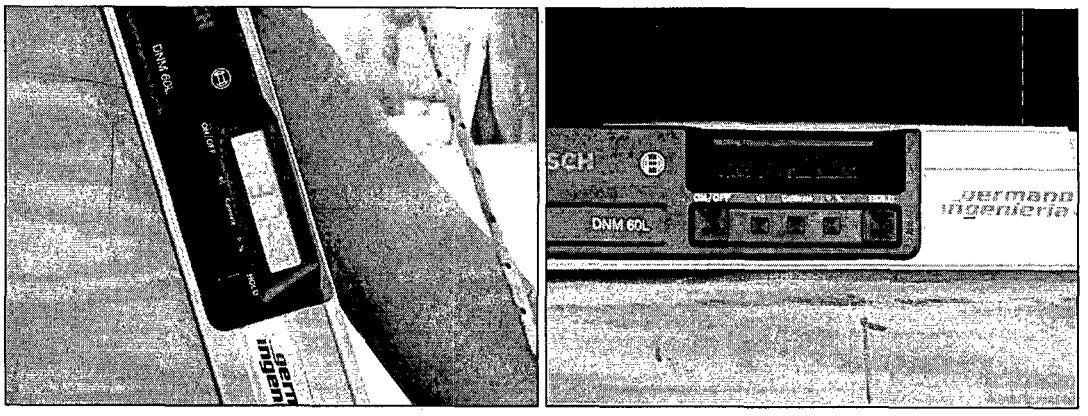

Figure 10: Inclinometer readings (2 planes)

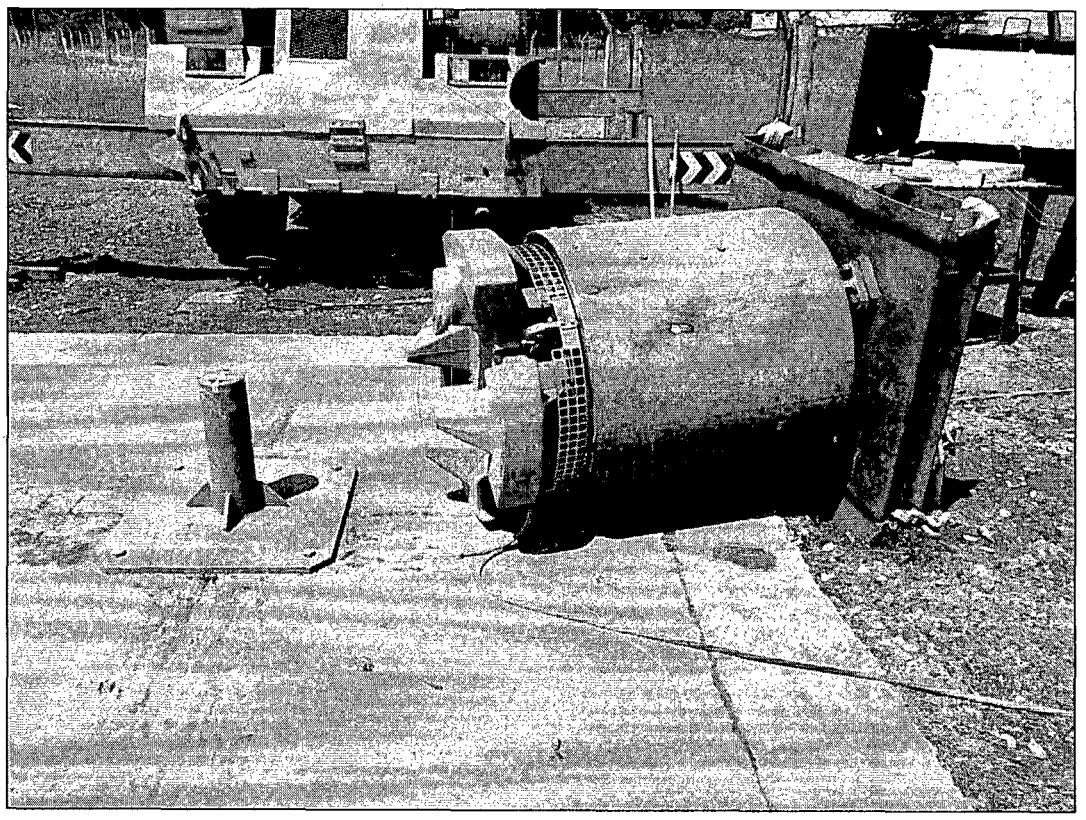

Figure 11: After drop

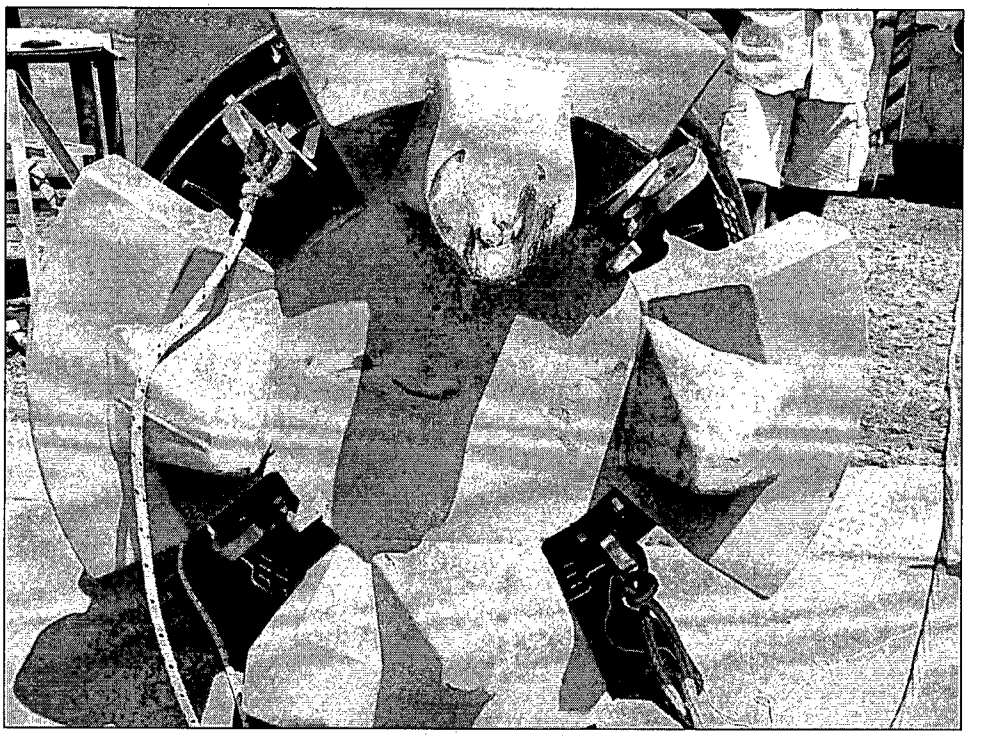

Figure 12: Damage to top shield

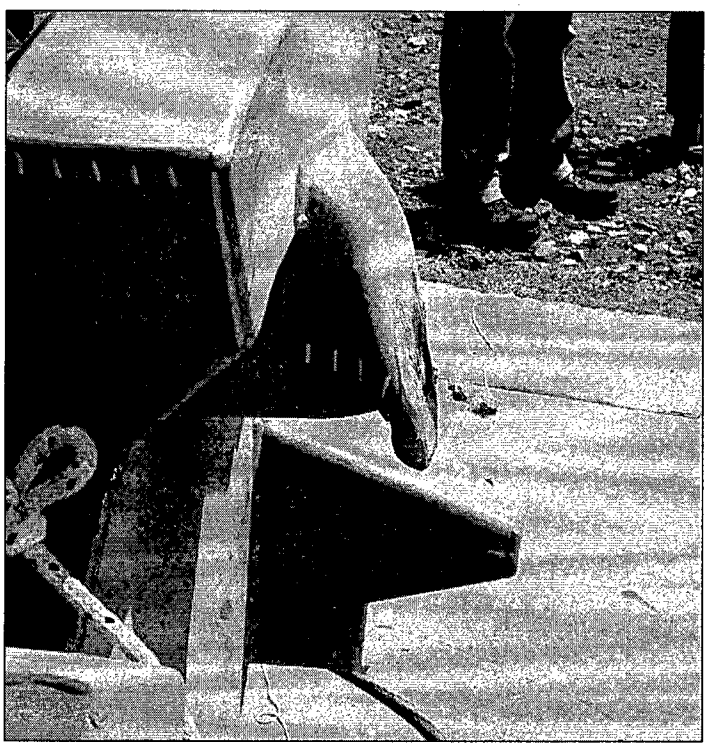

Figure 13: Damage to top shield cone

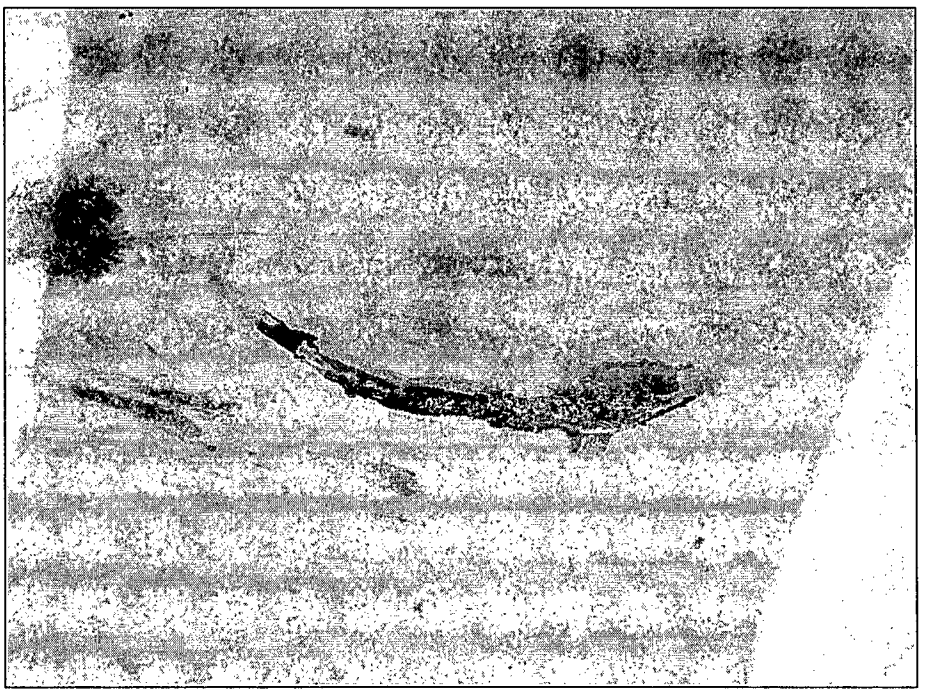

Figure 14: Damage to top shield (secondary impact)

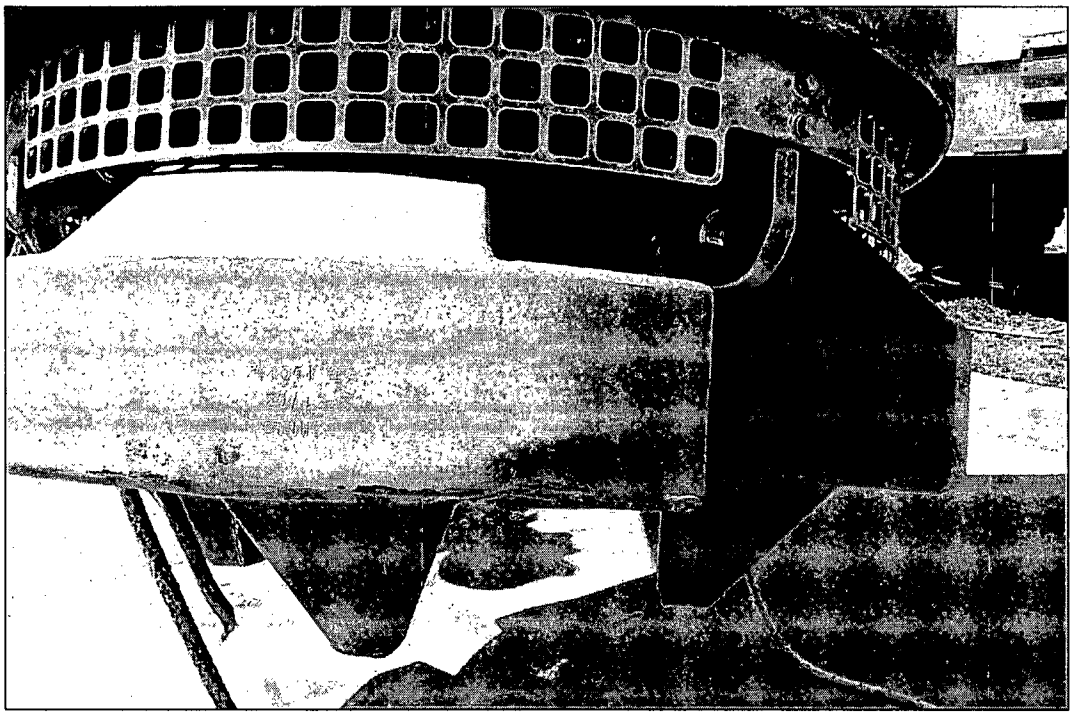

Figure 15: Damage to top shield (secondary impact)

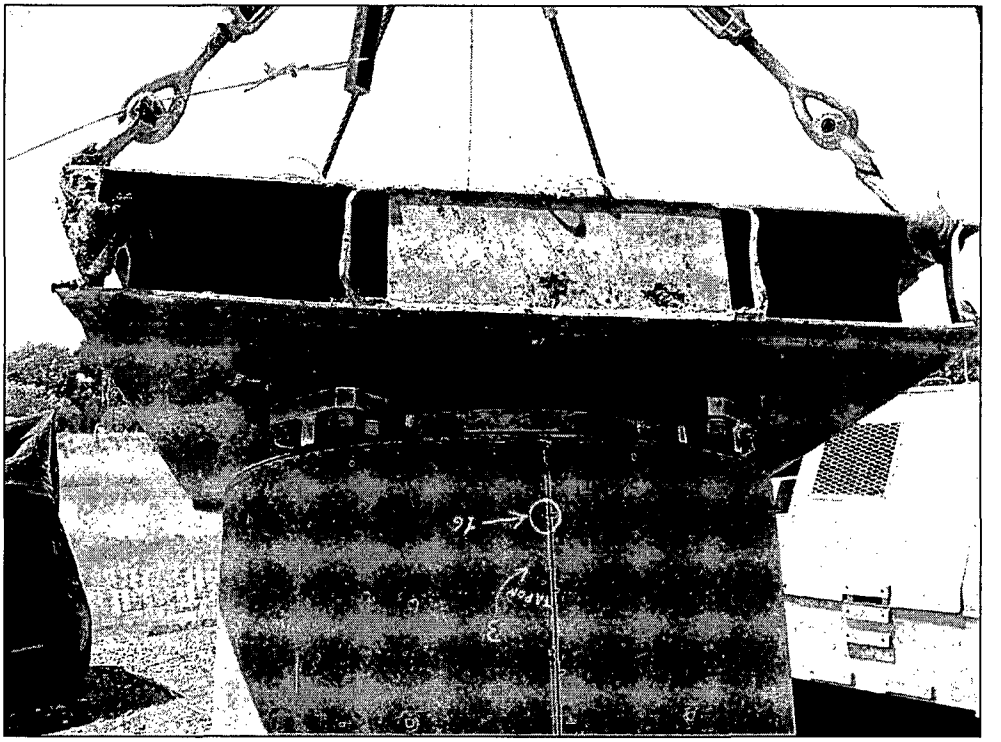

Figure 16: Damage to pallet (secondary impact)

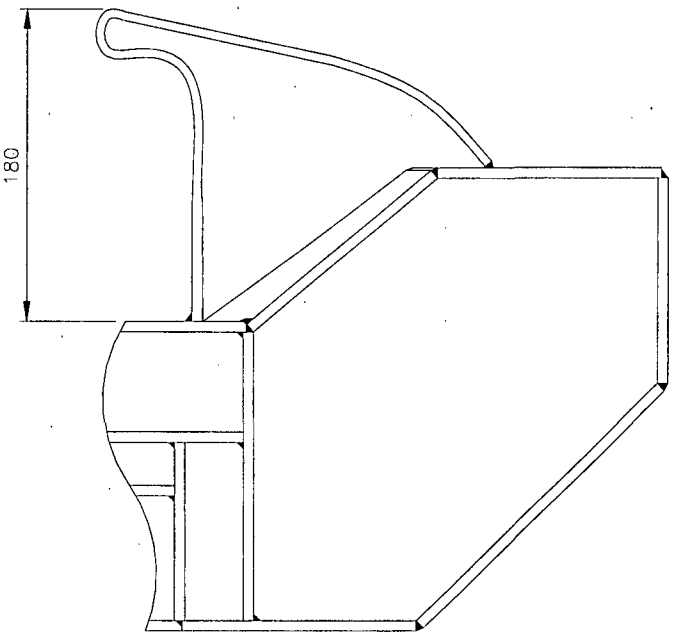

Figure 17: Damage to cone

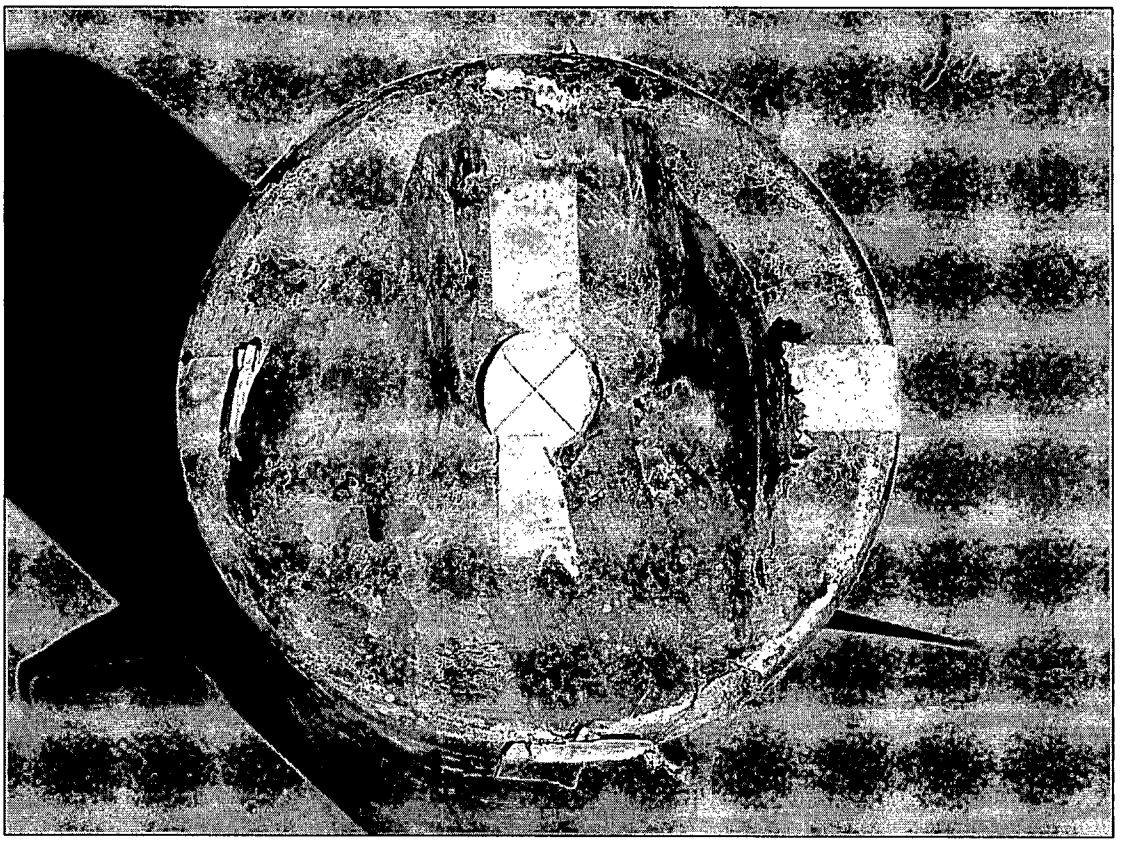

Figure 18: Condition of punch

Reviss Services (UK) Ltd **Drop Test Checklist (OP225)**	RTR: 245 Date: 20/11/08
Test Description: 1.0m Punch Test: Angled Inverted (IAEA Type B)	
1. Confirm all personnel are aware of safety rules	✓
2. Test Plan/issue	RTM 118 issue 2, Drop 11.
3. Specimen Design/Serial No/Drg No.	3981/01 (flask & jacket)*
4. Height gauge Identity/Drg No.	1.030m (R8083/005 issue A).
5. Target Identity/Drg No.	R8085/001 issue B.
6. Punch Identity/Drg No.	R8099/002 issue A.
7. Penetration bar Identity/Drg No.	N/A
8. Other Inclinometer Bosch DNM 60L	(cal. due 30/09/09).
9. Specimen prepared correctly	See RTR 244 and below**.
10. Specimen orientated correctly	73.8° & 0.4° on jacket.
11. Photograph just above target	✓
12. Raise to correct height	✓ 1.030m.
13. Release specimen	✓
14. Photograph in situ	✓
15. Photograph damage	✓
16. Confirm correct execution of drop	✓
17. Pass/Fail (if, applicable see Test Plan)	PASS (fit to continue).

18. Notes

* ~~Pallet and top shield are 3981/02~~ DWR Pallet is 3981/01, top shield is 3981/02.

** Pallet nuts retorqued to 150 N.m. Jacket and top shield bolts and nuts replaced with new and torqued to 80 N.m. Grill screws to 20 N.m. Wrench: Norbar TT300: 2008/189666 (cal. due 27/10/11).

- Impact cone crushed to height of 180mm above inner surface.
- Minor damage to supporting segment, inner surface and edge of pallet from secondary impacts.
- No other damage externally visible.
- Pallet, jacket, top shield and grill securely attached.

19. Signed: DW Rogers	Date: 20/11/08
20. Witnessed: Michael Nixon	Date: 20/11/08

REVISS

REVISS Services
Technical and Manufacturing Group

Test Report No. RTR 246

3981/01
9.0m Free Drop Test – Angled Inverted

Author:		**Reviewer:**	
Name	P J G Robbins	Name	D W Rogers
Signature		Signature	
Date	03/07/09	Date	03/07/09

1. PURPOSE AND SCOPE

The purpose of this document is to record the performance of the R7021 specimen, 3981/01, in an IAEA drop test for Type B radioactive materials package designs. The full test programme is discussed, justified and detailed in the test plan, RTM 118.

2. DESCRIPTION

2.1 DESIGN

The outer components of the R7021, a cylindrical, insulated jacket, a top shield (with energy absorbing structures and insulation), and a pallet, are constructed predominantly from carbon steel. There is also a stainless steel grill around the top of the jacket to restrict access to hot surfaces. The flask is a stainless steel, lead shielded, upright, finned cylinder with a conventional plug type closure in the top and thermal insulation built into its top and bottom corners. The closure has a vent point and the cavity has a drain tube to allow the flask to be operated in ponds as well as in cells. The cylindrical cavity holds encapsulated radioactive material (solid cobalt metal) in a basket. Although primarily intended to carry Special Form capsules, the flask has a containment system as it may also be used to carry non-Special Form encapsulated cobalt. The closure and the vent and drain plugs are therefore equipped with testable O-ring seals. In addition, to prevent the migration of coarse solids outside the shielded volume, the top of the drain tube is fitted with a mesh filter and a spring gasket is used to seal the gap under the closure around the top of the cavity.

2.2 TEST

9.0 m Drop Test – Angled Inverted (Drop 12, RTM 118). Drop I test for Type B packages (paras. 656 & 727(b), TS-R-1).

2.3 TEST INTENT

To generate the maximum tensile stresses in the closure fixings and vent plug and maximise the risk of crush damage to these components.

2.4 PASS/FAIL CRITERIA

The pallet, top shield and jacket shall be secure after the test in order for the specimen to continue to the next test. For internal inspection see IR 0675.

2.5 TARGET

The R8085 target (Drawing No R8085/001) consists of a 50mm thick steel plate bonded to reinforced concrete of dimensions 4m square x 3m deep set flush with the ground. The total mass, 113000 kg, exceeds the RTM 118 minimum requirement of 45000 kg by 150%.

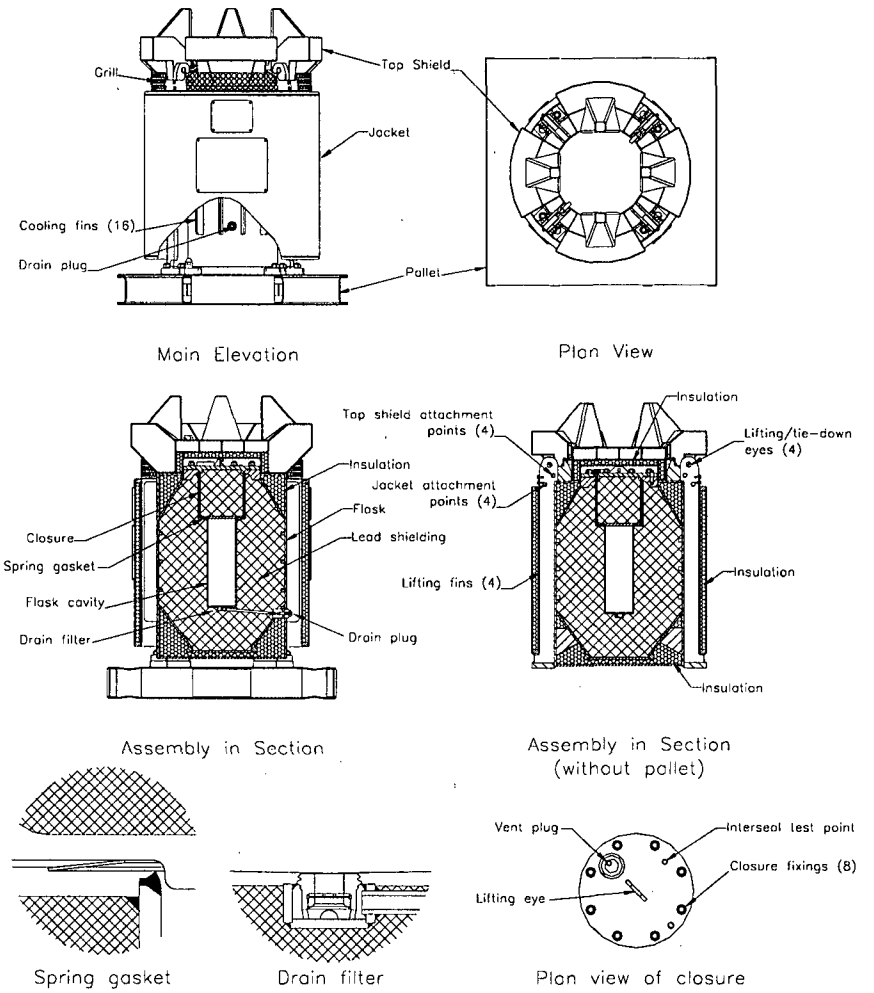

Figure 1: R7021 Constructional Details

2.6 SPECIMEN DETAILS (SEE ALSO IR 0674)

- Identity: 3981/01.
- Contents: A basket containing 48 stainless steel rods.
- Weight: 4374 kg.
- Existing Damage: See IR 0674 & RTR 244 & 245.

2.7 TEST PROCEDURE

As the weight of the container assembly was less than the design maximum gross weight (4500kg), the drop height was increased pro rata to compensate. The test height was therefore (4500/4374) x 9.0 = 9.26m.

The test was conducted in accordance with OP 225. The specified angle was 17° ± 2° from the vertical. All key actions were recorded on the test record sheet (attached).

3. RESULTS

- The test was executed correctly Figures 2-5). The angle measured for the drop was 73.0° from the horizontal, i.e. 17.0° from the vertical (Figure 6).
- The pallet, jacket, top shield and grill were all securely attached (Figure 7).
- The impact cone was completely crushed, the adjacent cones were partially crushed (mean height above the inner surface 155 & 160mm and the opposite cone was slightly crushed, height 210mm (Figures 8-10 & 14).
- The impact quadrant was crushed and folded over the grill which was slightly distorted (Figures 11-13).
- There was a slight depression of the flask top corner under the impact quadrant but no gap under the top shield.
- No other damage to the specimen or fixings was visible.

See Illustrations for photographic record.

4. CONCLUSIONS

The R7021 test specimen, 3981/01, was fit to continue to the next test.

5. REFERENCES

- IR 0674: 3981/01 Assembly Prior to Accident Conditions Drop Testing, REVISS Services (UK) Ltd.
- IR 0675: 3981/01 Inspection After Accident Conditions Drop Testing, REVISS Services (UK) Ltd.
- OP 225: Drop Testing Procedure, REVISS Services (UK) Ltd.
- R8085/001 issue B: Drop Test Target, REVISS Services (UK) Ltd.
- RTM 118: Test Plan for the R7021 Transport Container, REVISS Services (UK) Ltd.
- RTR 244: 1.0m Punch Test – Angled Inverted, REVISS Services (UK) Ltd.
- RTR 245: 1.0m Punch Test – Angled Inverted, REVISS Services (UK) Ltd.
- TS-R-1: Safety Standards Series, Regulations for the Safe Transport of Radioactive Material 1996 Edition (As amended 2003), IAEA, Vienna.

6. ATTACHMENTS

RTR 246: Drop Test Checklist, REVISS Services (UK) Ltd.

7. ILLUSTRATIONS

page
Figure 2: Test action sequence – Angle 1 6
Figure 3: Test action sequence – Angle 2 7
Figure 4: Above target 8
Figure 5: 9.26m above target 8
Figure 6: Inclinometer readings (2 planes) 9
Figure 7: After drop 9
Figure 8: Damage to top shield cones 10
Figure 9: Deformation of top shield cones 10
Figure 10: Deformation of top shield cones 11
Figure 11: Deformation of top shield quadrant 11
Figure 12: Deformation of top shield quadrant 12
Figure 13: Distortion of top shield quadrant sides 12
Figure 14: Deformation of cones 13

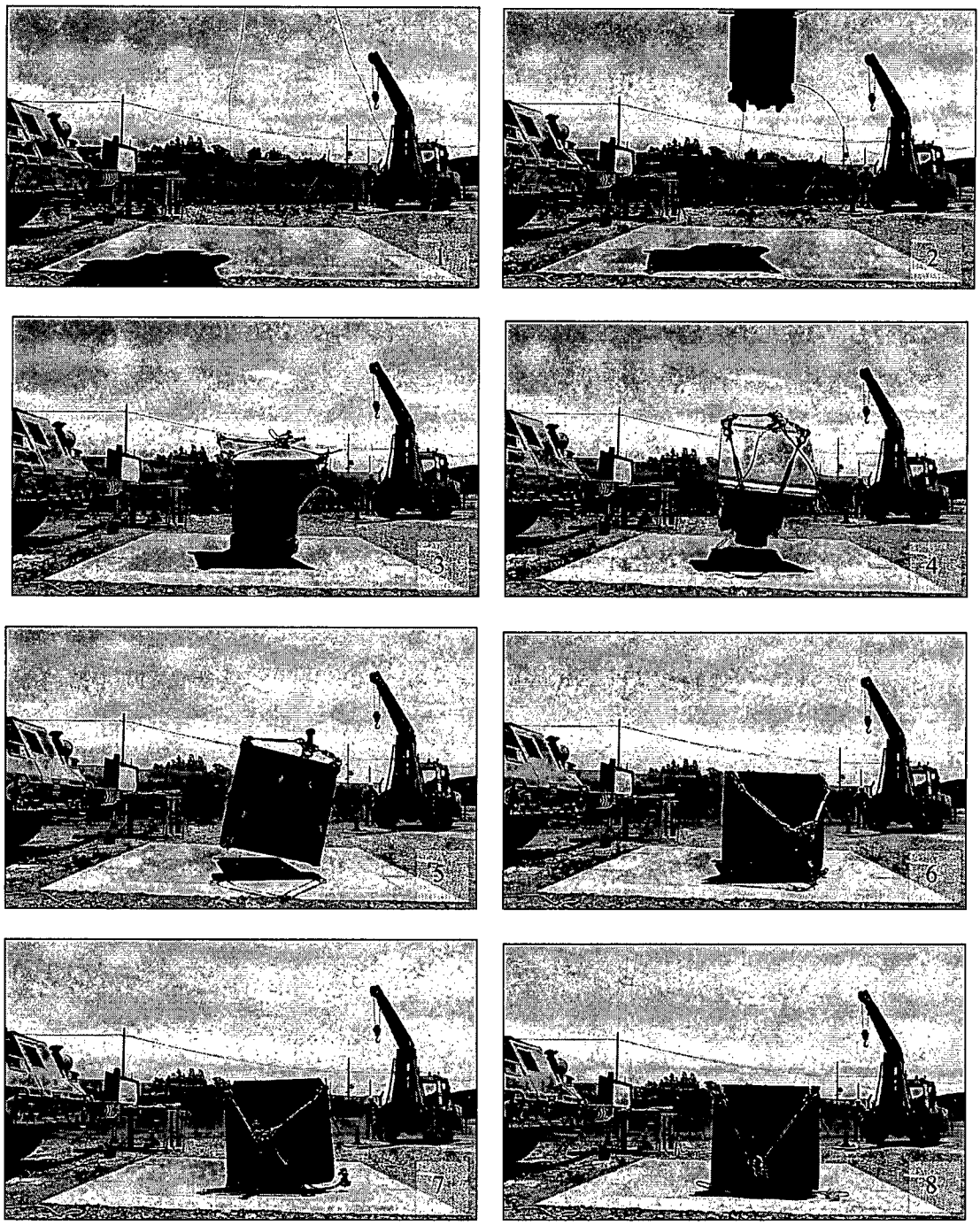

Figure 2: Test action sequence – Angle 1

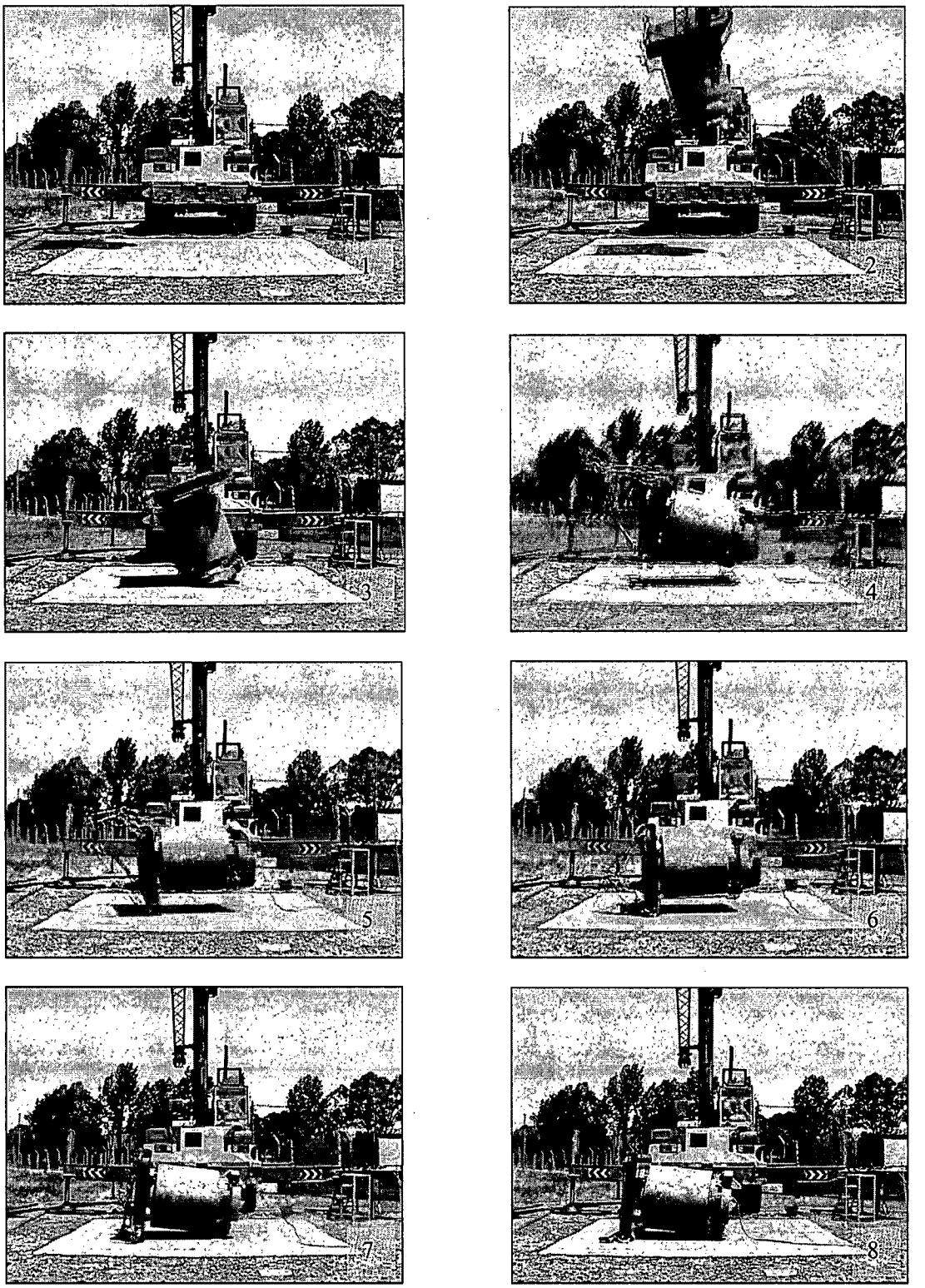

Figure 3: Test action sequence – Angle 2

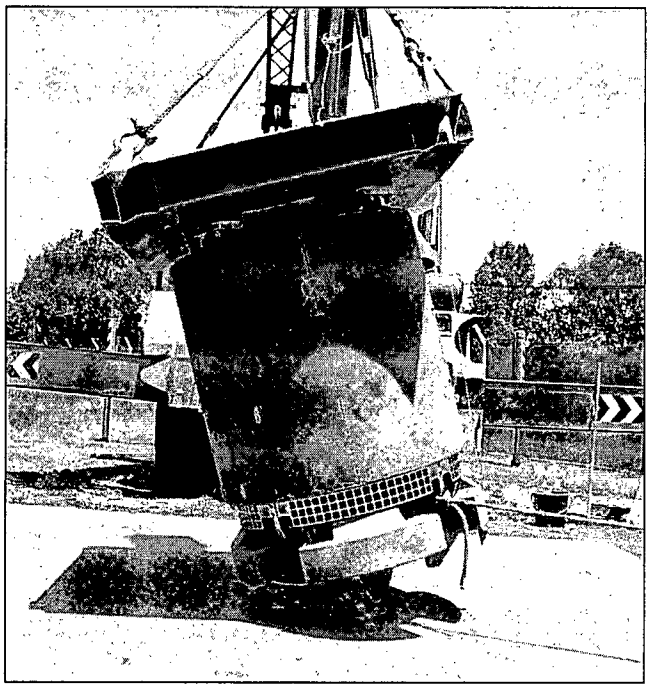

Figure 4: Above target

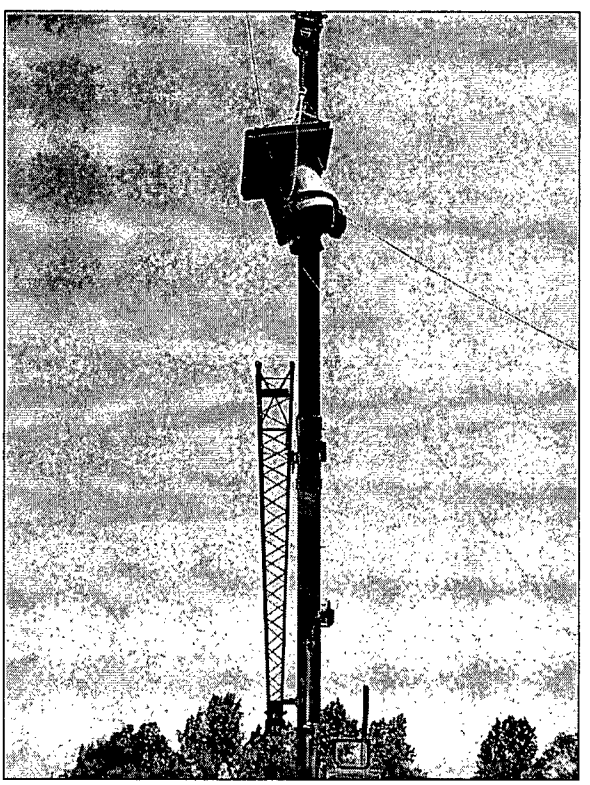

Figure 5: 9.26m above target

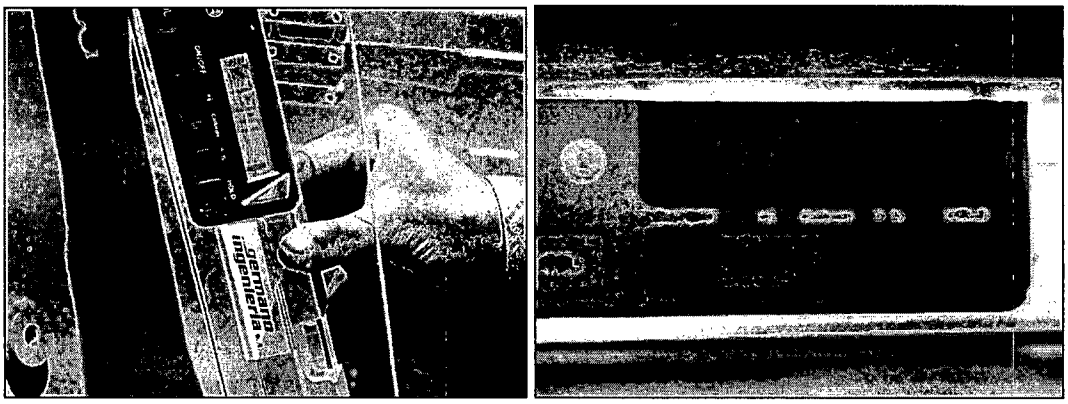

Figure 6: Inclinometer readings (2 planes)

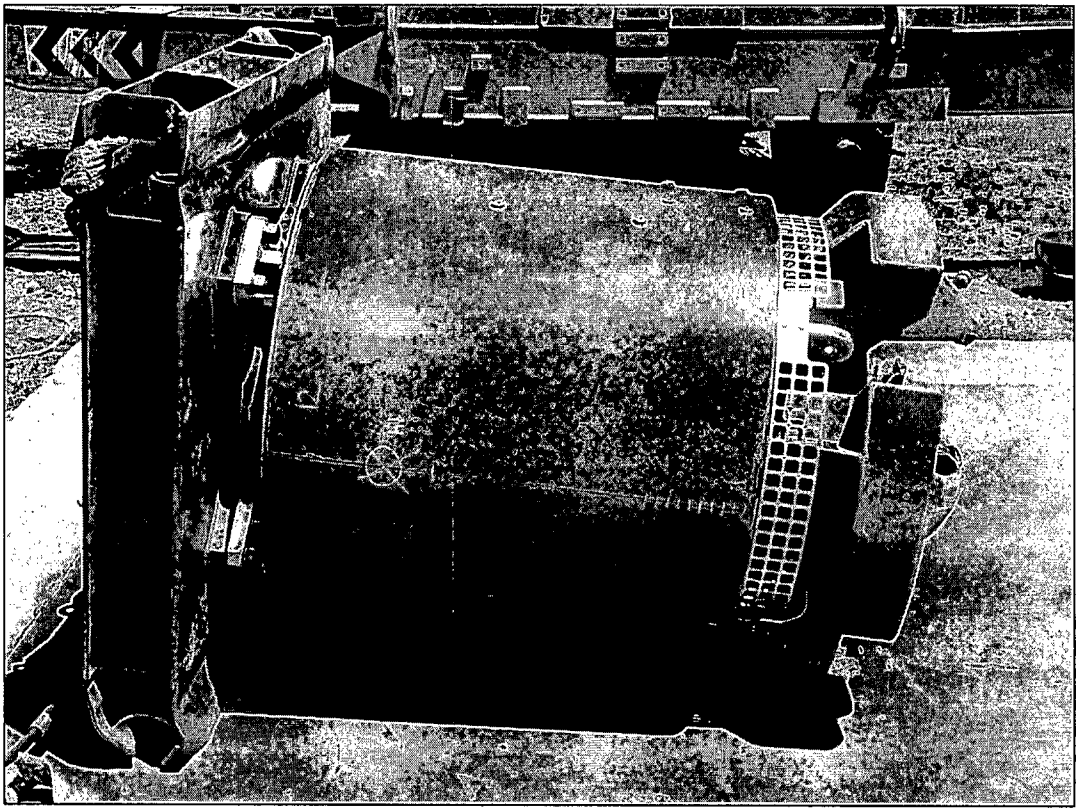

Figure 7: After drop

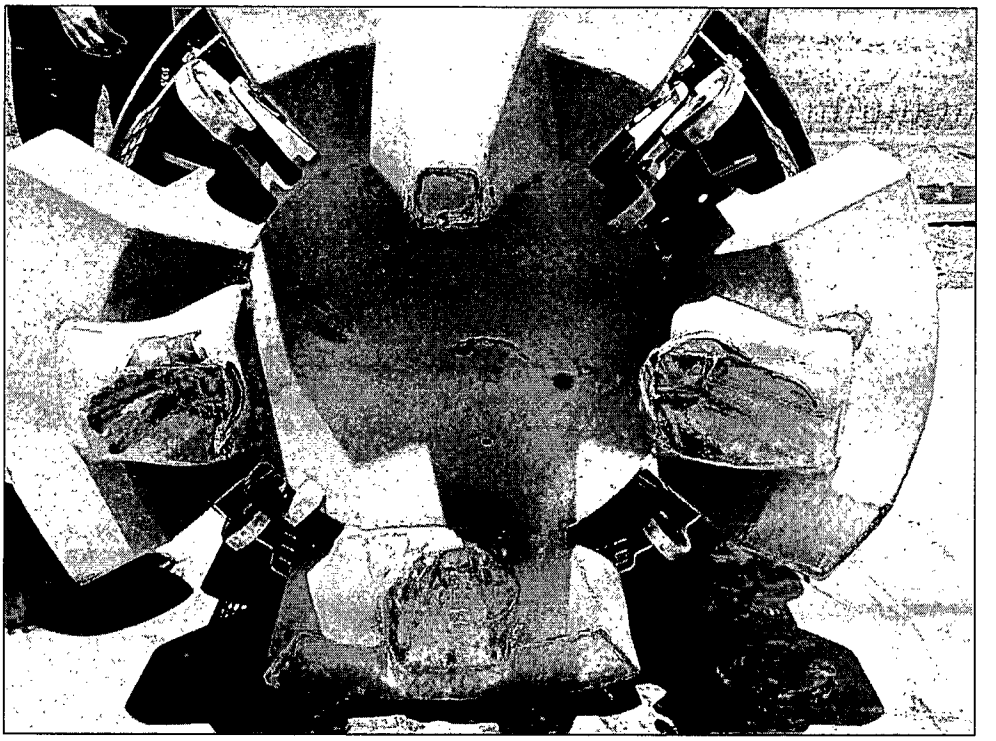

Figure 8: Damage to top shield cones

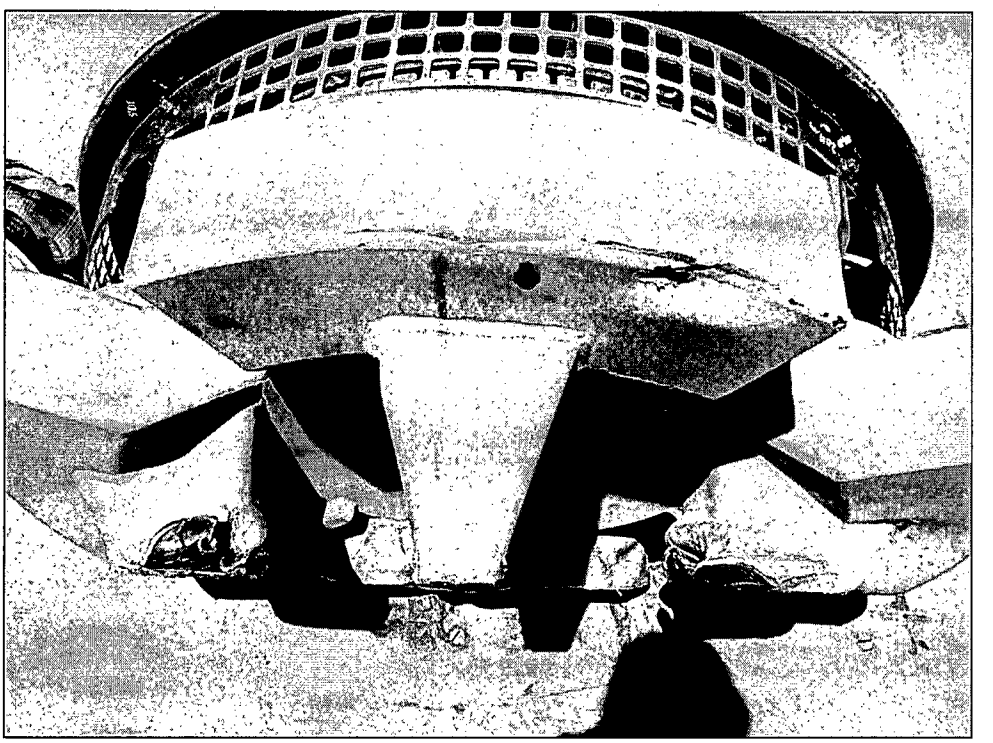

Figure 9: Deformation of top shield cones

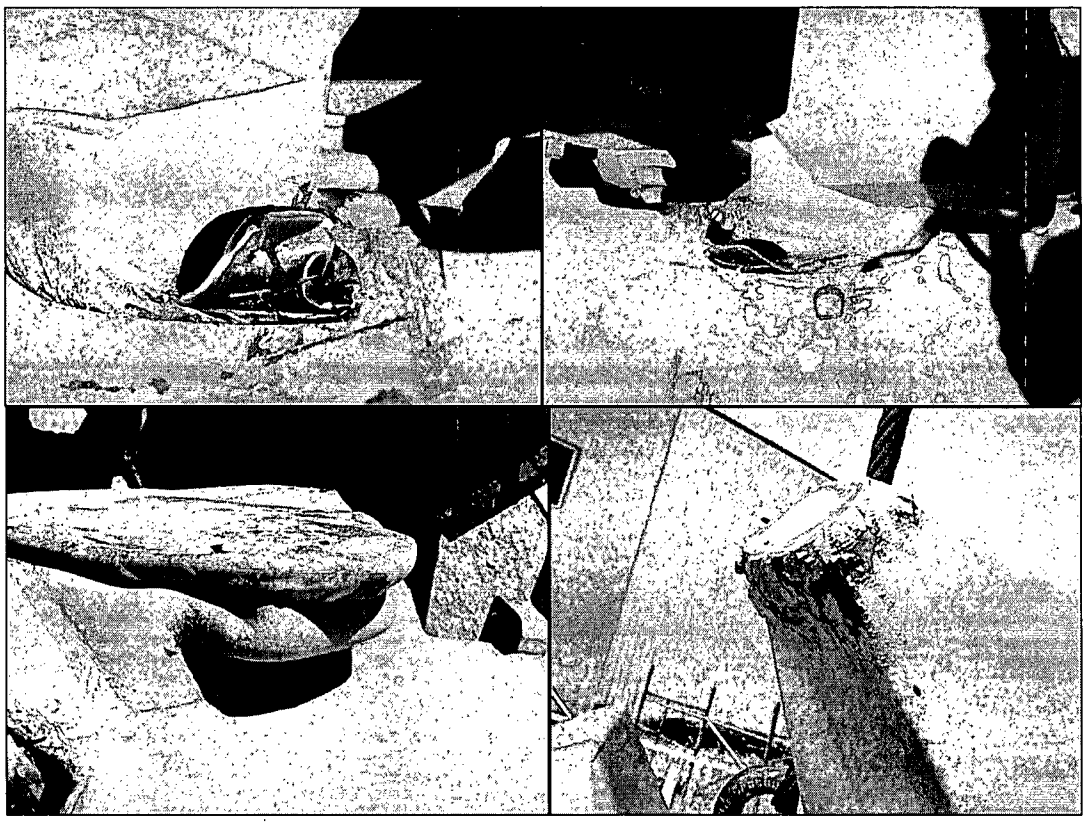

Figure 10: Deformation of top shield cones

Figure 11: Deformation of top shield quadrant

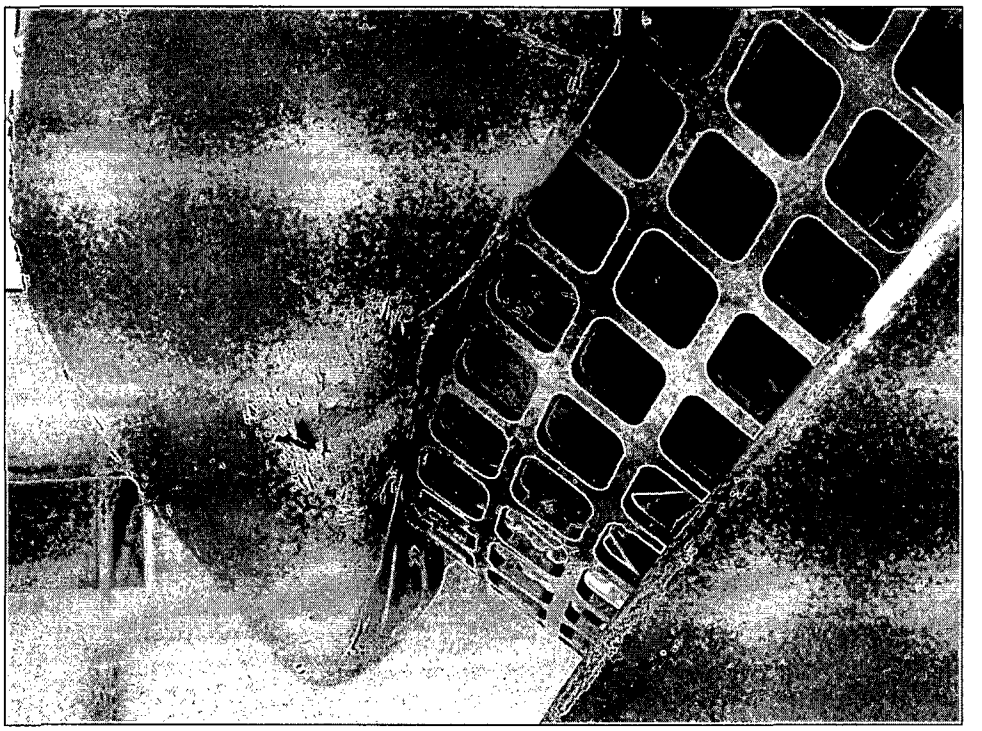

Figure 12: Deformation of top shield quadrant

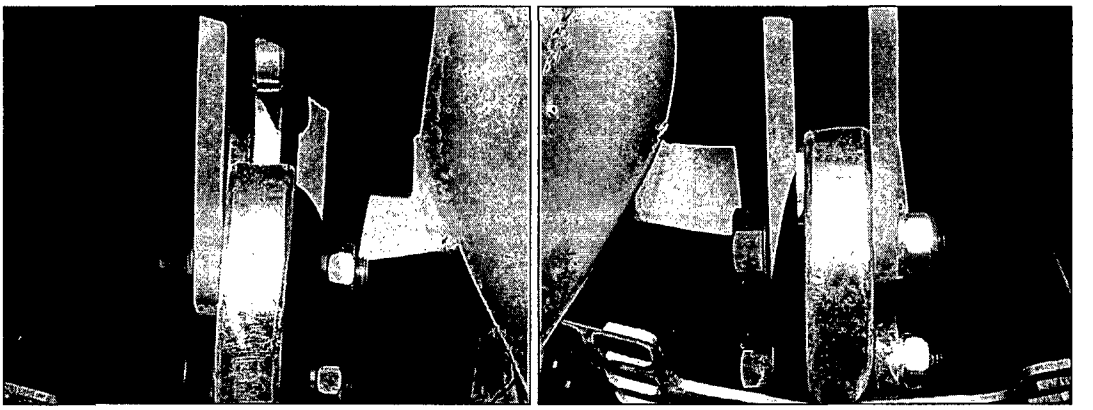

Figure 13: Distortion of top shield quadrant sides

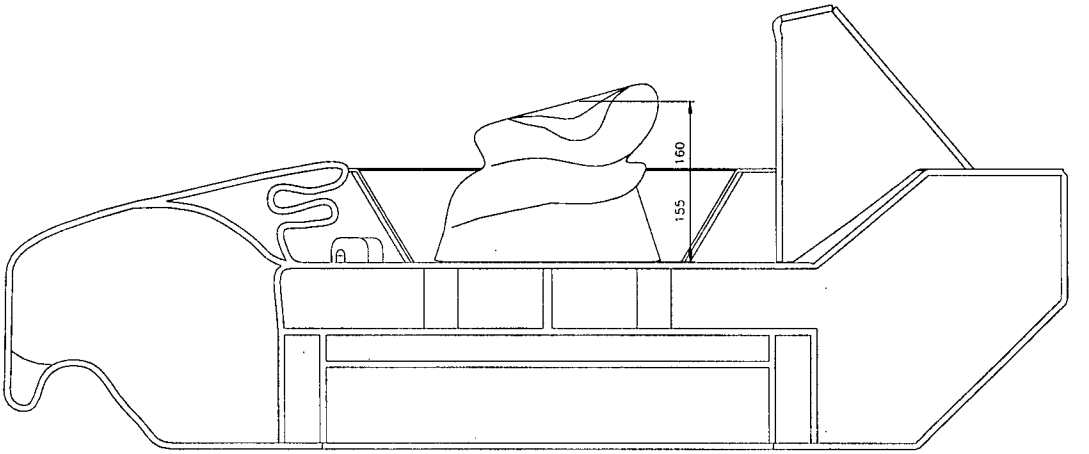

Figure 14: Deformation of cones

Reviss Services (UK) Ltd **Drop Test Checklist (OP225)**	RTR: 246 Date: 20/11/08
Test Description: 9-0m Drop = Angled Inverted (IAEA Type B).	
1. Confirm all personnel are aware of safety rules	✓
2. Test Plan/issue	RTM 118 issue 2, Drop 12.
3. Specimen Design/Serial No/Drg No.	3981/01 (top shield 02).
4. Height gauge Identity/Drg No.	9.26m (GT-8, cal due 11/09).
5. Target Identity/Drg No.	R8085/001 issue B.
6. Punch Identity/Drg No.	N/A
7. Penetration bar Identity/Drg No.	N/A
8. Other Inclinometer Bosch DNM 60L	(Cal. due 30/09/09).
9. Specimen prepared correctly	See RTR 245.
10. Specimen orientated correctly	73.0° & 0.05° on the jacket.
11. Photograph just above target	✓
12. Raise to correct height	✓ 9.26m.
13. Release specimen	✓
14. Photograph in situ	✓
15. Photograph damage	✓
16. Confirm correct execution of drop	✓
17. Pass/Fail (if, applicable see Test Plan)	PASS (fit to continue).

18. Notes

- Top shield cone and upper quadrant crushed. Lower quadrant distorted. Adjacent cones median height above inner surface - 155 & 160mm. Opposite cone - 210 mm.
- Two adjacent quadrants slightly distorted.
- Grill slightly distorted.
- Very slight swelling of flask wall under impact area. No change to gap under top shield.
- Pallet, jacket, top shield and grill securely attached.
- No other damage visible externally.

19. Signed: D W Rayes	Date: 20/11/08
20. Witnessed: Michael Nixon	Date: 20/11/08

REVISS Services
Technical and Manufacturing Group

Test Report No. RTR 247

3981/01
1.0m Punch Test – Angled Inverted

Author:		**Reviewer:**	
Name	P J G Robbins	Name	D W Rogers
Signature		Signature	
Date	02/07/09	Date	02/07/09

1. PURPOSE AND SCOPE

The purpose of this document is to record the performance of the R7021 specimen, 3981/01, in an IAEA drop test for Type B radioactive materials package designs. The full test programme is discussed, justified and detailed in the test plan, RTM 118.

2. DESCRIPTION

2.1 DESIGN

The outer components of the R7021, a cylindrical, insulated jacket, a top shield (with energy absorbing structures and insulation), and a pallet, are constructed predominantly from carbon steel. There is also a stainless steel grill around the top of the jacket to restrict access to hot surfaces. The flask is a stainless steel, lead shielded, upright, finned cylinder with a conventional plug type closure in the top and thermal insulation built into its top and bottom corners. The closure has a vent point and the cavity has a drain tube to allow the flask to be operated in ponds as well as in cells. The cylindrical cavity holds encapsulated radioactive material (solid cobalt metal) in a basket. Although primarily intended to carry Special Form capsules, the flask has a containment system as it may also be used to carry non-Special Form encapsulated cobalt. The closure and the vent and drain plugs are therefore equipped with testable O-ring seals. In addition, to prevent the migration of coarse solids outside the shielded volume, the top of the drain tube is fitted with a mesh filter and a spring gasket is used to seal the gap under the closure around the top of the cavity.

2.2 TEST

1.0 m Punch Test – Angled Inverted (Drop 13, RTM 118). Drop II test for Type B packages (paras. 656 & 727(b), TS-R-1).

2.3 TEST INTENT

To cause maximum distortion of the jacket and damage flask insulation in the top corner.

2.4 PASS/FAIL CRITERIA

The pallet, top shield and jacket shall be secure in order for the specimen to continue to the next test. For internal inspection see IR 0675.

2.5 TARGET

The R8085 target (Drawing No R8085/001) consists of a 50mm thick steel plate bonded to reinforced concrete of dimensions 4m square x 3m deep set flush with the ground. The total mass, 113000 kg, exceeds the RTM 118 minimum requirement of 45000 kg by 150%.

The punch (Drg. No. R8099/002) met RTM 118 requirements and was securely fastened to the target with four M24 screws.

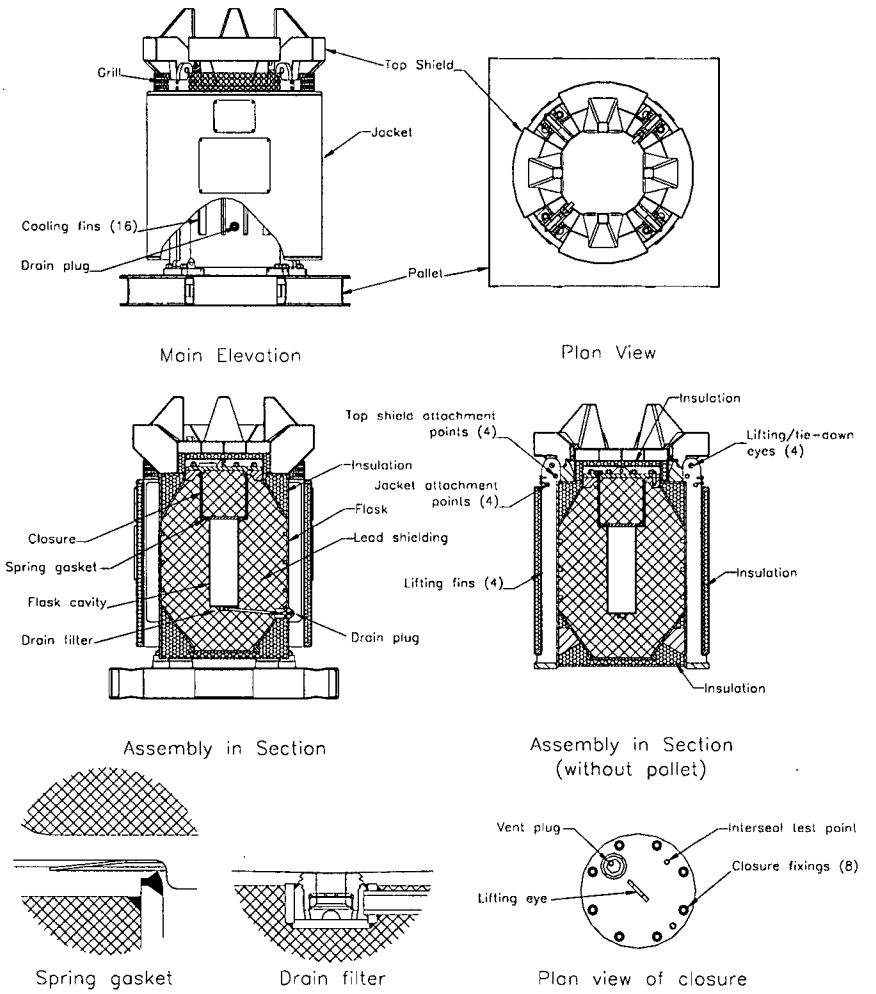

Figure 1: R7021 Constructional Details

2.6 SPECIMEN DETAILS (SEE ALSO IR 0674)

- Identity: 3981/01.
- Contents: A basket containing 48 stainless steel rods.
- Weight: 4374 kg.
- Existing Damage: See IR 0674 & RTR 244 to 246.

2.7 TEST PROCEDURE

As the weight of the container assembly was less than the design maximum gross weight (4500kg), the drop height was increased pro rata to compensate. The test height was therefore (4500/4374) x 1.0 = 1.030m.

The test was conducted in accordance with OP 225. The specified angle was 41° ± 2° from the horizontal. All key actions were recorded on the test record sheet (attached).

3. RESULTS

- The test was executed correctly (Figures 2-5). The angle measured on the jacket was 41.2° from the horizontal (Figure 6).
- The pallet, jacket, top shield and grill remained securely attached (Figure 7).
- There was localised jacket and grill distortion (Figures 8 & 9).
- There was localised cracking of the outer, upper circumferential jacket weld (Figure 11).
- The jacket lifting lug was slightly crushed against the side of the flask (Figures 10 & 14).
- The pallet suffered minor damage from secondary impact (Figures 12 & 13).
- The punch showed good impact location and no significant deformation (Figure 15).
- There was no other externally visible damage.

See Illustrations for photographic record.

4. CONCLUSIONS

The R7021 test specimen, 3981/01, was fit to continue to the next test.

5. REFERENCES

- IR 0674: 3981/01 Assembly Prior to Accident Conditions Drop Testing, REVISS Services (UK) Ltd.
- IR 0675: 3981/01 Inspection After Accident Conditions Drop Testing, REVISS Services (UK) Ltd.
- OP 225: Drop Testing Procedure, REVISS Services (UK) Ltd.
- R8085/001 issue B: Drop Test Target, REVISS Services (UK) Ltd.
- R8099/002 issue A: Drop Test Punch, REVISS Services (UK) Ltd.
- RTM 118: Test Plan for the R7021 Transport Container, REVISS Services (UK) Ltd.
- RTR 244: 1.0m Punch Test – Angled Inverted, REVISS Services (UK) Ltd.
- RTR 245: 1.0m Punch Test – Angled Inverted, REVISS Services (UK) Ltd.
- RTR 246: 9.0m Free Drop Test – Angled Inverted, REVISS Services (UK) Ltd.
- TS-R-1: Safety Standards Series, Regulations for the Safe Transport of Radioactive Material 1996 Edition (As amended 2003), IAEA, Vienna.

6. ATTACHMENTS

RTR 247: Drop Test Checklist, REVISS Services (UK) Ltd.

7. ILLUSTRATIONS

page
Figure 2: Test action sequence – Angle 1 6
Figure 3: Test action sequence – Angle 2 7
Figure 4: 1.030m above target 8
Figure 5: 1.030m above target (with height gauge) 8
Figure 6: Inclinometer readings (2 planes) 9
Figure 7: After drop 9
Figure 8: Distortion of jacket and grill 10
Figure 9: Distortion of jacket and grill 10
Figure 10: Distortion of lifting lug 11
Figure 11: Jacket weld failure 11
Figure 12: Damage to pallet (secondary impact) 12
Figure 13: Damage to pallet (secondary impact) 12
Figure 14: Distortion of lifting lug 13
Figure 15: Condition of punch 13

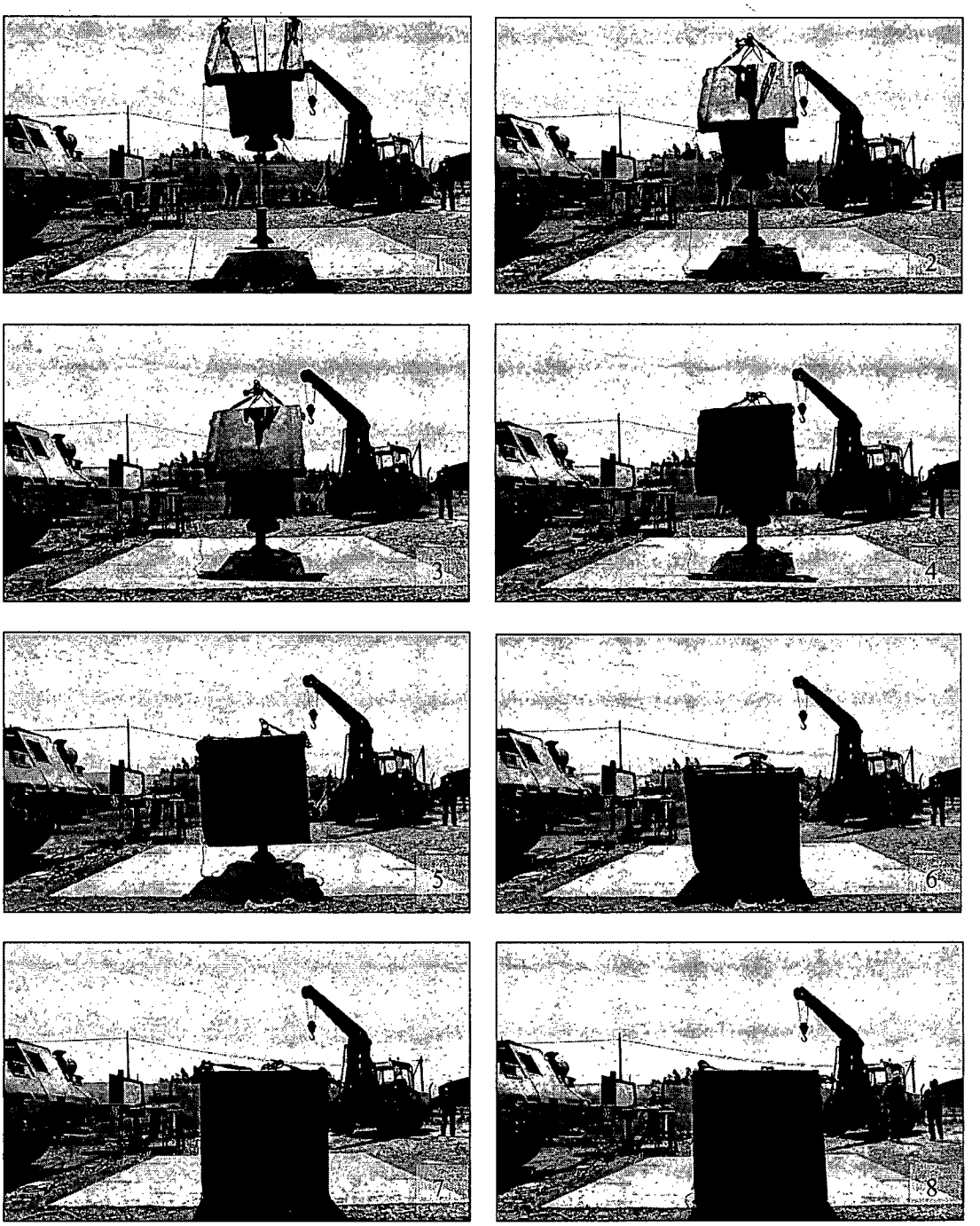

Figure 2: Test action sequence – Angle 1

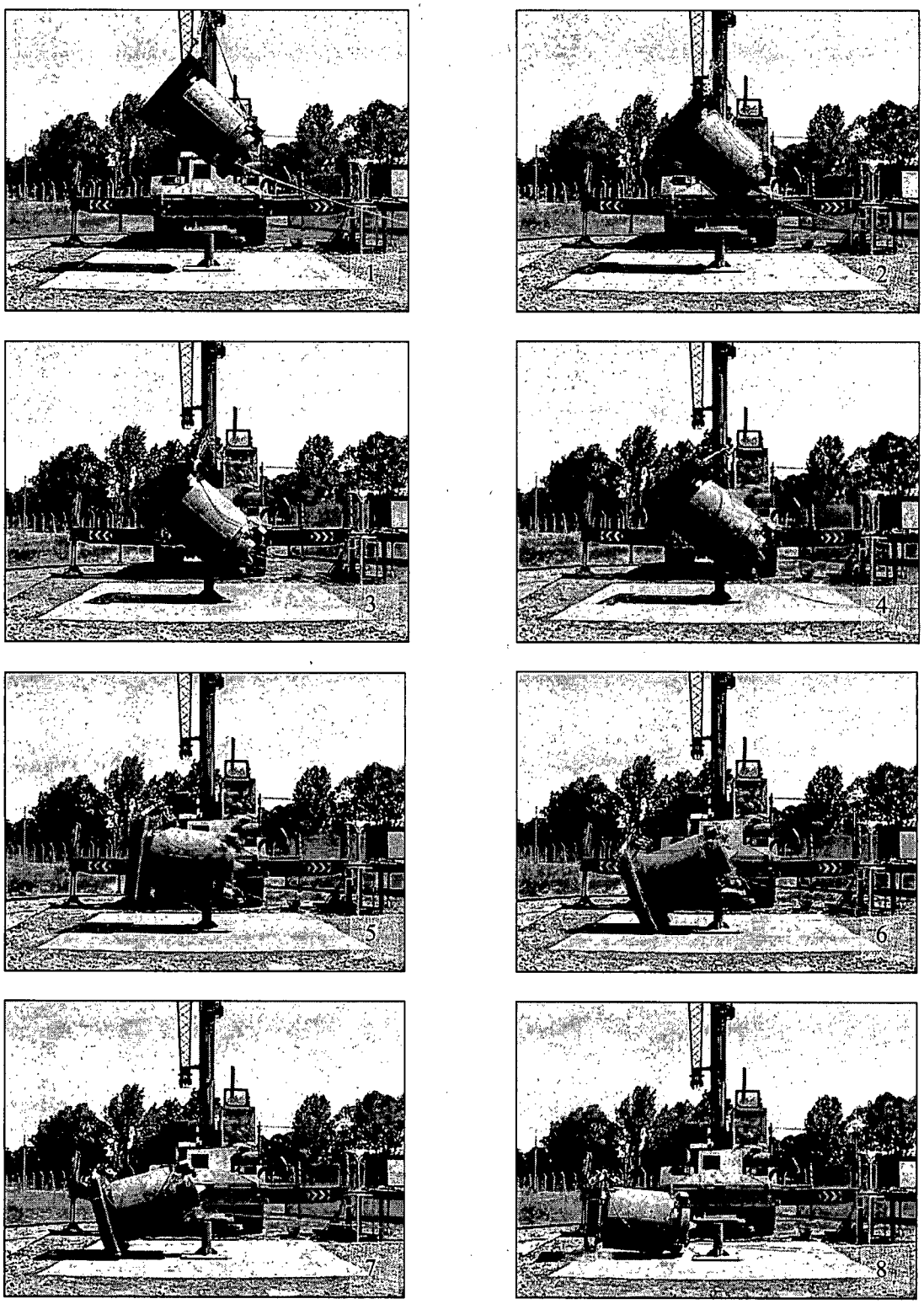

Figure 3: Test action sequence – Angle 2

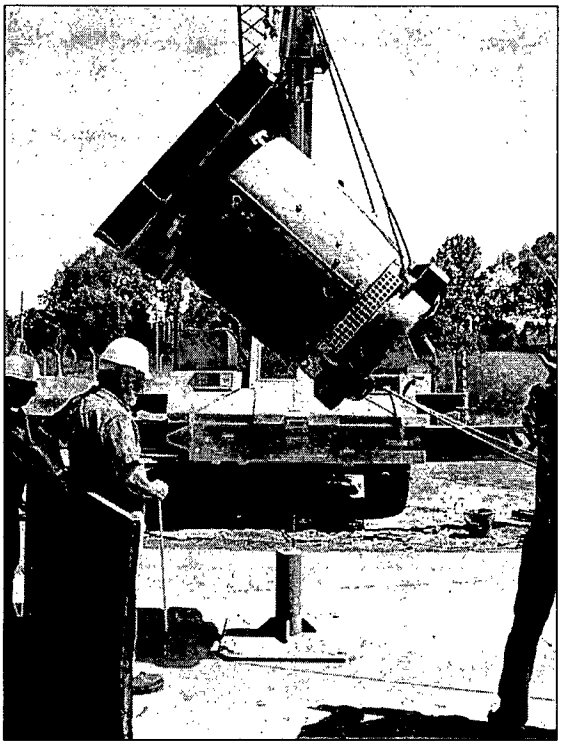

Figure 4: 1.030m above target

Figure 5: 1.030m above target (with height gauge)

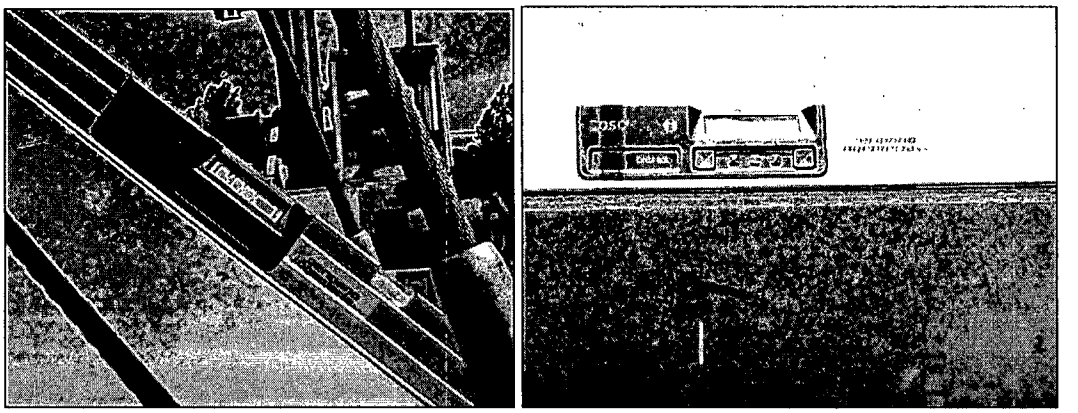

Figure 6: Inclinometer readings (2 planes)

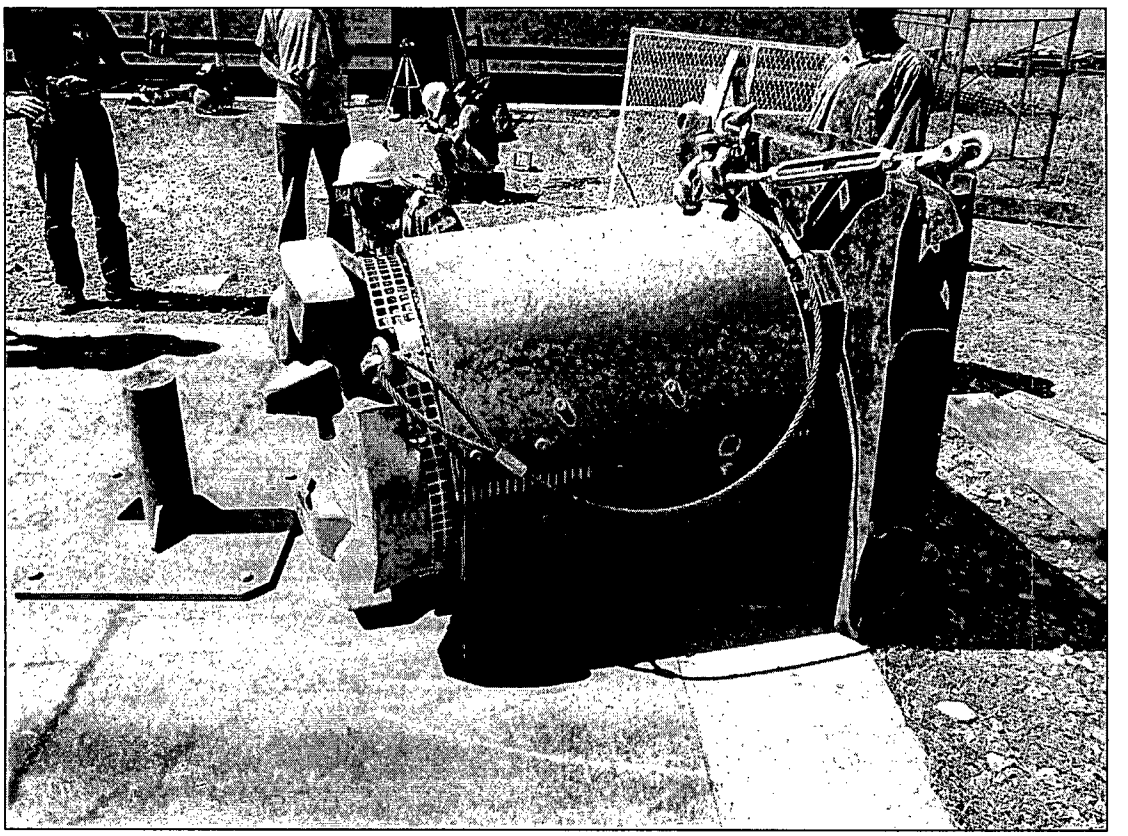

Figure 7: After drop

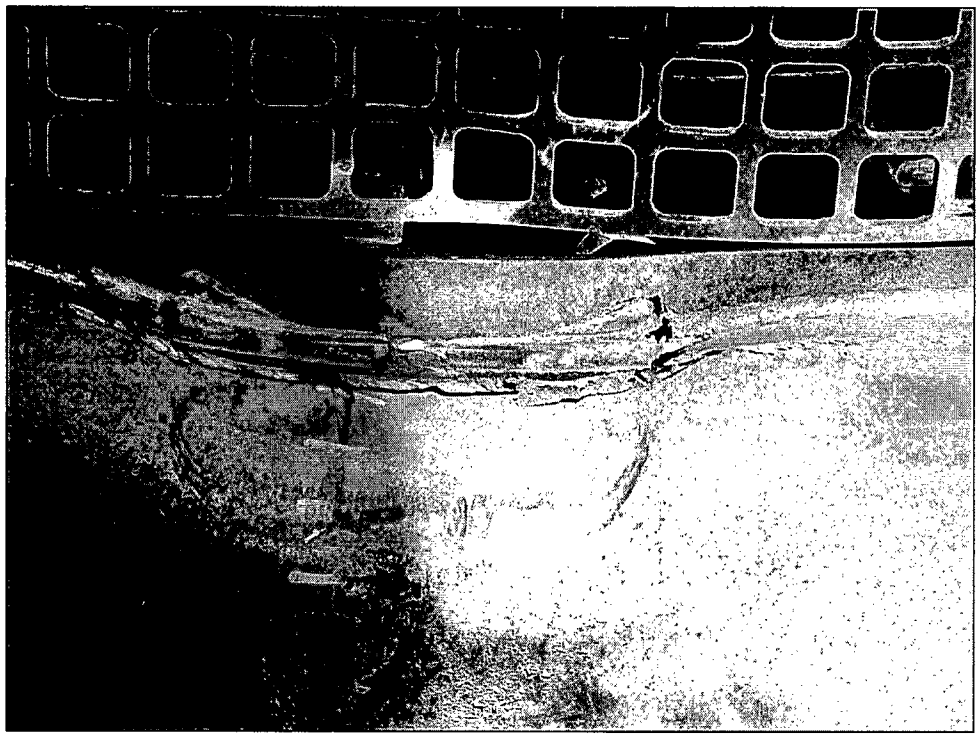

Figure 8: Distortion of jacket and grill

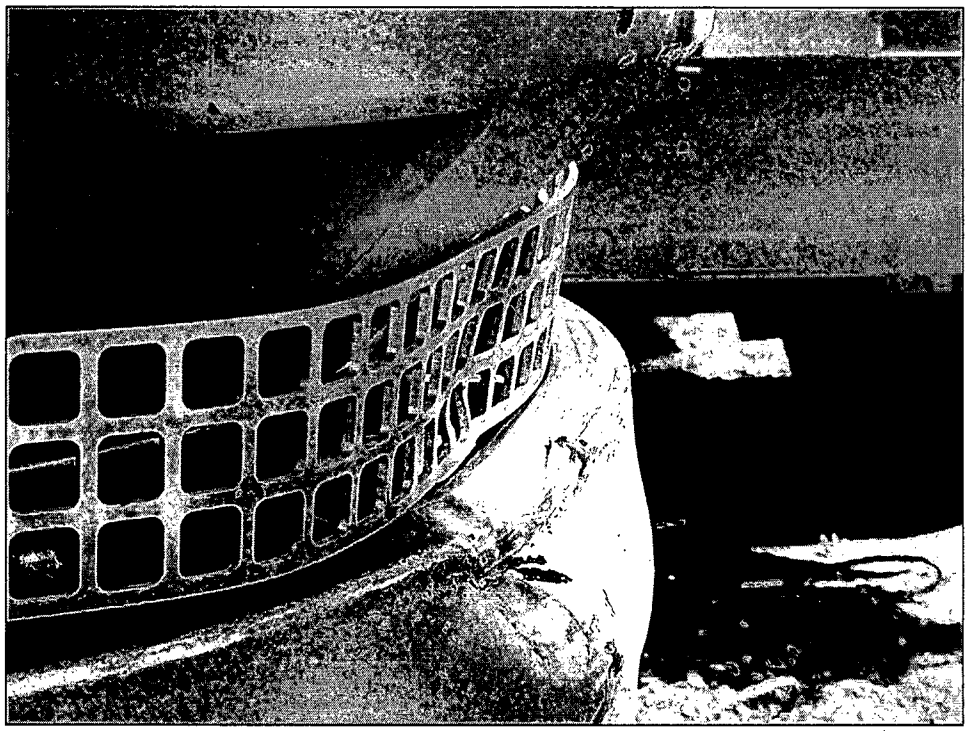

Figure 9: Distortion of jacket and grill

Figure 10: Distortion of lifting lug

Figure 11: Jacket weld failure

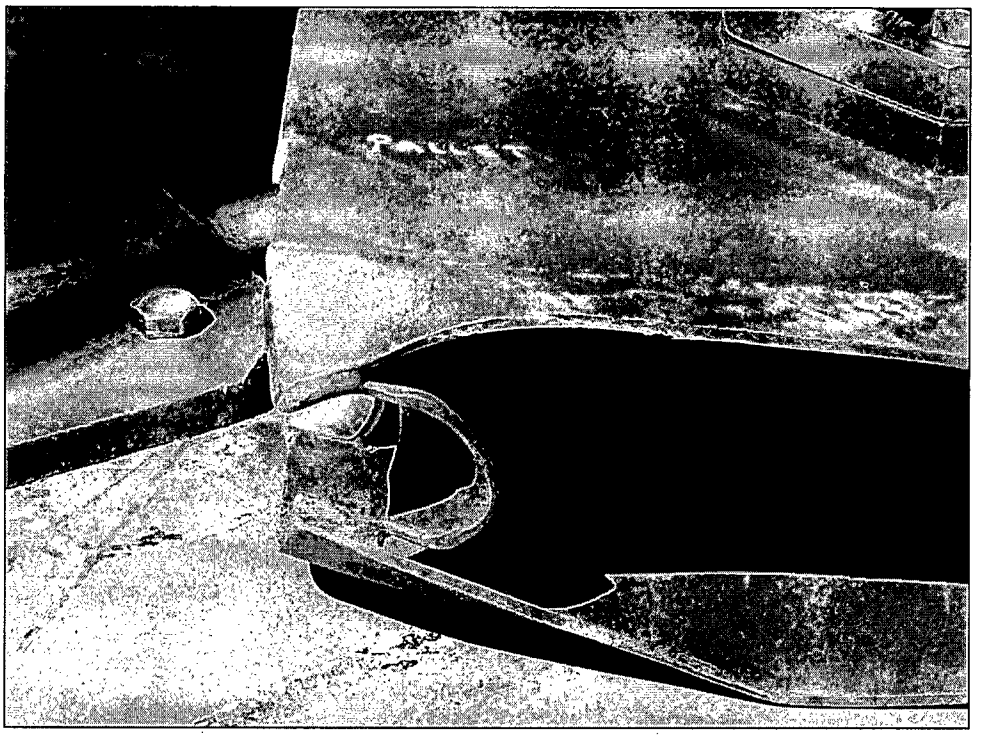

Figure 12: Damage to pallet (secondary impact)

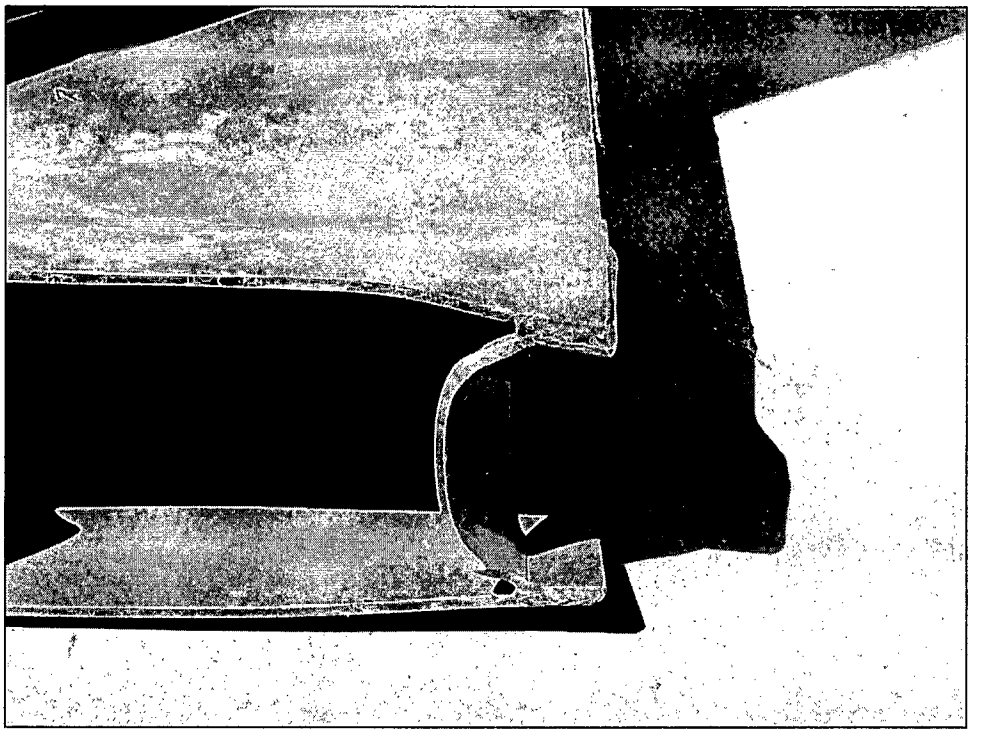

Figure 13: Damage to pallet (secondary impact)

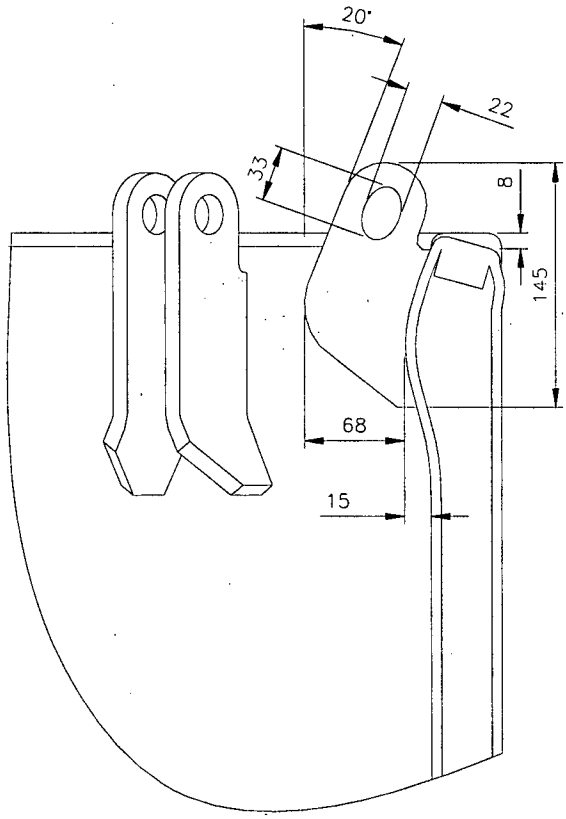

Figure 14: Distortion of lifting lug

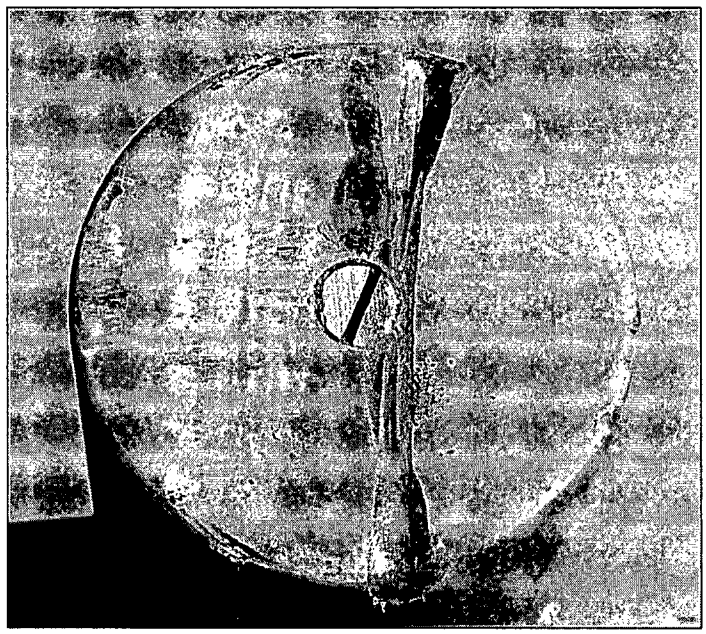

Figure 15: Condition of punch

Reviss Services (UK) Ltd **Drop Test Checklist (OP225)**	RTR: 247 Date: 20/11/08
Test Description: 1·0m Punch Test: Angled Inverted onto Jacket (IAEA Type B).	
1. Confirm all personnel are aware of safety rules	✓
2. Test Plan/issue	RTM118 issue 2, Drop 13.
3. Specimen Design/Serial No/Drg No.	3981/01 (top shield 02).
4. Height gauge Identity/Drg No.	1·030m (R8083/005 issue A).
5. Target Identity/Drg No.	R8085/001 issue B.
6. Punch Identity/Drg No.	R8099/002 issue A (new punch).
7. Penetration bar Identity/Drg No.	N/A
8. Other Inclinometer Bosch DNM 60L	(cal. due 30/09/09).
9. Specimen prepared correctly	See RTR 246
10. Specimen orientated correctly	41·2° & 0·2° on jacket & pallet.
11. Photograph just above target	✓
12. Raise to correct height	✓ 1·030m
13. Release specimen	✓
14. Photograph in situ	✓
15. Photograph damage	✓
16. Confirm correct execution of drop	✓ Impact line across centre of punch.
17. Pass/Fail (if, applicable see Test Plan)	PASS (fob to continue).

18. Notes

- Localised distortion of jacket. Depth
- Jacket lifting lug slightly crushed into side of flask.
- Flask fins each side of lifting lug bent outwards slightly at top.
- Grill deformed inwards slightly.
- No other damage visible externally.
- Pallet, jacket, top shield and grill securely attached.

19. Signed: D W Rogers	Date: 20/11/08
20. Witnessed: Michael N. [illegible]	Date: 20/11/08

REVISS

REVISS Services
Technical and Manufacturing Group

Test Report No. RTR 248

3981/01
1.0m Punch Test – Angled Side

Author:		**Reviewer:**	
Name	P J G Robbins	Name	D W Rogers
Signature		Signature	
Date	03/07/09	Date	03/07/09

1. PURPOSE AND SCOPE

The purpose of this document is to record the performance of the R7021 specimen, 3981/01, in an IAEA drop test for Type B radioactive materials package designs. The full test programme is discussed, justified and detailed in the test plan, RTM 118.

2. DESCRIPTION

2.1 DESIGN

The outer components of the R7021, a cylindrical, insulated jacket, a top shield (with energy absorbing structures and insulation), and a pallet, are constructed predominantly from carbon steel. There is also a stainless steel grill around the top of the jacket to restrict access to hot surfaces. The flask is a stainless steel, lead shielded, upright, finned cylinder with a conventional plug type closure in the top and thermal insulation built into its top and bottom corners. The closure has a vent point and the cavity has a drain tube to allow the flask to be operated in ponds as well as in cells. The cylindrical cavity holds encapsulated radioactive material (solid cobalt metal) in a basket. Although primarily intended to carry Special Form capsules, the flask has a containment system as it may also be used to carry non-Special Form encapsulated cobalt. The closure and the vent and drain plugs are therefore equipped with testable O-ring seals. In addition, to prevent the migration of coarse solids outside the shielded volume, the top of the drain tube is fitted with a mesh filter and a spring gasket is used to seal the gap under the closure around the top of the cavity.

2.2 TEST

1.0 m Punch Test – Angled Side (Drop 14, RTM 118). Drop II test for Type B packages (paras. 656 & 727(b), TS-R-1).

2.3 TEST INTENT

To penetrate the jacket and damage the flask.

2.4 PASS/FAIL CRITERIA

The pallet, top shield and jacket shall be secure in order for the specimen to continue to the next test. For internal inspection see IR 0675.

2.5 TARGET

The R8085 target (Drg. No. R8085/001) consists of a 50mm thick steel plate bonded to reinforced concrete of dimensions 4m square x 3m deep set flush with the ground. The total mass, 113000 kg, exceeds the RTM 118 minimum requirement of 45000 kg by 150%.

The punch (Drg. No. R8099/002) met RTM 118 requirements and was securely fastened to the target with four M24 screws.

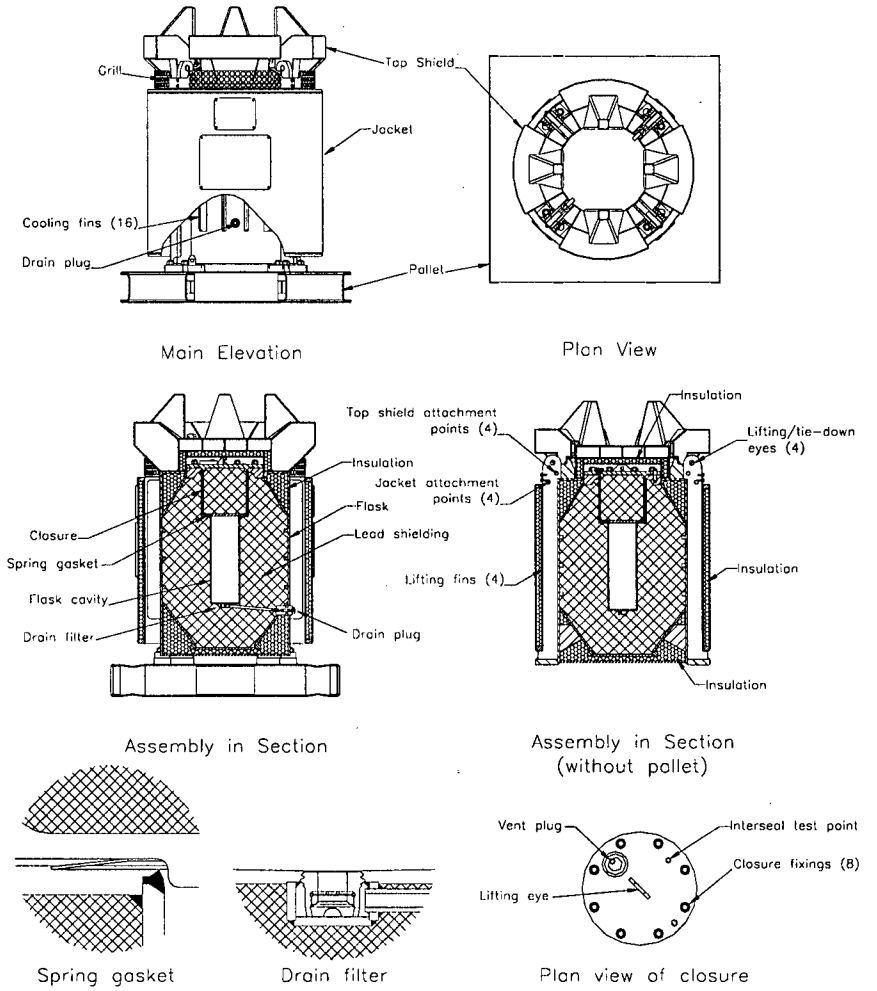

Figure 1: R7021 Constructional Details

2.6 SPECIMEN DETAILS (SEE ALSO IR 0674)

- Identity: 3981/01.
- Contents: A basket containing 48 stainless steel rods.
- Weight: 4374 kg.
- Existing Damage: See IR 0674 & RTRs 244 to 247.

2.7 TEST PROCEDURE

As the weight of the container assembly was less than the design maximum gross weight (4500kg), the drop height was increased pro rata to compensate. The test height was therefore (4500/4374) x 1.0 = 1.030m.

The test was conducted in accordance with OP 225. The specified angle was 25° ± 2° from the horizontal. All key actions were recorded on the test record sheet (attached).

3. RESULTS

- The test was executed correctly (Figures 2-5). The angle measured for the drop was 25.6° from the horizontal (Figure 6). The pallet edge went very close to the punch mounting before recovering slightly but the high speed footage showed that it did not actually touch it (Figure 7).
- The pallet, jacket, top shield and grill remained securely attached (Figure 8).
- The jacket outer and inner skins were partially sheared through. The outer skin was depressed to a maximum of 114mm. The inner skin was 4-5mm from the flask wall at the tip. The outer skin was sheared for 60% of punch diameter (Figures 9-11).
- The flask fins behind the hole in the jacket were distorted outwards locally (Figure 9).
- The punch showed no significant damage (Figure 12).

See Illustrations for photographic record.

4. CONCLUSIONS

The R7021 test specimen, 3981/01, was fit to continue to the next test.

5. REFERENCES

- IR 0674: 3981/01 Assembly Prior to Accident Conditions Drop Testing, REVISS Services (UK) Ltd.
- IR 0675: 3981/01 Inspection After Accident Conditions Drop Testing, REVISS Services (UK) Ltd.
- OP 225: Drop Testing Procedure, REVISS Services (UK) Ltd.
- R8085/001 issue B: Drop Test Target, REVISS Services (UK) Ltd.
- R8099/002 issue A: Drop Test Punch, REVISS Services (UK) Ltd.
- RTM 118: Test Plan for the R7021 Transport Container, REVISS Services (UK) Ltd.
- RTR 244: 1.0m Punch Test – Angled Inverted, REVISS Services (UK) Ltd.
- RTR 245: 1.0m Punch Test – Angled Inverted, REVISS Services (UK) Ltd.
- RTR 246: 9.0m Free Drop Test – Angled Inverted, REVISS Services (UK) Ltd.
- RTR 247: 1.0m Punch Test – Angled Inverted, REVISS Services (UK) Ltd.
- TS-R-1: Safety Standards Series, Regulations for the Safe Transport of Radioactive Material 1996 Edition (As amended 2003), IAEA, Vienna.

6. ATTACHMENTS

RTR 248: Drop Test Checklist, REVISS Services (UK) Ltd.

7. ILLUSTRATIONS

page
Figure 2: Test action sequence – Angle 1 6
Figure 3: Test action sequence – Angle 2 7
Figure 4: Above target 8
Figure 5: 1.030m above punch (with height gauge) 8
Figure 6: Inclinometer readings (2 planes) 9
Figure 7: High speed image showing lowest point of initial impact 9
Figure 8: After drop 10
Figure 9: Impact point and jacket penetration 10
Figure 10: Distortion of jacket 11
Figure 11: Punch penetration 12
Figure 12: Condition of punch 12

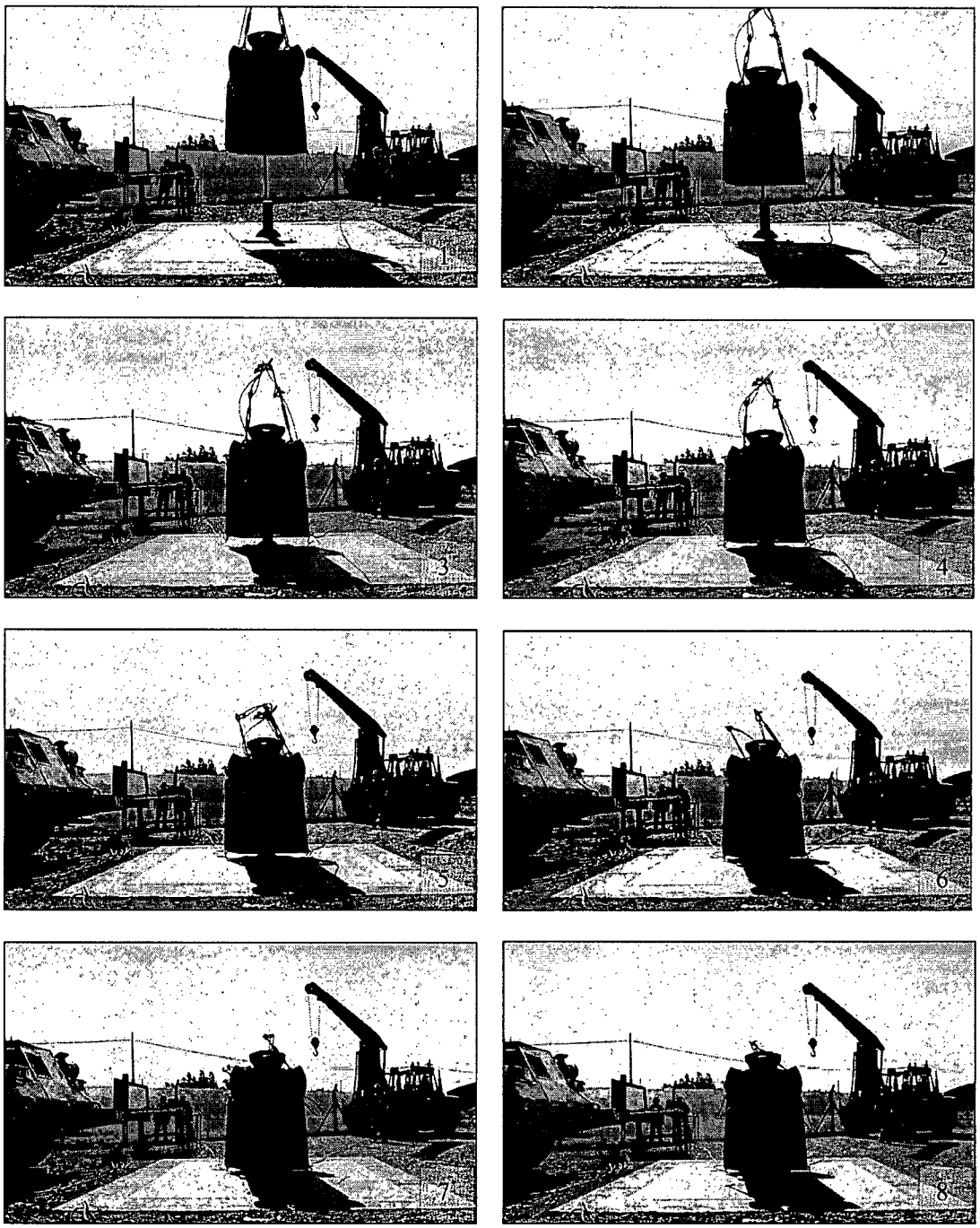

Figure 2: Test action sequence – Angle 1

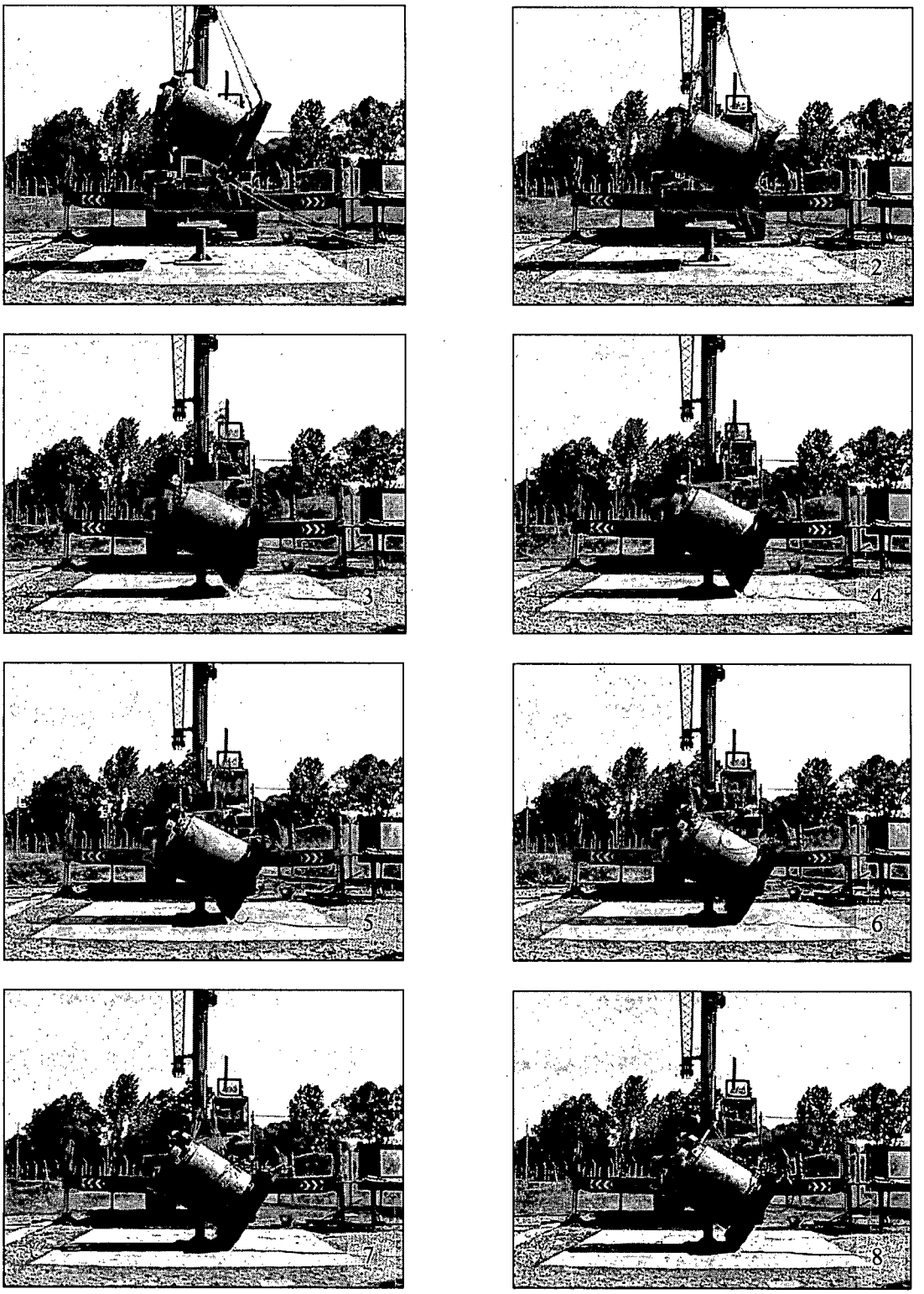

Figure 3: Test action sequence – Angle 2

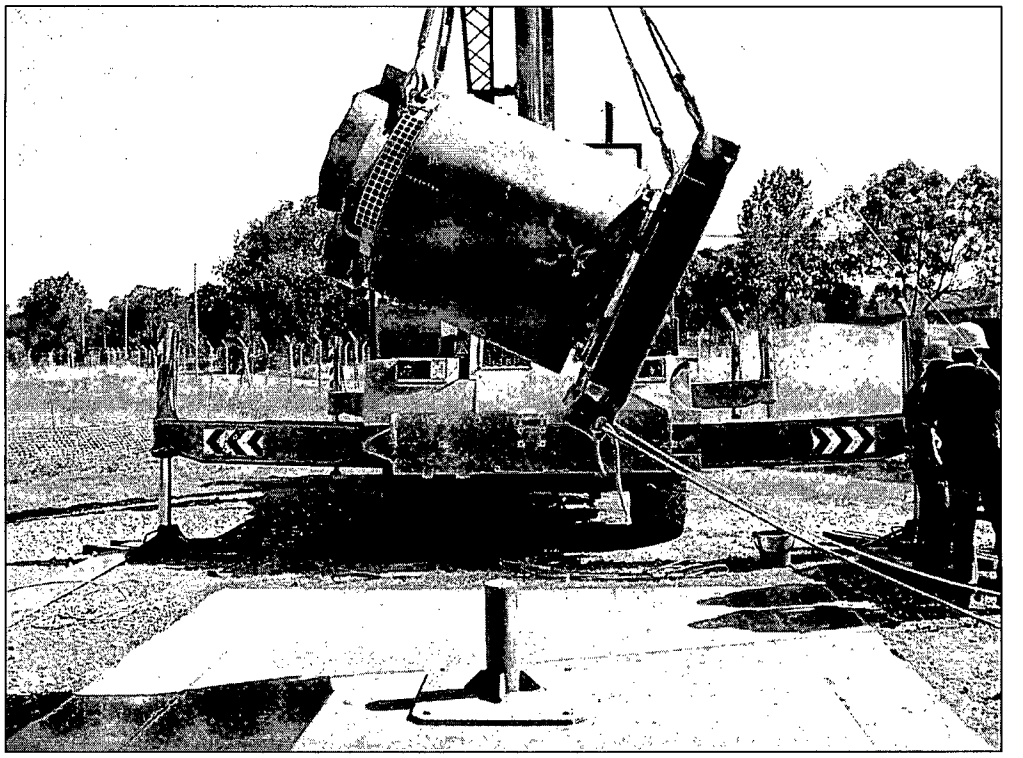

Figure 4: Above target

Figure 5: 1.030m above punch (with height gauge)

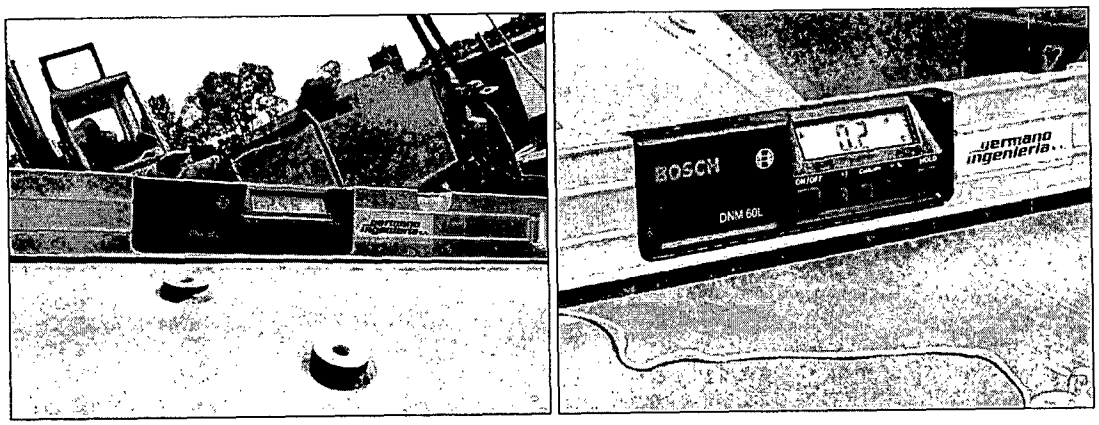

Figure 6: Inclinometer readings (2 planes)

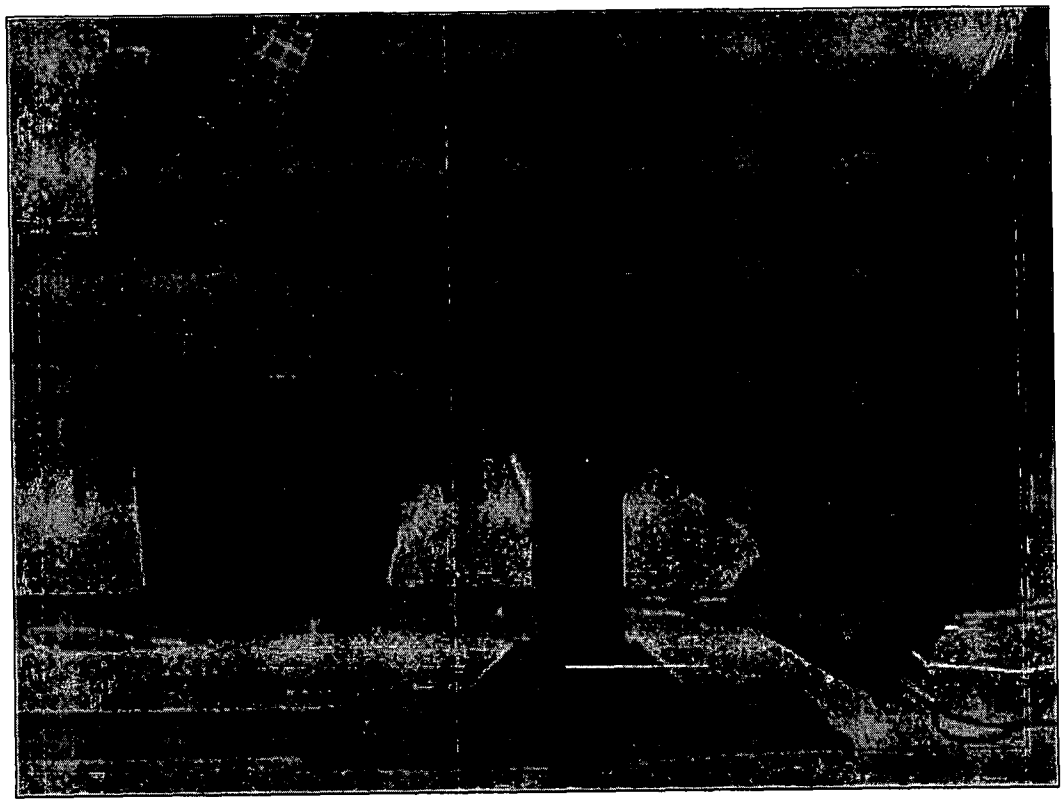

Figure 7: High speed image showing lowest point of initial impact

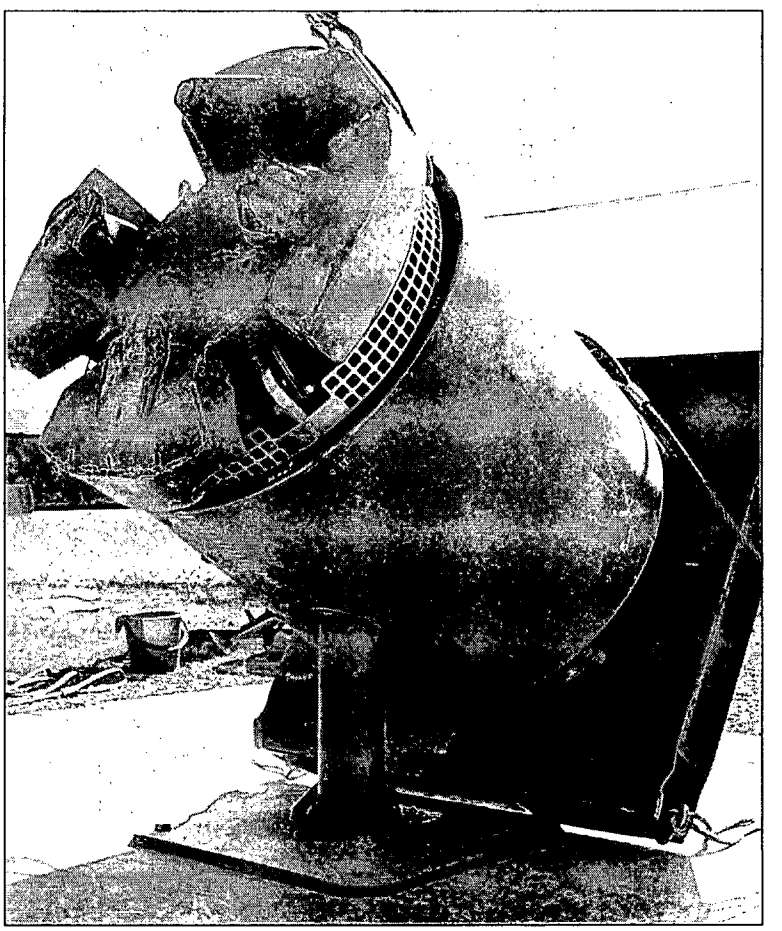

Figure 8: After drop

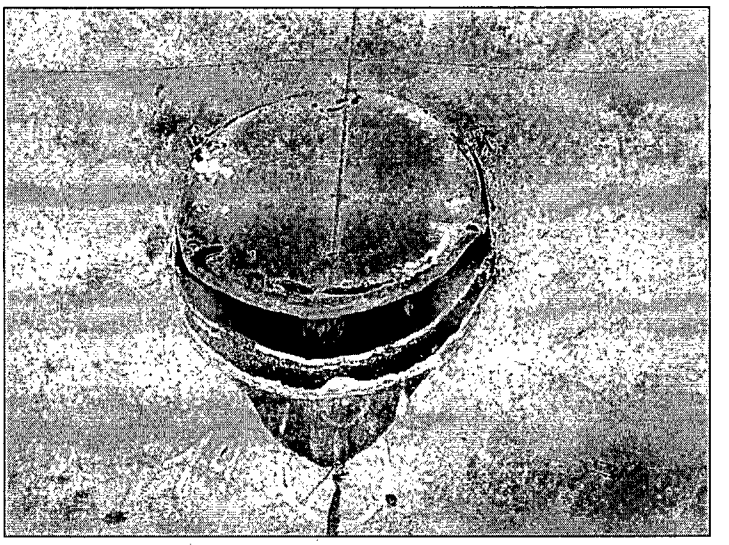

Figure 9: Impact point and jacket penetration

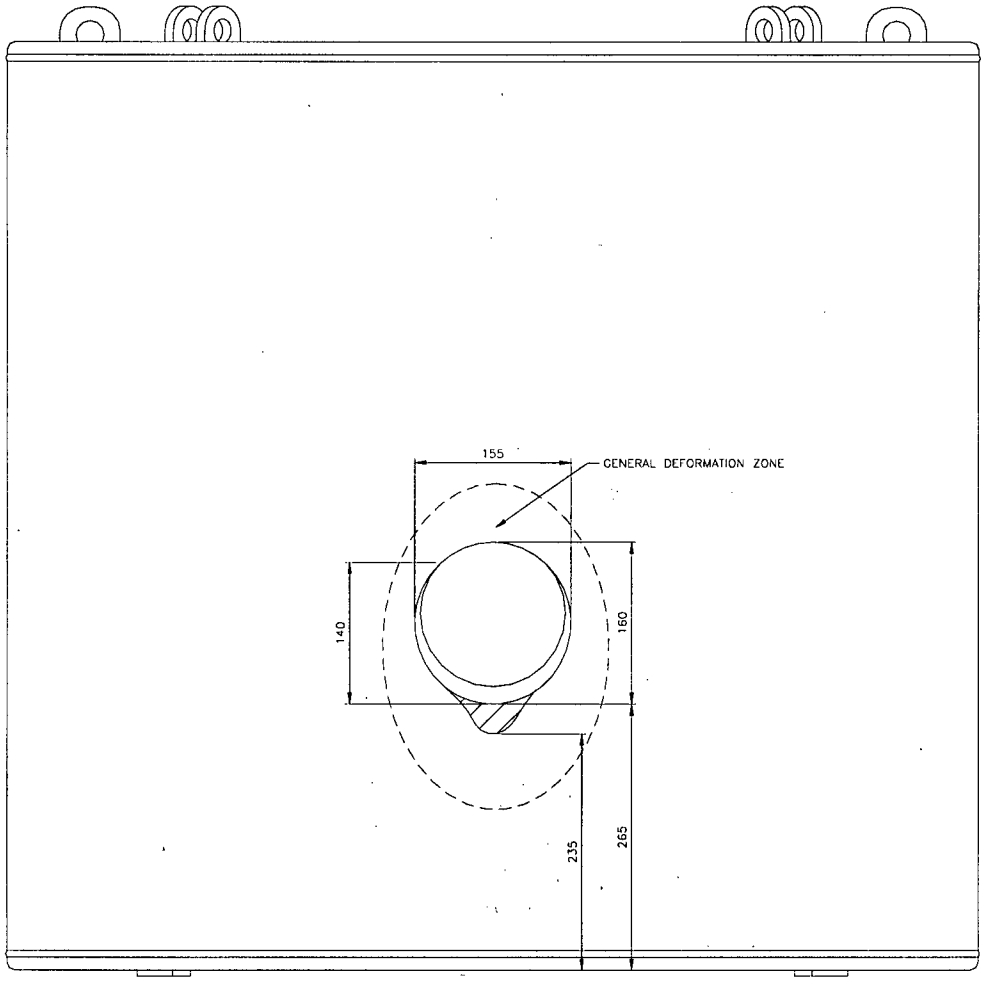

Figure 11: Punch penetration

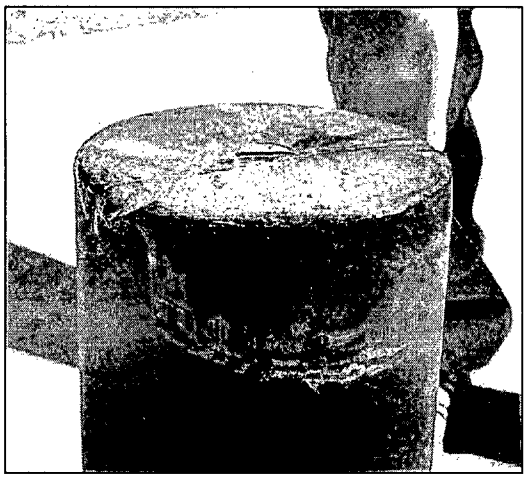

Figure 12: Condition of punch

Reviss Services (UK) Ltd **Drop Test Checklist (OP225)**	RTR: 248 Date: 20/11/08
Test Description: 1-0m Punch Test - Angled Side (IAEA Type B).	
1. Confirm all personnel are aware of safety rules	✓
2. Test Plan/issue	RTM118 issue 2, Drop 14.
3. Specimen Design/Serial No/Drg No.	3981/01 (top shield 02).
4. Height gauge Identity/Drg No.	1.030m (R8083/005 issue A).
5. Target Identity/Drg No.	R8085/001 issue B.
6. Punch Identity/Drg No.	R8099/002 issue A.
7. Penetration bar Identity/Drg No.	N/A
8. Other Inclinometer Bosch DNM 60L	(cal. due 30/09/09).
9. Specimen prepared correctly	See RTR 247
10. Specimen orientated correctly	25.6° ± 0.2° on jacket & pallet.
11. Photograph just above target	✓
12. Raise to correct height	✓ 1.030m.
13. Release specimen	✓
14. Photograph in situ	✓
15. Photograph damage	✓
16. Confirm correct execution of drop	✓ Impact point on aiming mark.
17. Pass/Fail (if, applicable see Test Plan)	PASS (fit to continue).

18. Notes

- Jacket outer skin and inner skin partially sheared. Outer skin depressed 114mm max. Inner skin 4-5 mm from flask wall at trip. Outer skin sheared for ~60% of punch diameter.
- Punch witness mark 60mm max from top.
- Flask fins behind hole in jacket folded outwards locally.

19. Signed: [signature]	Date: 20/11/08
20. Witnessed: [signature]	Date: 20/11/08

REVISS Services
Technical and Manufacturing Group

Test Report No. RTR 249

3981/01
9.0m Free Drop Test – Side Horizontal

Author:		**Reviewer:**	
Name	P J G Robbins	Name	D W Rogers
Signature		Signature	
Date	03/07/09	Date	03/07/09

1. PURPOSE AND SCOPE

The purpose of this document is to record the performance of the R7021 specimen, 3981/01, in an IAEA drop test for Type B radioactive materials package designs. The full test programme is discussed, justified and detailed in the test plan, RTM 118.

2. DESCRIPTION

2.1 DESIGN

The outer components of the R7021, a cylindrical, insulated jacket, a top shield (with energy absorbing structures and insulation), and a pallet, are constructed predominantly from carbon steel. There is also a stainless steel grill around the top of the jacket to restrict access to hot surfaces. The flask is a stainless steel, lead shielded, upright, finned cylinder with a conventional plug type closure in the top and thermal insulation built into its top and bottom corners. The closure has a vent point and the cavity has a drain tube to allow the flask to be operated in ponds as well as in cells. The cylindrical cavity holds encapsulated radioactive material (solid cobalt metal) in a basket. Although primarily intended to carry Special Form capsules, the flask has a containment system as it may also be used to carry non-Special Form encapsulated cobalt. The closure and the vent and drain plugs are therefore equipped with testable O-ring seals. In addition, to prevent the migration of coarse solids outside the shielded volume, the top of the drain tube is fitted with a mesh filter and a spring gasket is used to seal the gap under the closure around the top of the cavity.

2.2 TEST

9.0 m Drop Test – Side Horizontal (Drop 15, RTM 118). Drop I test for Type B packages (paras. 656 & 727(b), TS-R-1).

2.3 TEST INTENT

- To subject the closure fixings to the maximum shear load.
- To damage the drain plug.
- To subject the pallet fixings to the maximum shear load.
- To subject the top shield fixings to the maximum shear load.
- To crush the jacket.
- To displace the spring gasket.

2.4 PASS/FAIL CRITERIA

The pallet, top shield and jacket shall be secure in order for the specimen to continue to the next test. For internal inspection see IR 0675.

2.5 TARGET

The R8085 target (Drg. No. R8085/001) consists of a 50mm thick steel plate bonded to reinforced concrete of dimensions 4m square x 3m deep set flush with the ground. The total mass, 113000 kg, exceeds the RTM 118 minimum requirement of 45000 kg by 150%.

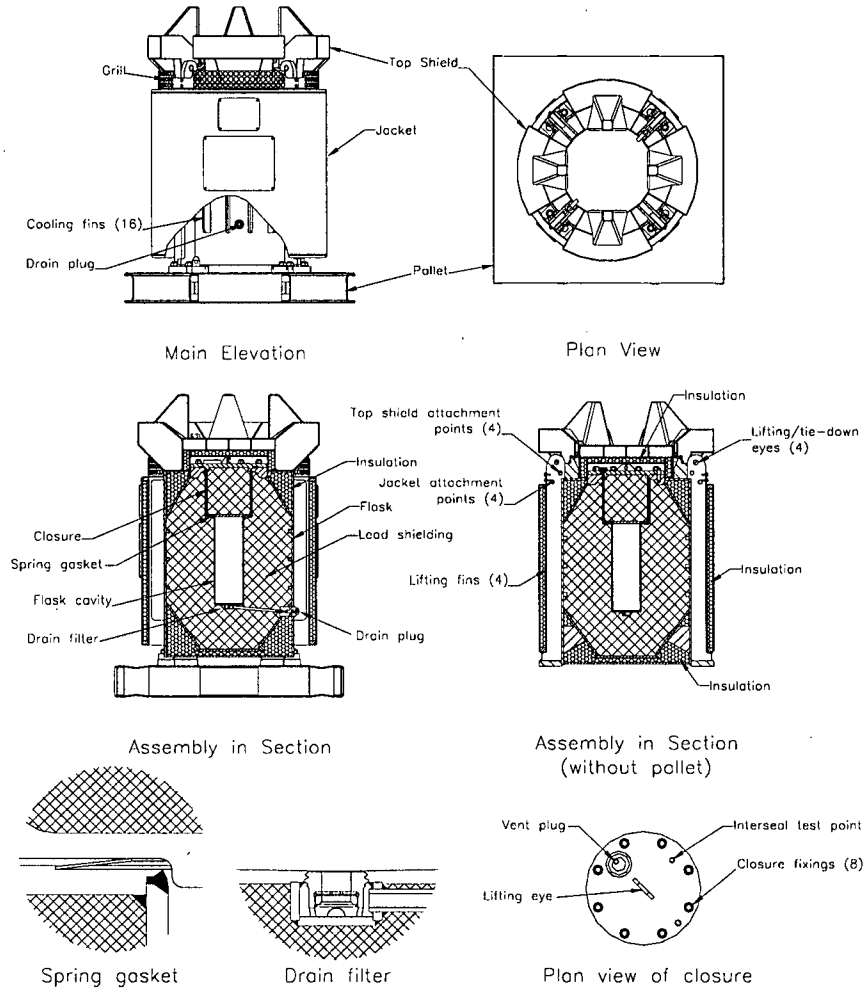

Figure 1: R7021 Constructional Details

2.6 SPECIMEN DETAILS (SEE ALSO IR 0674)

- Identity: 3981/01.
- Contents: A basket containing 48 stainless steel rods.
- Weight: 4374 kg.
- Existing Damage: See IR 0674 & RTRs 244 to 248.

2.7 TEST PROCEDURE

As the weight of the container assembly was less than the design maximum gross weight (4500kg), the drop height was increased pro rata to compensate. The test height was therefore (4500/4374) x 9.0 = 9.26m.

The test was conducted in accordance with OP 225. The specified angle was 0° ± 2° to the horizontal to generate "slap-down" impact. All key actions were recorded on the test record

sheet (attached). The

3. RESULTS

- The test was executed correctly (Figures 2-5).
- The angles measured off the pallet and jacket were 0.5° & 0.2° from the horizontal (Figure 6).
- The pallet, jacket, top shield and grill remained securely attached (Figure 7).
- The lowermost top shield quadrant was flattened and buckled upwards (Figures 10-14 & 20).
- The jacket had a triangular flat approximately 500mm wide and 600mm deep (Figures 18 & 19).
- The grill followed the contour of the jacket (Figures 12 & 13).
- Two lengths of the jacket inner top circumferential weld had sprung at its attachment points (Figure 15).
- The jacket outer top circumferential weld had sprung over the width of the flat (Figure 13).
- The top of the flask fins were buckled inwards behind the jacket together, to a lesser extent, with the outer wall of the flask. No cracks were visible (Figure 16).
- The side of the pallet was crushed (Figures 8, 9 & 21).
- One flask foot nut was loose (Figure 17).

See Illustrations for photographic record.

4. CONCLUSIONS

The R7021 test specimen, 3981/01, was fit to continue to the next test.

5. REFERENCES

- IR 0674: 3981/01 Assembly Prior to Accident Conditions Drop Testing, REVISS Services (UK) Ltd.
- IR 0675: 3981/01 Inspection After Accident Conditions Drop Testing, REVISS Services (UK) Ltd.
- OP 225: Drop Testing Procedure, REVISS Services (UK) Ltd.
- R8085/001 issue B: Drop Test Target, REVISS Services (UK) Ltd.
- RTM 118: Test Plan for the R7021 Transport Container, REVISS Services (UK) Ltd.
- RTR 244: 1.0m Punch Test – Angled Inverted, REVISS Services (UK) Ltd.
- RTR 245: 1.0m Punch Test – Angled Inverted, REVISS Services (UK) Ltd.
- RTR 246: 9.0m Free Drop Test – Angled Inverted, REVISS Services (UK) Ltd.
- RTR 247: 1.0m Punch Test – Angled Inverted, REVISS Services (UK) Ltd.
- RTR 248: 1.0m Punch Test – Angled Side, REVISS Services (UK) Ltd.
- TS-R-1: Safety Standards Series, Regulations for the Safe Transport of Radioactive Material 1996 Edition (As amended 2003), IAEA, Vienna.

6. ATTACHMENTS

RTR 249: Drop Test Checklist, REVISS Services (UK) Ltd.

7. ILLUSTRATIONS

page
Figure 2: Test action sequence – Angle 1 6
Figure 3: Test action sequence – Angle 2 7
Figure 4: Above target 8
Figure 5: Above target 8
Figure 6: Inclinometer readings (2 planes) 9
Figure 7: After drop 9
Figure 8: Crushing of the pallet 10
Figure 9: Crushing of the pallet 10
Figure 10: Deformation of top shield quadrant 11
Figure 11: Deformation of top shield quadrant 11
Figure 12: Flattening of top shield quadrant, jacket and grill 12
Figure 13: Flattening of top shield quadrant, jacket and grill 12
Figure 14: Damage to top shield quadrant 13
Figure 15: Jacket weld failure 13
Figure 16: Buckling of flask fins 14
Figure 17: Flask feet 14
Figure 18: Jacket distortion 15
Figure 19: Jacket distortion 16
Figure 20: Top shield distortion 17
Figure 21: Pallet distortion 17

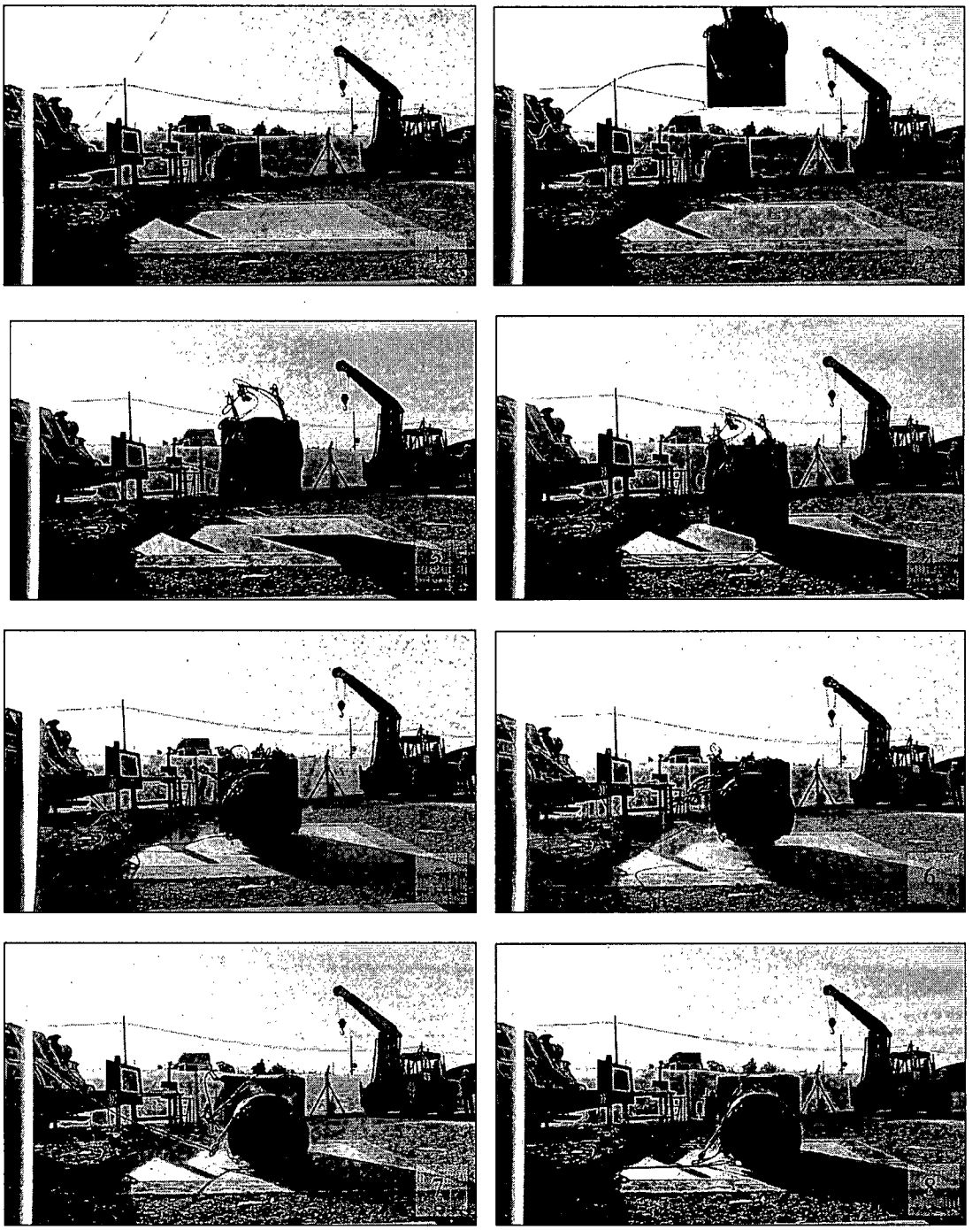

Figure 2: Test action sequence – Angle 1

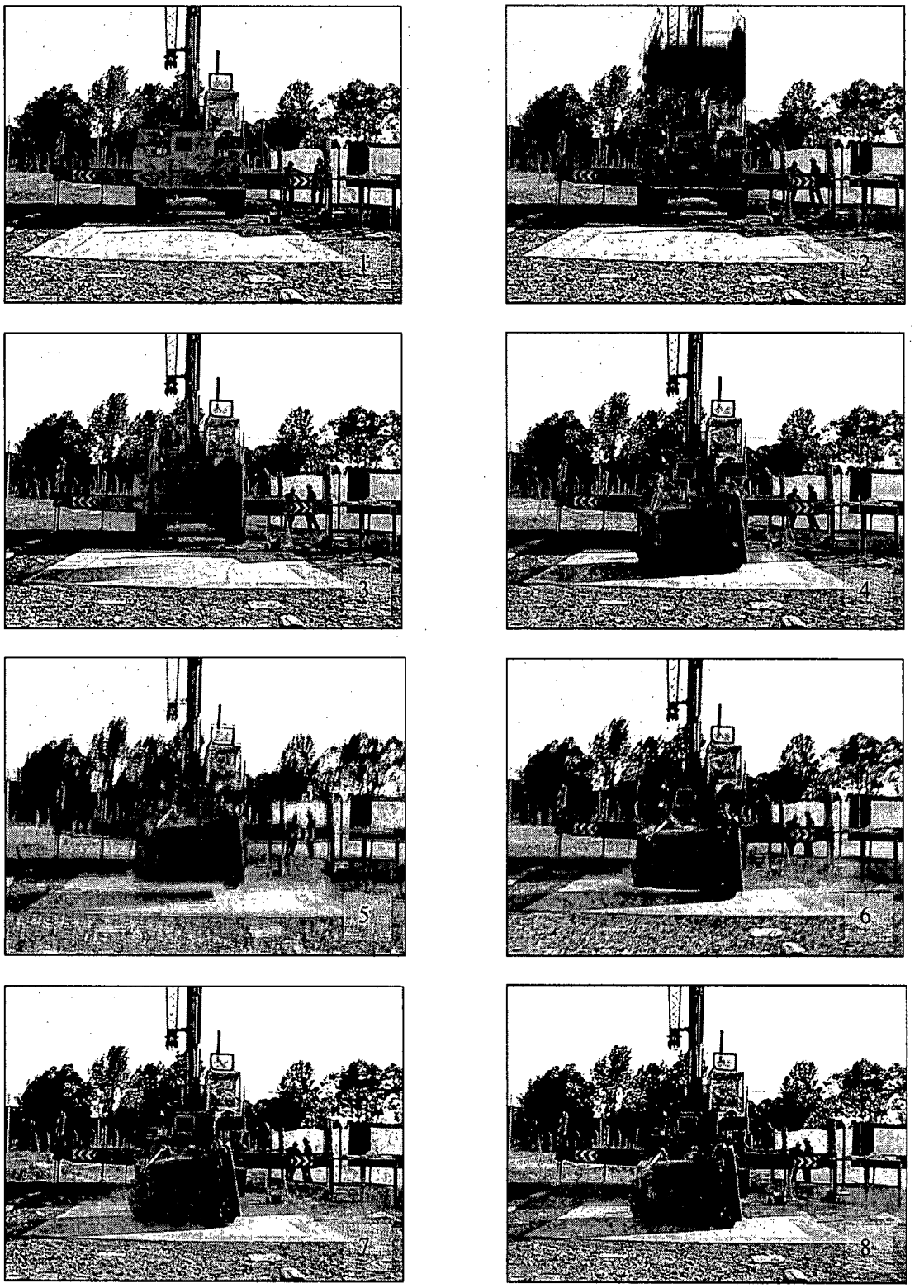

Figure 3: Test action sequence – Angle 2

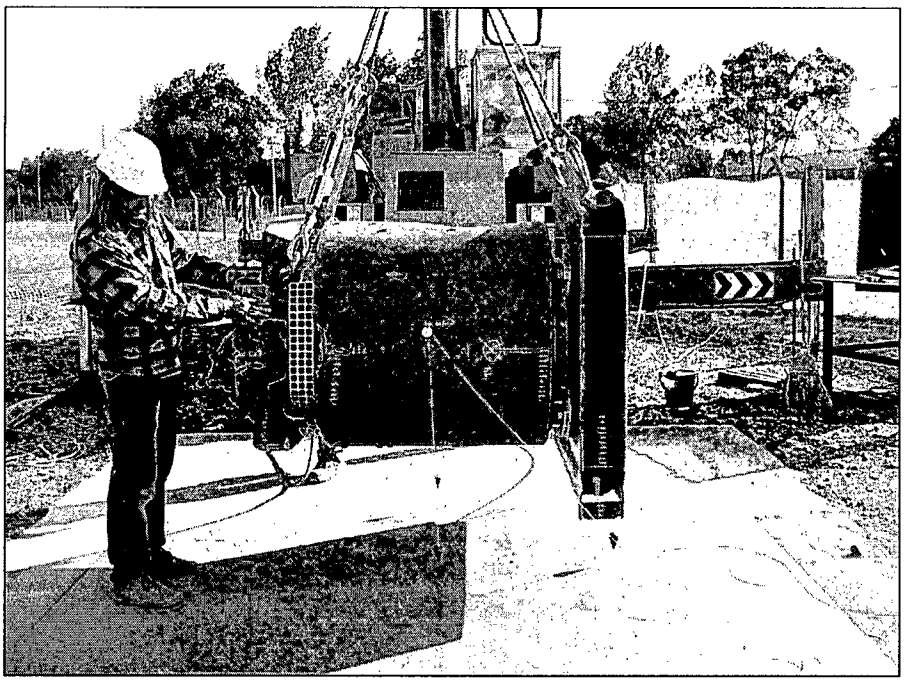

Figure 4: Above target

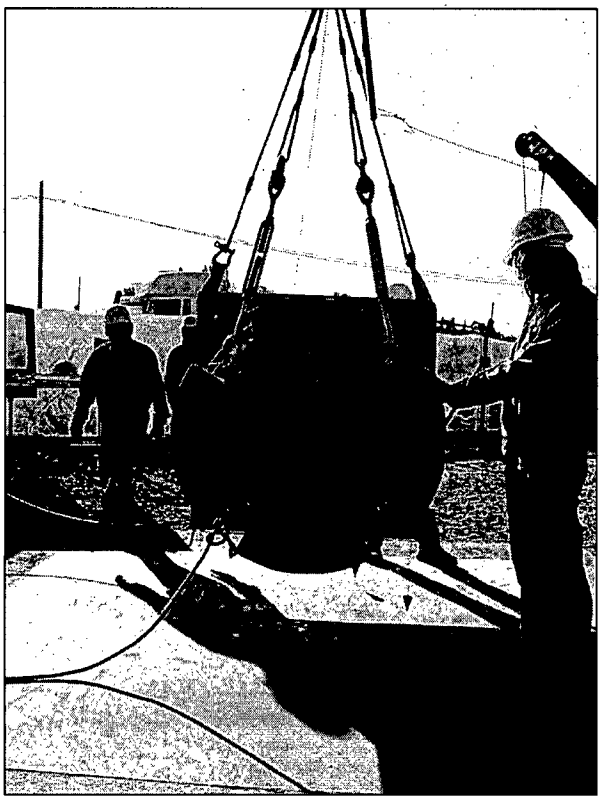

Figure 5: Above target

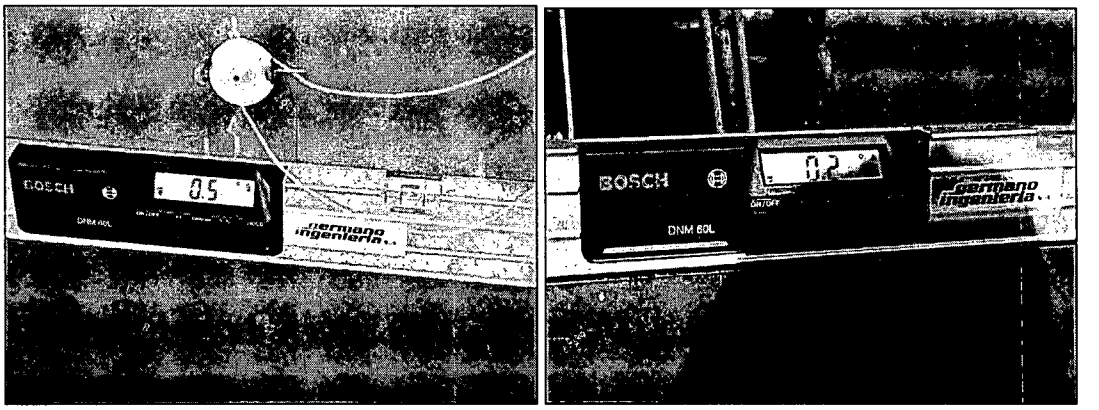

Figure 6: Inclinometer readings (2 planes)

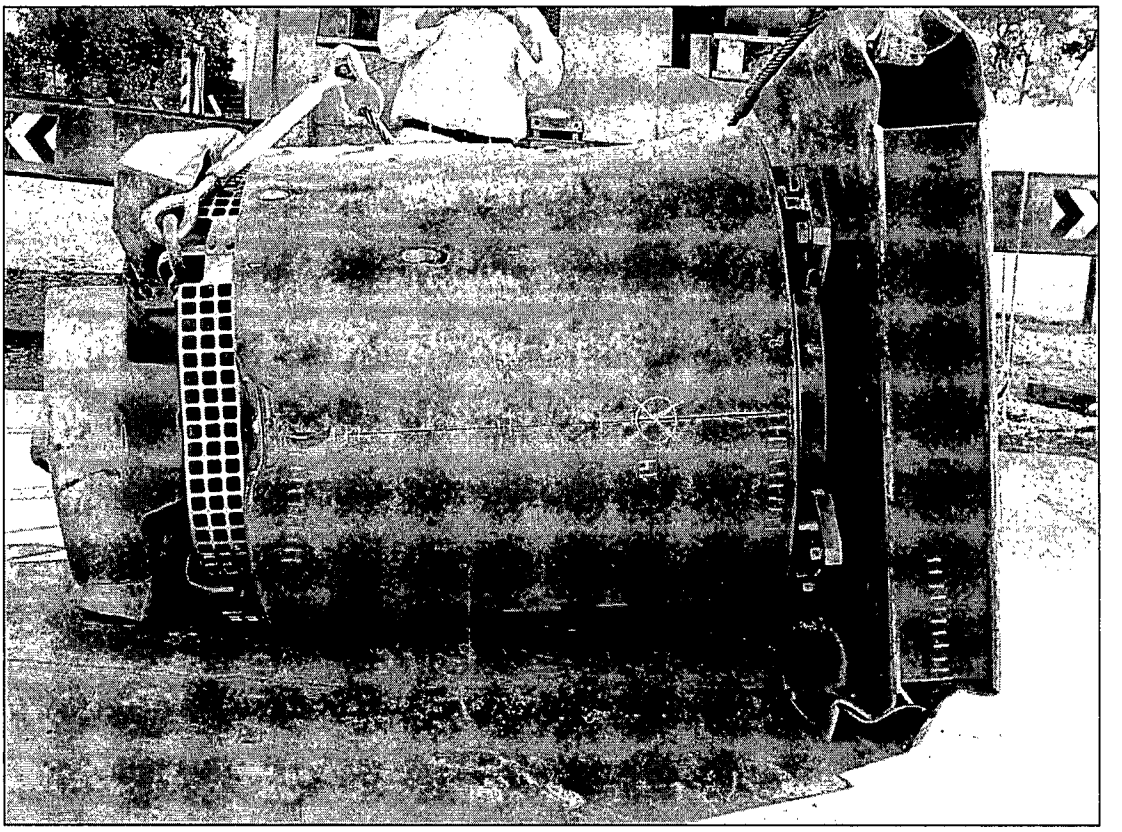

Figure 7: After drop

Figure 8: Crushing of the pallet

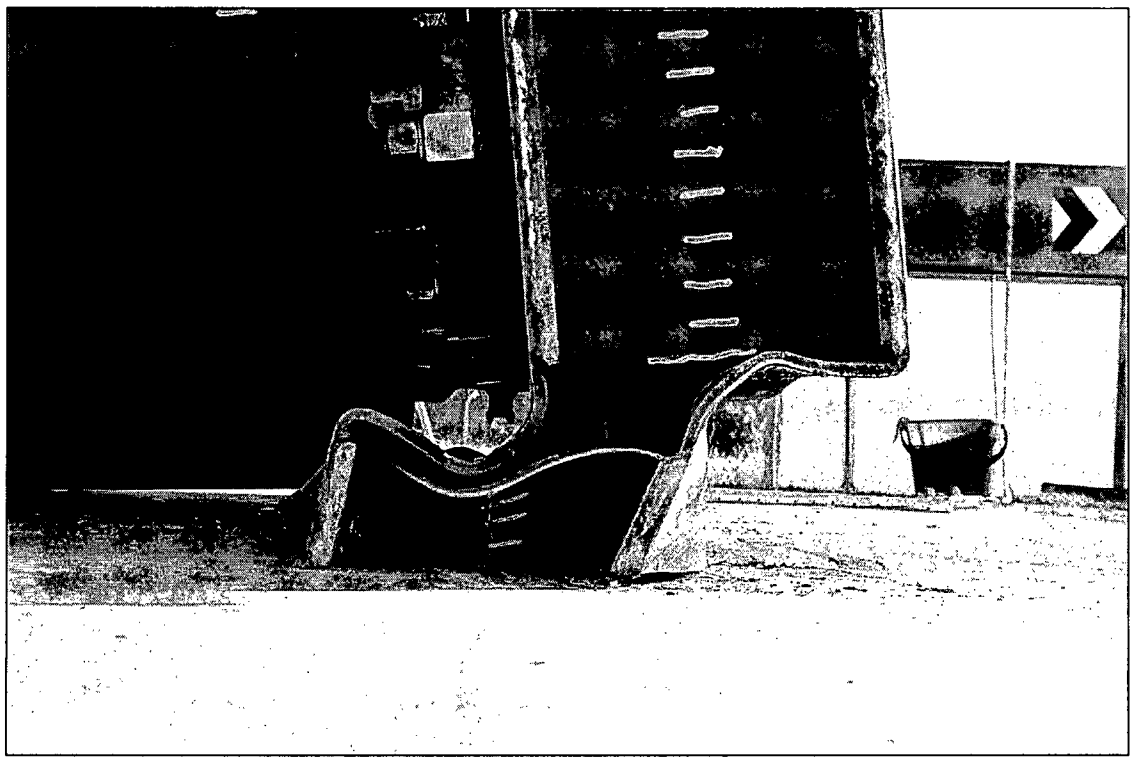

Figure 9: Crushing of the pallet

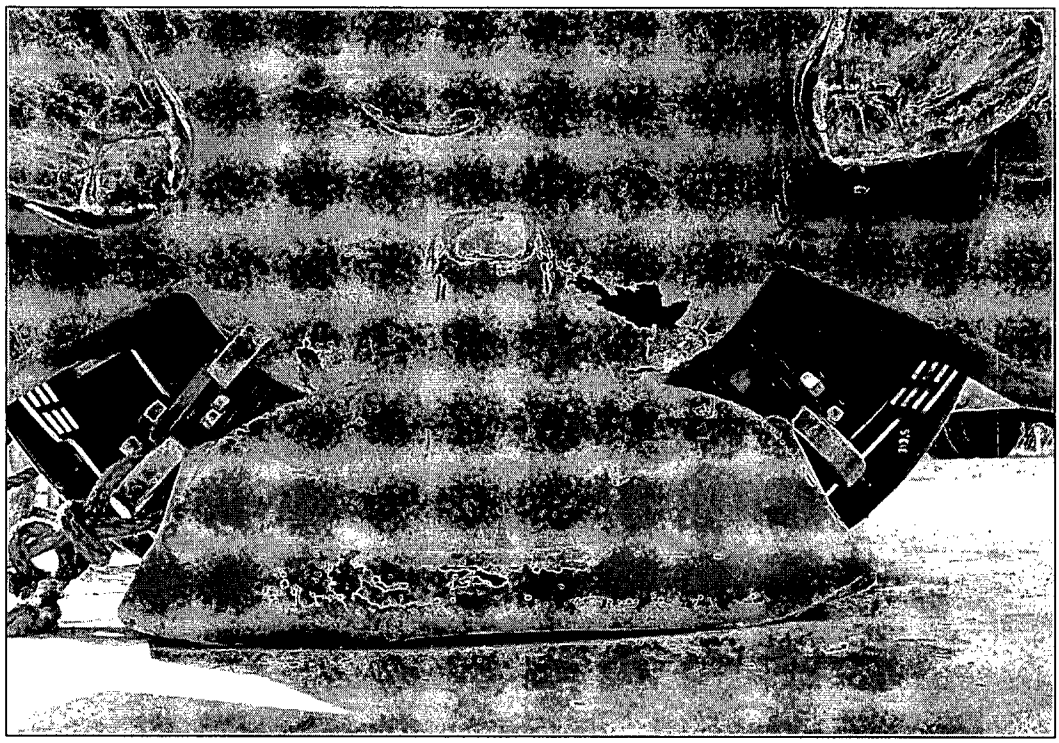

Figure 10: Deformation of top shield quadrant

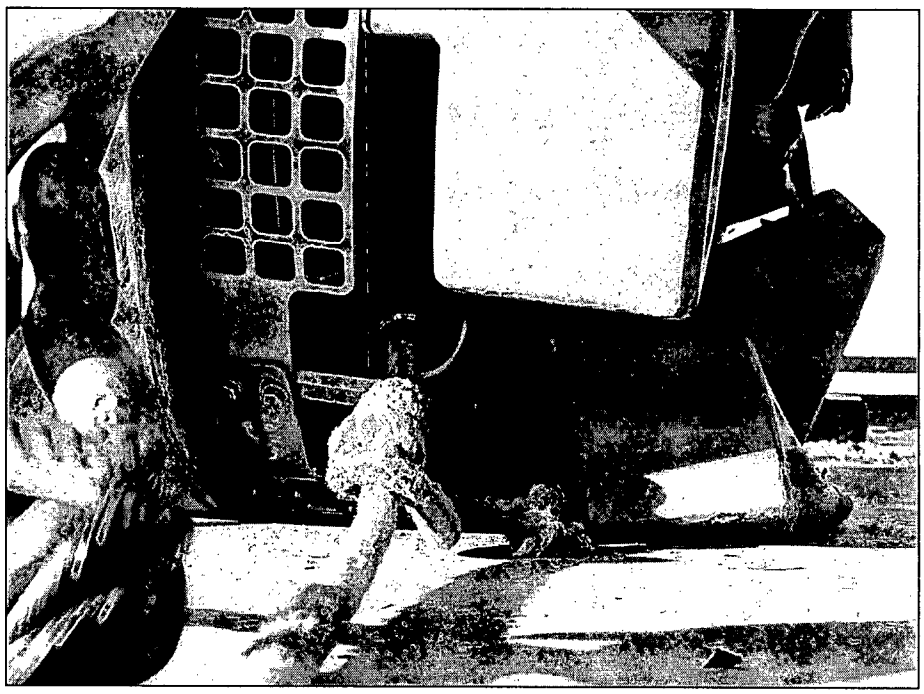

Figure 11: Deformation of top shield quadrant

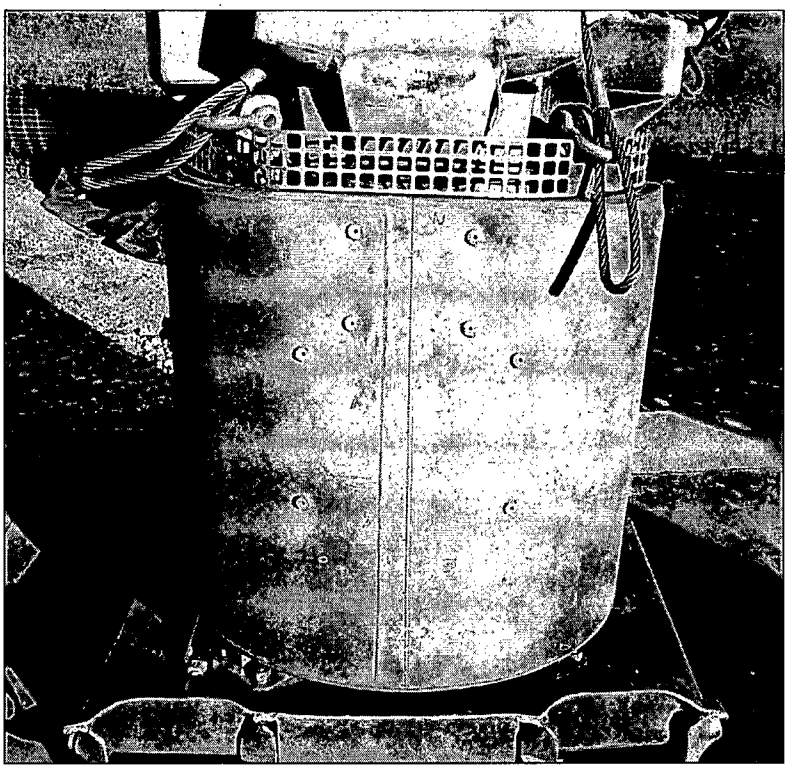

Figure 12: Flattening of top shield quadrant, jacket and grill

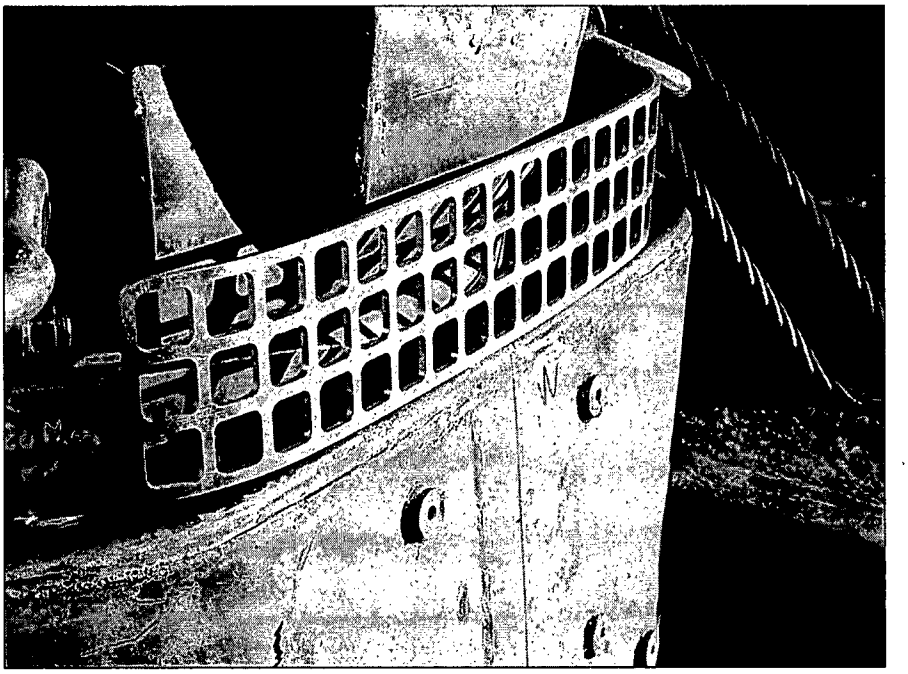

Figure 13: Flattening of top shield quadrant, jacket and grill

Figure 14: Damage to top shield quadrant

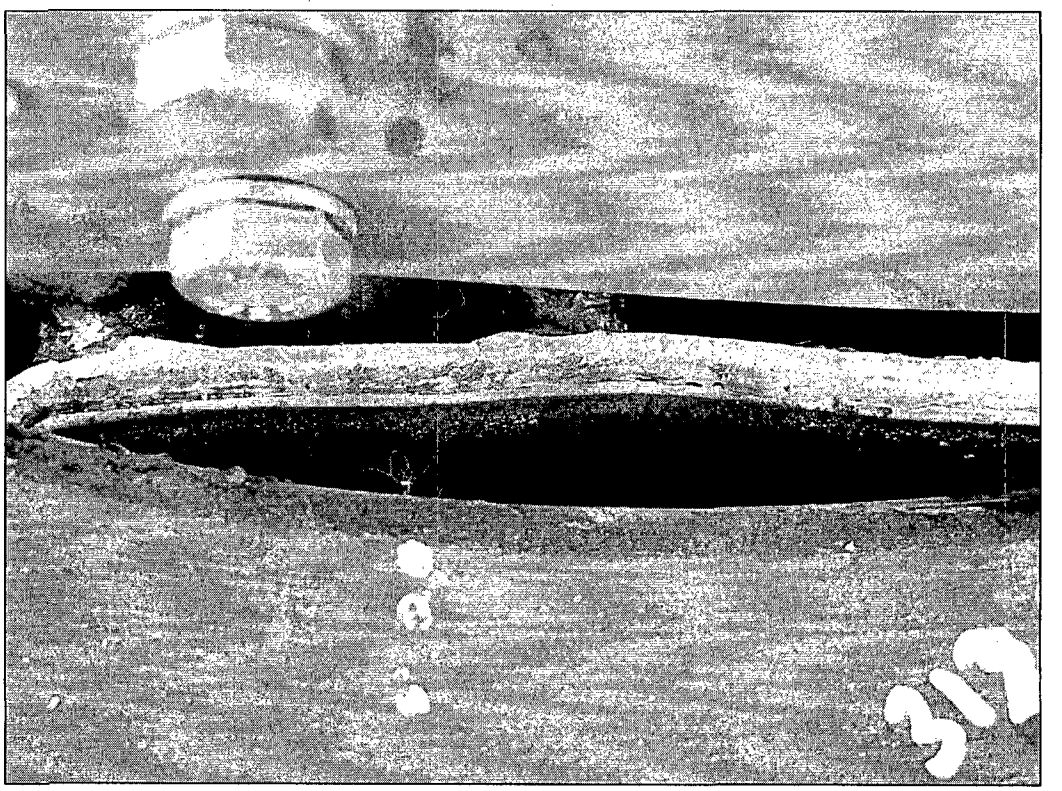

Figure 15: Jacket inner weld failure

Figure 16: Buckling of flask fins

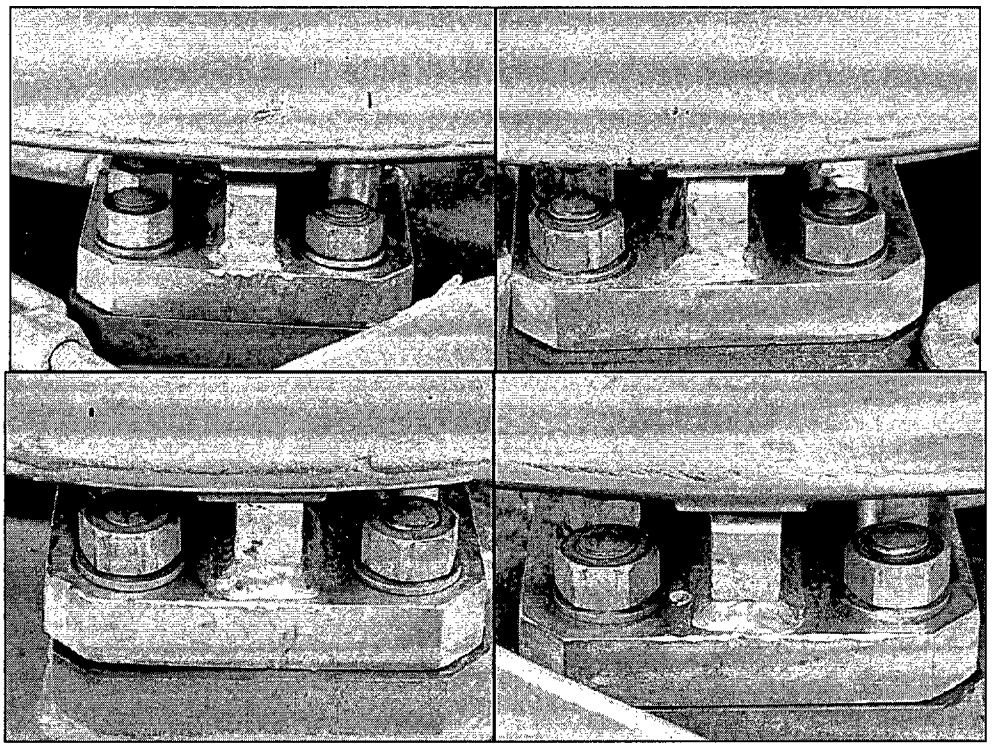

Figure 17: Flask feet

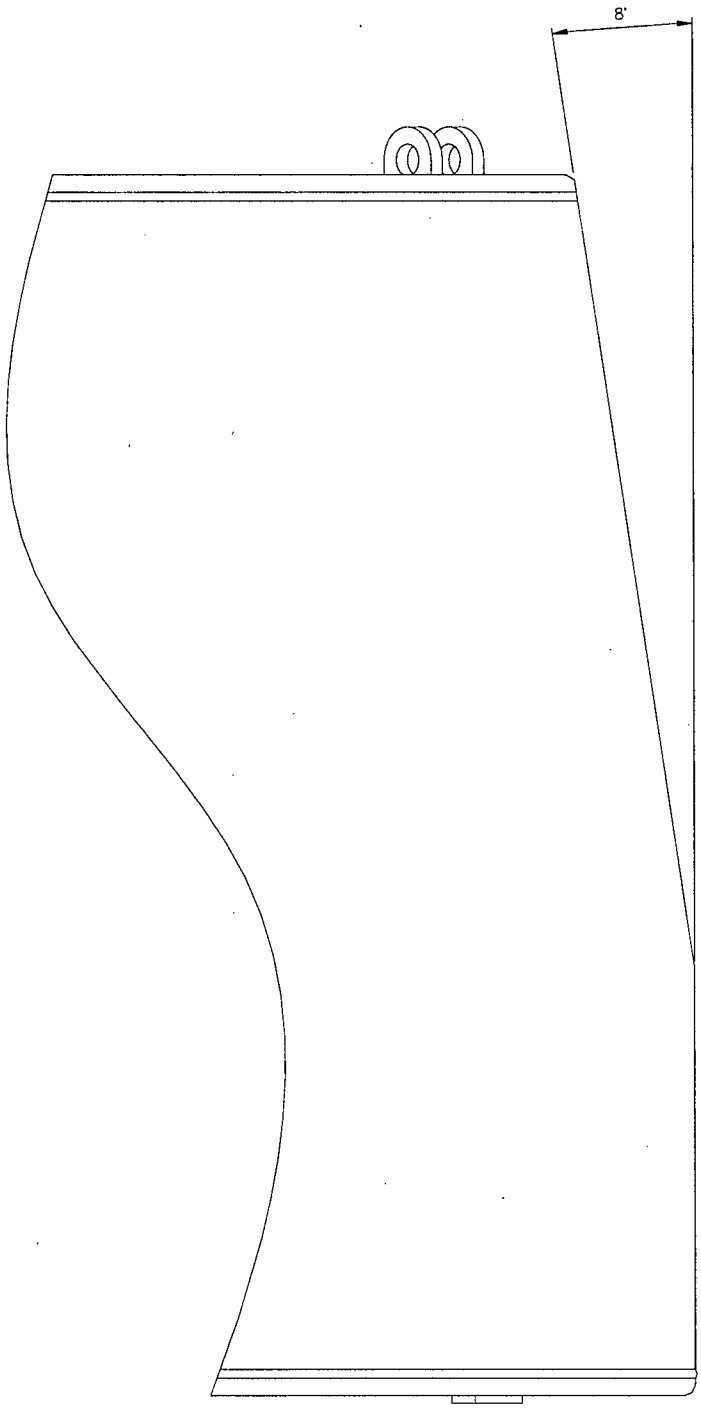

Figure 18: Jacket distortion

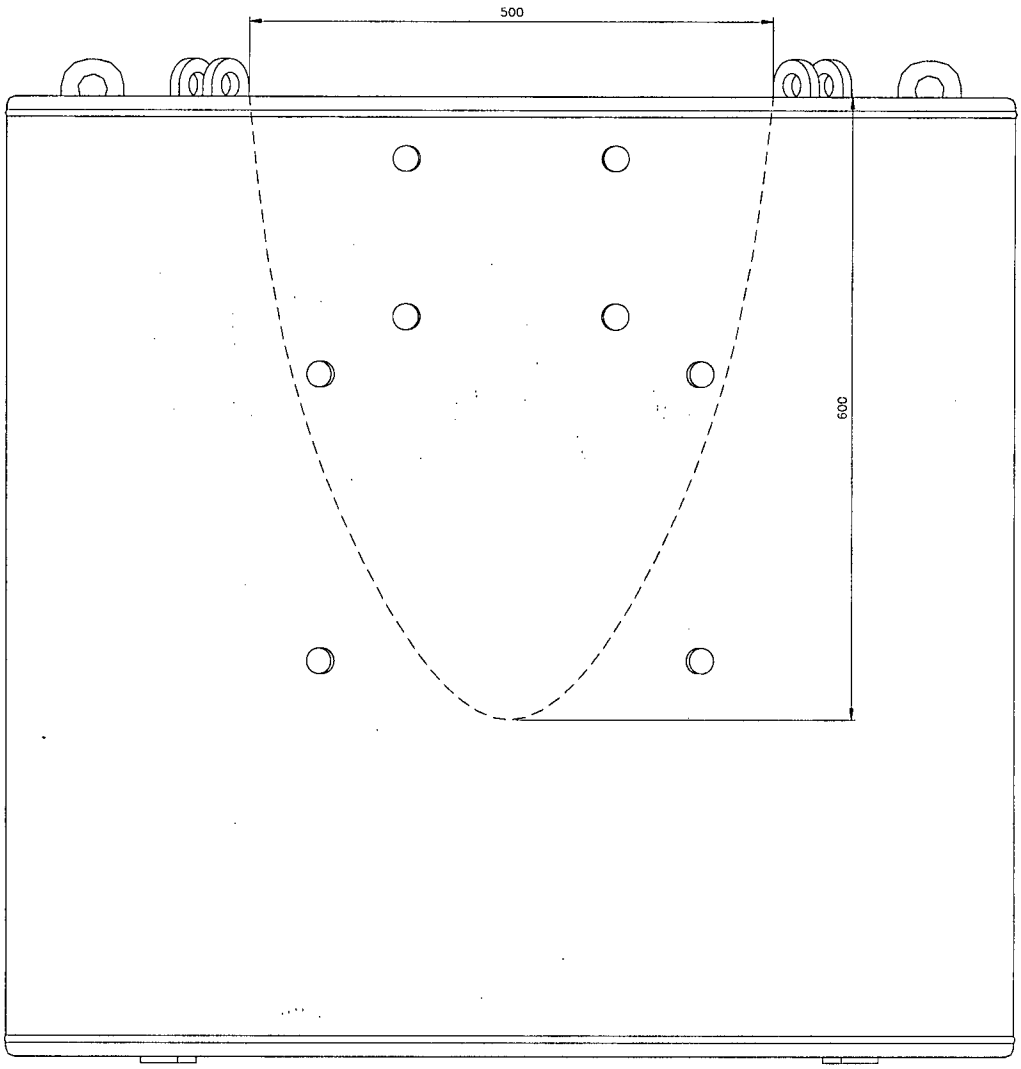

Figure 19: Jacket distortion

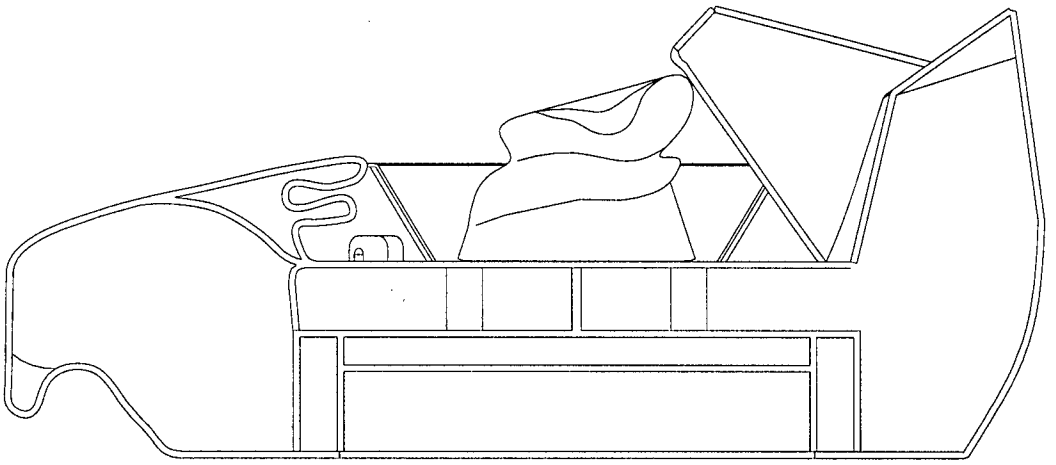

Figure 20: Top shield distortion

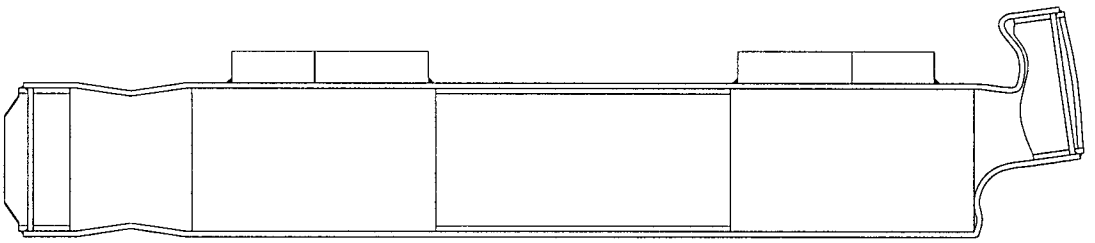

Figure 21: Pallet distortion

Reviss Services (UK) Ltd **Drop Test Checklist (OP225)**	RTR: ~~248~~ 249 (DW2) Date: 20/11/08
Test Description: 9.0m Drop Test: Side Horizontal (Type B).	
1. Confirm all personnel are aware of safety rules	✓
2. Test Plan/issue	RTM118 issue 2, Drop 15.
3. Specimen Design/Serial No/Drg No.	3981/01 (top shield 02).
4. Height gauge Identity/Drg No.	9.26m (GT-8, cal. due 11/09).
5. Target Identity/Drg No.	R8085/001 issue B.
6. Punch Identity/Drg No.	N/A
7. Penetration bar Identity/Drg No.	N/A
8. Other Inclinometer: Bosch DNM 60L	(cal. due 30/09/09).
9. Specimen prepared correctly	See RTR 248.
10. Specimen orientated correctly	0.5° & 0.2° on jacket and pallet.
11. Photograph just above target	✓
12. Raise to correct height	✓ 9.26m
13. Release specimen	✓
14. Photograph in situ	✓
15. Photograph damage	✓
16. Confirm correct execution of drop	✓
17. Pass/Fail (if, applicable see Test Plan)	PASS (fit to continue).

18. Notes

- Pallet side crushed. Two lengths of inner skin weld sprung at top.
- Jacket has triangular flat 500mm wide x 600mm deep.
- Top shield quadrant flattened and buckled upwards.
- Grill follows contour of jacket
- Flask fins buckled inwards over quadrant. Outer wall also. No cracks visible.
- Pallet, jacket, top shield and grill securely attached.
- No other damage visible externally.
- One flask foot nut loose.

19. Signed: D W Rogers	Date: 20/11/08
20. Witnessed: Richard Nixon	Date: 20/11/08

REVISS Services
Technical and Manufacturing Group

Test Report No. RTR 250

3981/01
1.0m Punch Test – Angled Side

Author:		**Reviewer:**	
Name	P J G Robbins	Name	D W Rogers
Signature		Signature	
Date	03/07/09	Date	03/07/09

1. PURPOSE AND SCOPE

The purpose of this document is to record the performance of the R7021 specimen, 3981/01, in an IAEA drop test for Type B radioactive materials package designs. The full test programme is discussed, justified and detailed in the test plan, RTM 118.

2. DESCRIPTION

2.1 DESIGN

The outer components of the R7021, a cylindrical, insulated jacket, a top shield (with energy absorbing structures and insulation), and a pallet, are constructed predominantly from carbon steel. There is also a stainless steel grill around the top of the jacket to restrict access to hot surfaces. The flask is a stainless steel, lead shielded, upright, finned cylinder with a conventional plug type closure in the top and thermal insulation built into its top and bottom corners. The closure has a vent point and the cavity has a drain tube to allow the flask to be operated in ponds as well as in cells. The cylindrical cavity holds encapsulated radioactive material (solid cobalt metal) in a basket. Although primarily intended to carry Special Form capsules, the flask has a containment system as it may also be used to carry non-Special Form encapsulated cobalt. The closure and the vent and drain plugs are therefore equipped with testable O-ring seals. In addition, to prevent the migration of coarse solids outside the shielded volume, the top of the drain tube is fitted with a mesh filter and a spring gasket is used to seal the gap under the closure around the top of the cavity.

2.2 TEST

1.0 m Punch Test – Angled Side (Drop 16, RTM 118). Drop II test for Type B packages (paras. 656 & 727(b), TS-R-1).

2.3 TEST INTENT

To penetrate the jacket and damage the drain plug.

2.4 PASS/FAIL CRITERIA

The pallet, top shield and jacket shall be secure in order for the specimen to continue to the next test. For internal inspection see IR 0675.

2.5 TARGET

The R8085 target (Drawing No R8085/001) consists of a 50mm thick steel plate bonded to reinforced concrete of dimensions 4m square x 3m deep set flush with the ground. The total mass, 113000 kg, exceeds the RTM 118 minimum requirement of 45000 kg by 150%.

The punch (Drg. No. R8099/002) met RTM 118 requirements and was securely fastened to the target with four M24 screws. The punch was extended by 100mm to 600mm (by welding on a section from a second punch) to avoid any risk of the specimen contacting the target (Figure 4).

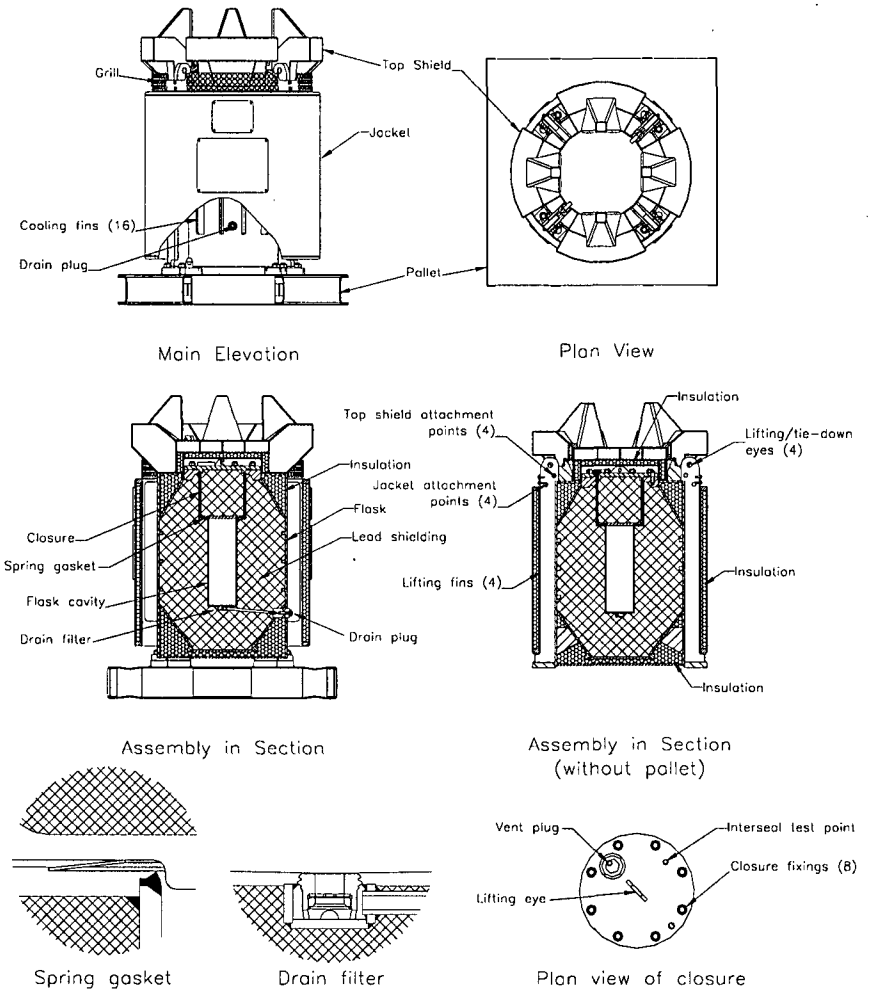

Figure 1: R7021 Constructional Details

2.6 SPECIMEN DETAILS (SEE ALSO IR 0674)

- Identity: 3981/01.
- Contents: A basket containing 48 stainless steel rods.
- Weight: 4374 kg.
- Existing Damage: See IR 0674 & RTRs 244 to 249.

2.7 TEST PROCEDURE

As the weight of the container assembly was less than the design maximum gross weight (4500kg), the drop height was increased pro rata to compensate. The test height was therefore (4500/4374) x 1.0 = 1.030m.

The specified angle was 35° from the horizontal and the impact point 120mm from the base of the jacket however, on review with the DfT engineer, these were changed to 37° and 90mm to

maximise the likelihood of the punch damaging the drain plug (see also CF757C).

The test was conducted in accordance with OP 225. All key actions were recorded on the test record sheet (attached).

3. RESULTS

- The test was executed correctly (Figures 2, 3, 5 6). The angle measured on the jacket was 37.0° from the horizontal (Figure 7).
- The pallet, jacket, top shield and grill were all securely attached (Figure 8).
- The outer skin of the jacket was indented to a depth of approximately 85mm with no cracking or shearing (Figures 9-11). The inner skin was clear of the drain plug by approximately 10mm.
- The punch showed no significant damage (Figure 12).
- No other damage was visible externally.

See Illustrations for photographic record.

4. CONCLUSIONS

The R7021 test specimen, 3981/01, was fit to continue to the next test.

5. REFERENCES

- IR 0674: 3981/01 Assembly Prior to Accident Conditions Drop Testing, REVISS Services (UK) Ltd.
- IR 0675: 3981/01 Inspection After Accident Conditions Drop Testing, REVISS Services (UK) Ltd.
- OP 225: Drop Testing Procedure, REVISS Services (UK) Ltd.
- R8085/001 issue B: Drop Test Target, REVISS Services (UK) Ltd.
- R8099/002 issue A: Drop Test Punch, REVISS Services (UK) Ltd.
- RTM 118: Test Plan for the R7021 Transport Container, REVISS Services (UK) Ltd.
- RTR 244: 1.0m Punch Test – Angled Inverted, REVISS Services (UK) Ltd.
- RTR 245: 1.0m Punch Test – Angled Inverted, REVISS Services (UK) Ltd.
- RTR 246: 9.0m Free Drop Test – Angled Inverted, REVISS Services (UK) Ltd.
- RTR 247: 1.0m Punch Test – Angled Inverted, REVISS Services (UK) Ltd.
- RTR 248: 1.0m Punch Test – Angled Side, REVISS Services (UK) Ltd.
- RTR 249: 9.0m Free Drop Test – Side Horizontal, REVISS Services (UK) Ltd.
- CF757C: Deviations from Drop Test Plan, RTM 118 issue 2, REVISS Services (UK) Ltd.
- TS-R-1: Safety Standards Series, Regulations for the Safe Transport of Radioactive Material 1996 Edition (As amended 2003), IAEA, Vienna.

6. ATTACHMENTS

RTR 250: Drop Test Checklist, REVISS Services (UK) Ltd.

7. ILLUSTRATIONS

page
Figure 2: Test action sequence – Angle 1 6
Figure 3: Test action sequence – Angle 2 7
Figure 4: Extended punch 8
Figure 5: Above target 8
Figure 6: 1.030m above target (with height gauge) 9
Figure 7: Inclinometer readings (2 planes) 9
Figure 8: After drop 10
Figure 9: Impact point and jacket indentation 10
Figure 10: Measurement of indentation 11
Figure 11: Punch damage 11
Figure 12: Punch after test 12

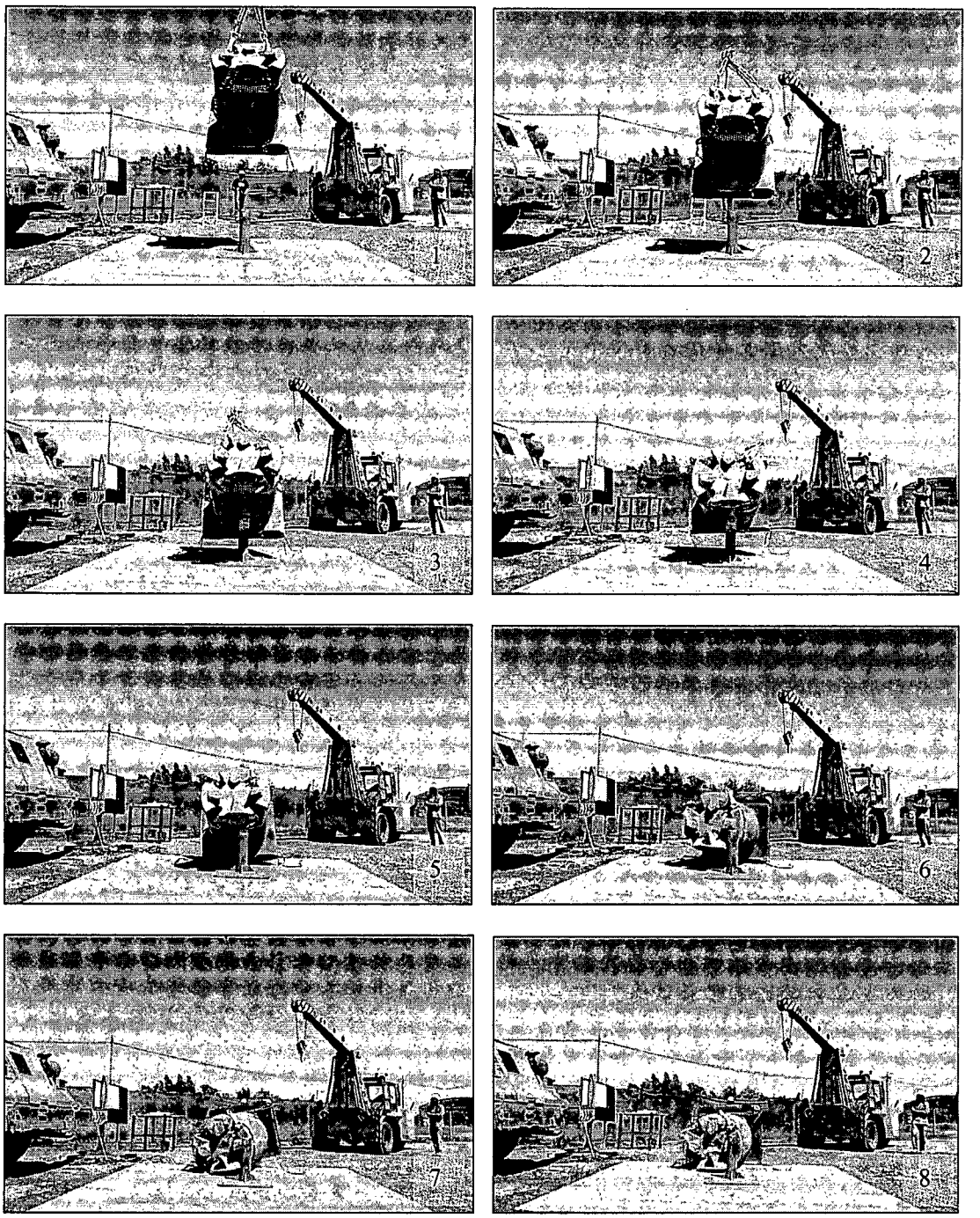

Figure 2: Test action sequence – Angle 1

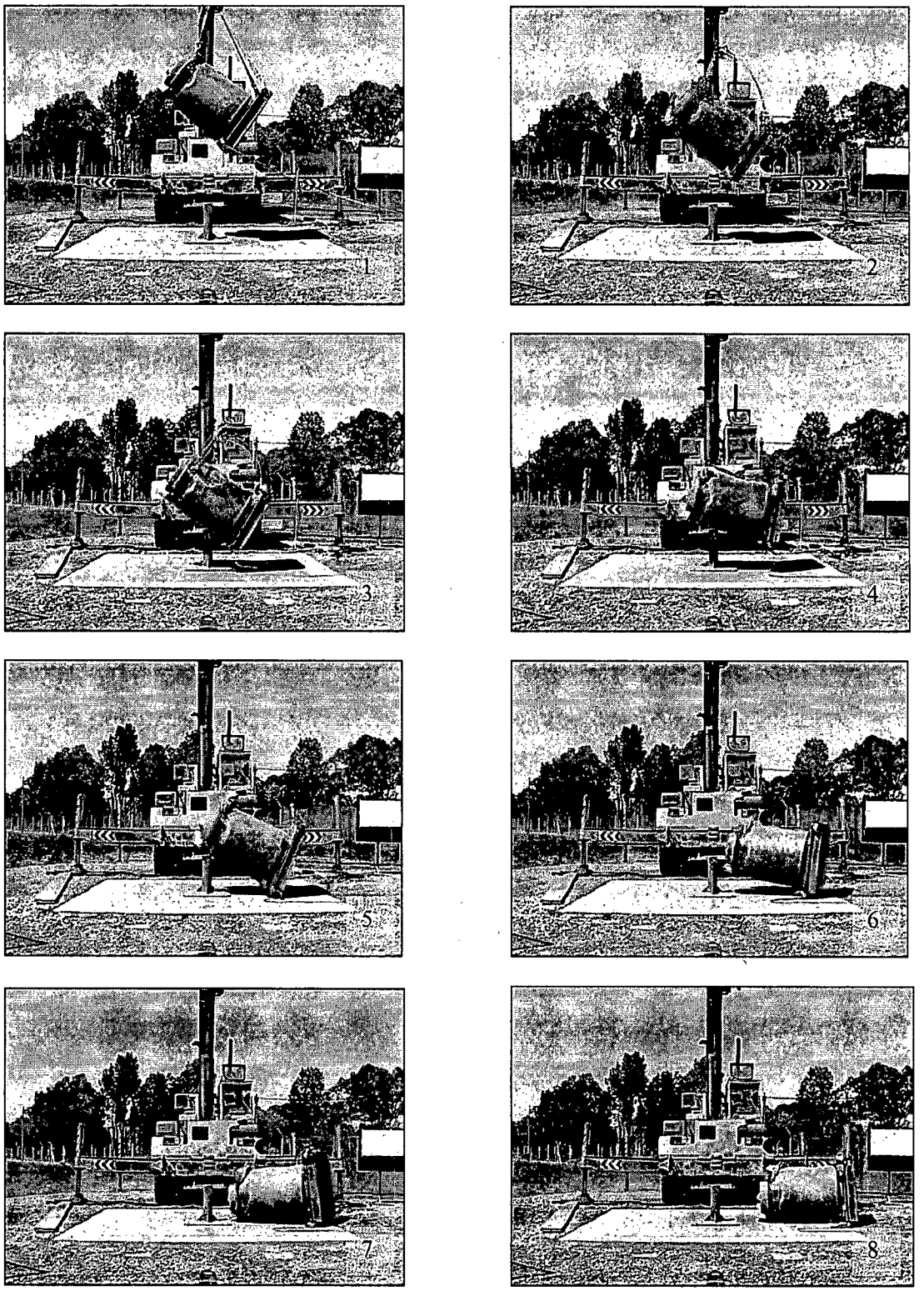

Figure 3: Test action sequence – Angle 2

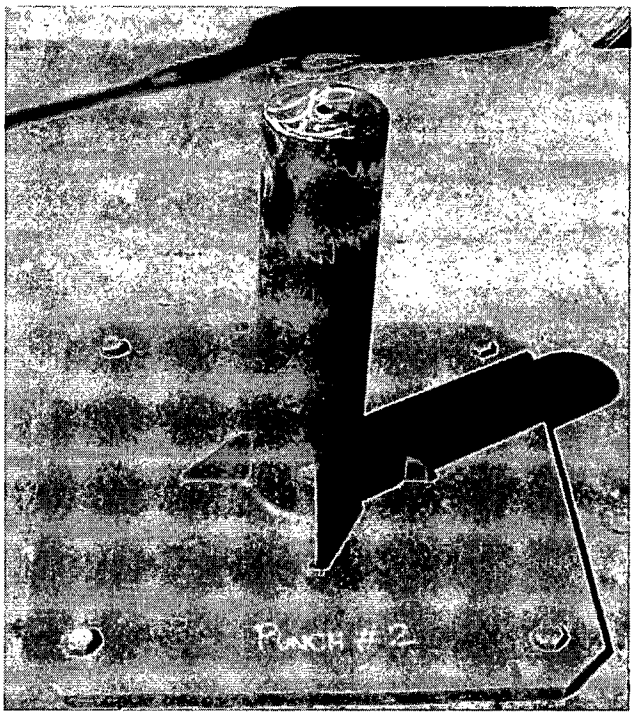

Figure 4: Extended punch

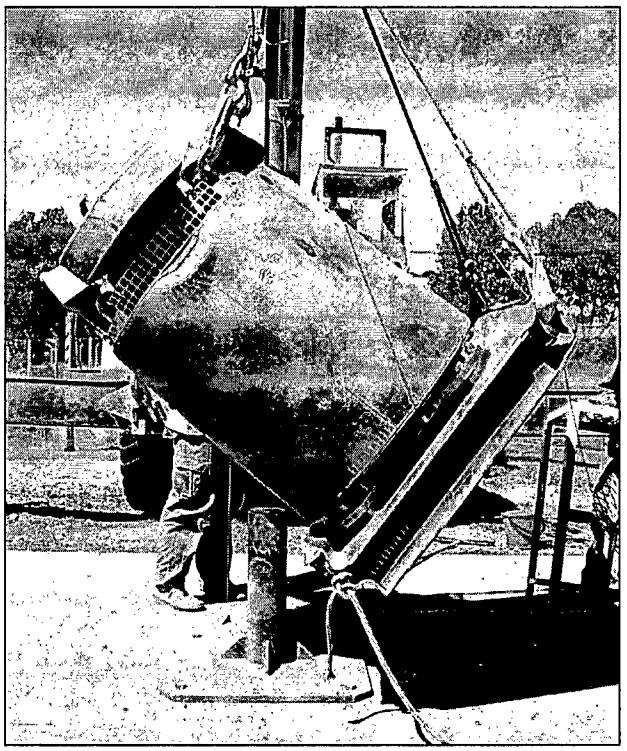

Figure 5: Above target

Figure 6: 1.030m above target (with height gauge)

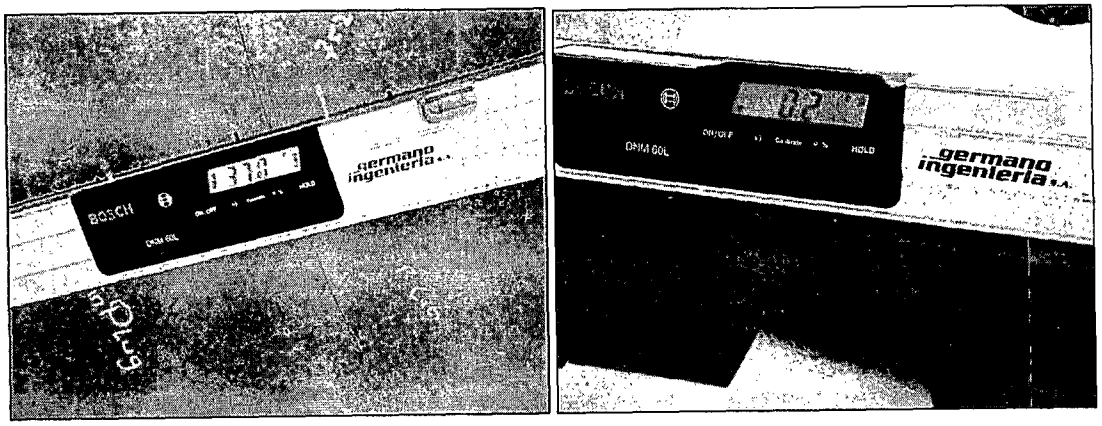

Figure 7: Inclinometer readings (2 planes)

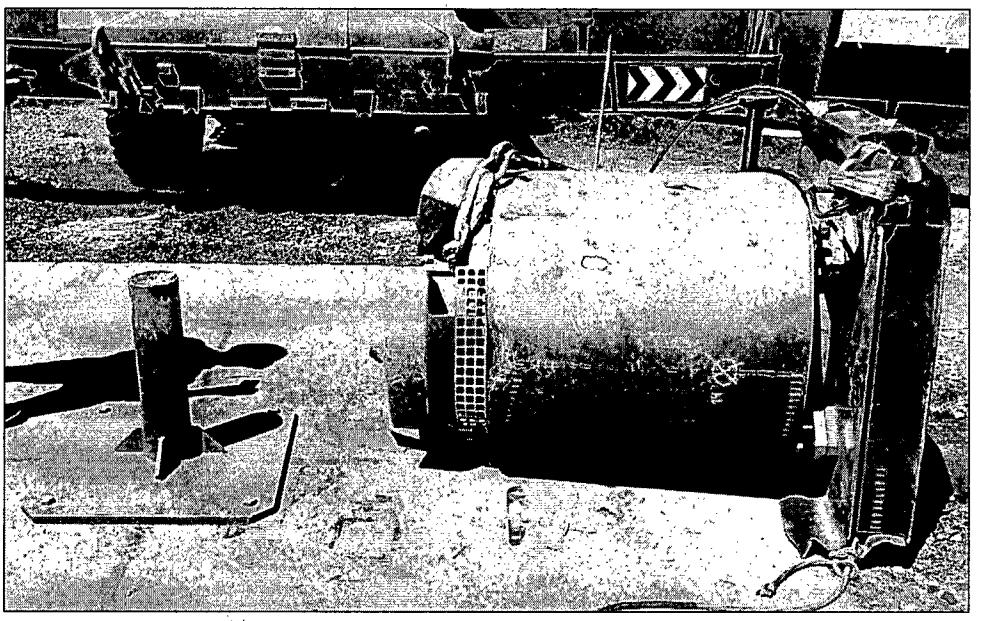

Figure 8: After drop

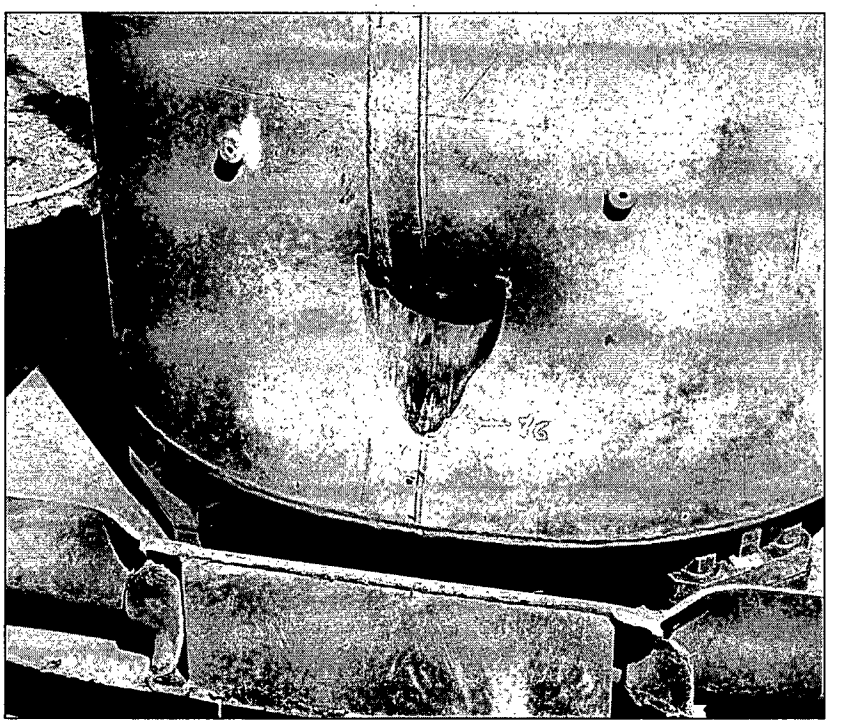

Figure 9: Impact point and jacket indentation

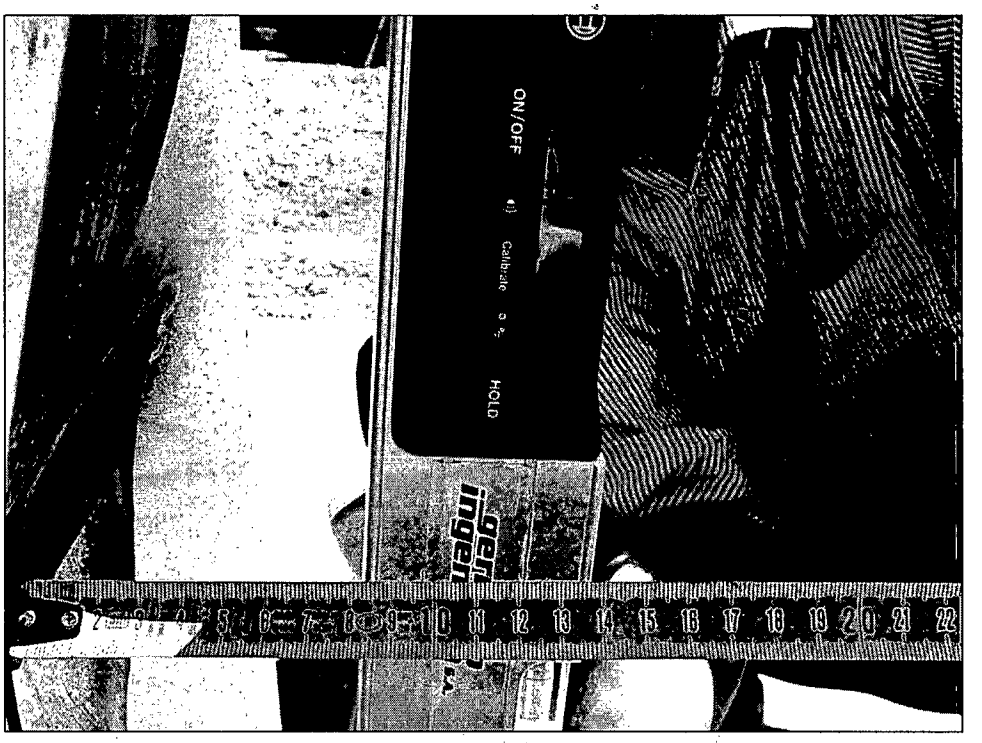

Figure 10: Measurement of indentation

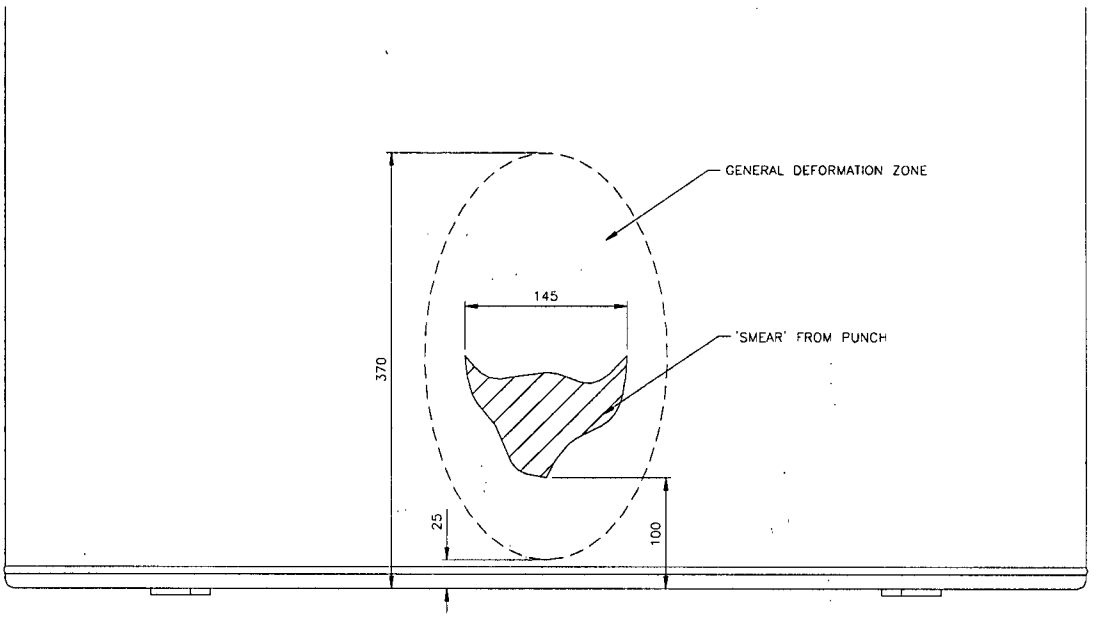

Figure 11: Punch damage

Figure 12: Punch after test

Reviss Services (UK) Ltd **Drop Test Checklist (OP225)**	RTR: 250 Date: 21/11/08
Test Description: 1-0m Punch Test : Angled Side over Drain Plug (IAEA Type B).	
1. Confirm all personnel are aware of safety rules	✓
2. Test Plan/issue	RTM 118 issue 2, Drop 16.
3. Specimen Design/Serial No/Drg No.	3981/01 (top shield 02).
4. Height gauge Identity/Drg No.	1.030m (R8083/005 issue A).
5. Target Identity/Drg No.	R8085/001 issue B
6. Punch Identity/Drg No.	R8099/002 issue A. *
7. Penetration bar Identity/Drg No.	N/A
8. Other Inclinometer = Bosch DNM 60L	(cal. due 30/09/09).
9. Specimen prepared correctly	See RTR 249.
10. Specimen orientated correctly	37.0° ± 0.2° on jacket + pallet **
11. Photograph just above target	✓
12. Raise to correct height	✓ 1.030m.
13. Release specimen	✓
14. Photograph in situ	✓
15. Photograph damage	✓
16. Confirm correct execution of drop	✓ Impact point 10mm above aiming mark Acceptable.
17. Pass/Fail (if, applicable see Test Plan)	Pass (fit to continue).

18. Notes

* Extended by 100mm to 600mm using section from second punch to avoid any risk of pallet contacting ground before package stops descending.
* Dimension "120" to aiming mark changed to 90mm to ensure impact with corner of drain plug. 35° changed to 37° to maintain CoG over point of impact (see also CF757C).
- Outer skin of jacket indented to a depth ~ 85mm (no cracking or shearing. Inner skin clear of drain plug by ~ 10mm.
- No other damage visible externally.
- Pallet, jacket, top shield and grill securely attached.

19. Signed: D W Rogers	Date: 21/11/08
20. Witnessed: Michael Nizza	Date: 21/11/08

REVISS Services
Technical and Manufacturing Group

Test Report No. RTR 251

3981/01
1.0m Punch Test – Angled Inverted

Author:		**Reviewer:**	
Name	P J G Robbins	Name	D W Rogers
Signature		Signature	
Date	03/07/09	Date	03/07/09

1. PURPOSE AND SCOPE

The purpose of this document is to record the performance of the R7021 specimen, 3981/01, in an IAEA drop test for Type B radioactive materials package designs. The full test programme is discussed, justified and detailed in the test plan, RTM 118.

2. DESCRIPTION

2.1 DESIGN

The outer components of the R7021, a cylindrical, insulated jacket, a top shield (with energy absorbing structures and insulation), and a pallet, are constructed predominantly from carbon steel. There is also a stainless steel grill around the top of the jacket to restrict access to hot surfaces. The flask is a stainless steel, lead shielded, upright, finned cylinder with a conventional plug type closure in the top and thermal insulation built into its top and bottom corners. The closure has a vent point and the cavity has a drain tube to allow the flask to be operated in ponds as well as in cells. The cylindrical cavity holds encapsulated radioactive material (solid cobalt metal) in a basket. Although primarily intended to carry Special Form capsules, the flask has a containment system as it may also be used to carry non-Special Form encapsulated cobalt. The closure and the vent and drain plugs are therefore equipped with testable O-ring seals. In addition, to prevent the migration of coarse solids outside the shielded volume, the top of the drain tube is fitted with a mesh filter and a spring gasket is used to seal the gap under the closure around the top of the cavity.

2.2 TEST

1.0 m Punch Test – Angled Inverted (Drop 17, RTM 118). Drop II test for Type B packages (paras. 656 & 727(b), TS-R-1).

2.3 TEST INTENT

To generate the maximum shear load in one of the jacket fixings. The test plan allowed for a final unspecified test depending on it had performed prior to that point. It was agreed with the DfT engineer that this test would be a repeat of RTR 247, but with the specimen rotated approximately 45° about its vertical axis to put the impact point as close as possible to the jacket fixing in order to generate the maximum shear load in that component.

2.4 PASS/FAIL CRITERIA

The pallet, top shield and jacket shall be secure. For stripdown and internal inspection see IR 0675.

2.5 TARGET

The R8085 target (Drg. No. R8085/001) consists of a 50mm thick steel plate bonded to reinforced concrete of dimensions 4m square x 3m deep set flush with the ground. The total mass, 113000 kg, exceeds the RTM 118 minimum requirement of 45000 kg by 150%.

The punch (Drg. No. R8099/002) met RTM 118 requirements and was securely fastened to the target with four M24 screws. The punch had been extended by 100mm to 600mm for the

previous test, RTR 250.

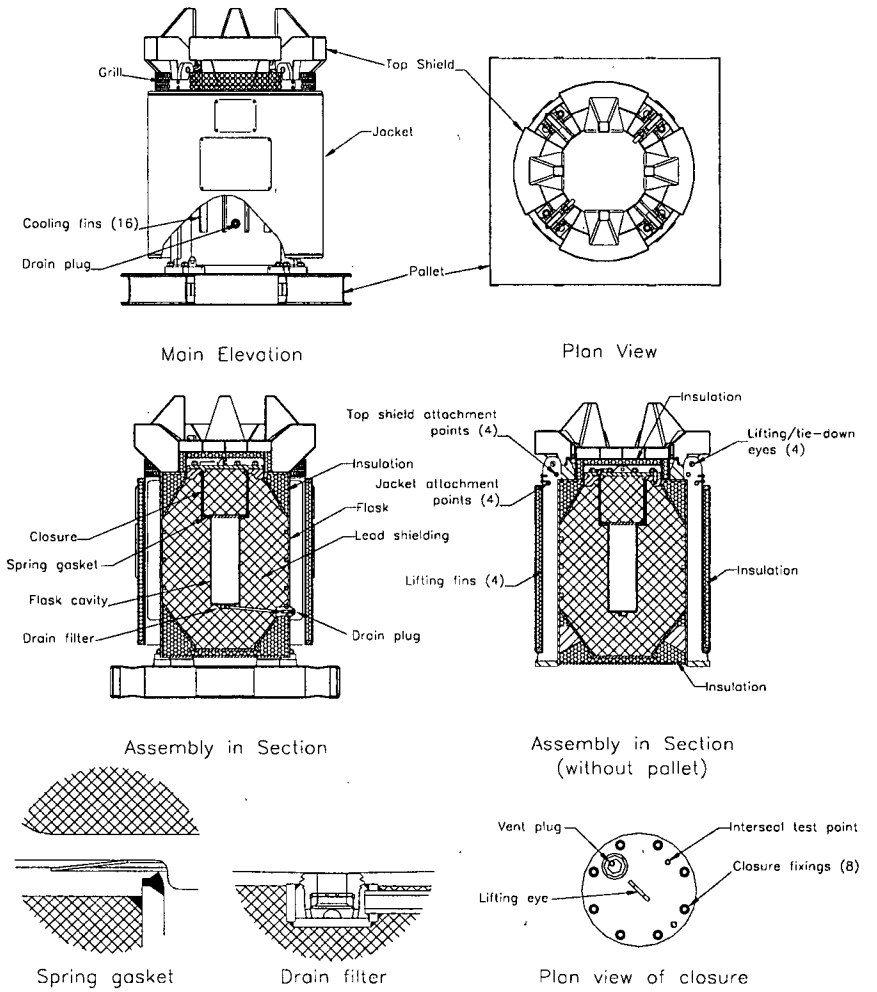

Figure 1: R7021 Constructional Details

2.6 SPECIMEN DETAILS (SEE ALSO IR 0674)

- Identity: 3981/01.
- Contents: A basket containing 48 stainless steel rods.
- Weight: 4374 kg.
- Existing Damage: See IR 0674 & RTR 244 to 250.

2.7 TEST PROCEDURE

As the weight of the container assembly was less than the design maximum gross weight (4500kg), the drop height was increased pro rata to compensate. The test height was therefore

(4500/4374) x 1.0 = 1.030m.

The test was conducted in accordance with OP 225. The specified angle was 41° ± 2° from the horizontal. All key actions were recorded on the test record sheet (attached).

3. RESULTS

- The test was executed correctly (Figures 2-5). The angle measured for the drop was 42.4° from the horizontal (Figure 6).
- The pallet, jacket, top shield and grill remained securely attached (Figure 7).
- The jacket fixing was secure and intact, the top of the jacket was distorted 30mm down and 50mm inwards in the impact area and the grill was slightly distorted (Figures 8-10).
- No other damage was visible externally.
- The punch showed correct impact positioning and no significant damage (Figure 11)

See Illustrations for photographic record.

4. CONCLUSIONS

The R7021 test specimen, 3981/01, was fit to continue to the next test.

5. REFERENCES

- IR 0674: 3981/01 Assembly Prior to Accident Conditions Drop Testing, REVISS Services (UK) Ltd.
- IR 0675: 3981/01 Inspection After Accident Conditions Drop Testing, REVISS Services (UK) Ltd.
- OP 225: Drop Testing Procedure, REVISS Services (UK) Ltd.
- R8085/001 issue B: Drop Test Target, REVISS Services (UK) Ltd.
- R8099/002 issue A: Drop Test Punch, REVISS Services (UK) Ltd.
- RTM 118: Test Plan for the R7021 Transport Container, REVISS Services (UK) Ltd.
- RTR 244: 1.0m Punch Test – Angled Inverted, REVISS Services (UK) Ltd.
- RTR 245: 1.0m Punch Test – Angled Inverted, REVISS Services (UK) Ltd.
- RTR 246: 9.0m Free Drop Test – Angled Inverted, REVISS Services (UK) Ltd.
- RTR 247: 1.0m Punch Test – Angled Inverted, REVISS Services (UK) Ltd.
- RTR 248: 1.0m Punch Test – Angled Side, REVISS Services (UK) Ltd.
- RTR 249: 9.0m Free Drop Test – Side Horizontal, REVISS Services (UK) Ltd.
- RTR 250: 1.0m Punch Test – Angled Side, REVISS Services (UK) Ltd.
- TS-R-1: Safety Standards Series, Regulations for the Safe Transport of Radioactive Material 1996 Edition (As amended 2003), IAEA, Vienna.

6. ATTACHMENTS

RTR 251: Drop Test Checklist, REVISS Services (UK) Ltd.

7. ILLUSTRATIONS

page
Figure 2: Test action sequence – Angle 1 6
Figure 3: Test action sequence – Angle 2 7
Figure 4: 1.030m above target 8
Figure 5: 1.030m above target (with height gauge) 8
Figure 6: Inclinometer reading 9
Figure 7: After drop 9
Figure 8: Jacket and grill distortion 10
Figure 9: Jacket and grill distortion 10
Figure 10: Jacket distortion 11
Figure 11: Condition of punch 11

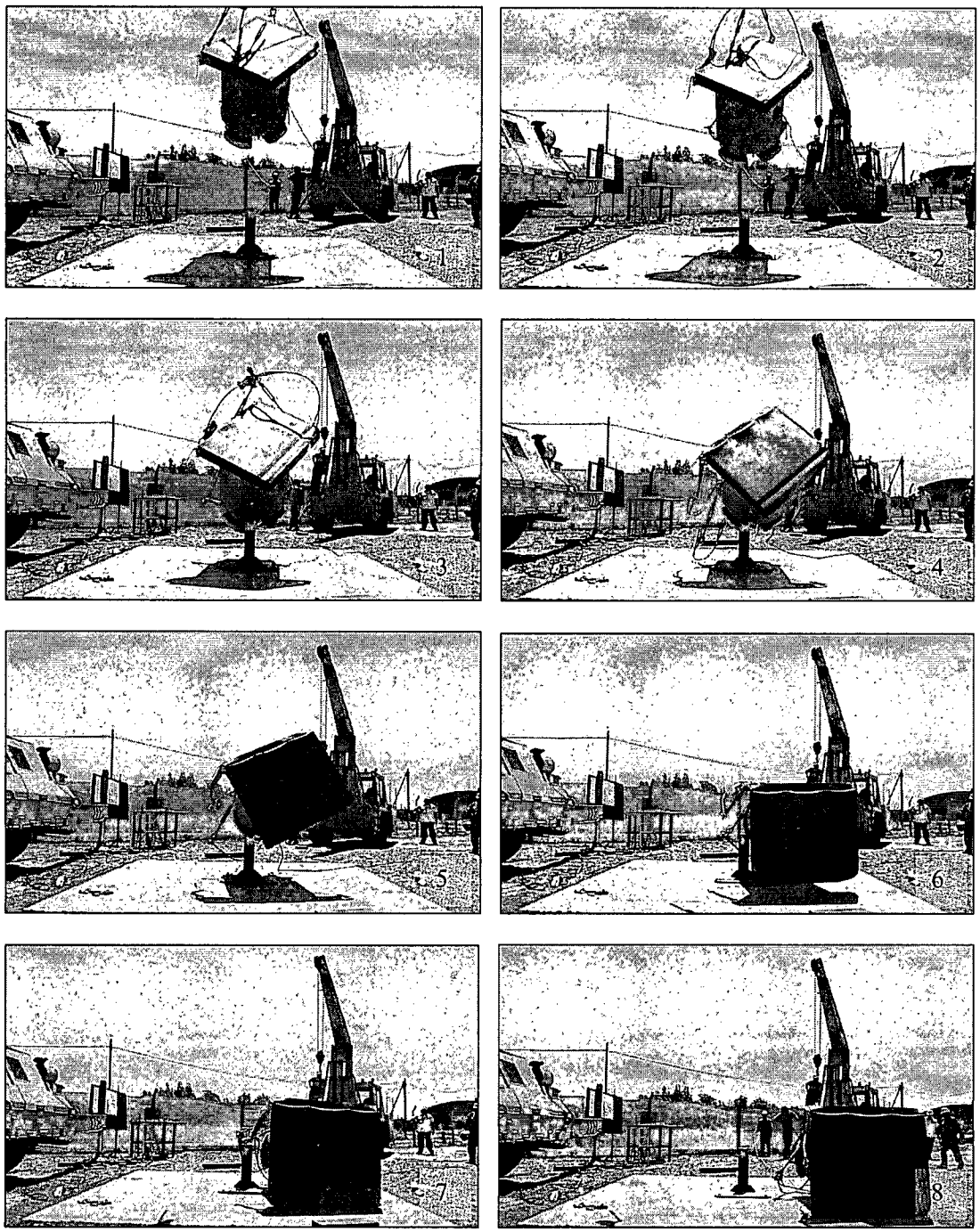

Figure 2: Test action sequence – Angle 1

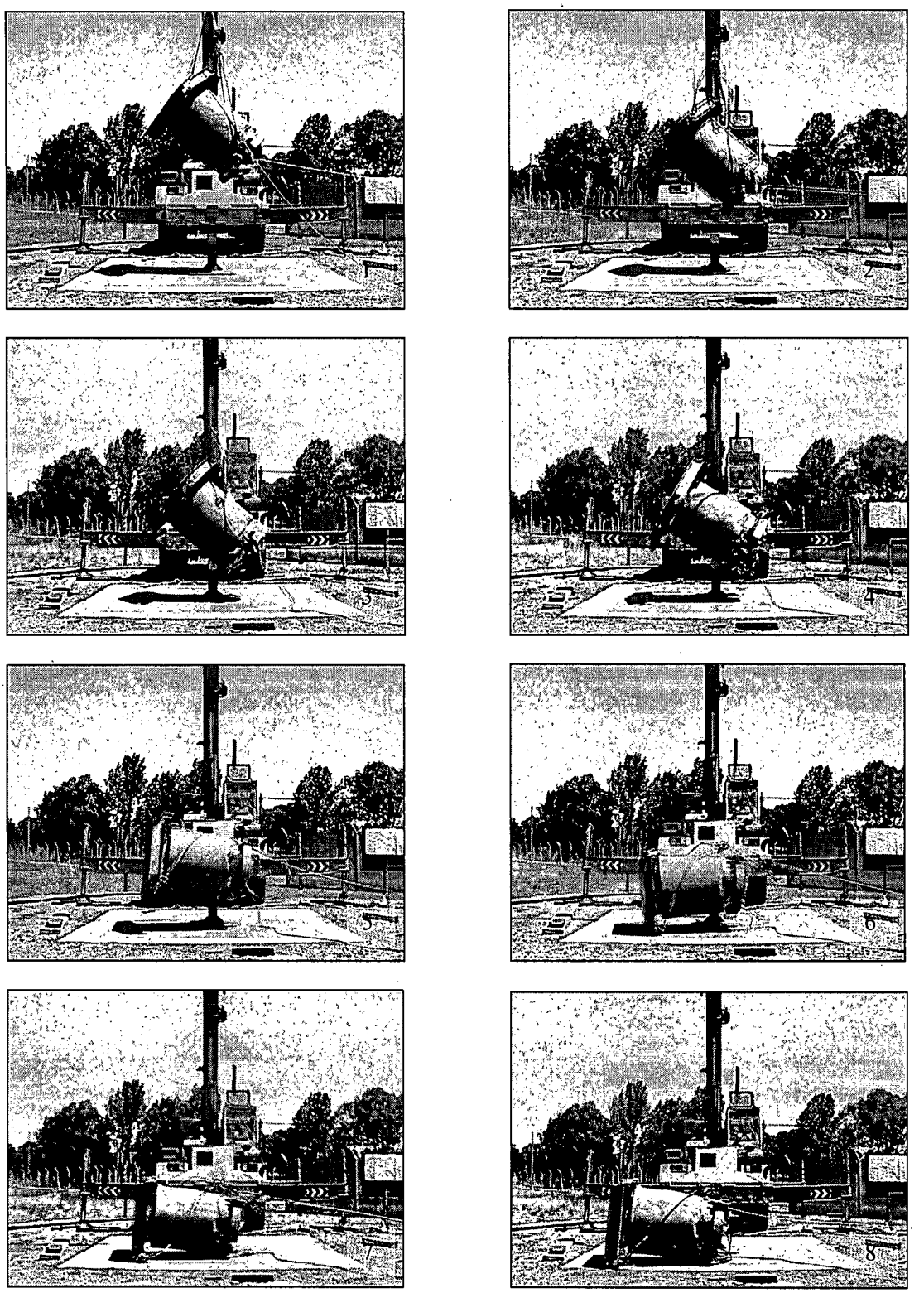

Figure 3: Test action sequence – Angle 2

Figure 4: 1.030m above target

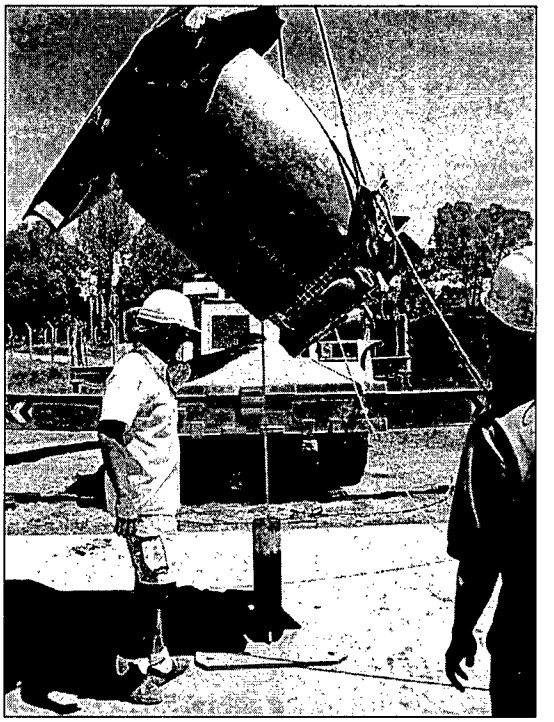

Figure 5: 1.030m above target (with height gauge)

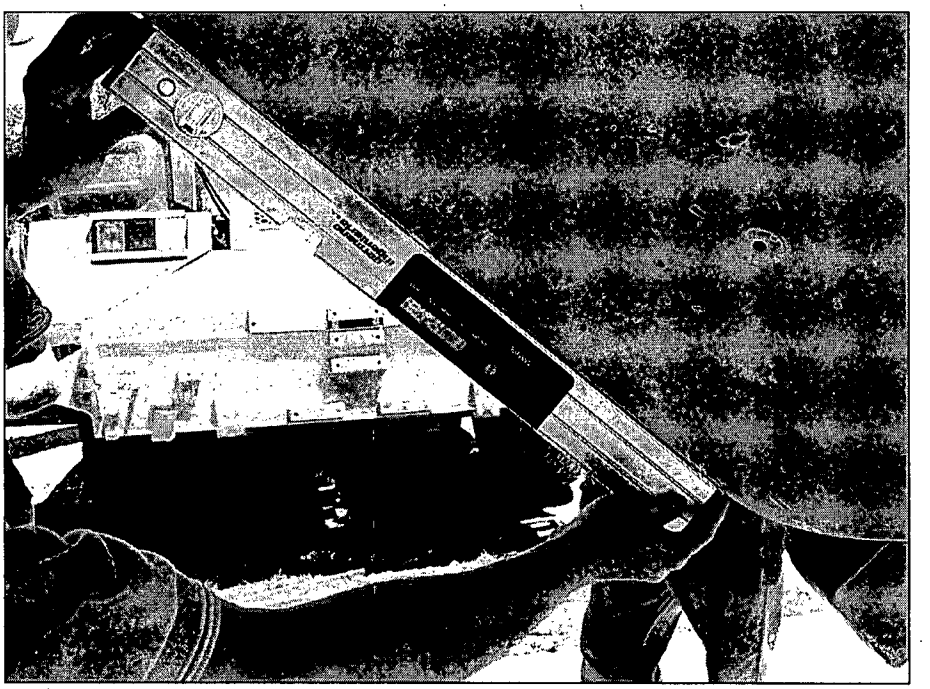

Figure 6: Inclinometer reading

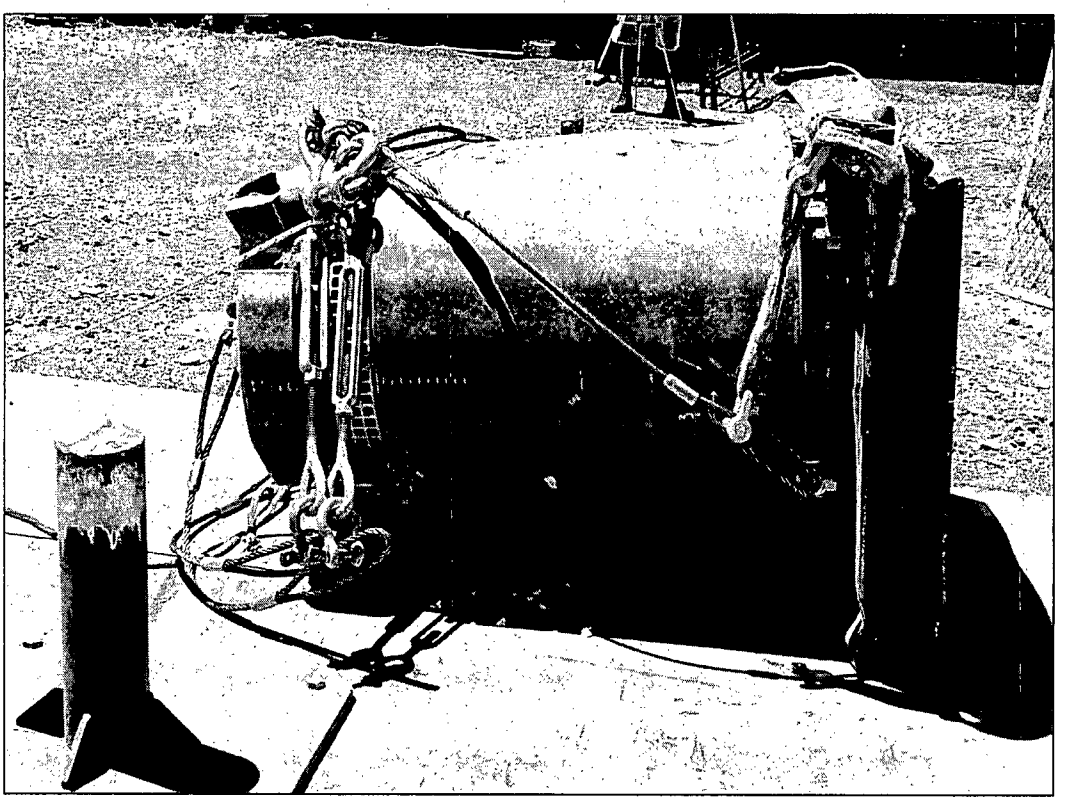

Figure 7: After drop

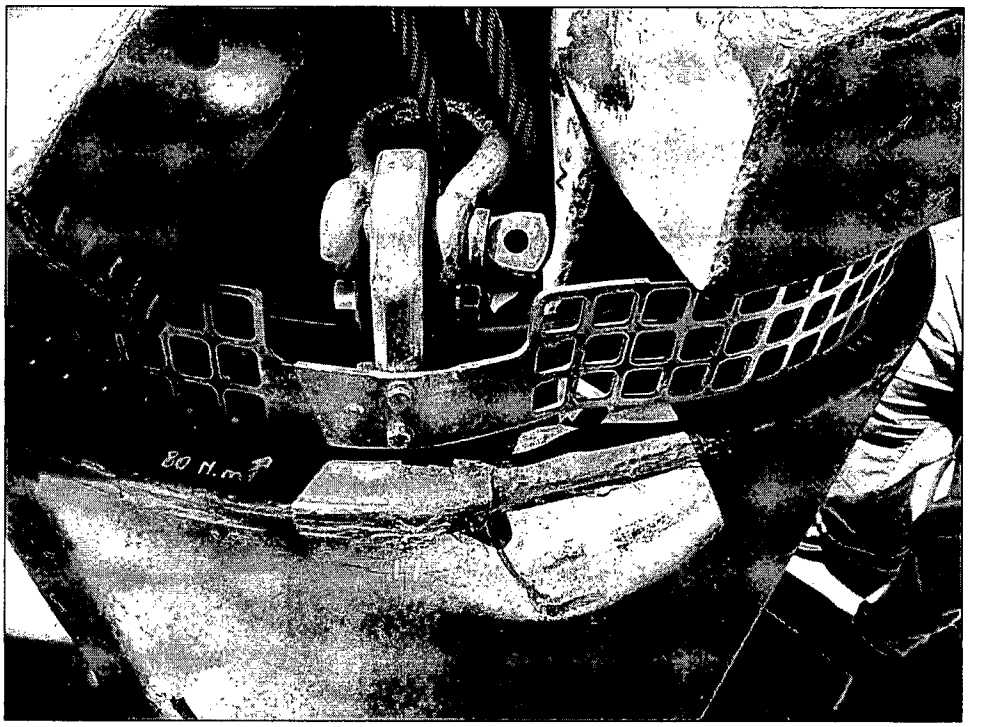

Figure 8: Jacket and grill distortion

Figure 9: Jacket and grill distortion

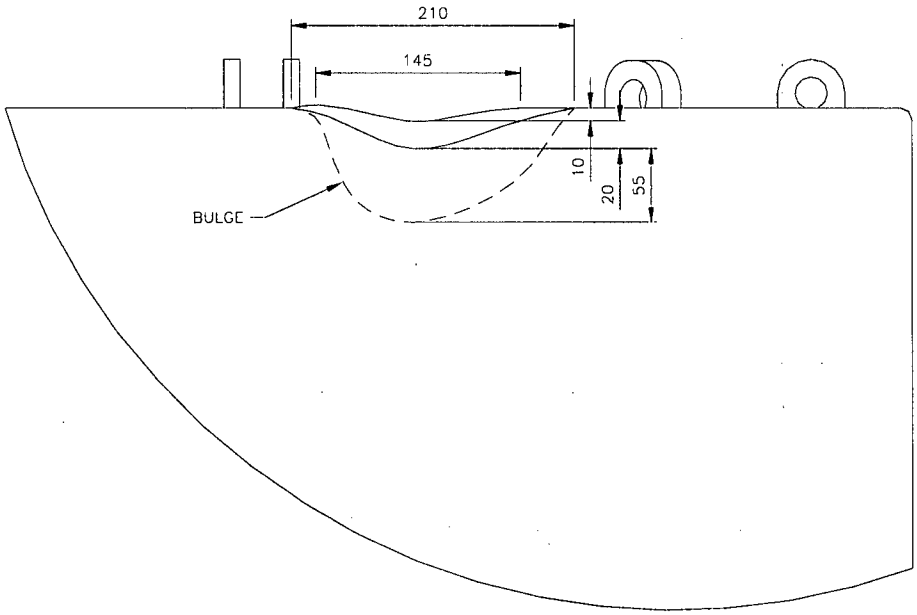

Figure 10: Jacket distortion

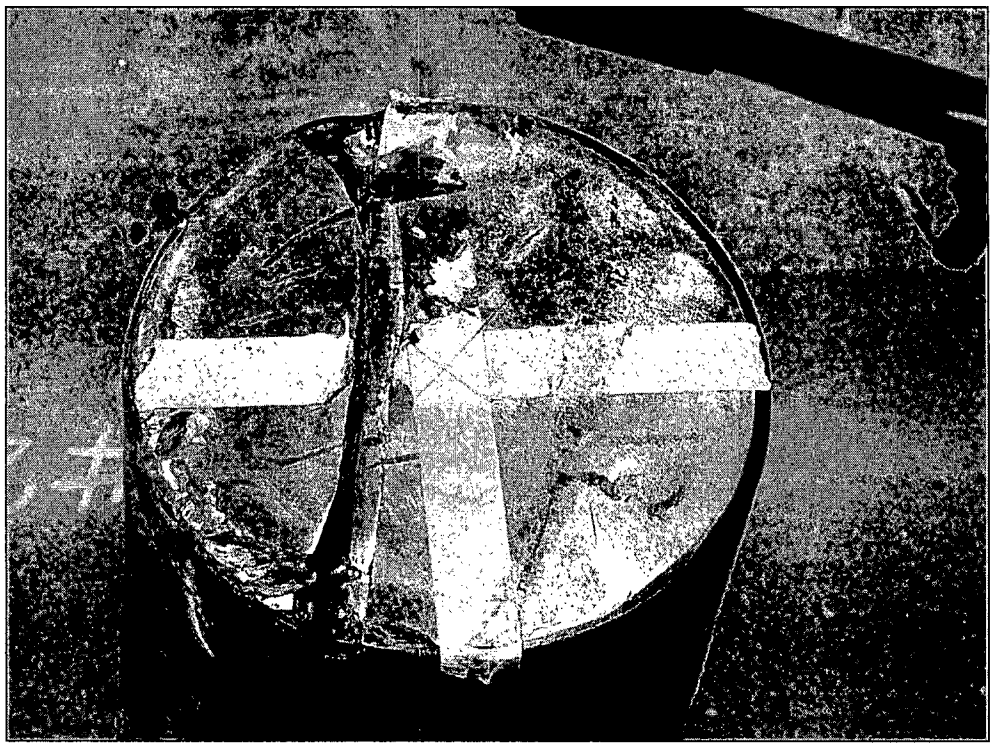

Figure 11: Condition of punch

Reviss Services (UK) Ltd **Drop Test Checklist (OP225)**	RTR: 251 Date: 21/11/08
Test Description: 1·0m Punch Test - Angled inverted onto Jacket (IAEA Type B).	
1. Confirm all personnel are aware of safety rules	✓
2. Test Plan/issue	RTM118 issue 2, Drop 17.
3. Specimen Design/Serial No/Drg No.	3981/01 (top shield 02).
4. Height gauge Identity/Drg No.	1·030m (R8083/005 issue A).
5. Target Identity/Drg No.	R8085/001 issue B.
6. Punch Identity/Drg No.	R8099/002 issue A *
7. Penetration bar Identity/Drg No.	N/A
8. Other Inclinometer: Bosch DNM 60L (cal. due 30/09/09).	
9. Specimen prepared correctly	See RTR 250.
10. Specimen orientated correctly	42·4° ± 0·5° jacket **
11. Photograph just above target	✓
12. Raise to correct height	✓
13. Release specimen	✓
14. Photograph in situ	✓
15. Photograph damage	✓
16. Confirm correct execution of drop	✓ Central on aiming line & punch
17. Pass/Fail (if, applicable see Test Plan)	Pass (fit to continue).

18. Notes

* Lengthened to 600mm for previous test, RTR 250.

** Agreed with Iain Davidson (DfT) to repeat Drop 13 but aim as close as possible to flask fin in order to transfer maximum energy into single jacket fixing point.

- Nearest jacket bolt secure and intact. Top of jacket distorted 30mm down and 50mm inwards in impact area.
- Grill slightly distorted.
- No other damage visible externally.
- Pallet, jacket, top shield and grill securely attached.

19. Signed: D W Reyes	Date: 21/11/08
20. Witnessed: Michael Nixon	Date: 21/11/08

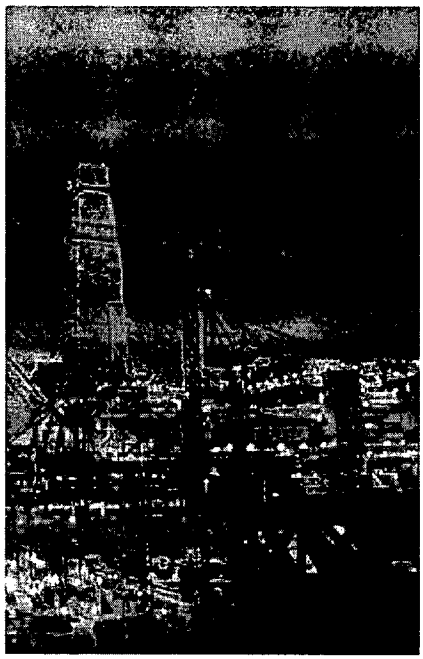
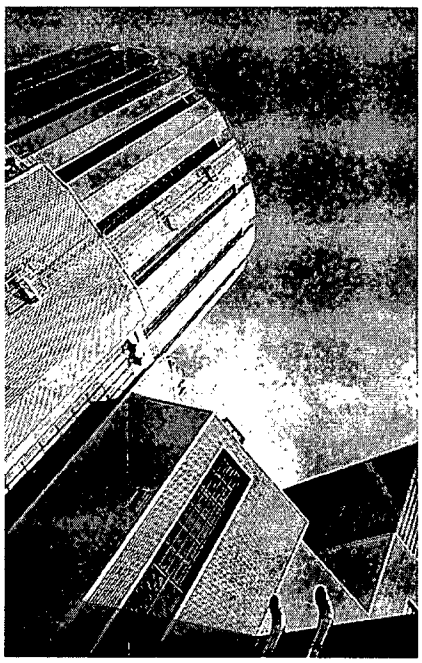
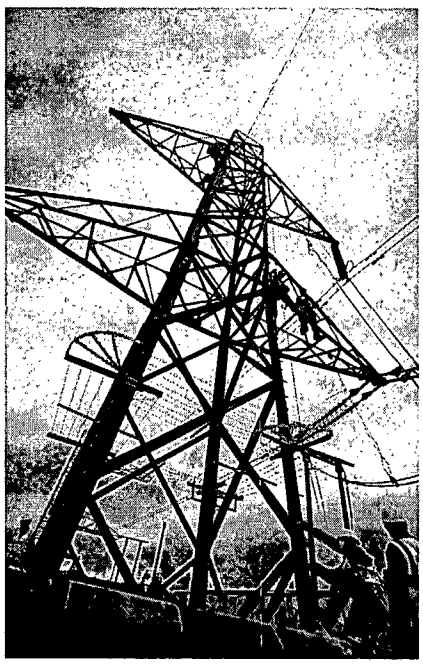

Impact Assessment of the REVISS R7021 Flask

A Sean Duvall
Senior Impact and Dynamics Specialist
Engineering Simulation Team

C15578/TR/0002
Issue 2
July 2010

DOCUMENT ISSUE RECORD
(engineering documents)

amec

Document Title :	Impact Assessment of the REVISS R7021 Flask
Project Reference:	REVISS R7021; Project Reference Number - 15578

Purpose of Issue : Approved Issue 02

Security Class : None

Issue	Description of Amendment	Originator/ Author	Checker	Approver	Date
1	Original Issue	A S Duvall	A Lamb	P Edwards	21/01/10.
2	Included comments from Reviss, DfT and Peer review	A S Duvall	A Lamb	P Edwards	25/06/2010

Total number of pages:	Intro:	11	Text	41	Tables	7	Figures	178	Appendices	

Previous issues of this document shall be destroyed or marked **SUPERSEDED**

© AMEC Nuclear UK Limited 2010

This report was prepared exclusively for REVISS by AMEC Nuclear UK Limited (AMEC). The quality of information, conclusions and estimates contained herein is consistent with the level of effort involved in AMEC's services and based on: i) information available at the time of preparation, ii) data supplied by outside sources and iii) the assumptions, conditions and qualifications set forth in this report. This report is intended to be used by REVISS only, subject to the terms and conditions of its contract with AMEC. Any other use of, or reliance on, this report by any third party is at that party's sole risk.

Distribution: REVISS, EDMS

3050aDec07 Controlling Procedure ProcessNet 9.7.1

I

CONTENTS

EXECUTIVE SUMMARY IX

1.0 INTRODUCTION 1-1

2.0 DESCRIPTION OF BENCHMARKING FINITE ELEMENT MODEL 2-1
- 2.1 Material properties 2-2
- 2.2 Method of analysis – cumulative damage 2-2
- 2.3 Modelling assumptions 2-3
  - 2.3.1 Gravity 2-3
  - 2.3.2 Initial Velocity 2-3
  - 2.3.3 Contact definitions 2-3
  - 2.3.4 Rigidwall definitions 2-3
  - 2.3.5 Element formulation 2-4
  - 2.3.6 Material definition 2-4
  - 2.3.7 Boundary conditions 2-4
  - 2.3.8 Summary of masses 2-4

3.0 THERMAL CONTRACTION ANALYSIS 3-1

4.0 COMPARISON OF RESULTS 4-1
- 4.1 Drop test 1 – 1.2 m vertical upright 4-1
- 4.2 Drop test 2 – 1.2 m horizontal 4-1
- 4.3 Drop test 3 – 1.2 m vertical inverted 4-1
- 4.4 Drop test 4 – 1.0 m penetration onto jacket 4-1
- 4.5 Drop test 5 – 1.0 m punch on to pallet 4-2
- 4.6 Drop test 6 – 9.0 m vertical upright 4-2
- 4.7 Drop test 7 – 1.0 m punch on to pallet opposite Drop 5 position 4-2
- 4.8 Drop test 8 – 1.0 m punch on to top shield over vent plug 4-2
- 4.9 Drop test 9 – 9.0 m vertical inverted 4-3
- 4.10 Drop test 10 – 1.0 m punch on to top shield opposite vent plug 4-3
- 4.11 Drop test 11 – 1.0 m angled inverted 4-3
- 4.12 Drop test 12 – 9.0 m angled inverted 4-3
- 4.13 Drop test 13 – 1.0 m punch angled inverted on to jacket corner 4-3
- 4.14 Drop test 14 – 1.0 m punch on to jacket opposite drain plug 4-3
- 4.15 Drop test 15 – 9.0 m horizontal 4-4
- 4.16 Drop test 16 – 1.0 m punch on to jacket over drain plug 4-4
- 4.17 Drop test 17 – 1.0 m punch angled inverted 4-4
- 4.18 Predicted stresses and strains in key components 4-4
  - 4.18.1 Drain tube, drain and weld 4-4
  - 4.18.2 Closure bolts, pallet bolts, jacket bolts and top shield bolts 4-6
  - 4.18.3 Containment boundary and associated welds 4-6
  - 4.18.4 Comparison of displacement, velocity and acceleration traces 4-7

5.0 DISCUSSION OF BENCHMARKING ANALYSES 5-1

6.0 IMPROVEMENTS TO THE BENCHMARKING FINITE ELEMENT MODEL 6-1

7.0 CONCLUSIONS OF BENCHMARKING ANALYSES 7-1

8.0 DESCRIPTION OF ORIENTATION FINITE ELEMENT MODEL 8-1
- 8.1 Modelling assumptions 8-1
  - 8.1.1 Gravity 8-1
  - 8.1.2 Initial velocity 8-1
  - 8.1.3 Contact definitions 8-1
  - 8.1.4 Rigidwall definitions 8-1
  - 8.1.5 Material definition 8-2
  - 8.1.6 Boundary conditions 8-2
  - 8.1.7 Summary of masses 8-2

8.2 Orientations for analysis ... 8-2
8.3 Material modelling discussion ... 8-3

9.0 RESULTS OF ORIENTATION ANALYSIS ... 9-1

10.0 CONCLUSIONS FROM ORIENTATION ANALYSIS ... 10-1
10.1 Off horizontal – 115° by 000° ... 10-1
10.2 Horizontal – 090° by 045° ... 10-1
10.3 Inclined base – 035° by 045° ... 10-1
10.4 Vertical upright (drop 6) – 000° by 000° ... 10-1
10.5 Vertical inverted (drop 9) – 180° by 000° ... 10-1
10.6 Angled inverted (drop 12) – 163° by 000° ... 10-1
10.7 Horizontal (drop 15) – 090° by 000° ... 10-1
10.8 Punch into opening between top shield and flask ... 10-2
10.9 Punch on to drain plug area ... 10-2
10.10 Punch on to vent plug area ... 10-2

11.0 DESCRIPTION OF DETAILED FINITE ELEMENT MODEL ... 11-1
11.1 Material properties ... 11-2
11.2 Modelling assumptions ... 11-2
11.2.1 Gravity ... 11-2
11.2.2 Initial velocity ... 11-2
11.2.3 Contact definitions ... 11-2
11.2.4 Target definitions ... 11-3
11.2.5 Element formulation ... 11-3
11.2.6 Boundary conditions ... 11-3
11.2.7 Summary of masses ... 11-3

12.0 RESULTS OF DETAILED IMPACT ANALYSES ... 12-1
12.1 Off horizontal – 115° by 000° ... 12-1
12.2 Horizontal – 090° by 045° ... 12-2
12.3 Inclined base – 035° by 045° ... 12-3
12.4 Vertical upright (drop 6) – 000° by 000° ... 12-4
12.5 Vertical inverted (drop 9) – 180° by 000° ... 12-4
12.6 Angled inverted (drop 12) – 163° by 000° ... 12-5
12.7 Horizontal (drop 15) – 090° by 000° ... 12-6
12.8 Punch into opening between top shield and flask ... 12-7
12.9 Punch on to drain plug area ... 12-8
12.10 Punch on to vent plug area ... 12-8

13.0 DISCUSSION OF DETAILED IMPACT ANALYSES ... 13-1
13.1 Impact performance of the pallet and pallet connections ... 13-1
13.2 Impact performance of the jacket ... 13-1
13.3 Impact performance of the top shield ... 13-2
13.4 Impact performance of the closure bolts ... 13-2
13.5 Impact performance of the shoulder bolts ... 13-2
13.6 Impact performance of the flask body ... 13-3
13.7 Impact performance of the drain tube assembly and containment boundary ... 13-3
13.8 Impact performance general discussion ... 13-3

14.0 IMPACT PERFORMANCE OF THE R7021 TRANSPORT FLASK ... 14-1

15.0 REFERENCES ... 15-2

TABLES

Table 1: Drawings used for benchmarking and orientation model creation....1
Table 2: Drawings used for orientation and detailed model creation....2
Table 3: Material properties used in benchmarking analyses....3
Table 4: Material properties used in orientation and detailed analyses....5
Table 5: Strains predicted in closure bolts, pallet bolts, jacket bolts and top shield bolts. 6
Table 6: Summary of detailed analysis results. 7

FIGURES

Figure 1: Finite element model and mesh....1
Figure 2: Details of mesh in pallet....1
Figure 3: Pallet bolted connections and dowel....2
Figure 4: Flask showing fins and details of internal structure. 2
Figure 5: Drain tube and details of drain tube weld and drain point 3
Figure 6: Closure details and top of flask....4
Figure 7: Top of flask showing shock absorbing features....4
Figure 8: Shock absorber and jacket connections 5
Figure 9: Drop 1 – comparison 1....6
Figure 10: Drop 1 – comparison 2....7
Figure 11: Drop 2 – comparison 1....8
Figure 12: Drop 2 – comparison 2....9
Figure 13: Drop 2 – comparison 3....10
Figure 14: Drop 2 – comparison 4....11
Figure 15: Drop 2 – comparison 5....12
Figure 16: Drop 2 – comparison 6....13
Figure 17: Drop 3 – comparison 1....14
Figure 18: Drop 3 – comparison 2....15
Figure 19: Drop 3 – comparison 3....16
Figure 20: Drop 5 – comparison 1....17
Figure 21: Drop 5 – comparison 2....18
Figure 22: Drop 5 – comparison 3....19
Figure 23: Drop 6 – comparison 1....20
Figure 24: Drop 6 – comparison 2....21
Figure 25: Drop 6 – comparison 3....22
Figure 26: Drop 6 – comparison 4....23
Figure 27: Drop 7 – comparison 1....24
Figure 28: Drop 7 – comparison 2....25
Figure 29: Drop 8 – comparison 1....26
Figure 30: Drop 8 – comparison 2....27
Figure 31: Drop 8 – comparison 3....28
Figure 32: Drop 9 – comparison 1....29
Figure 33: Drop 9 – comparison 2....30
Figure 34: Drop 9 – comparison 3....31
Figure 35: Drop 9 – comparison 4....32
Figure 36: Drop 10 – comparison 1....33
Figure 37: Drop 10 – comparison 2....34
Figure 38: Drop 10 – comparison 3....35
Figure 39: Drop 11 – comparison 1....36
Figure 40: Drop 11 – comparison 2....37
Figure 41: Drop 11 – comparison 3....38

Figure 42: Drop 12 – comparison 1 39
Figure 43: Drop 12 – comparison 2 40
Figure 44: Drop 12 – comparison 3 41
Figure 45: Drop 12 – comparison 4 42
Figure 46: Drop 12 – comparison 5 43
Figure 47: Drop 12 – comparison 6 44
Figure 48: Drop 12 – comparison 7 45
Figure 49: Drop 13 – comparison 1 46
Figure 50: Drop 13 – comparison 2 47
Figure 51: Drop 13 – comparison 3 48
Figure 52: Drop 14 – comparison 1 49
Figure 53: Drop 14 – comparison 2 50
Figure 54: Drop 14 – comparison 3 51
Figure 55: Drop 15 – comparison 1 52
Figure 56: Drop 15 – comparison 2 53
Figure 57: Drop 15 – comparison 3 54
Figure 58: Drop 15 – comparison 4 55
Figure 59: Drop 15 – comparison 5 56
Figure 60: Drop 15 – comparison 6 57
Figure 61: Drop 15 – comparison 7 58
Figure 62: Drop 15 – comparison 8 59
Figure 63: Drop 15 – comparison 9 60
Figure 64: Drop 15 – comparison 10 61
Figure 65: Drop 15 – comparison 11 62
Figure 66: Drop 16 – comparison 1 63
Figure 67: Drop 16 – comparison 2 64
Figure 68: Drop 17 – comparison 1 65
Figure 69: Drop 17 – comparison 2 66
Figure 70: Drop 17 – comparison 3 67
Figure 71: Strain component from drop test 1 68
Figure 72: Strain component from drop test 2 68
Figure 73: Strain component from drop test 3 69
Figure 74: Strain component from drop test 5 69
Figure 75: Strain component from drop test 6 70
Figure 76: Strain component from drop test 7 70
Figure 77: Strain component from drop test 8 71
Figure 78: Strain component from drop test 9 71
Figure 79: Strain component from drop test 10 72
Figure 80: Strain component from drop test 11 72
Figure 81: Strain component from drop test 12 73
Figure 82: Strain component from drop test 13 73
Figure 83: Strain component from drop test 14 74
Figure 84: Strain component from drop test 15 74
Figure 85: Strain component from drop test 16 75
Figure 86: Strain component from drop test 17 75
Figure 87: Final predicted effective plastic strains in closure bolts 76
Figure 88: Final predicted effective plastic strains in pallet bolts 76
Figure 89: Final predicted effective plastic strains in jacket bolts 77
Figure 90: Final predicted effective plastic strains in top shield bolts 77
Figure 91 Containment boundary strains - Inner wall components 78
Figure 92 Containment boundary strains -Closure components 79
Figure 93: Drop 6 – comparison of displacement. 80
Figure 94: Drop 6 – comparison of velocity. 81
Figure 95: Drop 6 – comparison of acceleration. 82

Figure 96: Drop 9 – comparison of displacement. 83
Figure 97: Drop 9 – comparison of velocity. 84
Figure 98: Drop 9 – comparison of acceleration. 85
Figure 99: Drop 12 – comparison of displacement. 86
Figure 100: Drop 12 – comparison of velocity. 87
Figure 101: Drop 12 – comparison of acceleration. 88
Figure 102: Drop 15 – comparison of displacement. 89
Figure 103: Drop 15 – comparison of velocity. 90
Figure 104: Drop 15 – comparison of acceleration. 91
Figure 105: Energy plots for Drop 1 92
Figure 106: Energy plots for Drop 2 92
Figure 107: Energy plots for Drop 3 93
Figure 108: Energy plots for Drop 5 93
Figure 109: Energy plots for Drop 6 94
Figure 110: Energy plots for Drop 7 94
Figure 111: Energy plots for Drop 8 95
Figure 112: Energy plots for Drop 9 95
Figure 113: Energy plots for Drop 10 96
Figure 114: Energy plots for Drop 11 96
Figure 115: Energy plots for Drop 12 97
Figure 116: Energy plots for Drop 13 97
Figure 117: Energy plots for Drop 14 98
Figure 118: Energy plots for Drop 15 98
Figure 119: Energy plots for Drop 16 99
Figure 120: Energy plots for Drop 17 99
Figure 121: Comparison of cone mesh. 100
Figure 122: Comparison of cone deformation. 100
Figure 123: Refined mesh and weld representation in pallet. 101
Figure 124: Improved deformation in pallet. 101
Figure 125: Refined mesh for punch analysis. 102
Figure 126: Predicted tearing of outer jacket wall 102
Figure 127: Predicted tearing of inner jacket wall. 103
Figure 128: Secondary damage to weld area of top shield quadrant. 103
Figure 129: Analysis of drop 15 with modified representation of top shield. 104
Figure 130: Analysis of drop 15 showing cut section. 104
Figure 131: Orientation finite element model 105
Figure 132: Pallet connection axial force of orientation models. 106
Figure 133: Pallet connection shear force of orientation models. 106
Figure 134: Closure connection shear force of orientation models. 107
Figure 135: Top shield connection axial force of orientation models. 107
Figure 136: Rigid wall normal force of orientation models. 108
Figure 137: Global acceleration of orientation models. 108
Figure 138: Detailed finite element model. 109
Figure 139: Section through detailed finite element model 109
Figure 140: Mesh of pallet for detailed finite element model 110
Figure 141: Internal structure and welds in pallet for detailed finite element model. 110
Figure 142: Mesh in foot, studs and dowel for detailed finite element model. 111
Figure 143: Mesh in top shield for detailed finite element model. 111
Figure 144: Details of internal mesh of top shield and welds in detailed finite element model. 112
Figure 145: Mesh in shoulder bolts for detailed finite element model. 112
Figure 146: Details of mesh and additional plate in jacket for detailed finite element model. 113
Figure 147: Details of mesh in fins for detailed finite element model. 113
Figure 148: Mesh of closure and studs for detailed finite element model. 114
Figure 149: Section showing mesh of internal lead of detailed finite element model. 114

Figure 150: Mesh showing shrinkage of lead after cool down for detailed finite element model.....115
Figure 151: Detailed finite element model of drain tube and outer tube.....115
Figure 152: Section through drain tube, outer tube and welds for detailed finite element model.....116
Figure 153: Initial impact orientation – Run 01.....116
Figure 154: Final deformation – Run 01.....117
Figure 155: Deformation of flask – Run 01.....117
Figure 156: Deformation of pallet – Run 01.....118
Figure 157: Deformation of top shield – Run 01.....118
Figure 158: Deformation of underside of top shield – Run 01.....119
Figure 159: Effective plastic strain in pallet connections – Run 01.....119
Figure 160: Effective plastic strain in dowels – Run 01.....120
Figure 161: Effective plastic strain in shoulder bolts – Run 01.....120
Figure 162: Effective plastic strain in flask wall – Run 01.....121
Figure 163: Effective plastic strain in closure studs – Run 01.....121
Figure 164: Effective plastic strain in outer tube – Run 01.....122
Figure 165: Effective plastic strain in drain tube – Run 01.....122
Figure 166: Energy histories – Run 01.....123
Figure 167: Global acceleration of flask – Run 01.....123
Figure 168: Initial impact orientation – Run 02.....124
Figure 169: Final deformation – Run 02.....124
Figure 170: Deformation of flask – Run 02.....125
Figure 171: Deformation of pallet – Run 02.....125
Figure 172: Deformation of top shield – Run 02.....126
Figure 173: Deformation of underside of top shield – Run 02.....126
Figure 174: Effective plastic strain in pallet connections – Run 02.....127
Figure 175: Effective plastic strain in shoulder bolts – Run 02.....127
Figure 176: Effective plastic strain in dowels – Run 02.....128
Figure 177: Effective plastic strain in flask wall – Run 02.....128
Figure 178: Effective plastic strain in closure studs – Run 02.....129
Figure 179: Effective plastic strain in outer tube – Run 02.....129
Figure 180: Effective plastic strain in drain tube – Run 02.....130
Figure 181: Energy histories – Run 02.....130
Figure 182: Global acceleration of flask – Run 02.....131
Figure 183: Initial impact orientation – Run 03.....131
Figure 184: Final deformation – Run 03.....132
Figure 185: Deformation of flask – Run 03.....132
Figure 186: Deformation of pallet – Run 03.....133
Figure 187: Effective plastic strain in pallet connections – Run 03.....134
Figure 188: Effective plastic strain in dowels – Run 03.....135
Figure 189: Effective plastic strain in shoulder bolts – Run 03.....135
Figure 190: Effective plastic strain in flask wall – Run 03.....136
Figure 191: Effective plastic strain in closure studs – Run 03.....136
Figure 192: Effective plastic strain in outer tube – Run 03.....137
Figure 193: Effective plastic strain in drain tube – Run 03.....137
Figure 194: Energy histories – Run 03.....138
Figure 195: Global acceleration of flask – Run 03.....138
Figure 196: Initial impact orientation – Run 04.....139
Figure 197: Final deformation – Run 04.....139
Figure 198: Deformation of flask – Run 04.....140
Figure 199: Deformation of pallet – Run 04.....141
Figure 200: Effective plastic strain in pallet connections – Run 04.....142
Figure 201: Effective plastic strain in dowels – Run 04.....143
Figure 202: Effective plastic strain in flask wall – Run 04.....143
Figure 203: Effective plastic strain in closure studs – Run 04.....144

Figure 204: Effective plastic strain in outer tube – Run 04 144
Figure 205: Effective plastic strain in drain tube – Run 04 145
Figure 206: Energy histories – Run 04 145
Figure 207: Global acceleration of flask – Run 04 146
Figure 208: Initial impact orientation – Run 05 146
Figure 209: Final deformation – Run 05 147
Figure 210: Deformation of top shield – Run 05 147
Figure 211: Effective plastic strain in pallet connections – Run 05 148
Figure 212: Effective plastic strain in dowels – Run 05 148
Figure 213: Effective plastic strain in shoulder bolts – Run 05 149
Figure 214: Effective plastic strain in flask wall – Run 05 149
Figure 215: Effective plastic strain in closure studs – Run 05 150
Figure 216: Effective plastic strain in outer tube – Run 05 150
Figure 217: Effective plastic strain in drain tube – Run 05 151
Figure 218: Energy histories – Run 05 151
Figure 219: Global acceleration of flask – Run 05 152
Figure 220: Initial impact orientation – Run 06 152
Figure 221: Final deformation – Run 06 153
Figure 222: Deformation of top shield – Run 06 153
Figure 223: Deformation of top shield absorbers removed – Run 06 154
Figure 224: Deformation of underside of top shield – Run 06 154
Figure 225: Effective plastic strain in closure studs – Run 06 155
Figure 226: Effective plastic strain in outer tube – Run 06 155
Figure 227: Effective plastic strain in drain tube – Run 06 156
Figure 228: Energy histories – Run 06 156
Figure 229: Global acceleration of flask – Run 06 157
Figure 230: Initial impact orientation – Run 07 157
Figure 231: Final deformation – Run 07 158
Figure 232: Deformation of flask – Run 07 158
Figure 233: Deformation of pallet – Run 07 159
Figure 234: Deformation of pallet side view – Run 07 159
Figure 235: Deformation of top shield – Run 07 160
Figure 236: Deformation of underside of top shield – Run 07 160
Figure 237: Effective plastic strain in pallet connections – Run 07 161
Figure 238: Effective plastic strain in dowels – Run 07 161
Figure 239: Effective plastic strain in shoulder bolts – Run 07 162
Figure 240: Effective plastic strain in flask wall – Run 07 162
Figure 241: Effective plastic strain in closure studs – Run 07 163
Figure 242: Effective plastic strain in outer tube – Run 07 163
Figure 243: Effective plastic strain in drain tube – Run 07 164
Figure 244: Energy histories – Run 07 164
Figure 245: Global acceleration of flask – Run 07 165
Figure 246: Initial impact orientation – Punch 01 165
Figure 247: Final deformation – Punch 01 166
Figure 248: Deformation of underside of top shield – Punch 01 166
Figure 249: Effective plastic strain in shoulder bolts – Punch 01 167
Figure 250: Effective plastic strain in drain tube – Punch 01 167
Figure 251: Velocity profile showing rotation after impact – Punch 01 168
Figure 252: Energy histories – Punch 01 169
Figure 253: Initial impact orientation – Punch 02 169
Figure 254: Final deformation – Punch 02 170
Figure 255: Final deformation section-through centre of drain plug – Punch 02 170
Figure 256: Deformation of flask close-up – Punch 02 171
Figure 257: Effective plastic strain in jacket outer wall – Punch 02 171

Figure 258: Effective plastic strain in jacket additional plate – Punch 02 172
Figure 259: Effective plastic strain in jacket inner wall – Punch 02....172
Figure 260: Effective plastic strain in flask fins – Punch 02 173
Figure 261: Effective plastic strain in outer tube – Punch 02 173
Figure 262: Effective plastic strain in drain tube – Punch 02 174
Figure 263: Energy histories – Punch 02 174
Figure 264: Initial impact orientation – Punch 03 175
Figure 265: Final deformation section through impact point – Punch 03 175
Figure 266: Deformation of flask – Punch 03 176
Figure 267: Effective plastic strain in top shield under punch– Punch 03....176
Figure 268: Effective plastic strain in outer tube – Punch 03 177
Figure 269: Effective plastic strain in drain tube – Punch 03 177
Figure 270: Energy histories – Punch 03 178

EXECUTIVE SUMMARY

Following a series of drop tests on the REVISS R7021 flask, finite element analysis has been completed to determine the effects of the drops on the internal components. An internal drain tube weld failed during the final drop test sequence and although all other components passed the testing, a number of areas were identified where improved performance would be beneficial. Finite element analysis has been used, without prior access to the drop test results, to provide a benchmark modelling approach which has been used to determine the effects of a number of design changes.

In general, excellent agreement has been obtained between the observed and predicted deformations. A number of improvements to the model have been made to provide better agreement based on the observed data.

An orientation analysis has been used to determine the worst case impact orientations for the flask. The latest flask design has been analysed at these worse case impact orientations before being subjected to a number of punch tests.

The top shield and pallet act to protect the flask from gross deformation. They also act to reduce accelerations of the contents and flask as a whole and will be retained following regulatory impact tests.

The modifications made to the flask since the drop testing are minor but all improve the impact performance of the flask.

The containment area remains predominately elastic, with localised plastic deformation due to surface contact or minor movement of the lead. The maximum predicted effective plastic strain in the drain tube is 1.0% demonstrating that containment will not be lost.

The shielding performance will not be affected due to regulatory impacts.

The analysis predicts that the flask can survive both a regulatory 9 m drop on to a rigid target and a regulatory 1m punch test in any orientation with no loss of containment.

1.0 INTRODUCTION

The REVISS R7021 radioactive material transport flask has been subjected to a series of seventeen drop tests to prove the design for subsequent licensing under the IAEA regulations, as described in TS-R-1 (Ref. 1). The seventeen drops are described in detail in the REVISS test plan (Ref. 2). An inspection of the flask after drop 10 showed that the containment boundary remained leaktight. However, after the final test inspection it was revealed that the weld connecting the drain tube to the drain point had failed.

Finite element analysis has been introduced to this project to assist in defining the causes of the drain tube weld failure and to provide demonstration that the proposed design changes increase the safety and reliability of the flask.

Finite element models have been created to simulate the entire series of drop tests with cumulative damage being passed on between each simulation. The details of the damage observed in the drop tests, except for the knowledge that the drain tube weld had failed, was unknown by the analyst until the simulation of drop 12 had started.

The finite element models were then refined in certain areas to provide a more detailed simulation of the deformation and material failure particularly in areas subjected to the punch tests, where tearing of material was observed.

The results from the benchmarking analyses have been used to improve the design with minor modification to the top shield, pallet and jacket. The drain tube and associated welds have been modified to improve their performance during impact. These improvements have been included in a detailed finite element model. A simplified representation of the flask has been built and used to determine the worst impact orientations with respect to safety criteria. The worst case orientations, along with some of the original drop test orientations, have been analysed with the detailed improved finite element model.

2.0 DESCRIPTION OF BENCHMARKING FINITE ELEMENT MODEL

The benchmarking finite element model has been constructed in Patran (Ref. 3) using the drawings from Table 1. The finite element model and mesh discretisation are shown in Figure 1.

The details of the pallet are shown in Figure 2. It can be seen that for this analysis the mesh of the pallet bolting plates, and that of the top plate of the pallet, are non-continuous. The weld that connects the top plate to the bolted plate is represented by solid elements, which are tied to the top surface of the pallet top plate. The weld detail of the internal support structure of the pallet is not explicitly modelled and it was assumed that these welds did not fail. Therefore, the internal structure is modelled as continuous with the top and base plates of the pallet.

The pallet connection bolts, washers and dowels are shown in Figure 3. The bolt thread is continuous with the pallet bolting plate and the minimum thread diameter has been modelled for the bolt shank.

Figure 4 shows the flask and the details of the internal structure. The external fins and support fins are modelled in detail and the mesh is continuous as welds in this area are large and no significant failure would be expected. The cut section shows the internal structure including the lead retaining rings. It should be noted that the complexity of modelling the drain tube has resulted in some discontinuities in the mesh of the lead. The effect of these should be minimal and these areas of lead have been tied together where possible.

The drain tube and the internal containment boundary are shown in Figure 5. A close up of the drain tube and drain point is also shown. The drain tube weld can be seen in pink in the close up image. The complex geometry and requirement to refine this area resulted in the drain tube weld controlling the analysis timestep.

The top of the closure attached to the flask by the bolts can be seen in Figure 6. The additional mass blocks are shown in red. The vent plug guard, shown in blue, is tied to the top of the closure and does not have a continuous mesh with the closure. A preload in the closure and pallet studs was included by introducing an initial axial stress in the shank of the studs for the first analysis.

Figure 7 shows the flask with the outer jacket and the shock absorber attached. Initial analyses assumed that all the plates in the shock absorber were fully welded. Following discussions with REVISS, after a number of analyses had been completed, this was found to be incorrect and the weld detail corrected accordingly where possible. In some cases the mesh was not sufficiently detailed to enable welds to be corrected. These changes are discussed in detail in Section 6.0. The bolts connecting the jacket and the shock absorber to the flask are shown in Figure 8.

The contents have been modelled as a single cylinder with steel properties and mass adjusted accordingly.

The grill, spring gasket, drain filter and O rings have not been modelled.

The model consists entirely of 8-noded high order solid elements. The flat target has been represented by a rigid wall and the punch has been explicitly modelled using 8-noded solid elements.

2.1 Material properties

The material properties have been derived from the initial material test data supplied to AMEC by REVISS on 7th April 2009. In most cases this test data only consisted of the material yield strength, an ultimate tensile strength and an elongation at failure in tension. In some cases a 1% proof stress was available. The engineering values obtained from the tensile tests have been used to obtain a representative true stress/strain curve which can be used in the finite element analysis. It has been assumed that the ultimate tensile stress occurs at 70% of the final elongation, based on observations from similar tensile load/displacement curves. The material data used for the analyses are shown in Table 3.

The available material data has been used in the LS-DYNA (Ref. 4) piecewise linear plasticity material model, type 24, which allows a plastic stress strain curve to be defined. With this material option, and high order solid elements, it is only possible to define failure based on effective plastic strain. This can result in failure of elements when under compression only and gives unrealistic results. Therefore, failure of elements during the analysis is not permitted in these analyses and it is necessary to review the predicted stresses and strain at the end of the analysis to determine if failure would have occurred.

2.2 Method of analysis – cumulative damage

The R7021 was subjected to a sequence of seventeen drops. The original pallet was replaced after drop 4. The flask was then subjected to a further six drops. After drop 10 the original pallet was re-attached along with a new shock absorber. The flask was then subjected to a further seven drops. It is assumed that the cumulative damage accrued from the series of drops was the main cause of the drain tube weld failure. As such the analyses attempt to replicate the seventeen drops with the damage, in the form of deformation, stress and strains, being carried on from one drop to the next.

This approach does present some problems in the analysis. In practice there is additional damage, albeit minor, due to the secondary impacts as the flask rebounds. The typical duration of the initial impact for this type of flask is around 0.05 seconds. The secondary impact may not occur for up to 0.5 seconds later and in some cases even longer. An impact analysis of this duration would result in run time of weeks and add little to the overall results. Therefore, only the initial impact up to the point of rebound has been analysed and no secondary damage was accrued.

It should be noted that the elastic stresses that exist during the impact would largely be relieved after the impact and items would "settle" before the next impact. To replicate this would require extensive analysis time and it is concluded that passing the elastic stresses on to the next analysis will not significantly affect the

overall results of the impact. This will result in some deformation measurement being different to the physical drop tests as no "springback" has been allowed but these differences should be minimal. To minimise the affects of springback, the 9 m drop analyses are run until the internal energy has reached a steady value. In the punch tests and 1.2 m drops the effects of springback are minimal. The associated variation in deformation depends upon the flexibility of the item, being larger in the plates in the pallet than elsewhere in the flask. The elastic deformation of the pallet plates following a flat base drop can be of the order of 10 mm.

Any spurious deformations, due to contact or modelling errors, are therefore also carried through and this can result in some high strains being apparent in every analysis once the error occurs. It is possible to correct some minor errors in the modelling but this can have adverse affects on the stress state and can lead to instability in the analysis model.

2.3 Modelling assumptions

2.3.1 Gravity

Gravity has been applied to all analyses using the *LOAD_BODY definition cards in LS-DYNA (Ref. 4). A constant value of 9.81 m/s^2 is applied for the duration of the impact.

2.3.2 Initial Velocity

The initial velocity is based on the enhanced height for each impact analysis. The enhanced heights are based on the given mass of the flask (4374 kg) against the maximum stated mass of the flask (4500 kg). This results in a factor of 1.0288 being applied to the drop height. A drop height of 1 m becomes 1.03 m, a drop height of 1.2 m becomes 1.24 m and a drop height of 9 m becomes 9.26 m. These equate to initial velocities of 4.495 m/s, 4.932 m/s and 13.479 m/s respectively.

2.3.3 Contact definitions

In general, the AUTOMATIC_SINGLE_SURFACE contact definition has been used. In addition a number of TIED_SURFACE_TO_SURFACE contact definitions have been used where the mesh is not continuous, e.g. the make weights on the closure and the pallet feet to the pallet top plate. Contact friction for all cases is set to zero to maximise the relative movement. The exact values of friction are unknown but it is unlikely to make any significant difference to the flask behaviour.

2.3.4 Rigidwall definitions

The impact target is not explicitly modelled but is represented by a RIGIDWALL_PLANAR definition. This provides an infinitely large, smooth impact surface. Contact friction is set to zero in all cases. In the detailed finite element model, presented in Section 11.0, the contact friction was set to 0.2 but found to have limited influence on results. The most likely orientation to provide noticeable

differences is the 9 m flat lid impact (drop 9), where the shock absorber cones slid under the flask during the impact.

2.3.5 Element formulation

The default solid element type in LS-DYNA (Ref. 4) is a single integration point element. This can prove unstable and result in hourglass modes being formed. These hourglass modes are zero energy modes where the element deforms but does not absorb any energy. To avoid this problem, the type 2, fully integrated selective reduced (S/R) solid element is used. This element formulation takes longer to compute but provides a more accurate result with less possibility of the analysis failing due to excessive spurious distortion.

2.3.6 Material definition

In the benchmarking finite element model, the PIECEWISE_LINEAR_PLASTICITY, mat 24, model has been used for all components. No failure mechanisms have been used so components will continue to strain and deform even when their tensile strain is above the material failure strain. This material option is used as it provides the best representation based on the available material data.

The improved material data obtained from REVISS (Ref. 5) at the beginning of July 2009, summarised in Table 4, was used in the detailed finite element model as it was not possible to back fit in the cumulative set of analyses.

2.3.7 Boundary conditions

A full 3-D model with no symmetry planes has been created. There are no boundary conditions required.

2.3.8 Summary of masses

The following masses are taken from the LS-DYNA finite element model for the first analysis. The masses in brackets are taken from the Inspection Report (Ref. 6)

- Flask body 3381.5kg (3416kg)
- Contents 17.6kg (17.92kg)
- Closure including lead 157.1kg (158kg)
- Jacket 270.7kg (322kg)
- Top shield 176.5kg (196kg)
- Pallet 238.0kg (262kg)
- Bolts, nuts, dowels, etc 32.3kg

- Total mass of finite element model 4273.9kg (4374kg)

It should be noted that the items used to calculate the masses of the FE model and the Inspection report may not correspond directly.

The FE model is approximately 100kg under weight, 2.3%. This will not have a significant effect on the analysis results.

3.0 THERMAL CONTRACTION ANALYSIS

The construction of the flask is such that the steel components are manufactured and, when almost complete, the flask void is filled with molten lead. During the cooling process the lead will contract, as will the flask after expanding due to the heat of the lead. The different rates of thermal contraction, of the lead and the steel, result in gaps forming between the lead and the steel in certain areas. This gap allows the lead to move around, albeit only by a few millimetres, within the flask and is considered to be a contributory factor to the failure of the drain tube weld.

In order to predict the size of this gap, the finite element model utilises an elastic-plastic material model with an added thermal coefficient of expansion. The model is set to an initial temperature and allowed to "cool" by 305°C from 325°C as advised by REVISS (Ref. 7). A thermal coefficient of expansion of 17.3×10^{-6} was used for the steel and 29.0×10^{-6} was used for the lead.

The resultant geometry is then used as the starting geometry for the impact analysis. A gap of approximately 1.25 mm was predicted between the outer edge of the lead and the inner edge of the outer wall of the flask.

4.0 COMPARISON OF RESULTS

The results from the analysis are compared with the images from the drop test result reports (Ref. 6). In subsection 4.18 the predicted stresses and strains in key components are reported. In line with the drop test procedure a new pallet was used for drops 5 to 10 after which the original deformed pallet from drops 1 to 4 was refitted and used for drops 11 to 17. A new top shield was used for drops 11 to 17.

4.1 Drop test 1 – 1.2 m vertical upright

Figure 9 and Figure 10 show the deformation of the inner webs of the pallet. The extent of deformation is similar but the main deformation occurs on the lower edge of the inner support and is predicted to occur on the upper edge of the inner support. There is no other significant deformation observed.

4.2 Drop test 2 – 1.2 m horizontal

Figure 11 shows the deformation of the impact edge of the pallet. In both cases the leading edges have bent inwards towards each other. The predicted deformation shows some movement of the leading edge away from the flask not observed in the impact. Figure 12 shows favourable agreement in deformation mode and size. Figure 13 shows similar agreement but the edge of the internal support has formed a double buckle which may be due to some minor deformation from drop 1 or slight variation in the impact attitude. Figure 14 shows favourable agreement but Figure 15 shows that the upper plate of the shock absorber "quadrant" does not deform to the extent observed. This has been subsequently identified as a modelling assumption error whereby the vertical internal plates in the quadrant were modelled as fully welded to the upper horizontal plate giving the quadrant greater strength. This is also shown in Figure 16 however, the angle of the deformed quadrant from the horizontal compares favourably. The error in the fully welded plates in the quadrant was only identified after drop 5 was completed and corrected as best as possible for drop 6 by manual removal of elements around the weld.

4.3 Drop test 3 – 1.2 m vertical inverted

Figure 17, Figure 18 and Figure 19 all show good agreement between the observed deformation of the shock absorber cones and the predicted results. A more refined mesh around the tips of the cones would probably result in an improved prediction of the deformation.

4.4 Drop test 4 – 1.0 m penetration onto jacket

There is no significant damage to the flask from this impact test. It was considered that the drop of the punch onto the flask would not affect the strains in the flask apart from locally around the point of impact and therefore this impact was not simulated.

4.5 Drop test 5 – 1.0 m punch on to pallet

Figure 20 shows the observed and predicted deformation of the edge of the pallet. The observed deformation shows a non symmetrical result. The lower plate shows a crease from the point of impact to the edge which is possibly due to the partial failure of the weld on the internal short support. This did not occur on the plate, which can be seen, but on the plate partially hidden by the upright side plate. Figure 21 shows the penetration of the punch in to the pallet space. Figure 22 compares the extent of the tear in the base plate with the predicted plastic strains in the base plate.

A maximum strain in excess of 25%, compared to the failure strain of 28%, is predicted over a large area. As this is predominately a tensile strain this is likely to cause failure. The detailed finite element model analyses, presented in Section 12.0, show better agreement as failure based on stress state and strain can be used on a refined mesh.

4.6 Drop test 6 – 9.0 m vertical upright

Figure 23 shows reasonable agreement in the deformation mode of the pallet but the predicted extent of deformation is less than observed. Figure 24 and Figure 25 show that the collapse of the internal supports is under predicted. This is due to discrepancies in the physical welding which is not reproduced in the finite element representation. Subsequent inspection of the pallet has shown that a large number of welds failed during this drop test, which allowed the internal supports to rotate and collapse more readily than if the welds had held. Figure 26 shows a similar deformation mode but the predicted extent of deformation is less than observed.

4.7 Drop test 7 – 1.0 m punch on to pallet opposite Drop 5 position

Figure 27 and Figure 28 show similar agreement to that of drop 5. The predicted plastic strains in the pallet base are in excess of 33%, compared to the failure strain of 28%, over a large area and failure would be expected.

4.8 Drop test 8 – 1.0 m punch on to top shield over vent plug

Figure 29 and Figure 30 show good agreement with the extent of deformation. The predicted strains local to the point of impact are in excess of 62%, compared to the failure strain of 28%, and local failure of the top plate would be expected. Figure 31 shows that the predicted depression in the top plate is approximately 47 mm compared to the observed value of 50 mm. The extent of deformation is partly controlled by the vertical plates that are beneath the top plate. These were initially assumed to be fully welded but discussions with REVISS has shown that they are not welded to the top plate. This error was corrected for drop 11 onwards.

4.9 Drop test 9 – 9.0 m vertical inverted

Figure 32 shows less predicted deformation than observed but it is not known if this deformation was consistent on all four quadrants or due to the slight offset of impact angle. Figure 33 and Figure 34 show good agreement between observed and predicted deformation modes. The tight folds observed in the cones are not fully captured. This is partly due to the mesh size used and also the amount of weld around the base of the cone. The weld around the base ensures that the wide edge of the cone remains upright and forces the buckle towards the thin edge of the cone. A refined representation of the weld around the base of the cone will result in an improved visual agreement. Figure 35 shows that the predicted final height of the cones is approximately 90 mm compared to the observed heights of between 95 mm and 115 mm.

4.10 Drop test 10 – 1.0 m punch on to top shield opposite vent plug

Figure 36, Figure 37 and Figure 38 show similar agreement to drop test 8 with predicted strains in excess of 75%, compared to the failure strain of 28%. The observed penetration of 55 mm is accurately predicted.

4.11 Drop test 11 – 1.0 m angled inverted

Figure 39 and Figure 40 show good agreement in the deformation mode and extent of deformation. Figure 41 shows that the observed final height of the cone was 180 mm compared to the predicted height of 160 mm.

4.12 Drop test 12 – 9.0 m angled inverted

Figure 42, Figure 43, Figure 44, Figure 45, Figure 46 and Figure 47 all show similarly good agreement. The tight folds and the local tearing are not predicted due to the mesh size used and the lack of failure criteria. Figure 48 shows that the predicted height of the central cones at the end of the impact is approximately 130 mm. The observed deformation of the central cones was between 155 mm and 160 mm.

4.13 Drop test 13 – 1.0 m punch angled inverted on to jacket corner

Figure 49 and Figure 50 show good agreement on the extent of deformation. The grill was omitted from all the analyses as it was considered not to offer any significant resistance or strength during the impacts. Figure 51 shows that strains in excess of 44%, compared to the failure strain of 28%, are predicted in the jacket weld area and failure is likely.

4.14 Drop test 14 – 1.0 m punch on to jacket opposite drain plug

Figure 52 shows the plastic strain at the point of impact to be distributed over a large area. The general deformation shown in Figure 53 compares well and the detail shown in Figure 54 indicates that typically plastic strains are around 13%, compared to the failure strain of 28%. Although this may appear low, it should be

noted that the mesh size at the point of impact is relatively large and the plastic strain is spread over a large area. A refined mesh would result in more localised strains being predicted. These localised strains would be higher and more likely to cause failure. A more refined mesh was used in subsequent punch analyses in the detailed finite element model, presented in Section 11.0. The centre of the predicted strain is in a similar position to the observed start of failure.

4.15 Drop test 15 – 9.0 m horizontal

Figure 55 shows that the predicted deformation agrees with observed deformation of the leading edge of the pallet. The mesh does not fully capture the bending and the mesh should be refined in this area. Figure 56 and Figure 57 show slightly less deformation predicted in the quadrant but slightly more on the shock absorber top plate. This may be due to differences in the weld details within the shock absorber. Figure 58 shows good agreement in the deformation of the jacket. It should be noted that it would appear the jacket is 90 degrees out of position on the finite element model and this impact struck one of the lifting points which slightly affects the deformation around the top of the flask. Figure 59 shows failure of the weld in the quadrant. Strains in excess of 28%, the failure strain, are predicted in this area and failure would be predicted. Figure 60 shows high strains predicted on the inside top of the jacket in excess of 84%, however this is affected by the jacket lifting point. Figure 61 shows good agreement with respect to the deformation of the fins. Figure 62 and Figure 63 show that the jacket is not predicted to deform to the same extent as observed again this is due to the lifting point resisting the deformation. Figure 64 and Figure 65 show generally good agreement but the failure of the weld on the quadrant and the coarse mesh on the pallet limit the agreement. These items, along with the position of the lifting point, are addressed in subsequent analyses.

4.16 Drop test 16 – 1.0 m punch on to jacket over drain plug

Figure 66 and Figure 67 show the deformation due to the punch. The predicted area of deformation is similar to that observed. A refined mesh is required to capture the sharp angle of deformation due to the edge of the punch.

4.17 Drop test 17 – 1.0 m punch angled inverted

The exact position of the punch for drop 17 was not detailed in the original documentation. Figure 68 and Figure 69 show that the analysis point of impact was more central than the test location but the deformation of the jacket is similar. Figure 70 shows reasonable agreement between the predicted deformation and that observed.

4.18 Predicted stresses and strains in key components

4.18.1 Drain tube, drain and weld

The analyses simulate the seventeen drop tests and the damage to the drain tube, drain and weld are cumulative. In order to assist the design process it is possible to

estimate the amount of plastic strain increase in the drain tube, drain and weld area for each drop. These values are shown in Figure 71 to Figure 86 and tabulated below. The predicted effective plastic strains for the weld and drain tube towards the centre of the flask are given separately from those of the outer weld, drain and drain tube are where the failure occurred during drop testing.

	Plastic strain in inner weld and drain tube	Cumulative plastic strain in inner weld and drain tube	Plastic strain in outer weld, drain and drain tube	Cumulative plastic strain in outer weld, drain and drain tube
Drop test 1	11.5	11.5	2.6	2.6
Drop test 2	3.8	15.3	17.9	20.5
Drop test 3	1.2	16.5	3.4	23.9
Drop test 4		16.5		23.9
Drop test 5	1.7	18.2	1.9	25.8
Drop test 6	5.5	23.7	4.0	29.8
Drop test 7	0.3	24.0	1.0	30.8
Drop test 8	3.4	27.4	5.0	35.8
Drop test 9	1.2	28.6	4.6	40.4
Drop test 10	0.7	29.3	3.7	44.1
Drop test 11	1.8	31.1	0.3	44.4
Drop test 12	2.6	33.7	2.2	46.6
Drop test 13	2.3	36.0	3.6	50.2
Drop test 14	2.3	38.3	4.4	54.6
Drop test 15	8.8	47.1	13.9	68.5
Drop test 16	1.0	48.1	0.5	69.0
Drop test 17	2.5	50.6	5.9	74.9

This gives a clear indication that the side drops, drops 2 and 15, generate the large strains in the drain tube and weld area. Drop 1, flat on to base, also generates

large strains which are probably due to settlement of the lead and initial gaps being taken up. These initial strains may well occur for any initial impact orientation.

4.18.2 Closure bolts, pallet bolts, jacket bolts and top shield bolts

The damage to the bolts is cumulative over the simulated seventeen drop tests. In order to assist the design process it is possible to estimate the amount of plastic strain increase in the bolts for each drop. These are shown in Table 5. Plots of the cumulative effective plastic strain at the end of the drop test sequence are shown in Figure 87 for the closure bolts, Figure 88 for the pallet bolts, Figure 89 for the jacket bolts and Figure 90 for the top shield bolts.

During the simulation of drop 15, some minor contact problems generated excessive deformation in the jacket bolts after which they were converted to a rigid material for subsequent analyses. The contact problems arose due to a build up of deformation over the previous analyses. It should be noted that in the drop tests the jacket and top shield fixings were changed between drops 10 and 11 but not during the analysis as this may have generated more significant problems with contacts. The subsequent analyses are punch tests and do not challenge the jacket bolts. The results presented for the jacket bolts are taken from the end of drop test 15 with the localised excessive strain removed from the contour plot.

The highest strain increases in the closure bolts occur during drop 9 and drop 15, the 9 m vertical inverted and 9 m horizontal impacts. This is also the case for the pallet bolts because the pallet starts to rebound before the flask thereby placing the studs in to tension. In all cases the strains predicted in the closure bolts are localised surface strains and no permanent elongation of the closure bolts is predicted.

The highest strain increase in the jacket bolts occurs during drop 14 and 15, a 1 m punch on to the jacket side and the 9 m horizontal impact. The 9 m horizontal impact and drop 2, the 1.2 m horizontal impact, generate the highest strain increase in the top shield bolts.

4.18.3 Containment boundary and associated welds

Figure 91 shows the predicted final cumulative strains in the inner wall containment boundary. The highest strains, up to 32%, are predicted around the drain tube to inner wall weld. The top of the inner wall, where it is welded to the lid bolt flange area, is subjected to cumulative plastic strains up to 2.3%. Plastic strains are below 0.7% at the connection where the diameter of the inner wall decreases.

Figure 92 shows the predicted final cumulative strains in the closure. The maximum plastic strain of 1.1% occurs in the base of the closure and is compressive due to the contents striking the underside of the closure. The predicted strain in the area of the weld between the top plate of the closure and sides of the closure is 0.2% and in the base weld the strain is under 0.2%.

4.18.4 Comparison of displacement, velocity and acceleration traces

The displacement, velocity and acceleration plots generated from the high speed films are compared with the rigid body motion of components from the finite element models.

Figure 93, Figure 94 and Figure 95 are for drop 6, Figure 96, Figure 97 and Figure 98 are for drop 9, Figure 99, Figure 100 and Figure 101 are for drop 12 and Figure 102, Figure 103 and Figure 104 are for drop 15.

In general, there is good agreement in the displacement plots and the velocity plots. The number of data points collected from the high speed film limits the available data and cannot accurately capture the peak accelerations. However, it is noted that the general trend in most of the acceleration plots is similar and the accelerations are of a similar order.

5.0 DISCUSSION OF BENCHMARKING ANALYSES

In general, the agreement between the "blind" benchmarking finite element analyses and the observed data is good. There are two key points that cause the differences

- The mesh density in areas of high deformation, such as the cones and the pallet
- The failure of material due to tearing.

In both cases these have been addressed. New material data and a new material model are available and will be utilised in both the orientation and the detailed analyses. The mesh density was selected and considered to be sufficient at the start of the analysis. Ideally, a number of 9 m drops would have been completed to assess the deformation patterns, the mesh would then be refined and the analyses re-run. With the requirement to assess the cumulative damage this was not possible.

The energy plots for the analyses are shown in Figure 105 to Figure 120.

In all cases, the hourglassing energy is zero, as would be expected with higher order elements. The sliding interface energy for drops 5, 7 and 9 show some variation from zero but there are no sudden jumps in the energy plots for any of the analyses. The kinetic energy for drops 5, 7, 14 and 16 remains relatively high after the initial impact as the flask rotates off the punch. In all other cases the kinetic energy is close to zero and the rebound energy is minimal.

6.0 IMPROVEMENTS TO THE BENCHMARKING FINITE ELEMENT MODEL

In order to obtain improved agreement, a number of aspects have been addressed in the benchmarking finite element model. These are the deformation mode of the cones in the 9 m lid impact, the representation of the welds in the pallet in the base impact, the tearing of the jacket in the punch test and the failure of the top shield quadrant in the side impact.

Figure 121 shows a number of different representations of the cones. The original mesh is shown in the bottom right corner and the mesh is refined towards the top of the image. The three on the right have a square corner and the three on the left have curved corners. It is clear from Figure 122 that as the mesh is refined the deformation becomes smoother and a better agreement with the deformation observed in the drop tests is obtained. The overall energy absorbed in the deformation modes is not significantly different for the six cases shown but a refined mesh with weld representation should be used in subsequent analyses.

The weld detail on the drop test model of the uprights to the horizontal plates in the pallets was as indicated on the drawings. A study of the actual welds has allowed a more representative finite element model to be utilised. A refined mesh has also been introduced to capture the plastic hinge details in the uprights. The refined model is shown in Figure 123. Figure 124 shows the deformed shape indicating greater collapse of the uprights, as observed in the drop tests. The main reason for the original differences is the representation of the welds, which did not perform as the design intent, but showed significant failure where smaller welds were used in the drop test model than specified on the drawings. Greater detail to weld specification and inspection can be supported by utilising a range of analyses with differing weld sizes and strengths.

Figure 125 shows a significantly refined mesh in the area of the punch. The original coarse mesh, and material model utilised, captured the deformation but could not predict the failure of the material. An improved material model, which can predict the failure of material combined with the refined mesh, provides the results shown in Figure 126 and Figure 127. These both clearly show a hole in the outer and inner jacket walls. The predicted hole is not identical to that observed, as failure can only occur where the mesh allows and some lateral failure occurs. A more refined mesh would again add greater detail but will result in longer analysis times. A localised refined mesh should be used for punch analyses.

The deformation of the quadrant, which strikes the target in drop 15, the flat side impact, shows gross failure of a number of welds. This failure has not been captured in the finite element analyses; however a study of the photographs from the previous impacts and a review of the video footage indicated that some significant deformation occurred to this area before drop 15. Figure 9 in RTR 246, reproduced here as Figure 128, clearly shows some secondary impact damage to the edge of the quadrant after drop test 12.

A number of analyses have been completed for the 9 m flat side impact. Figure 129 and Figure 130 show the results from two analyses. It is apparent that the detail of the internal welding of the top shield components is key in predicting the deformation mode. The position of the stitch welds should be defined or continuous welding used in preference. However, continuous weld will cause the quadrant to stiffen further and therefore more likely to rotate as a rigid item. The central ribs, immediately above the lid, may add stiffness to the central section and resist some of the rigid body motion but this remains to be determined. An analysis with all internal quadrant ribs removed, but assuming no failure, showed a rigid rotation of the quadrant for the flat side impact. It is the opinion of the author that the suppression of this rigid body motion is key to the design of the top shield shock absorber and that the rotation is highly dependant upon weld failure.

7.0 CONCLUSIONS OF BENCHMARKING ANALYSES

In general, the agreement between the benchmarking finite element analyses and the observed data is excellent. Improvements will be made to the finite element model to obtain better agreement in some areas. A refined mesh will be utilised in areas of high deformation where significant material folding occurs. Material failure will be included in areas subjected to the punch tests and to represent some of the welded features where gross deformation is expected.

In general, the drop test flask performed as expected. Improvements will be made to the design to obtain lower accelerations and to ensure that the drain tube weld does not fail.

It is clear from the analyses that no single drop caused the failure of the drain tube weld and that the cumulative damage eventually caused the failure. A redesign of this area will ensure that the movement of the lead within the flask does not cause movement of the drain tube. It should be noted that the strains in the weld between the drain tube weld and the central cavity are also high.

The uprights in the pallet, if fully welded to each other, will perform as required. The addition of the strengthening uprights was negated by the weld connecting them to the pallet, which just acted as a hinge. A fully welded box section of the same dimensions could provide the necessary protection required in a more controllable manner.

The top shield performs reasonably well but some redesign is required to provide additional punch protection and energy absorption in lid and side impacts. At present the top shield quadrants do not collapse as required and the finite element analyses indicate that, based on no previous damage in the shield quadrants, they will hinge as a rigid body rather than crush as desired.

The jacket is subjected to punch tests which are shown to result in some tearing of the jacket walls. This tearing has not be explicitly captured in the analyses but to ensure it can be avoided some redesign is required to include local additional punch protection.

8.0 DESCRIPTION OF ORIENTATION FINITE ELEMENT MODEL

The orientation finite element model has been constructed in Patran (Ref. 3) using the drawings from Table 1 and Table 2. The drawings had not been finalised at the time the analysis was completed and some items were based on the original design. These include the top shield cones and minor modifications to the jacket. The details of the drain tube are not included in the orientation model.

The finite element model and mesh discretisation are shown in

Figure 131. The model is simplified compared to the benchmarking model.

8.1 Modelling assumptions

The main components which deform during impact, the pallet, the top shield and the jacket, are constructed using thin shell elements. A large portion of the flask, the majority of the lead and some of the flask walls, are treated as rigid as they were not observed to deform significantly during the impact. No preloads are applied in any components as the results from these analyses are for comparison with each other.

8.1.1 Gravity

Gravity has been applied for all analyses using the *LOAD_BODY definition cards in LS-DYNA (Ref. 4). A constant value of 9.81 m/s^2 is applied for the duration of the impact.

8.1.2 Initial velocity

The initial velocity is based on the required drop height of 9 m giving a velocity of 13.288 m/s for all the analyses.

8.1.3 Contact definitions

Detailed items, such as the pallet studs, the closure studs and the shoulder bolts are replaced with TIED_SURFACE_TO_SURFACE interfaces and the forces are monitored at these locations for comparison. The pallet feet are also tied to the top of the pallet using a TIED_SURFACE_TO_SURFACE contact definition. All remaining contacts are defined using the AUTOMATIC_SINGLE_SURFACE contact definition. Contact friction is set to zero for all sliding contacts to provide maximum relative movement between components.

8.1.4 Rigidwall definitions

The impact target is represented by a RIGIDWALL_PLANAR definition with zero friction. The force on the rigidwall is monitored during the analysis.

8.1.5 Material definition

A material model based on the PIECEWISE_LINEAR_PLASTICITY model has been used for the analysis. This provides a more detailed failure model, where the stress state is evaluated in determining the material failure. The material will fail based on the effective plastic strain only if it is also in a predominantly tensile stress state. This means that a purely compressive strain will not cause element erosion and provides an improved failure criteria compared to the default PIECEWISE_LINEAR_PLASTICITY model. The material data summarised in Table 4, from Ref. 5, have been used for these analyses. A detailed discussion of the material model used is given in Section 8.3.

8.1.6 Boundary conditions

A full 3-D model with no symmetry planes has been created. There are no boundary conditions required.

8.1.7 Summary of masses

The following masses are taken from the LS-DYNA finite element model.. The masses in brackets are taken from the Inspection Report (Ref. 6)

- Flask body 3670.8kg (3416kg)
- Contents 25.3kg (17.92kg)
- Closure including lead 162.4kg (158kg)
- Jacket 308.8kg (322kg)
- Top shield 200.4kg (196kg)
- Pallet 238.3kg (262kg)
- Bolts, nuts, dowels, etc 13.3kg
- Total mass of finite element model 4619.2kg (4374kg)

It should be noted that the items used to calculate the masses of the FE model and the Inspection report may not correspond directly.

8.2 Orientations for analysis

A total of 325 analyses were completed for different orientations of the flask. The flask was rotated both around the vertical plane for angles of 0° to 45° and around the horizontal plane for angles of 0° to 180° which covers every possible impact orientation based on general symmetry of the flask. All the analyses were run until the initial impact had completed. In some cases the secondary impact was also included but where the impact angle is large the flask can take up to a second to

rotate to the secondary impact and these have not been included. The resulting secondary impact in these cases is normally less damaging than the initial impact.

8.3 Material modelling discussion

Material test data has been provided for the components used in the drop tests and for the production flasks. This test data usually consists of yield stress data and a failure at elongation. This limited data is obtained from a series of standard tensile tests. As steel is a ductile material the value of elongation failure is much lower that the true strain at failure due to the necking of the material. If the elongation failure strain were to be used in LS-DYNA the component would fail at considerably lower loads than in reality.

A more realistic approach is to calculate the true strain versus true stress curve and use this in the analysis. The true stress and true strain values are calculated based on information in Ref. 8. This document provides a method which can utilise the reduction in cross sectional area at failure (R_A) and the elongation at failure (ε) to generate a true stress-true strain curve.

$$\text{True strain } \epsilon = \ln(1+\varepsilon)$$

$$\text{True stress } \sigma_\epsilon = \sigma(1+\varepsilon)$$

This curve then provides the input to the LS-DYNA PIECEWISE-LINEAR material option.

In LS-DYNA there are a number of criteria that can be used to simulate material failure. The usual method is to compare the effective plastic strain (εffp) with the true strain failure calculated from the material data provided. When a material is in a tensile load this is acceptable and provides excellent agreement with tests, however in compression the analysis will mark finite elements as failed far too early as the failure criteria is based on tensile failure.

In pure compression material will not fail. It will only fail once a shear load exists, i.e. the principal stress become tensile. In LS-DYNA the combination of the current effective plastic strain and a requirement for a tensile load is the criteria for marking a finite element as failed. As such only if the principal stress is tensile and the current calculated effective plastic strain exceeds the true failure strain then mark the element as failed.

9.0 RESULTS OF ORIENTATION ANALYSIS

The results from the orientation analyses are presented in the form of force and acceleration comparisons. The values given are indicative of those that would occur and should not be taken as accurate predictions. This approach provides a series of analyses that can be compared with each other to indicate which orientations are the worst for a given criteria. The angle of rotation is indicted by the two numbers that give the horizontal rotation and the vertical rotation, for instance a side impact on to the flat edge of the pallet would be 090x000, a side impact on to the corner of the pallet would be 090x045 and an inverted impact on to the lid would be 180x000.

Figure 132 indicates that the peak axial force on the pallet connection occurs at angles of rotation about the horizontal of between 100° and 120° for all vertical rotations. The maximum occurs for a horizontal angle of 115° when the flask lands on the flat side of the pallet (115x000).

Figure 133 indicates that the peak shear force on the pallet connection occurs at angles of horizontal rotation of between 20° and 45° with the force increasing with vertical rotation. The maximum occurs for a horizontal angle of 35° when the flask lands on the corner of the pallet (035x045).

Figure 134 indicates that the peak shear force on the closure connection occurs at angles of horizontal rotation of between 90° and 95° with the maximum occurring for a side impact on to the corner of the pallet (090x045).

Figure 135 indicates that the peak force on the top shield connection occurs for a side impact when the flask lands on the corner of the pallet (090x045).

Figure 136 indicates that the peak force acting on the target occurs for a side impact when the flask lands on the corner of the pallet. Forces are also high for horizontal rotations of between 35° and 45° (090x045 and 035x045).

Figure 137 indicates that the peak accelerations occur for angles of rotation of between 20° and 45° with secondary maximums at 90° for some vertical rotations.

In addition to the above, the deformed shape of every analysis has been compared visually. In general the deformation is as expected. However for a number of orientations the top shield base plate is seen to deform and move away from the top surface of the flask and presents a gap close to the seal face. The largest observed gap occurs for an impact of 35° rotated by 45° (035x045).

10.0 CONCLUSIONS FROM ORIENTATION ANALYSIS

The series of orientation analyses indicate a number of worst case orientations to be considered for subsequent detailed finite element analysis.

10.1 Off horizontal – 115° by 000°

This orientation gives the highest axial loads on the pallet connections.

10.2 Horizontal – 090° by 045°

This orientation gives the highest shear loads on the closure connections, the highest loads on the top shield connections and the highest force on the target. It also provides the largest observed gap between the top shield base plate and the top of the flask.

10.3 Inclined base – 035° by 045°

This orientation gives the highest shear load on the pallet connections and the highest acceleration.

10.4 Vertical upright (drop 6) – 000° by 000°

This orientation provides the best direct comparison with the drop tests for the changes made to the pallet. It should be noted that the analysis will not address the normal handling impacts or any punch tests before the 9 m impact.

10.5 Vertical inverted (drop 9) – 180° by 000°

This orientation provides the best direct comparison with the drop tests for the changes made to the top shield. It should be noted that the analysis will not address the normal handling impacts or any punch tests before the 9 m impact.

10.6 Angled inverted (drop 12) – 163° by 000°

This orientation provides the worst deformation for subsequent punch analysis on to the vent point and the best direct comparison with the drop tests for the changes made to the top shield. It should be noted that the analysis will not address the normal handling impacts or any punch tests before the 9 m impact.

10.7 Horizontal (drop 15) – 090° by 000°

This orientation provides the worst impact orientation for the drain tube based on the observed failure from the benchmarking analysis.

10.8 Punch into opening between top shield and flask

This analysis follows drop 15 (subsection 10.7 above) and targets the gap produced between the top shield and the flask. The angle of impact is approximately 63° from vertical.

10.9 Punch on to drain plug area

This analysis follows drop 15 (subsection 10.7 above) and targets the drain plug. The angle of impact is 35° from vertical.

10.10 Punch on to vent plug area

This analysis follows drop 12 (subsection 10.6 above) and targets the vent plug. The angle of impact is 163° from vertical.

11.0 DESCRIPTION OF DETAILED FINITE ELEMENT MODEL

The detailed finite element model has been constructed in Patran (Ref. 3) using the drawings from Table 2. Figure 138 and Figure 139 show the detailed finite element model and a section though the model.

The details of the pallet are shown in Figure 140. It can be seen that the mesh of the pallet bolting plates and that of the top plate of the pallet are non-continuous. The weld that connects the top plate of the bolting plate is represented by solid elements, which are tied to the top surface of the pallet top plate. The internal structure of the pallet can be seen in Figure 141. It can be seen that the majority of the fillet weld detail is modelled explicitly. Full penetration welds are not modelled explicitly.

The pallet connection bolts and dowels are shown in Figure 142. The threads of the bolts and dowels are tied to the pallet bolting plate where necessary and the minimum thread diameter has been modelled for all threaded areas.

Figure 143 shows the top shield, with details of the internal structure shown in Figure 144. The majority of the fillet welds are modelled explicitly. The mesh is sufficiently refined to capture the gross deformation from impacts onto the top shield.

Figure 145 shows the shoulder bolts that connect the top shield and the jacket to the flask fins. The top of the jacket can also be seen in this figure. A section through the jacket base in Figure 146 shows the internal drain vent protection plate and the details of the welds in the jacket. The edges of the protection plate are tied to the jacket inner wall. The fillet weld is not modelled explicitly.

Figure 147 shows the detail of the cooling fins including the radius edges and the fillet welds along the length of the fins. The radius is modelled to give a more accurate representation of the deformation for the punch tests and where the jacket becomes deformed in side impacts.

The closure and associated studs are shown in Figure 148. The vent point has not been modelled as the benchmarking and subsequent analyses indicated that the punch to this area would not reach the vent plug. The studs are tied to the flask along the threaded section.

Figure 149 shows a section through the flask body showing the internal ribs, the inner wall, the voids at the top and base and the lead fill. In Figure 150, the gap formed between the lead and the outer wall can be seen. This gap is typically 1.25 mm and is introduced via the thermal contraction analysis, as described in Section 3.0.

Figure 151 and Figure 152 show details of the drain tube and outer tube. The weld details of both the drain tube and the outer tube are included.

The model consists entirely of 8-noded high order solid elements. The flat target has been represented by a rigidwall and the punch has been explicitly modelled using 8-noded solid elements.

11.1 Material properties

The material properties have been derived from material data provided by REVISS (Ref. 5) and based on British Standards data. A modified version of the PIECEWISE_LINEAR_PLASTICITY model has been used for all materials. The material data used is given in Table 4. The material model used allows elements to be removed from the analysis provided both the effective plastic strain has exceeded a given value, based on engineering elongation failure strain and reduction in area at failure, and the stress in the element is predominantly tensile. This ensures that elements do not fail under pure compression but will fail once a significant shear stress or pure tensile stress exists and the true strain failure value has been exceeded. The contacts are represented by a cylinder with steel properties and modified density. This provides pessimistic results as it will apply greater loads to the containment boundary during the impact.

In all cases the material properties used are based on the minimum specification values from the data provided by REVISS or from British Standards.

11.2 Modelling assumptions

11.2.1 Gravity

Gravity has been applied for all analyses using the *LOAD_BODY definition cards in LS-DYNA (Ref. 4). A constant value of 9.81 m/s^2 is applied for the duration of the impact.

11.2.2 Initial velocity

The initial velocity is based on the drop height. The 9 m impacts are given an initial velocity of 13.288 m/s and the 1 m punch tests are given an initial velocity of 4.429 m/s. The density of the flask lead was increased to ensure that the total mass of the flask was 4600 kg and therefore no enhancement of the initial velocity is required.

11.2.3 Contact definitions

In general, the AUTOMATIC_SINGLE_SURFACE contact definition has been used. In addition, a number of TIED_SURFACE_TO_SURFACE and one TIED_NODES_TO_SURFACE definitions have been used where the mesh is not continuous, e.g. the pallet feet to the pallet top plate. In all cases the mesh size on both surfaces is similar which results in a 1 to 1 relationship for the tied contact surfaces. Contact friction for all cases is set to 0.2 but no initial pre-stress has been applied to the bolted connections. Indications from the previous analyses are that strains in the closure studs will be negligible. A preload in the pallet studs would

reduce the relative movement of the flask feet and the pallet feet and therefore a pessimistic approach is to not include preload.

11.2.4 Target definitions

The impact target is represented by a RIGIDWALL_PLANAR definition. This provides an infinitely large, smooth impact surface. Contact friction is set to 0.2 in all cases. Sensitivity of the impact surface contact friction value is minimal and the only differences observed have been for a limited number of orientations which do not form part of the worst case selection.

11.2.5 Element formulation

The default element type in LS-DYNA (Ref. 4) is a single integration point solid element. This can prove unstable and result in hourglass modes being formed. To avoid hourglass modes the type 2, fully integrated selective reduced (S/R) solid element is used.

11.2.6 Boundary conditions

A full 3-D model with no symmetry planes has been created. There are no boundary conditions required.

11.2.7 Summary of masses

The following masses are taken from the LS-DYNA finite element model. The masses in brackets are taken from the Inspection Report (Ref. 6)

• Flask body	3670.8kg	(3416kg)
• Contents	25.3kg	(17.92kg)
• Closure including lead	162.4kg	(158kg)
• Jacket	308.8kg	(322kg)
• Top shield	200.4kg	(196kg)
• Pallet	238.3kg	(262kg)
• Bolts, nuts, dowels, etc	13.3kg	
• Total mass of finite element model	4619.2kg	(4374kg)

It should be noted that the items used to calculate the masses of the FE model and the Inspection report may not correspond directly.

12.0 RESULTS OF DETAILED IMPACT ANALYSES

The results are presented in the form of deformation, effective plastic strain, histories of energy and histories of acceleration. The main focus of the results are the connections and the drain tube. The results are summarised in Table 6. The results are discussed in Section 13.0.

12.1 Off horizontal – 115° by 000°

The orientation before impact is shown in Figure 153. The deformation at the end of the impact is shown in Figure 154. The impact face of the flask is shown in Figure 155.

Figure 156 shows a close up of the deformation of the pallet. It can be seen that the upper plate and lower plate have deformed downwards and that some minor failure of the top plate is predicted at the edges. Where the pallet top plate contacts the internal supports of the pallet, some failure is predicted. However, between the supports the pallet top plate bends smoothly and effective plastic strains are below 20%.

Figure 157 shows the deformation of the top shield. Only one quadrant is deformed and it can be seen that it is compressed downwards. A view of the underside of this quadrant is shown in Figure 158, which shows the buckling of the plates and some failure of the welds.

Figure 159 shows the predicted effective plastic strains in the pallet studs and weld. A maximum effective plastic strain of 2.6% is predicted in the weld and locally in the shank of some of the studs. The maximum predicted effective plastic strain in the pallet dowels of 14.2% is shown in Figure 160.

Figure 161 shows the predicted effective plastic strains in the shoulder bolts. The maximum of 1.3% occurs in only one of the bolts.

Figure 162 shows the predicted effective plastic strains in the flask wall. The maximum of 13.9% occurs locally where the feet are attached.

Figure 163 shows that the closure studs are predicted to remain elastic during the impact.

Figure 164 shows the predicted effective plastic strains in the drain tube system. A maximum of 4.1% is predicted in the outer tube, where it is connected to the drain plug assembly. It can be seen that the maximum, predicted in the drain tube itself, is 0.6%, as shown in Figure 165. This occurs where the drain tube is welded to the well.

Figure 166 shows that the initial kinetic energy is fully converted to internal energy, sliding interface energy and rigidwall (stonewall) energy, with the latter two due to friction. The hourglass energy is zero. The initial impact on to the top shield shows a gradual decrease in kinetic energy until the pallet strikes the target after 0.027

seconds. At this point the pallet deforms and absorbs energy until the flask comes to rest after 0.05 seconds.

Figure 167 shows that the peak acceleration of the flask is predicted to be 61g.

12.2 Horizontal – 090° by 045°

The orientation before impact is shown in Figure 168. The deformation at the end of the impact is shown in Figure 169 and Figure 170.

Figure 171 shows a close up of the deformation of the pallet. It can be seen that the upper and lower plates have buckled and some weld failure in this area is predicted.

Figure 172 shows the deformation of the top shield. Two of the quadrants have deformed with the top plate buckling upwards and the side plates inwards. The flask lifting fin has also struck the target and the top of the jacket has deformed pushing the fin into the corner cavity of the flask. The resulting deformation produces a small gap between the top shield and the flask, as shown in Figure 173.

Figure 174 shows the predicted effective plastic strains in the pallet studs and weld. A maximum effective plastic strain of 20% is predicted along the edge of the weld closest to the point of impact, but strain elsewhere in these components are all below 3%.

Figure 175 shows the predicted effective plastic strains in the shoulder bolts. The maximum of 7% occurs in the bolt that connects the top shield closest to the point of impact. The plastic strains in the other bolts connecting the top shield are below 1%.

Figure 176 shows the predicted effective plastic strains in the pallet dowels. A maximum of 9% occurs in the threaded part of the dowel.

Figure 177 shows the predicted effective plastic strain in the flask wall. A maximum plastic strain of 33% is predicted where the main lifting fin is pushed into the corner cavity. It should be noted that this is not part of the containment boundary.

Figure 178 shows the predicted effective plastic strain in the closure studs. A maximum plastic strain of below 0.1% is predicted in two of the studs.

Figure 179 shows the predicted effective plastic strain in the drain tube system. A maximum plastic strain of 5.2% is predicted in the outer tube, where it is connected to the drain plug assembly. It can be seen that the maximum predicted in the drain tube itself is 0.15%, as shown in Figure 180.

Figure 181 shows that the initial kinetic energy is fully converted to internal energy, sliding interface energy and rigidwall (stonewall) energy, with the latter two due to friction. The hourglass energy is zero. The initial impact involving the pallet shows a slow decrease in kinetic energy until the top shield strikes the target after 0.025

seconds. At this point the top shield deforms and absorbs energy until the flask comes to a rest after 0.044 seconds.

Figure 182 shows that the peak acceleration of the flask is predicted to be 95g.

12.3 Inclined base – 035° by 045°

The orientation before impact is shown in Figure 183. The deformation at the end of the impact is shown in Figure 184 and Figure 185.

Figure 186 shows the deformation of the pallet. It can be seen that the leading edges of the pallet have both deformed upwards with complex deformation modes in the deformed corner. Some local weld failure is predicted.

Figure 187 shows the predicted effective plastic strains in the pallet studs and weld. A plastic strain of 50% is predicted in the leading edge of the weld which is predominately compressive. The maximum predicted in the pallet studs is 4% in the three studs closest to the point of impact.

Figure 188 shows the effective plastic strain in the pallet dowels. A maximum plastic strain of 16% occurs in the threaded region of the dowel closest to the impact.

Figure 189 shows the predicted effective plastic strain in the shoulder bolts. A maximum of 5% is predicted in the four jacket connections with minimal strains predicted in the top shield connections.

Figure 190 shows the predicted effective plastic strain in the flask wall. The maximum of 45% occurs locally where the foot is pushed upwards in to the corner cavity and is predominately compressive. It should be noted that this is not part of the containment boundary.

Figure 191 shows that the closure studs are predicted to remain elastic during the impact.

Figure 192 shows the predicted effective plastic strains in the drain tube system. A maximum of 1.5% is predicted in the outer tube, where it is connected to the drain plug assembly. It can be seen that the maximum predicted in the drain tube itself is less than 0.02%, as shown in Figure 193.

Figure 194 shows that the initial kinetic energy is fully converted to internal energy, sliding interface energy and rigidwall (stonewall) energy with the latter two due to friction. The hourglass energy is zero. The loss of energy is reasonably smooth and increases in rate as more components start to deform. The flask comes to rest after 0.043 seconds.

Figure 195 shows the predicted peak acceleration of the flask to be 82g.

12.4 Vertical upright (drop 6) – 000° by 000°

The orientation before impact is shown in Figure 196. The deformation at the end of the impact is shown in Figure 197 and Figure 198.

Figure 199 shows a close up of the pallet and a section through the pallet. It can be seen that the internal sections have deformed in a complex mode due to the end plates and that some failure is predicted where the internal sections are deformed over the welds but continue to absorb energy as they are crushed further.

Figure 200 shows the predicted effective plastic strains in the pallet studs and weld. A maximum effective plastic strain of 46% occurs locally in the welds and is compressive in nature where the pallet top plate bends upwards and inwards. The maximum predicted effective plastic strain in the pallet studs is less than 1%.

Figure 201 shows that the maximum predicted effective plastic strain in the pallet dowels is 3% and occurs in the threaded area. This is due to the small rotation of the feet as the pallet top plate bends.

Figure 202 shows the predicted effective plastic strain in the flask wall. The maximum of 17% occurs locally where the feet are welded to the wall.

Figure 203 shows that the closure bolts are predicted to remain elastic during the impact.

Figure 204 shows the predicted effective plastic strain in the drain tube system. A maximum of 1.1% is predicted in the outer tube, where it is connected to the drain plug assembly. It can be seen that the maximum in the drain tube itself is less than 1%, as shown in Figure 205.

Figure 206 shows that the initial kinetic energy is fully converted to internal energy, sliding interface energy and rigidwall (stonewall) energy with the latter two due to friction. The hourglass energy is zero. The rate of energy transfer is smooth and the flask comes to rest after 0.017 seconds.

Figure 207 shows the acceleration of the flask. The peak acceleration is predicted to be 1110g and occurs as the flask initially strikes the target in a perfectly flat orientation. This acceleration only lasts for 70 microseconds. This is the only orientation that is likely to generate such a high acceleration. A secondary peak acceleration of 120g occurs near the end of the impact.

12.5 Vertical inverted (drop 9) – 180° by 000°

The orientation before impact is shown in Figure 208. The deformation at the end of the impact is shown in Figure 209.

Figure 210 shows a close up of the deformation of the top shield. It can be seen that the cones have compressed and that some tearing of the cones is predicted. This is minimal deformation observed elsewhere.

Figure 211 shows the predicted effective plastic strains in the pallet studs and weld. A maximum effective plastic strain of 2.2% is predicted in the weld with localised surface strains in the studs all less than 1%. The studs are placed in tension as the pallet starts to rebound before the flask.

Figure 212 shows the predicted effective plastic strains in the pallet dowels. A maximum plastic strain of less than 1% is predicted in the threaded area of the dowel. This strain is a localised surface strain due to the flexibility of the pallet plates generating small rotations in the feet during the impact.

Figure 213 shows the predicted effective plastic strains in the shoulder bolts. The maximum of 1.4% occurs in two of the jacket connectors with all other shoulder bolts less than 1%, due to the asymmetry of the flask and the complex deformation modes of the top shield.

Figure 214 shows the predicted effective plastic strains in the flask wall. There are minor plastic strain predicted where the top shield bears against the top of the flask. The maximum of 0.8% occurs internally where the lead bears against the hoop restraint rings.

Figure 215 shows the maximum predicted effective plastic strain in the closure bolts to be less than 0.07%.

Figure 216 shows the predicted effective plastic strain in the drain tube system. A maximum of 2.8% is predicted in the outer tube, where it is connected to the drain plug assembly. It can be seen that the maximum in the drain tube itself is less than 0.9%, as shown in Figure 217

Figure 218 shows that the initial kinetic energy is fully converted to internal energy, sliding interface energy and rigidwall (stonewall) energy with the latter two due to friction. The hourglass energy is zero. The rate of energy transfer is smooth and the flask comes to rest after 0.023 seconds.

Figure 219 shows that the peak acceleration of the flask is predicted to be 85g.

12.6 Angled inverted (drop 12) – 163° by 000°

The orientation before impact is shown in Figure 220. The deformation at the end of the impact is shown in Figure 221.

Figure 222 shows a close up of the top shield. It can be seen that all four cones have deformed with some tearing predicted in the three cones closest to the point of impact. Figure 223 shows that some tearing of the plate under the cones closest to the point of impact is predicted but this is limited by the internal ribs in the quadrant. Figure 224 shows that the outer curved plate of the quadrant closest to the point of impact bends out slightly as the angled plate that supports it deforms.

All the pallet components remain elastic.

Figure 225 shows the predicted effective plastic strains in the closure studs to be less than 0.005%.

Figure 226 shows the predicted effective plastic strain in the drain tube system. A maximum of 1.5% is predicted in the outer tube, where it is connected to the drain plug assembly. It can be seen that the maximum in the drain tube itself is less than 0.01%, as shown in Figure 227

Figure 228 shows that the initial kinetic energy is fully converted to internal energy, sliding interface energy and rigidwall (stonewall) energy with the latter two due to friction. The hourglass energy is zero. The rate of energy transfer is smooth and the flask comes to rest after 0.025 seconds.

Figure 229 shows the predicted peak acceleration of the flask to be 105g.

12.7 Horizontal (drop 15) – 090° by 000°

The orientation before impact is shown in Figure 230. The deformation at the end of the impact is shown in Figure 231. The impact face is shown in Figure 232.

Figure 233 shows a close up of the underside of the pallet and Figure 234 shows the final profile of the pallet. It can be seen that the top and base plates of the pallet move upwards together and that there is some general deformation of the plates due to the twisting motion of the flask.

Figure 235 shows a close up of the top shield. It can be seen that, the quadrant that strikes the target is deformed upwards and some weld failure is predicted. The quadrant rotates slightly and generates a gap between the top shield and the top of the flask. This can be seen in Figure 236. The top corner of the flask is also shown to deform as the jacket strikes the target and the fins are pushed in to the flask wall corner cavity.

Figure 237 shows the predicted effective plastic strains in the pallets studs and weld. A maximum effective plastic strain of 8.6% is predicted in two of the studs close to the point of impact and locally in areas of the weld. The predicted effective plastic strain in the other studs is less than 5%.

Figure 238 shows the predicted effective plastic strain in the pallet dowels. The maximum of 19% occurs in the threaded area of the dowels.

Figure 239 shows the predicted effective plastic strains in the shoulder bolts. The maximum plastic strain of 3% occurs in the top shield connections. The predicted plastic strains in the jacket connections are less than 0.7%.

Figure 240 shows the predicted effective plastic strains in the flask wall. The maximum plastic strain of 23% occurs where the fins deform the wall pushing it into the upper corner cavity and where the pallet feet are welded to the wall at the lower corner cavity.

Figure 241 shows that the predicted effective plastic strains in the closure bolts are less than 0.2%.

Figure 242 shows the predicted effective plastic strain in the drain tube system. A maximum of 8% is predicted in the outer tube, where it is connected to the drain plug assembly. It can be seen that the maximum in the drain tube itself is less than 0.2%, as shown in Figure 243.

Figure 244 shows that the initial kinetic energy is fully converted to internal energy, sliding interface energy and rigidwall (stonewall) energy with the latter two due to friction. The hourglass energy is zero. It can be seen that the flask strikes the pallet and rotates until the top shield strikes the target after 0.008 seconds. The rate of energy transfer increases after this time until the flask comes to rest after 0.024 seconds.

Figure 245 shows that the peak acceleration of the flask is predicted to be 90g.

12.8 Punch into opening between top shield and flask

The orientation before impact is shown in Figure 246. The deformation at the end of the impact is shown in Figure 247. The analysis is run until the flask has rebounded from the punch.

Figure 248 shows a close up of the deformation caused by both the initial 9 m impact and the subsequent punch in an attempt to open the existing gap between the top shield and the top of the flask. It can be seen that the punch does not generate much additional deformation compared to the 9 m impact deformation, as shown in Figure 236. The impact face has been pushed further back into the top shield but no additional failure of welds or plate materials is predicted.

Figure 249 shows the predicted effective plastic strain in the shoulder bolts. There has been a slight increase but the maximum strain is less than 3.8%.

Figure 250 shows the predicted effective plastic strain in the drain tube has increased to a maximum of less than 1%.

Figure 251 is a velocity profile plot at the end of the analysis which shows that the flask is now rotating away from the punch.

Figure 252 shows that the initial kinetic energy has not all been converted to internal energy as the flask continues to rotate away from the punch. The initial kinetic energy increase, and corresponding internal energy decrease, is due to stress relaxation, as the stress states were taken from the final state of the previous 9 m impact. The stored stresses in the material are relieved by the material moving and hence returning initial internal energy to kinetic energy. These stored initial stresses, using the *INITIAL_STRESS card, are not included in the internal energy calculation by LS-DYNA (Ref. 4) and therefore appear as negative internal energy when relieved.

12.9 Punch on to drain plug area

The orientation before impact is shown in Figure 253. The deformation at the end of the impact is shown in Figure 254. The analysis is run until the flask has rebound from the punch.

Figure 255 shows a section through the point of impact at the end of the impact. It can be seen that the deformation is limited and does not impinge on the drain plug. The inner surface of the jacket wall is 19mm away from the drain plug at the time of maximum deformation.

Figure 256 shows the deformation of the jacket due to the punch.

Figure 257, Figure 258 and Figure 259 show the predicted effective plastic strains in the jacket outer wall, jacket additional plate and the jacket inner wall respectively. It can be seen that the maximums of 33.2%, 13.7% and 16.5% are not predicted to result in any failure of the material.

Figure 260 shows the effective plastic strain predicted in the fins of the flask. The radius on the leading edge of the fins allows them to deform readily and assist in decreasing the predicted strains in the jacket walls. The maximum strain of 41% occurs on the leading edges of the two fins closest to the point of impact.

Figure 261 shows the predicted effective plastic strain in the drain tube system. A maximum of 10.1% is predicted in the outer tube, where it is connected to the drain plug assembly. It can be seen that the maximum in the drain tube itself is less than 0.4%, as shown in Figure 262.

Figure 263 shows that the initial kinetic energy is fully converted to internal energy, sliding interface energy and rigidwall (stonewall) energy with the latter two due to friction. The hourglass energy is zero. A large amount of energy is converted to sliding interface energy, as both the punch slides on the jacket wall and the fins resist moving outwards. A zero value of friction would allow the punch to slide more readily and also allow the fins to deform more readily, both of which would minimise the amount of deformation predicted by the punch.

12.10 Punch on to vent plug area

The orientation before impact is shown in Figure 264. The analysis is run until the flask has rebounded from the punch.

Figure 265 shows a section though the flask at the point of impact. It can be seen that the upper two horizontal plates of the top shield have deformed along with the cruciform in the upper section. The punch does not challenge the vent plug or any of the closure bolts and two of the four horizontal plates remain undeformed.

Figure 266 shows the deformation of the top shield and the indentation caused by the punch.

Figure 267 shows the predicted effective plastic strain in the upper horizontal plate and the cruciform in the upper section. The maximum plastic strain of 50% occurs on the underside of the upper plate where the edge of the punch strikes.

Figure 268 shows the predicted effective plastic strain in the drain tube system. A maximum of 1.6% is predicted in the outer tube, where it is connected to the drain plug assembly. It can be seen that the maximum in the drain tube itself is 0.01%, as shown in Figure 269

Figure 270 shows that the initial kinetic energy is fully converted to internal energy, sliding interface energy and rigidwall (stonewall) energy with the latter two due to friction. The hourglass energy is zero.

13.0 DISCUSSION OF DETAILED IMPACT ANALYSES

The impact performance of the major components are discussed and compared with the observed impact results. It should be noted that in all cases the predicted effective plastic strains in the containment area are well below both the true failure strain and the engineering elongation failure strain. A failure criterion has been included in the analyses, which removes failed finite elements in the top shield and pallet during the analysis.

The design is such that failure of some welds will not result in significantly different results, as the material cannot be released from the flask and still forms part of the energy absorption characteristics of the flask. This was observed in the drop tests, where failure occurred in the central components of the pallet, but continued to crush after failure.

There is no evidence of failure of any of the tied contact surfaces for any of the impacts. The energy histories indicate that all the analyses completed without any spurious jumps in the energy. A study of the output file reveals no errors or warnings during the analyses.

13.1 Impact performance of the pallet and pallet connections

The pallet has been assessed for a number of impact orientations. The main requirement is to remain attached to provide thermal protection and punch protection from underneath. The punch protection has been proven by test and the pallet design has not changed significantly post test. The main changes made are the inclusion of the formed bends on both sides and changes to channel construction. Both changes work to absorb energy in a more controlled manner. The 9 m impact in an upright position does not allow the pallet to fully crush the channels. Although some failure is predicted in the internal channels, the pallet limits the accelerations passed to the flask.

The pallet is connected to the flask via the studs and the welds. In all cases, the predicted strains in these components are not sufficient to cause failure that would result in the loss of the pallet. Any failure is localised to either one out of four of the welds or to a single stud.

The pallet dowels provide sufficient shear protection to limit the predicted strains in the studs without failing. High strains are predicted in the threaded area of some dowels but failure is not predicted.

13.2 Impact performance of the jacket

In general, the jacket is required for thermal protection and for punch protection. It does provide some energy absorption during 9 m impacts but this is a secondary function. Retention of the jacket is discussed in subsection 13.5. The punch protection of the jacket has been improved by the addition of plates in four locations over the drain plug. The requirement is to ensure that the punch cannot

penetrate the jacket and provide a problem for thermal protection. The punch test at an inclined angle on to the drain plug shows that none of the jacket walls are compromised. It is also worth noting that the locations of the strains in the jacket walls and the additional plate are such that if failure did occur the tearing of the material would not result in a hole being punched as observed in test, but that the inner wall is likely to tear longitudinally where it bears against the internal fins. The predicted strains for this impact are well below the true strain failure of the material of 61%.

13.3 Impact performance of the top shield

The top shield is required to remain attached to the flask, via the shoulder bolts, to provide thermal protection. It is also required to provide protection of the closure bolts and vent point for punch tests. A number of impact orientations result in deformation of the top shield and in some cases there is local failure of welds and some tearing of the plates in the cones. This failure is all within acceptable limits as it does not reduce the thermal performance of the top shield and still provides protection from punch tests.

The angled inverted impact, run 07, and the rotated side impact, run 02, generate a gap between the underside of the top shield and top of the flask. This gap is small, approximately 40 mm decreasing to zero at the seal face for a length of 200 mm, for the angled inverted impact. The gap for the rotated side impact is more complex, with a gap around half the circumference of up to 16 mm close to the seal face, and up to 40 mm at the outer edge in two locations for a length of 40 mm and almost zero elsewhere. These gaps will decrease post impact as the flask relaxes slightly and the top shield settles back on to the flask.

13.4 Impact performance of the closure bolts

The predicted strains in the closure bolts are surface strains for all impacts and in many cases the bolts remain elastic. The maximum seal face gap detected in the analyses is less than 0.4 mm and is transient with gaps returning to zero at the end of the impact. This occurs between the bolts and is due to flexure of the closure between the bolts and not due to elongation of the bolts.

The maximum predicted strains will not result in failure of, or permanent elongation of, the closure bolts and containment will not be lost due to failure of closure bolts.

13.5 Impact performance of the shoulder bolts

The shoulder bolts ensure that the jacket and the top shield remain in position. In all cases, the predicted strains in the shoulder bolts are well below the true strain failure value of 72.7%. Localised strains are predicted but the shoulder bolts will not fail during impact.

13.6 Impact performance of the flask body

The flask walls are predicted to deform and have high strains, however the components that undergo large deformation do not form part of the containment function and are remote from the containment area. Two main areas of the flask outer wall deform for a number of orientations. These are the outer corners of the walls, where the fins and the pallet feet are attached. Although some local failure of the material is observed in these locations, it is only on the surface and no through wall failure is predicted.

The inner walls, which form part of the containment system, do not undergo any plastic deformation and the containment system is not challenged due to deformation of the inner walls.

The external cooling fins act as shock absorbers for some side impacts. Any deformation to the fins is minimal and failure of the fins will not occur during impact.

13.7 Impact performance of the drain tube assembly and containment boundary

The drain tube assembly has been redesigned and improved by the addition of the outer guard tube. Although strains are predicted in both the outer and inner tubes, the inner drain tube is the containment boundary. The maximum strains predicted in the drain tube and associated items are below the failure strain of the material and significantly reduced from those predicted in the original design.

The inner drain tube vibrates with an amplitude of approximately 1 mm and does not strike the outer tube at any point during the impacts.

Loss of containment due to failure of the drain tube or associated items will not occur.

The containment boundary, which includes the drain plug, vent plug, drain tube, closure bolts, closure and flask inner wall, is subjected to minor surface strains due to contact. The majority of the containment boundary remains elastic for all the impacts considered.

Loss of containment due to failure of the containment boundary will not occur.

13.8 Impact performance general discussion

There is no gross failure of any components and deformation is limited to the pallet, jacket, top shield and associated items. The body of the flask, and especially the containment boundary, remain undeformed.

The movement of the lead in both the closure and the flask is limited and no lead slump is observed.

The shielding performance will not be affected due to regulatory impacts.

14.0 IMPACT PERFORMANCE OF THE R7021 TRANSPORT FLASK

The top shield and pallet act to protect the flask from gross deformation. They also act to reduce accelerations of the contents and flask as a whole and will be retained following regulatory impact tests.

The modifications made to the flask since drop testing are minor but all improve the impact performance of the flask.

The containment area remains predominately elastic, with localised plastic deformation due to surface contact or minor movement of the lead. The maximum predicted effective plastic strain in the drain tube is 1.0% demonstrating that containment will not be lost.

The shielding performance will not be affected due to regulatory impacts.

The analysis predicts that the flask can survive both a regulatory 9 m drop on to a rigid target and a regulatory 1m punch test in any orientation with no loss of containment.

15.0 REFERENCES

Ref. 1 Regulations for the Safe Transport of Radioactive Material, 2005 edition, TS-R-1, IAEA Safety Standards

Ref. 2 Test Plan for the R7021 Transport Container, REVISS Services Transport Container, RTM 118 Issue 2, 14/10/2008

Ref. 3 MSC Patran, Version 2008_r1 running under Redhat Linux 4

Ref. 4 LS-DYNA version 971, R3.2.1, Livermore Software Technology Corporation

Ref. 5 Material data received from REVISS. Drop Test Material certs, Email from P Robbins, 7th April 2009. Caparo Report, L91805 Issue 01, Email from P Robbins, 7th April 2009. Material data received from P Robbins, 2nd April 2009. Test report, RSL06797, Sheffield Testing Laboratories

Ref. 6 Drop test results reports from REVISS, Numbers, IR 0672, IR 0673, IR 0674, IR 0675, RTR 233, RTR 234, RTR 235, RTR 236, RTR 239, RTR 240, RTR 241, RTR 242, RTR 243, RTR 244, RTR 245, RTR 246, RTR 247, RTR 248, RTR 249, RTR 250 and RTR 251. Received 6th July 2009

Ref. 7 REVISS Project Meeting Minutes, GB/3981, 22nd May 2009

Ref. 8 Uniaxial True Stress-Strain after Necking, Yun Ling, AMP Journal of Technology Vol. 5 June, 1996

TABLES

Table 1: Drawings used for benchmarking and orientation model creation

Title	Drawing Number	Issue	Mod No.	Date
Assembly of capsule R2089	GA20890	F	DB267	22/06/06
Sub-assembly of capsule R2089	SA20890	D	DB072	01/02/00
Plug type 'B' for capsule R2089	D020892	B	DB072	15/12/99
Plug type 'A' for capsule R2089	D020893	B	DB072	15/12/99
Body for capsule R2089	D020894	B	DB072	15/12/99
Spacer for capsule R2089	D020895	A	DB072	01/02/00
R7021 container assembly	R7021/001	B	DB 262/2	22/10/08
Body (Sheets 1 to 6 of 6)	R7021/002	B	DB 262/2	22/10/08
Closure (Sheets 1 to 2 of 2)	R7021/003	B	DB 262/2	22/10/08
Pallet	R7021/004	B	DB 262/2	22/10/08
Top shield (Sheets 1 to 4 of 4)	R7021/005	B	DB 262/2	22/10/08
Jacket (sheets 1 to 2 of 2)	R7021/006	A	DB 262/1	18/01/08
Grill	R7021/007	A	DB 262/1	18/01/08
Drain plug	R7021/008	A	DB 262/1	18/01/08
Vent plug	R7021/009	A	DB 262/1	18/01/08
M20 locking pin	R7021/010	A	DB 262/1	18/01/08
M20 stud	R7021/011	A	DB 262/1	18/01/08
M24 stud	R7021/012	A	DB 262/1	18/01/08
M24 dowel	R7021/013	A	DB 262/1	18/01/08
M16 shoulder bolt	R7021/016	B	DB 262/2	21/10/08
Drain filter (Sheet 1 of 3)	R7021/017	A	DB 262/2	22/10/08
Filter body (Sheet 2 of 3)	R7021/017	A	DB 262/2	22/10/08
Mesh, washer and backing ring (Sheet 3 of 3)	R7021/017	A	DB 262/2	22/10/08
Spring gasket	R7021/018	A	DB 262/2	22/10/08
Assembly R8062 basket: 48 R2089 in R7008 (3750A)	R8062/001	B	DB 158	30/04/01
Base	R8062/002	B	DB 158	30/04/01
Handle	R8062/003	B	DB 158	30/04/01
Tie rod	P/8062/004	A	DB 087	02/12/99
Spacer disk	R8062/005	B	DB 158	30/04/01
Drop test target	R8085/001	B	DB 211/3	19/10/05
Target surface plate	R8085/002	B	DB 211/3	19/10/05
Punch for IAEA drop II test	R8099/002	A	DB 262	11/09/08

Table 2: Drawings used for orientation and detailed model creation

Title	Drawing Number	Issue	Mod No.	Date
R7021 Container assembly (Sheet 1 of 2)	R7021/001	C	DB 262/3	12/11/09
R7021 Container assembly (Sheet 2 of 2)	R7021/001	C	DB 262/4	12/11/09
Body (Sheet 1 of 6)	R7021/002	C	DB 262/4	09/11/09
Body (Sheet 2 of 6)	R7021/002	C	DB 262/4	09/11/09
Body (Sheet 3 of 6)	R7021/002	C	DB 262/4	09/11/09
Body (Sheet 4 of 6)	R7021/002	C	DB 262/4	09/11/09
Body (Sheet 5 of 6)	R7021/002	C	DB 262/4	09/11/09
Body (Sheet 6 of 6)	R7021/002	C	DB 262/4	09/11/09
Closure (Sheet 1 of 2)	R7021/003	C	DB 262/4	09/11/09
Closure (Sheet 2 of 2)	R7021/003	C	DB 262/4	09/11/09
Pallet (Sheet 1 of 2)	R7021/004	D	DB 262/4	02/11/09
Pallet (Sheet 2 of 2)	R7021/004	D	DB 262/4	02/11/09
Top Shield (Sheet 1 of 5)	R7021/005	D	DB 262/4	02/11/09
Top Shield (Sheet 2 of 5)	R7021/005	D	DB 262/4	02/11/09
Top Shield (Sheet 3 of 5)	R7021/005	D	DB 262/4	02/11/09
Top Shield (Sheet 4 of 5)	R7021/005	D	DB 262/4	02/11/09
Top Shield (Sheet 5 of 5)	R7021/005	D	DB 262/4	02/11/09
Jacket (Sheet 1 of 2)	R7021/006	D	DB 262/4	02/11/09
Jacket (Sheet 2 of 2)	R7021/006	D	DB 262/4	02/11/09
Grill	R7021/007	A	DB 262/1	18/01/08
Drain plug	R7021/008	B	DB 262/4	09/11/09
Vent plug	R7021/009	B	DB 262/4	09/11/09
M20 Locking pin	R7021/010	A	DB 262/1	18/01/08
M20 Stud	R7021/011	C	DB 262/4	10/11/09
M24 Stud	R7021/012	C	DB 262/4	11/11/09
M30 Dowel	R7021/013	B	DB 262/4	11/11/09
M16 Shoulder bolt	R7021/016	C	DB 262/4	10/11/09
Drain tube assembly	R7021/020	A	DB 262/4	06/11/09
Boss	R7021/021	A	DB 262/4	06/11/09
Well	R7021/022	A	DB 262/4	06/11/09
Outer tube	R7021/023	A	DB 262/4	06/11/09
Drain tube	R7021/024	A	DB 262/4	06/11/09
Outer tube	R7021/025	A	DB 262/4	06/11/09
Plug	R7021/026	A	DB 262/4	09/11/09

Table 3: Material properties used in benchmarking analyses

Part No.	LS-DYNA Component part description	Yield stress MPa	Ultimate Tensile Stress MPa	Elongation failure strain	True Stress (at 70% failure strain) MPa	70% of failure	True stress at failure MPa
1	Cooling fins	354	618	55%	855.93	0.385	957.9
2	Feet - Body	249	573	55%	793.605	0.385	888.15
3	Cone Section Top - Body	330	626	52%	853.864	0.364	951.52
4	Lead	18	20	50%	27	0.35	30
5	Lead around drain tube	18	20	50%	27	0.35	30
6	Large Fin - Body	354	618	55%	855.93	0.385	957.9
7	Rolled Cylinder - Body	335	639	57%	893.961	0.399	1003.23
8	Top Flange Ring-Body	251	536	74%	813.648	0.518	932.64
9	Web Plates - Body	354	618	55%	855.93	0.385	957.9
10	Weld Part 7 and 49	267	590	52%	804.76	0.364	896.8
11	Weld Part 7 and 49	267	590	52%	804.76	0.364	896.8
12	Closure Top Plate - Closure	253	574	58%	807.044	0.406	906.92
13	Lead in closure	18	20	50%	27	0.35	30
14	Weight Block - Closure	303	604	62%	866.136	0.434	978.48
15	Body Cylinder - Closure	386	661	52%	901.604	0.364	1004.72
16	Protection Ring - Closures	265	582	61%	830.514	0.427	937.02
17	Drain Tube Body	267	590	52%	804.76	0.364	896.8
18	Weld Part 17 and 49	267	590	52%	804.76	0.364	896.8
19	Outer and Inner Cylinder - Jacket	430	570	30%	689.7	0.21	741
20	Weld Part 19 and 21/24	430	570	30%	689.7	0.21	741
21	Outer and Inner Cylinder - Jacket	430	570	30%	689.7	0.21	741
22	Lug - Jacket	305	630	55%	872.55	0.385	976.5
23	Bottom Guide Lug - Jacket	275	588	76%	900.816	0.532	1034.88
24	Outer and Inner Cylinder - Jacket	430	570	30%	689.7	0.21	741
25	Outer and Inner Cylinder - Jacket	430	570	30%	689.7	0.21	741
26	Weld Part 25 and 21/24	430	570	30%	689.7	0.21	741
27	Top Guide Lug- Jacket	275	588	76%	900.816	0.532	1034.88
28	M16 bolt	640	880	12%	953.92	0.084	985.6
29	M16 washer	215	505	30%	611.05	0.21	656.5
30	M16 bolt	640	880	12%	953.92	0.084	985.6
31	M16 washer	215	505	30%	611.05	0.21	656.5
32	M20 nut	640	880	12%	953.92	0.084	985.6
33	M20 washer	215	505	30%	611.05	0.21	656.5
34	M20 stud	240	620	30%	750.2	0.21	806

Part No.	LS-DYNA Component part description	Yield stress MPa	Ultimate Tensile Stress MPa	Elongation failure strain	True Stress (at 70% failure strain) MPa	70% of failure	True stress at failure MPa
35	M24 dowel	205	515	30%	623.15	0.21	669.5
36	M24 nut	640	880	12%	953.92	0.084	985.6
37	M24 stud	640	880	12%	953.92	0.084	985.6
38	M24 washer	215	505	30%	611.05	0.21	656.5
39	Top & Bottom Plate - Pallet	426	566	27%	672.974	0.189	718.82
40	End Plate - Pallet	426	566	27%	672.974	0.189	718.82
41	Flask Mount Plate - Pallet	360	514	30%	621.94	0.21	668.2
42	Weld Part 41 and 43	360	514	27%	611.146	0.189	652.78
43	Top & Bottom Plate - Pallet	426	566	27%	672.974	0.189	718.82
44	Top Cap Plate - Top Shield	345	379	74%	575.322	0.518	659.46
45	Cone Half Right - Top Shield	345	379	74%	575.322	0.518	659.46
46	Fixing Lugs - Top Shield	257	571	62%	818.814	0.434	925.02
47	Middle Flange Plate - Top Shield	455	560	38%	708.96	0.266	772.8
48	Middle Flange Plate - Top Shield	455	560	38%	708.96	0.266	772.8
49	Drain Tube Entry Ring - body	267	590	52%	804.76	0.364	896.8

Table 4: Material properties used in orientation and detailed analyses

Material property	Stainless steel BS EN 10083-3 Grade 1.4307 (304L) for flask	Lead	Carbon steel for shoulder bolts	Plain form A Stainless steel for washers BS 4320	Stainless steel Grade A2-80 BS EN ISO 3506-1 for closure studs	Carbon steel Grade 8.8 BS 3692 for dowels and pallet studs	Carbon steel EN 10025 S355 J2+N for top shield, jacket and pallet
Young's modulus	$2x10^{11}$ N/m^2	$16x10^9$ N/m^2	$2x10^{11}$ N/m^2	$2x10^{11}$ N/m^2	$2x10^{11}$ N/m^2	$2x10^{11}$ N/m^2	$2x10^{11}$ N/m^2
Poisson's ratio	0.3	0.45	0.3	0.3	0.3	0.3	0.3
0.2% proof stress	200 MN/m^2	17 MN/m^2	890 MN/m^2	200 MN/m^2	600 MN/m^2	640 MN/m^2	400 MN/m^2
Ultimate tensile stress	500 MN/m^2	30 MN/m^2	950 MN/m^2	500 MN/m^2	800 MN/m^2	800 MN/m^2	570 MN/m^2
Elongation failure strain	0.45	0.50	0.10	0.45	0.12	0.12	0.28
Reduction in area at failure			0.45		0.52	0.46	
True effective plastic strain							
0.2%	0.0	0.0	0.0	0.0	0.0	0.0	0.0
1.0%	0.81%	0.69%	0.35%	0.81%	0.49%	0.48%	0.59%
UTS	24.26%	26.3%	39.2%	24.26%	7.53%	39.31%	34.02%
At failure	41.46%	45.4%	72.8%	41.46%	12.04%	72.88%	61.22%
True stress							
0.2%	200 MN/m^2	17 MN/m^2	896 MN/m^2	200 MN/m^2	603 MN/m^2	643 MN/m^2	402 MN/m^2
1.0%	414 MN/m^2	17.6 MN/m^2	900 MN/m^2	414 MN/m^2	620 MN/m^2	650 MN/m^2	409 MN/m^2
UTS	639 MN/m^2	39.1 MN/m^2	1415 MN/m^2	639 MN/m^2	867 MN/m^2	1191 MN/m^2	804 MN/m^2
at failure	739 MN/m^2	45.9 MN/m^2	1847 MN/m^2	739 MN/m^2	902 MN/m^2	1556 MN/m^2	1003 MN/m^2

Table 5: Strains predicted in closure bolts, pallet bolts, jacket bolts and top shield bolts.

Drop test	Closure bolts		Pallet bolts		Jacket bolts		Top shield bolts		Comments
	εffp	RF	**εffp**	RF	**εffp**	RF	**εffp**	RF	**RF – Reserve factor**
1	1.6	**7,50**	0.5	**24.0**	0.3	**33.3**	0.0		
2	8.6	**1.40**	6.9	**1.74**	2.9	**3.45**	13.8	**0.73**	
3	7.4	**1.62**	0.3	**40.0**	5.1	**1.96**	2.4	**4.17**	
4	-		-		-		-		Assumed to be zero
5	0.3	**40.0**	0.0		0.1	**100.**	0.1	**100.**	
6	1.2	**10.0**	1.0	**12.0**	0.4	**25.0**	1.5	**6.67**	
7	0.0		0.0		0.0		2.4	**4.17**	
8	4.5	**2.67**	0.1	**120,**	2.7	**3.70**	4.7	**2.13**	
9	22.1	**0.54**	11.5	**1.04**	6.1	**1.64**	0.1	**100.**	Pallet bolts - local surface strains only
10	0.7	**17.1**	0.0		2.0	**5.0**	0.5	**20.0**	
11	0.4	**30.0**	1.3	**9.23**	0.6	**16.7**	0.3	**33.3**	
12	4.2	**2.86**	0.1	**120.**	3.4	**2.94**	5.1	**1.96**	
13	4.0	**3.00**	0.2	**60.0**	4.0	**2.50**	2.0	**5.00**	Very high local deformation at one location due to contact problems
14	2.9	**4.14**	0.0		9.0	**1.11**	0.4	**25.0**	
15	14.1	**0.85**	28.7	**0.42**	26.4	**0.38**	15.3	**0.65**	
16	1.6	**7.50**	0.2	**60.0**	- #		1.3	**7.69**	# This component converted to rigid for this analysis
17	9.8	**1.22**	11.9 ‡	**1.01**	- #		10.3	**0.97**	‡ Local compressive strains on bolt heads

Table 6: Summary of detailed analysis results.

	Off horizontal 115x000	Horizontal 090x045	Inclined base 035x045	Vertical upright 000x000	Vertical inverted 180x000	Angled inverted 163x000	Horizontal 090x000
Comparative drop test in Table 5				Drop 6 value shown in brackets	Drop 9 value shown in brackets	Drop 12 value shown in brackets	Drop 15 value shown in brackets
Plastic strain							
Pallet weld	2.6%	20.0%	50.0%	46.0%	2.2%	0.3%	8.6%
Pallet stud	2.6%	3.0%	4.0%	1.0% (1.0%)	1.0% (11.5%)	elastic (0.1%)	8.6% (28.7%)
Pallet dowel	14.2%	9.0%	16.0%	3.0%	1.0%	elastic	19.0%
Shoulder bolt	1.3%	7.0%	5.0%	0.8%	1.4%	2.1%	3.0%
Outer wall	13.9%	33.0%	45.0%	17.0%	0.8%	8.0%	23.0%
Closure stud	elastic	0.1%	elastic	elastic (1.2%)	0.1% (22.1%)	0.0% (4.2%)	0.2% (14.1%)
Outer tube	4.1%	5.2%	1.5%	1.1%	2.8%	1.5%	8.0%
Drain tube	0.6%	0.2%	0.0%	1.0%	0.9%	0.0%	0.2%
Accelerations							
Peak	61g	95g	82g	1110g (120g)	85g	105g	90g
Average	26g	23g	21g	72g	71g	49g	48g

FIGURES

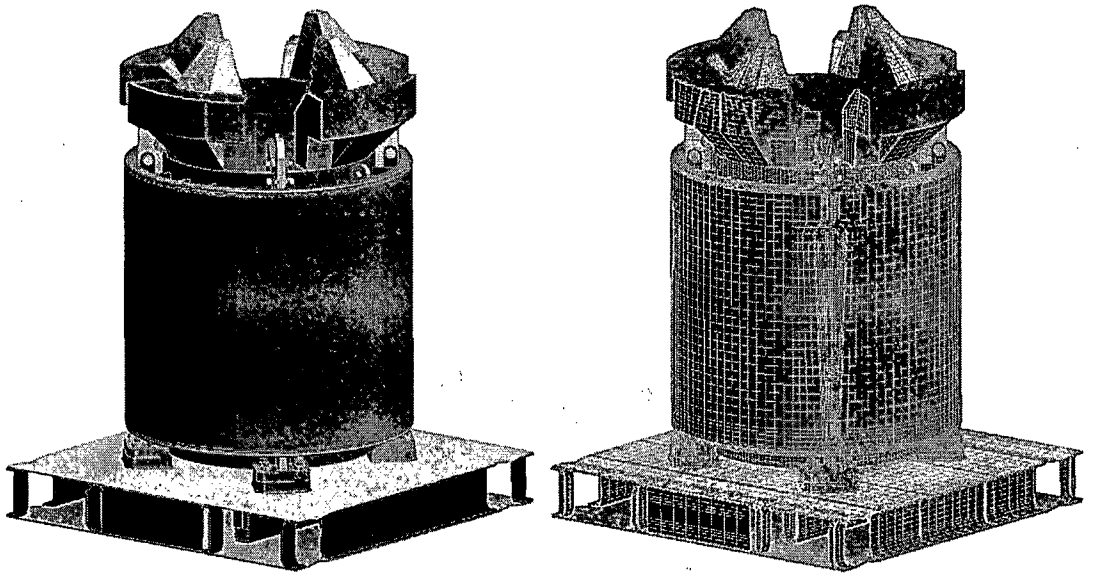

Figure 1: Finite element model and mesh

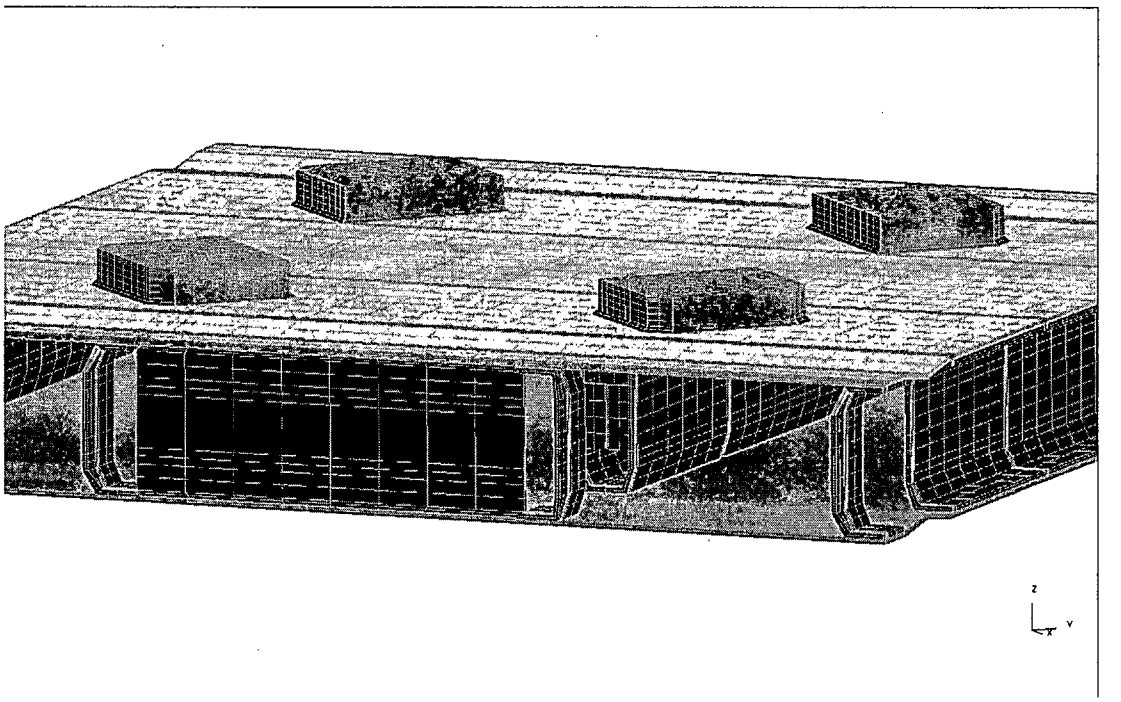

Figure 2: Details of mesh in pallet

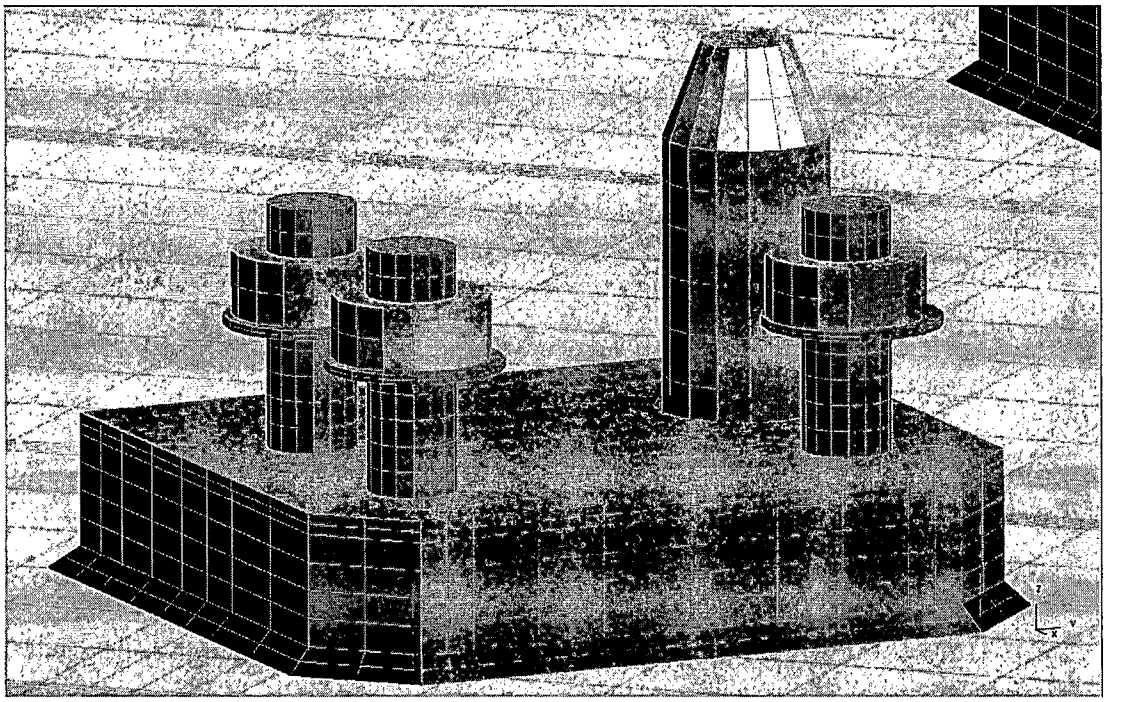

Figure 3: Pallet bolted connections and dowel

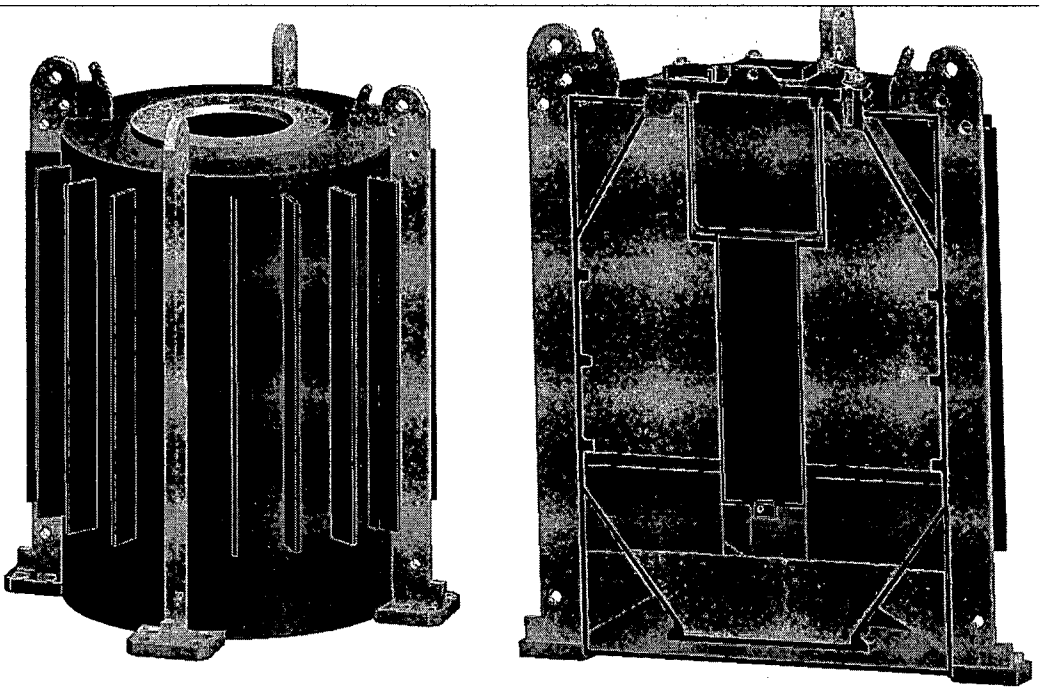

Figure 4: Flask showing fins and details of internal structure.

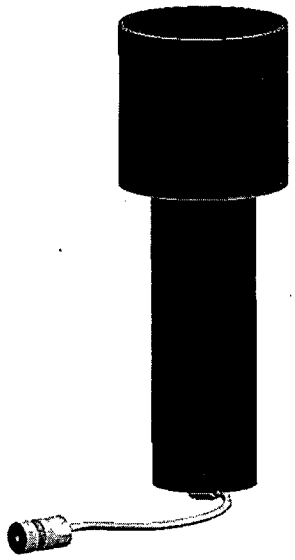

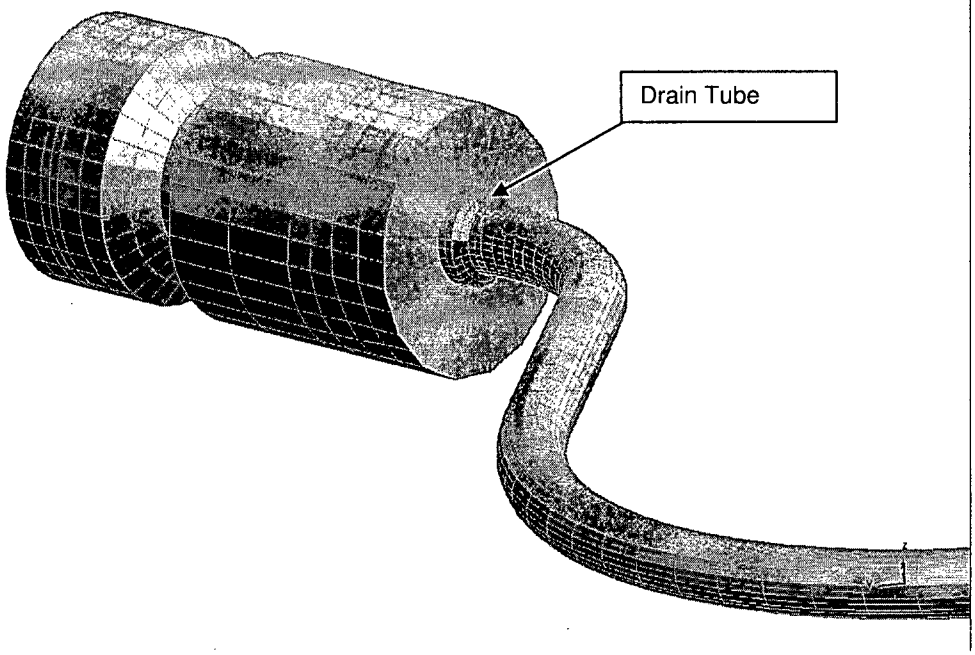

Figure 5: Drain tube and details of drain tube weld and drain point

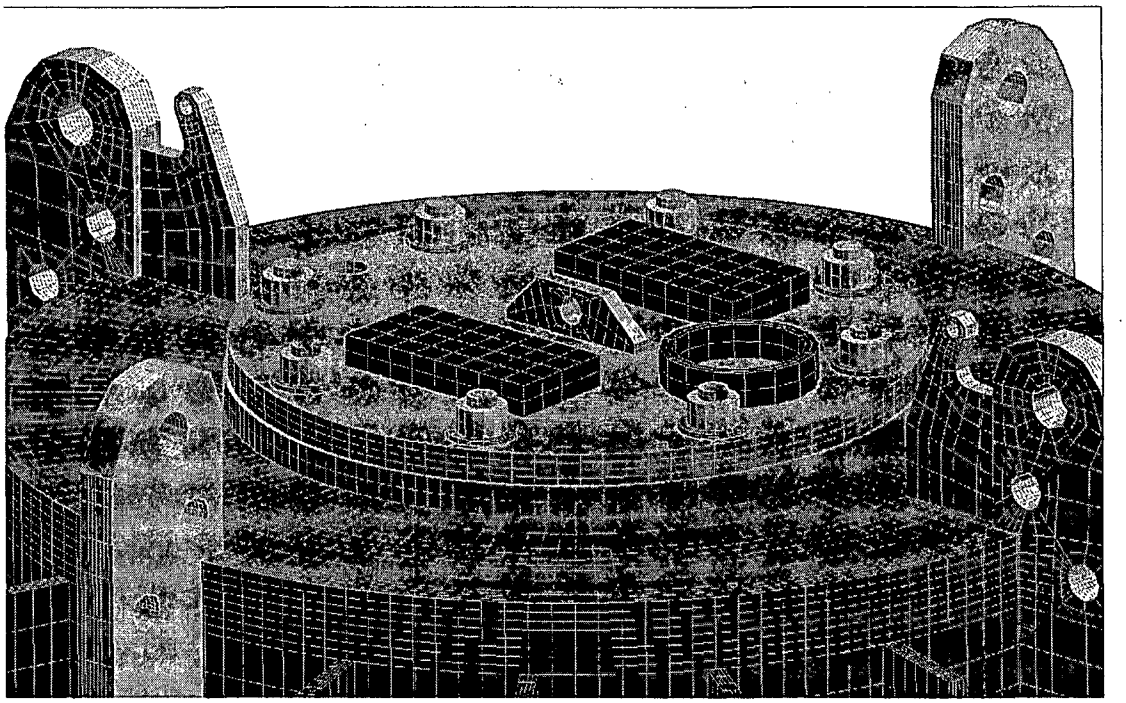

Figure 6: Closure details and top of flask

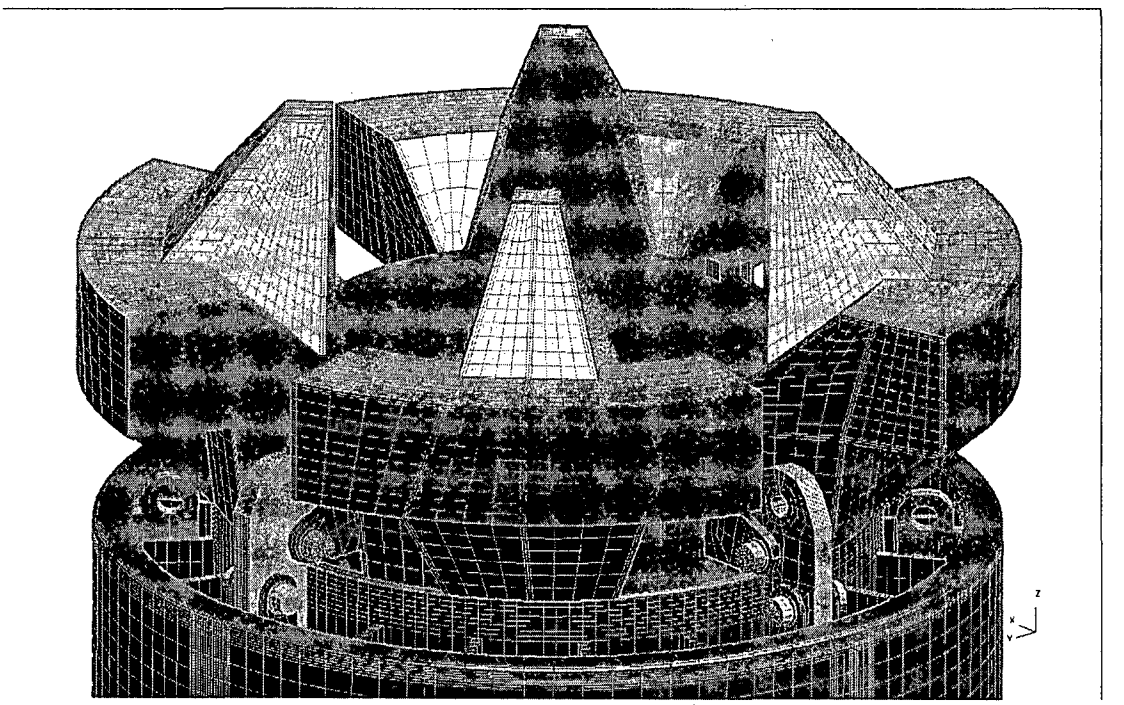

Figure 7: Top of flask showing shock absorbing features

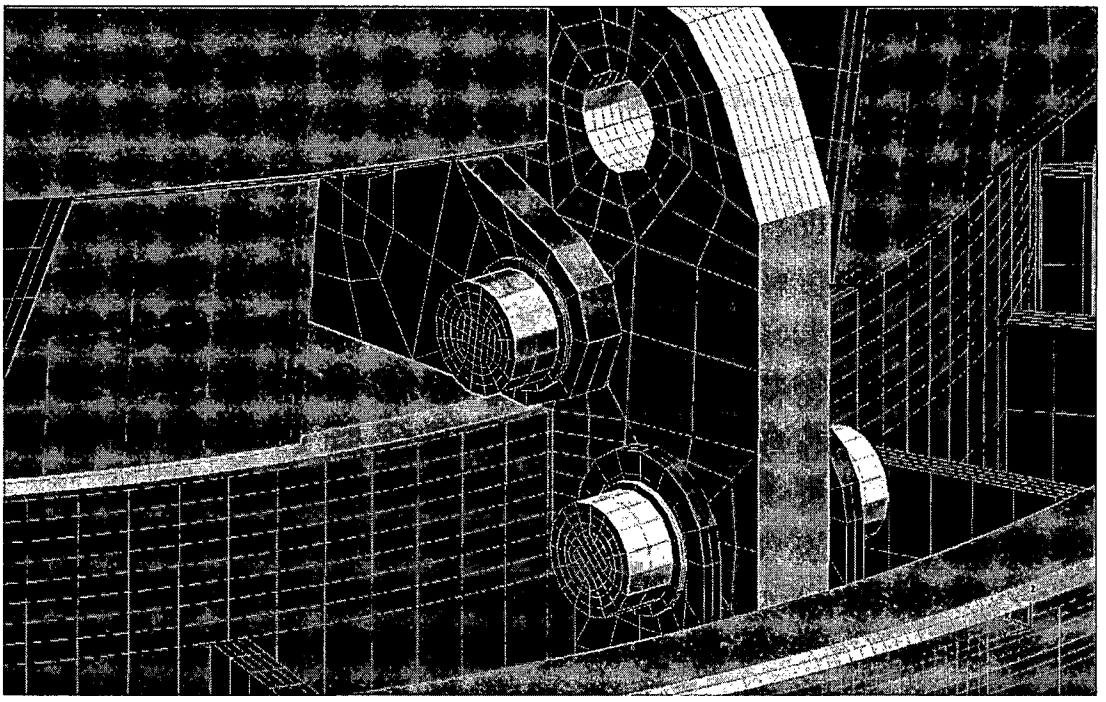

Figure 8: Shock absorber and jacket connections

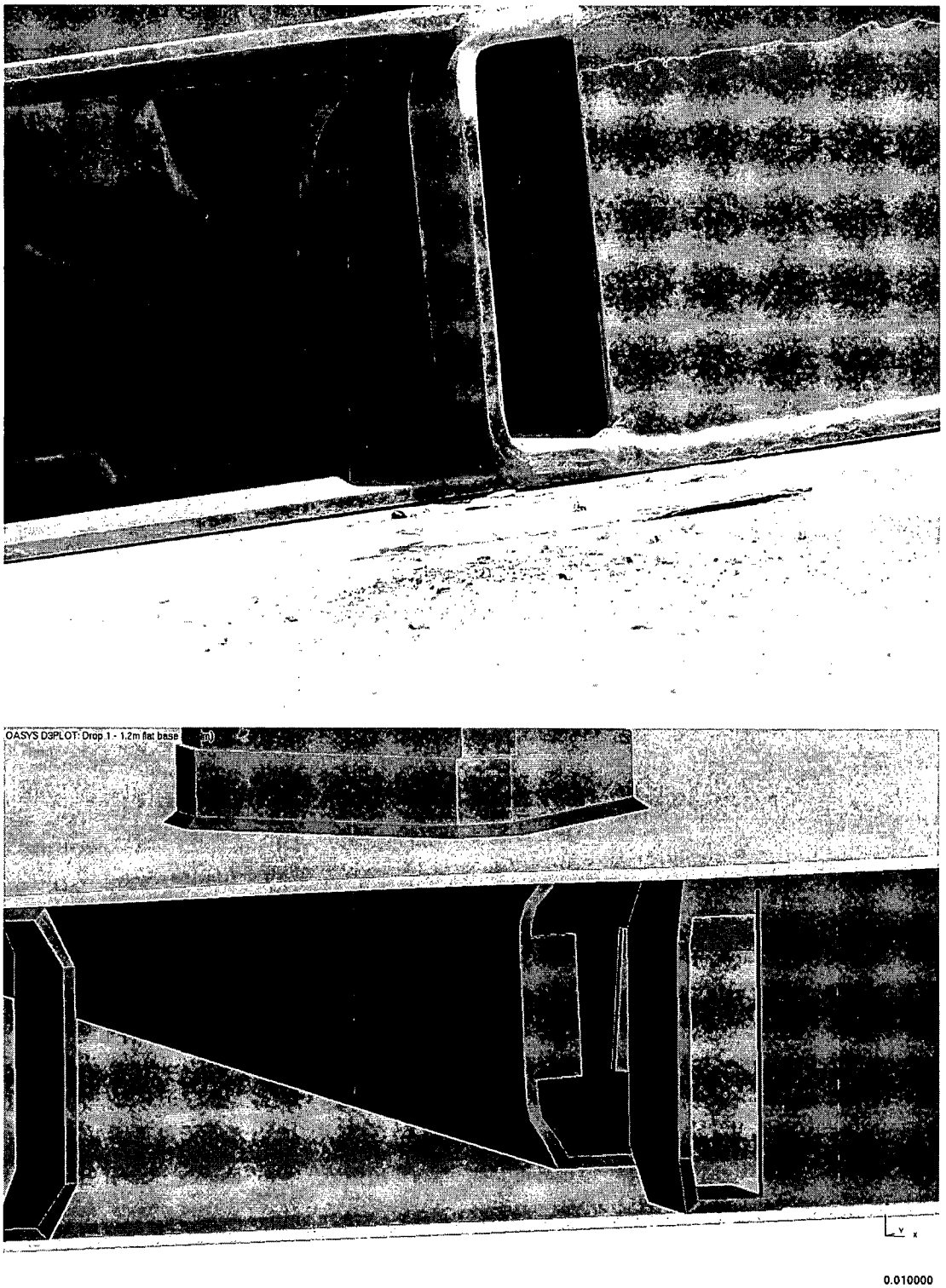

Figure 9: Drop 1 – comparison 1

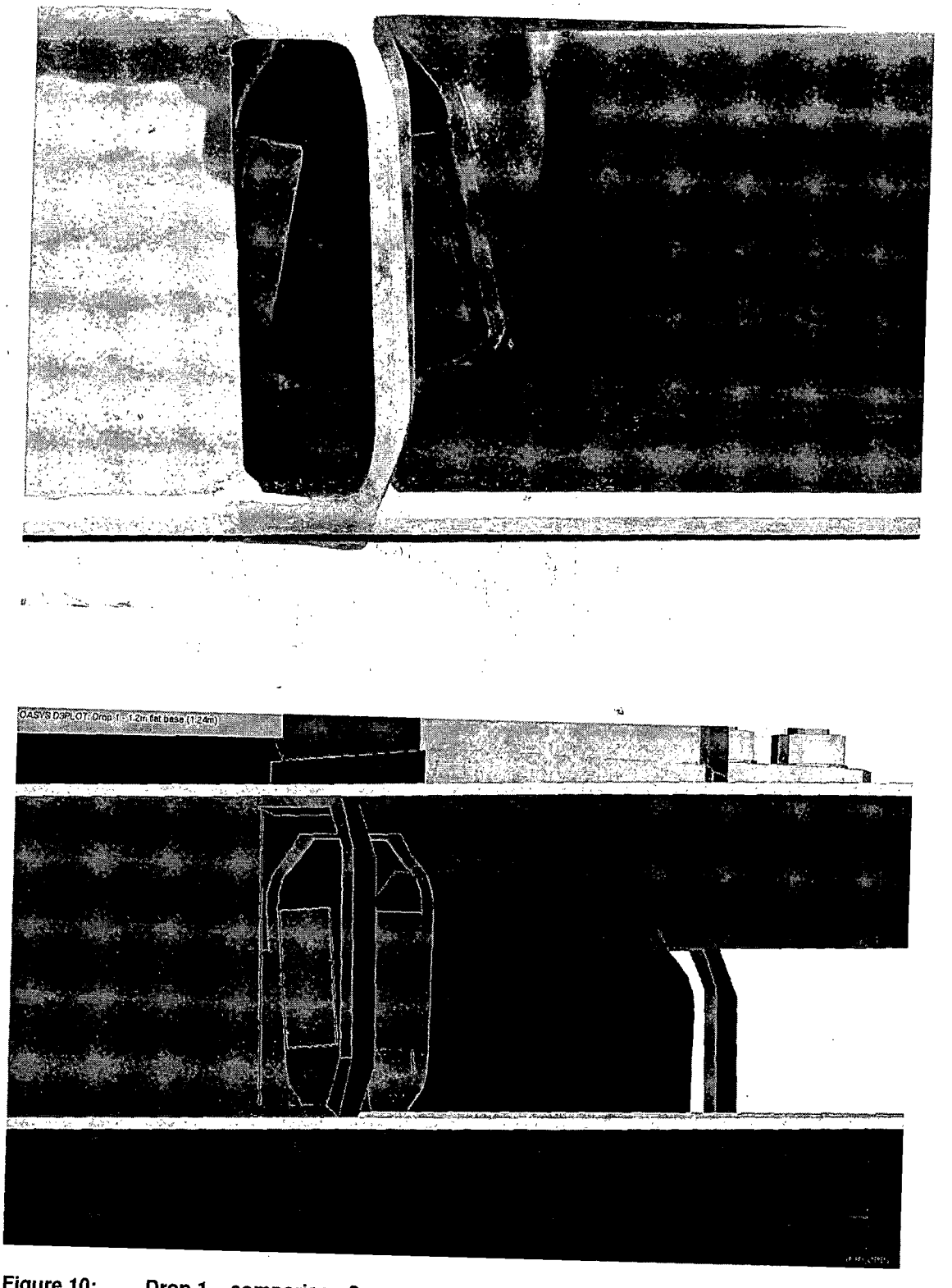

Figure 10: **Drop 1 – comparison 2**

Figure 11: Drop 2 – comparison 1

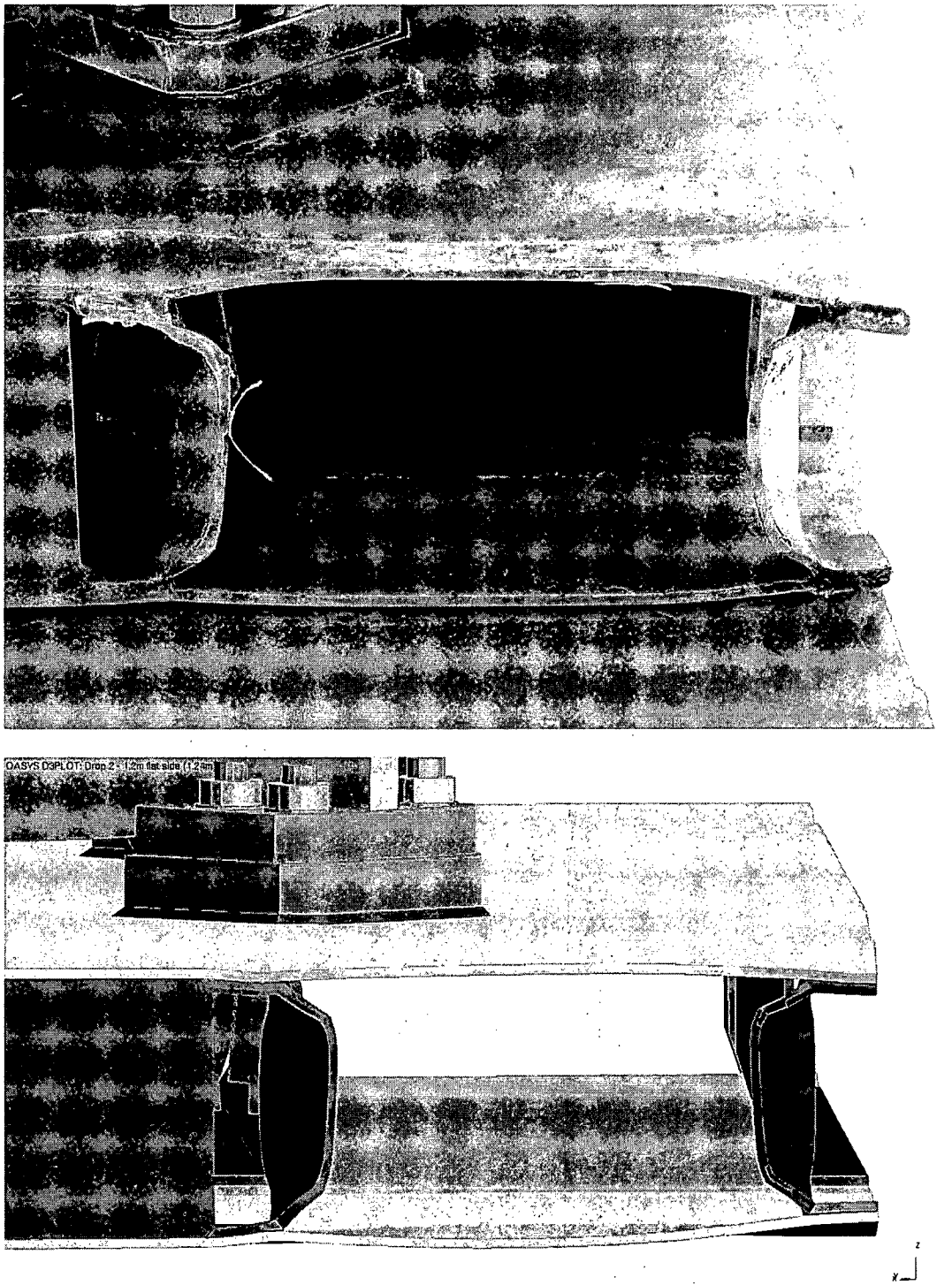

Figure 12: Drop 2 – comparison 2

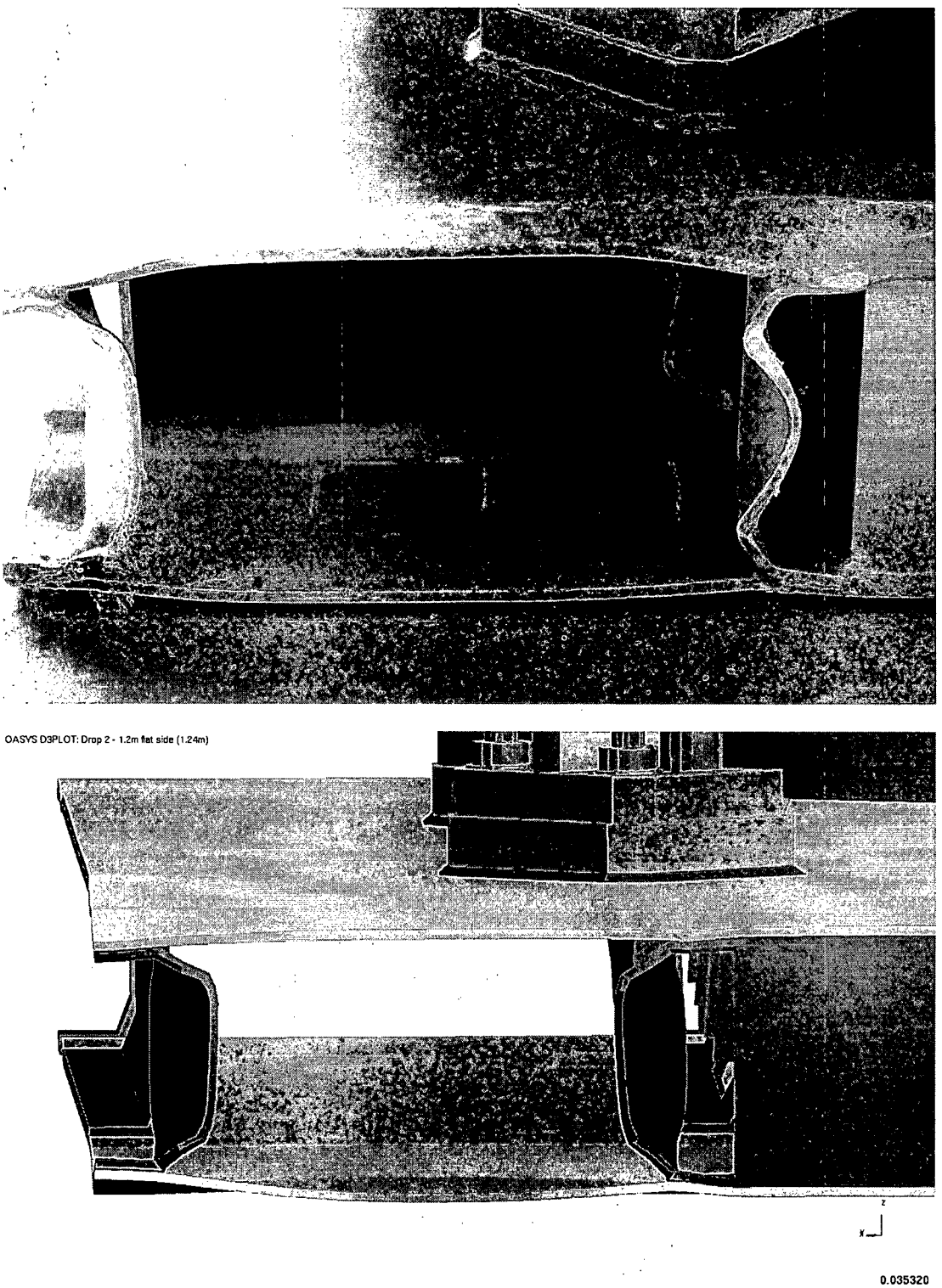

Figure 13: Drop 2 – comparison 3

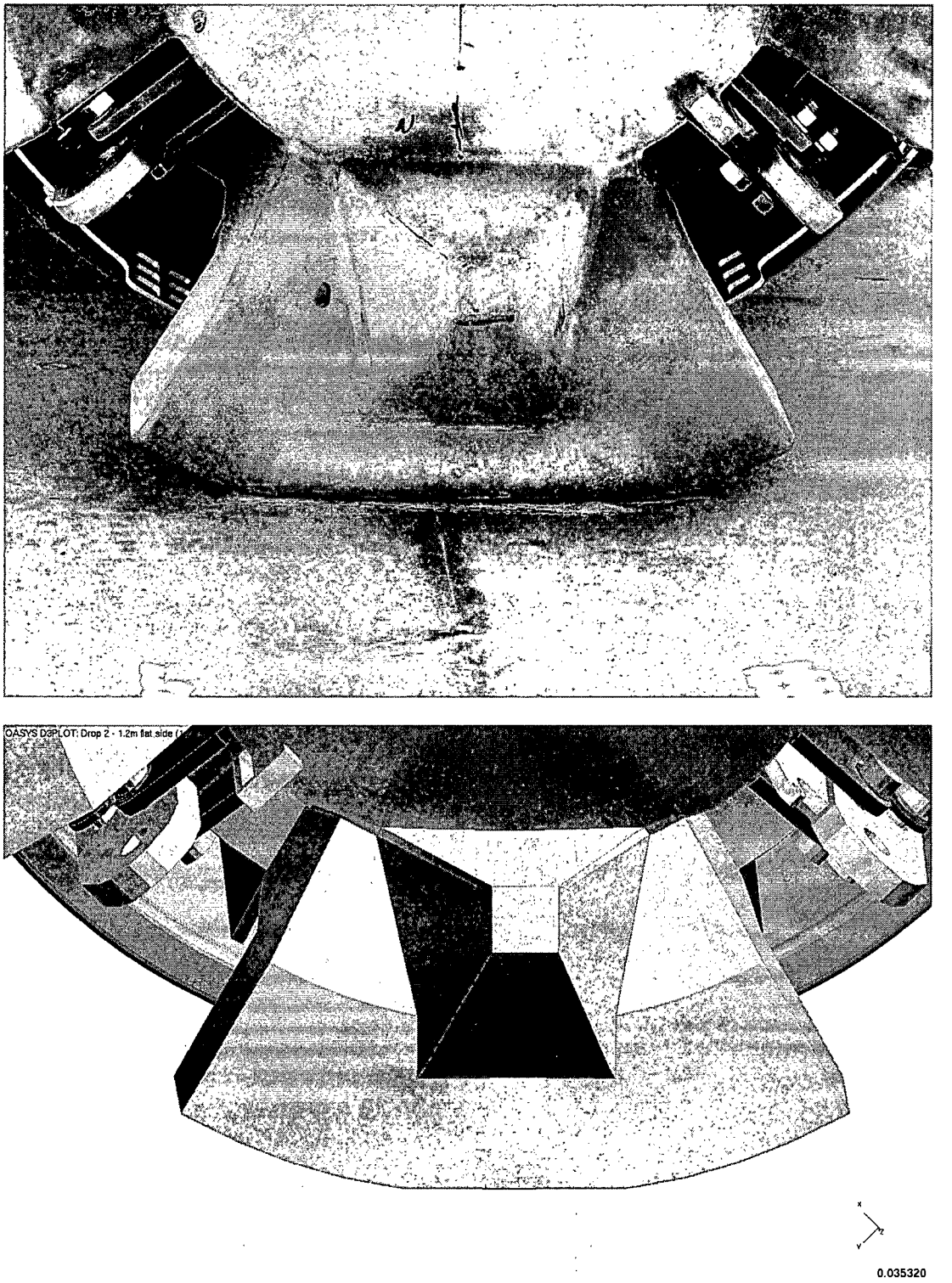

Figure 14: Drop 2 – comparison 4

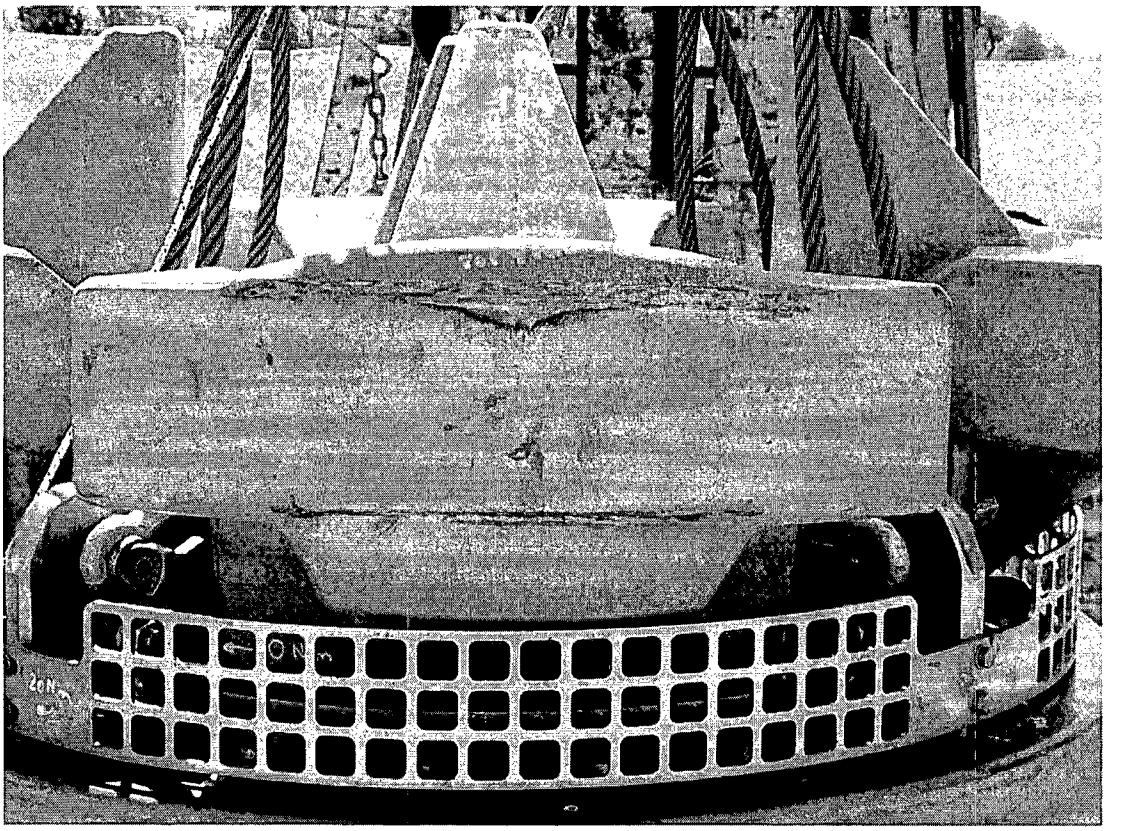

OASYS D3PLOT: Drop 2 - 1.2m flat side (1.24m)

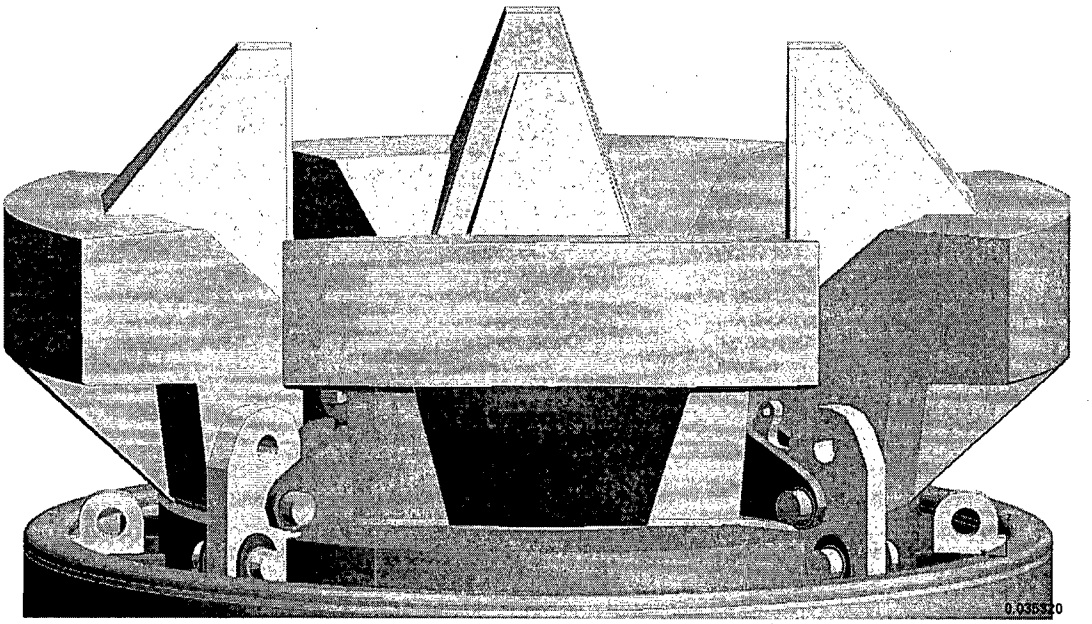

Figure 15: Drop 2 – comparison 5

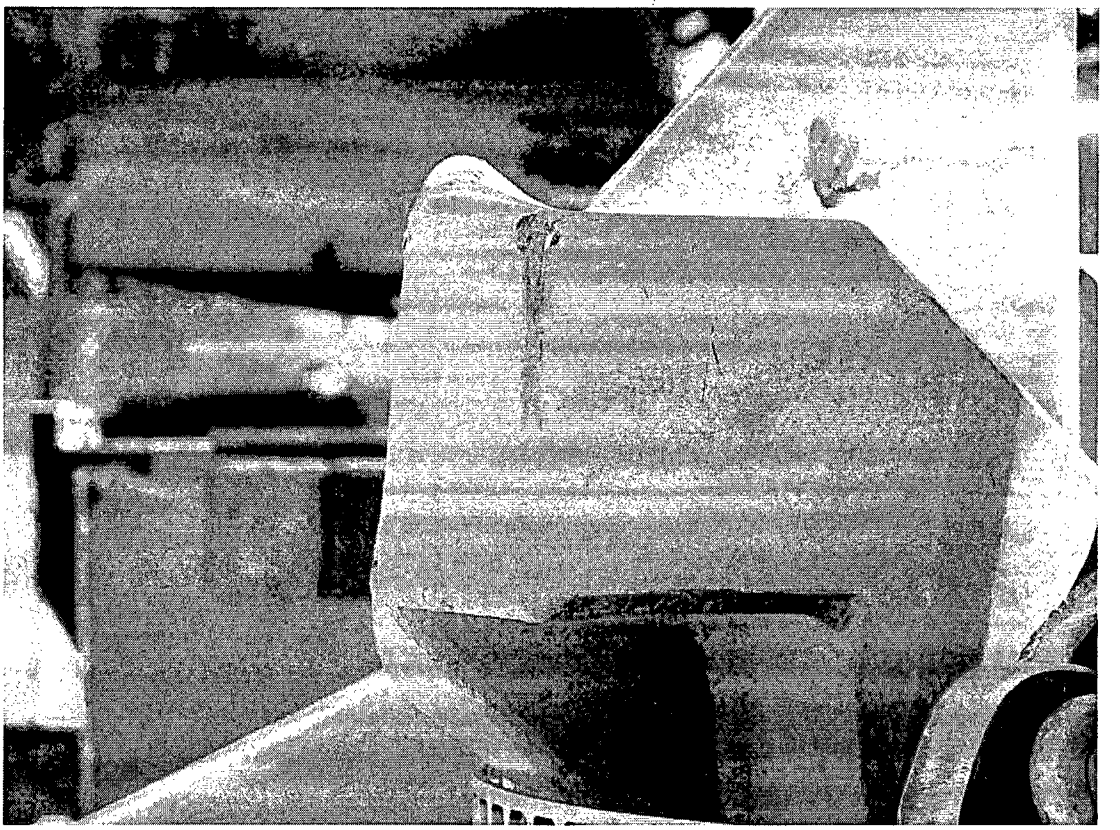

OASYS D3PLOT: Drop 2 - 1.2m flat side (1.24m)

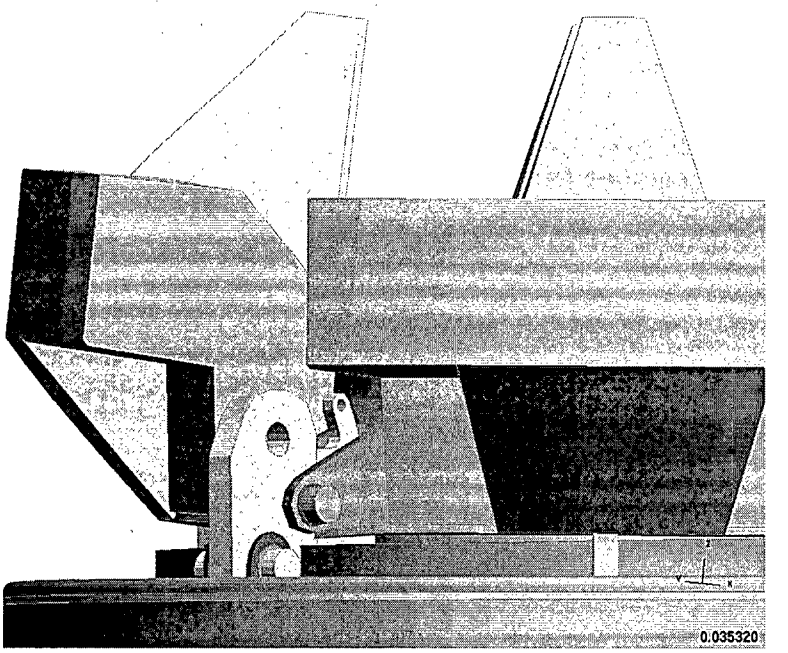

Figure 16: Drop 2 – comparison 6

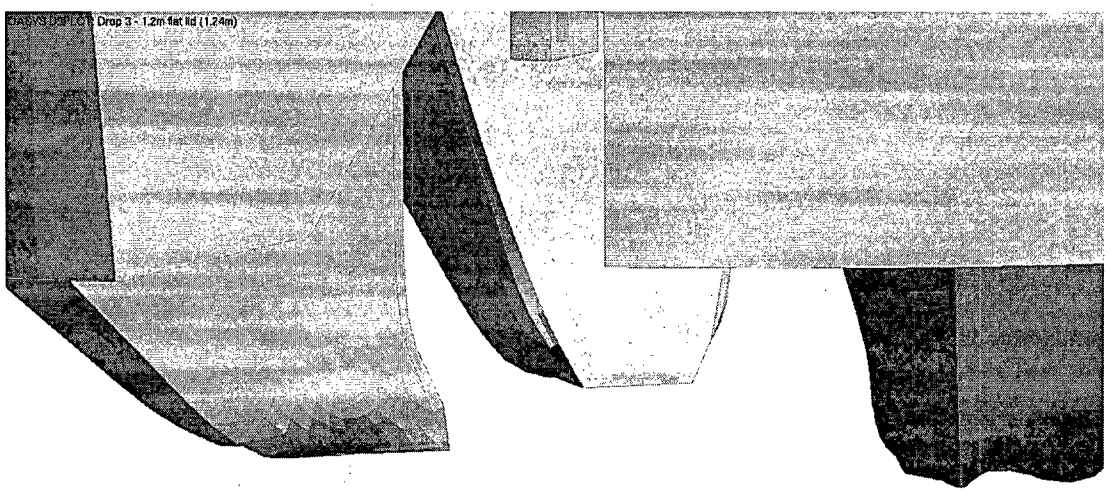

Figure 17: Drop 3 – comparison 1

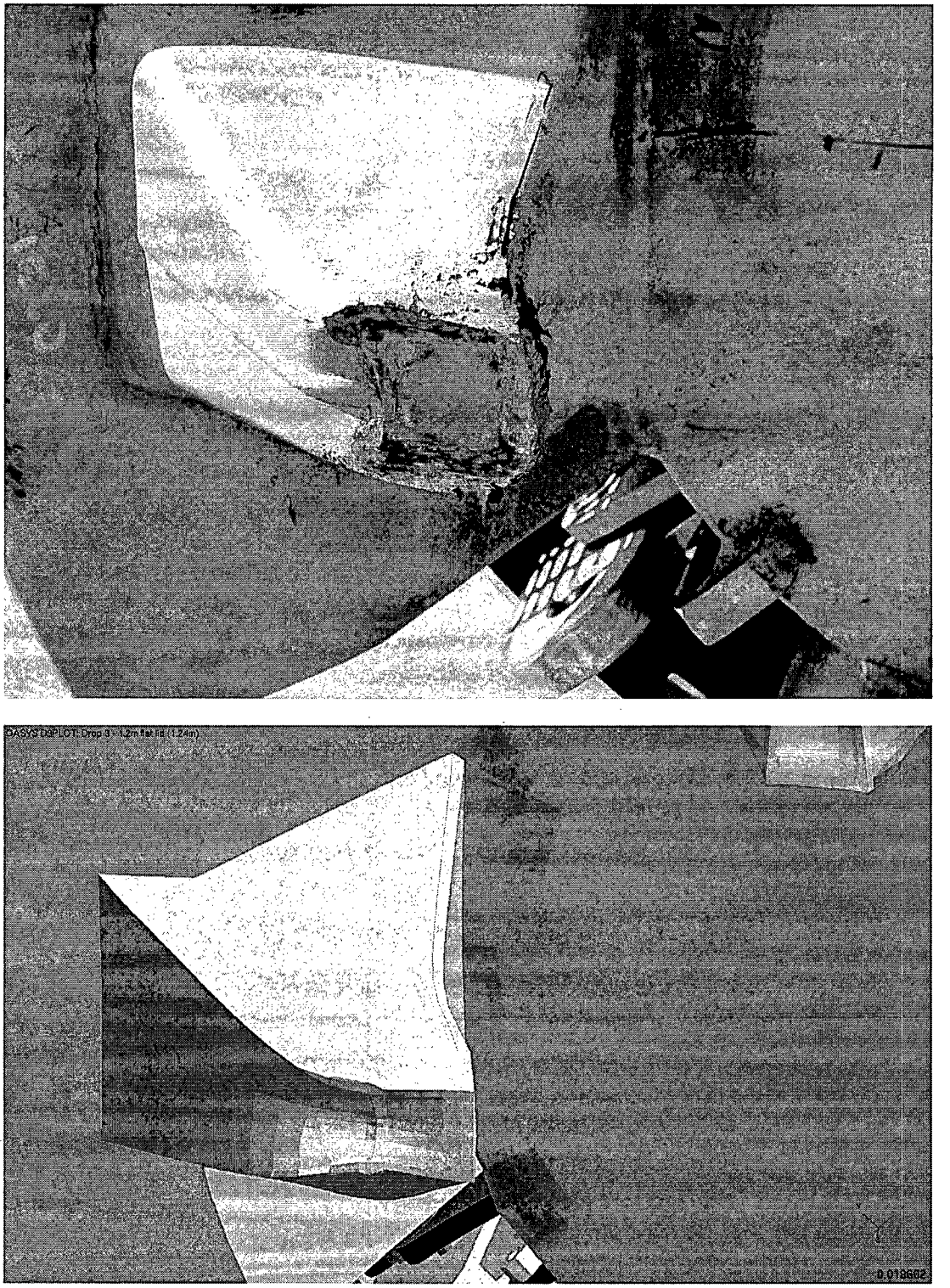

Figure 18: Drop 3 – comparison 2

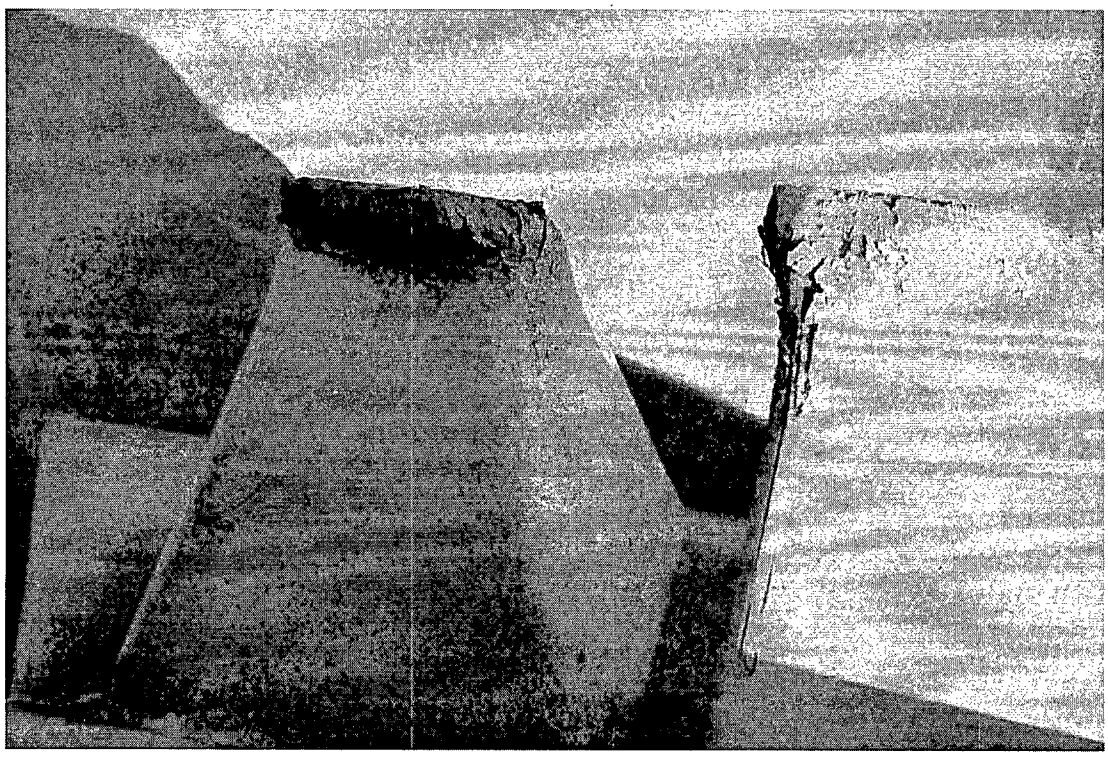

OASYS D3PLOT: Drop 3 - 1.2m flat lid (1.24m)

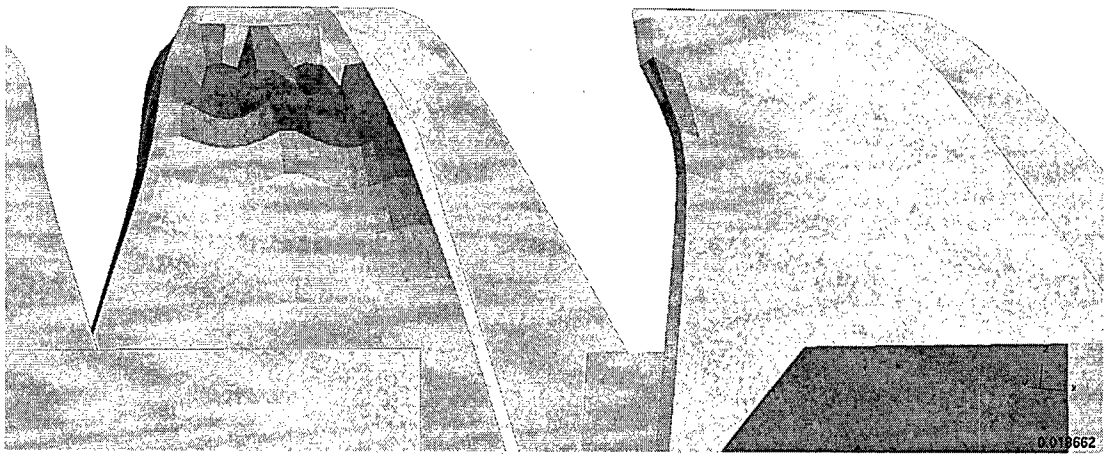

Figure 19: Drop 3 – comparison 3

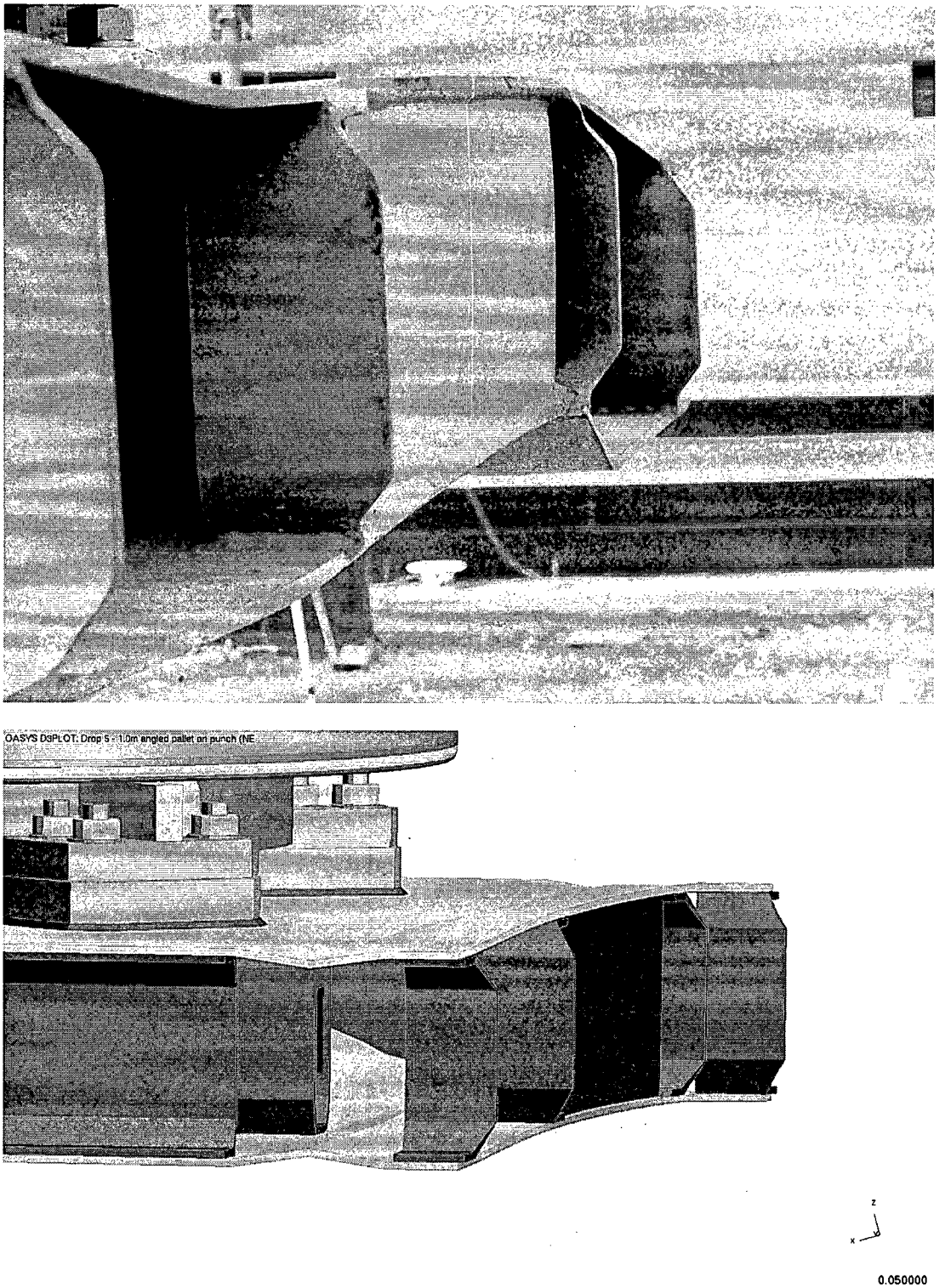

Figure 20: Drop 5 – comparison 1

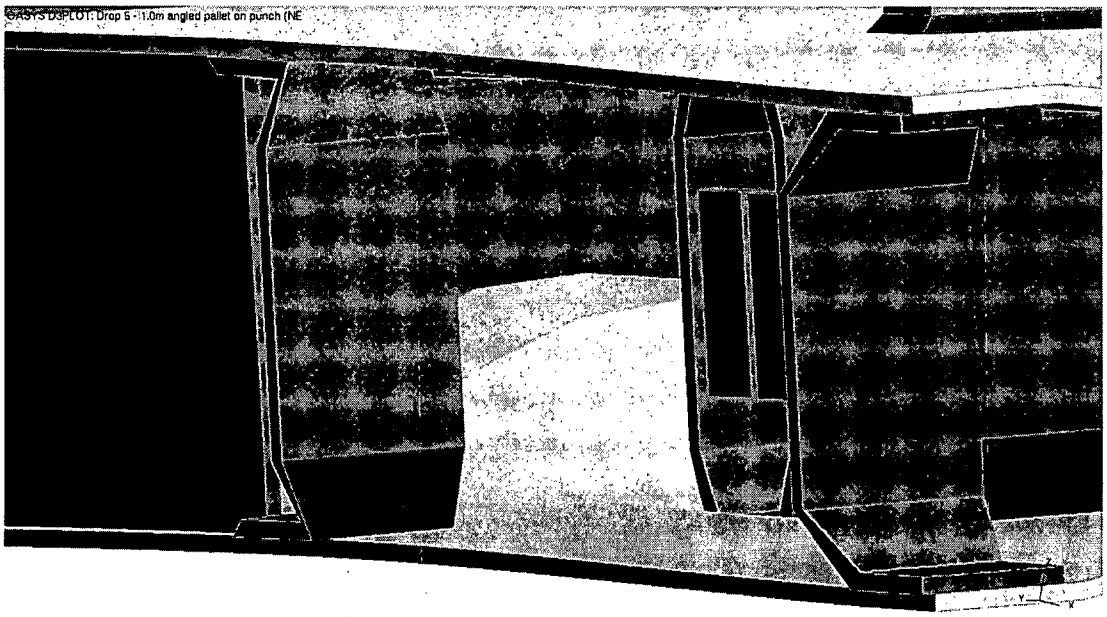

0.050000

Figure 21: Drop 5 – comparison 2

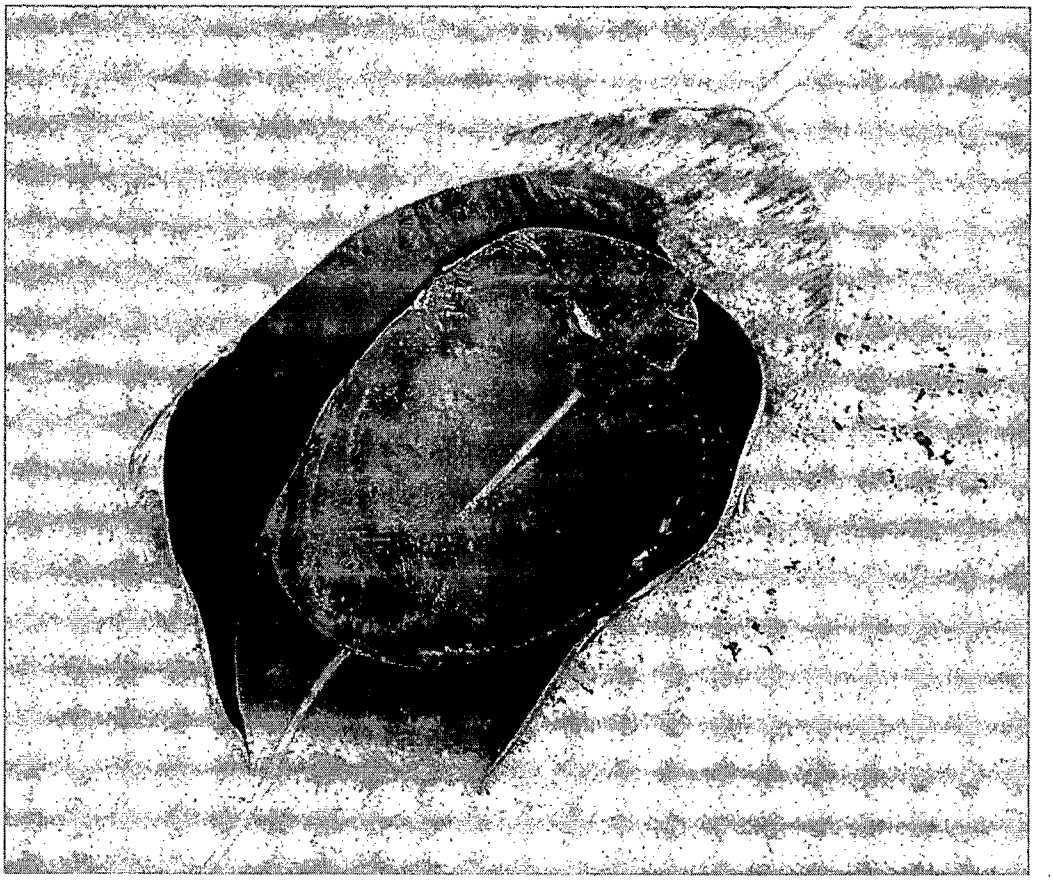

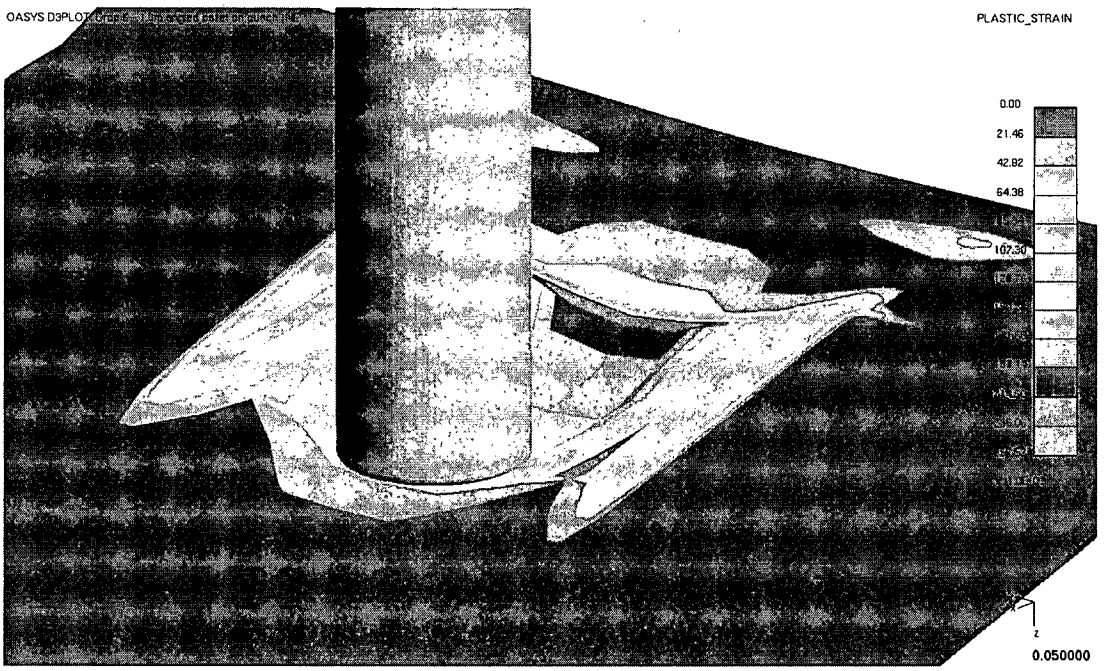

Figure 22: Drop 5 – comparison 3

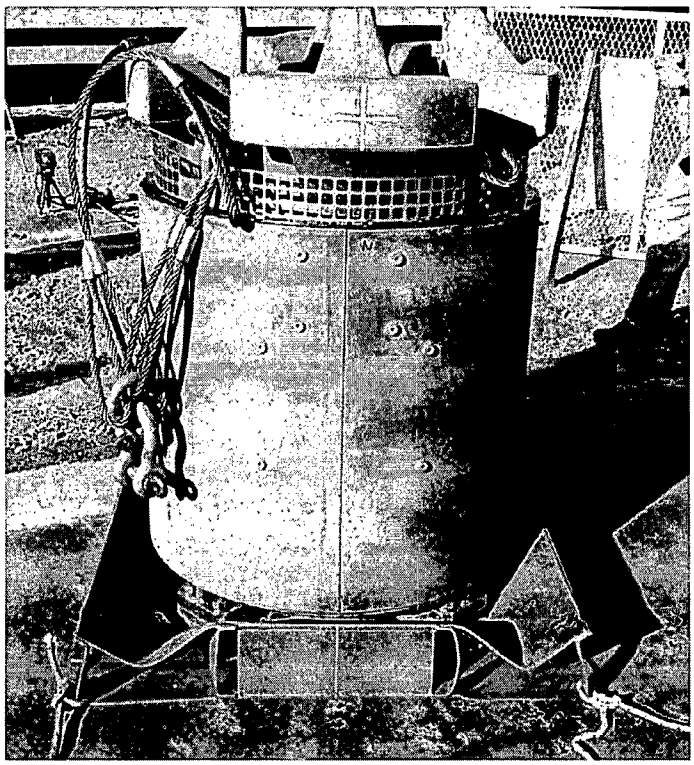

OASYS D3PLOT: Drop 6 - 8.0m flat base impact

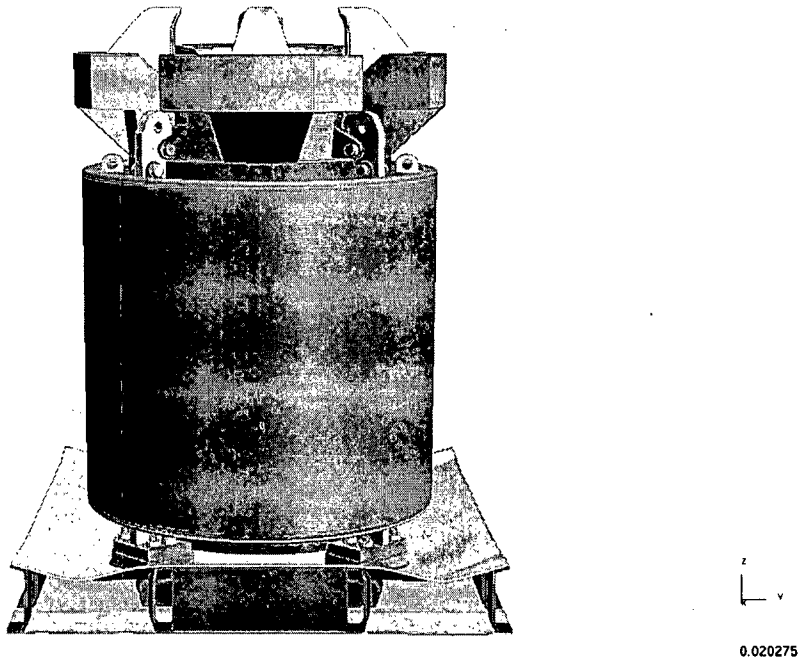

Figure 23: Drop 6 – comparison 1

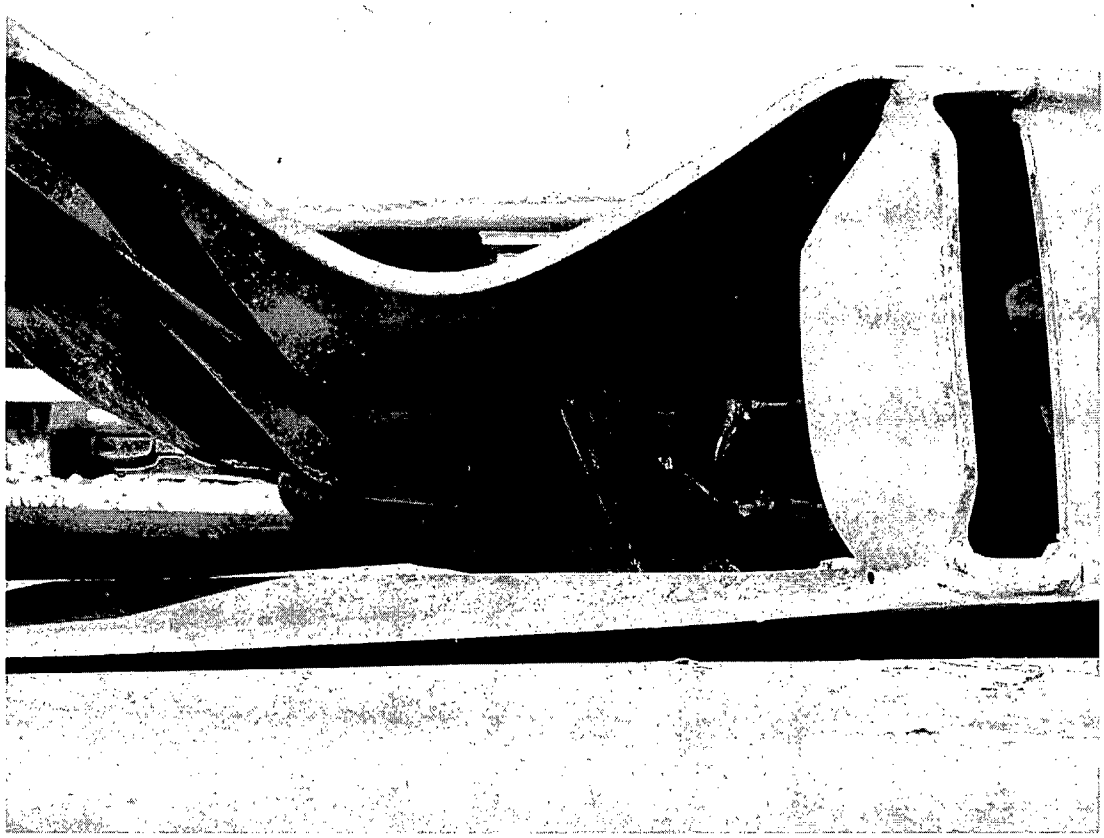

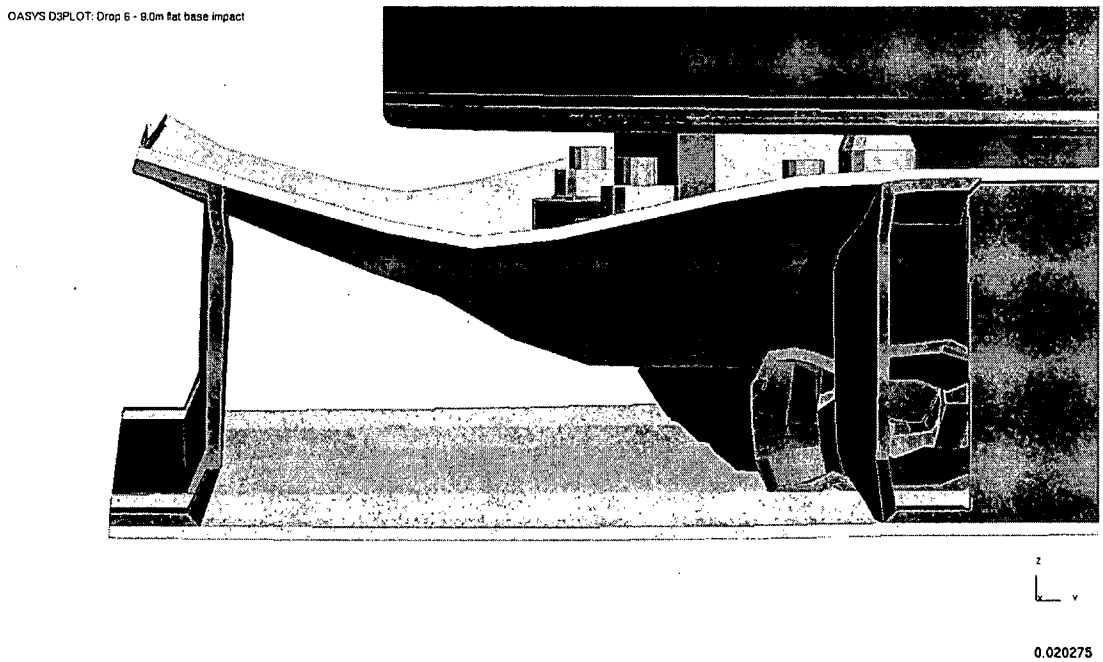

Figure 24: Drop 6 – comparison 2

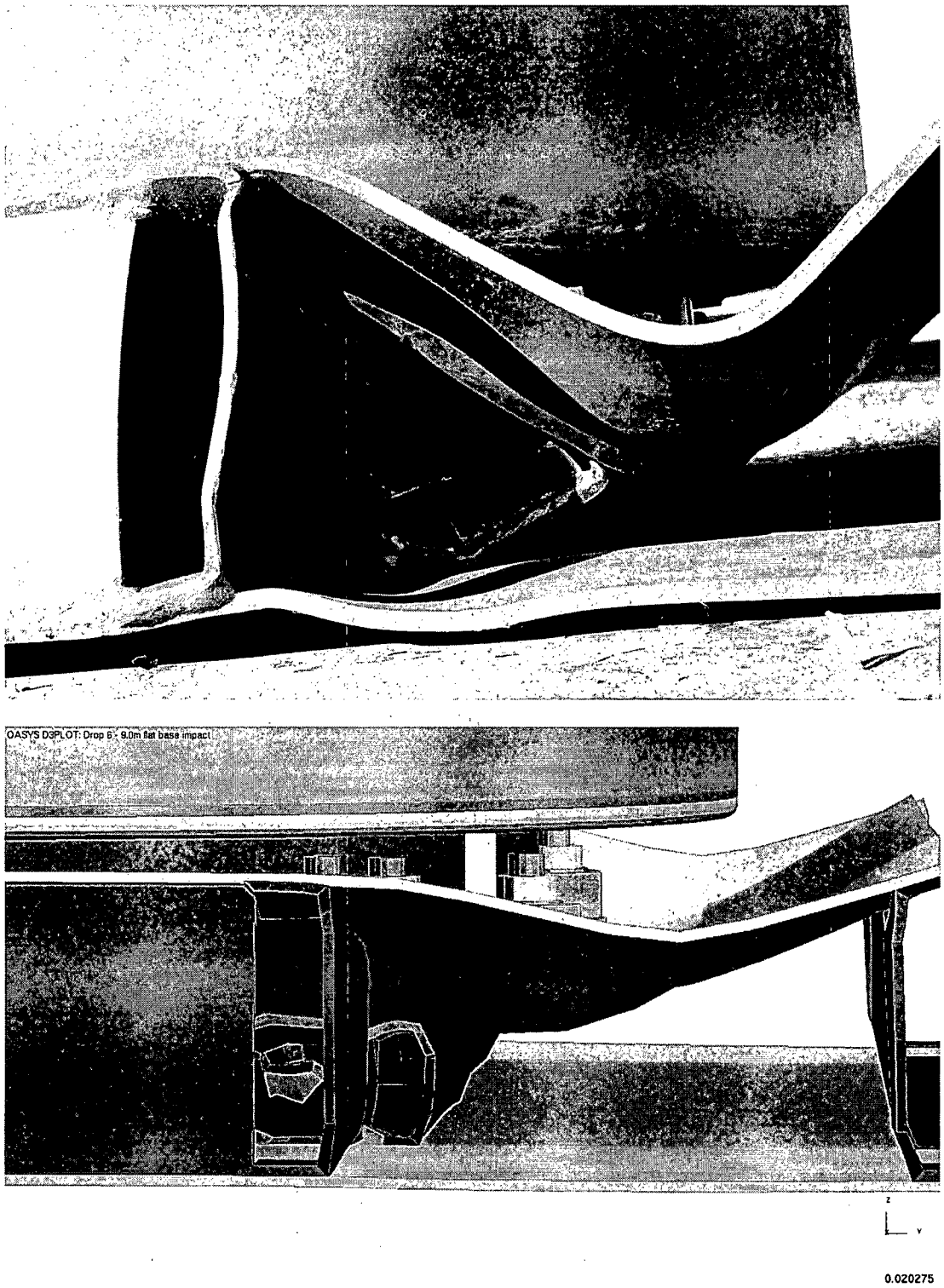

Figure 25: Drop 6 – comparison 3

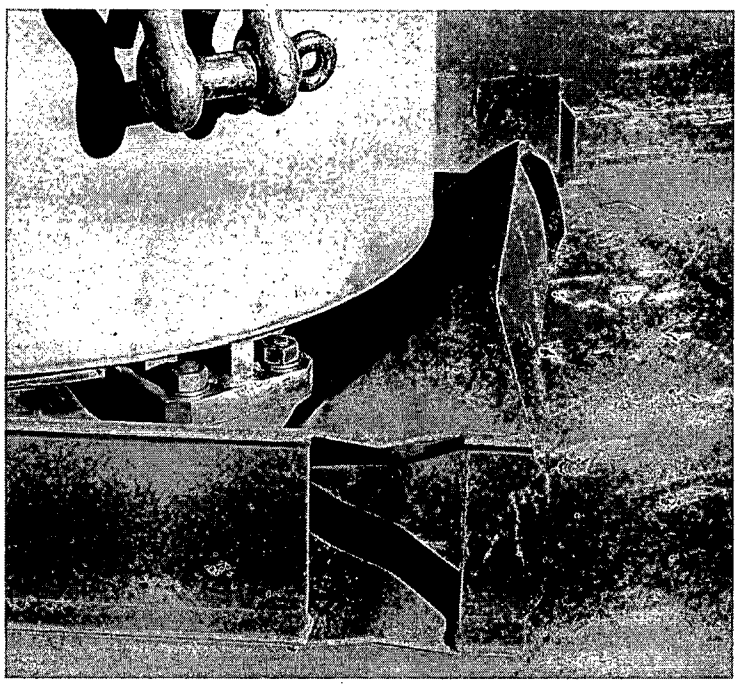

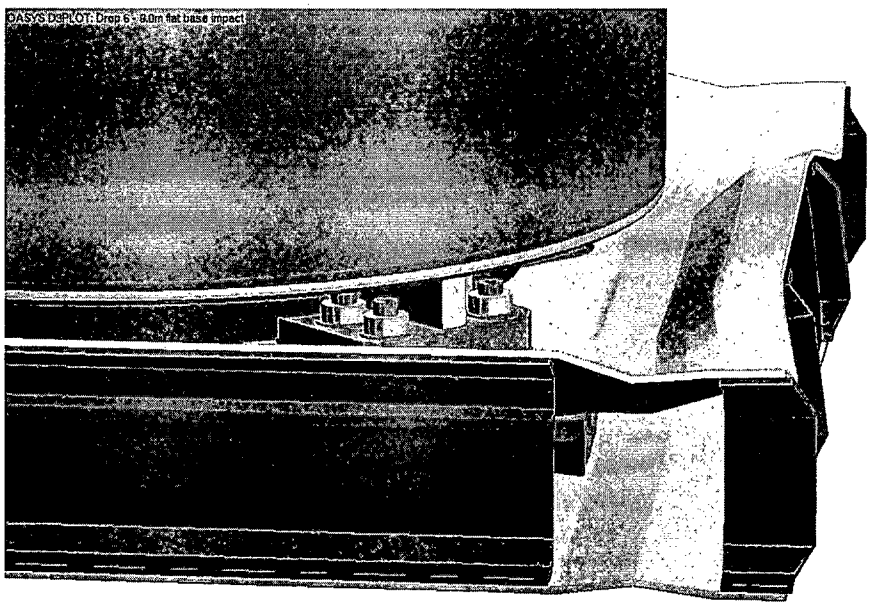

0.020275

Figure 26: Drop 6 – comparison 4

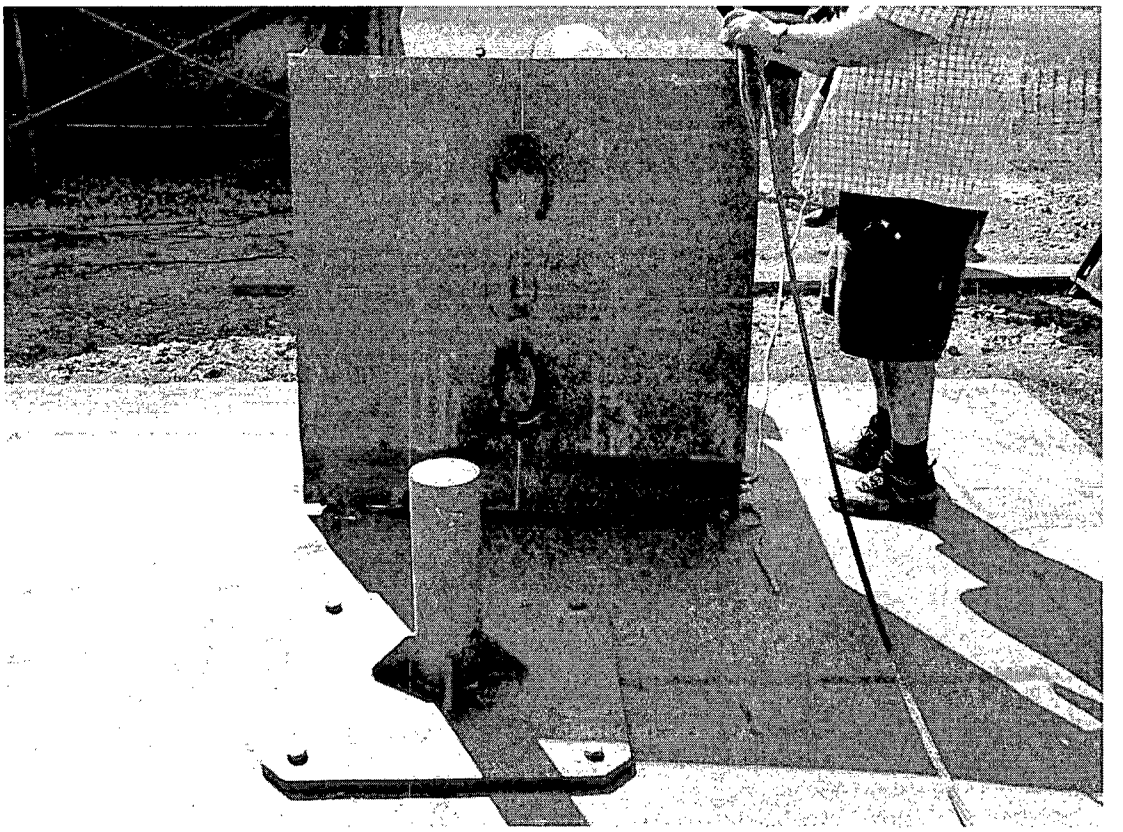

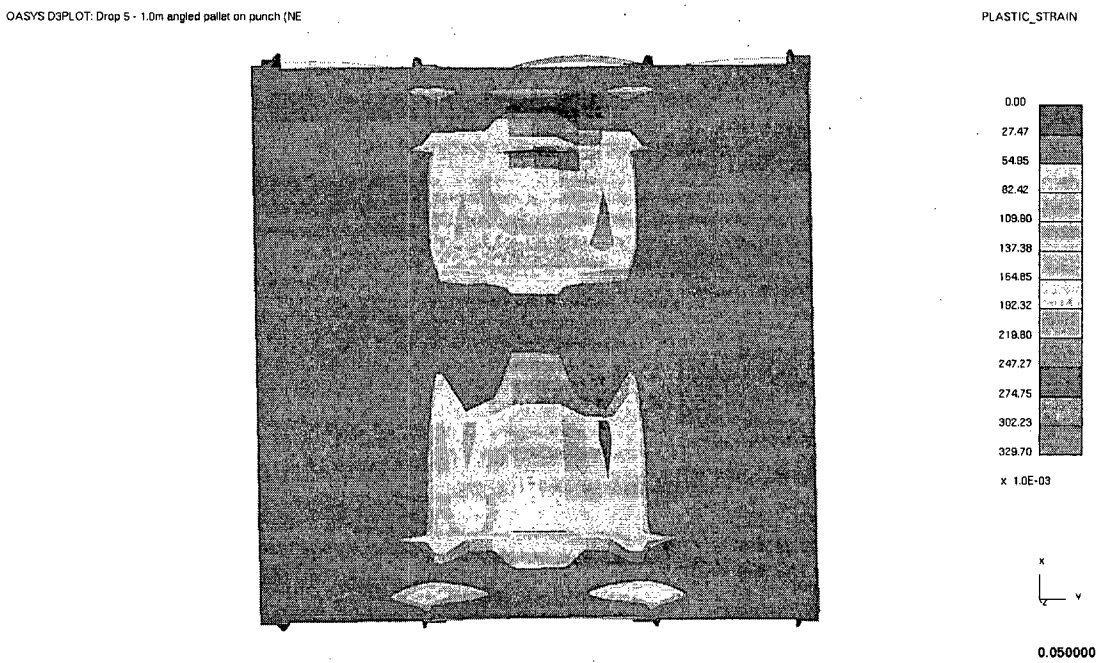

Figure 27: Drop 7 – comparison 1

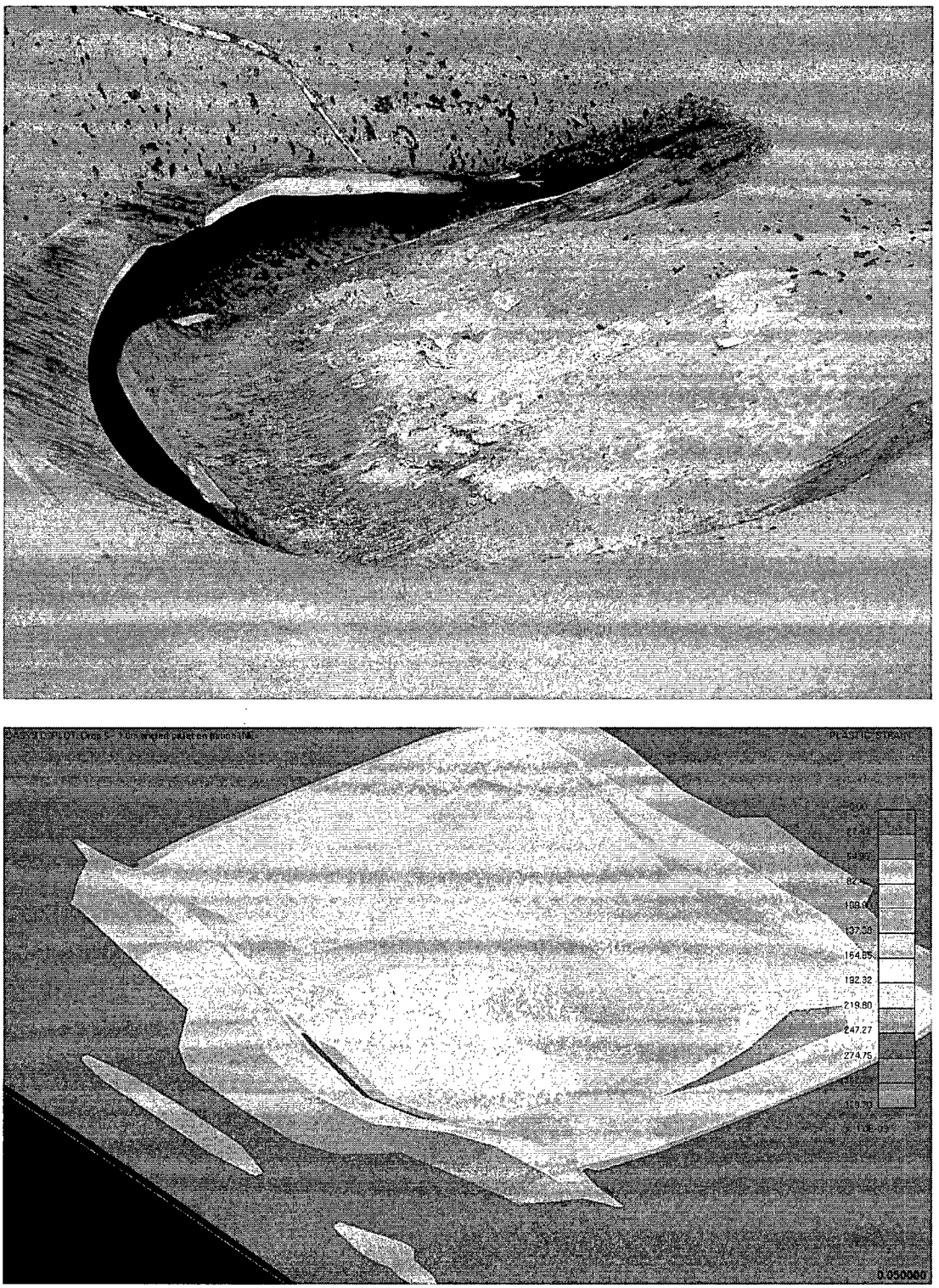

Figure 28: Drop 7 – comparison 2

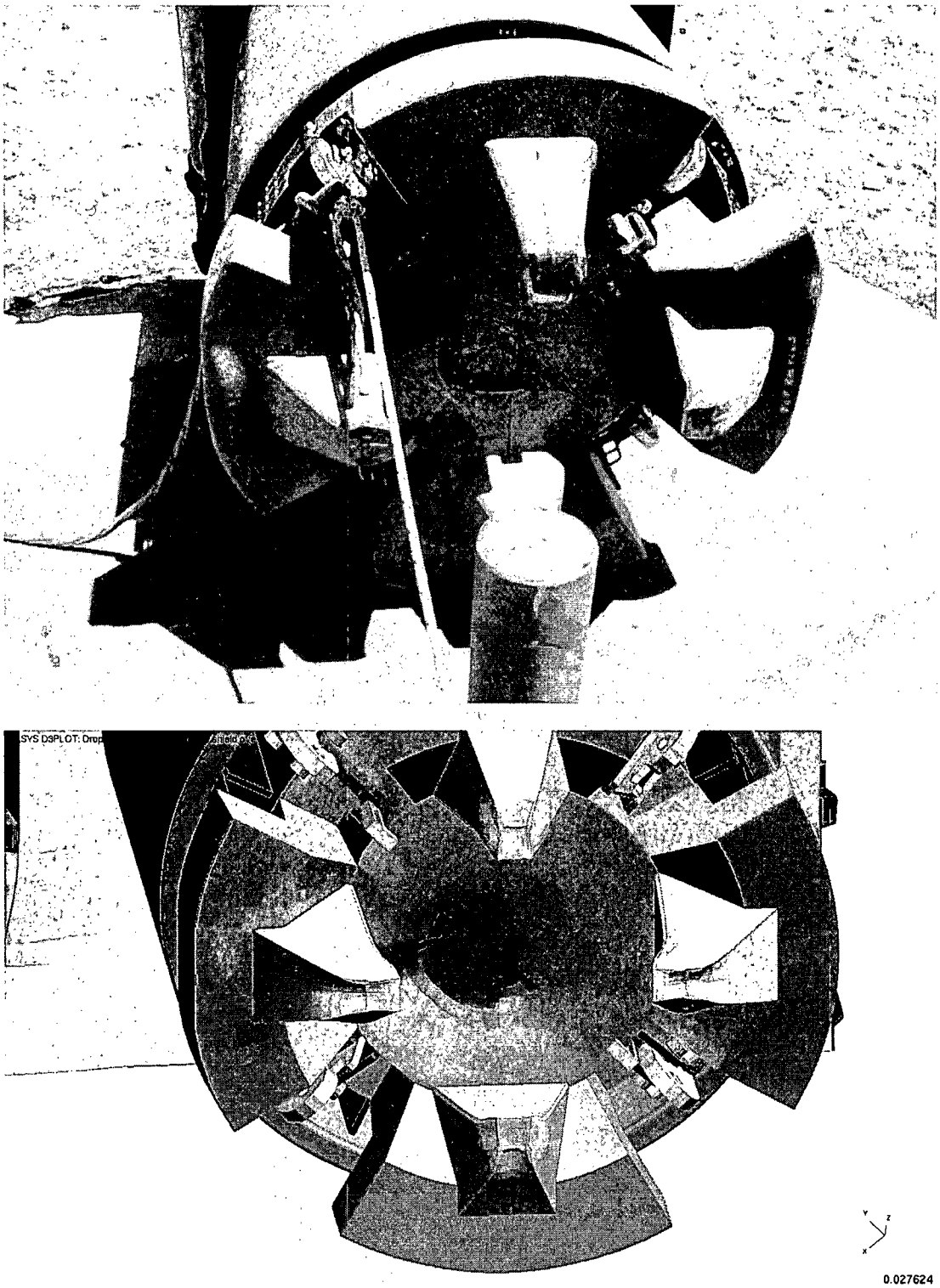

Figure 29: Drop 8 – comparison 1

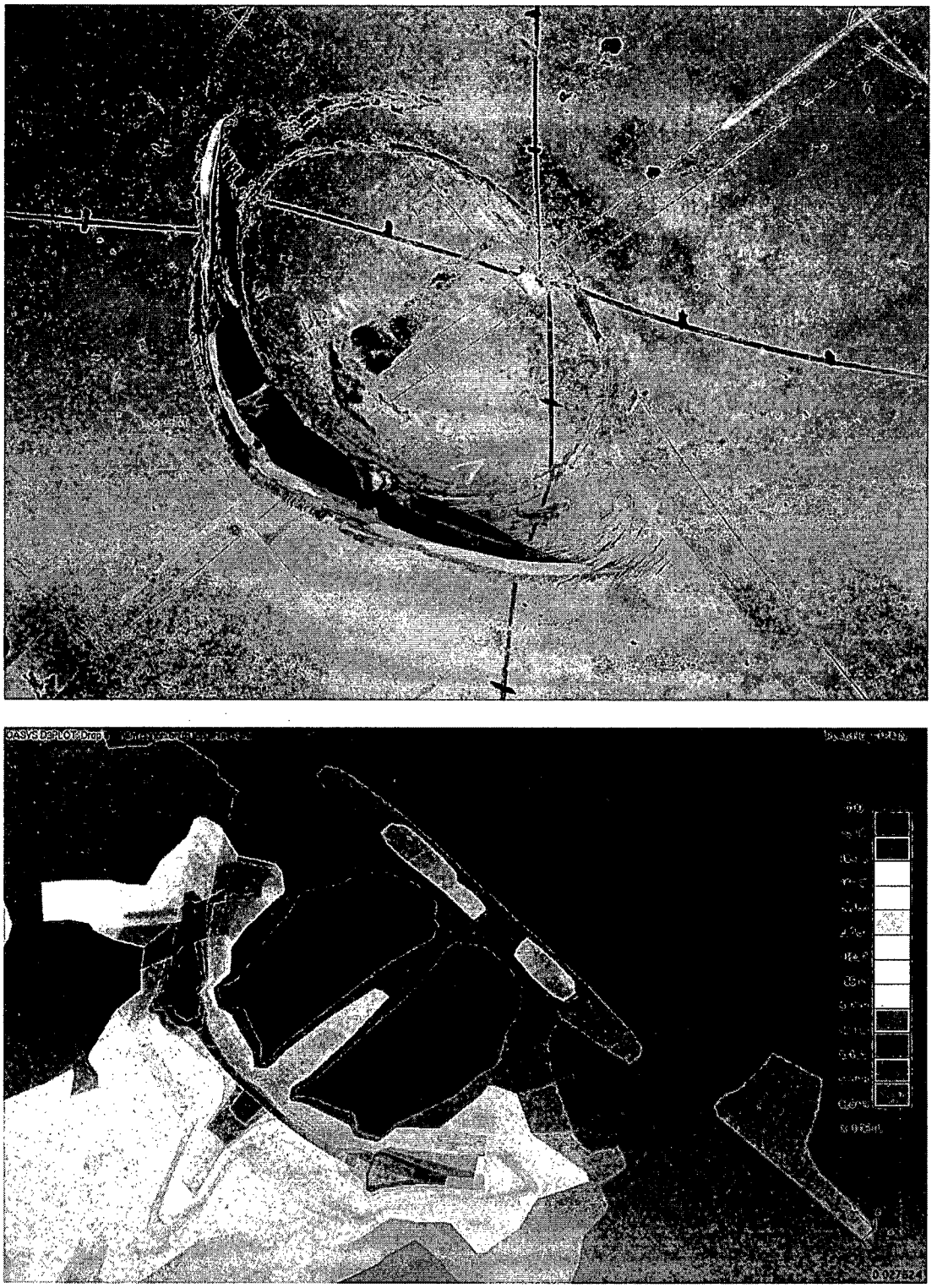

Figure 30: Drop 8 – comparison 2

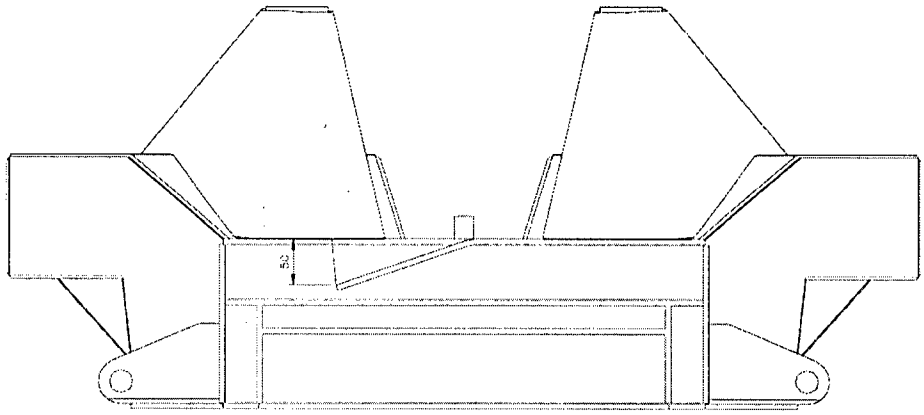

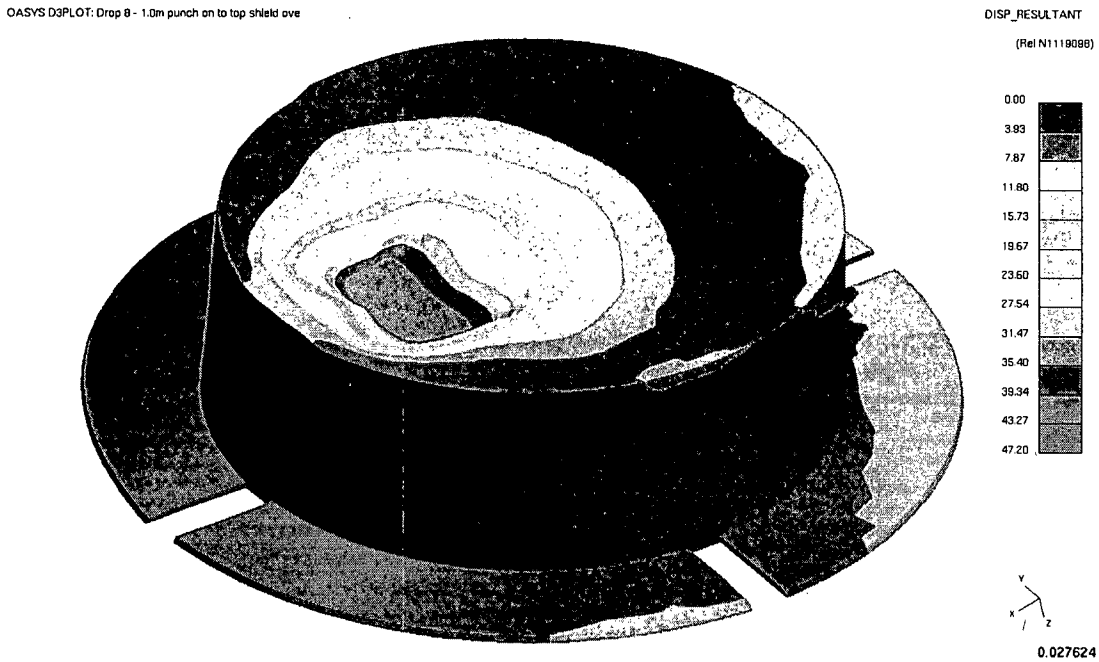

Figure 31: Drop 8 – comparison 3

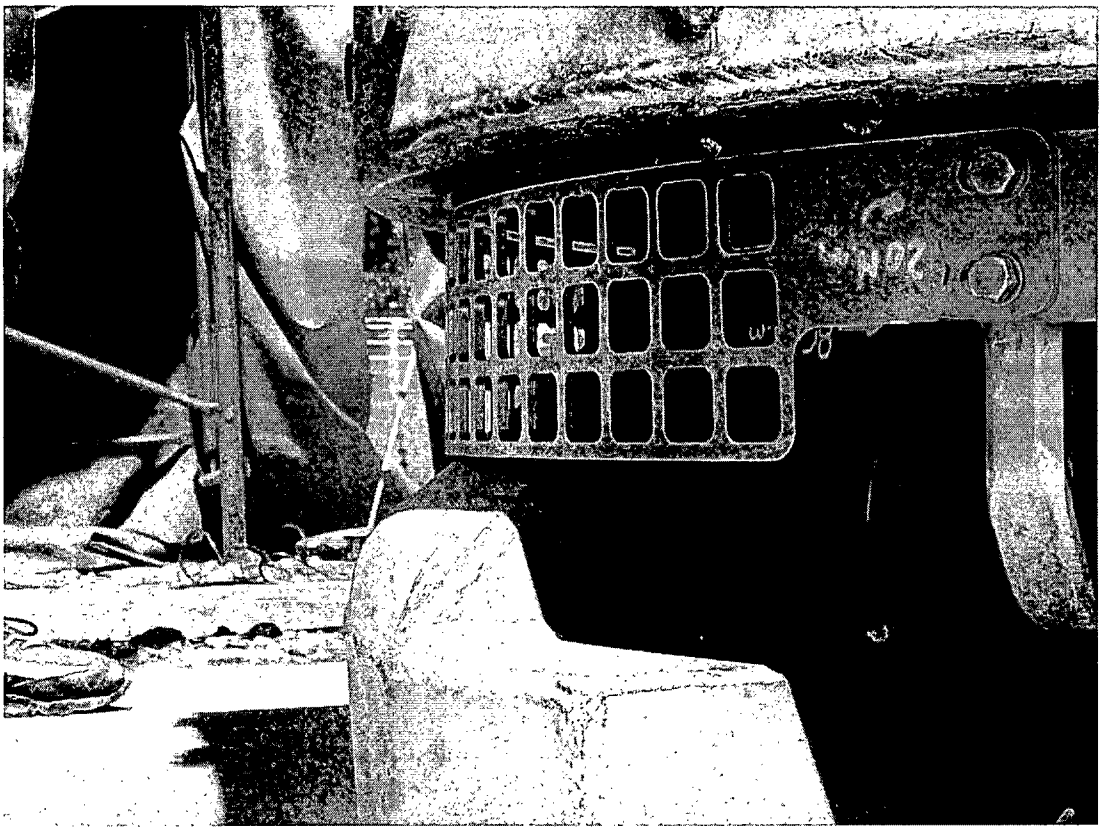

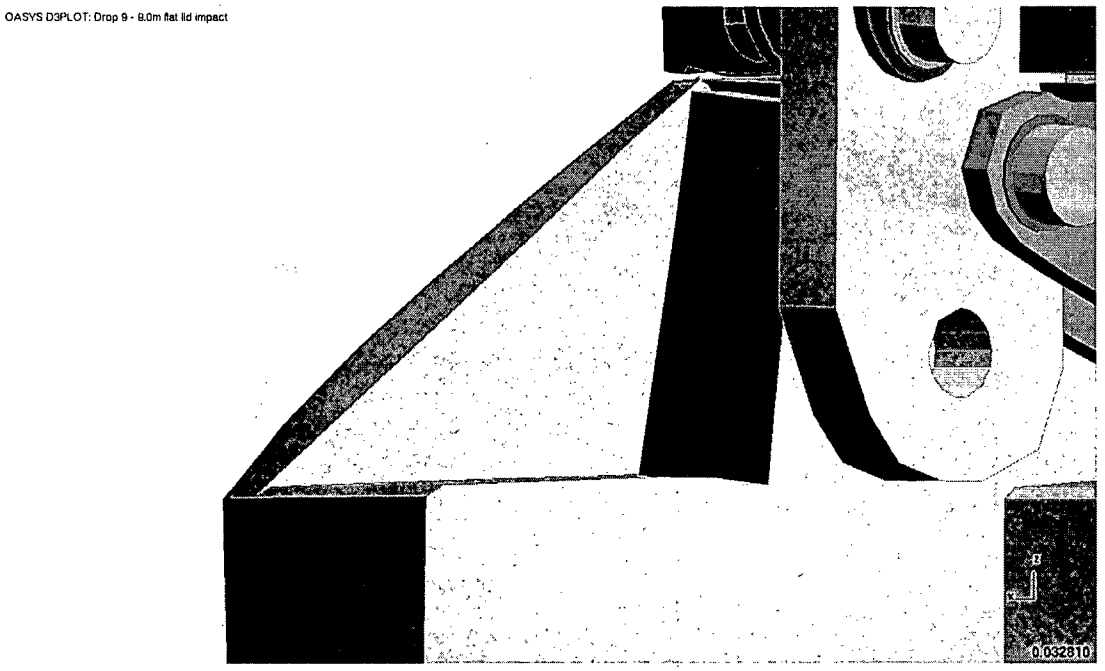

Figure 32: Drop 9 – comparison 1

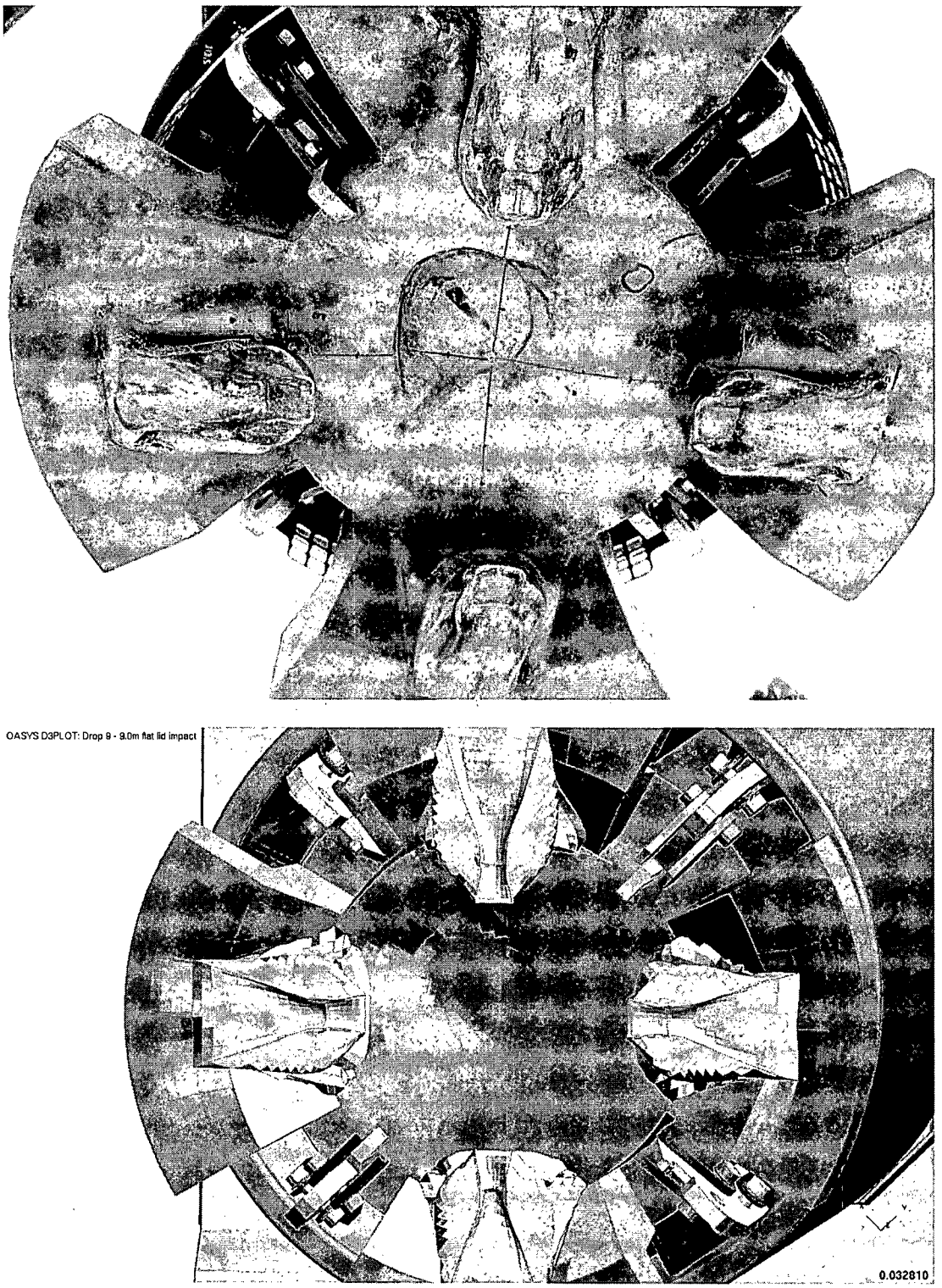

Figure 33: Drop 9 – comparison 2

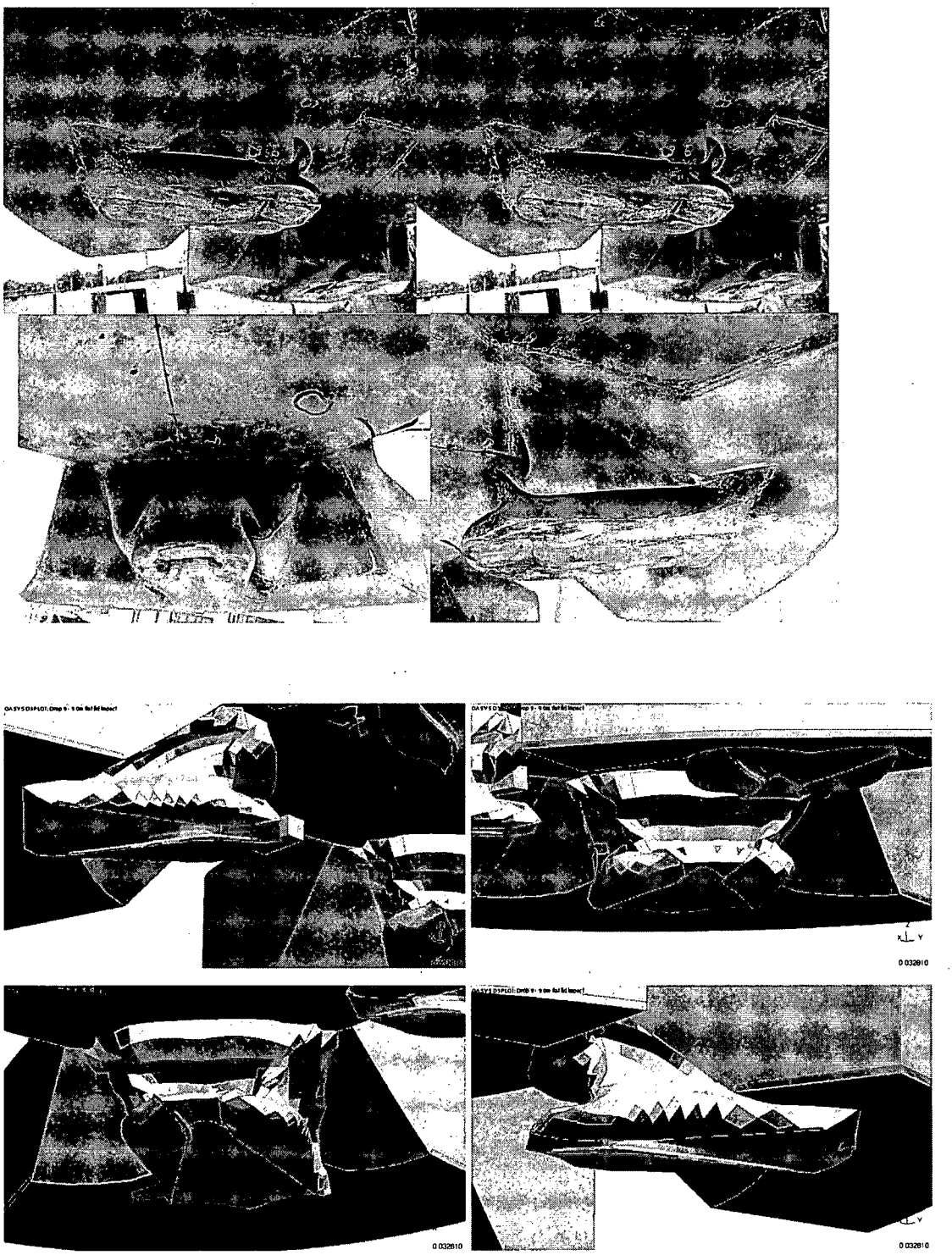

Figure 34: Drop 9 – comparison 3

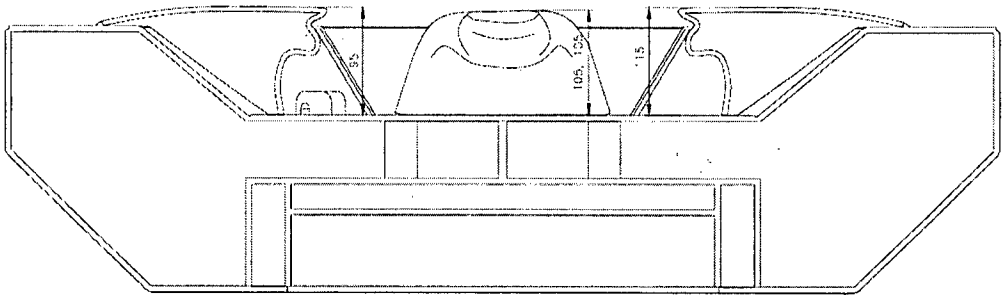

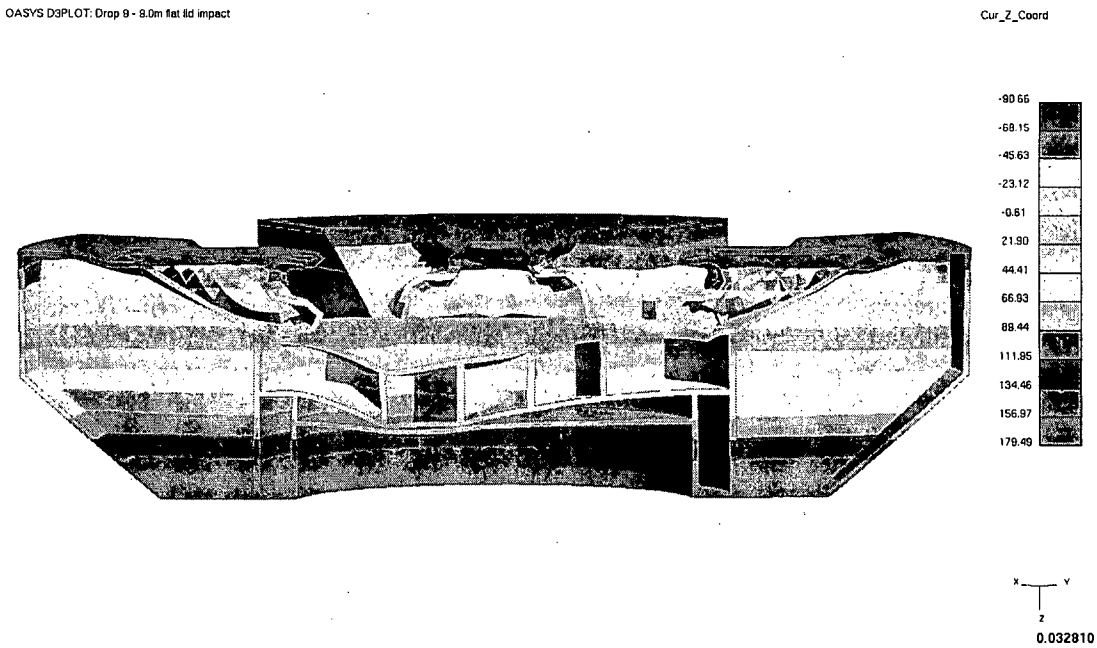

Figure 35: Drop 9 – comparison 4

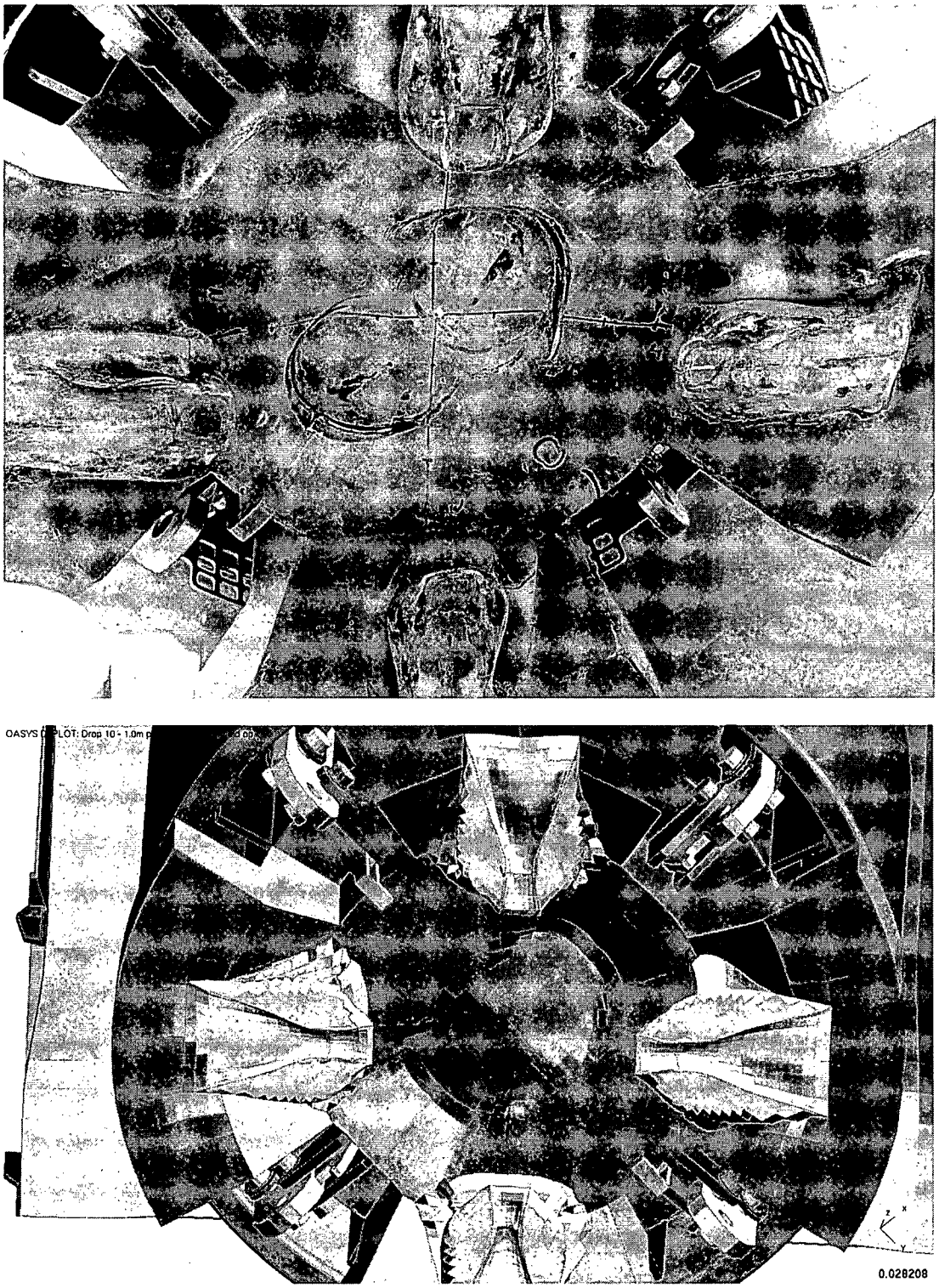

Figure 36: Drop 10 – comparison 1

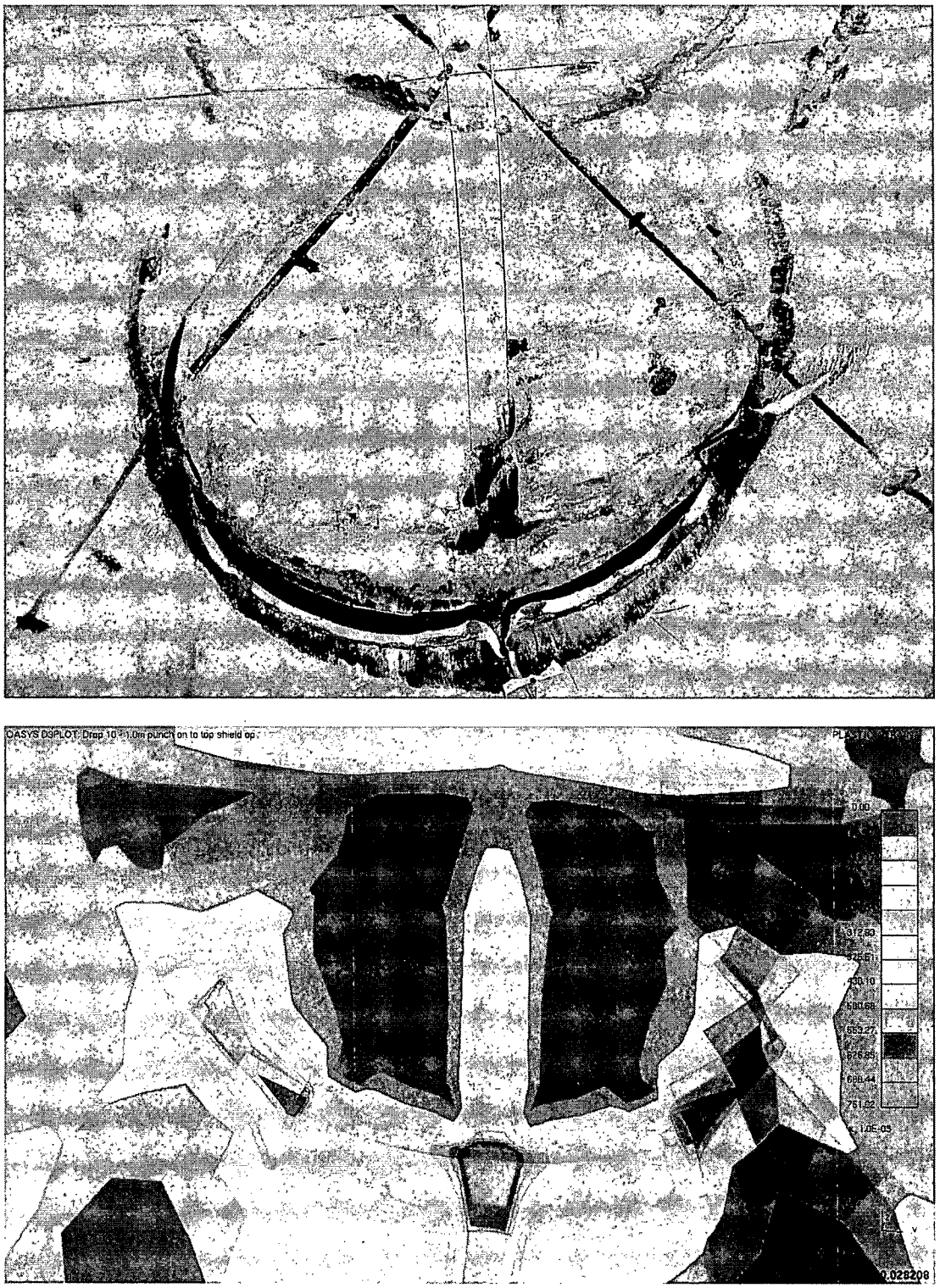

Figure 37: Drop 10 – comparison 2

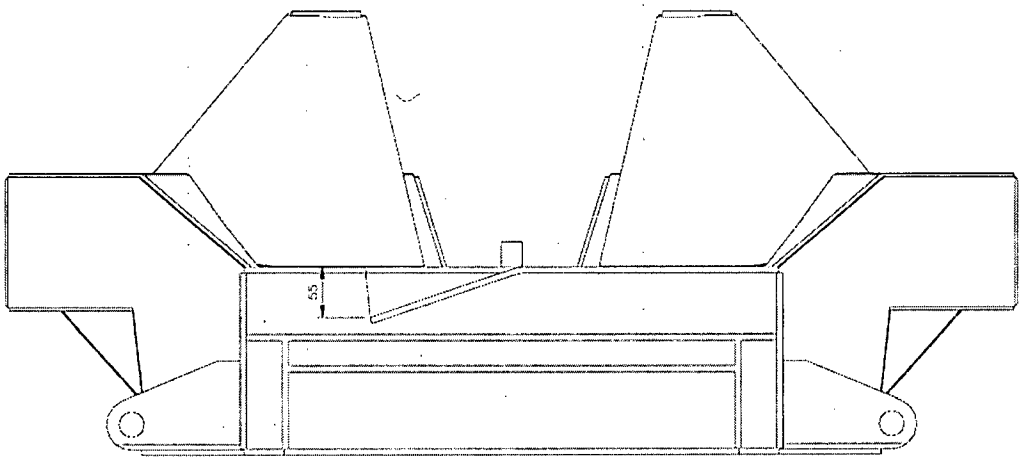

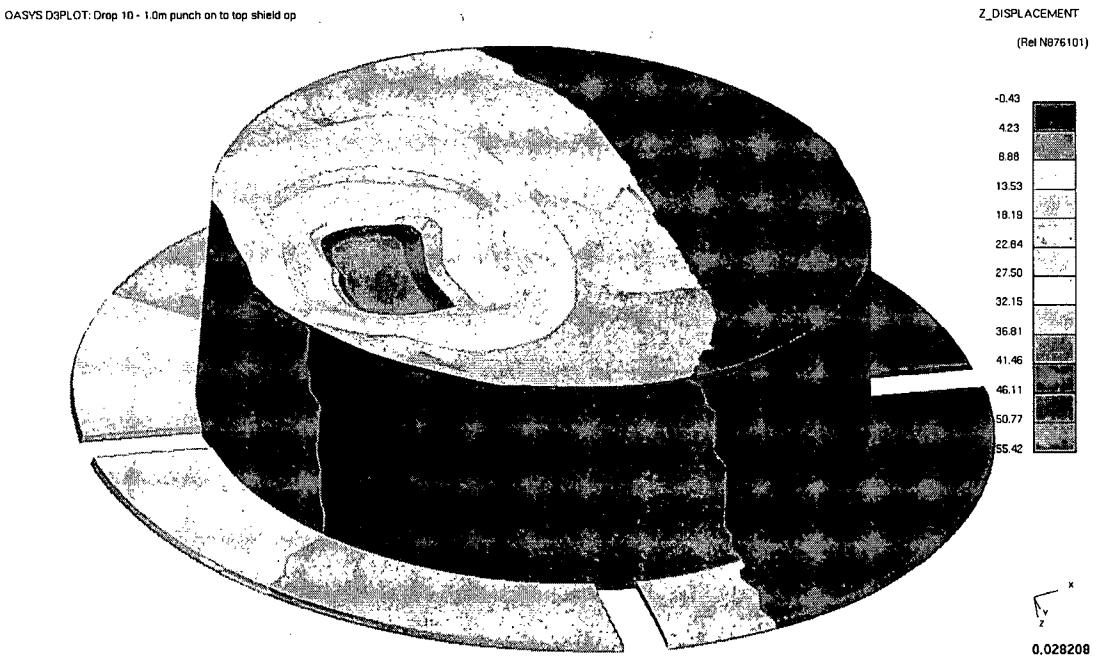

Figure 38: Drop 10 – comparison 3

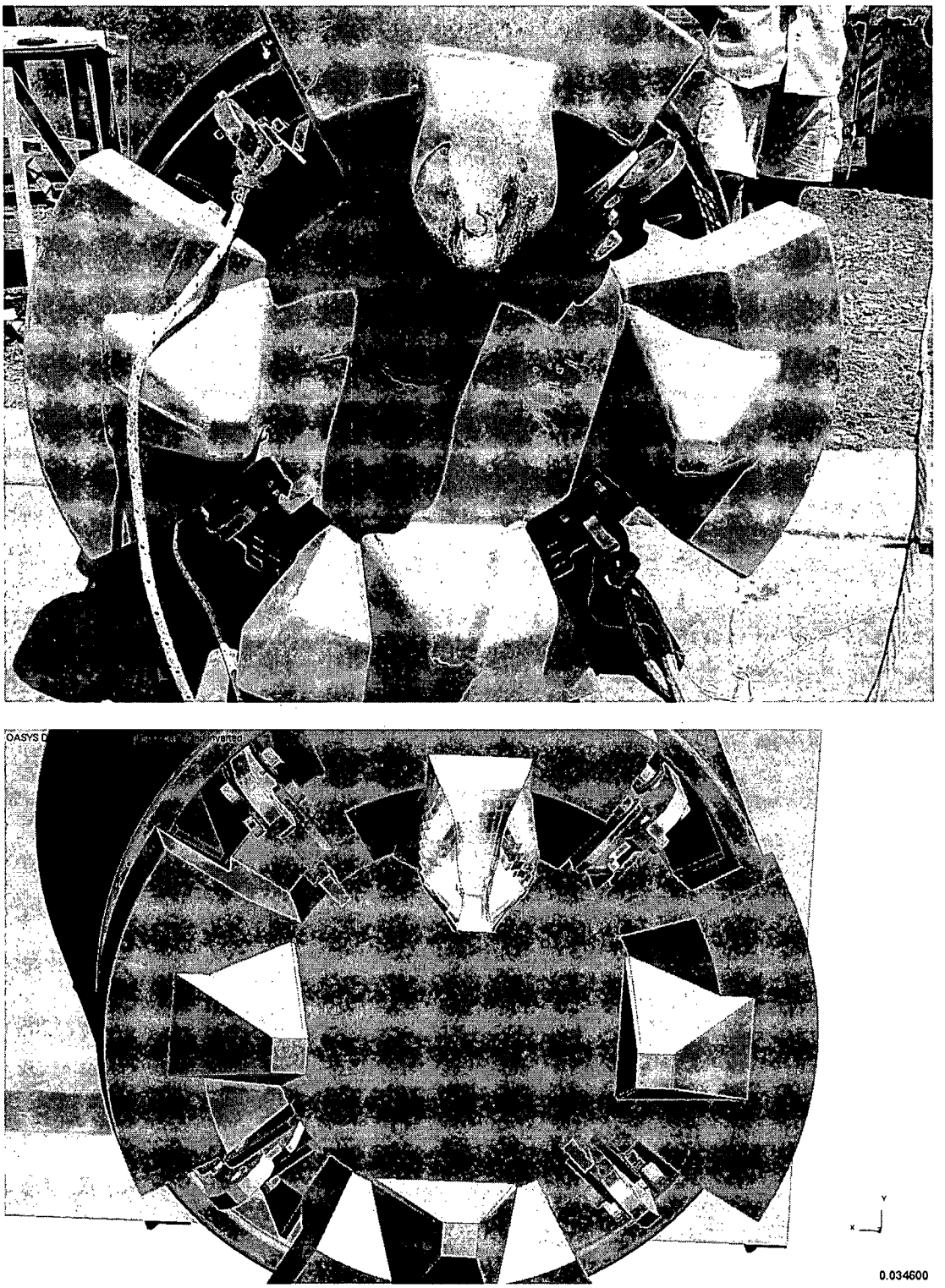

Figure 39: Drop 11 – comparison 1

Figure 40: Drop 11 – comparison 2

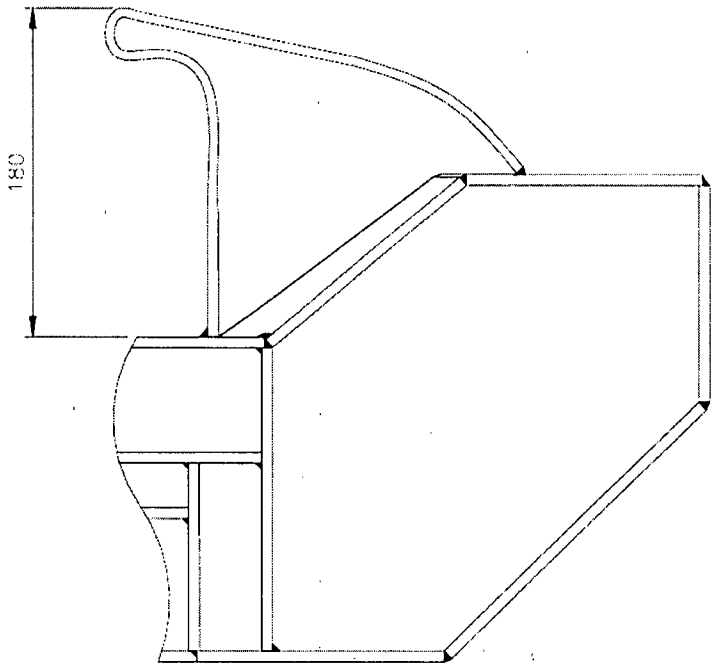

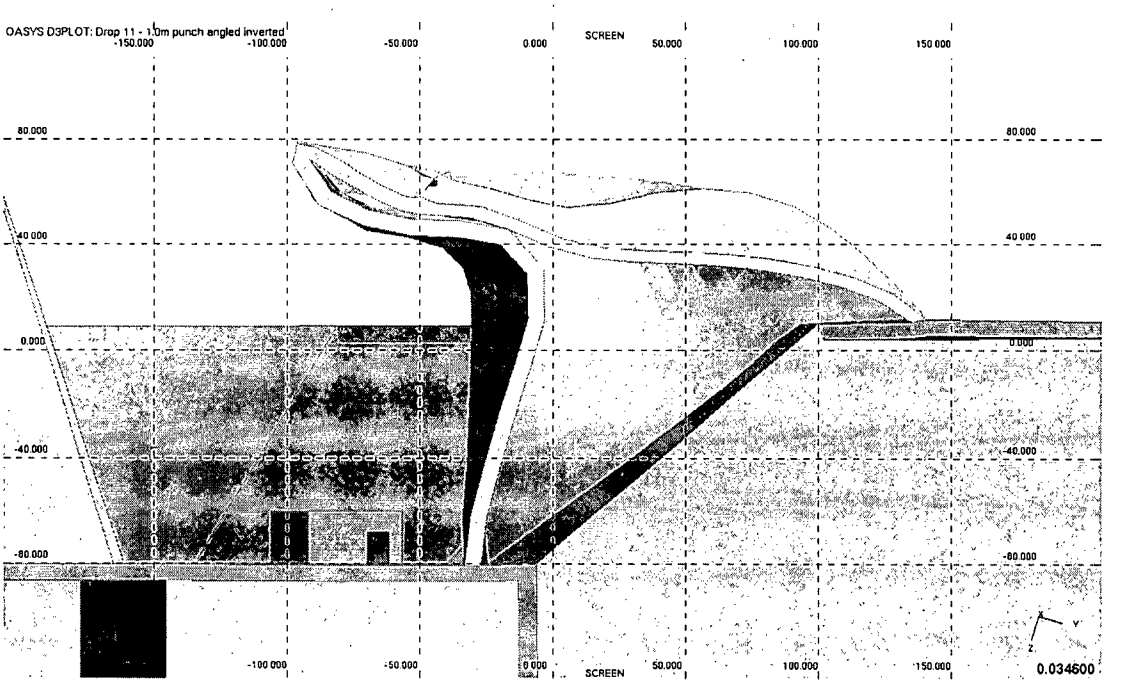

Figure 41: Drop 11 – comparison 3

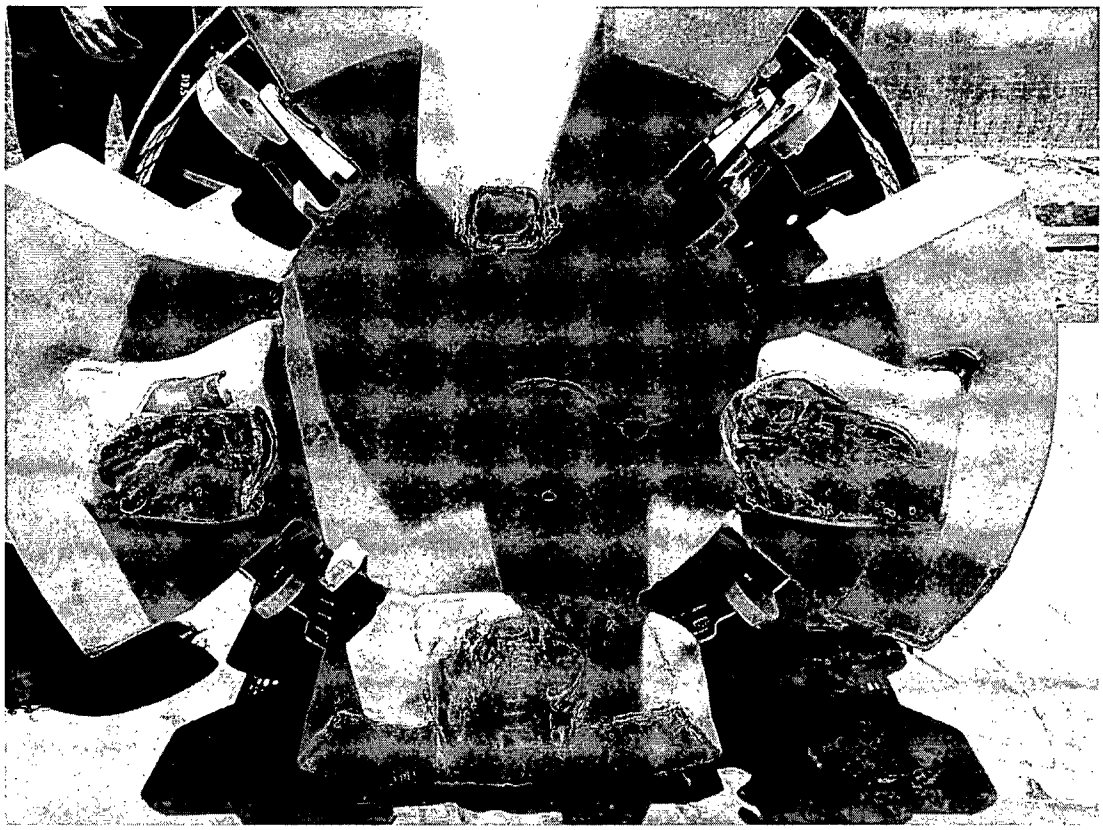

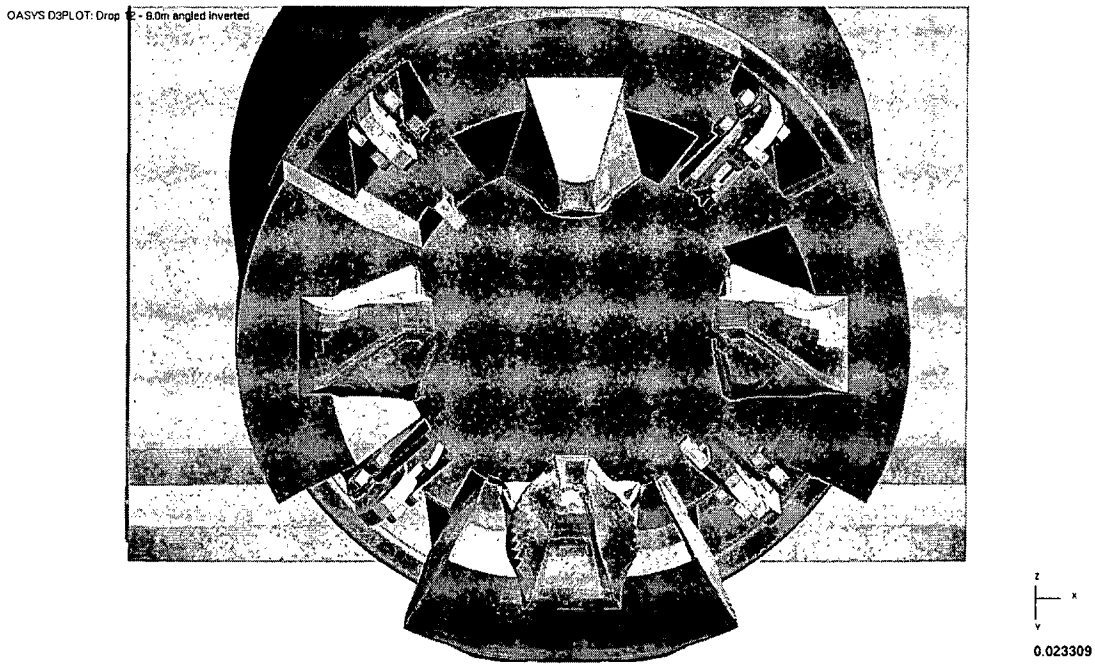

Figure 42: Drop 12 – comparison 1

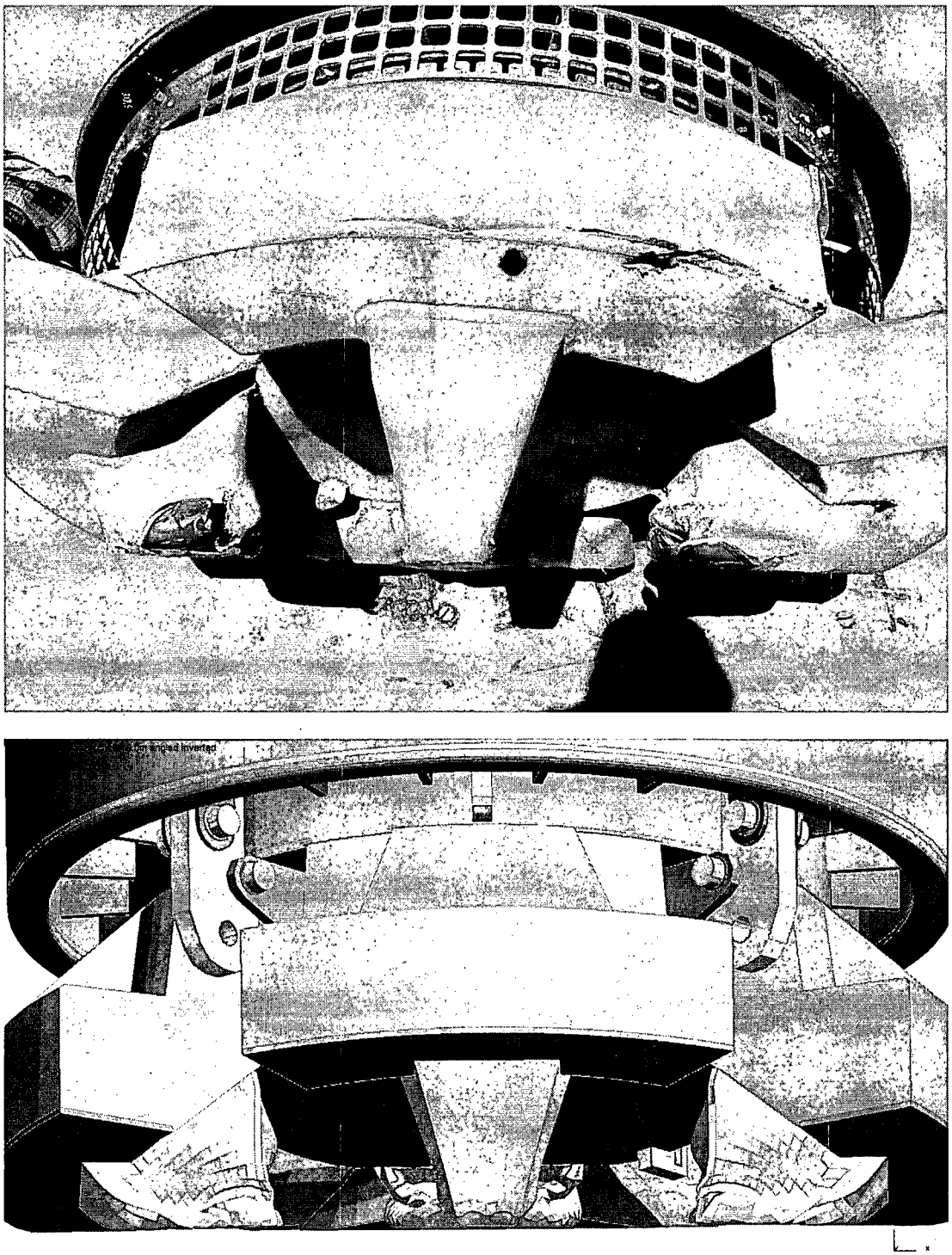

0.023309

Figure 43: Drop 12 – comparison 2

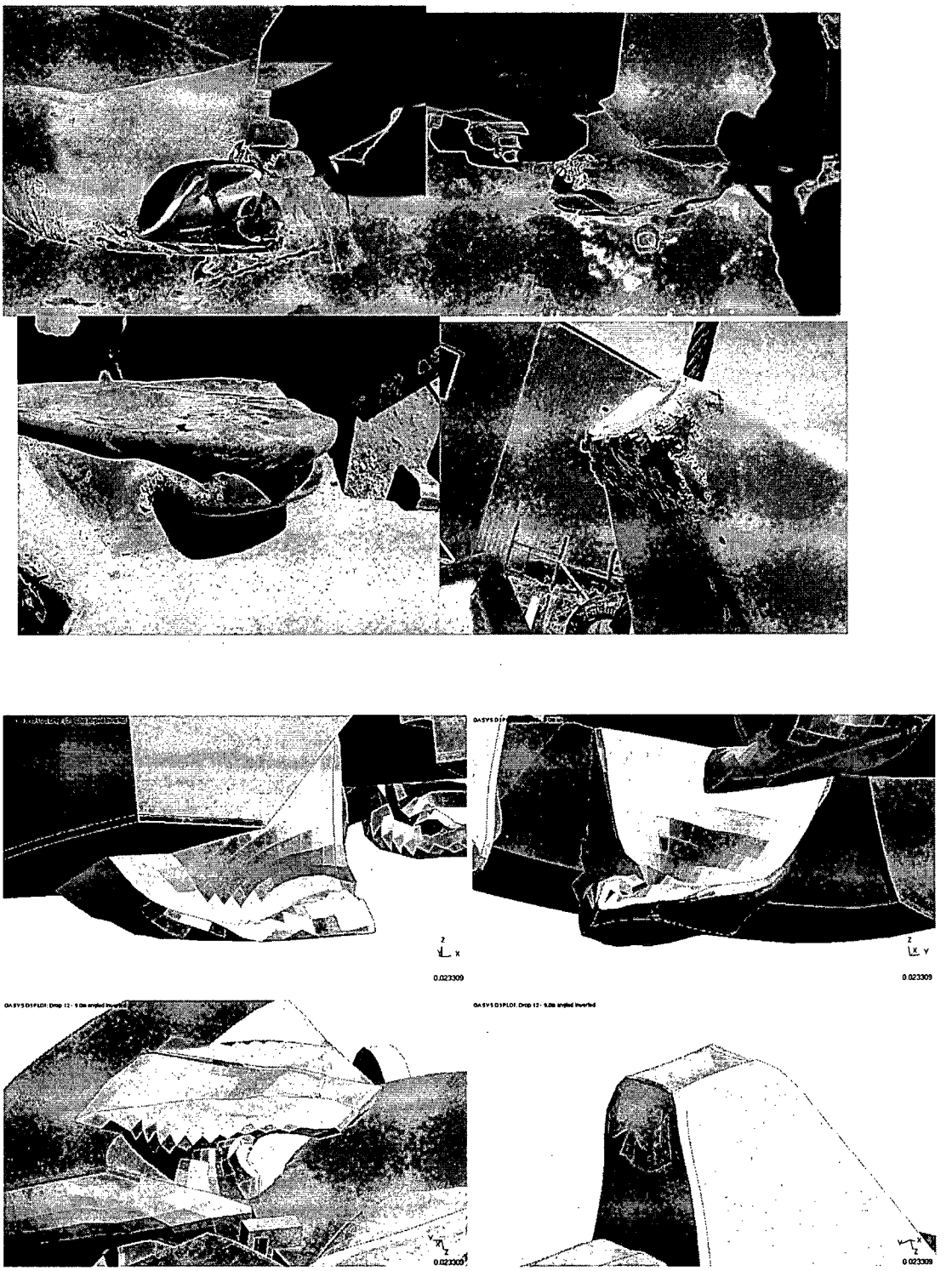

Figure 44: Drop 12 – comparison 3

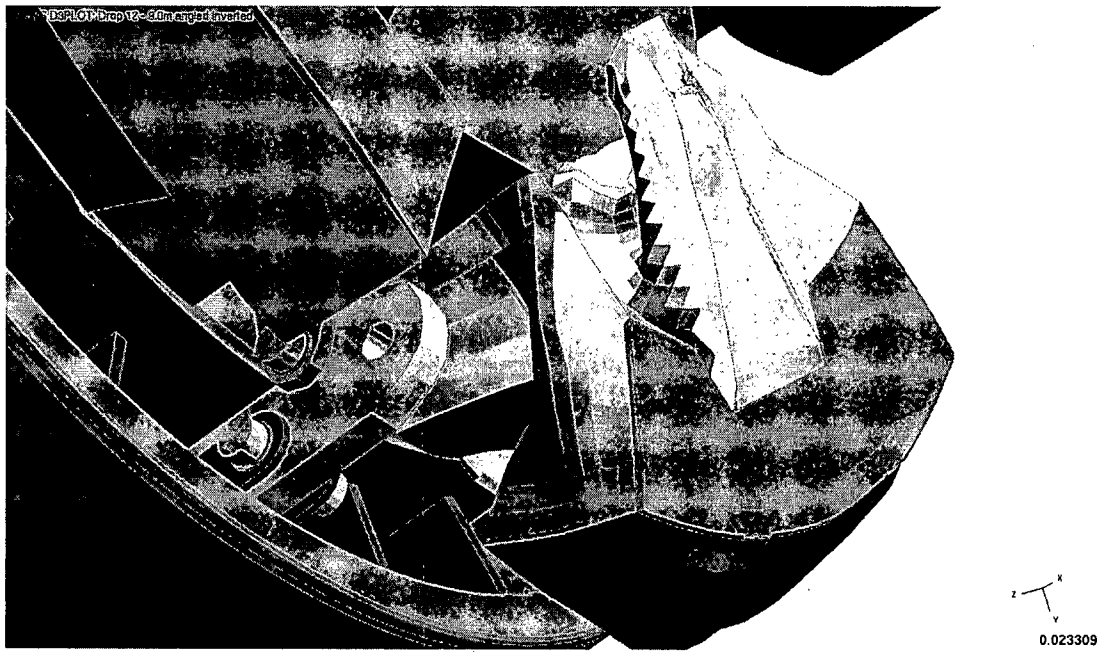

Figure 45: Drop 12 – comparison 4

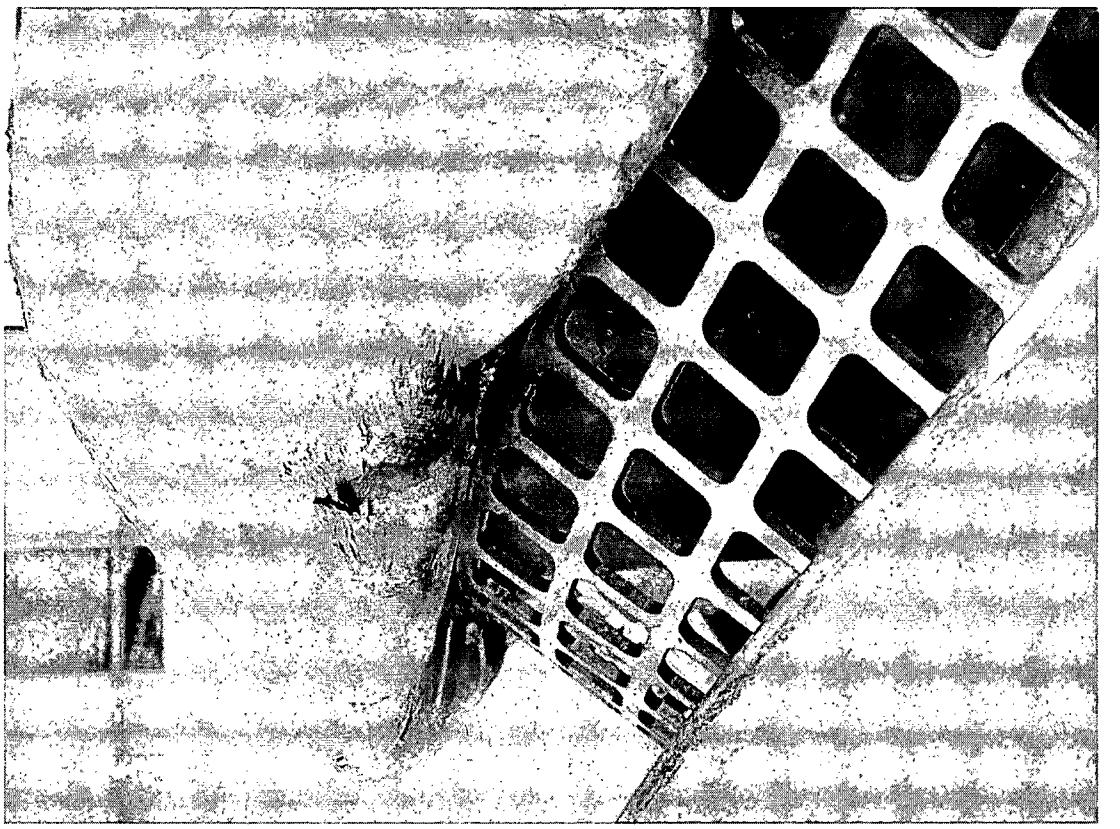

OASYS D3PLOT: Drop 12 - 9.0m angled inverted

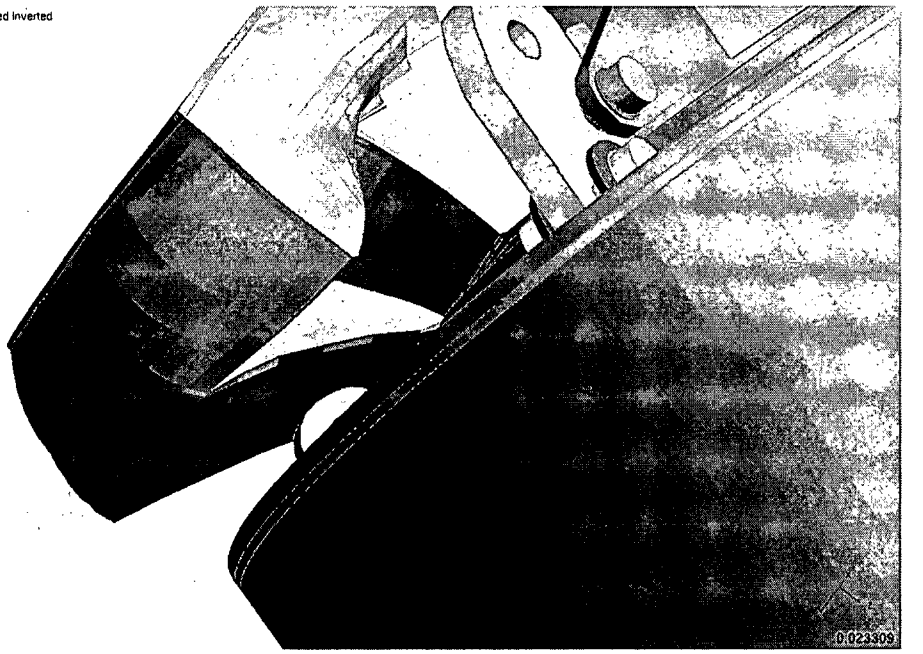

Figure 46: Drop 12 – comparison 5

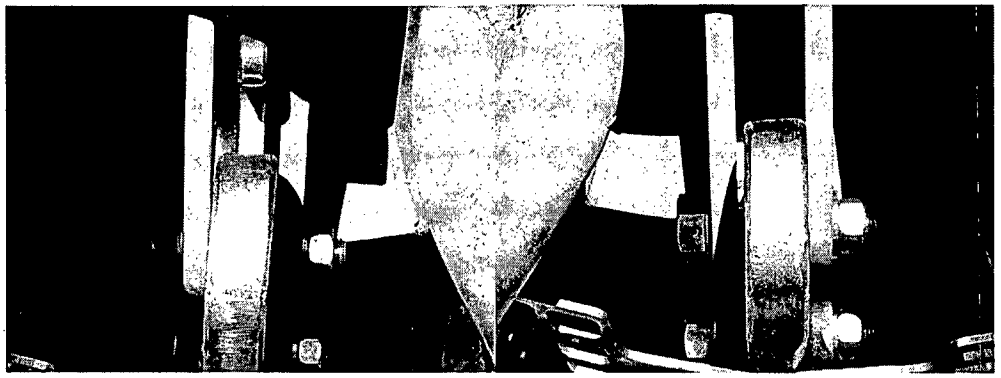

Figure 47: Drop 12 – comparison 6

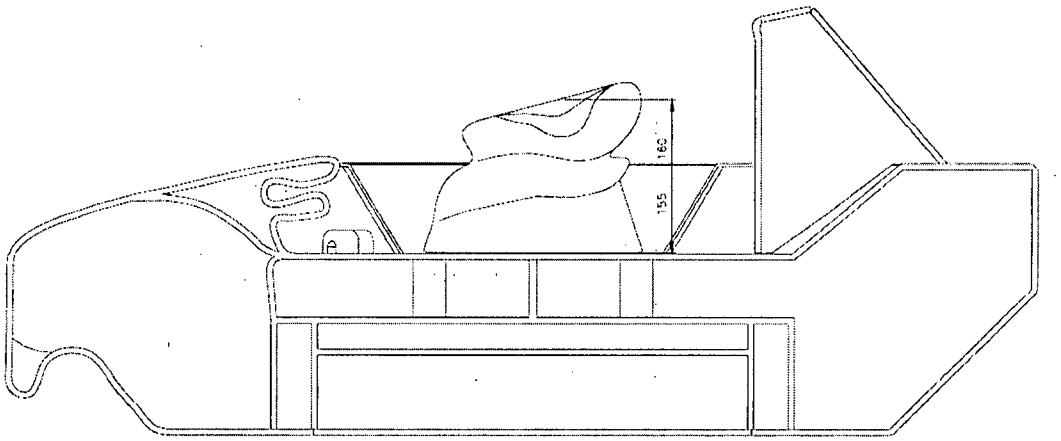

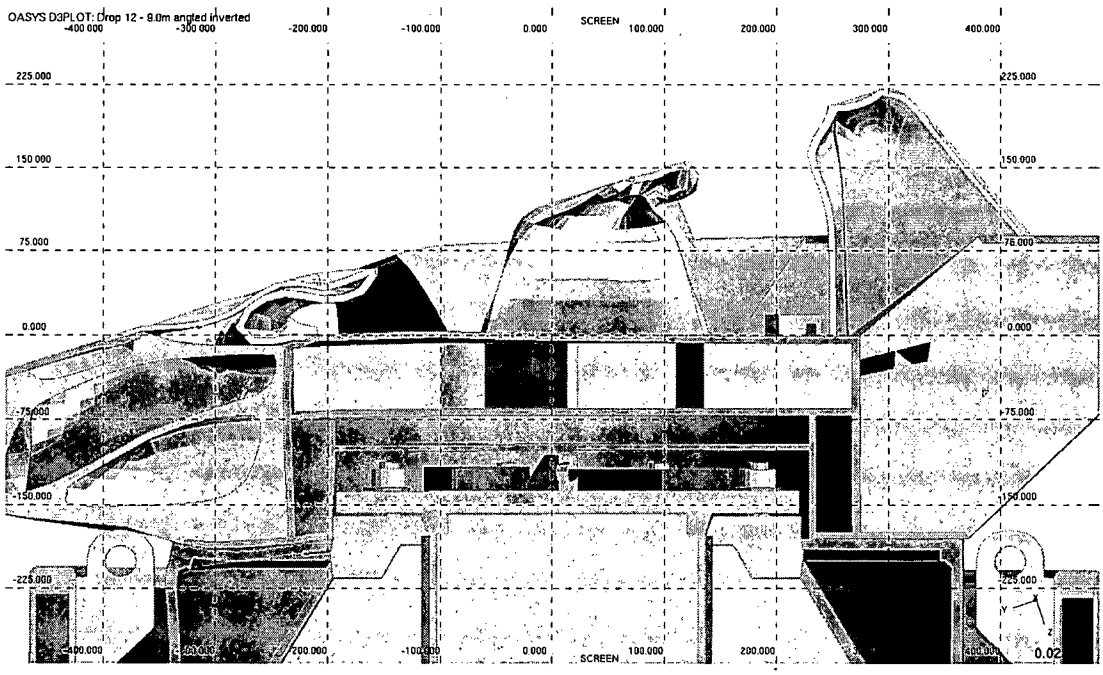

Figure 48: Drop 12 – comparison 7

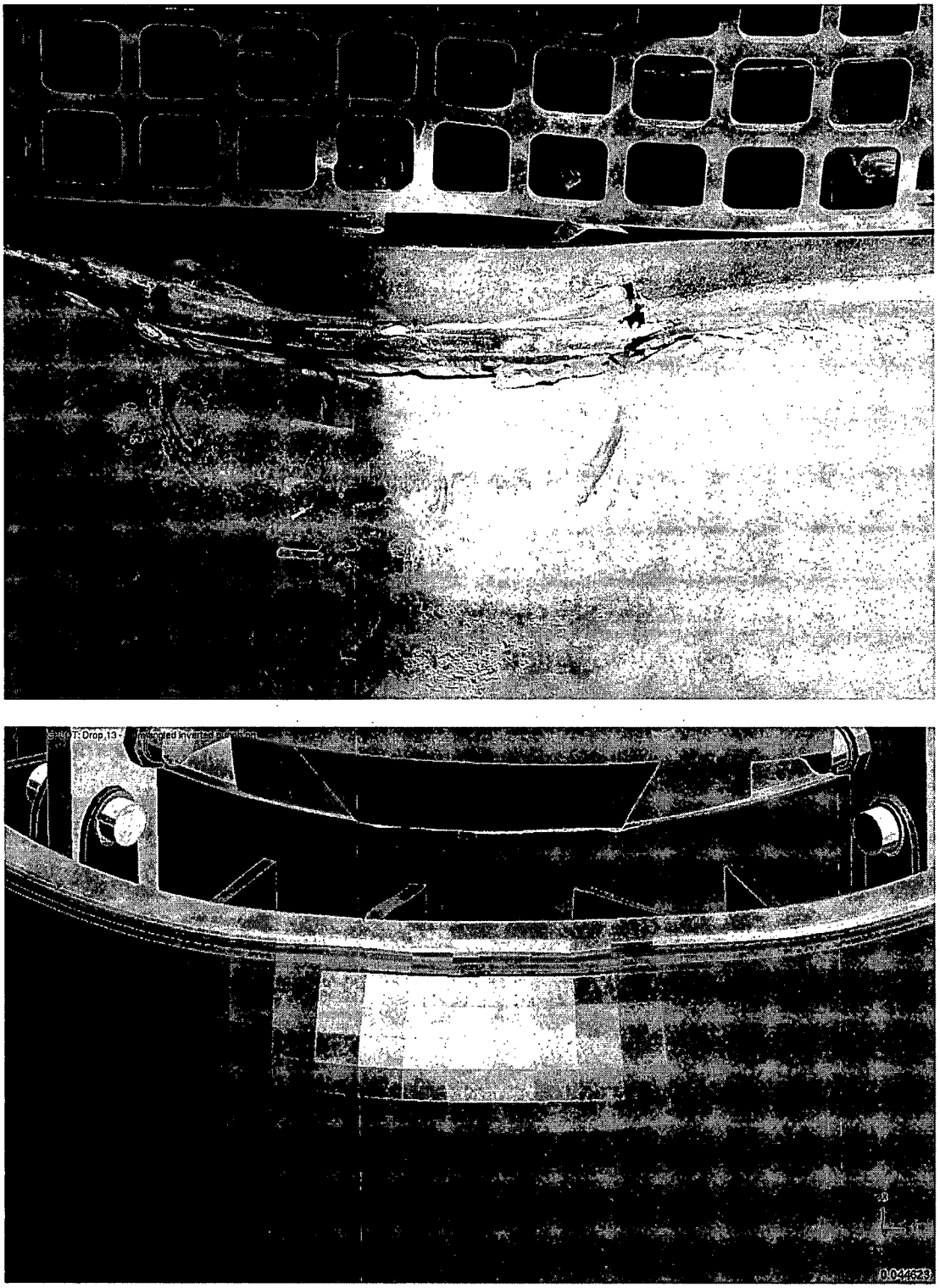

Figure 49: Drop 13 – comparison 1

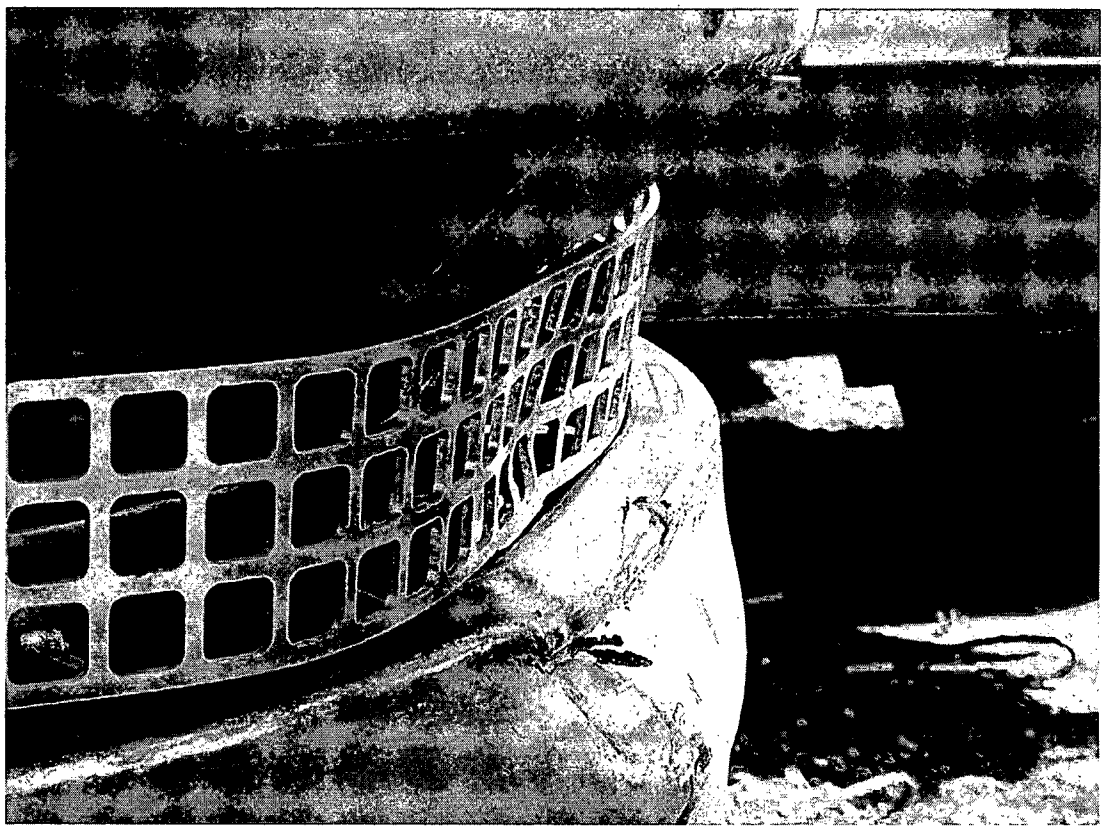

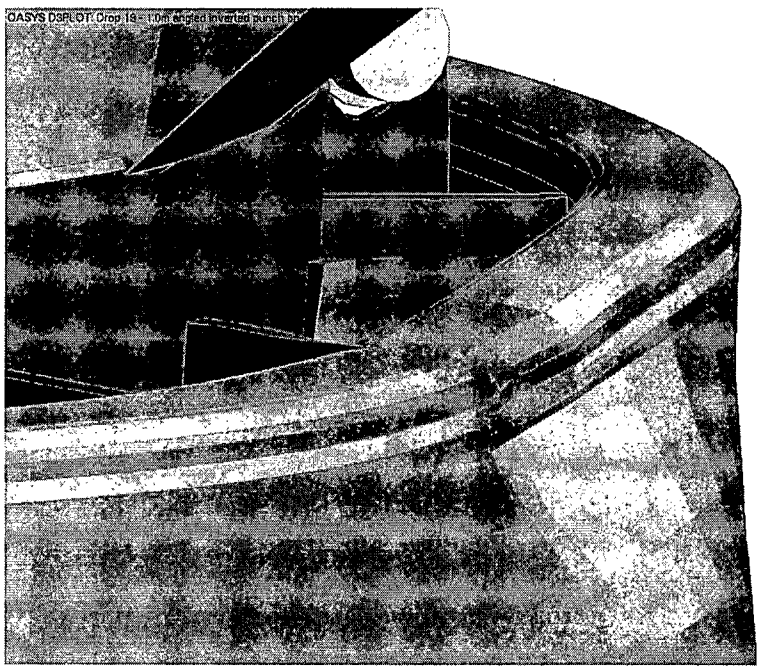

Figure 50: Drop 13 – comparison 2

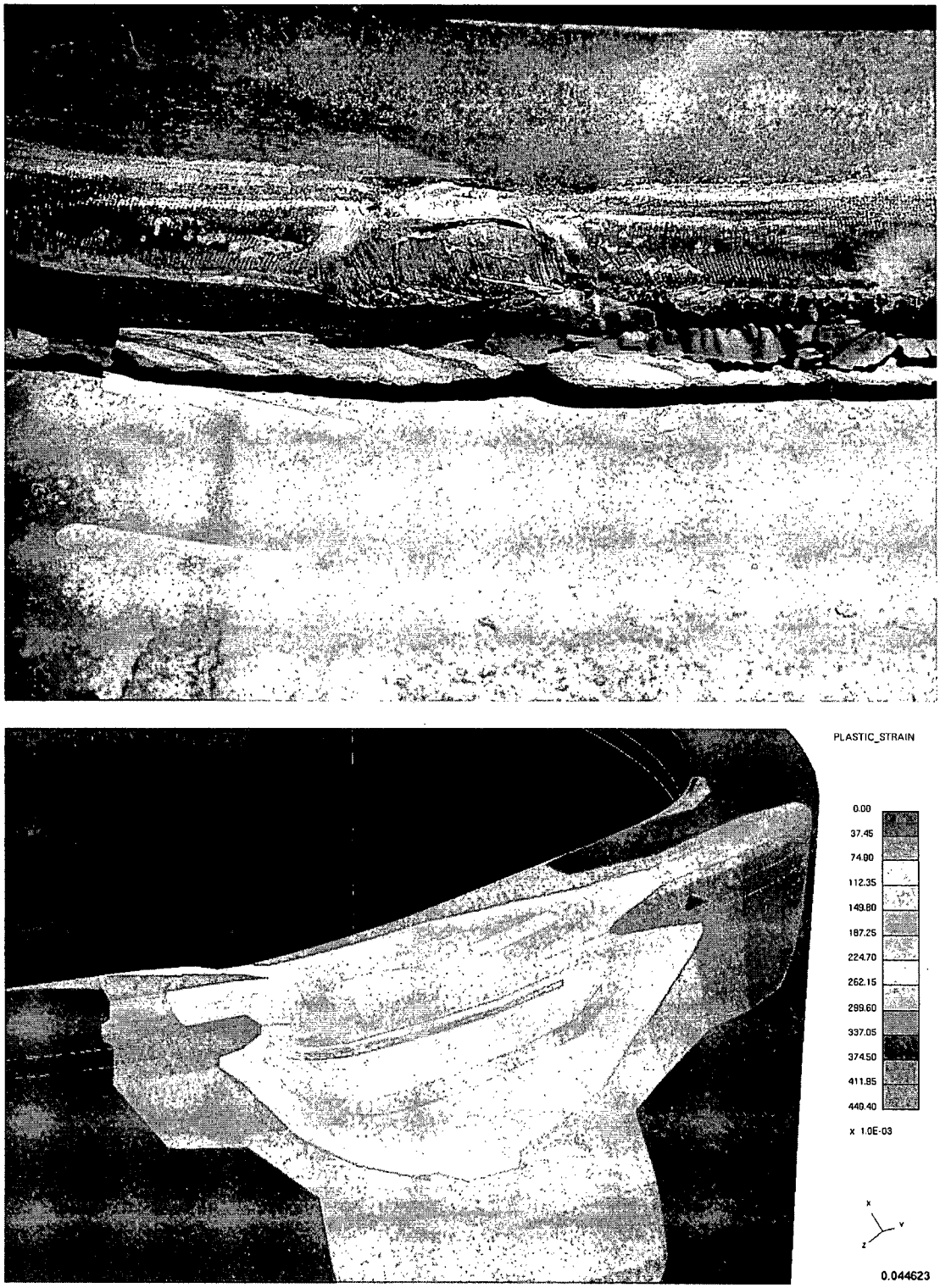

Figure 51: Drop 13 – comparison 3

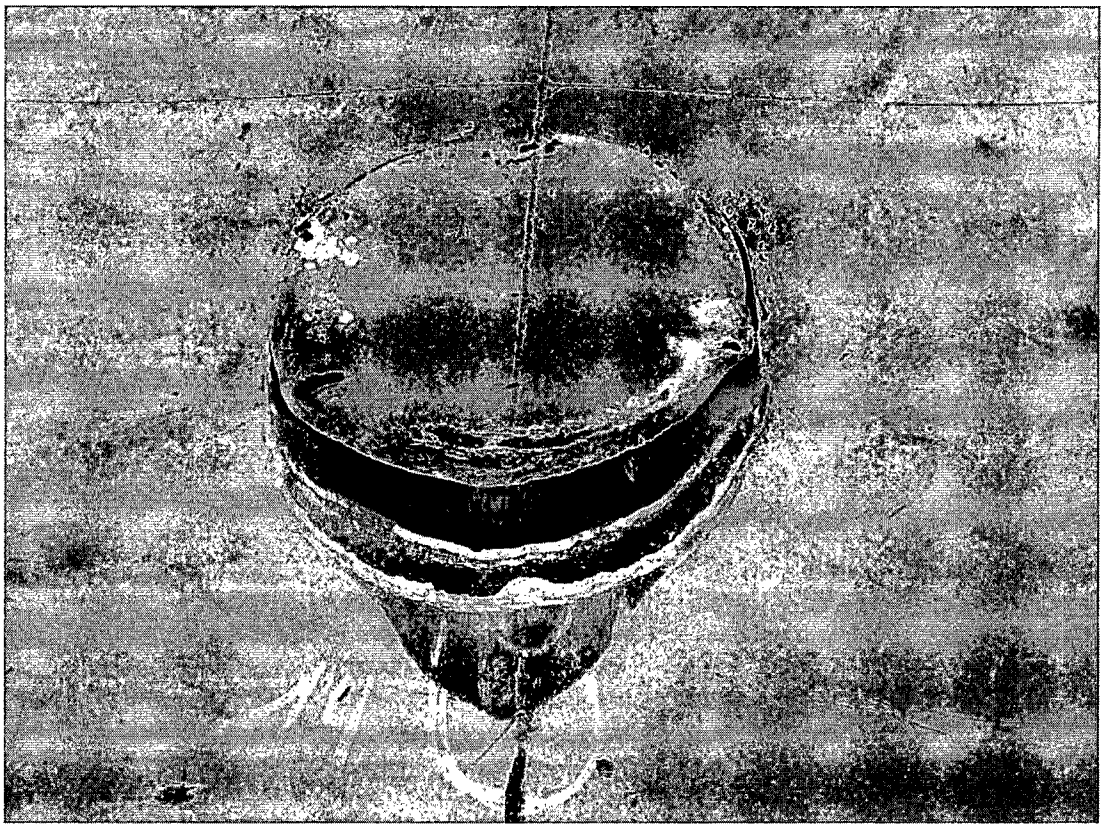

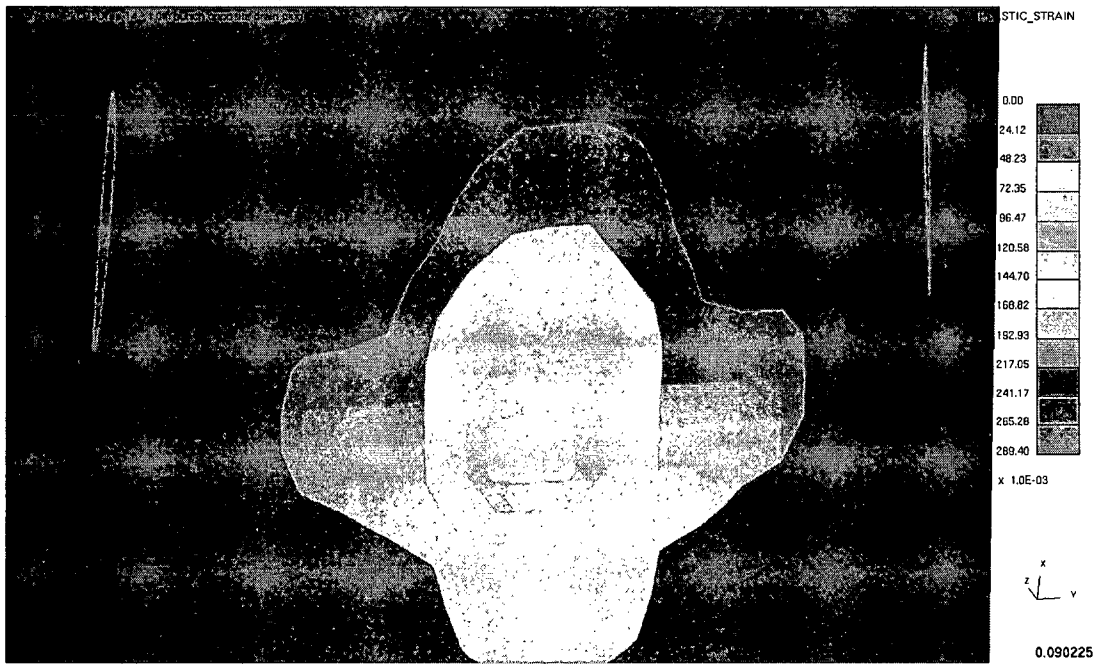

Figure 52: Drop 14 – comparison 1

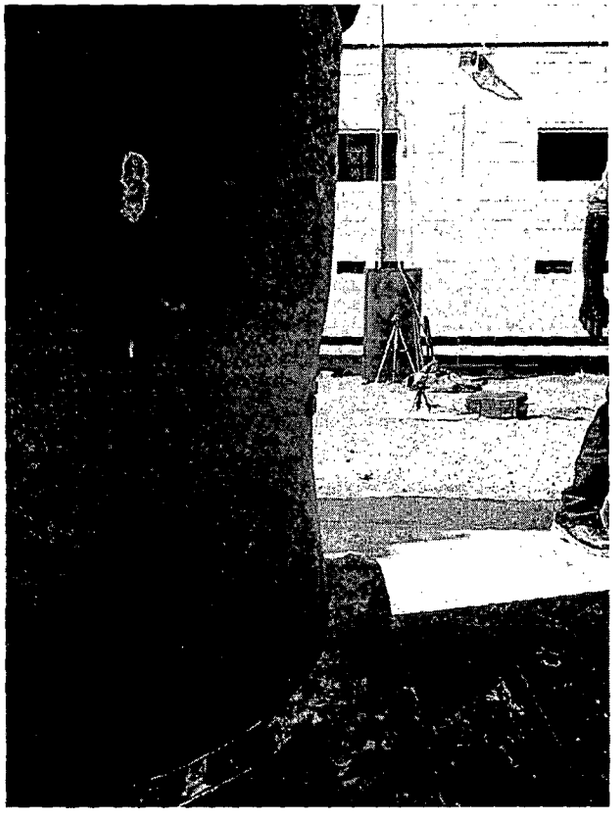

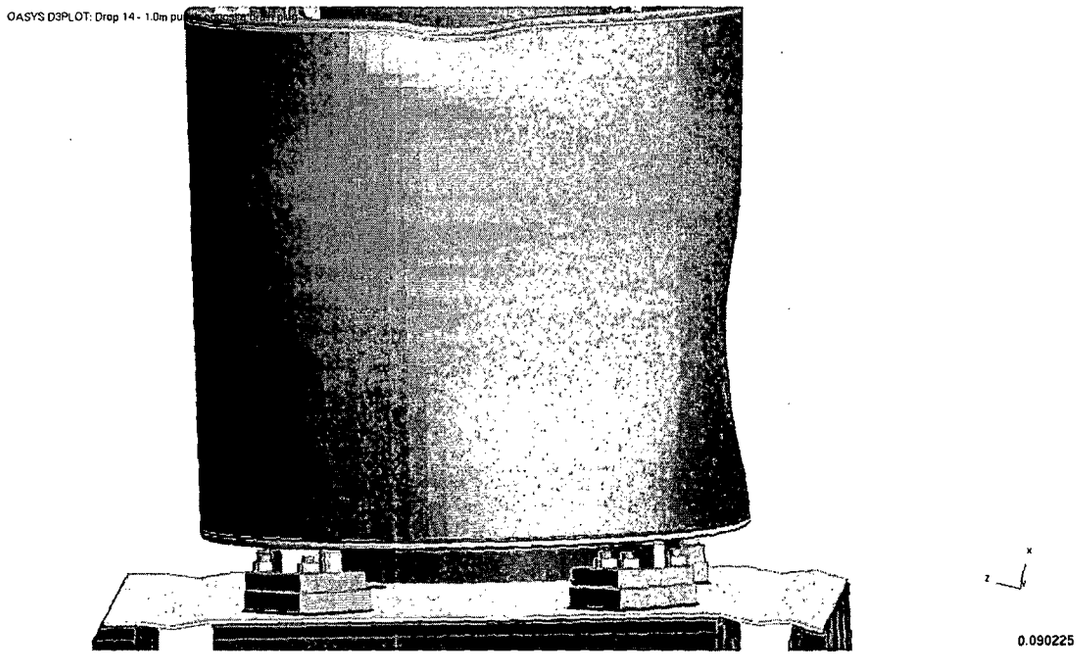

Figure 53: Drop 14 – comparison 2

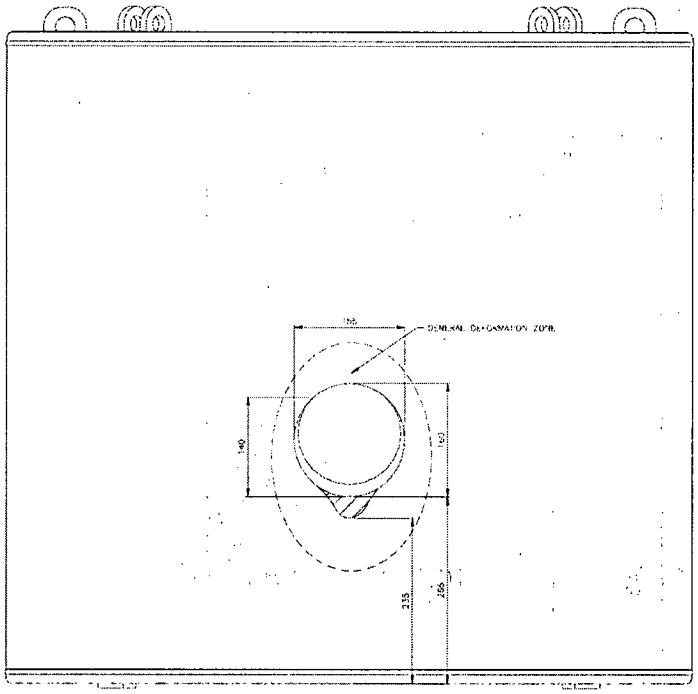

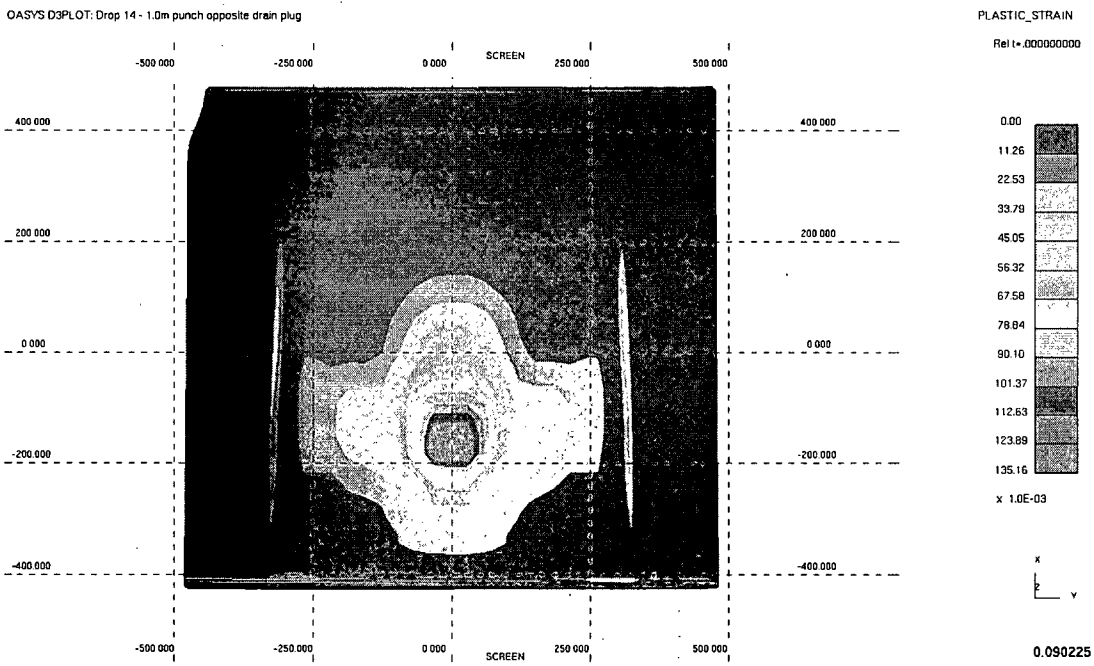

Figure 54: Drop 14 – comparison 3

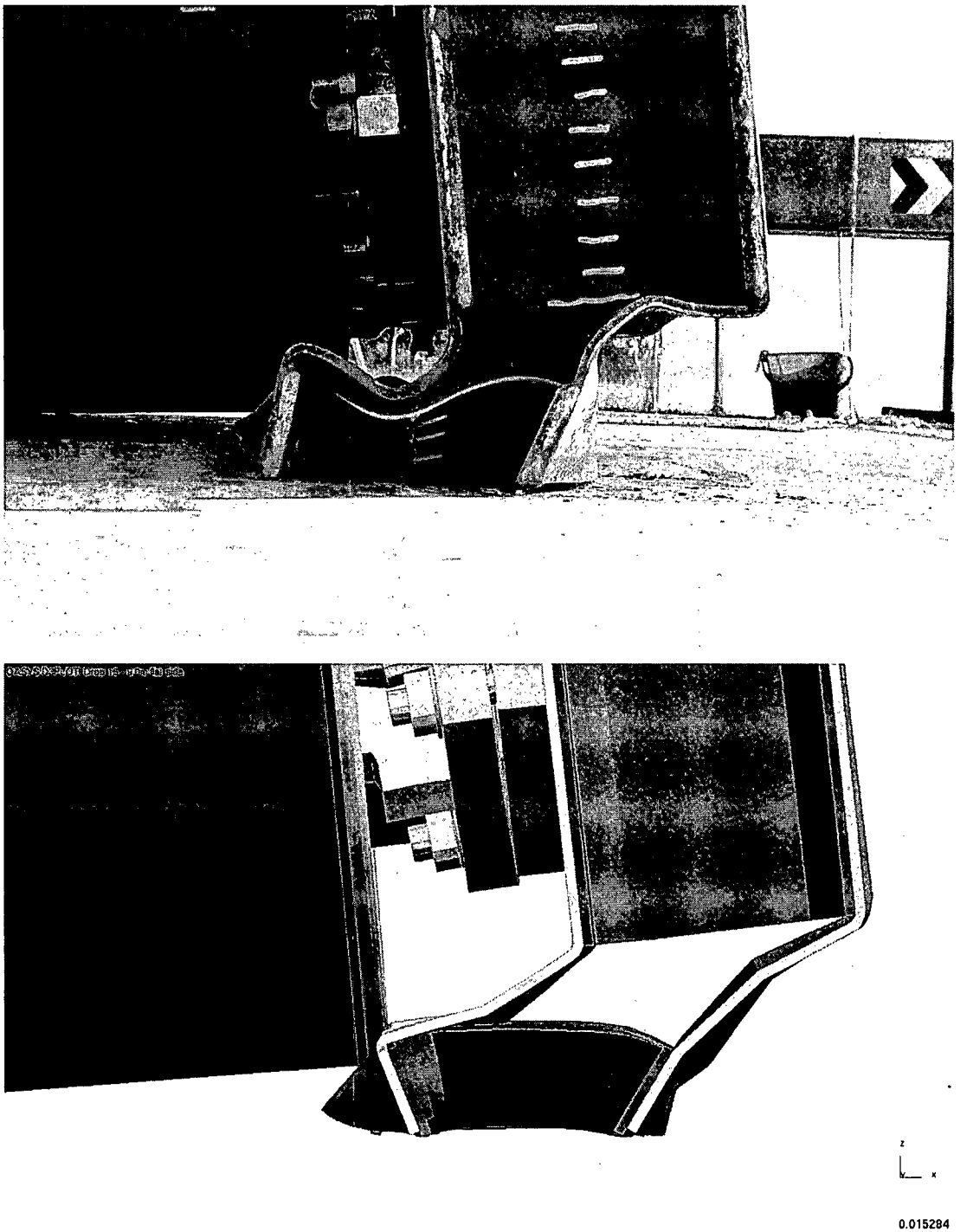

Figure 55: Drop 15 – comparison 1

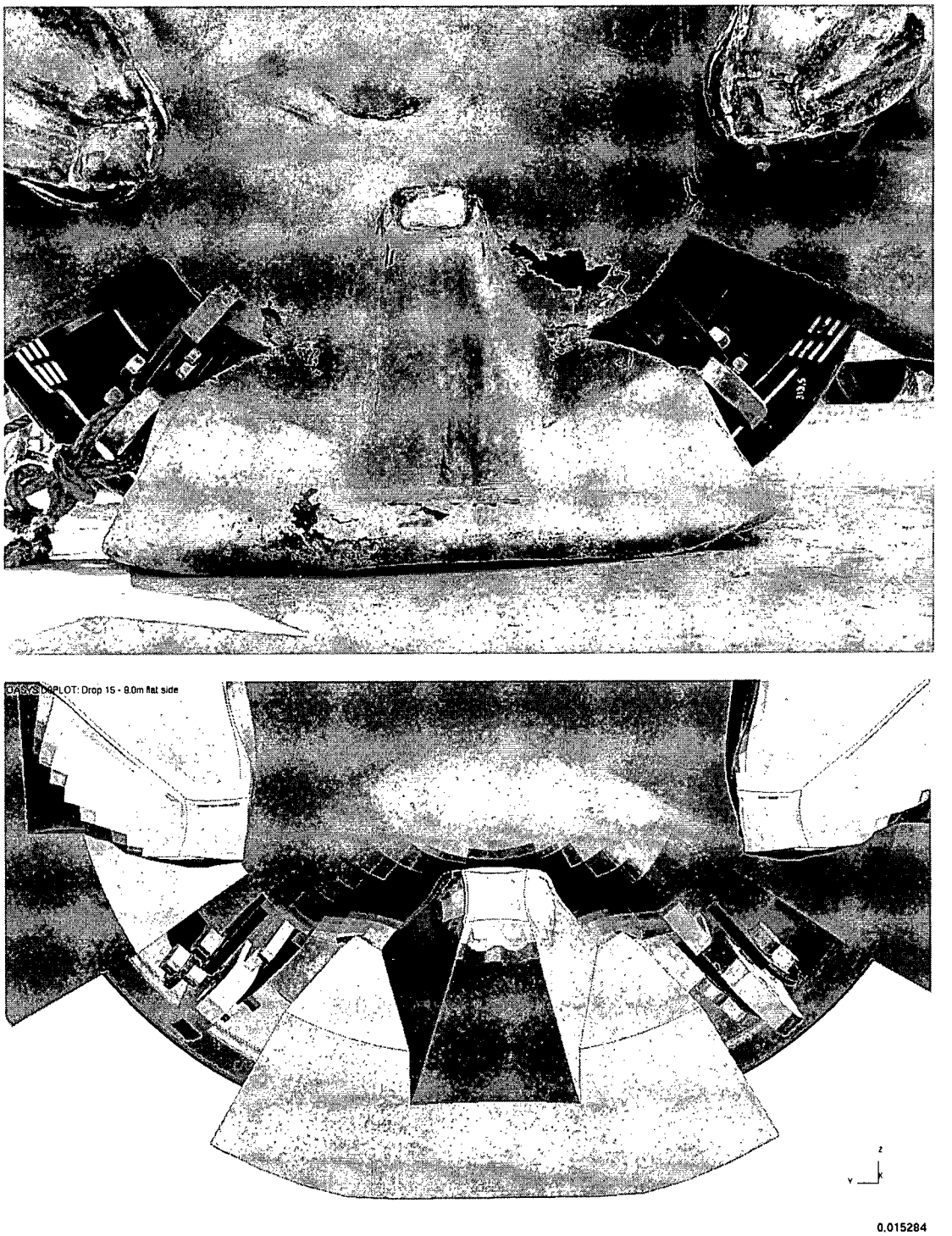

Figure 56: Drop 15 – comparison 2

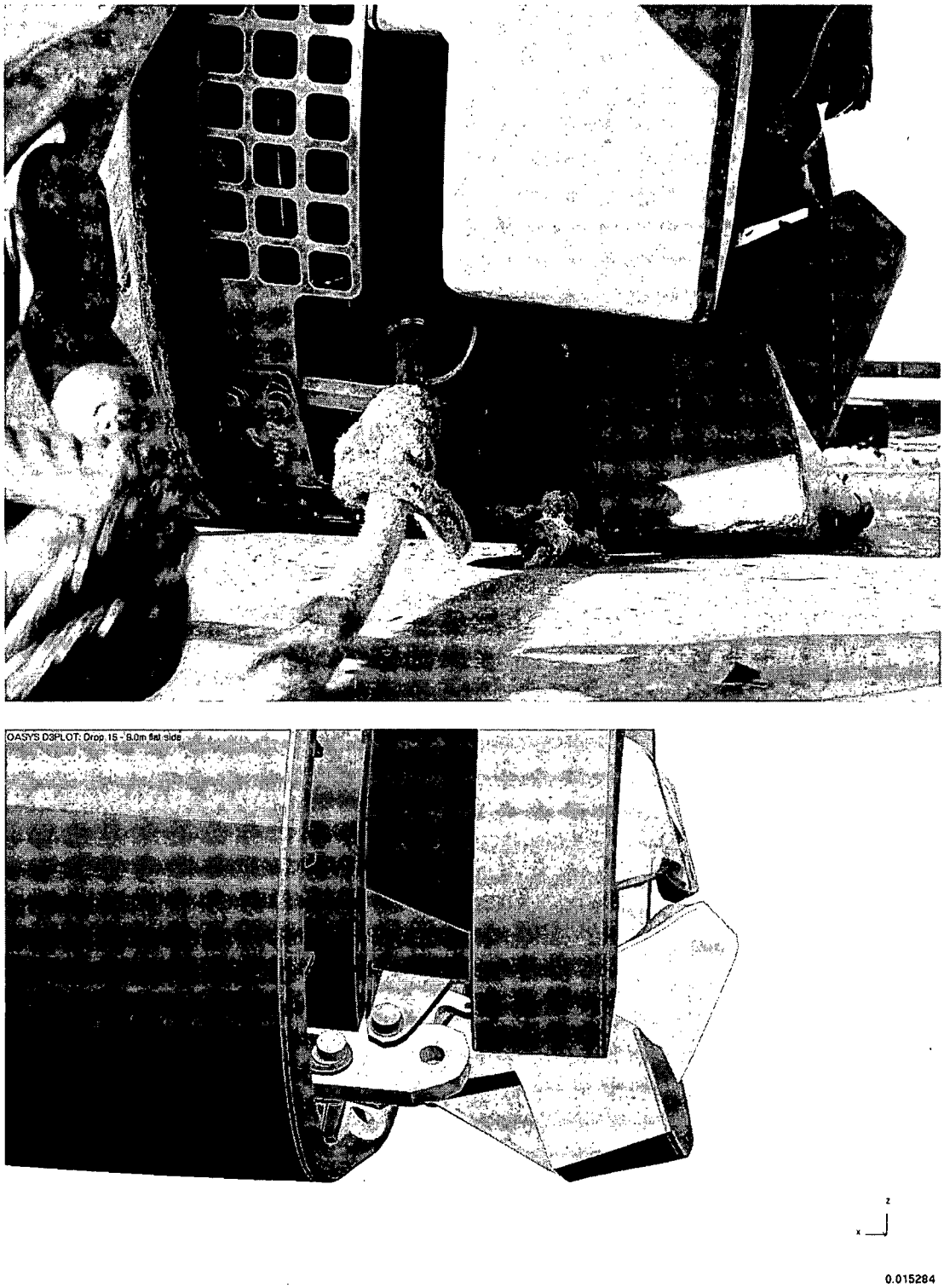

Figure 57: Drop 15 – comparison 3

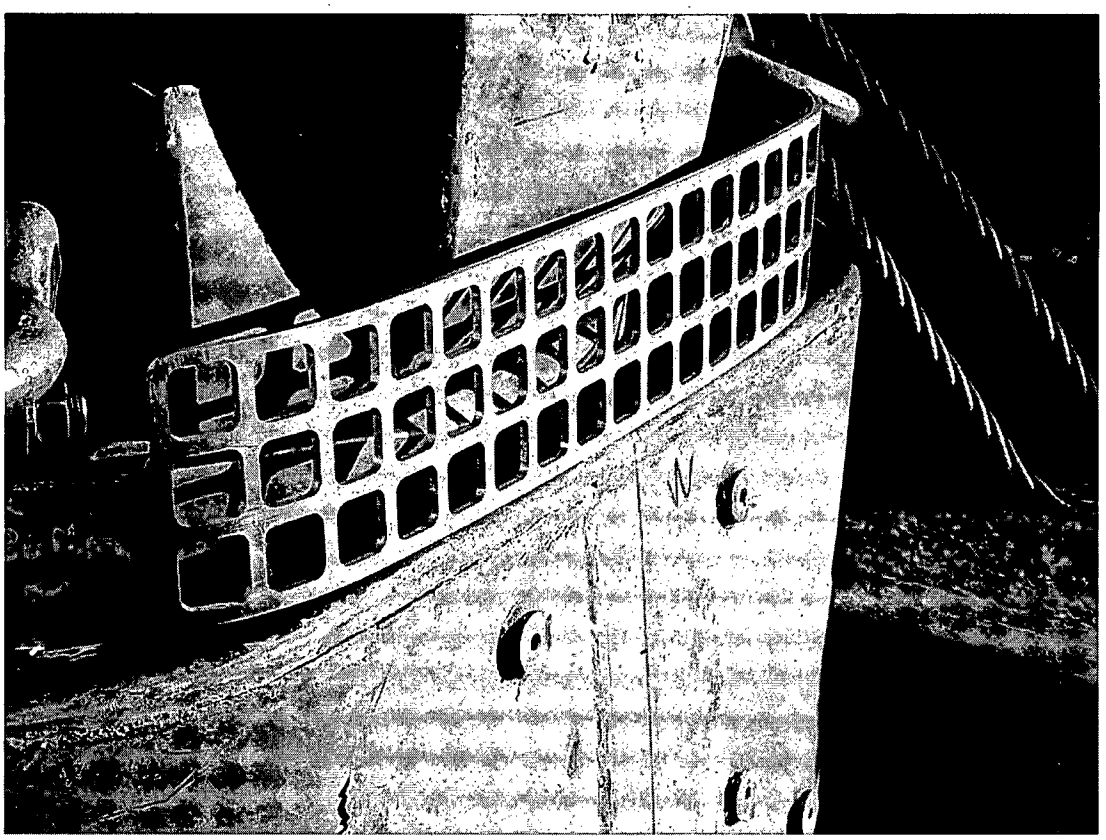

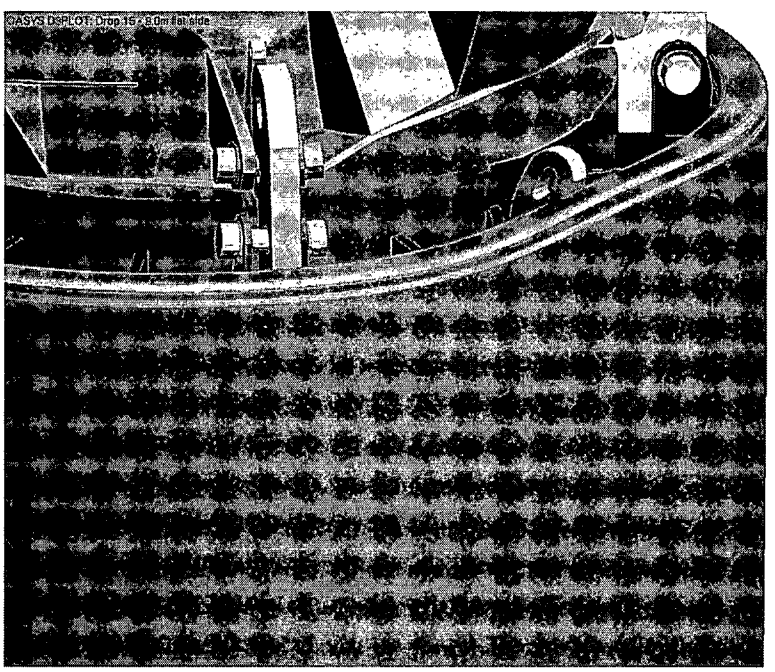

Figure 58: Drop 15 – comparison 4

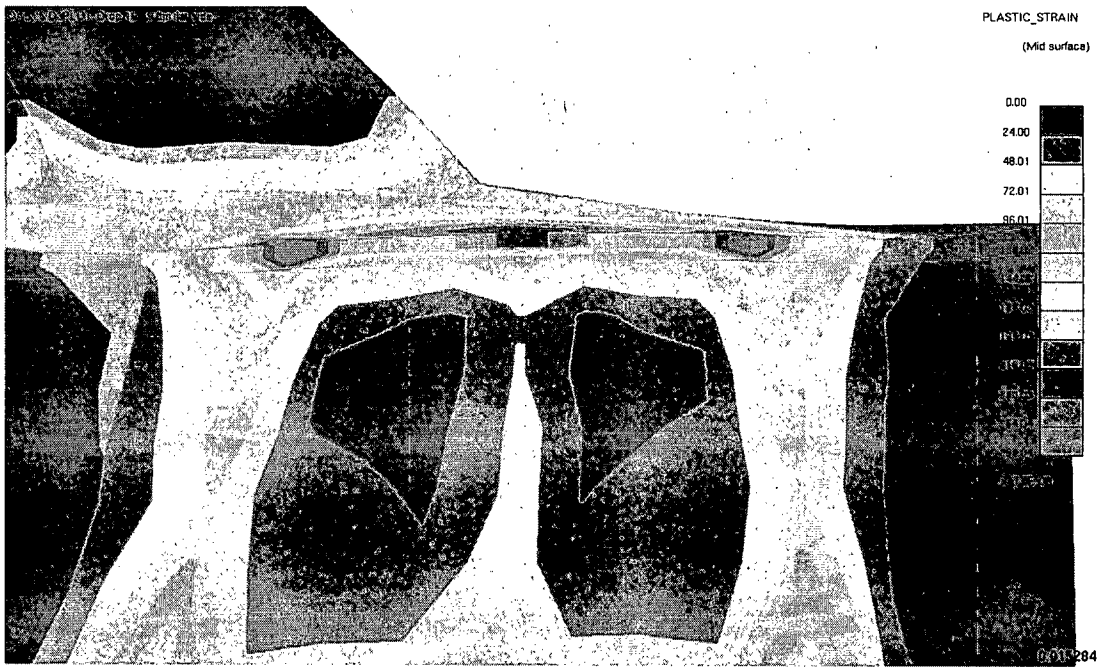

Figure 59: Drop 15 – comparison 5

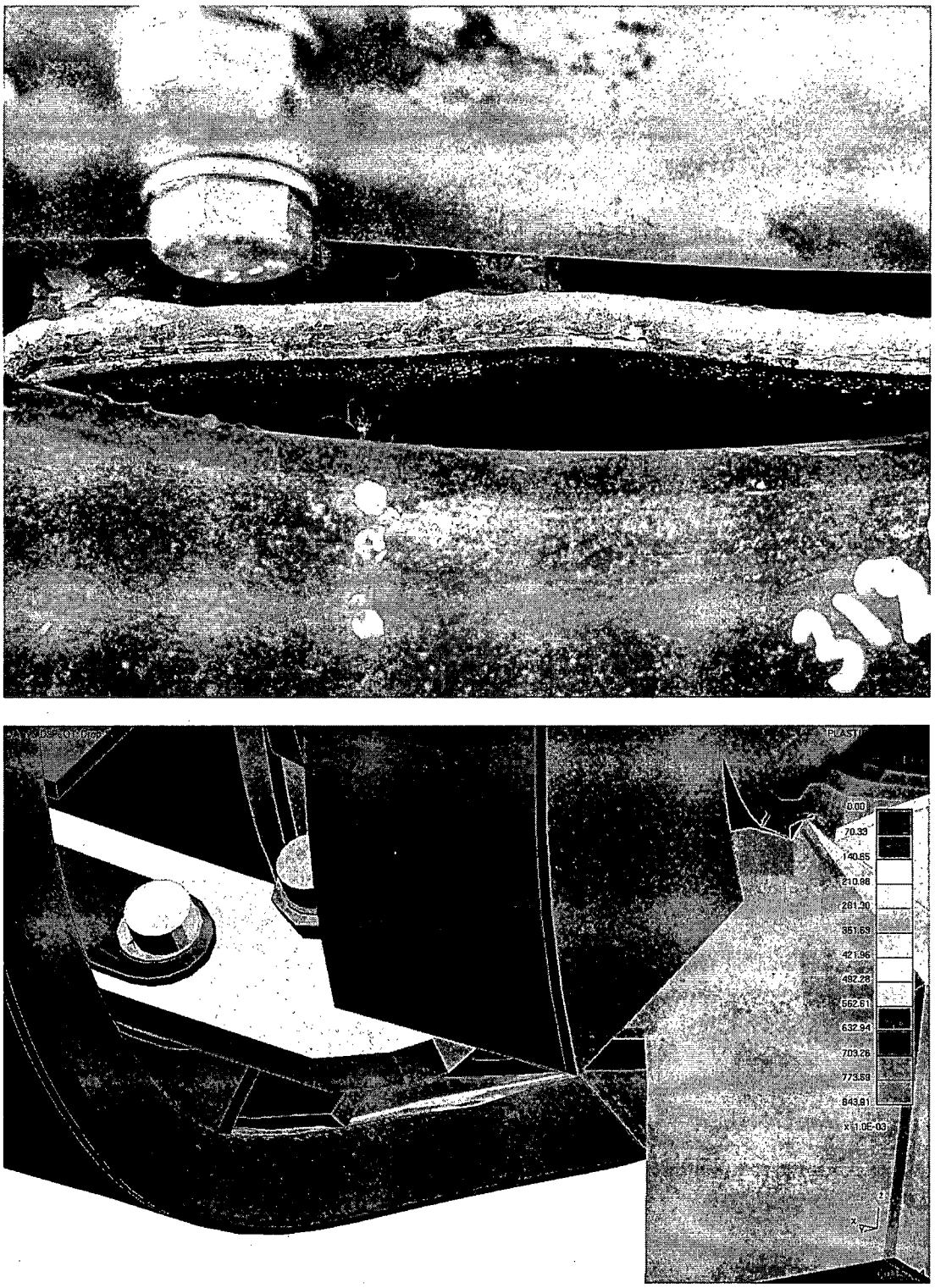

Figure 60: Drop 15 – comparison 6

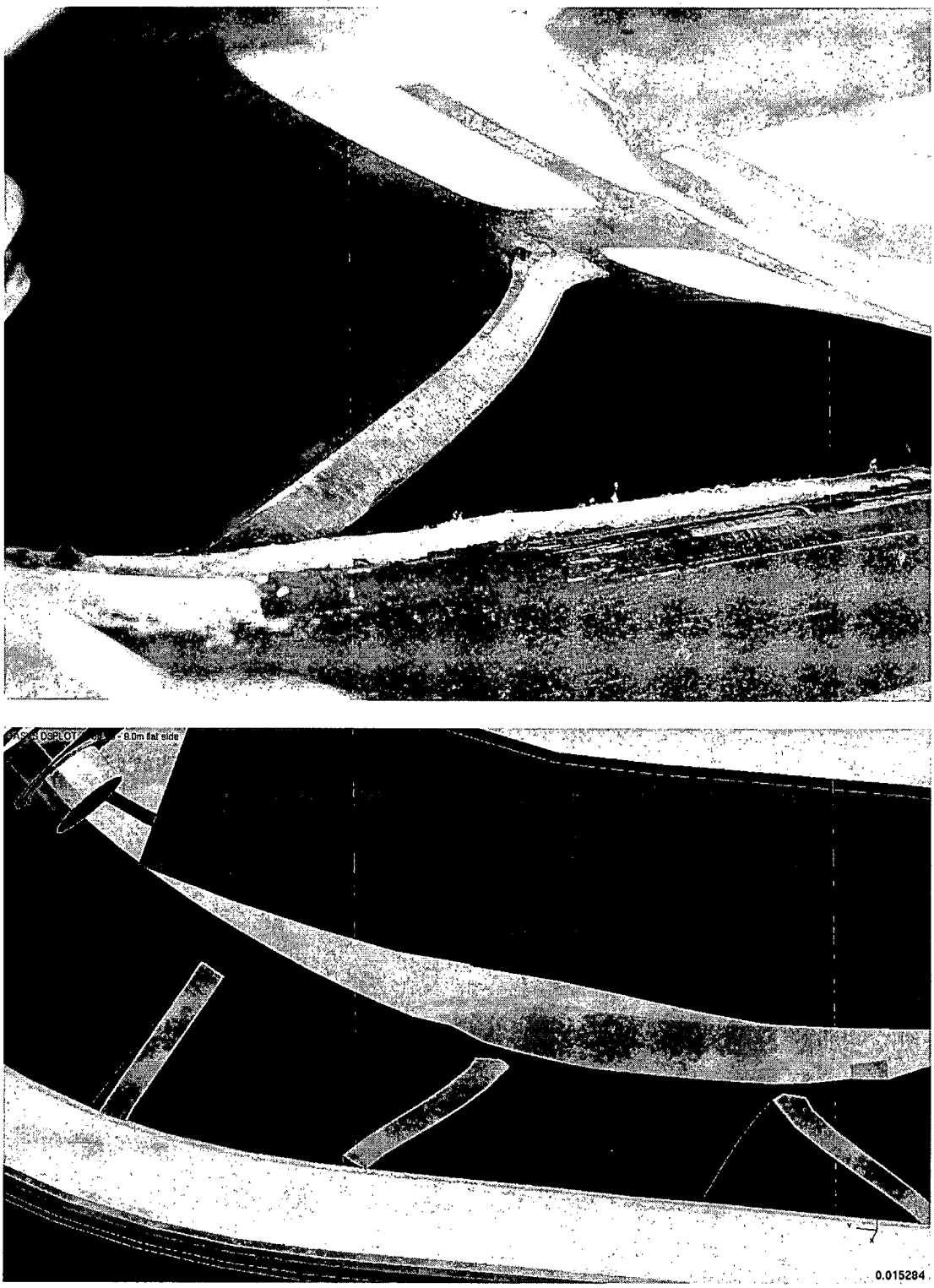

Figure 61: Drop 15 – comparison 7

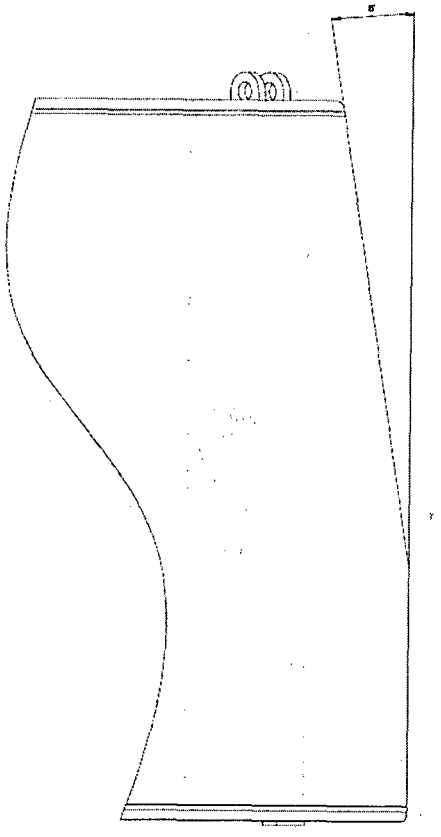

OASYS D3PLOT: Drop 15 - 9.0m flat side

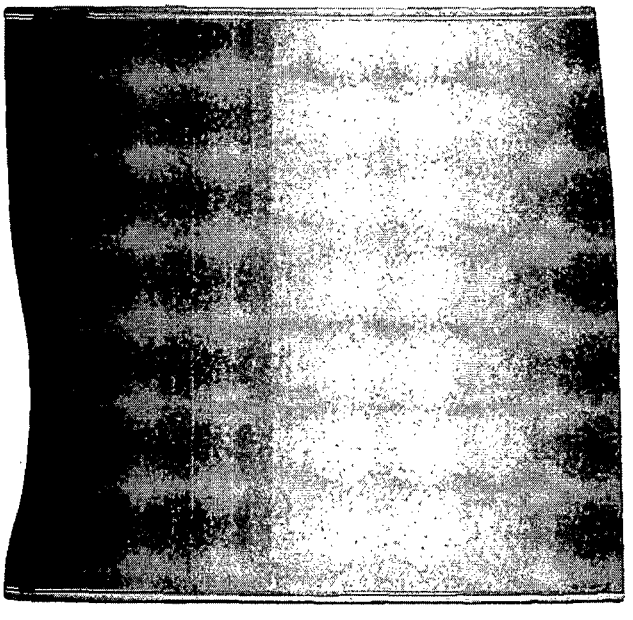

0.015284

Figure 62: Drop 15 – comparison 8

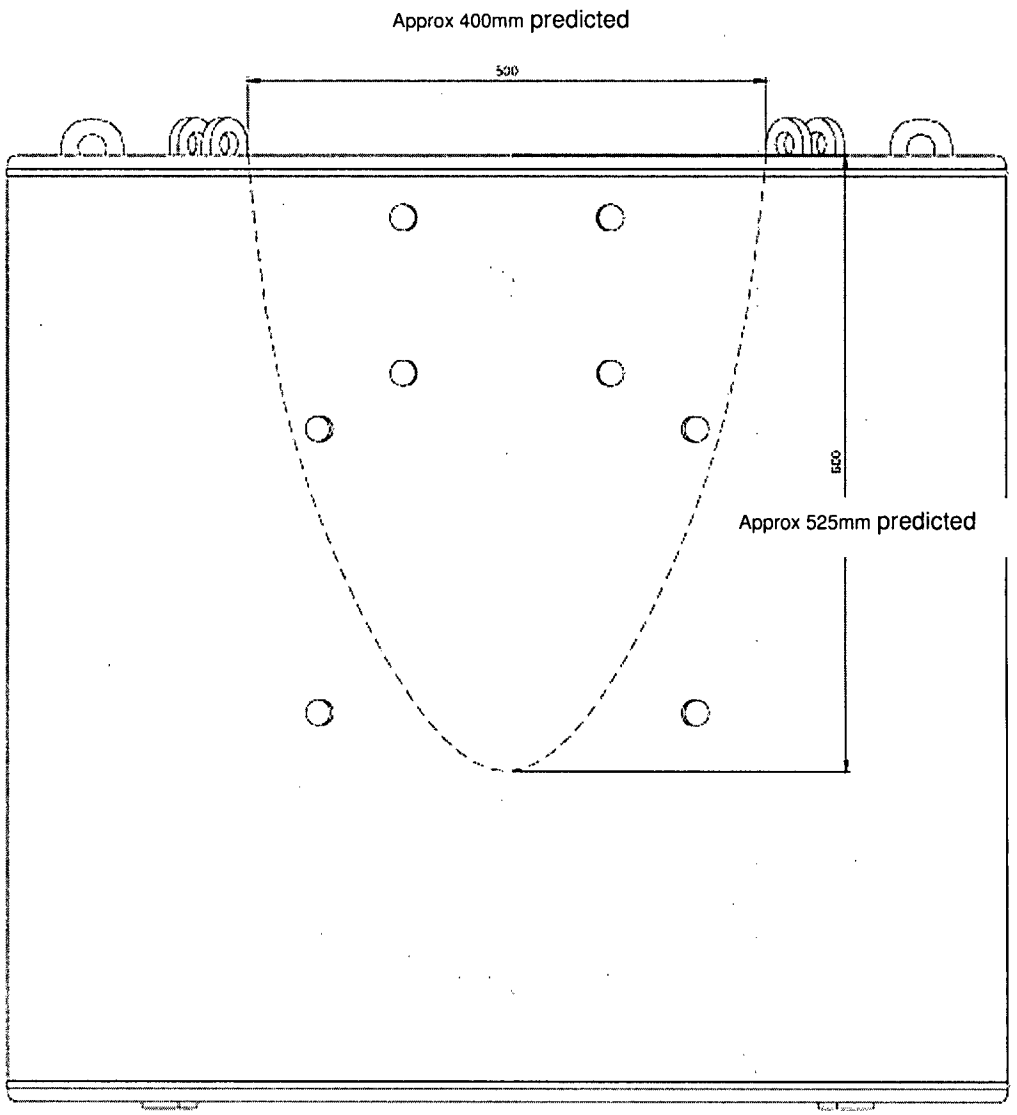

Figure 63: Drop 15 – comparison 9

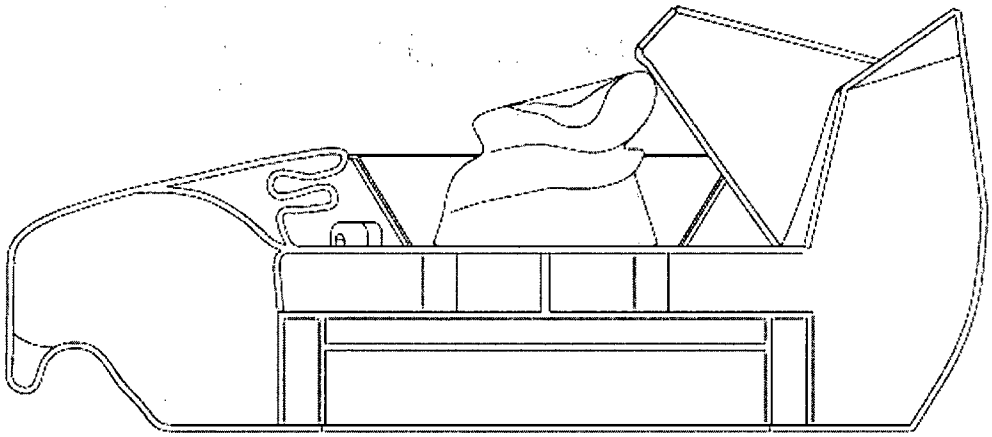

OASYS D3PLOT: Drop 15 - 9.0m flat side

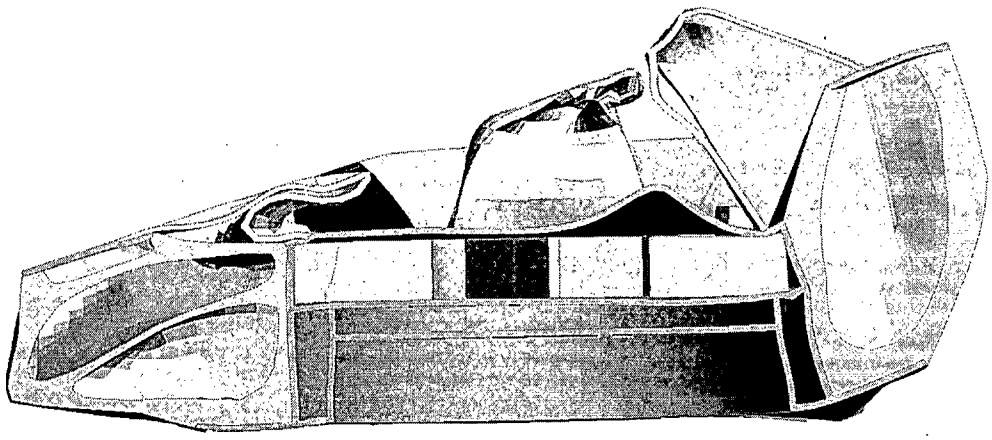

0.015284

Figure 64: Drop 15 – comparison 10

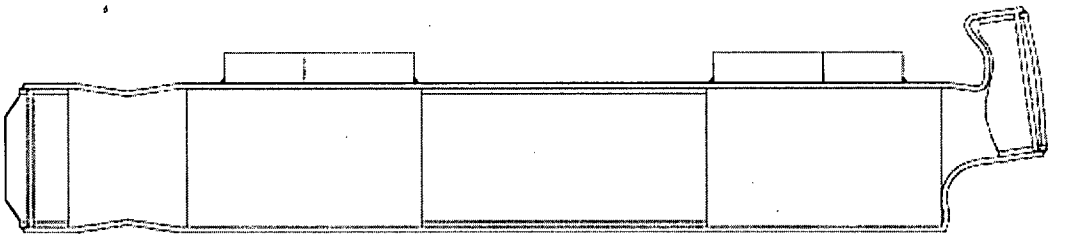

OASYS D3PLOT: Drop 15 - 9.0m flat side

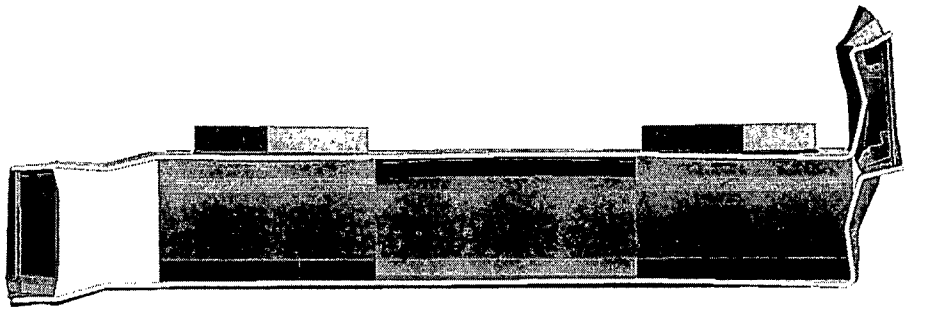

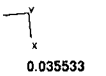

Figure 65: Drop 15 – comparison 11

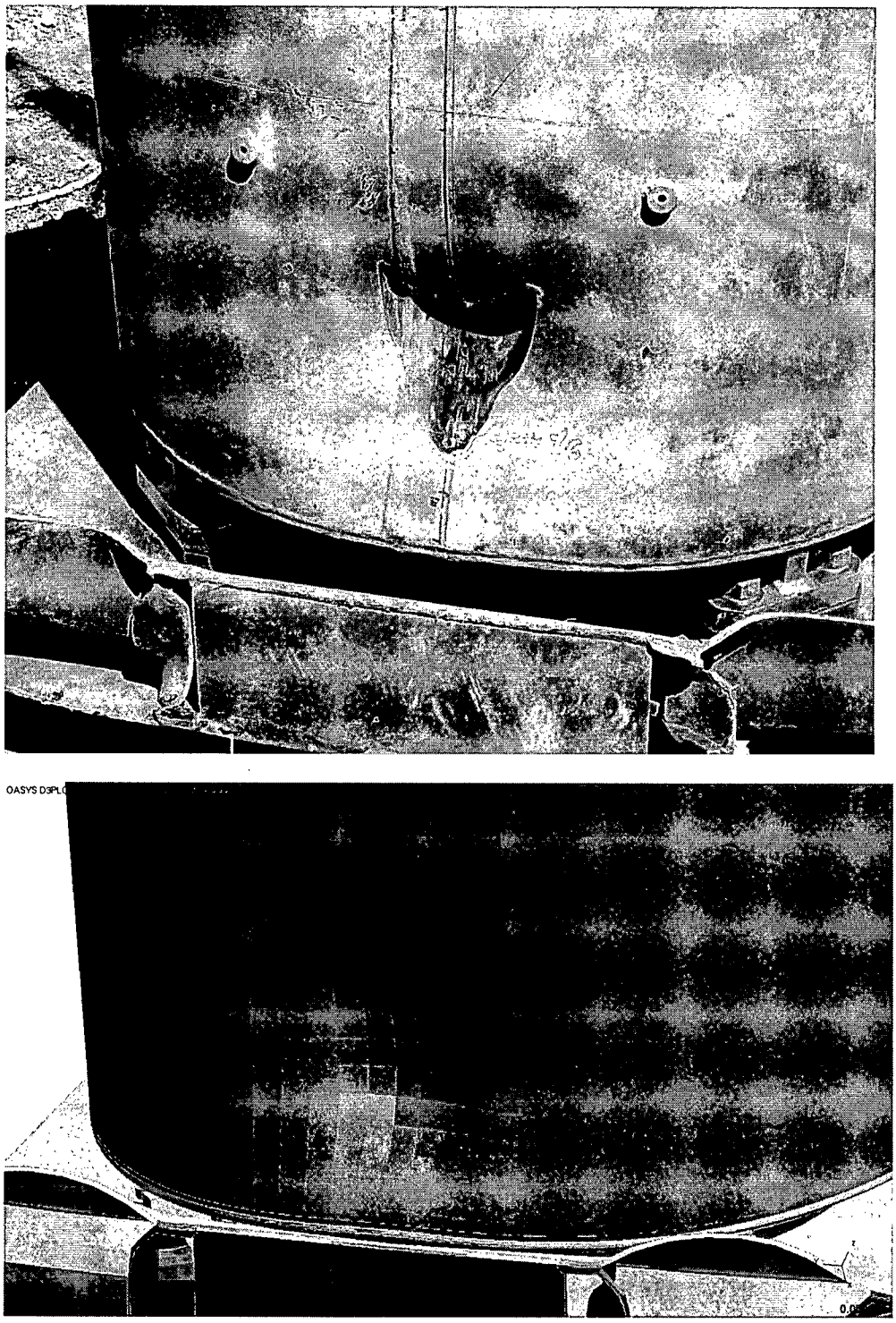

Figure 66: Drop 16 – comparison 1

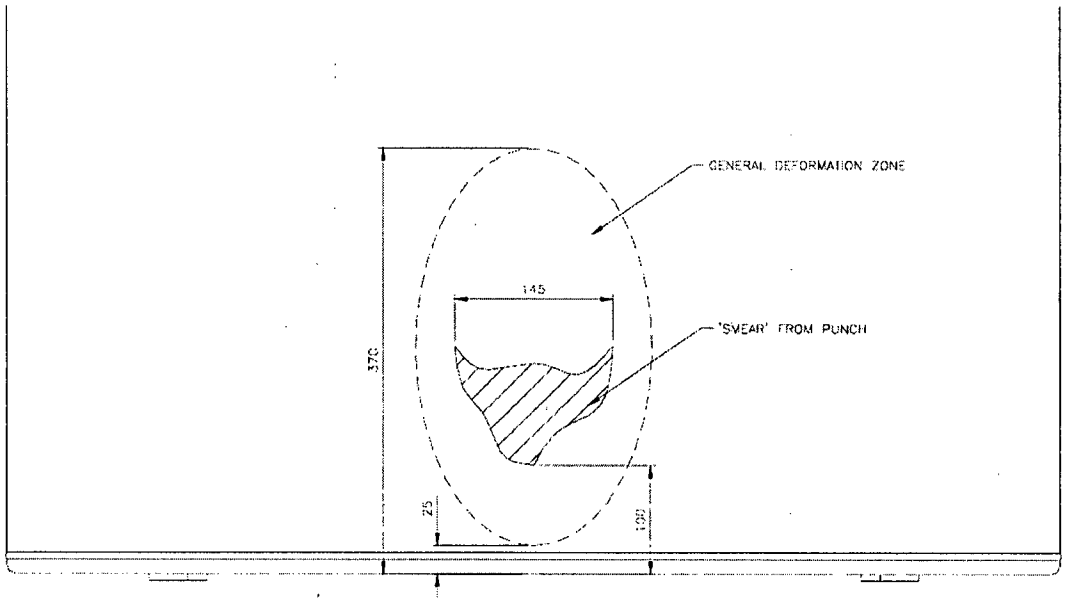

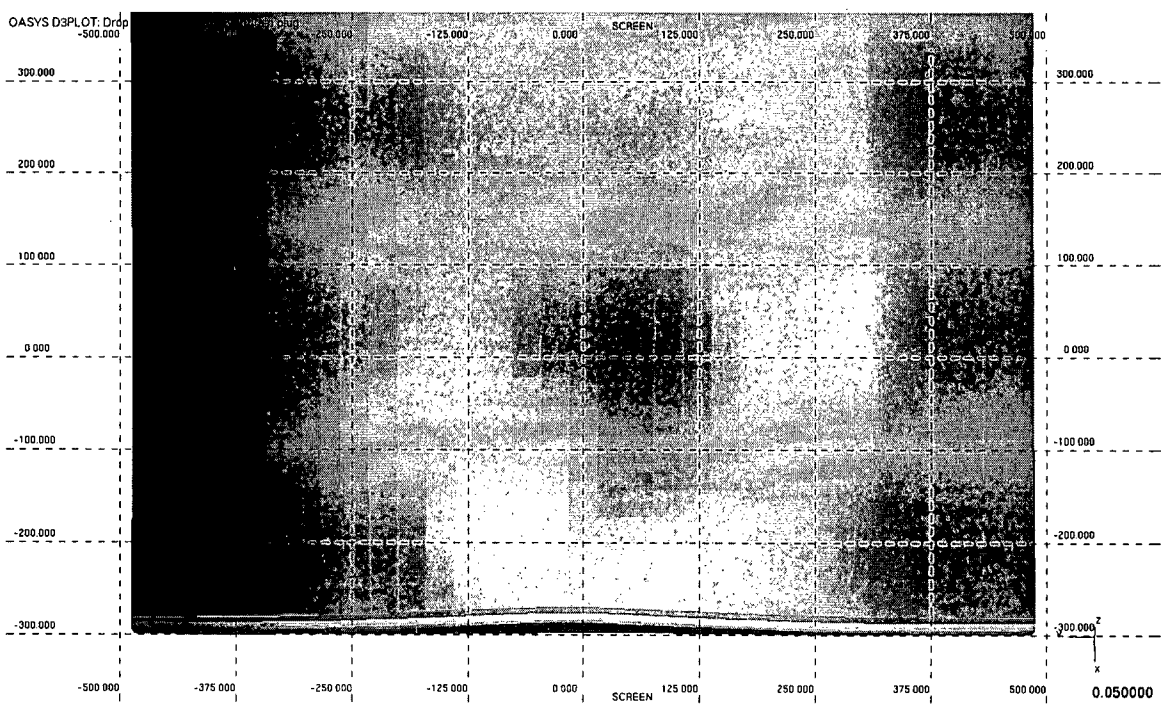

Figure 67: Drop 16 – comparison 2

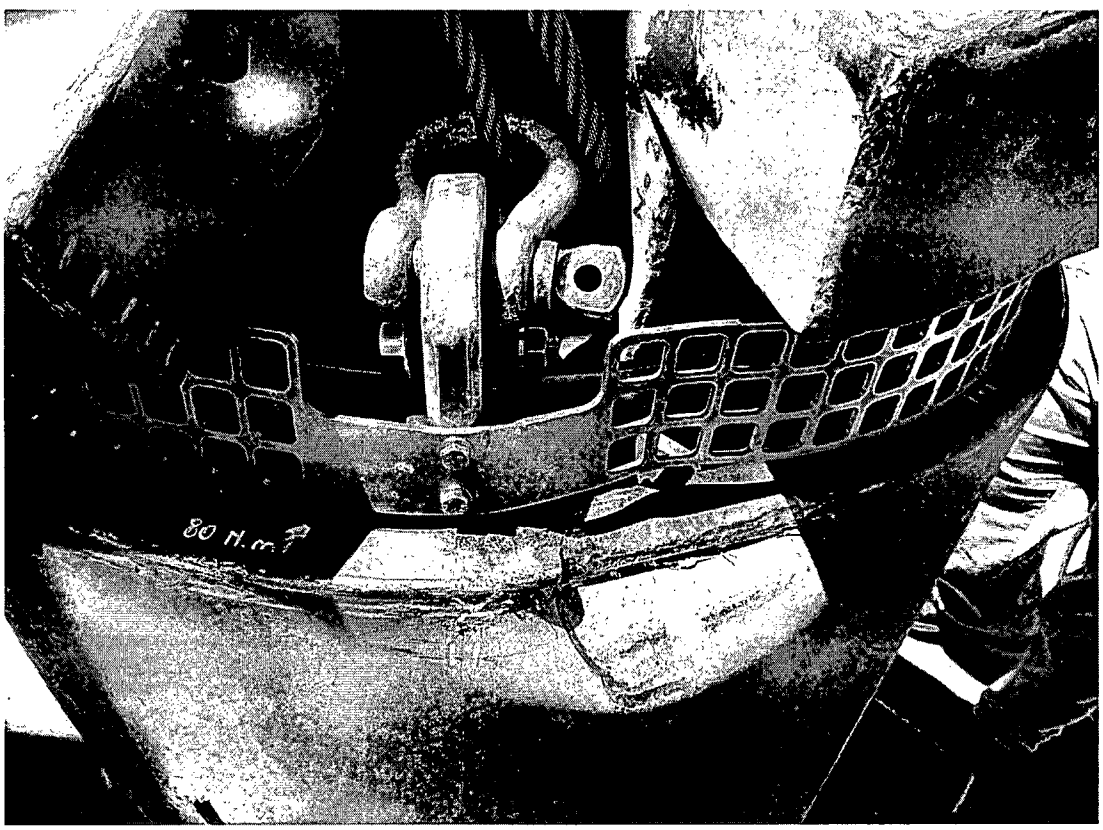

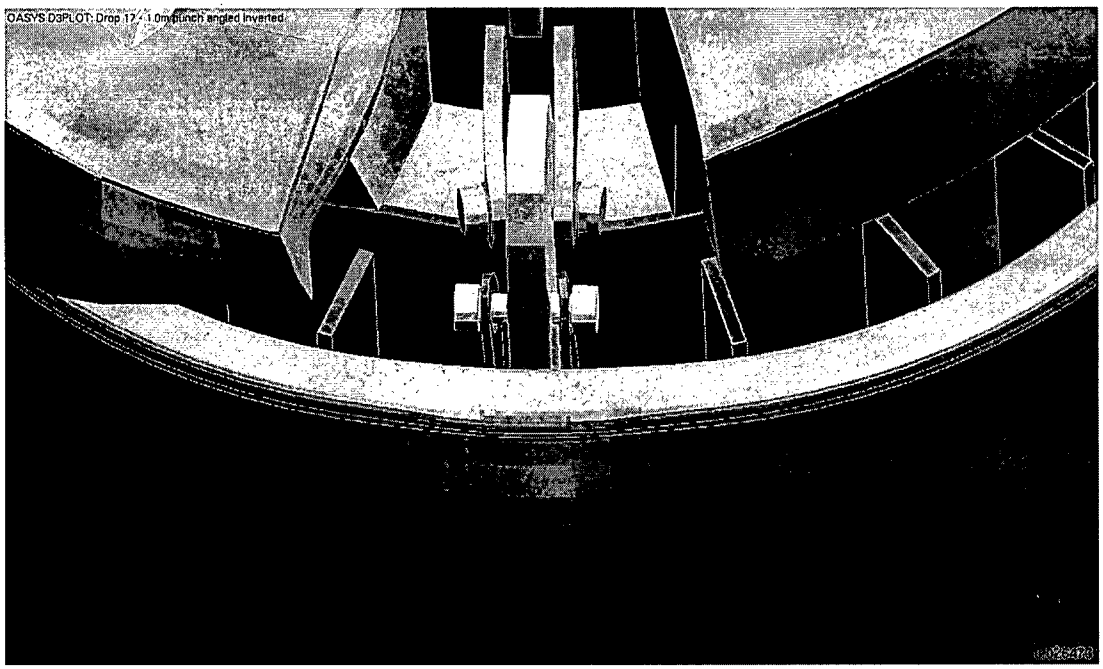

Figure 68: Drop 17 – comparison 1

Figure 69: Drop 17 – comparison 2

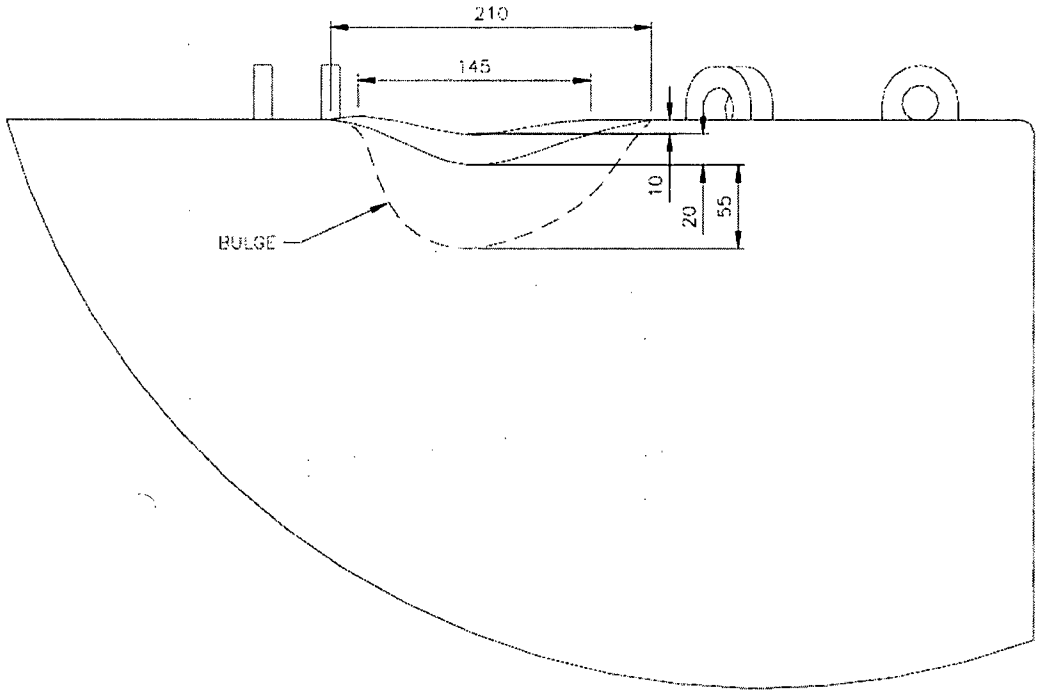

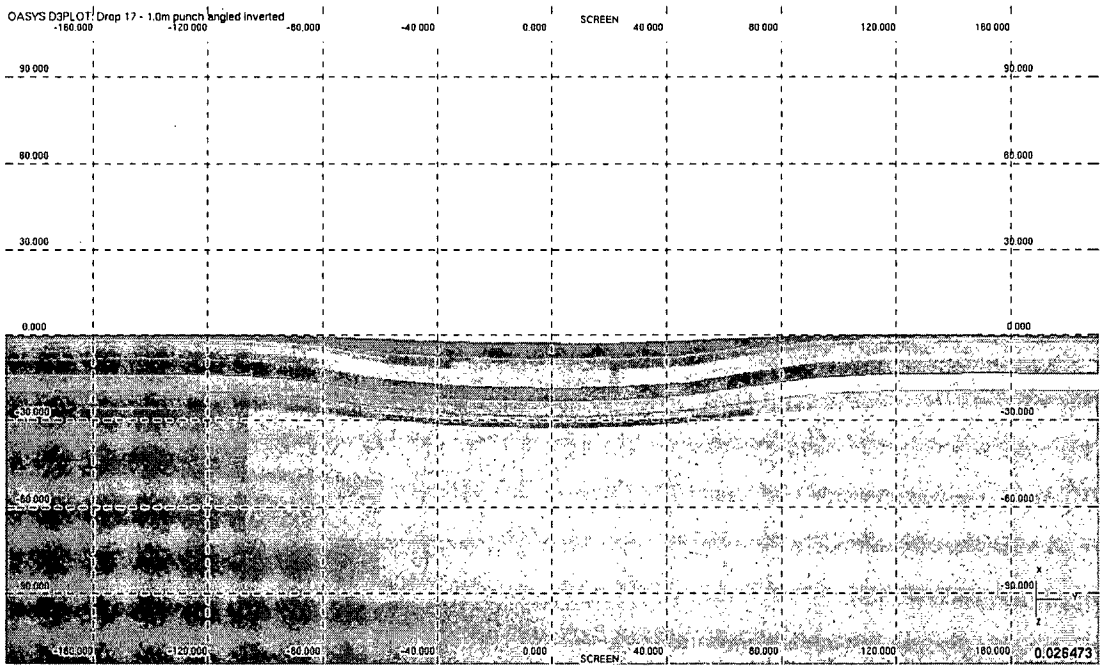

Figure 70: Drop 17 – comparison 3

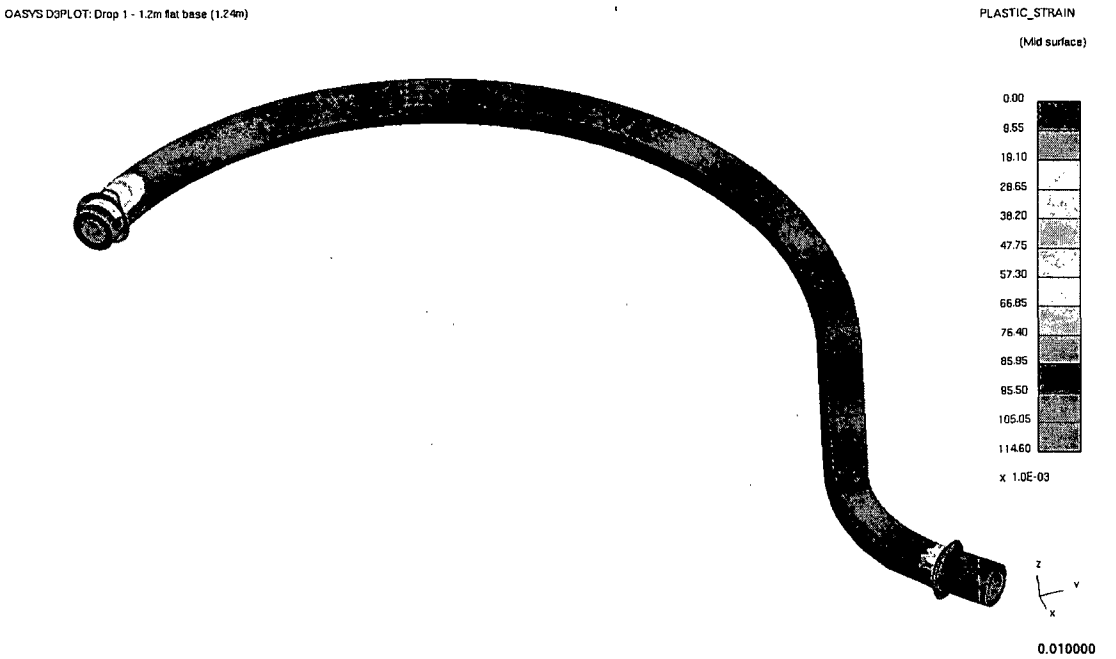

Figure 71: Strain component from drop test 1

Figure 72: Strain component from drop test 2

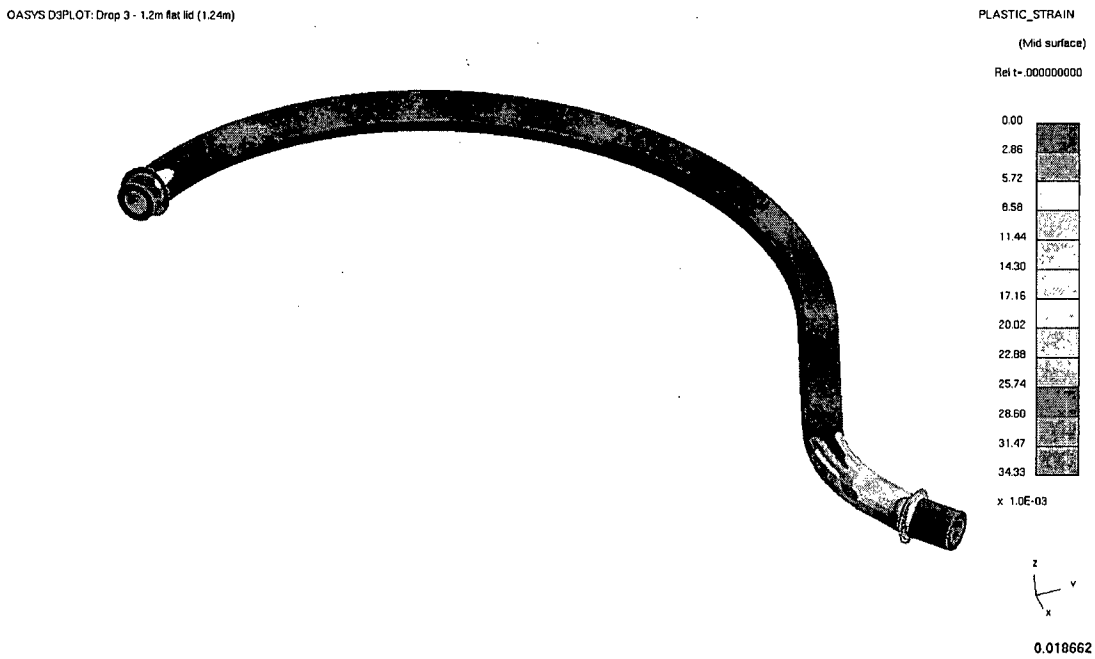

Figure 73: Strain component from drop test 3

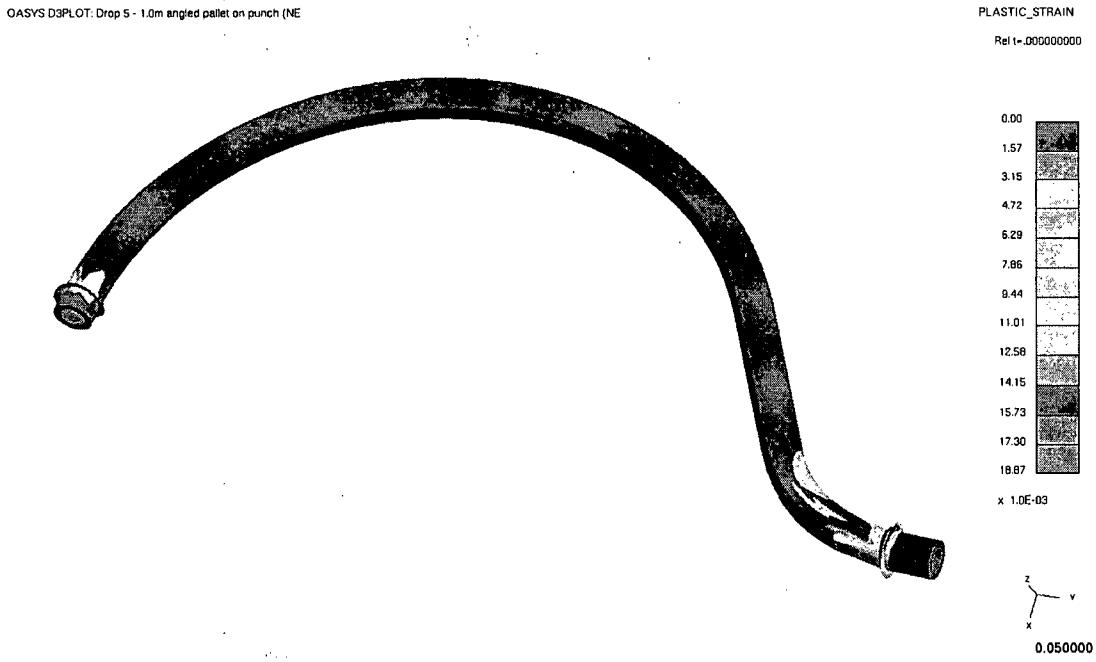

Figure 74: Strain component from drop test 5

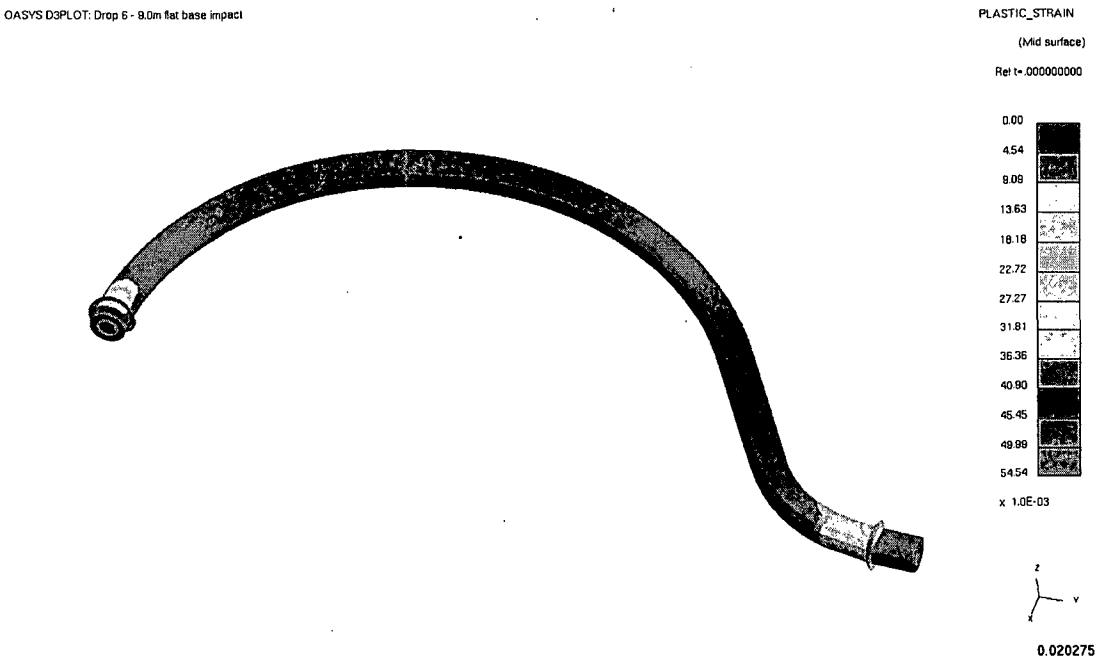

Figure 75: Strain component from drop test 6

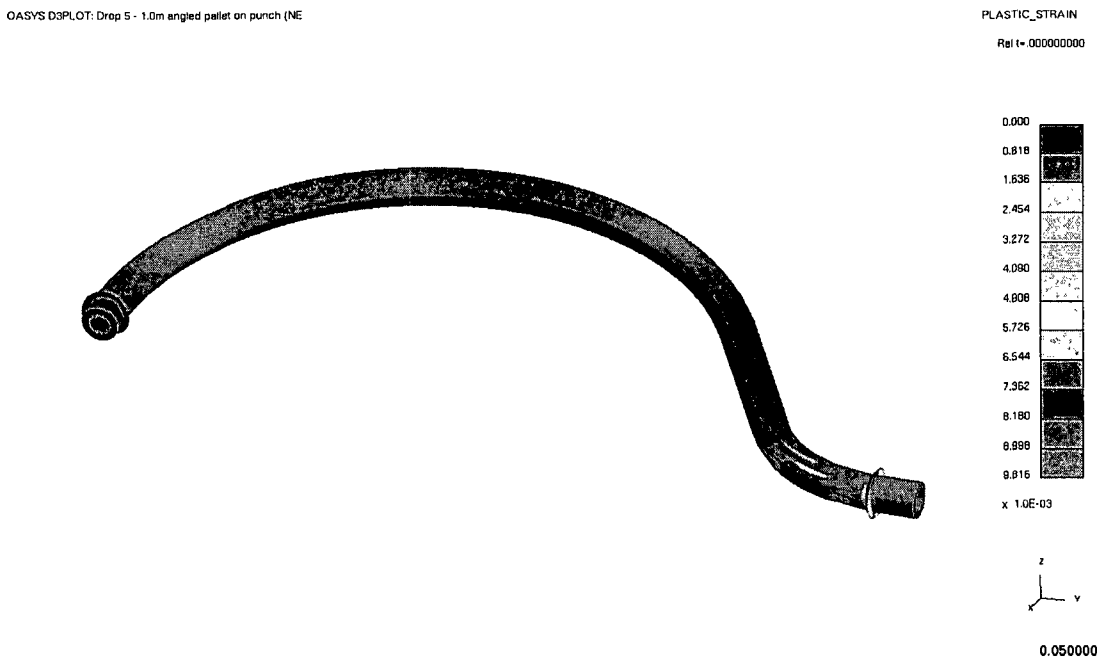

Figure 76: Strain component from drop test 7

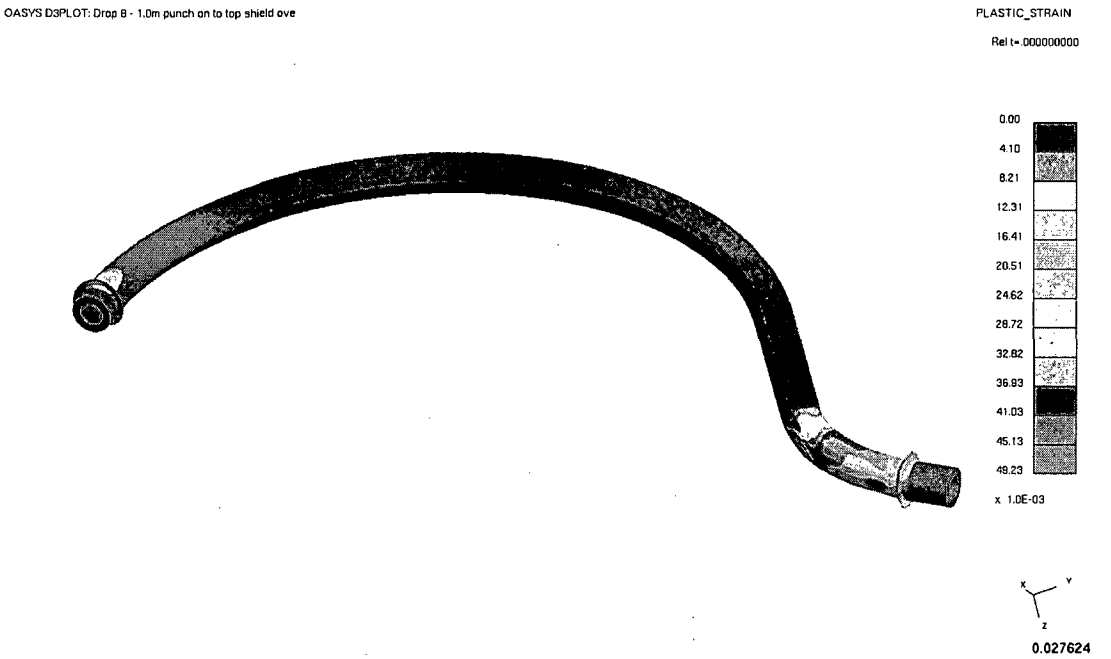

Figure 77: Strain component from drop test 8

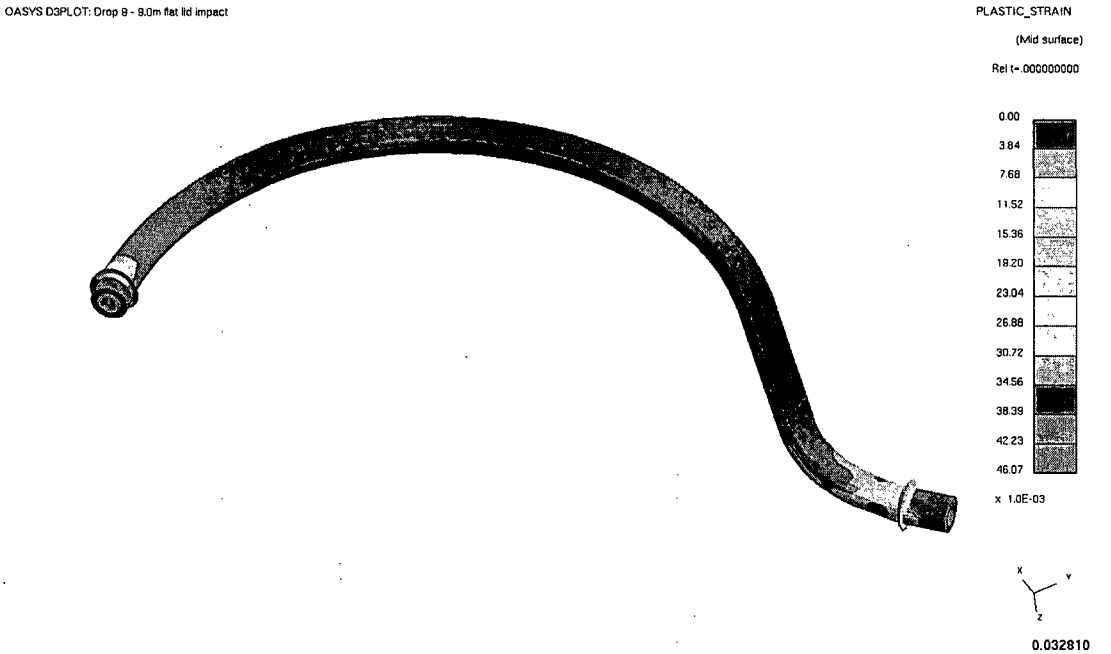

Figure 78: Strain component from drop test 9

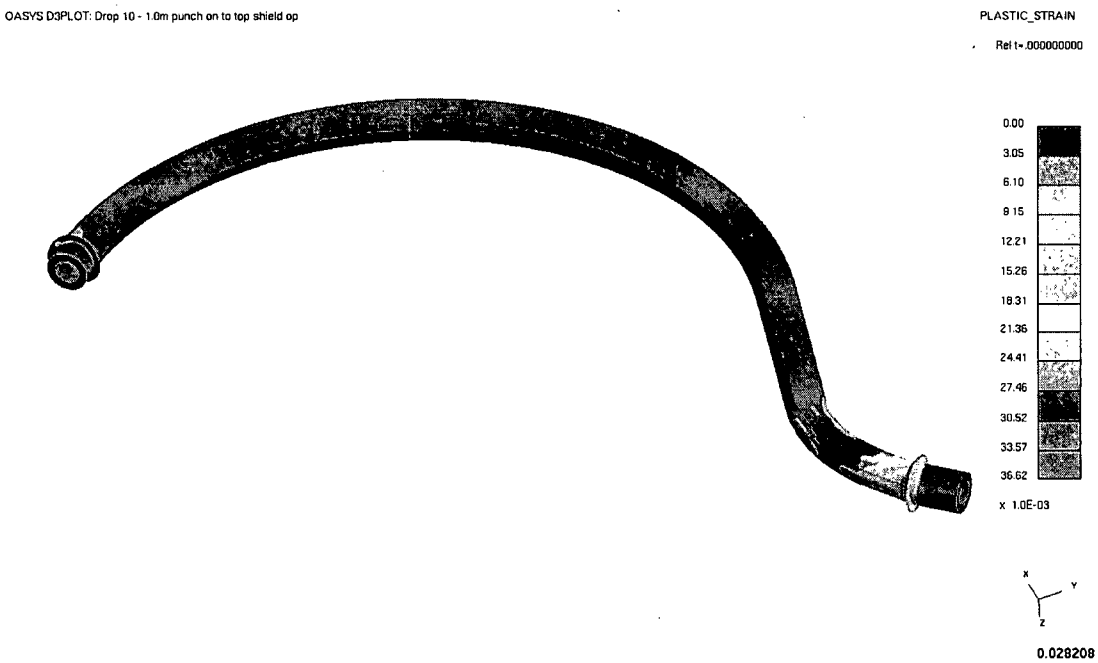

Figure 79: Strain component from drop test 10

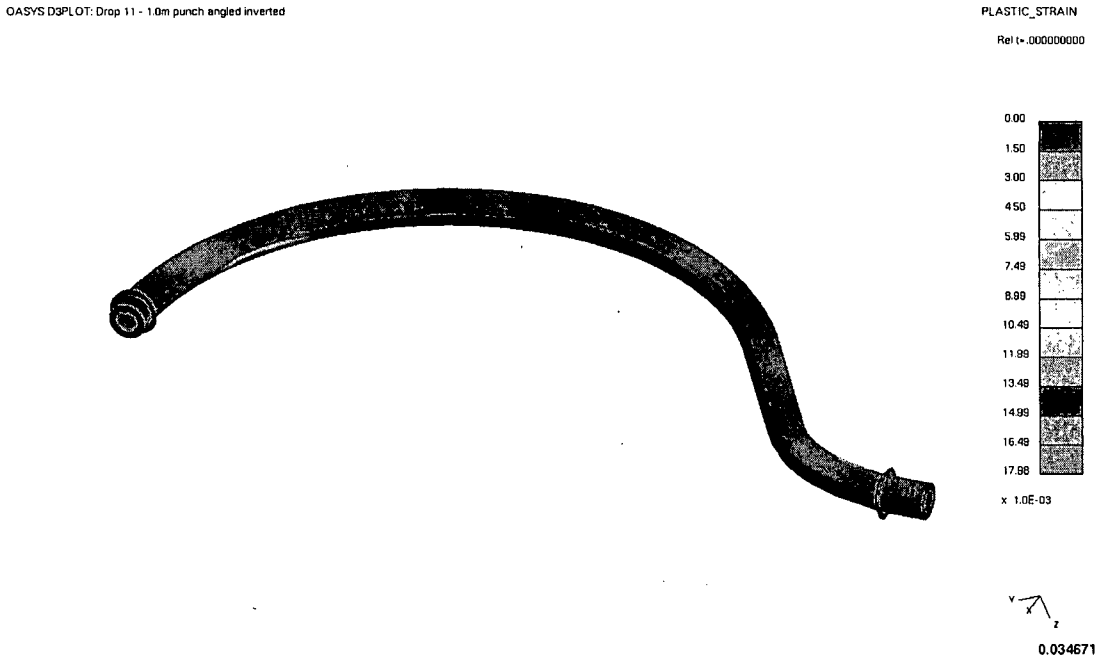

Figure 80: Strain component from drop test 11

Figure 81: Strain component from drop test 12

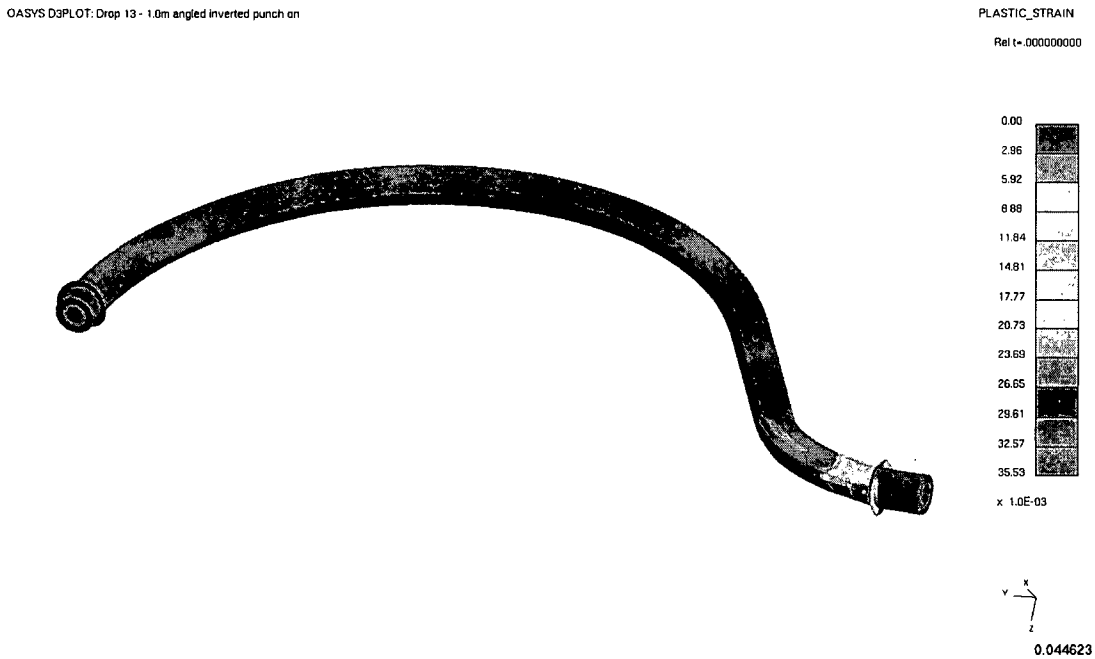

Figure 82: Strain component from drop test 13

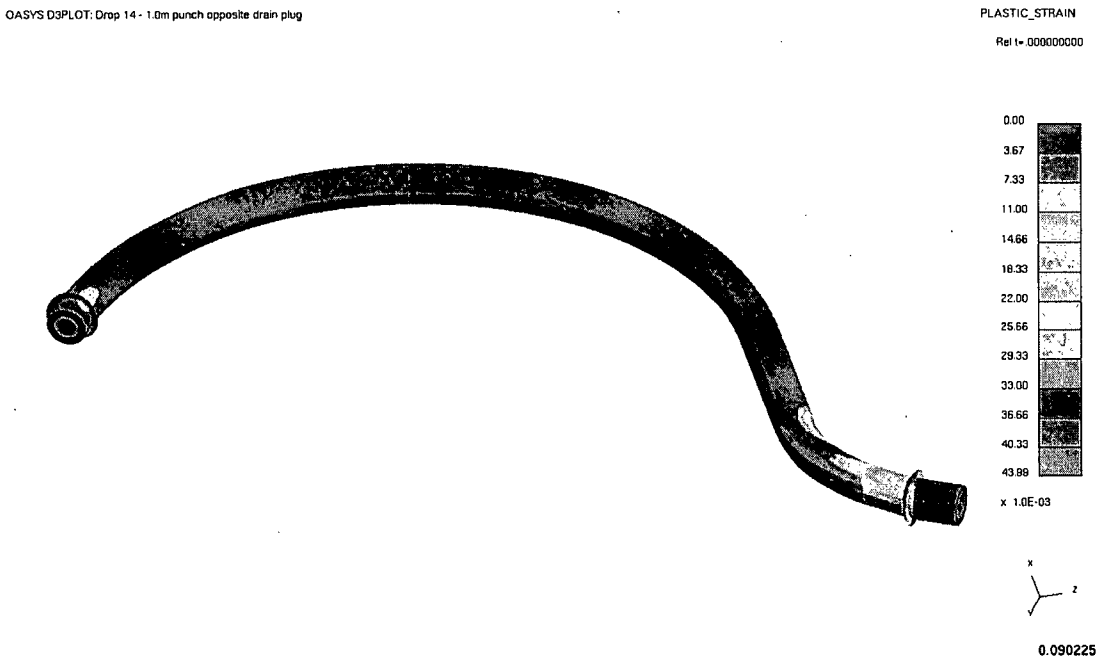

Figure 83: Strain component from drop test 14

Figure 84: Strain component from drop test 15

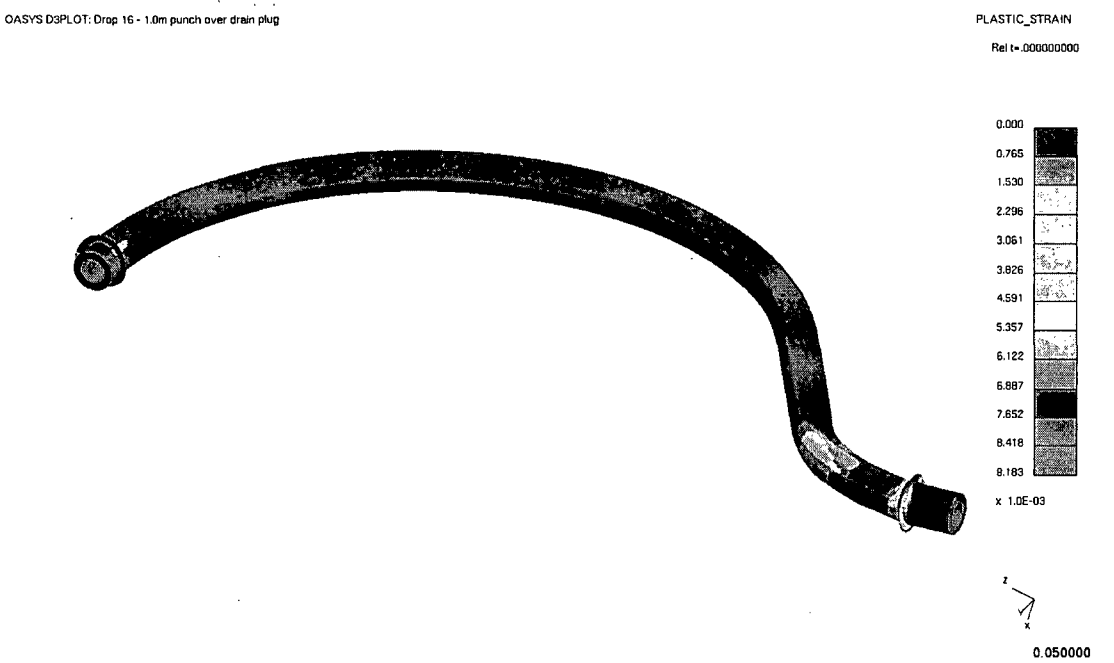

Figure 85: Strain component from drop test 16

Figure 86: Strain component from drop test 17

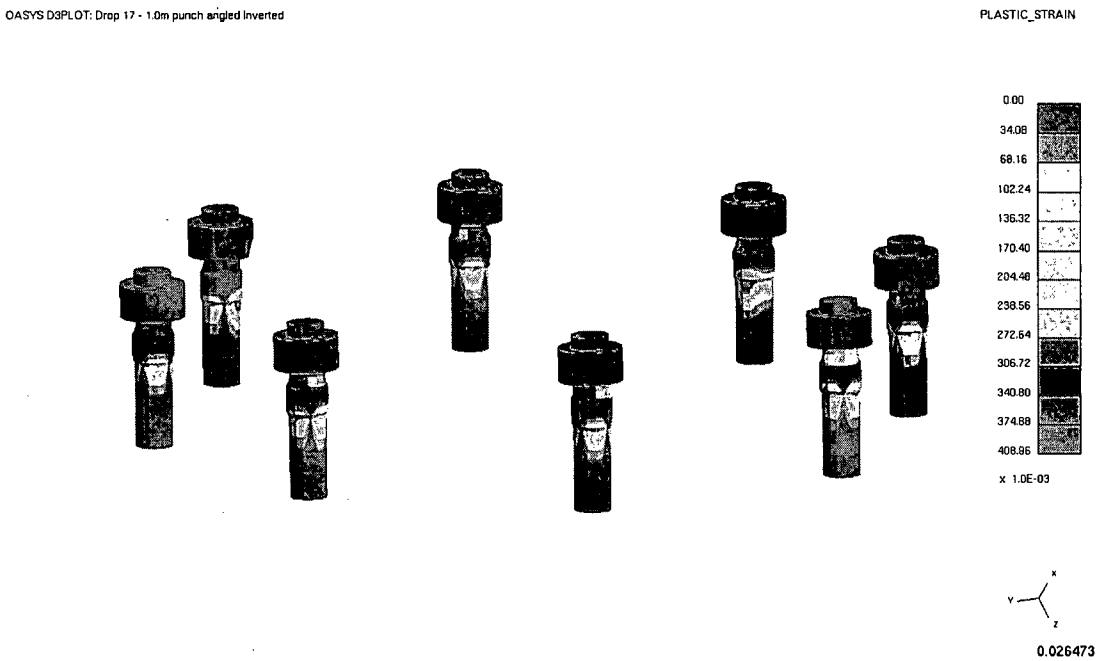

Figure 87: Final predicted effective plastic strains in closure bolts

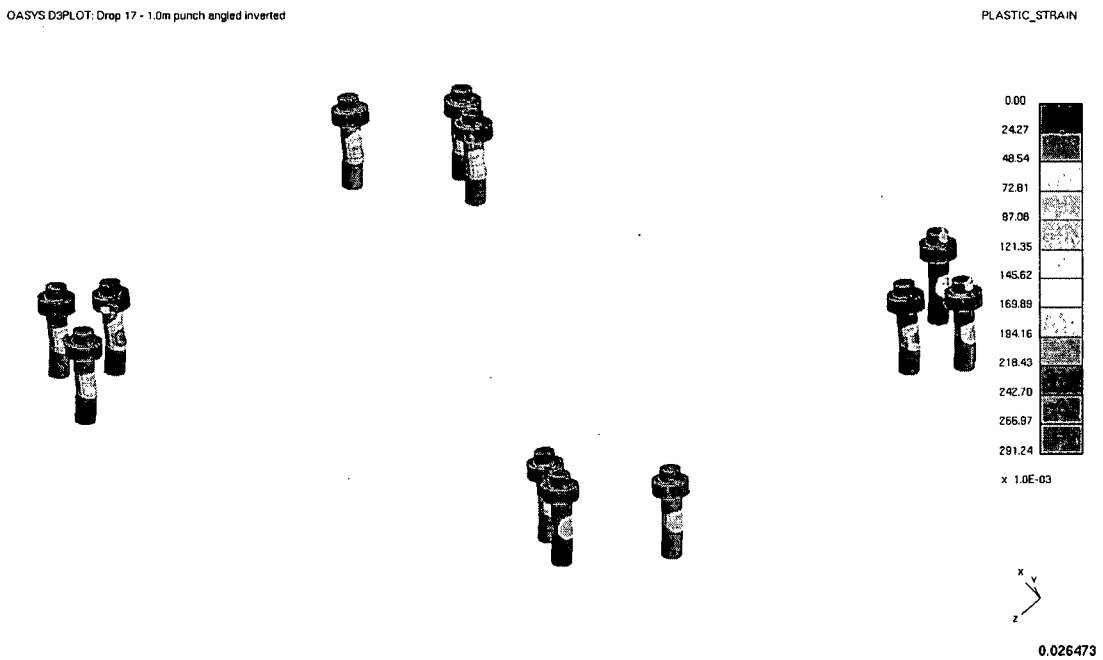

Figure 88: Final predicted effective plastic strains in pallet bolts

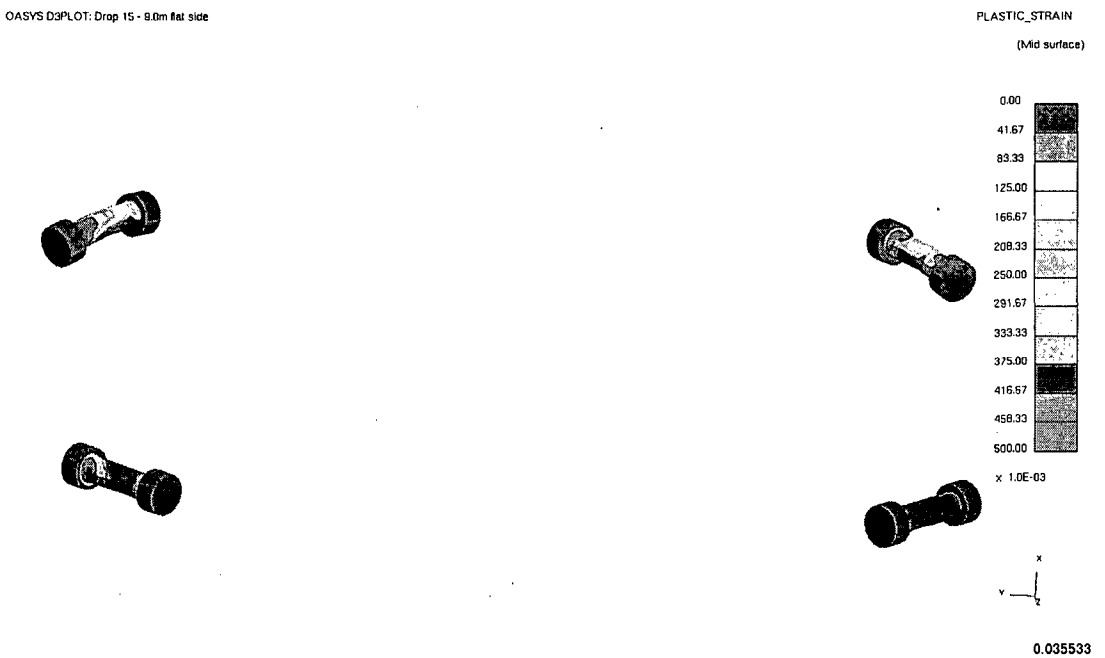

Figure 89: Final predicted effective plastic strains in jacket bolts

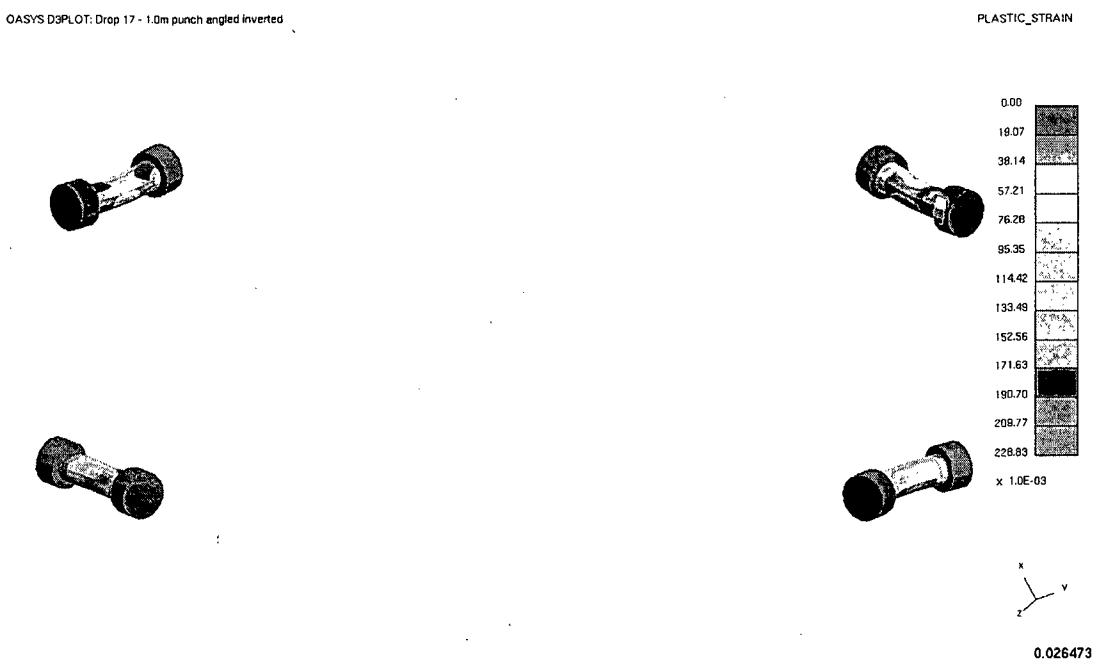

Figure 90: Final predicted effective plastic strains in top shield bolts

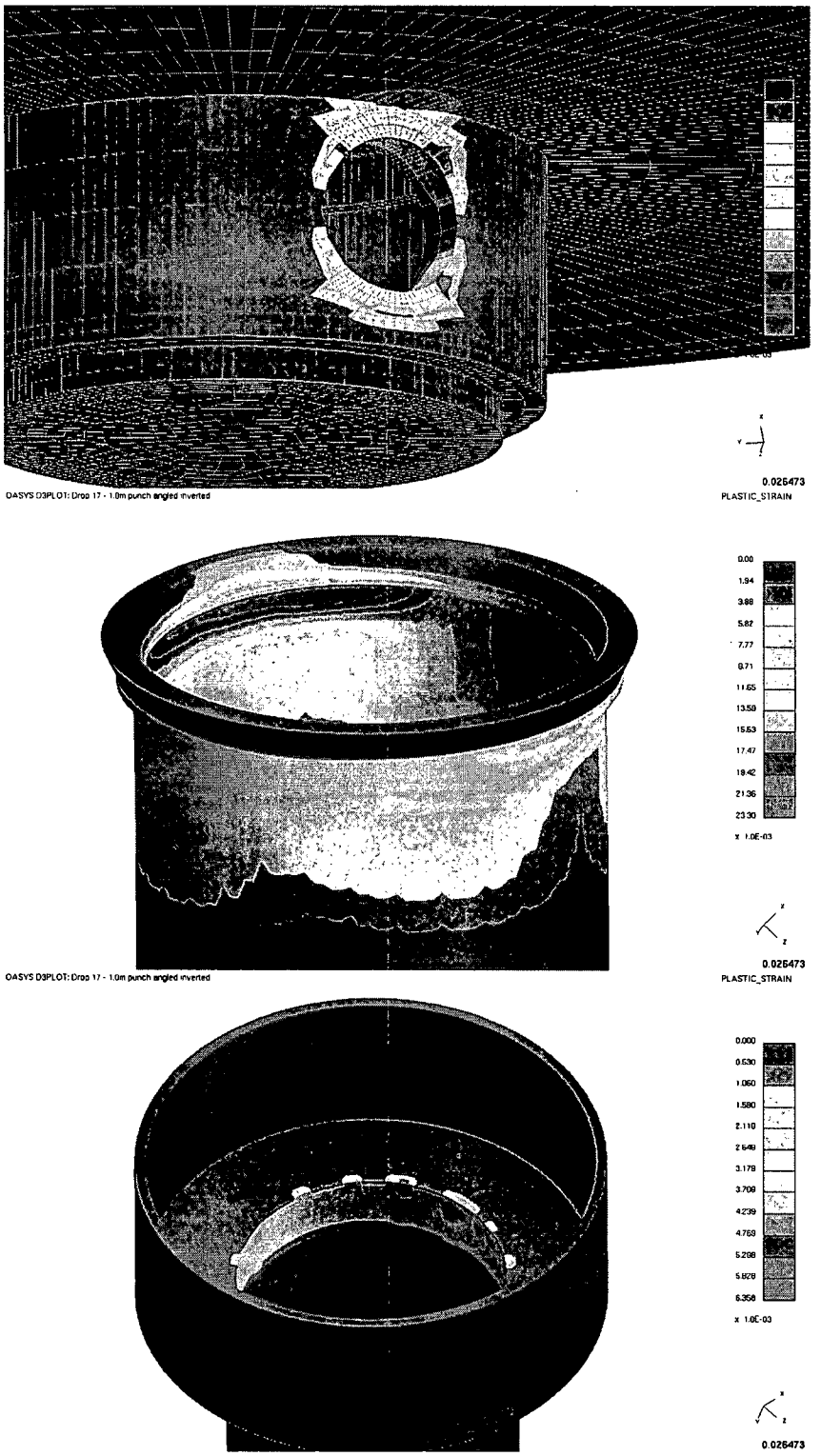

Figure 91 Containment boundary strains - Inner wall components

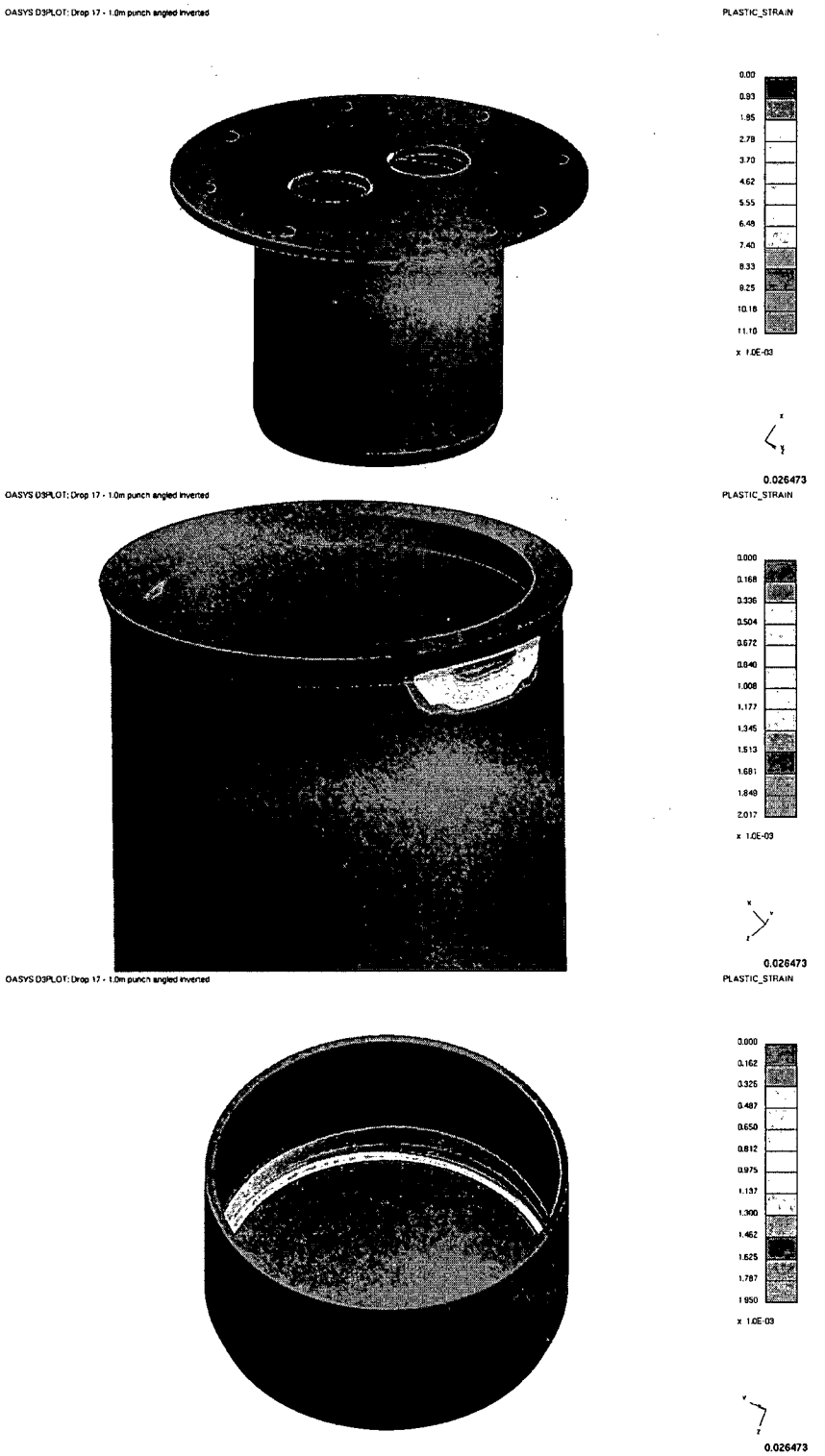

Figure 92 Containment boundary strains -Closure components

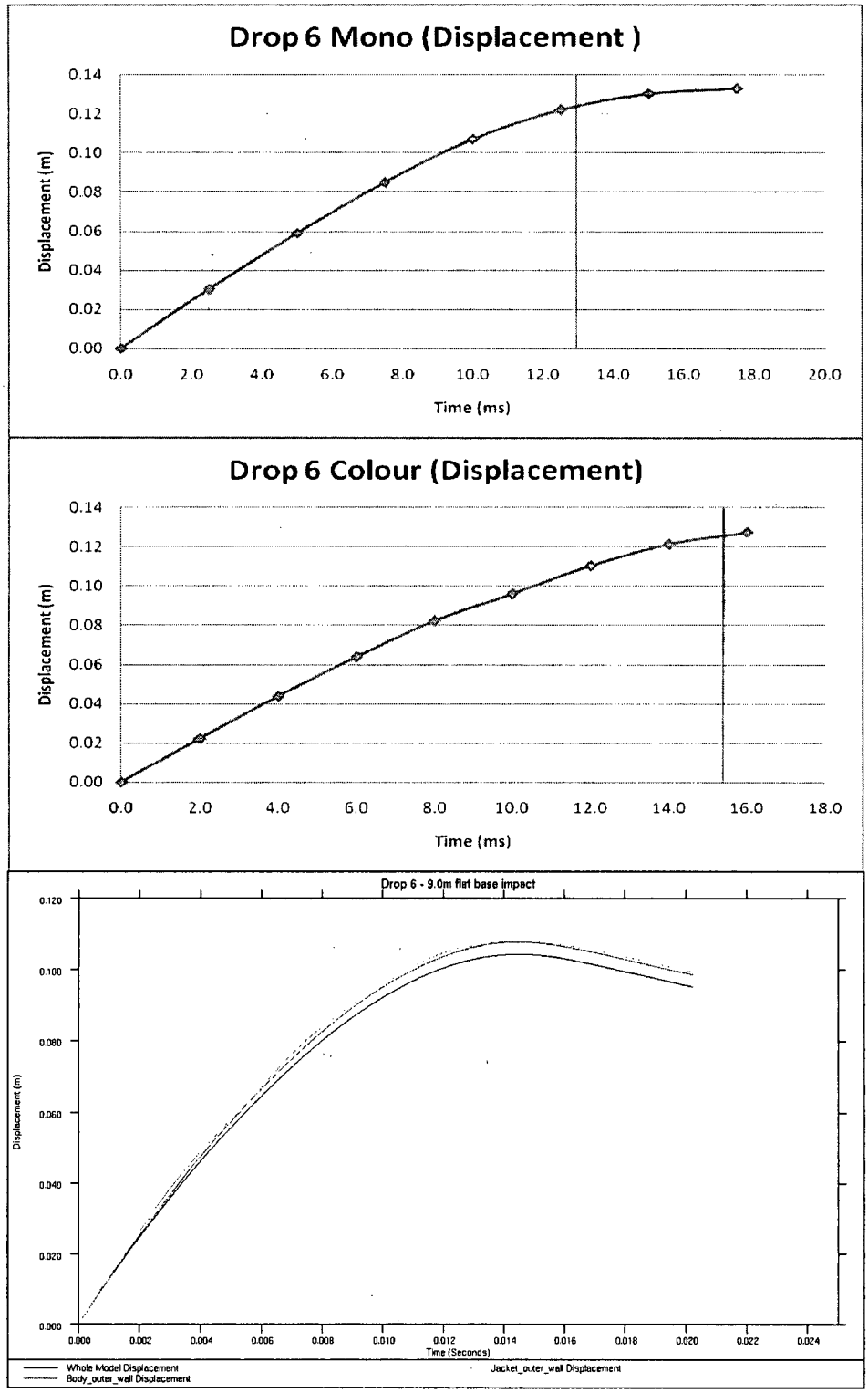

Figure 93: Drop 6 – comparison of displacement.

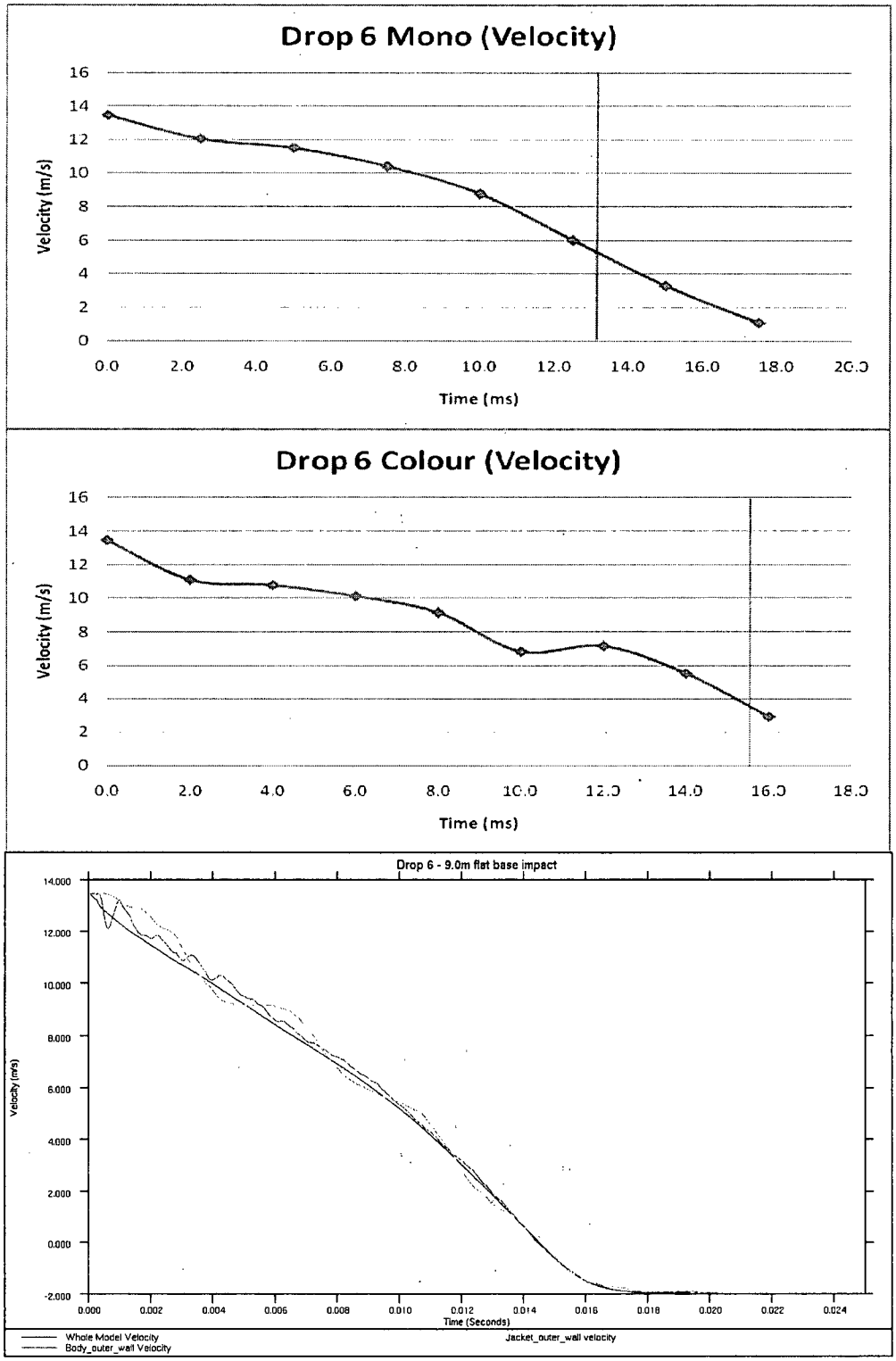

Figure 94: Drop 6 – comparison of velocity.

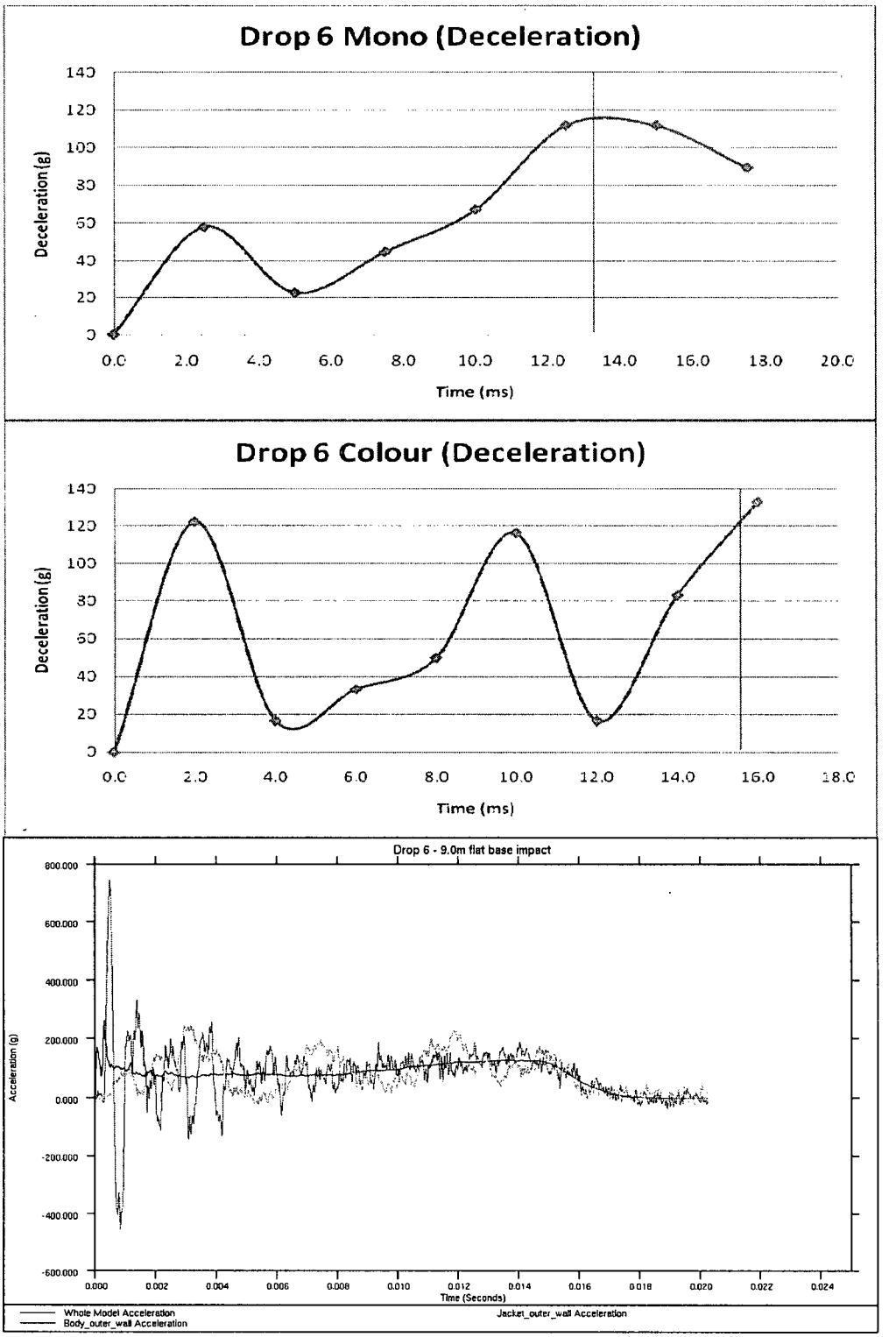

Figure 95: Drop 6 – comparison of acceleration.

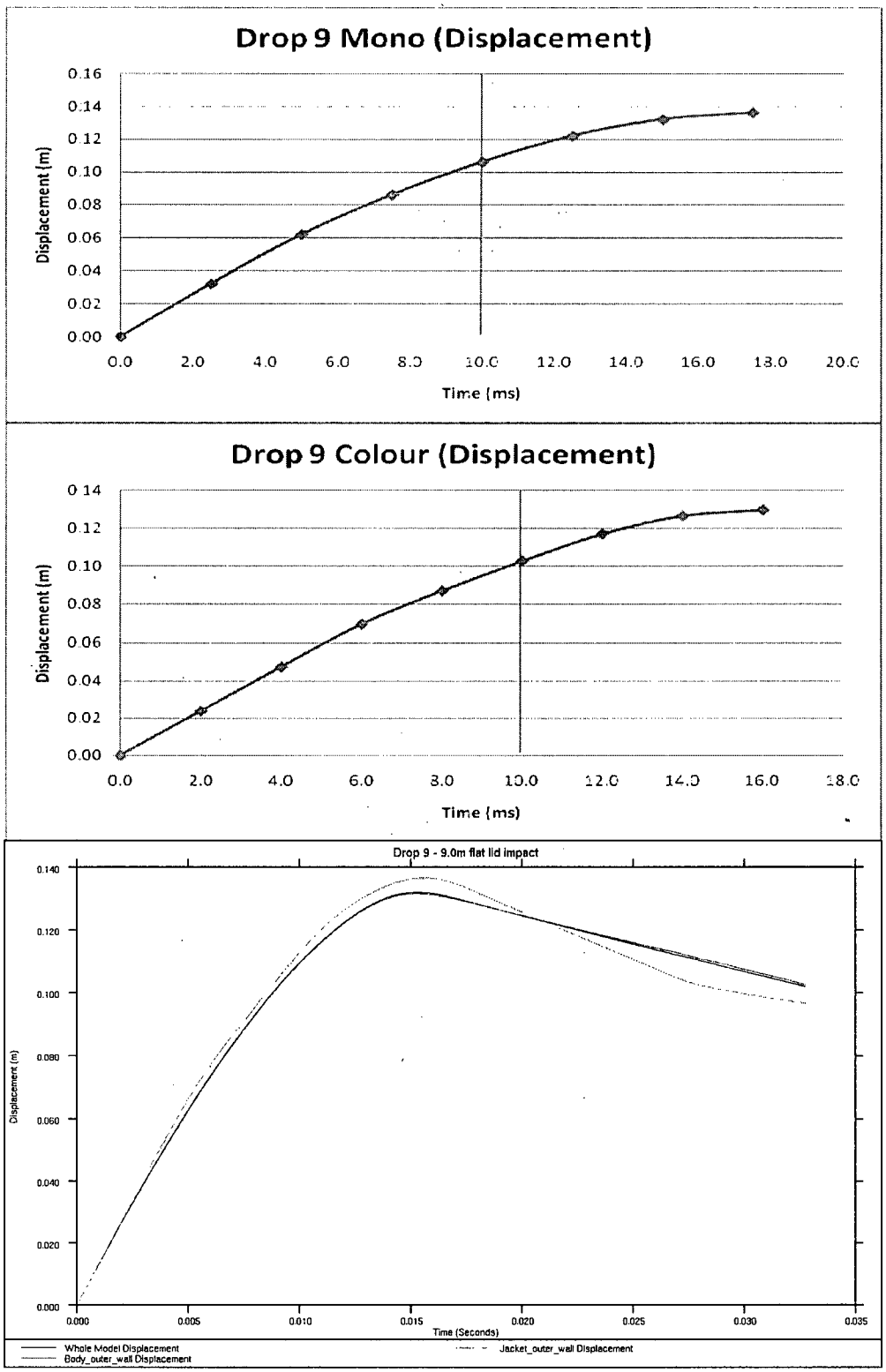

Figure 96: Drop 9 – comparison of displacement.

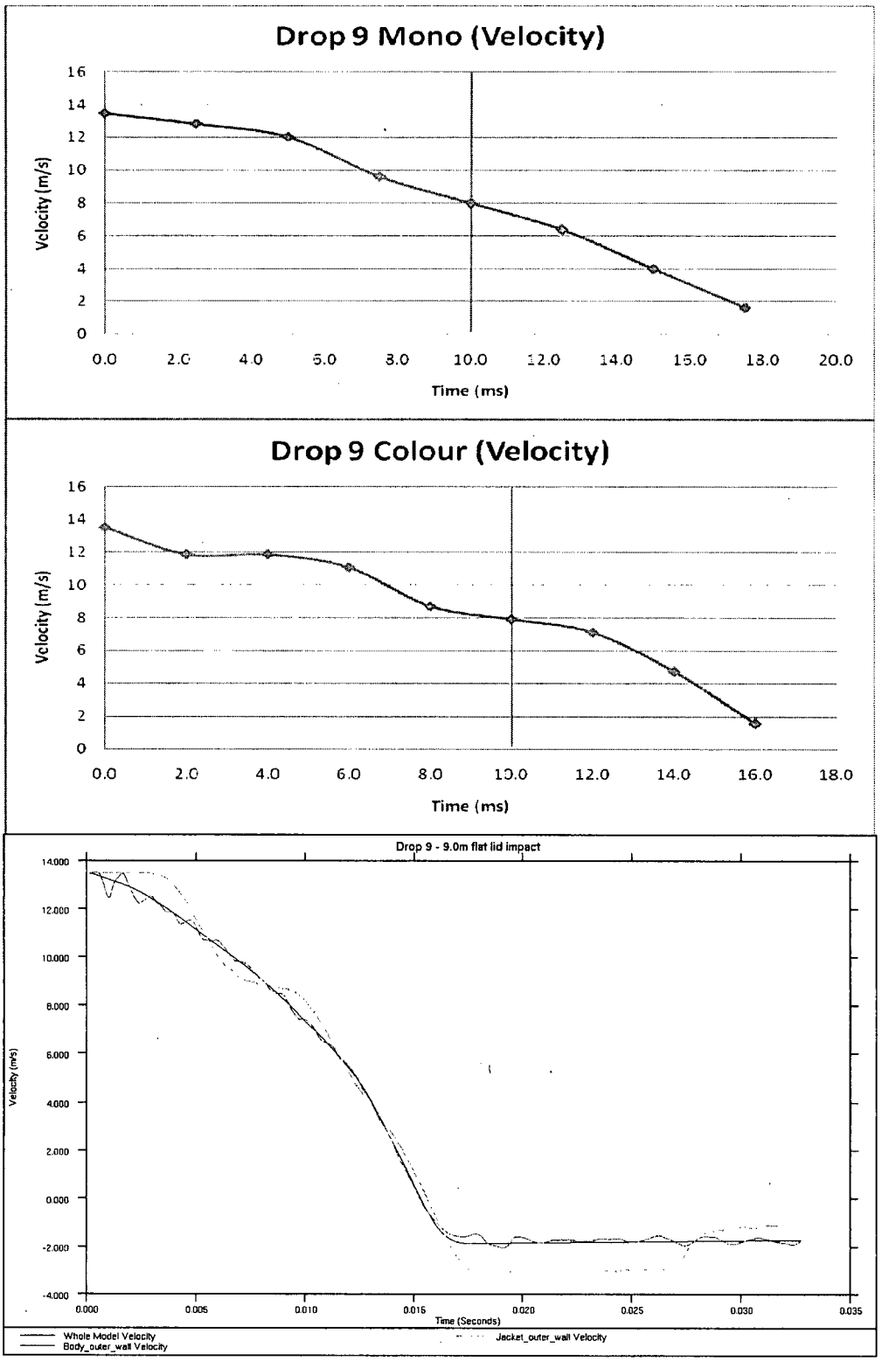

Figure 97: Drop 9 – comparison of velocity.

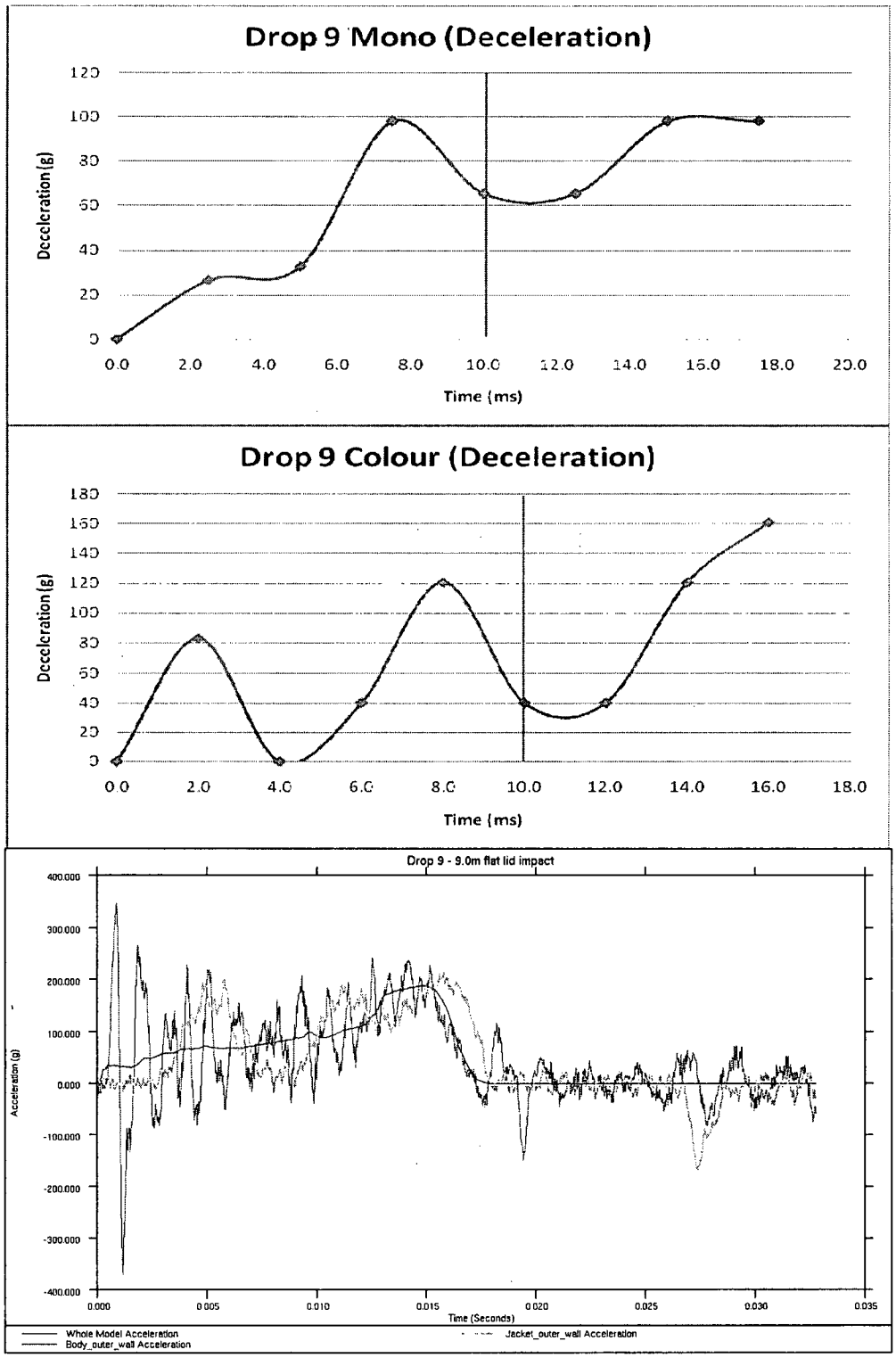

Figure 98: Drop 9 – comparison of acceleration.

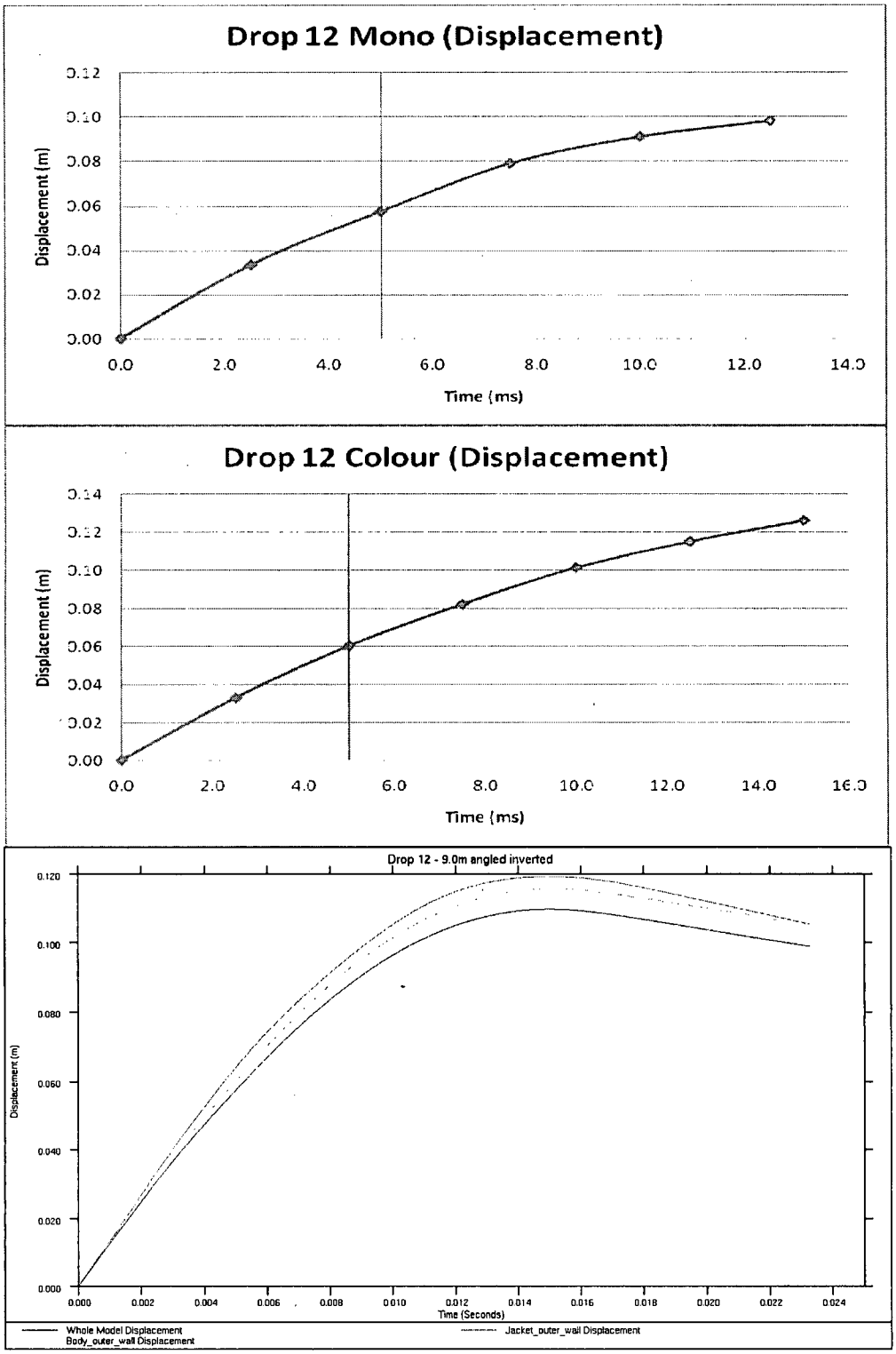

Figure 99: Drop 12 – comparison of displacement.

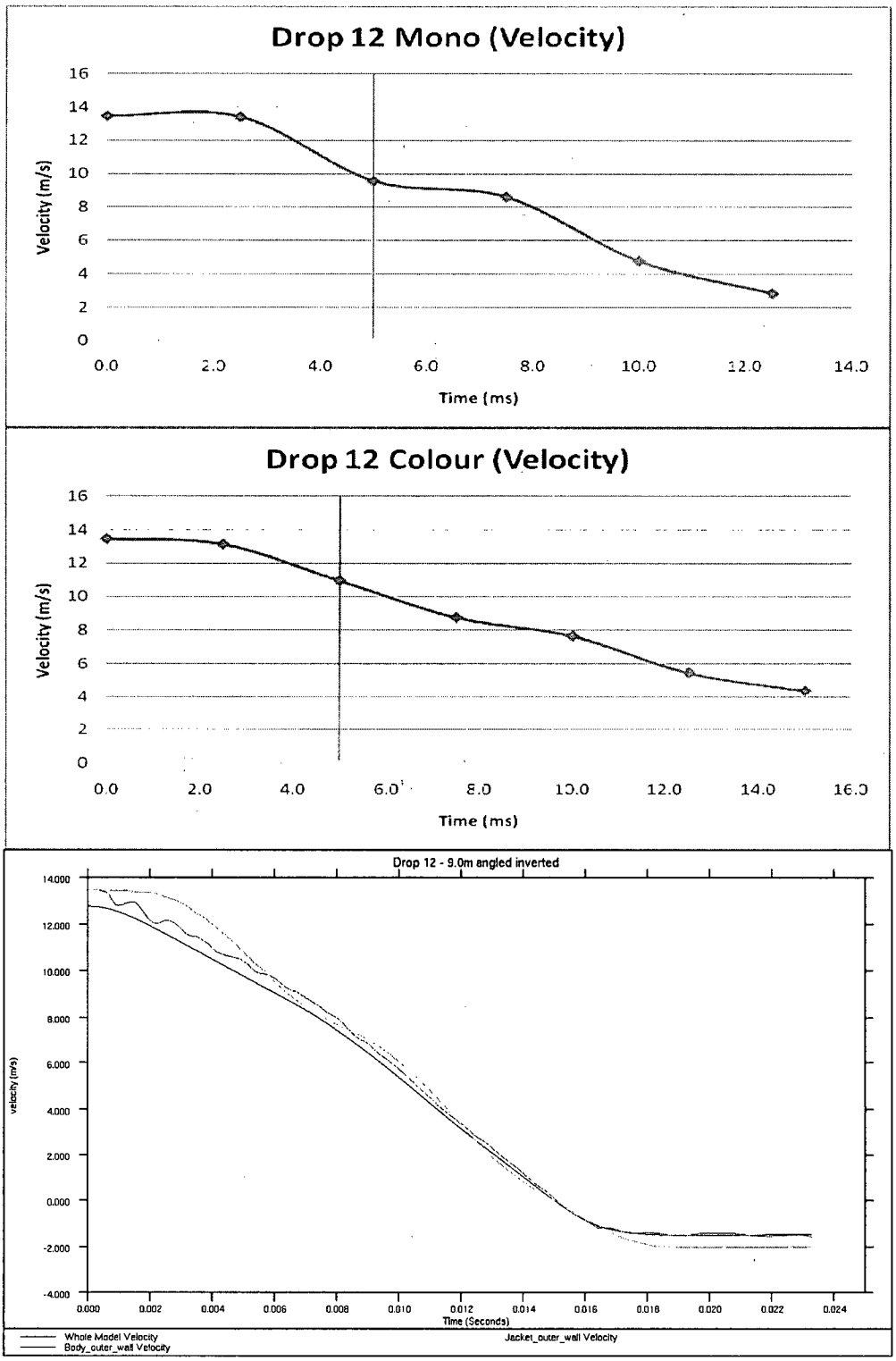

Figure 100: Drop 12 – comparison of velocity.

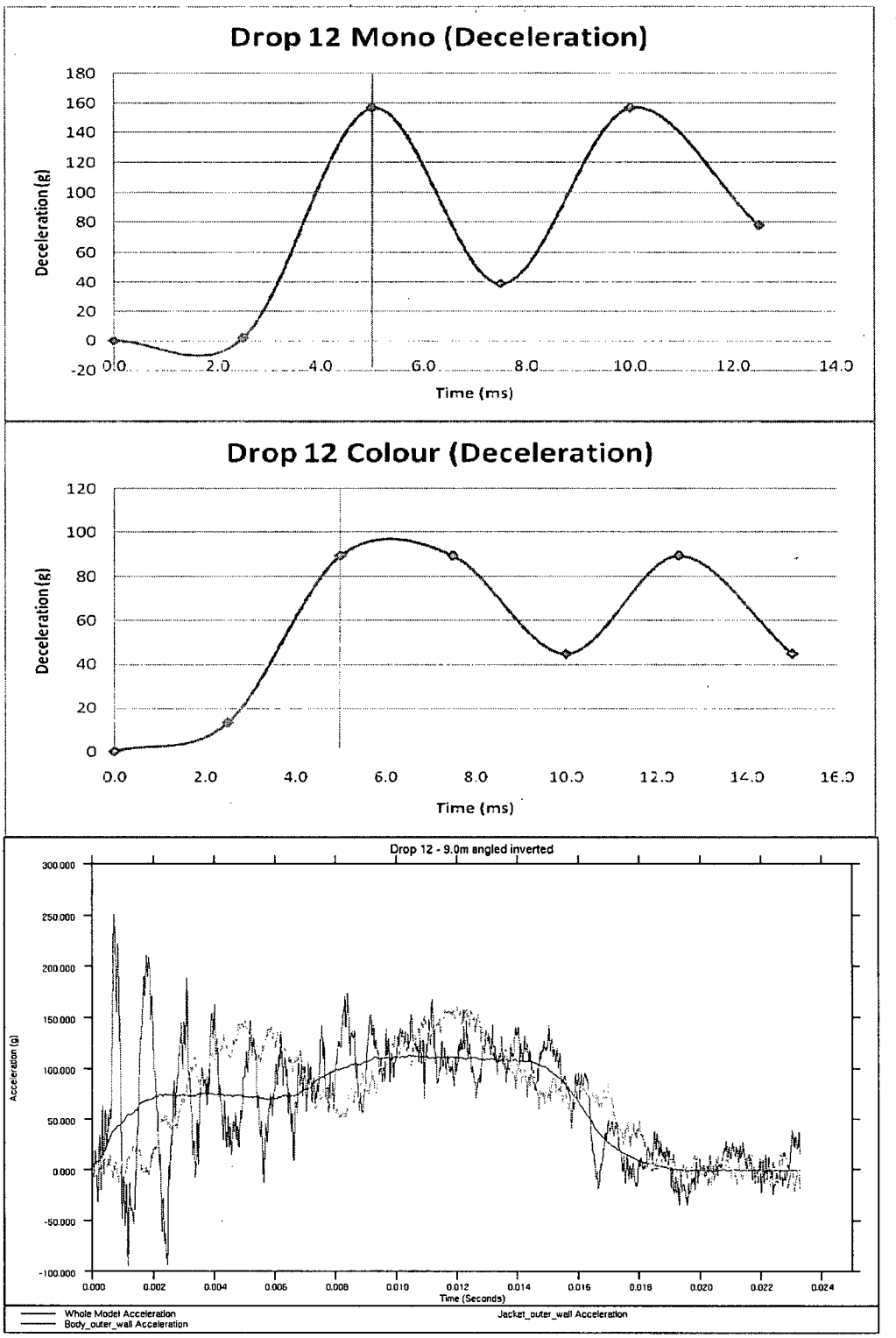

Figure 101: Drop 12 – comparison of acceleration.

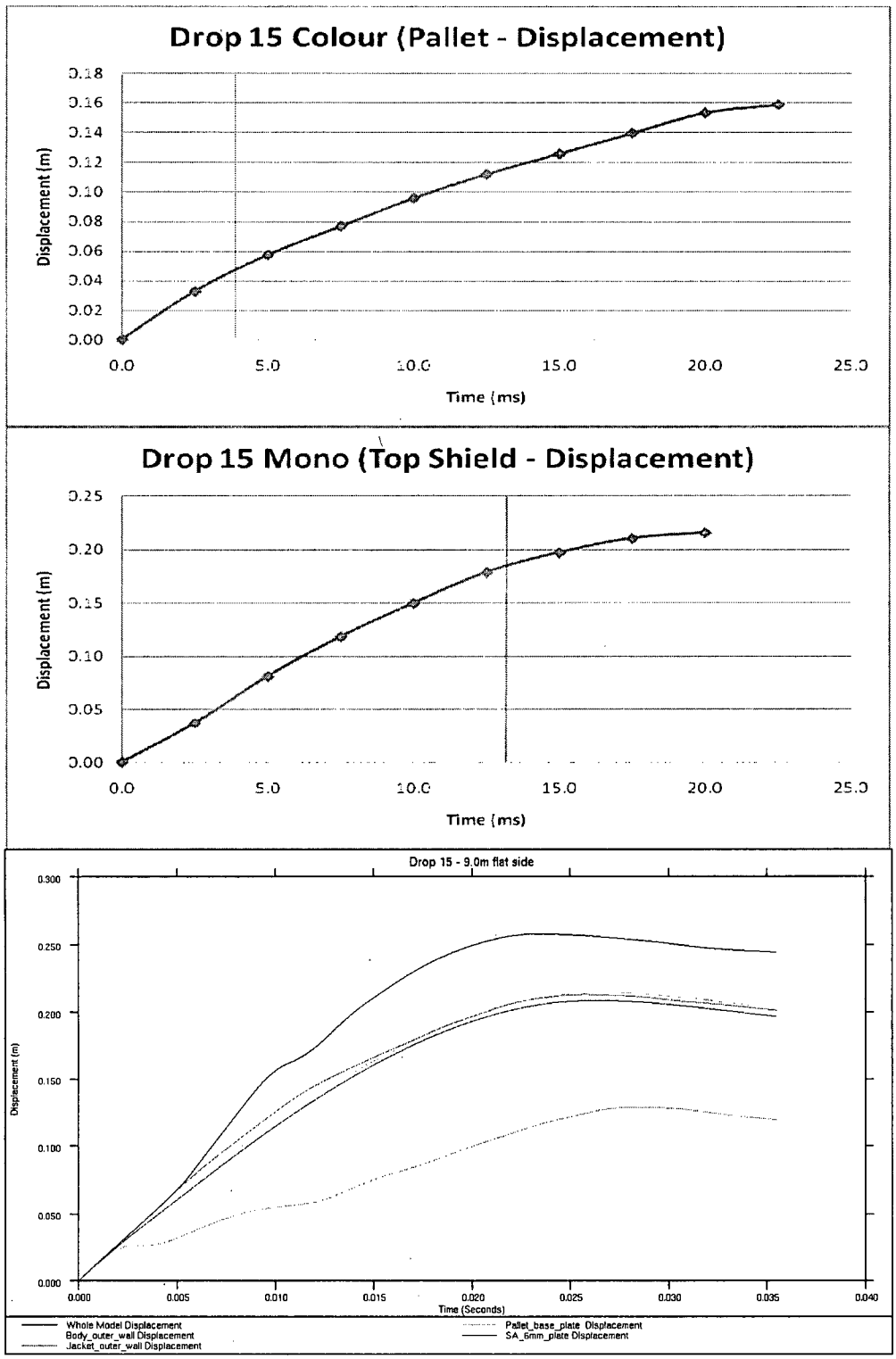

Figure 102: Drop 15 – comparison of displacement.

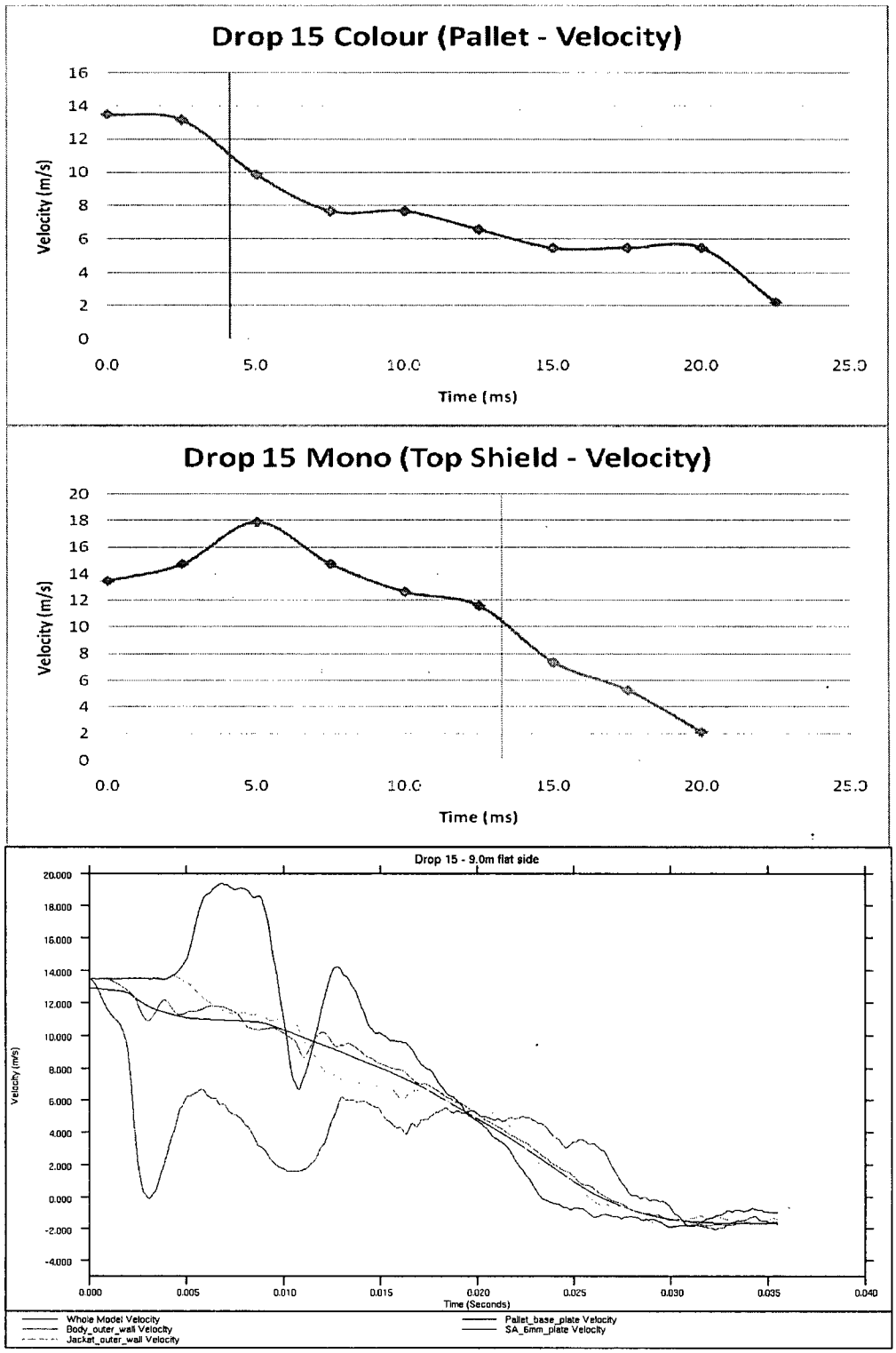

Figure 103: Drop 15 – comparison of velocity.

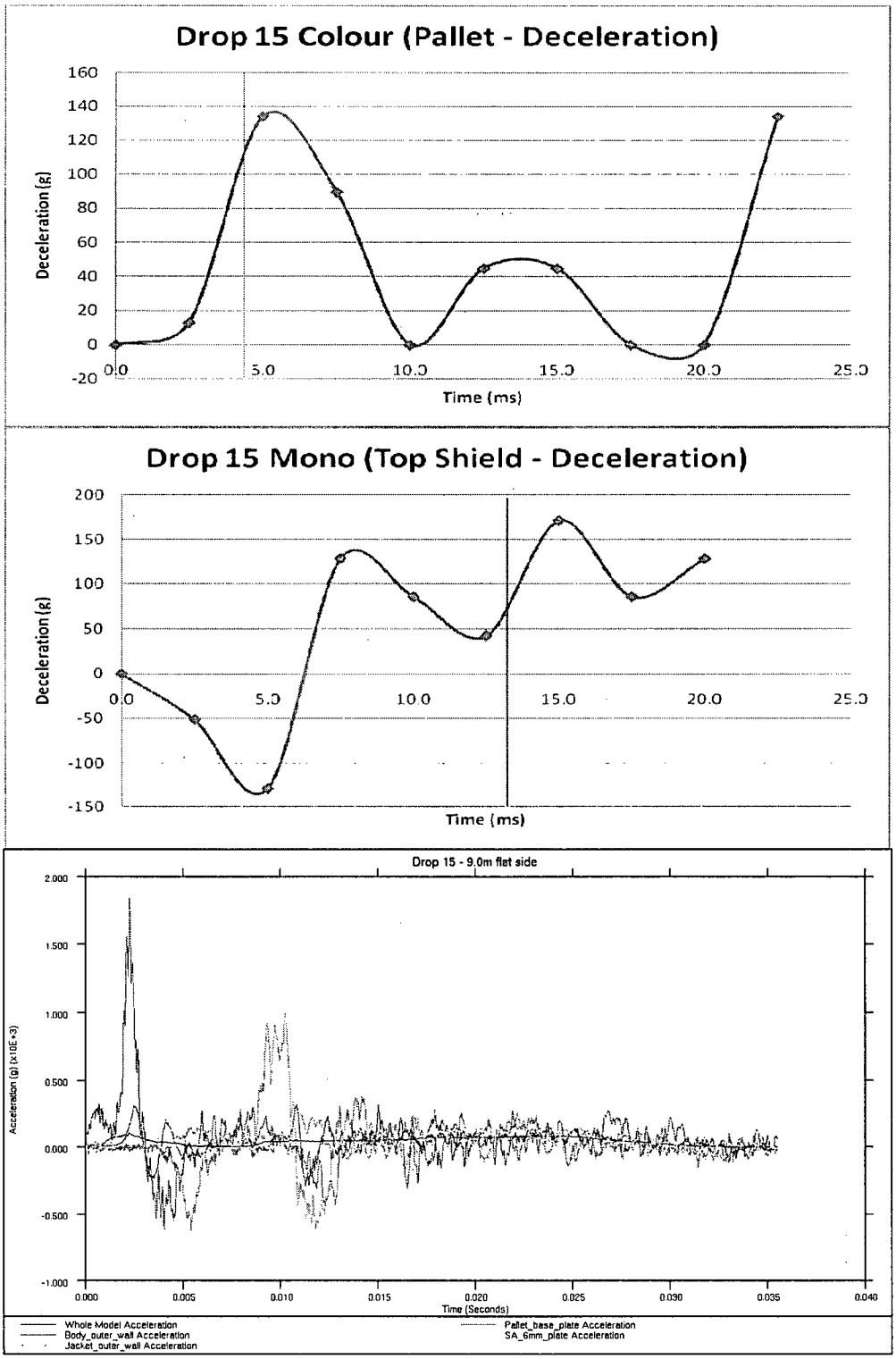

Figure 104: Drop 15 – comparison of acceleration.

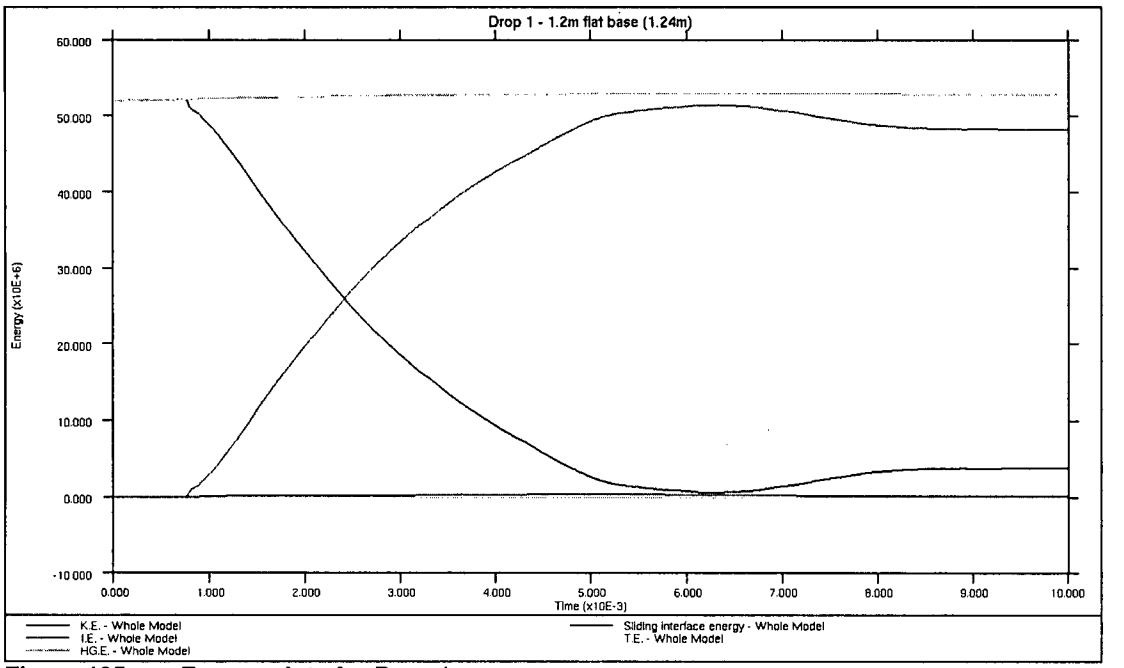

Figure 105: Energy plots for Drop 1

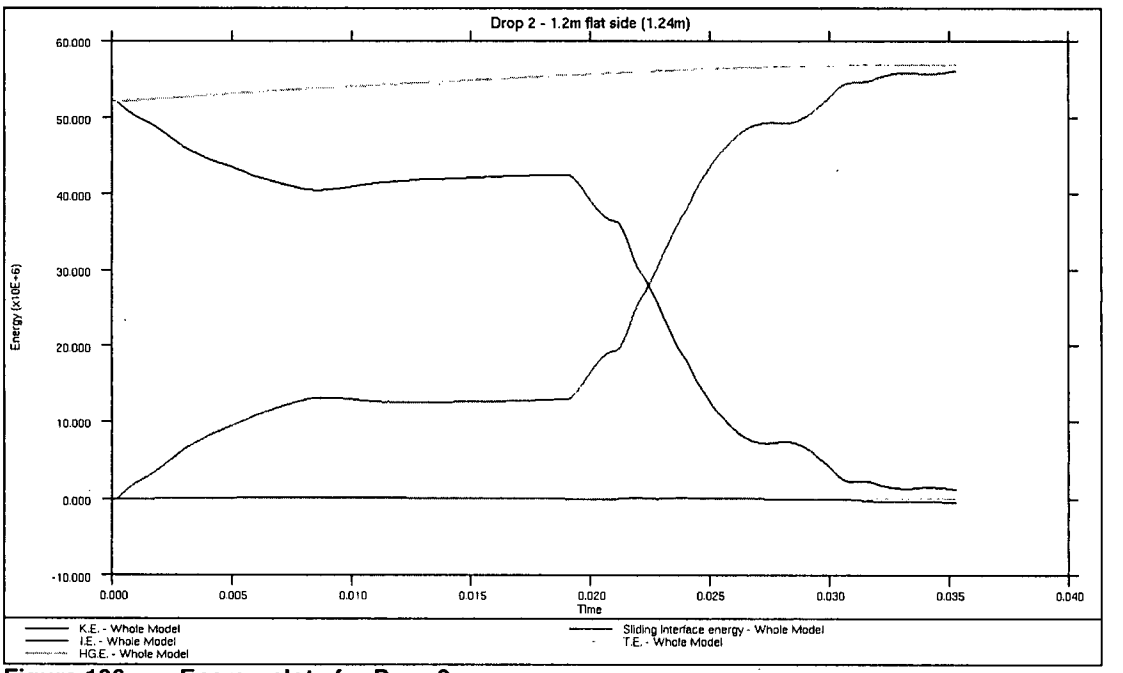

Figure 106: Energy plots for Drop 2

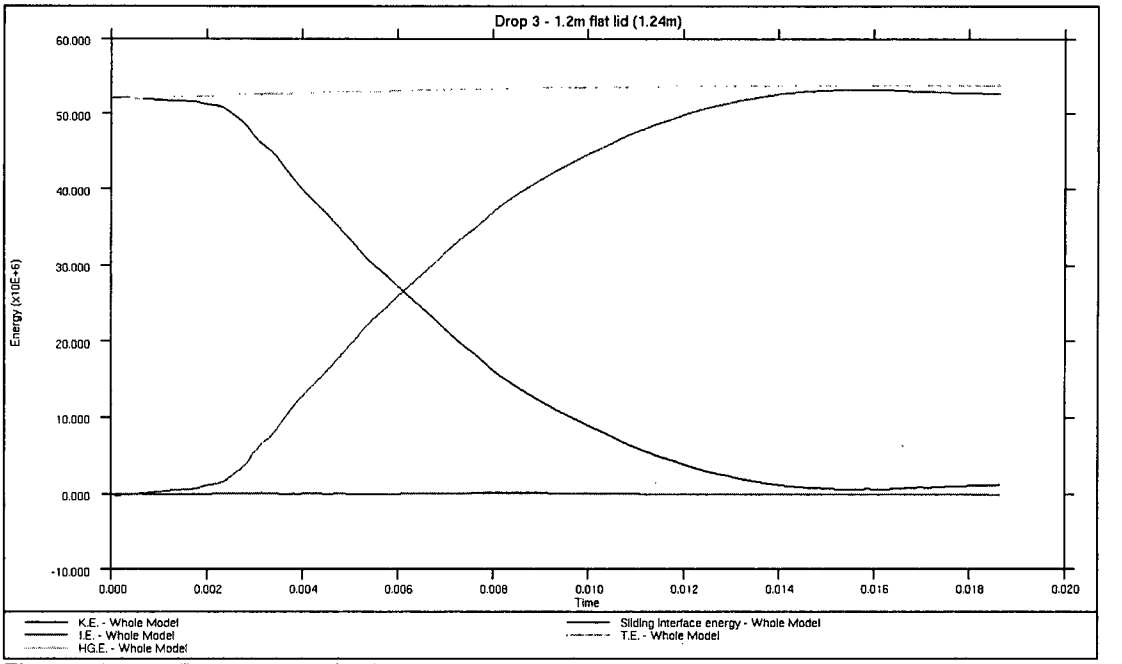

Figure 107: Energy plots for Drop 3

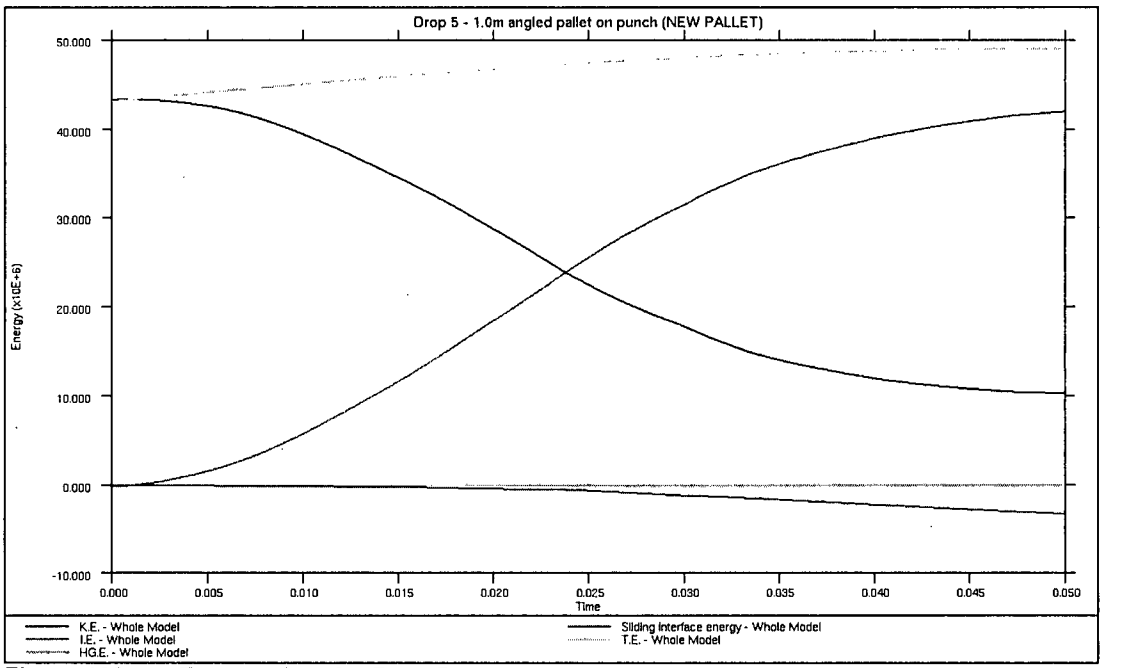

Figure 108: Energy plots for Drop 5

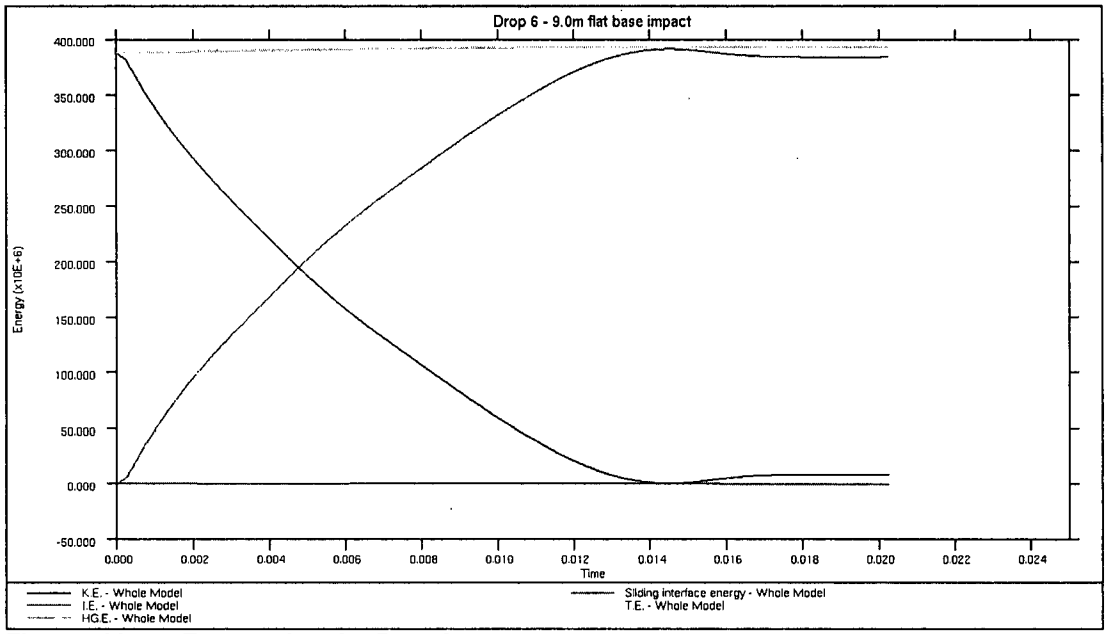

Figure 109: Energy plots for Drop 6

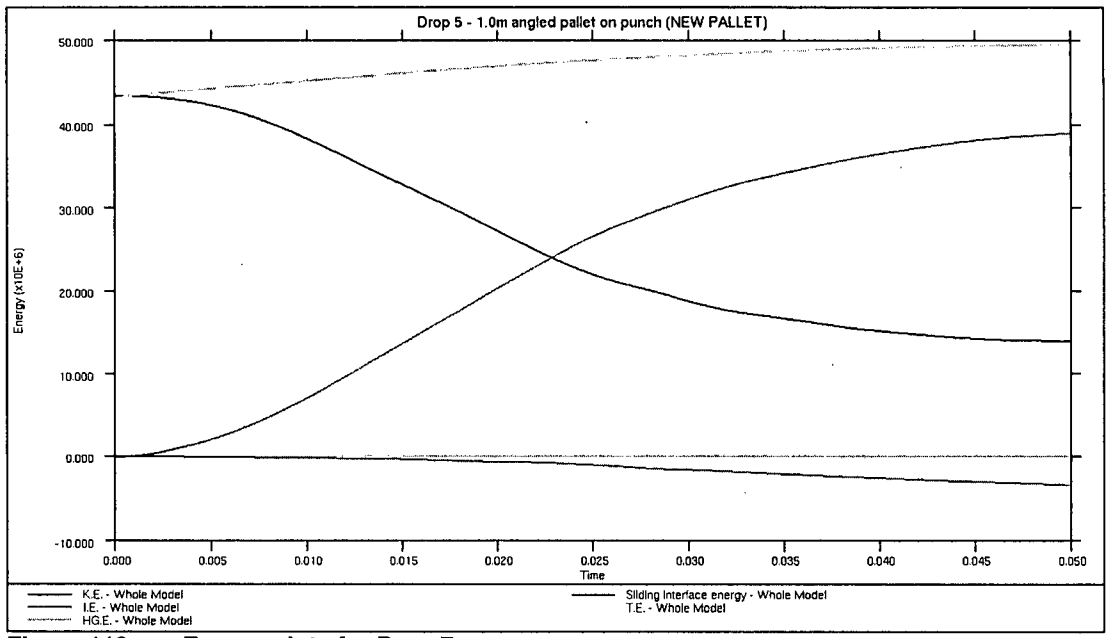

Figure 110: Energy plots for Drop 7

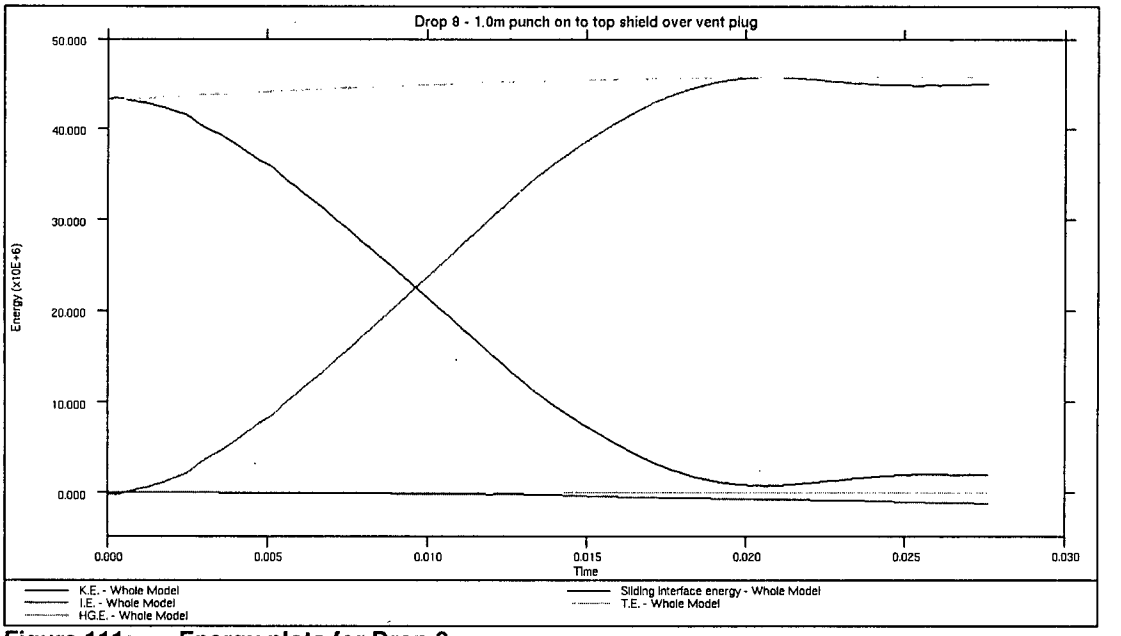

Figure 111: Energy plots for Drop 8

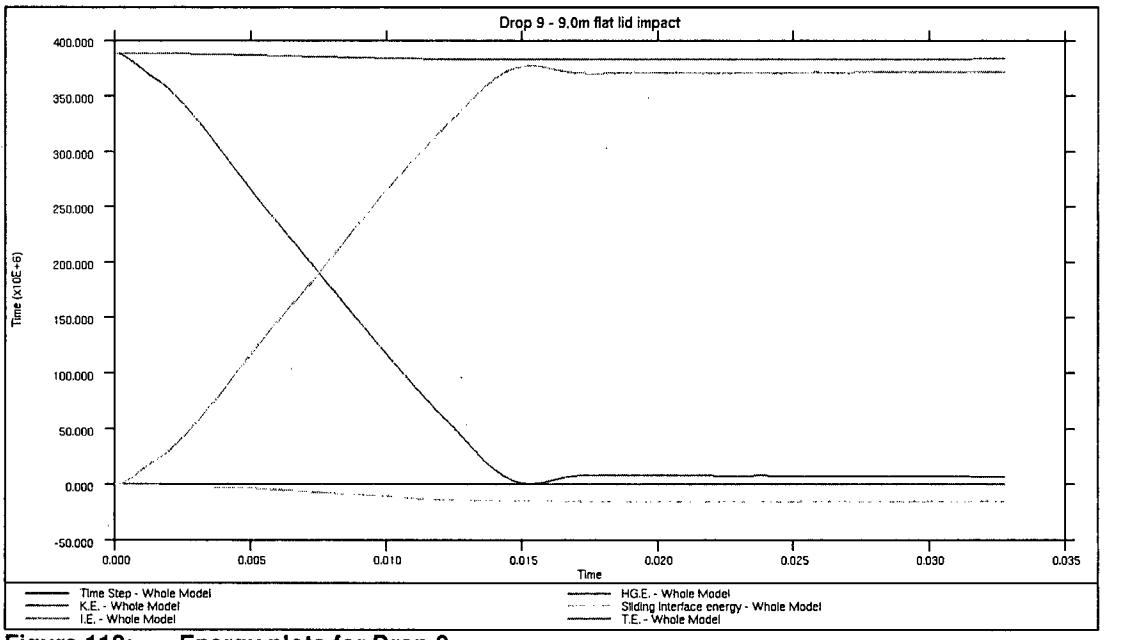

Figure 112: Energy plots for Drop 9

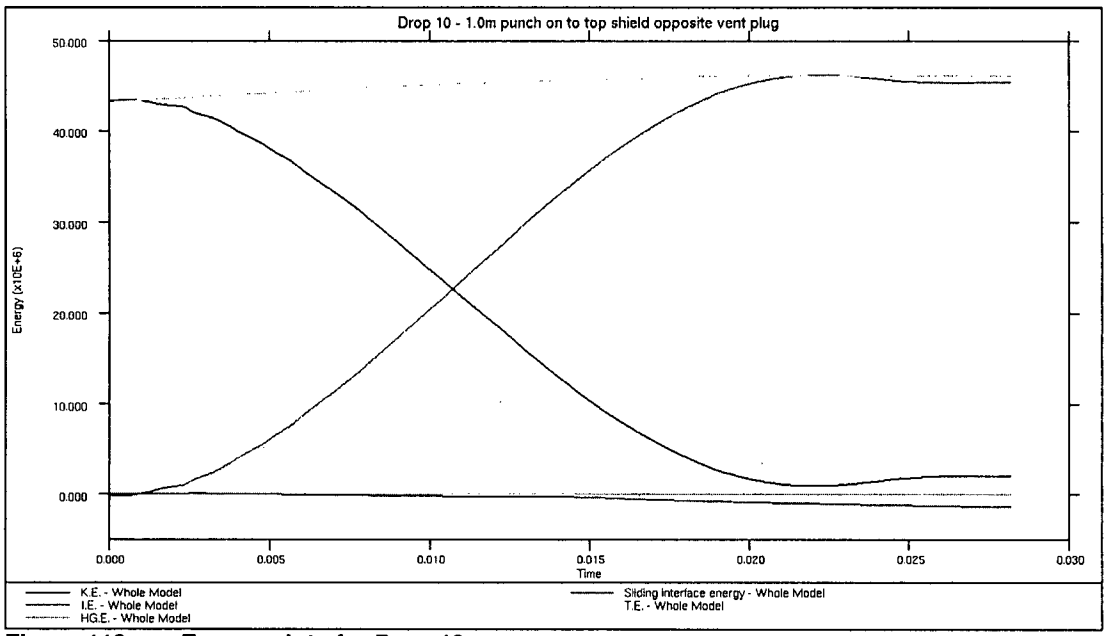

Figure 113: Energy plots for Drop 10

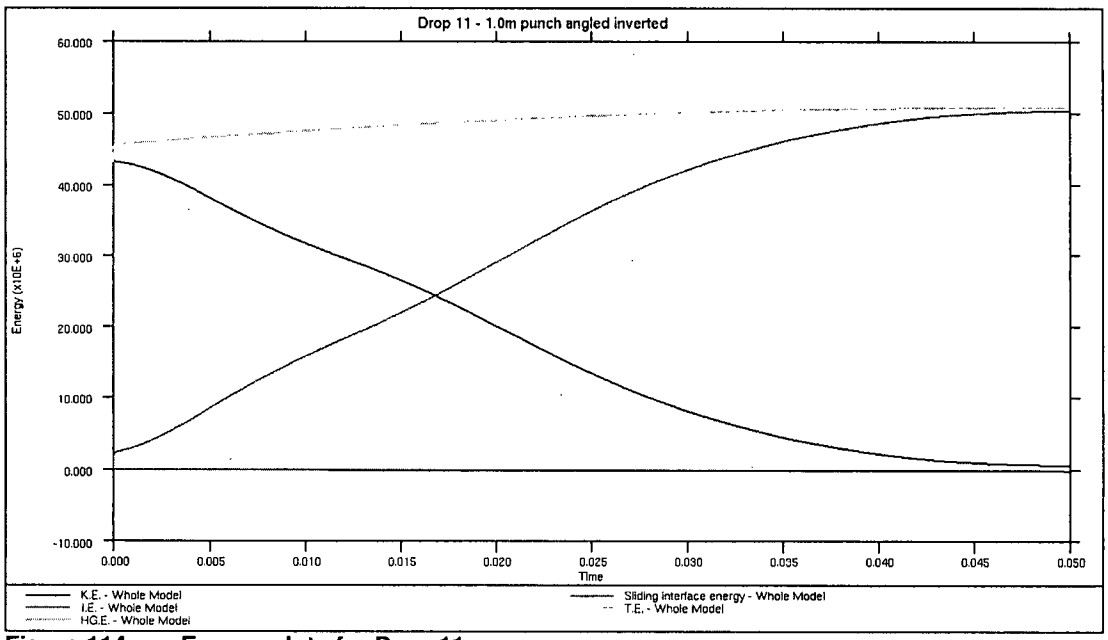

Figure 114: Energy plots for Drop 11

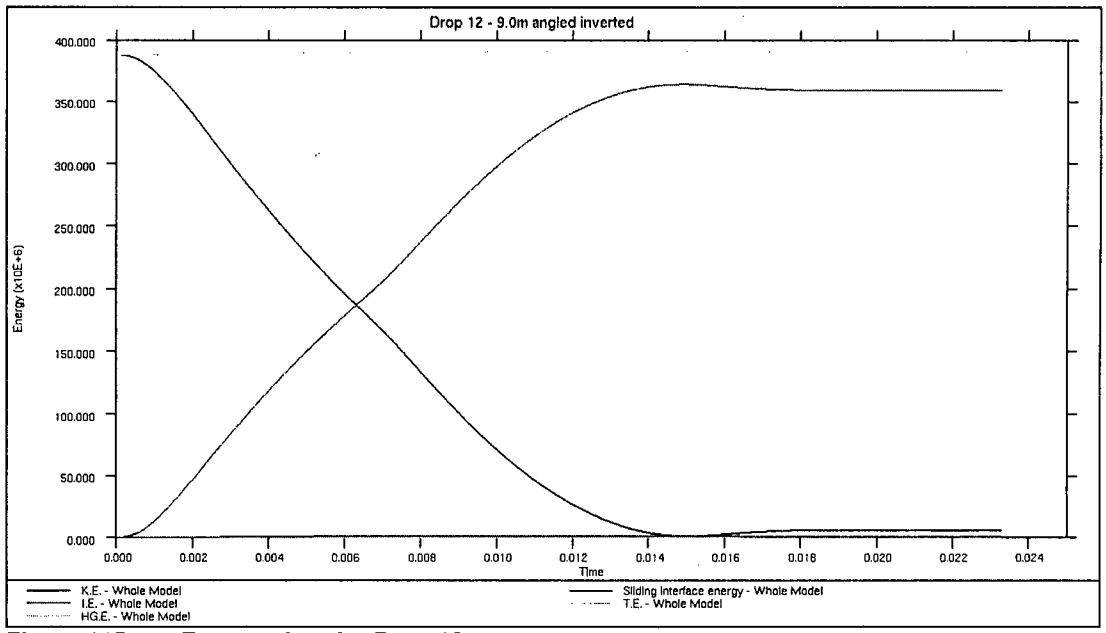

Figure 115: Energy plots for Drop 12

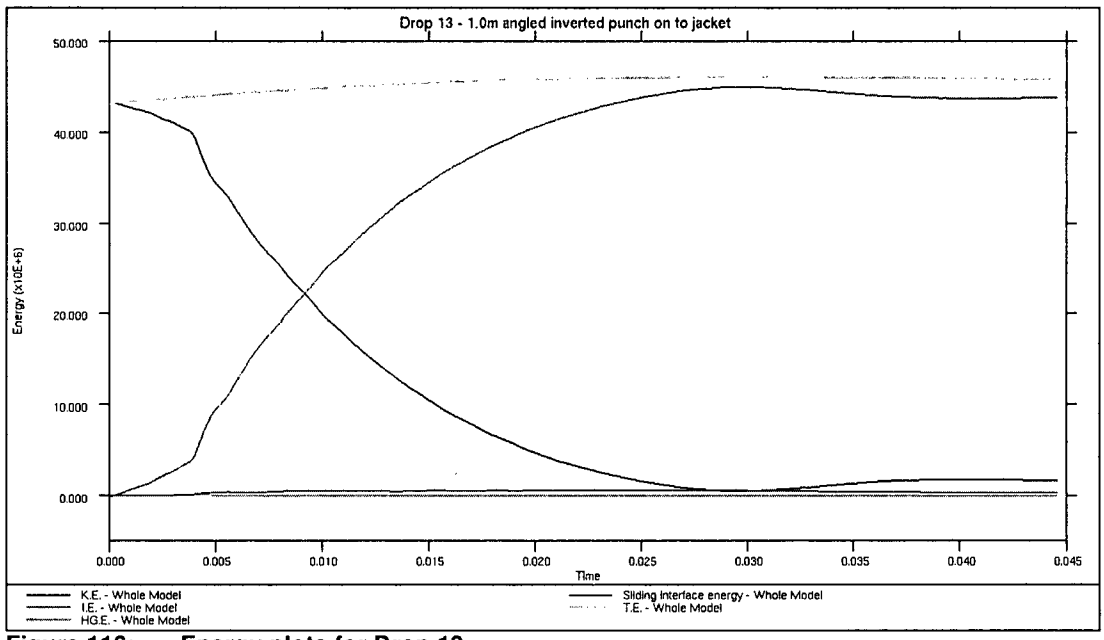

Figure 116: Energy plots for Drop 13

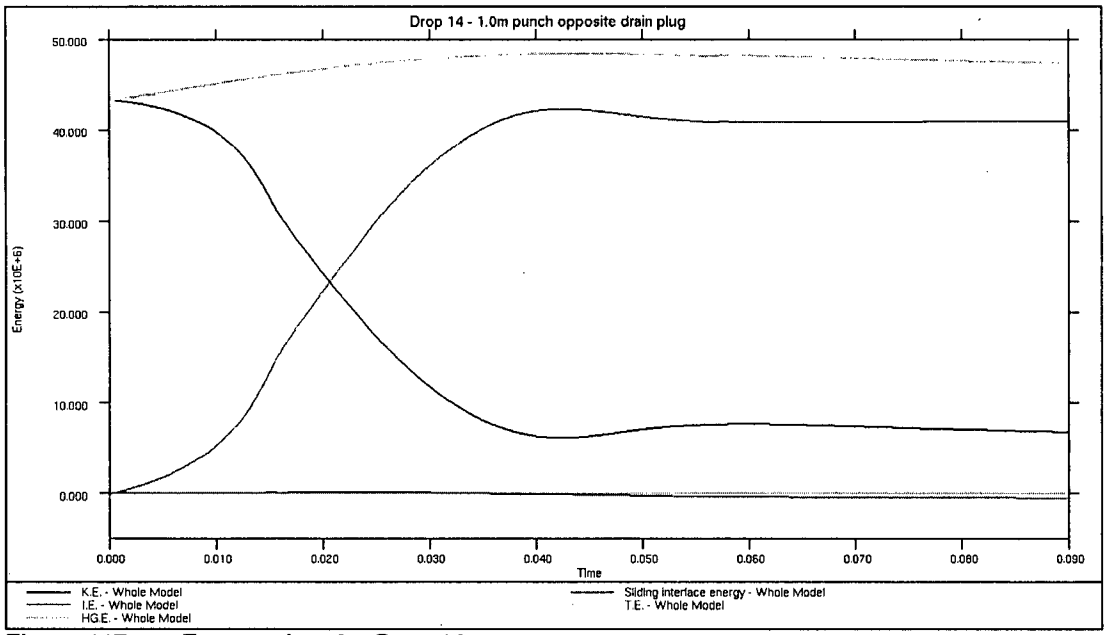

Figure 117: Energy plots for Drop 14

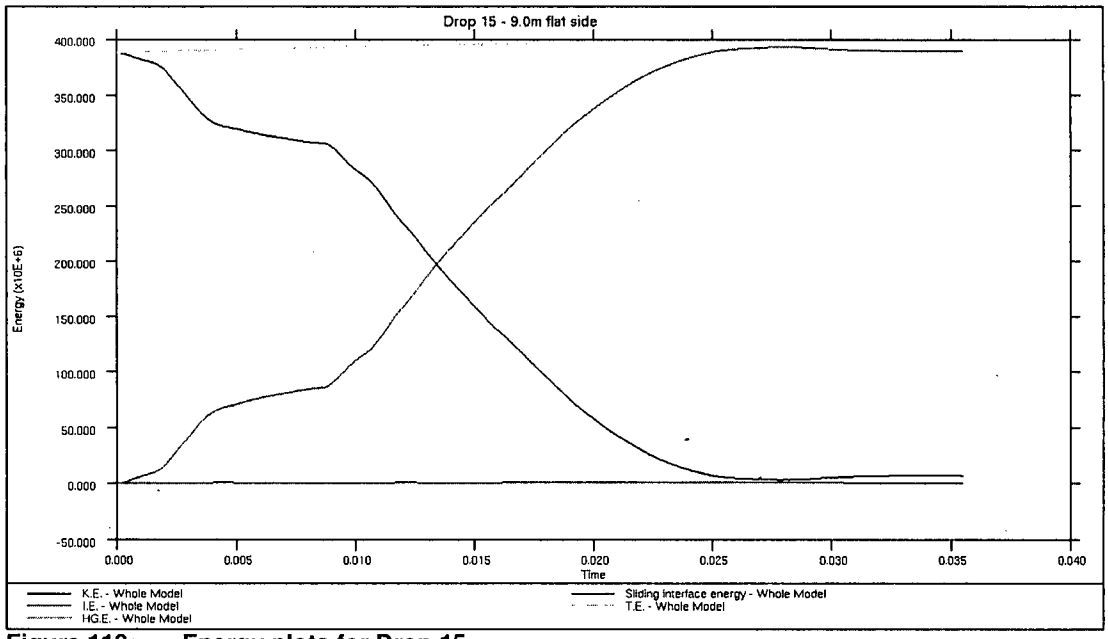

Figure 118: Energy plots for Drop 15

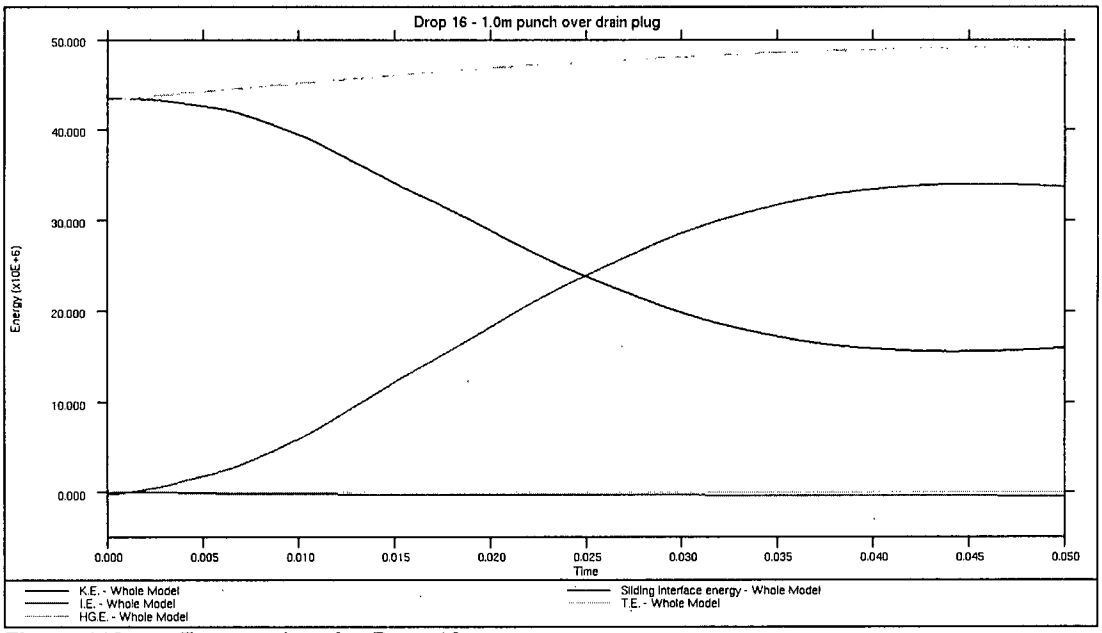

Figure 119: Energy plots for Drop 16

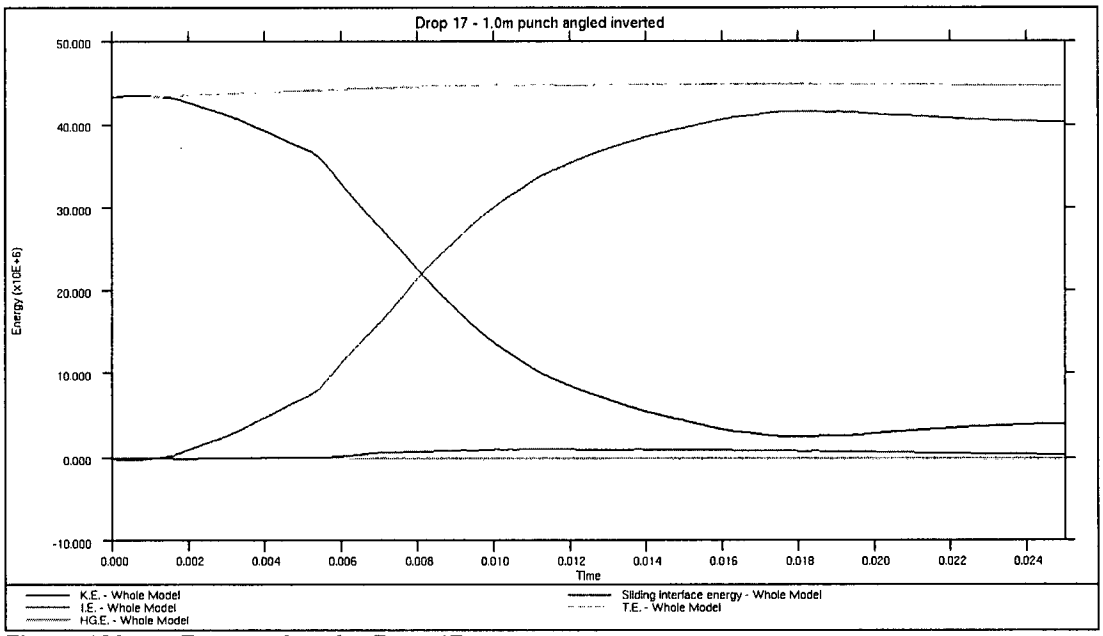

Figure 120: Energy plots for Drop 17

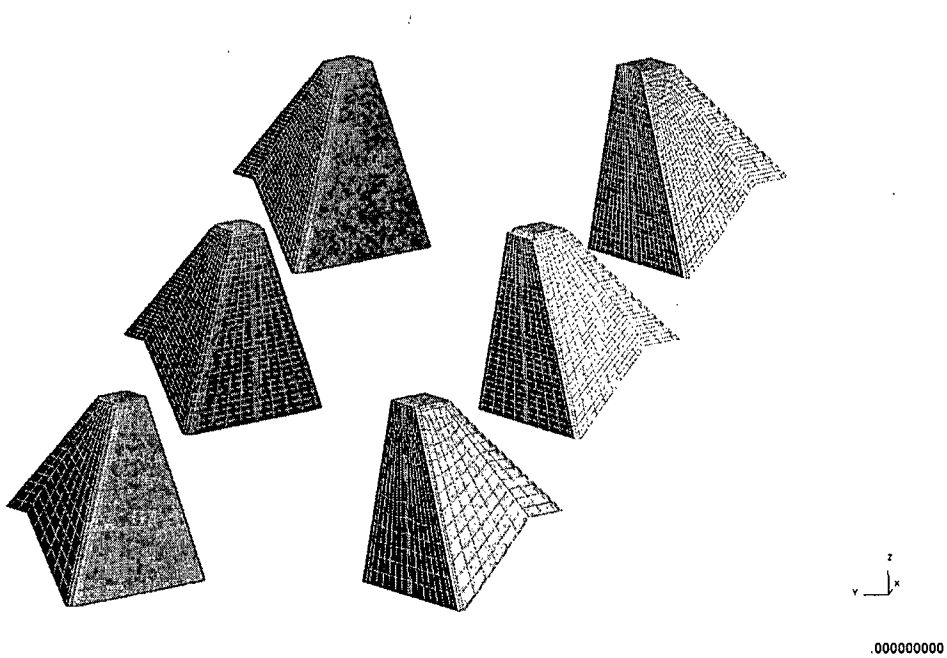

Figure 121: Comparison of cone mesh.

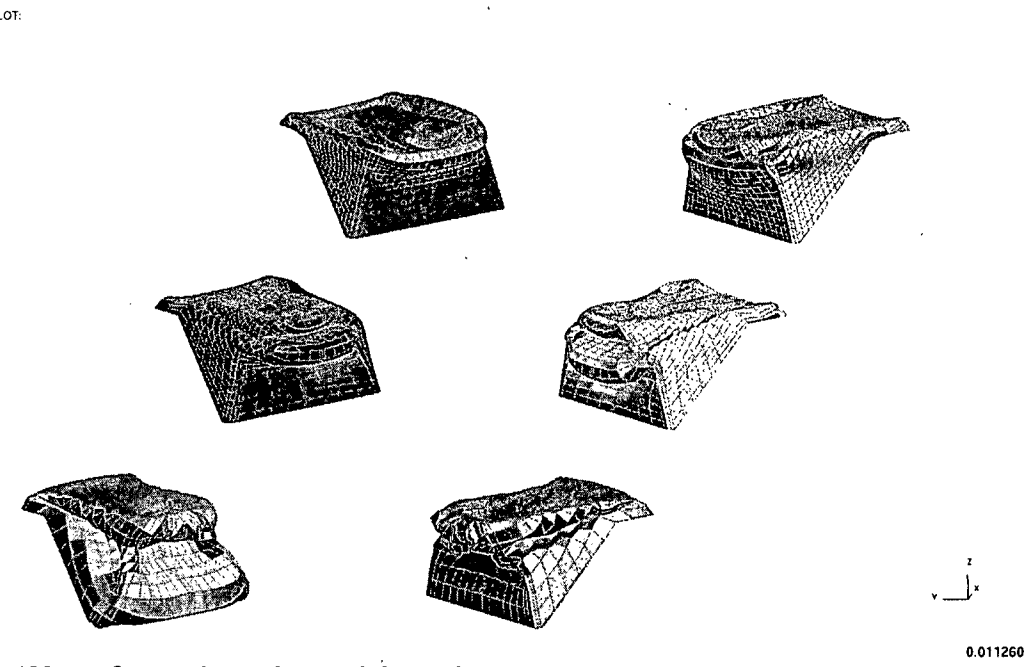

Figure 122: Comparison of cone deformation.

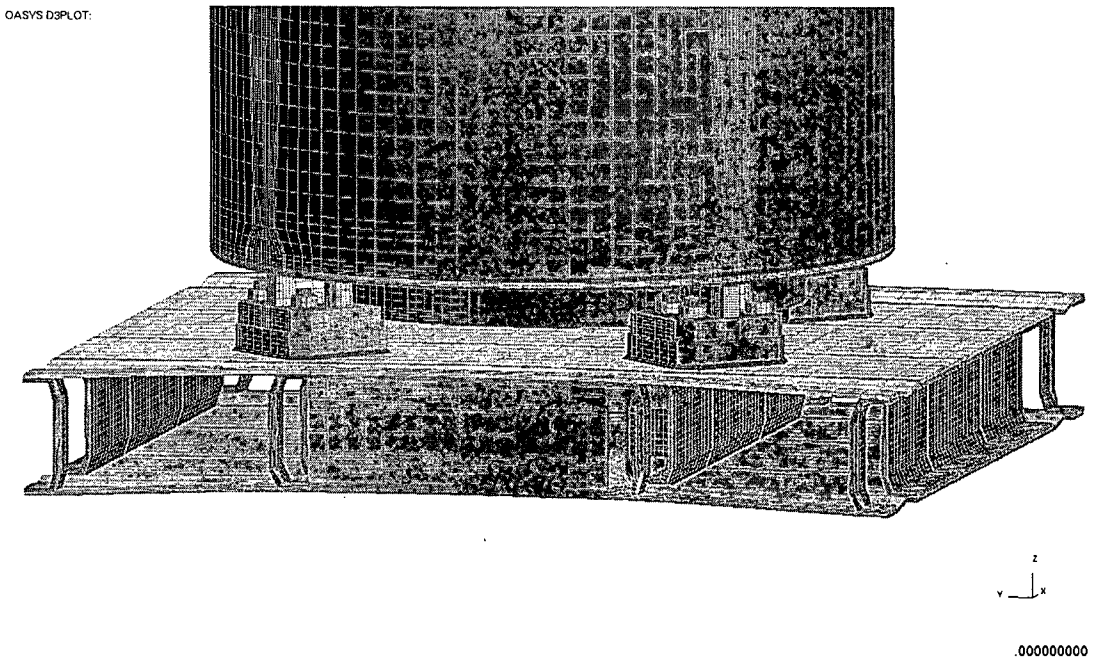

Figure 123: Refined mesh and weld representation in pallet.

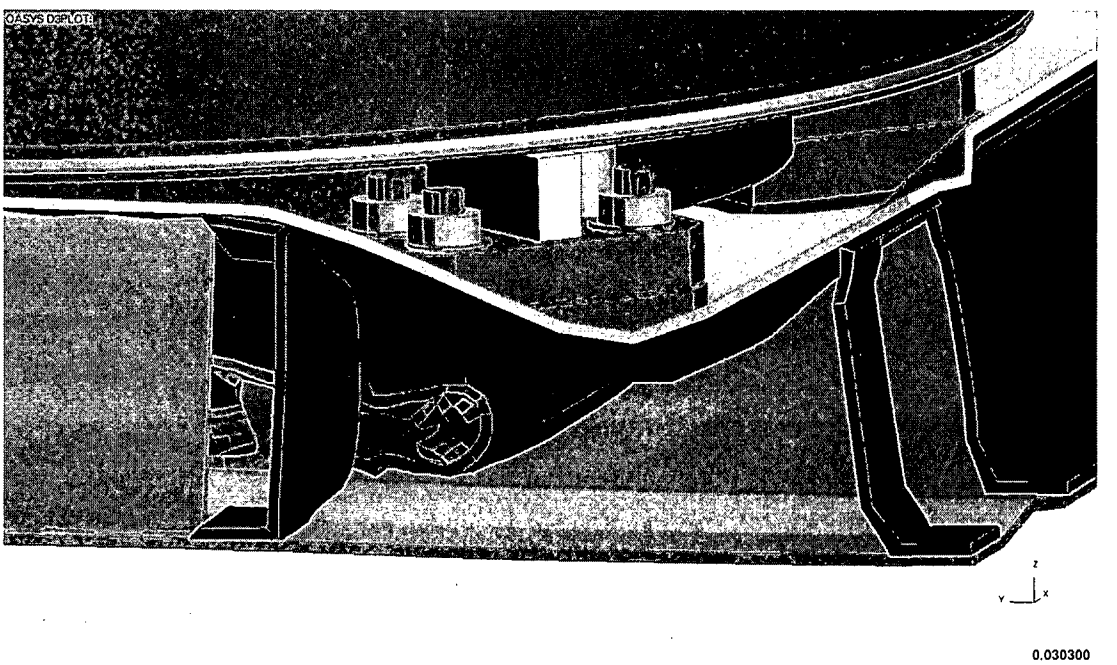

Figure 124: Improved deformation in pallet.

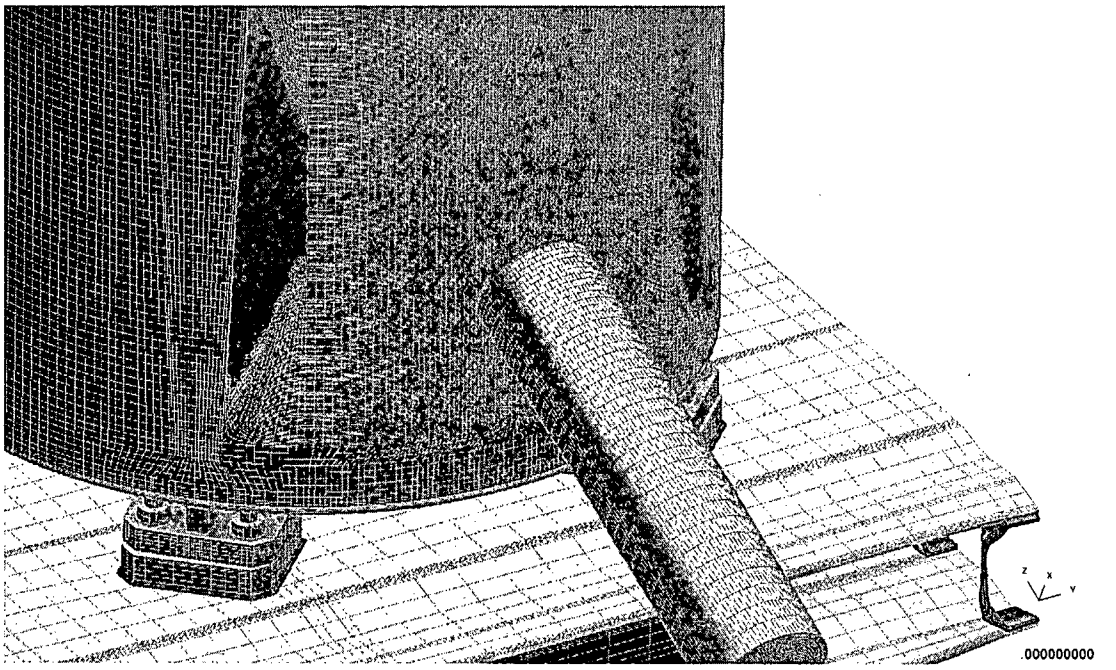

Figure 125: Refined mesh for punch analysis.

Figure 126: Predicted tearing of outer jacket wall

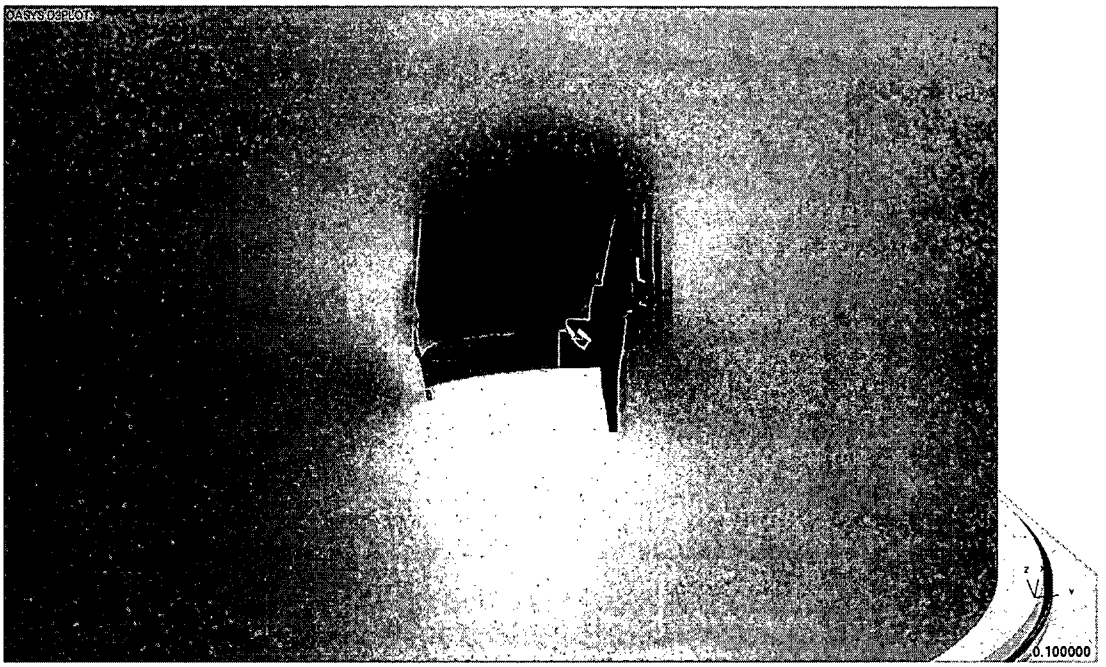

Figure 127: Predicted tearing of inner jacket wall.

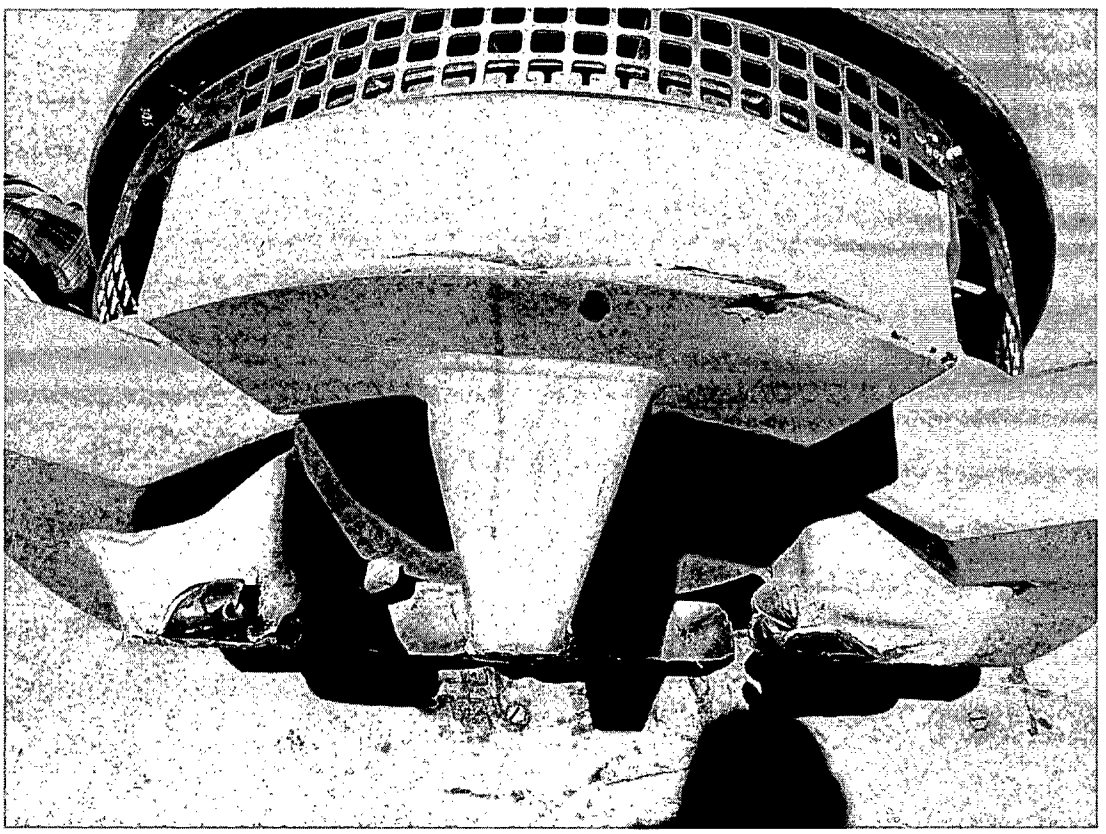

Figure 128: Secondary damage to weld area of top shield quadrant.

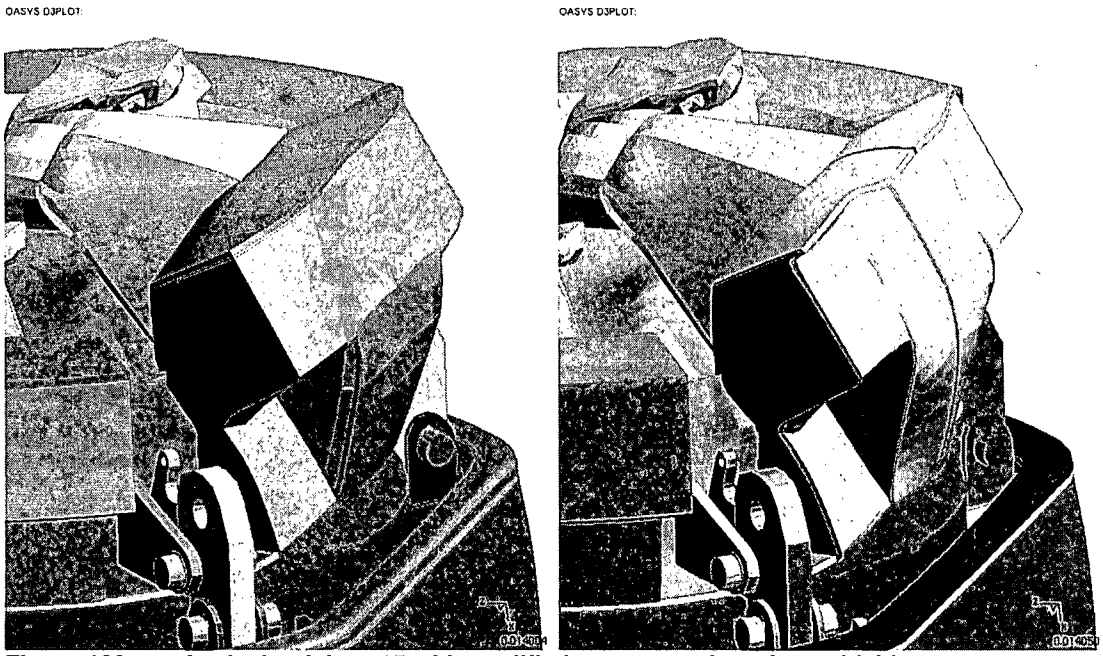

Figure 129: Analysis of drop 15 with modified representation of top shield.

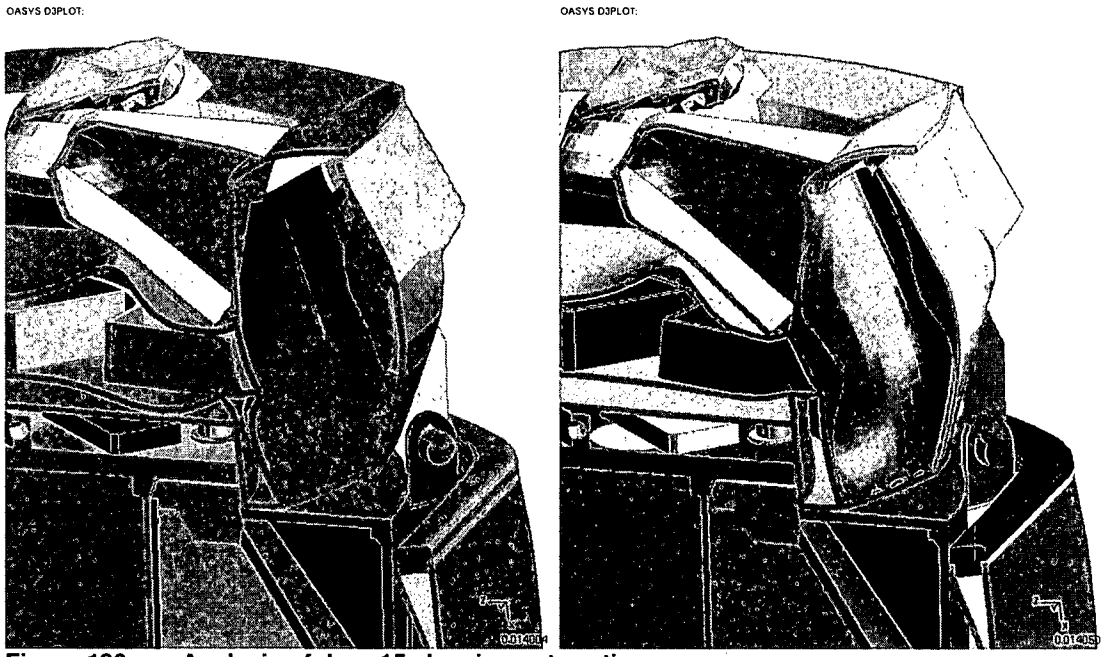

Figure 130: Analysis of drop 15 showing cut section.

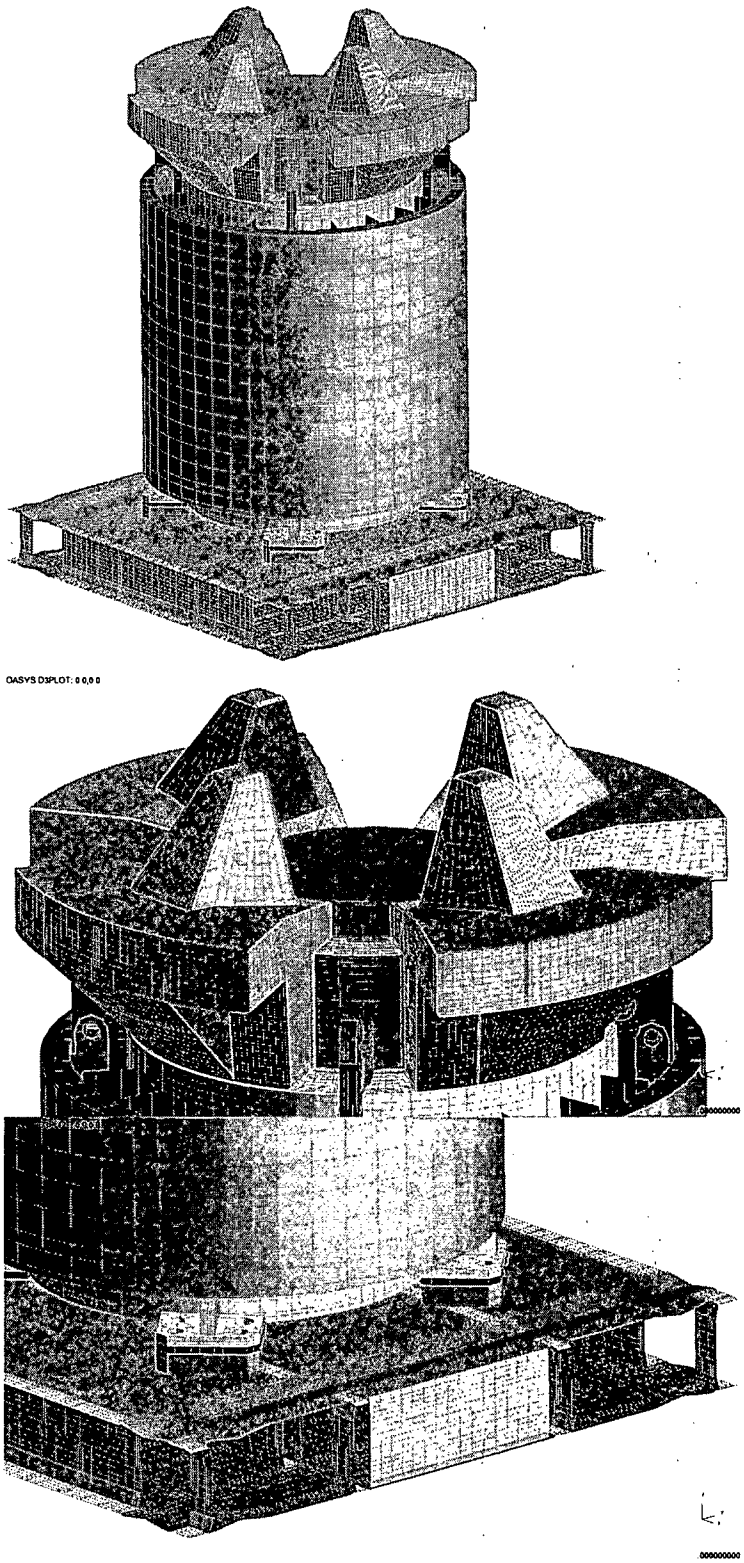

Figure 131: Orientation finite element model

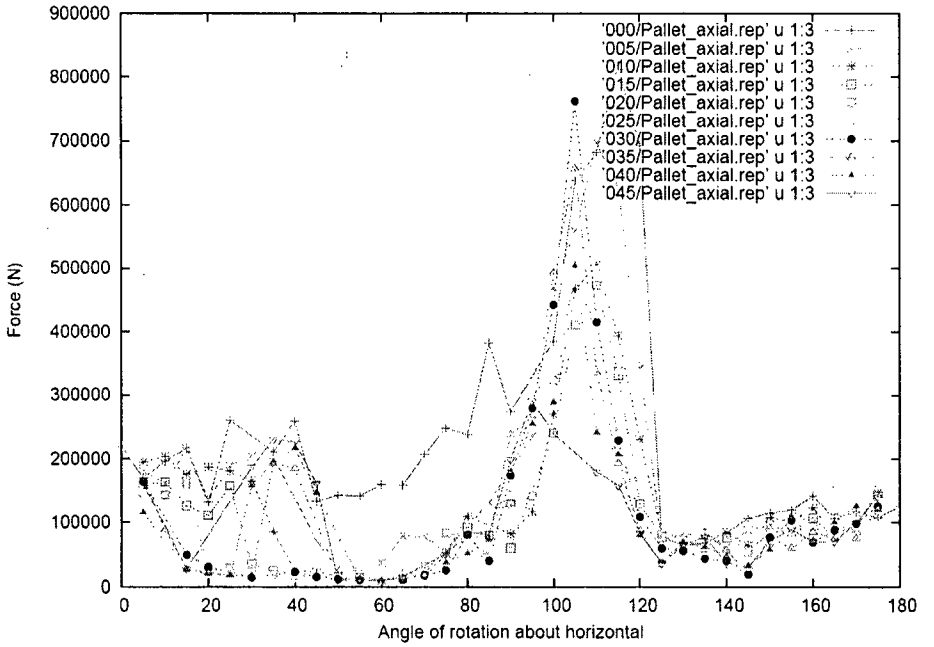

Figure 132: Pallet connection axial force of orientation models.

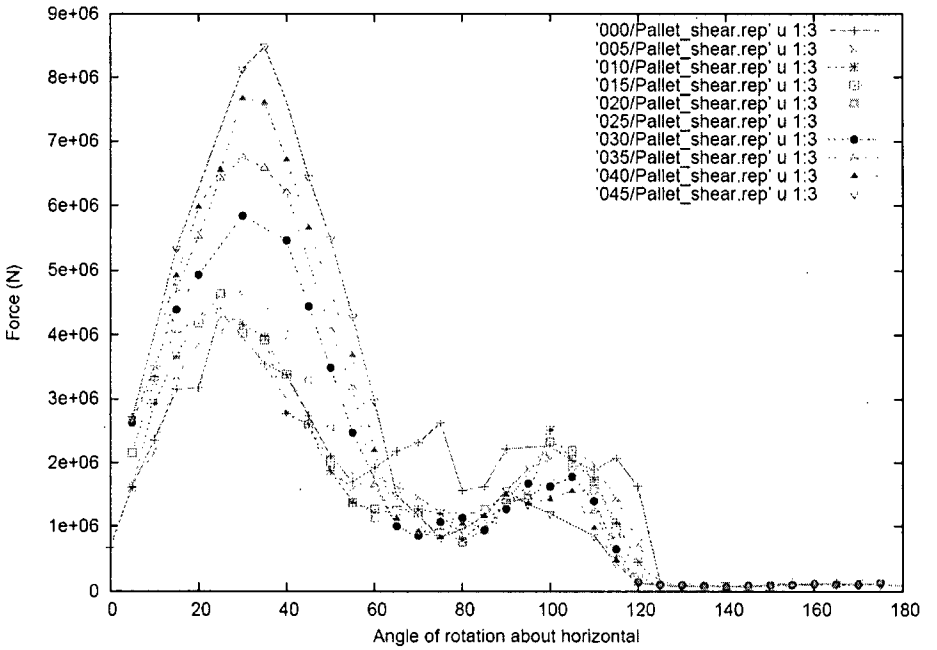

Figure 133: Pallet connection shear force of orientation models.

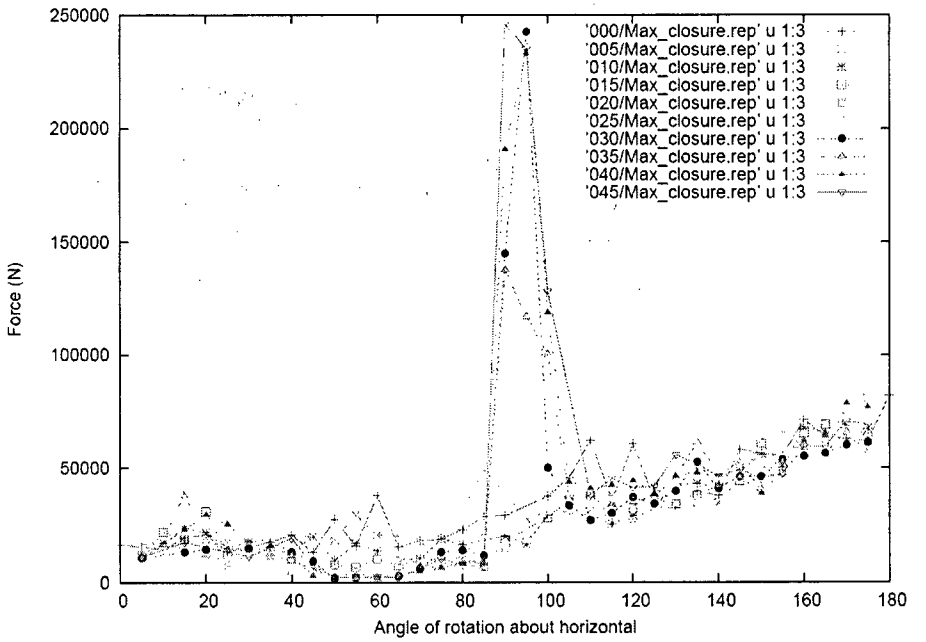

Figure 134: Closure connection shear force of orientation models.

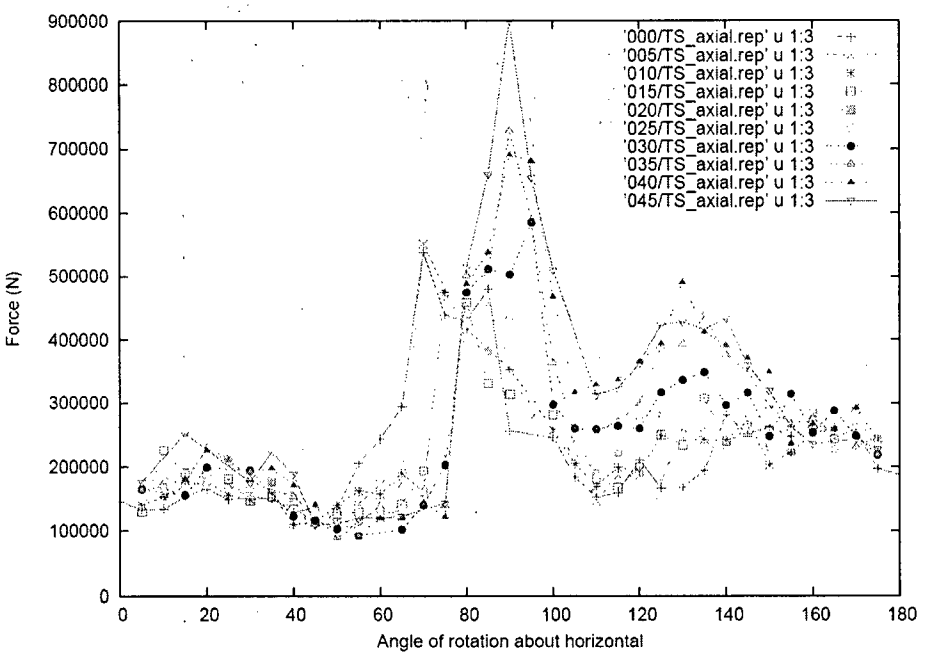

Figure 135: Top shield connection axial force of orientation models.

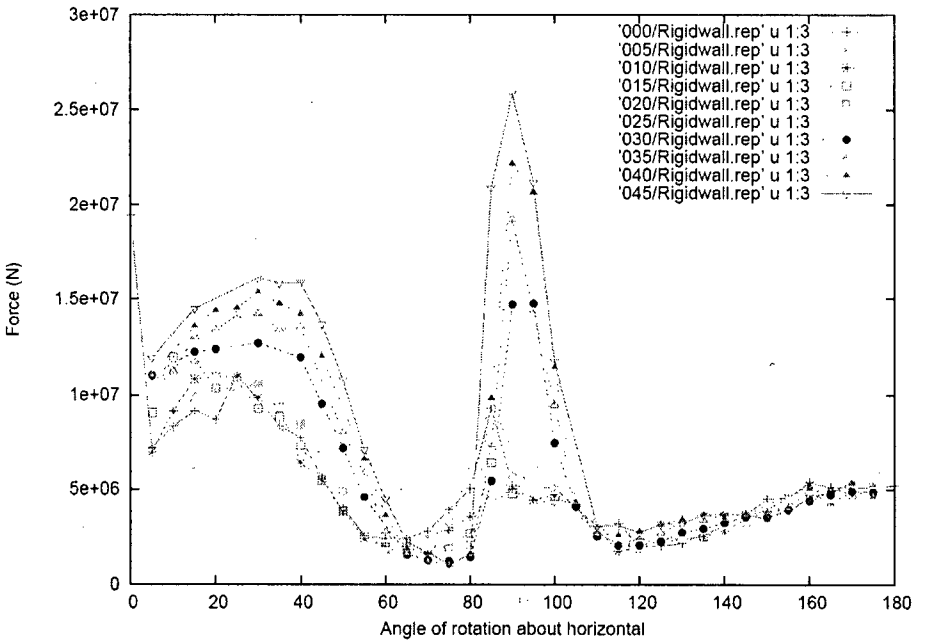

Figure 136: Rigid wall normal force of orientation models.

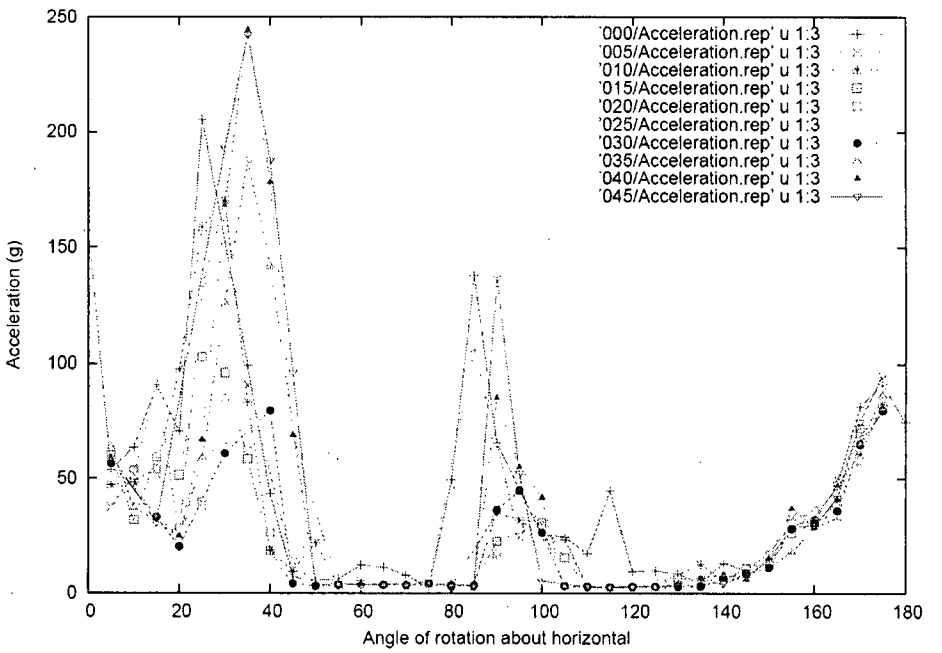

Figure 137: Global acceleration of orientation models.

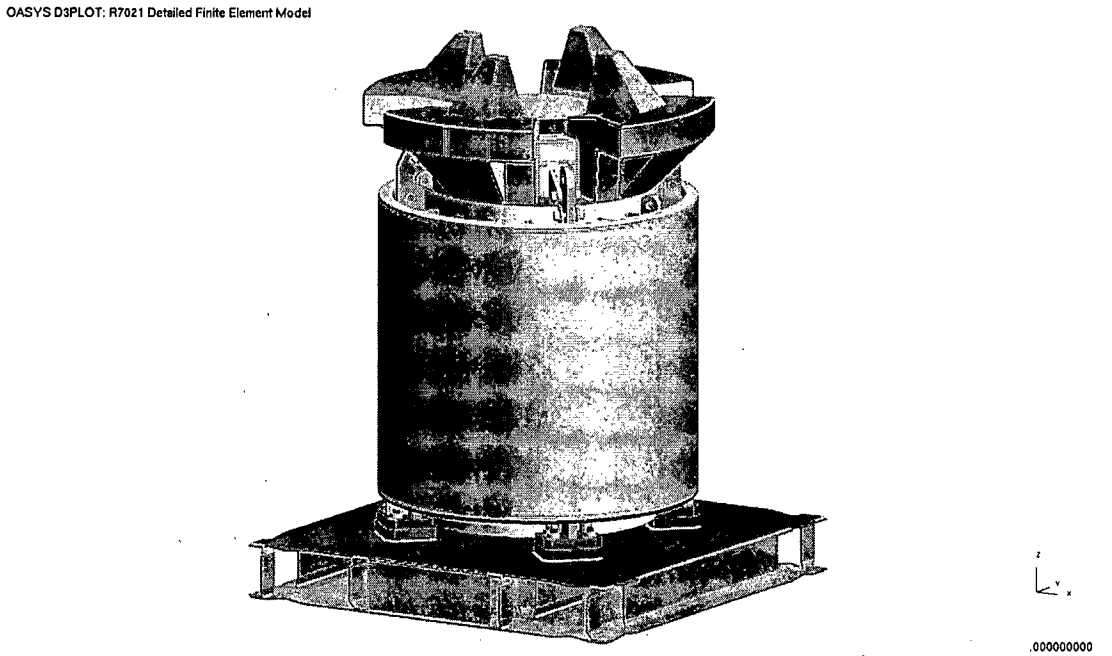

Figure 138: Detailed finite element model

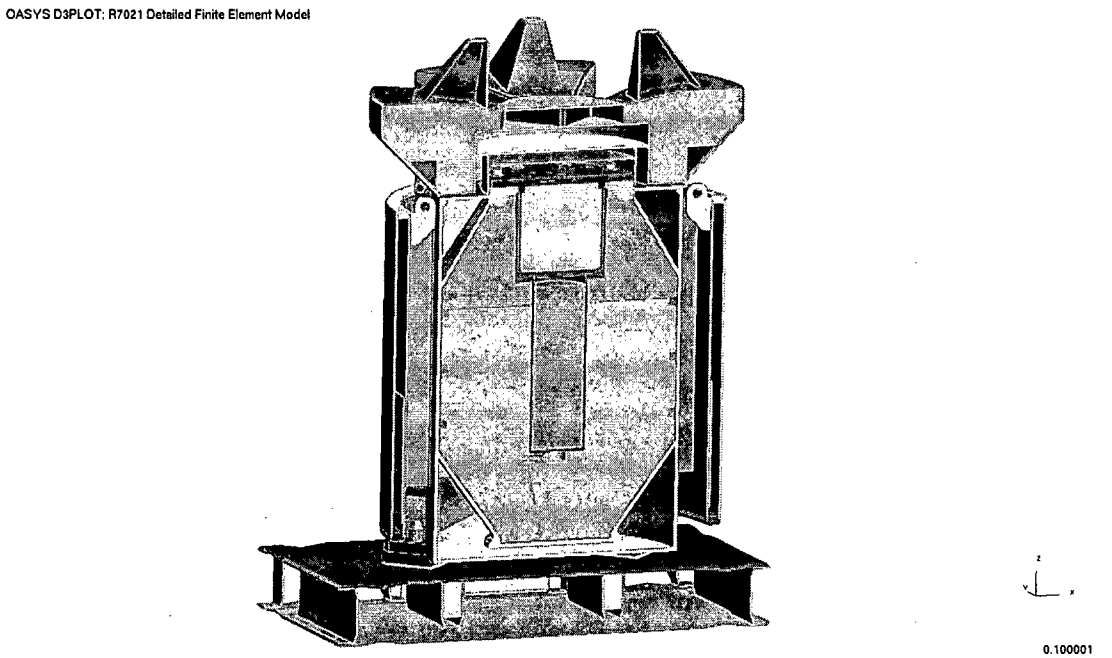

Figure 139: Section through detailed finite element model

OASYS D3PLOT: R7021 Detailed Finite Element Model

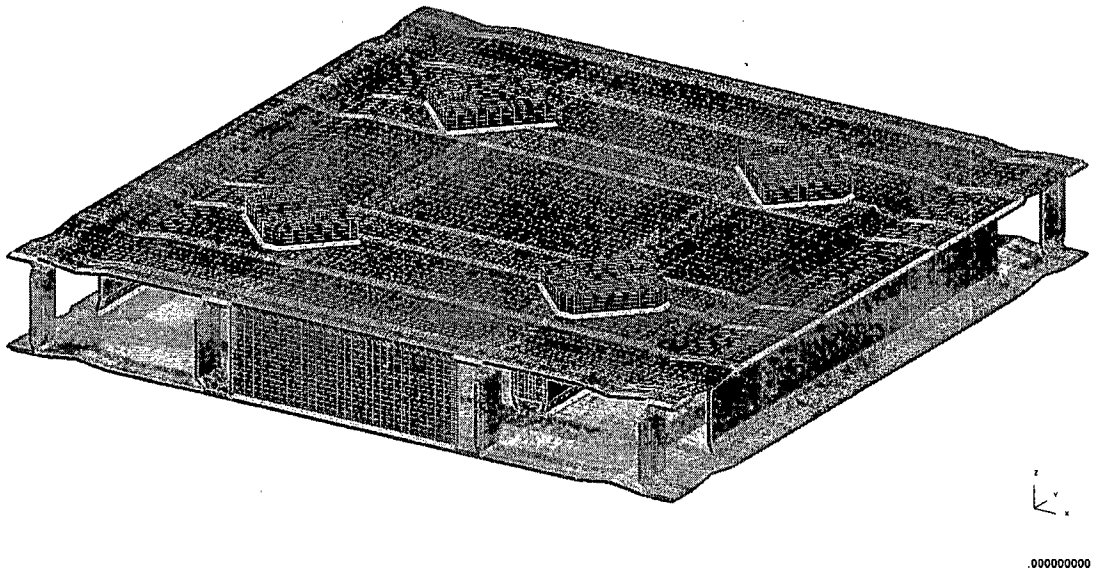

Figure 140: Mesh of pallet for detailed finite element model

OASYS D3PLOT: R7021 Detailed Finite Element Model

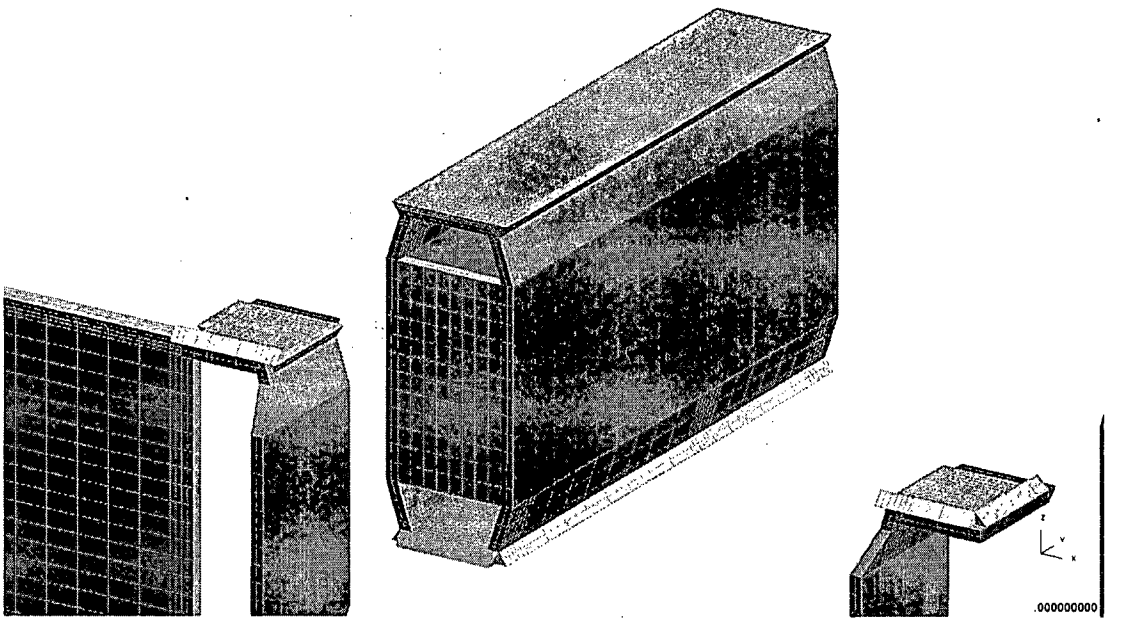

Figure 141: Internal structure and welds in pallet for detailed finite element model.

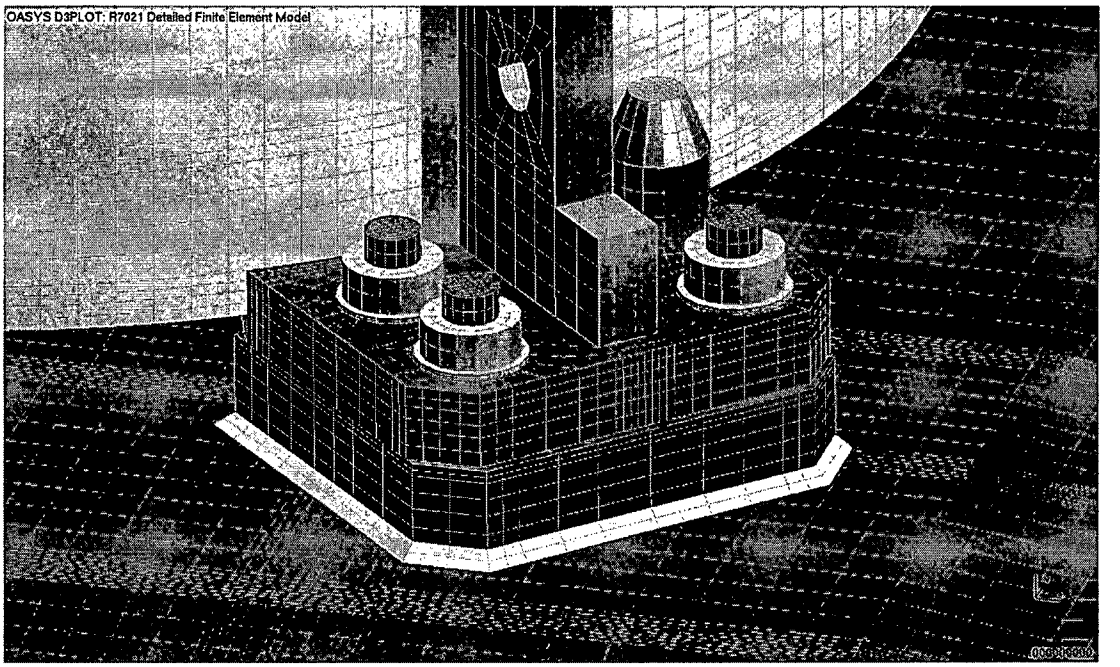

Figure 142: Mesh in foot, studs and dowel for detailed finite element model.

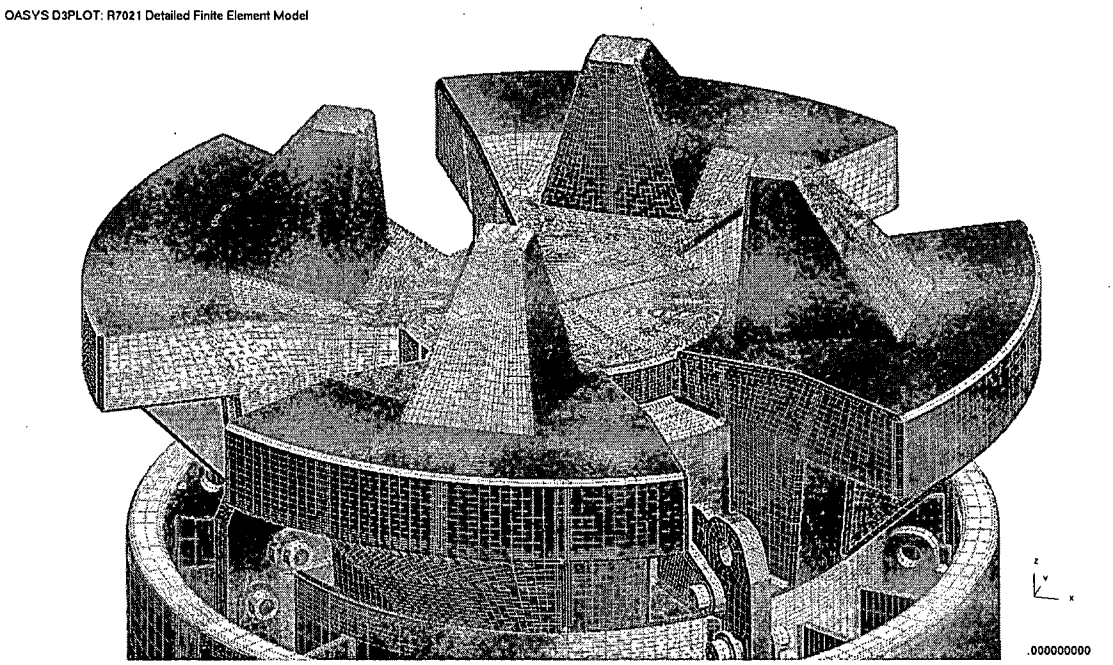

Figure 143: Mesh in top shield for detailed finite element model.

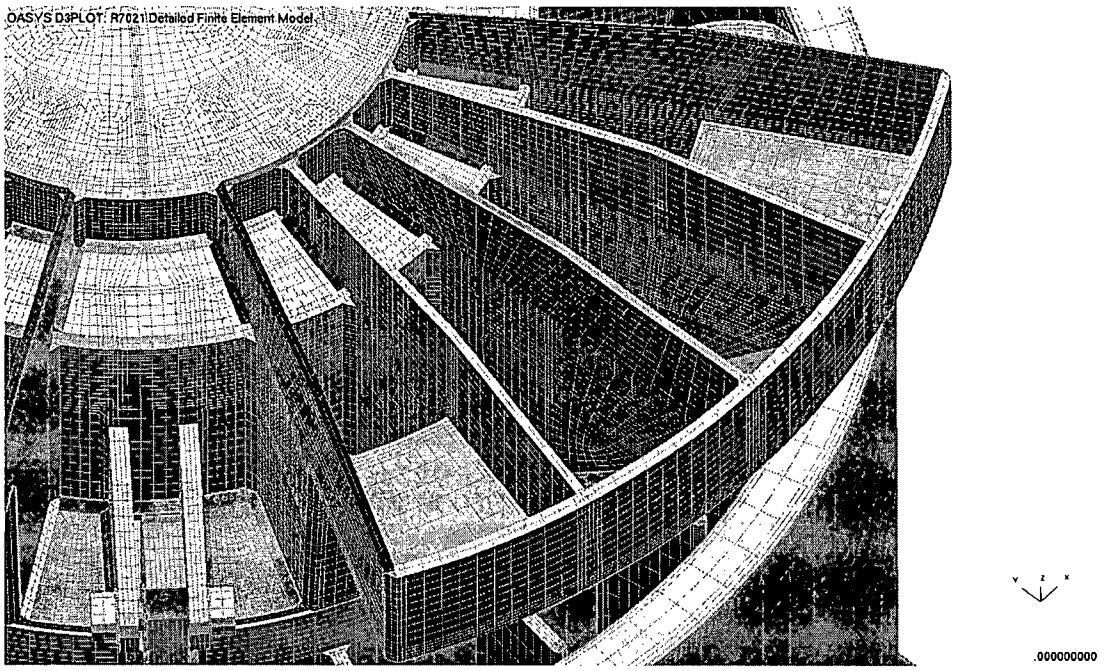

Figure 144: Details of internal mesh of top shield and welds in detailed finite element model.

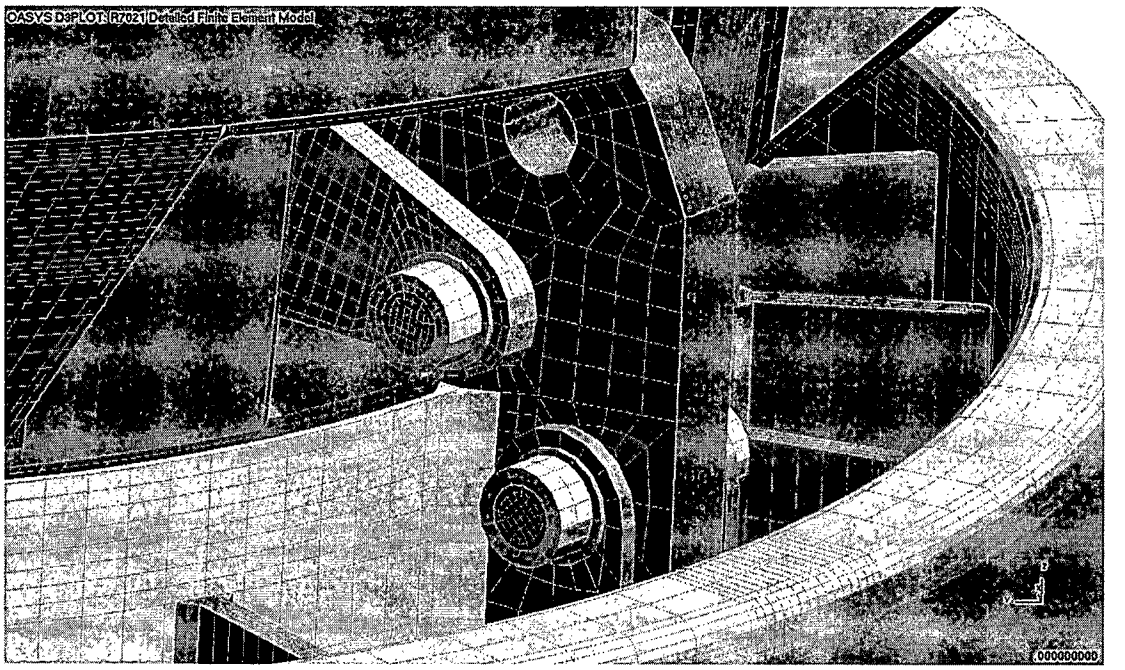

Figure 145: Mesh in shoulder bolts for detailed finite element model.

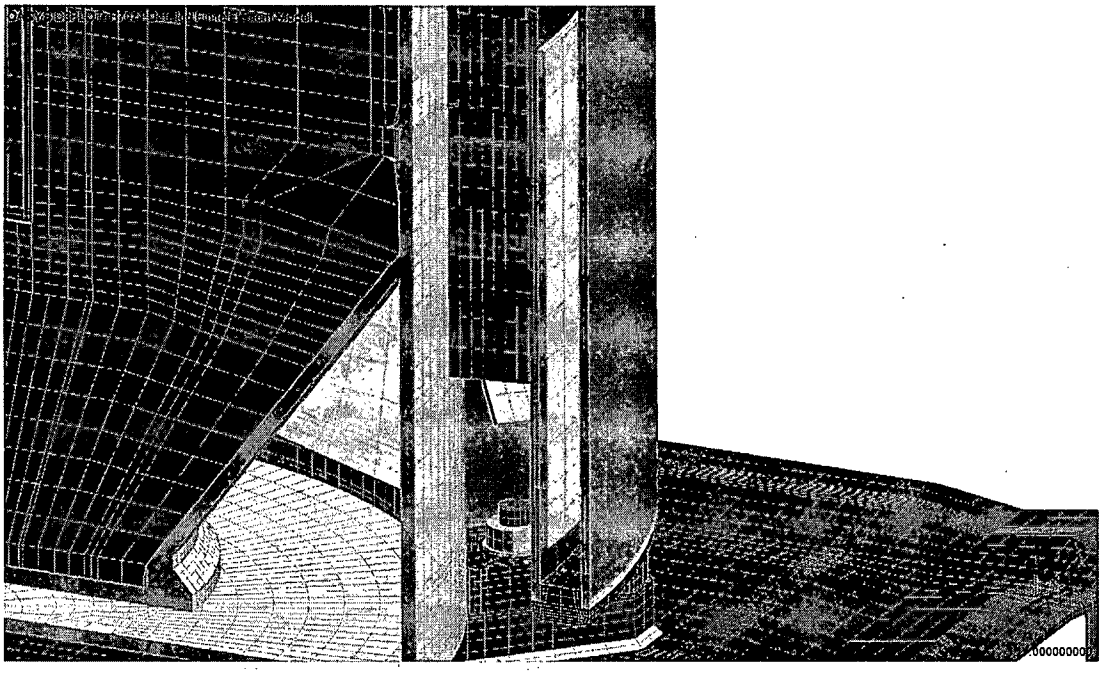

Figure 146: Details of mesh and additional plate in jacket for detailed finite element model.

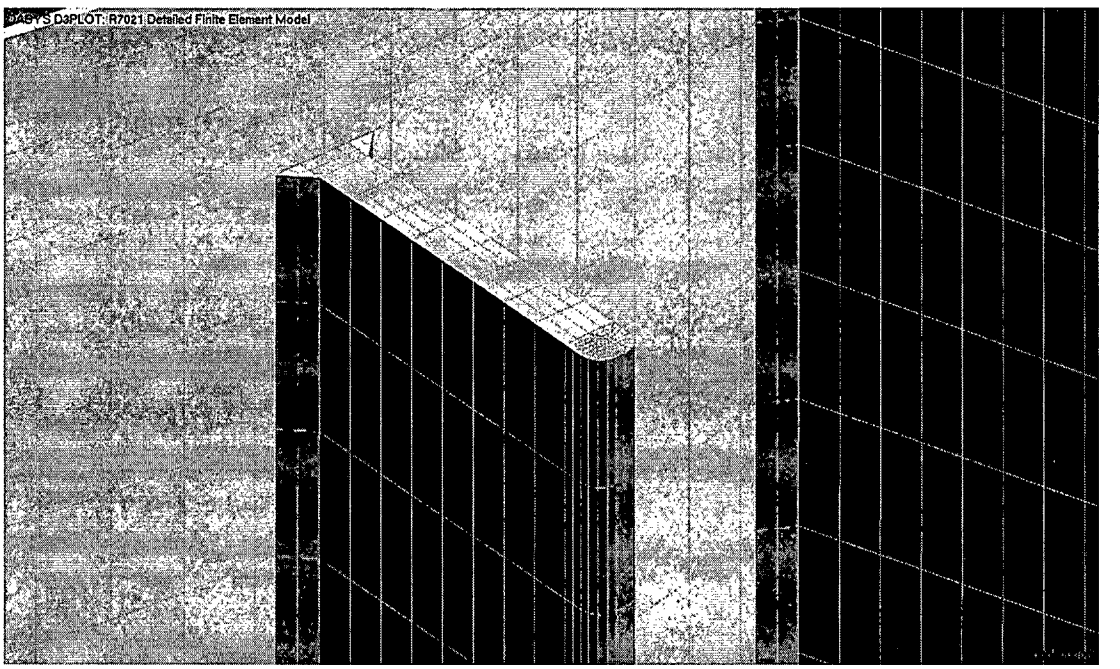

Figure 147: Details of mesh in fins for detailed finite element model.

OASYS D3PLOT: R7021 Detailed Finite Element Model

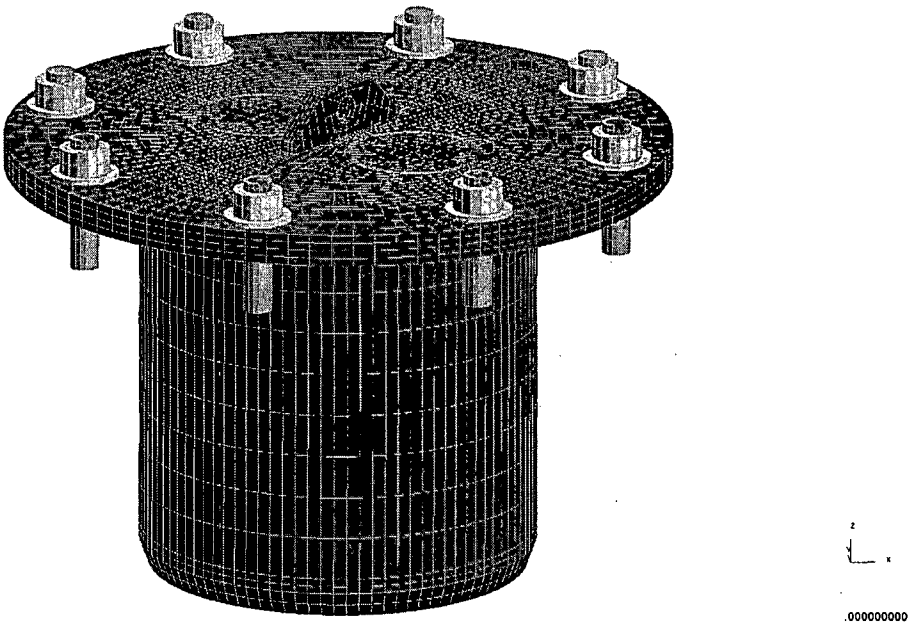

Figure 148: Mesh of closure and studs for detailed finite element model.

OASYS D3PLOT: R7021 Detailed Finite Element Model

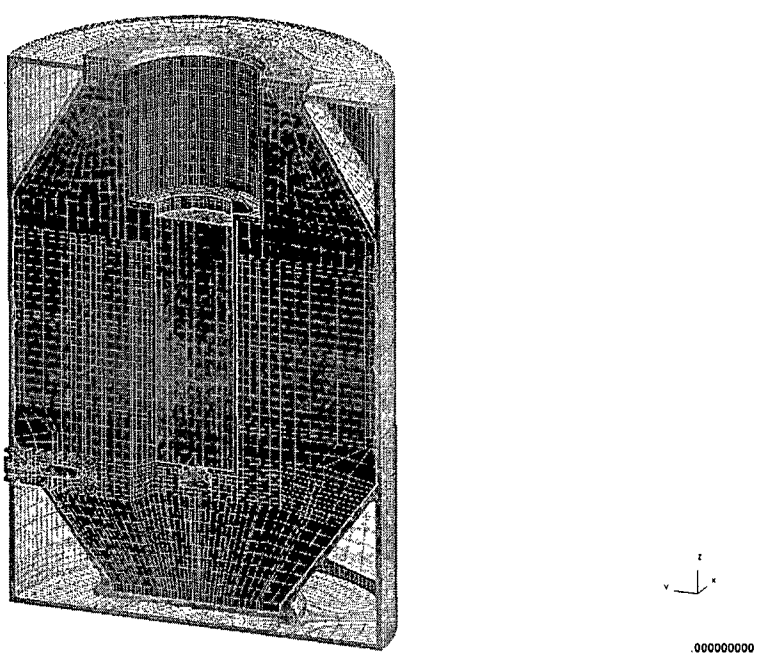

Figure 149: Section showing mesh of internal lead of detailed finite element model.

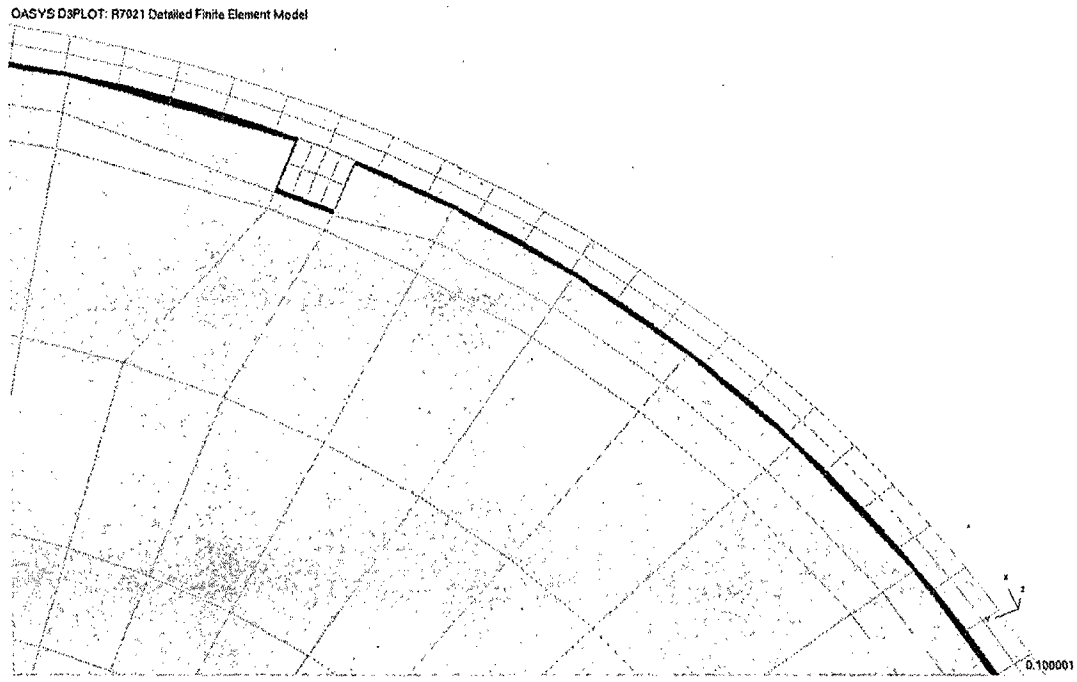

Figure 150: Mesh showing shrinkage of lead after cool down for detailed finite element model.

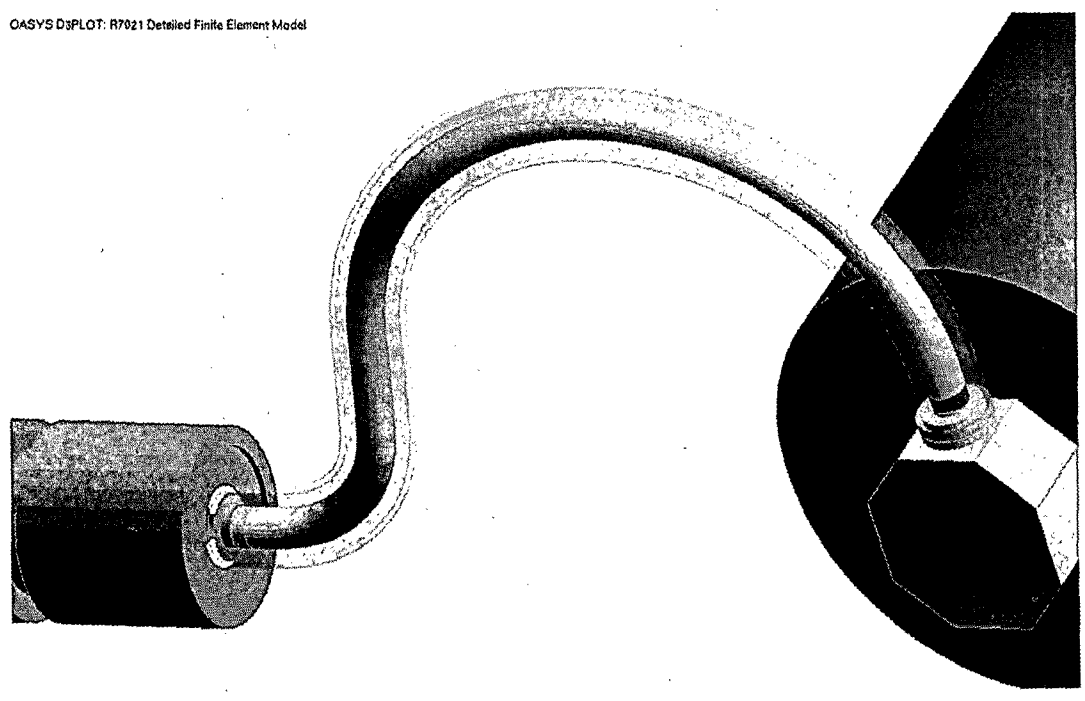

Figure 151: Detailed finite element model of drain tube and outer tube.

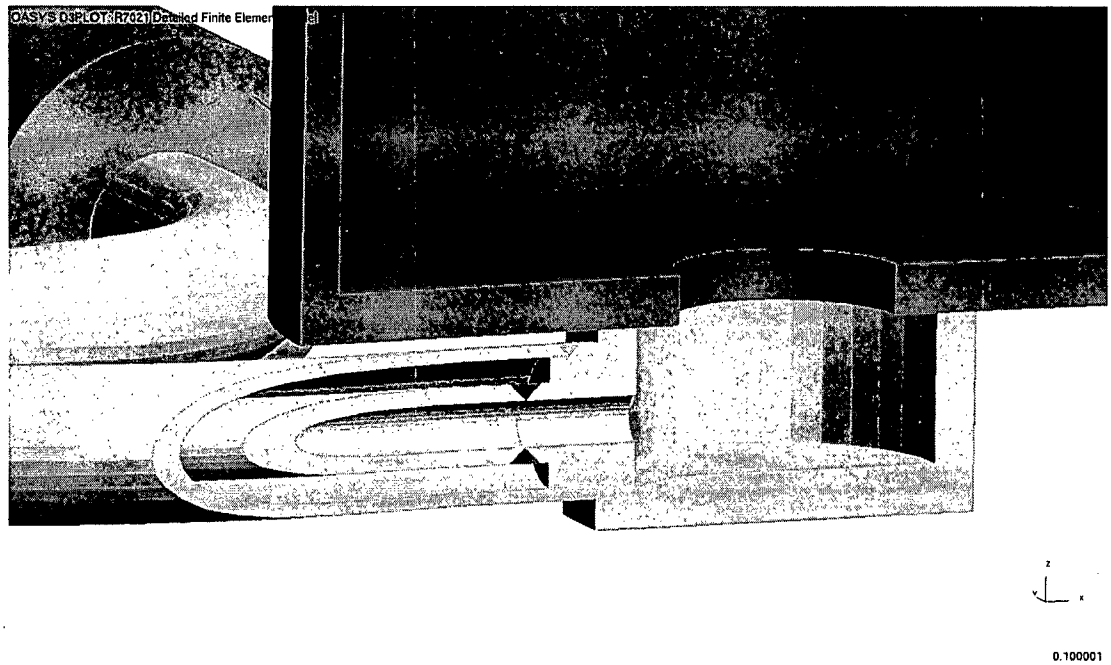

Figure 152: Section through drain tube, outer tube and welds for detailed finite element model.

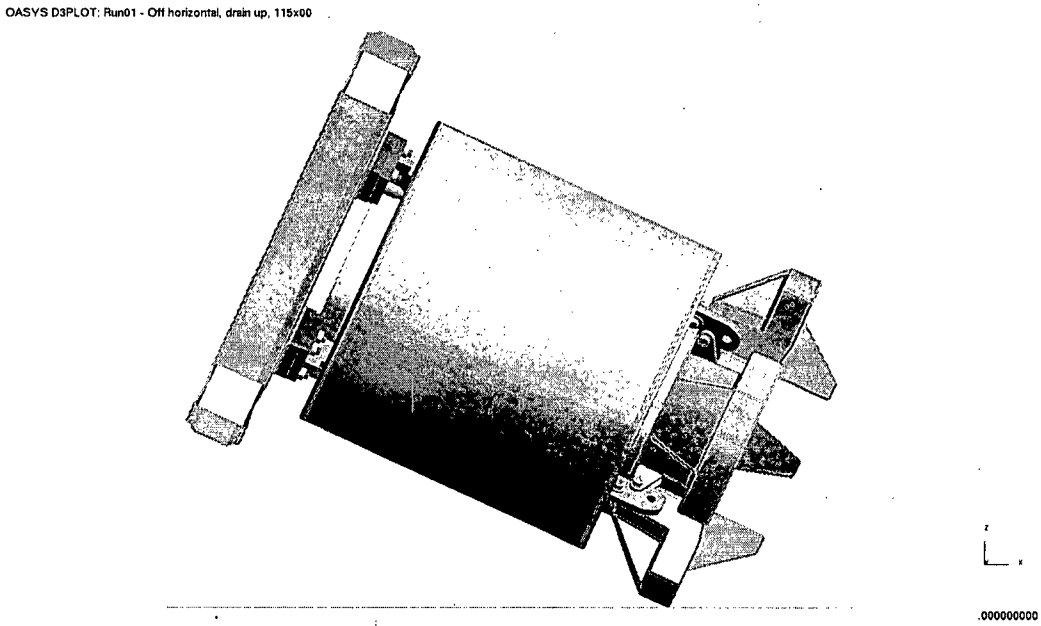

Figure 153: Initial impact orientation – Run 01.

OASYS D3PLOT: Run01 - Off horizontal, drain up, 115x00

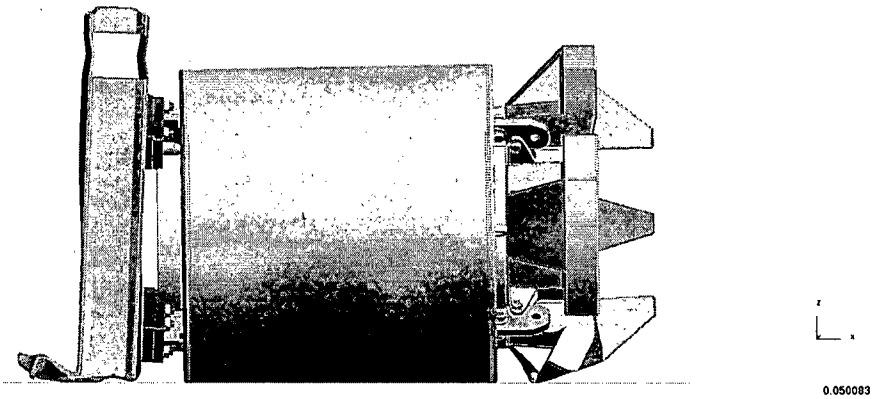

Figure 154: Final deformation – Run 01.

OASYS D3PLOT: Run01 - Off horizontal, drain up, 115x00

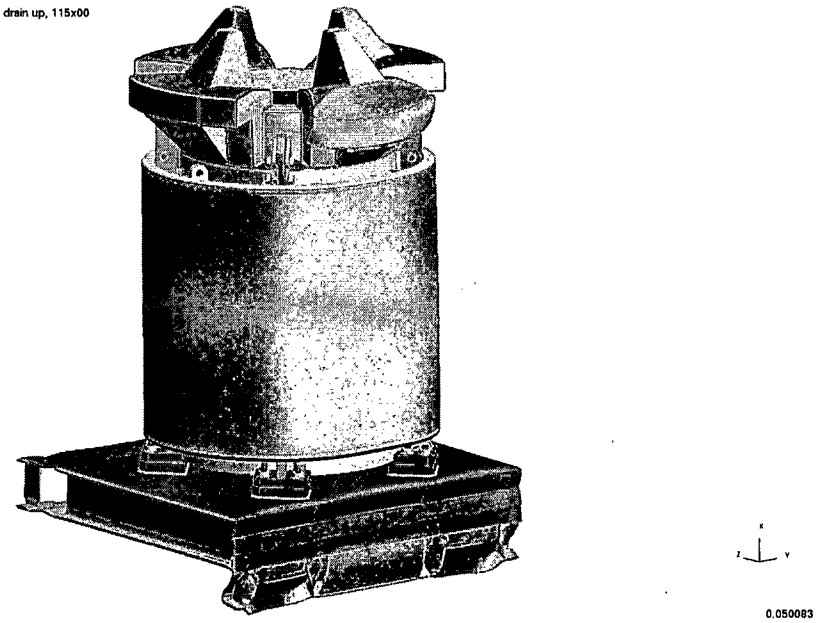

Figure 155: Deformation of flask – Run 01.

Figure 156: Deformation of pallet – Run 01.

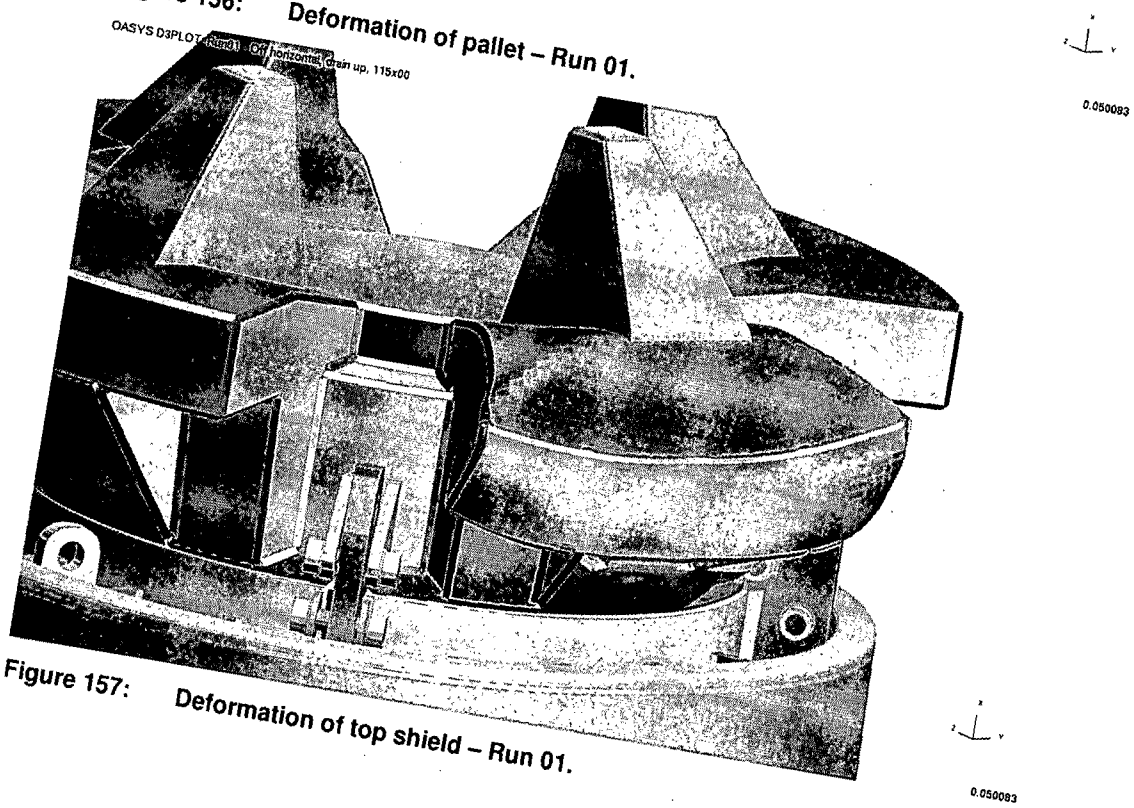

Figure 157: Deformation of top shield – Run 01.

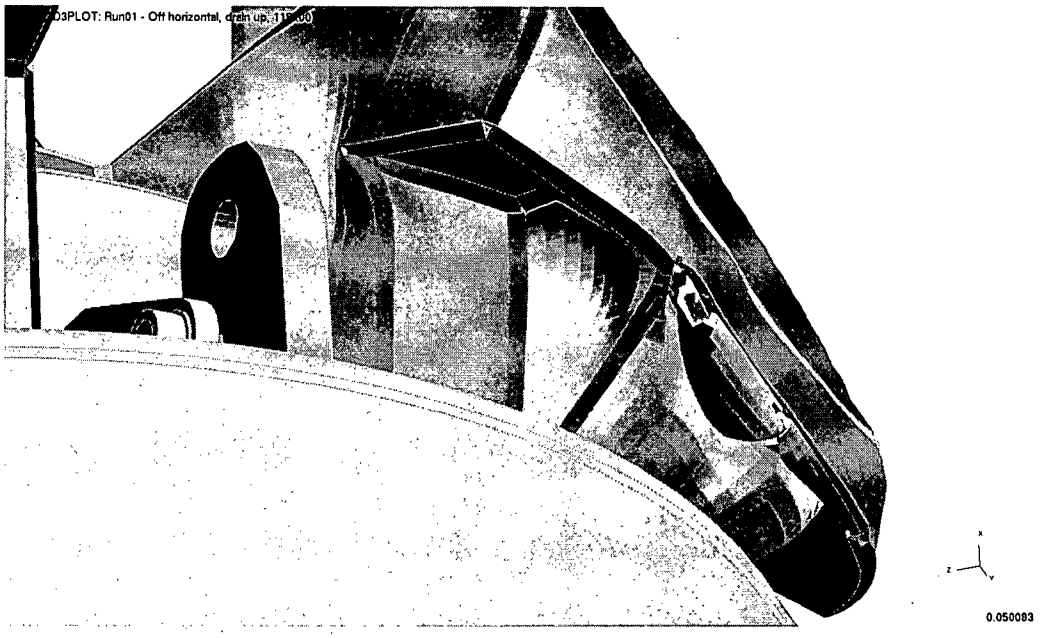

Figure 158: Deformation of underside of top shield – Run 01.

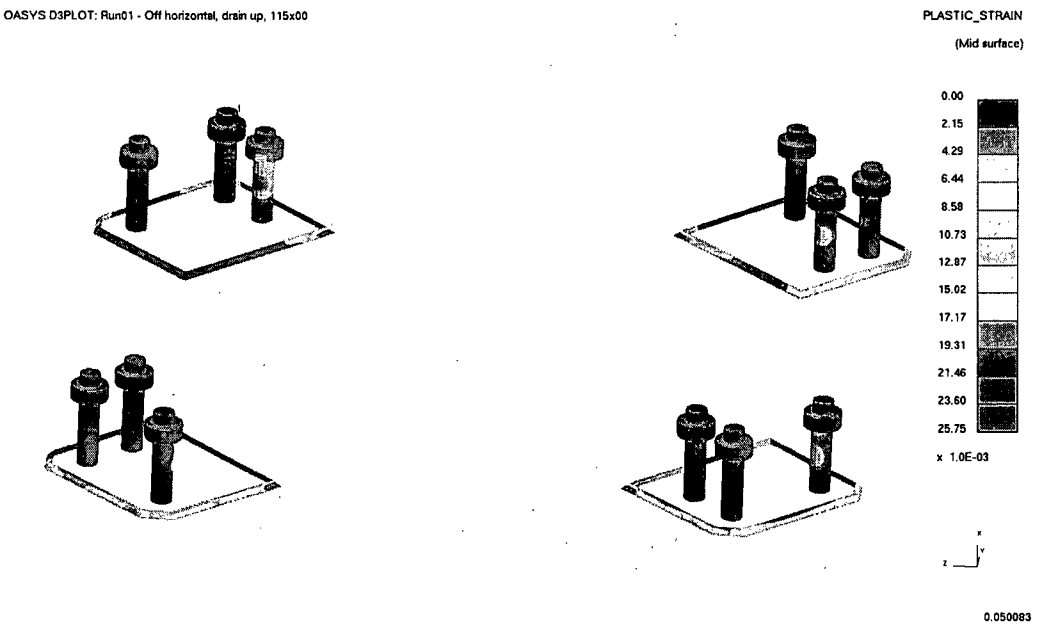

Figure 159: Effective plastic strain in pallet connections – Run 01.

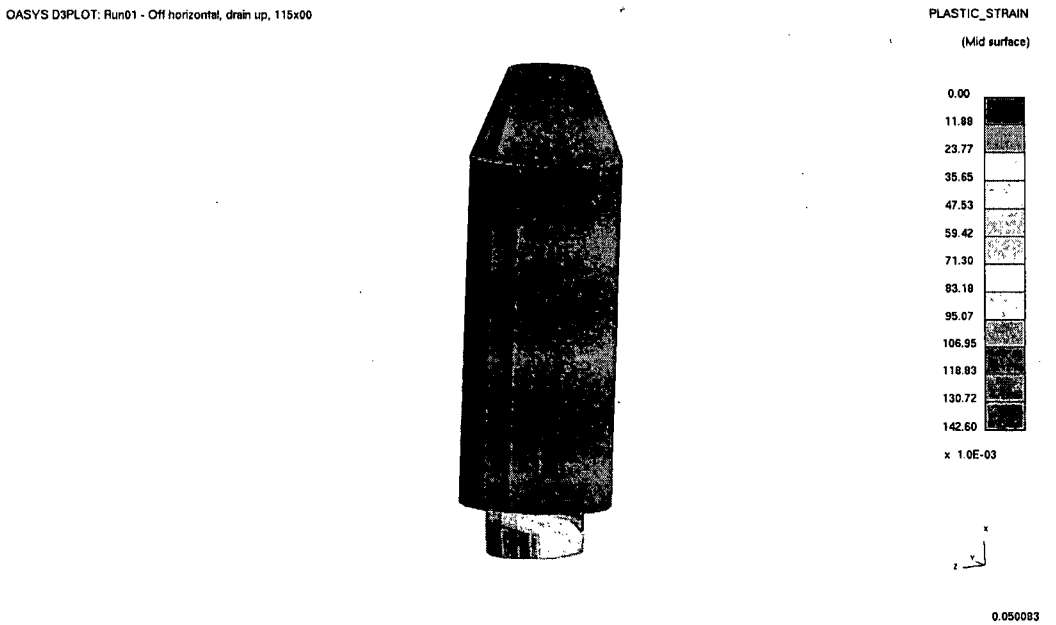

Figure 160: Effective plastic strain in dowels – Run 01.

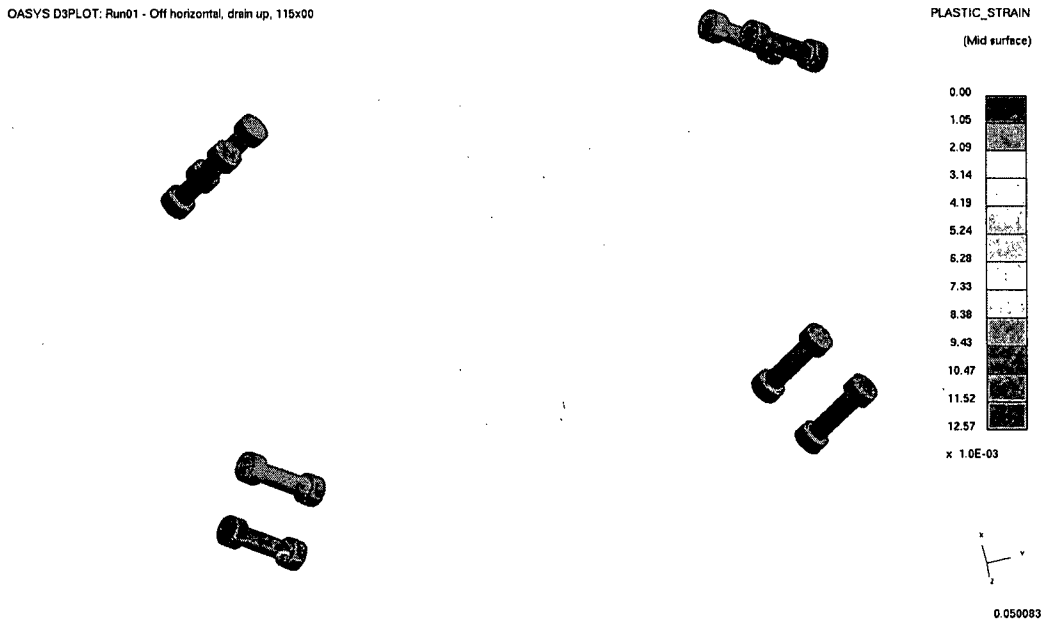

Figure 161: Effective plastic strain in shoulder bolts – Run 01.

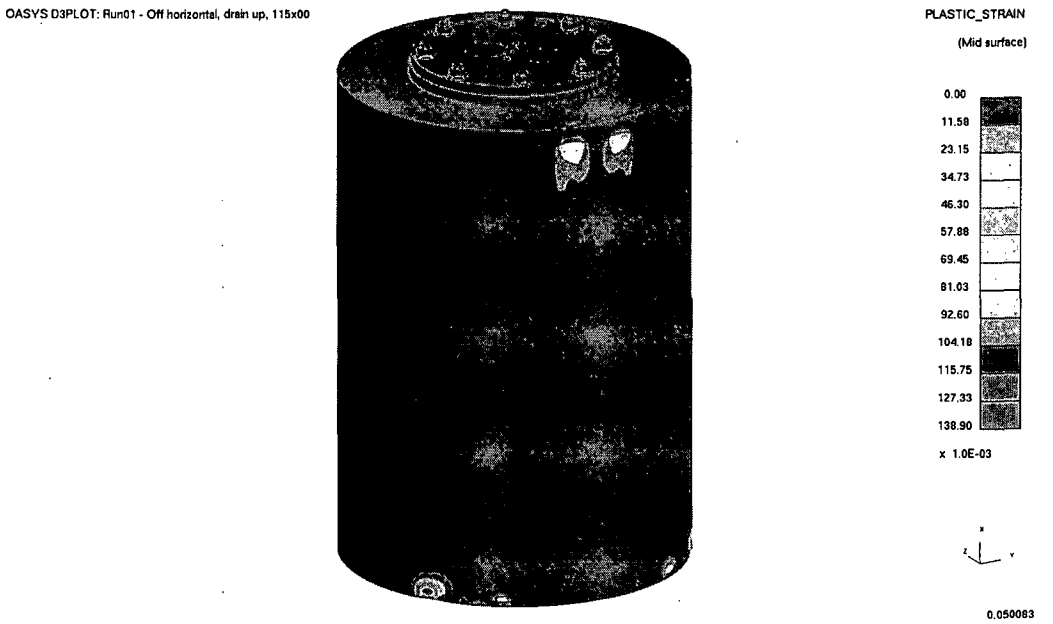

Figure 162: Effective plastic strain in flask wall – Run 01.

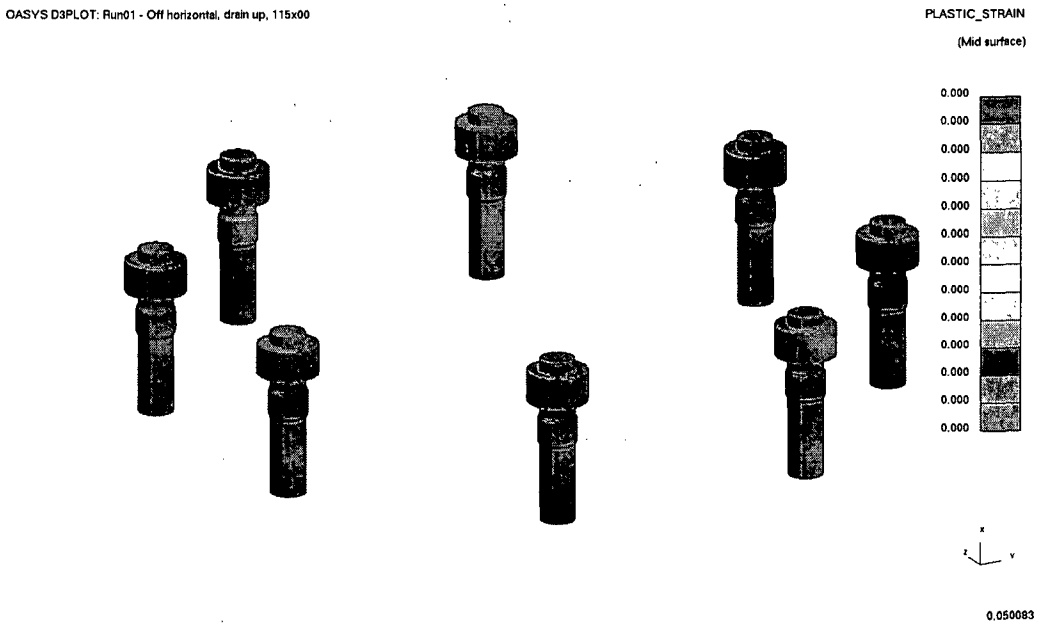

Figure 163: Effective plastic strain in closure studs – Run 01.

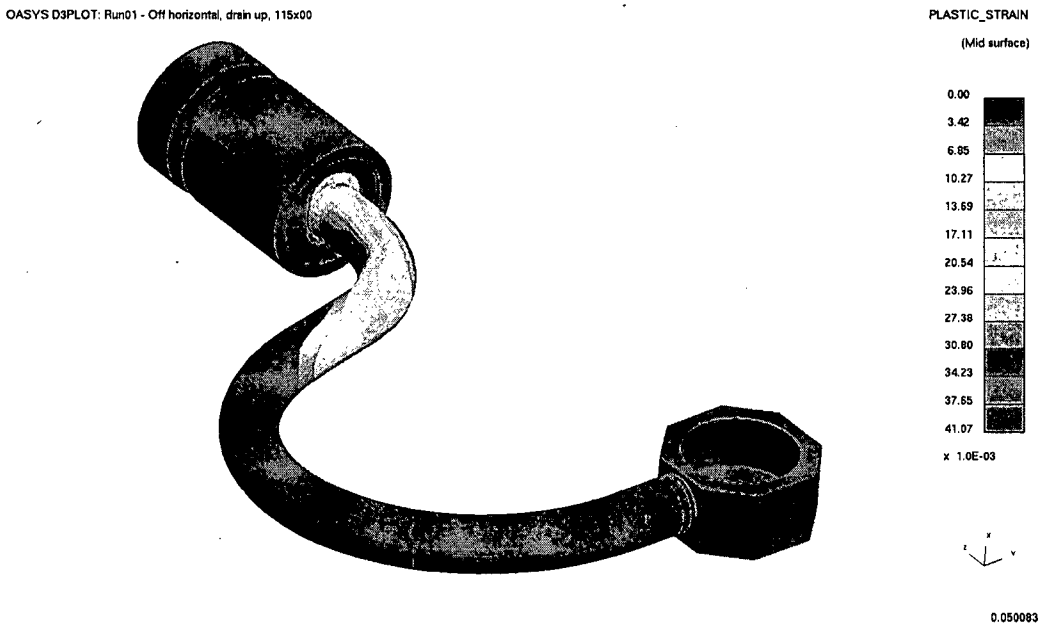

Figure 164: Effective plastic strain in outer tube – Run 01.

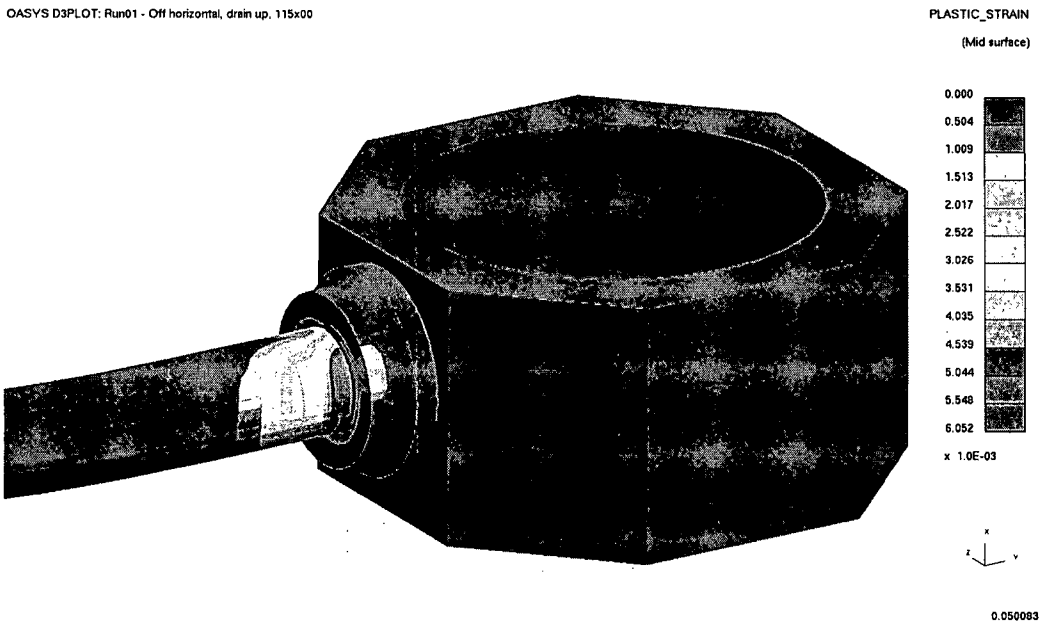

Figure 165: Effective plastic strain in drain tube – Run 01.

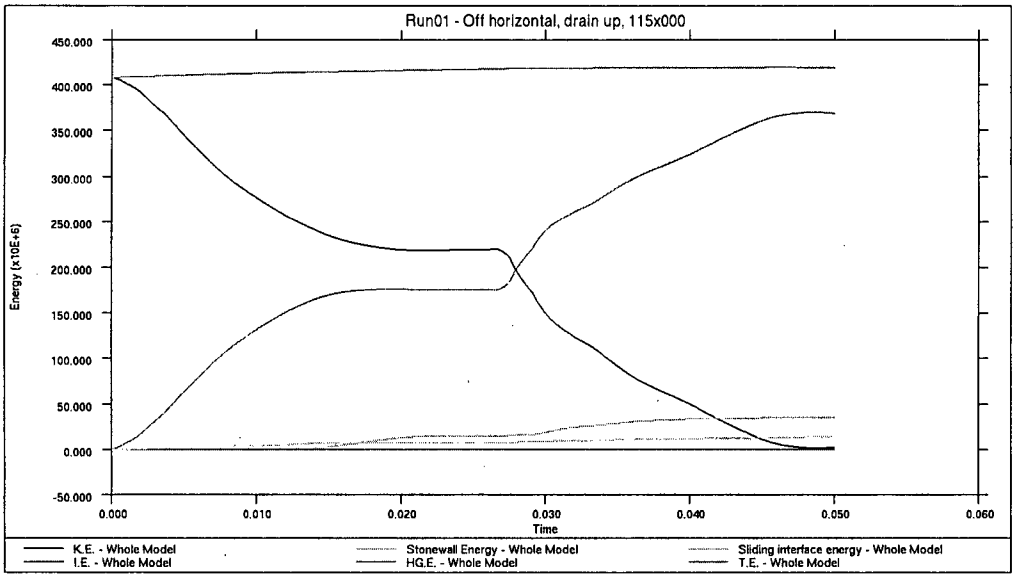

Figure 166: Energy histories – Run 01.

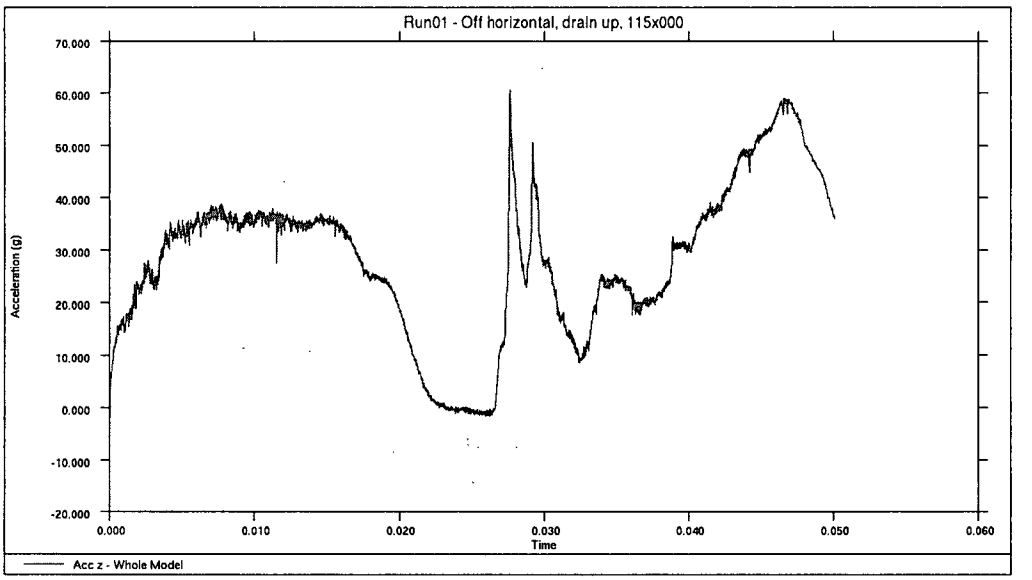

Figure 167: Global acceleration of flask – Run 01.

OASYS D3PLOT: Run 02 - Horizontal - drain down 090x045

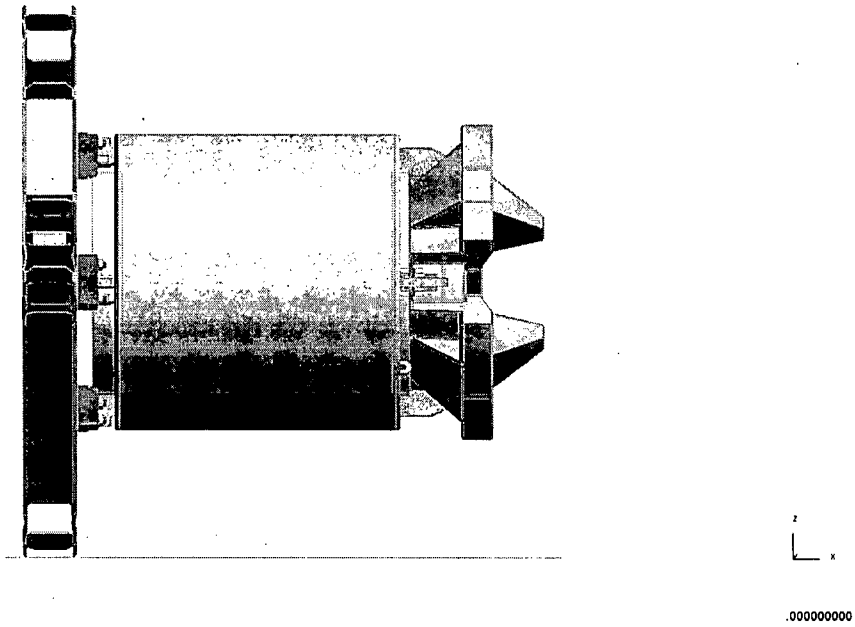

Figure 168: Initial impact orientation – Run 02

OASYS D3PLOT: Run 02 - Horizontal - drain down 090x045

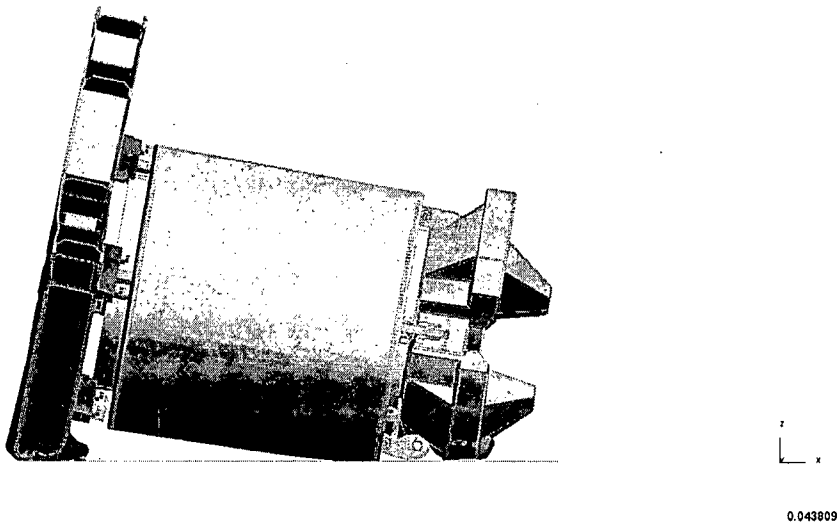

Figure 169: Final deformation – Run 02

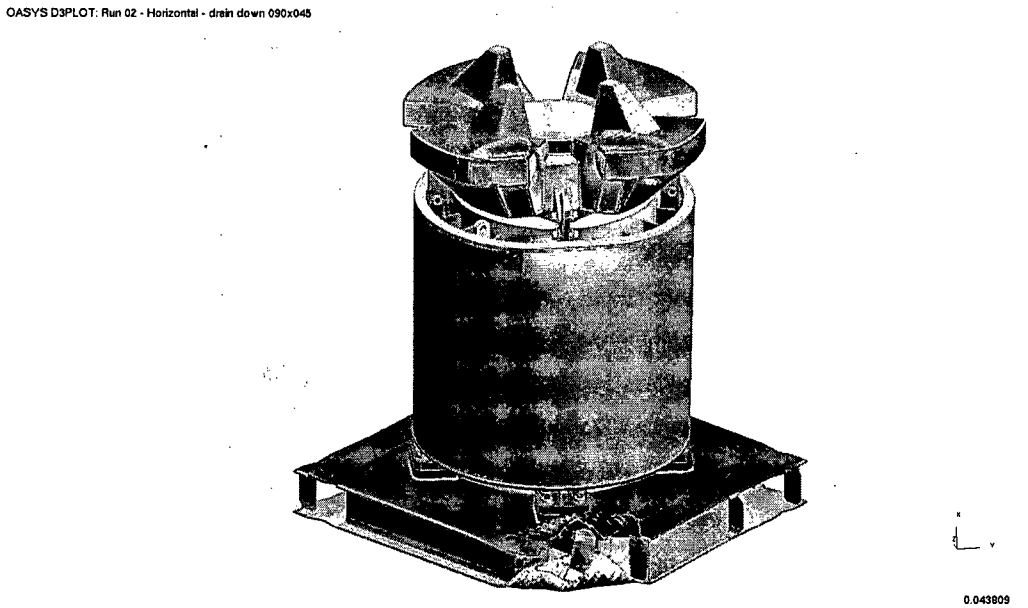

Figure 170: Deformation of flask – Run 02

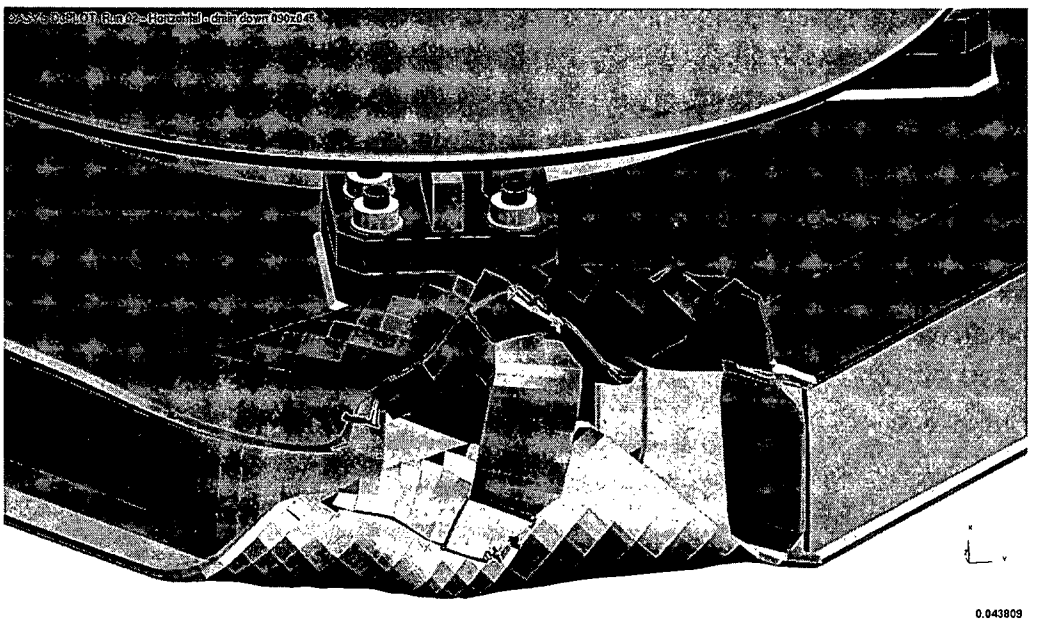

Figure 171: Deformation of pallet – Run 02

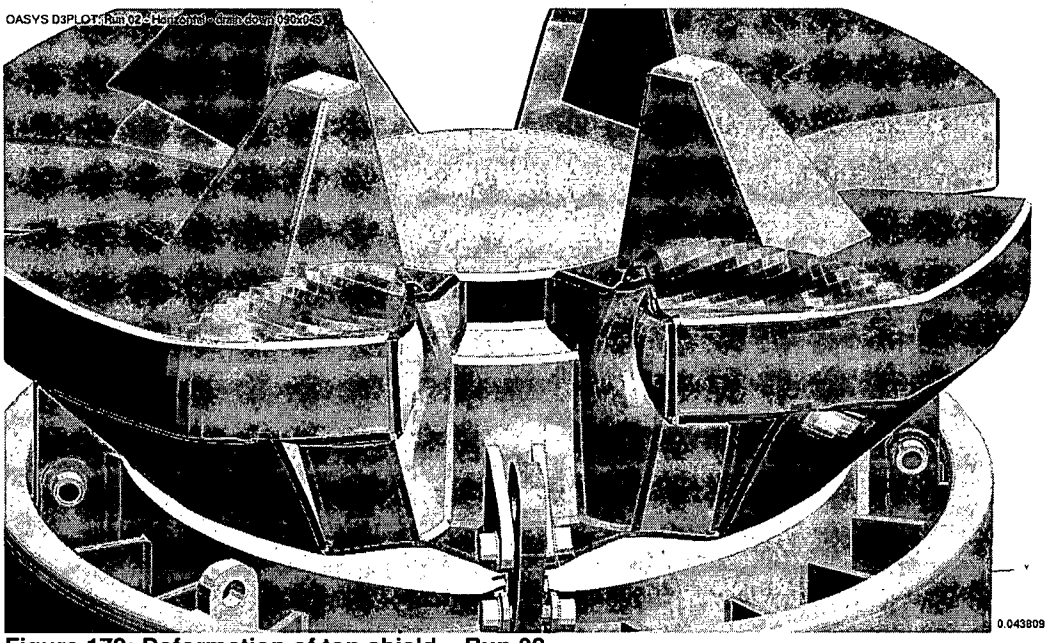

Figure 172: Deformation of top shield – Run 02

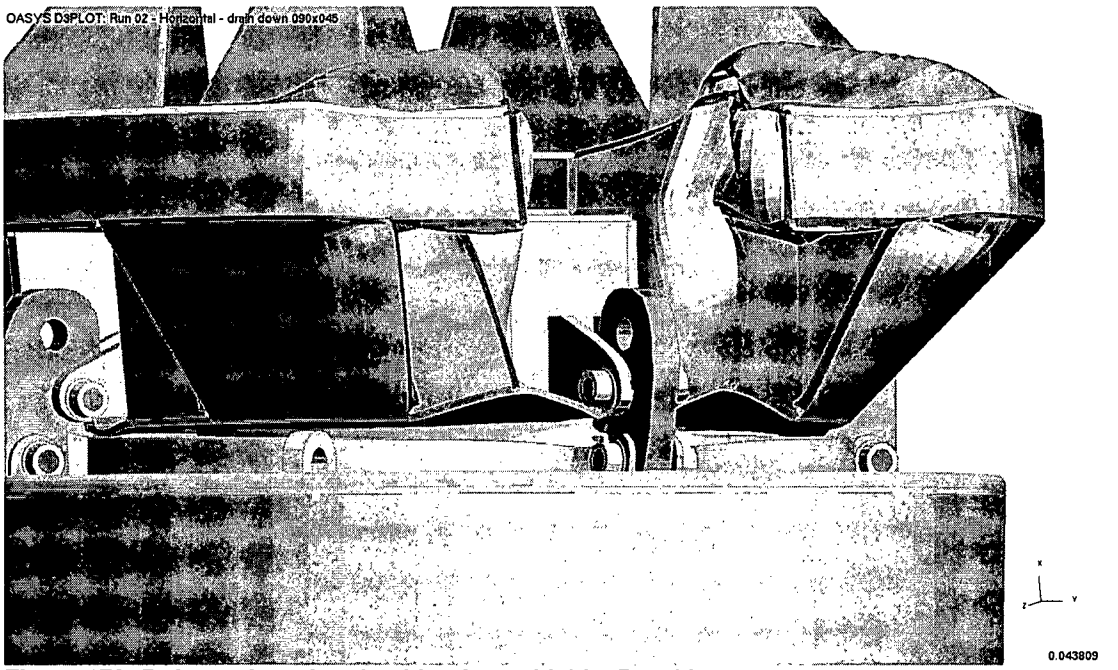

Figure 173: Deformation of underside of top shield – Run 02

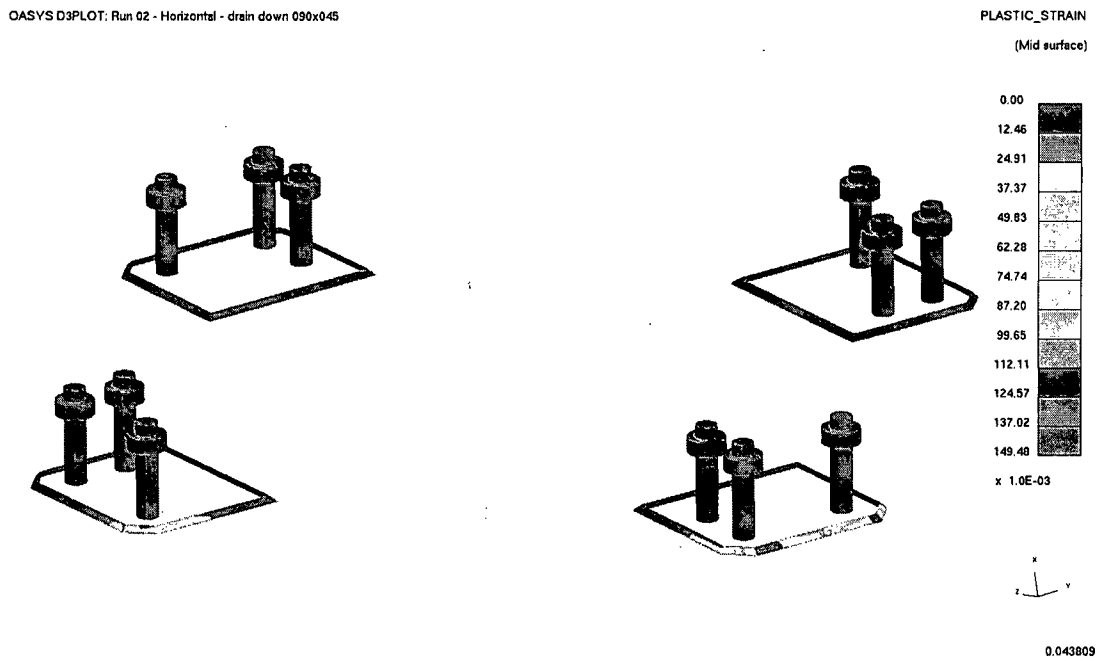

Figure 174: Effective plastic strain in pallet connections – Run 02

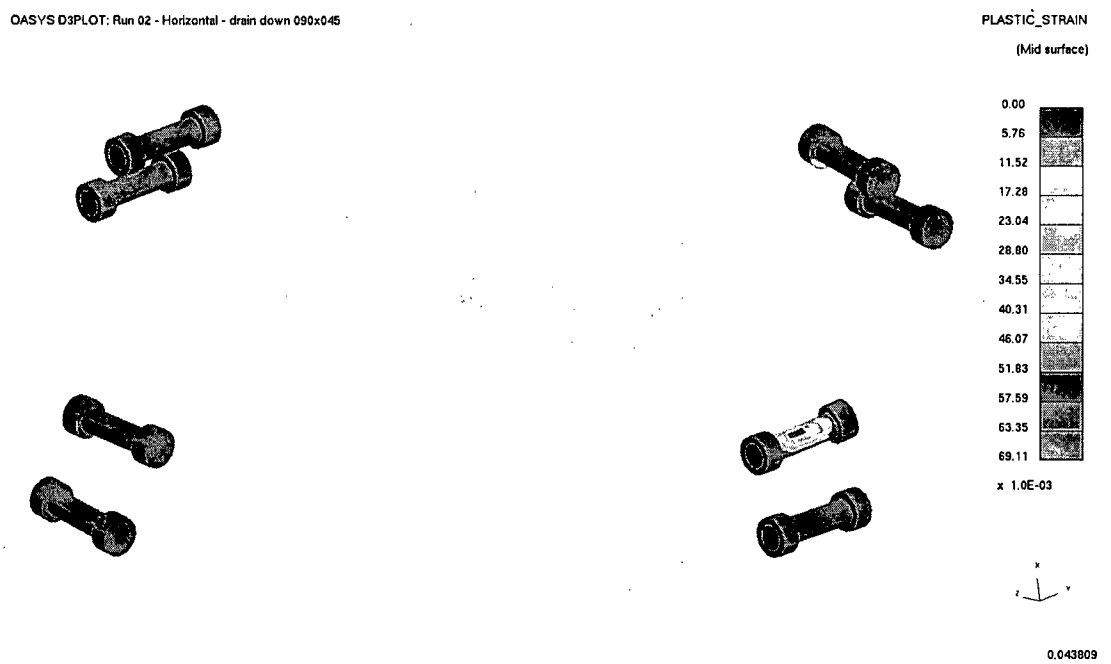

Figure 175: Effective plastic strain in shoulder bolts – Run 02

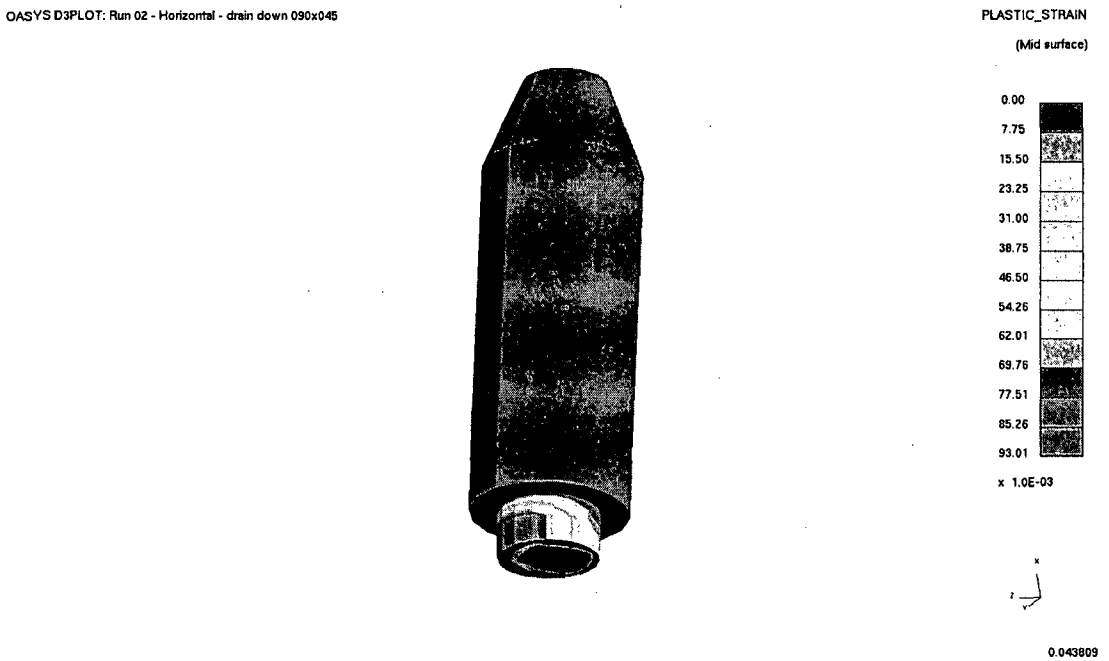

Figure 176: Effective plastic strain in dowels – Run 02

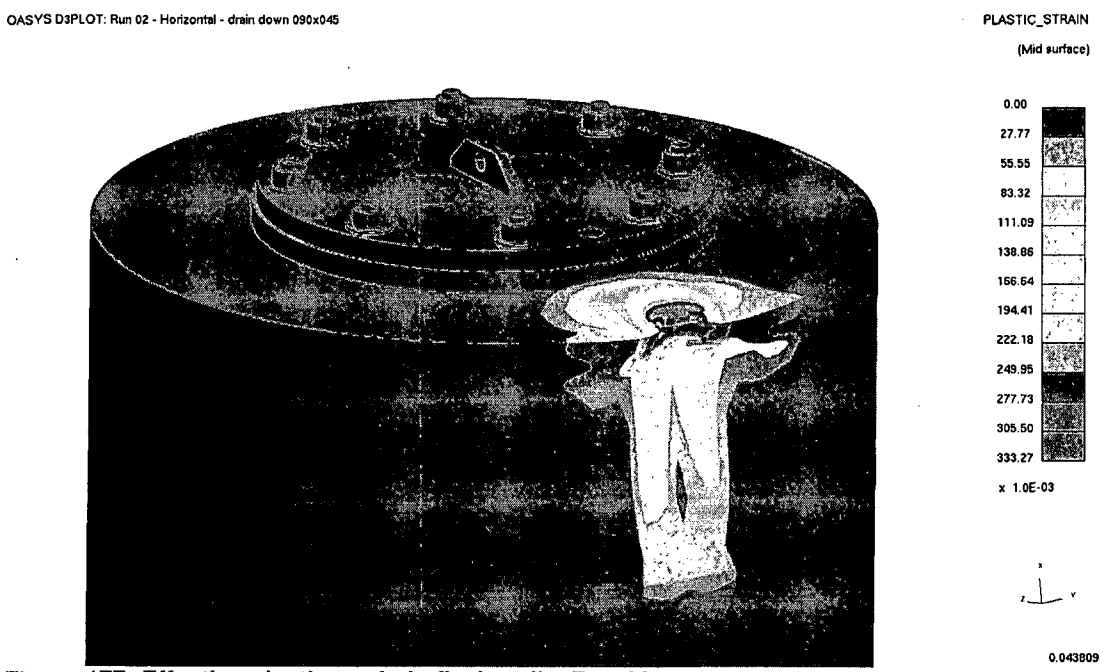

Figure 177: Effective plastic strain in flask wall – Run 02

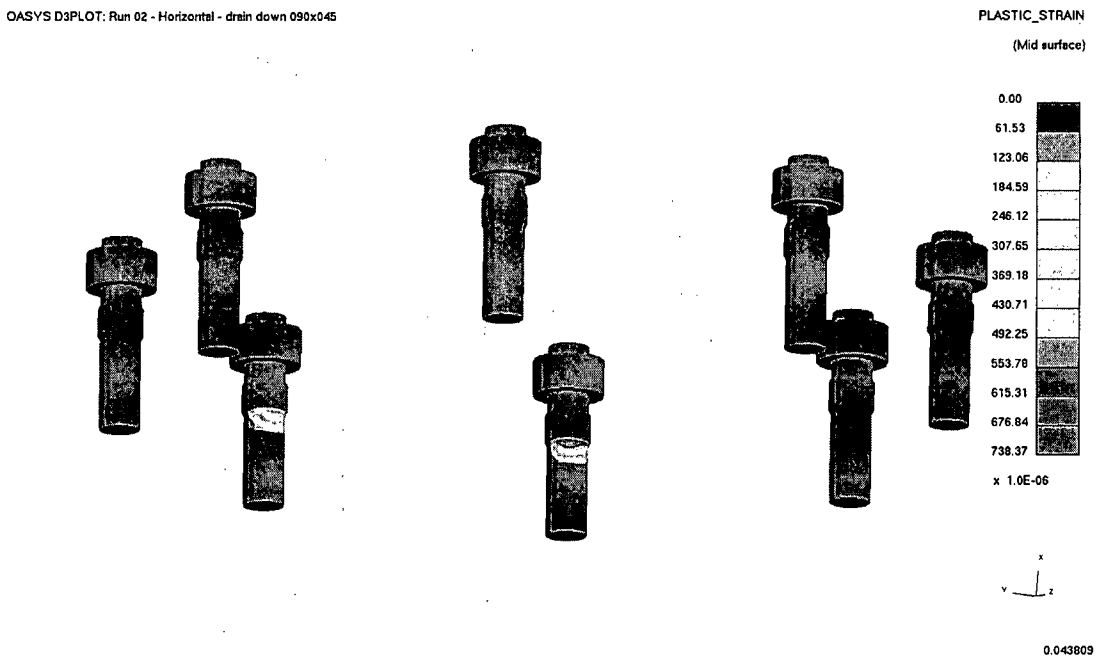

Figure 178: Effective plastic strain in closure studs – Run 02.

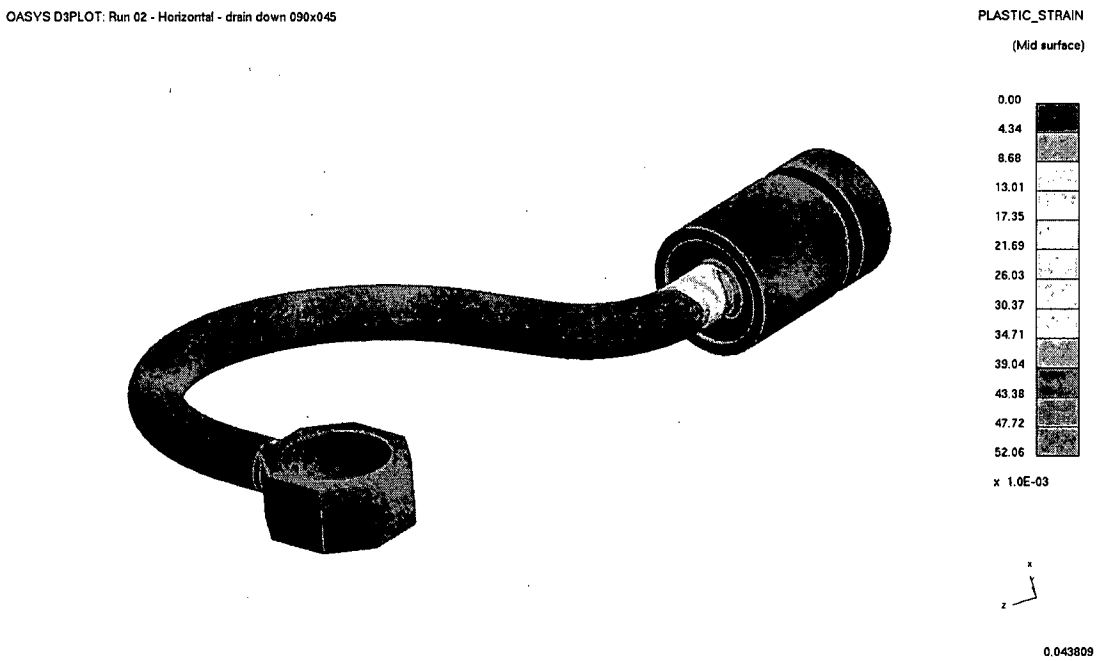

Figure 179: Effective plastic strain in outer tube – Run 02

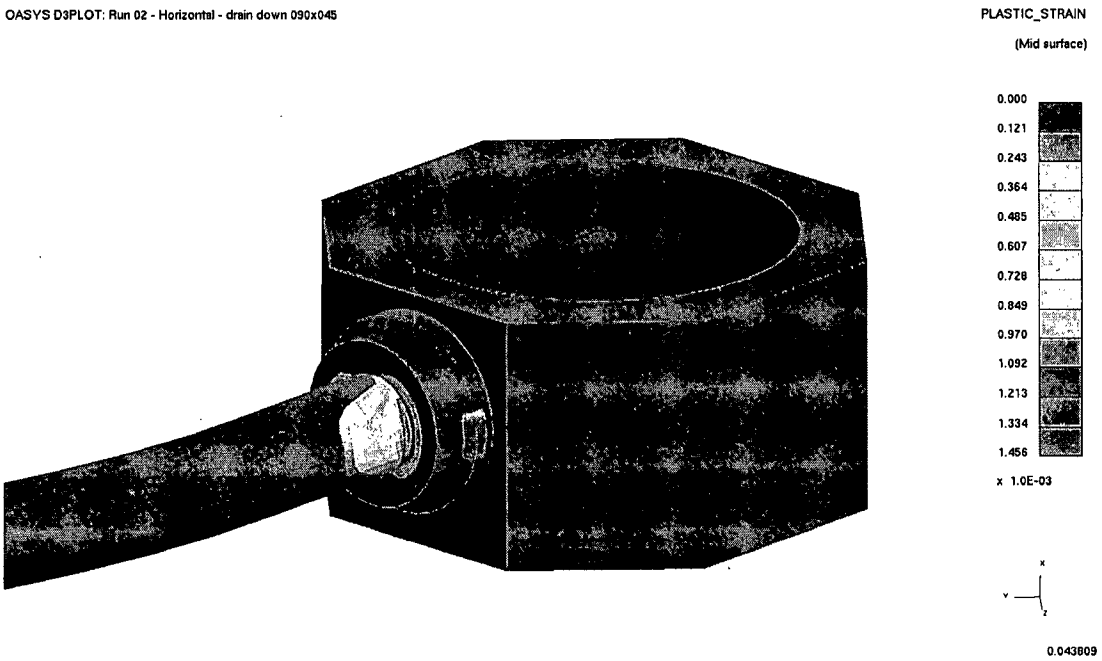

Figure 180: Effective plastic strain in drain tube – Run 02.

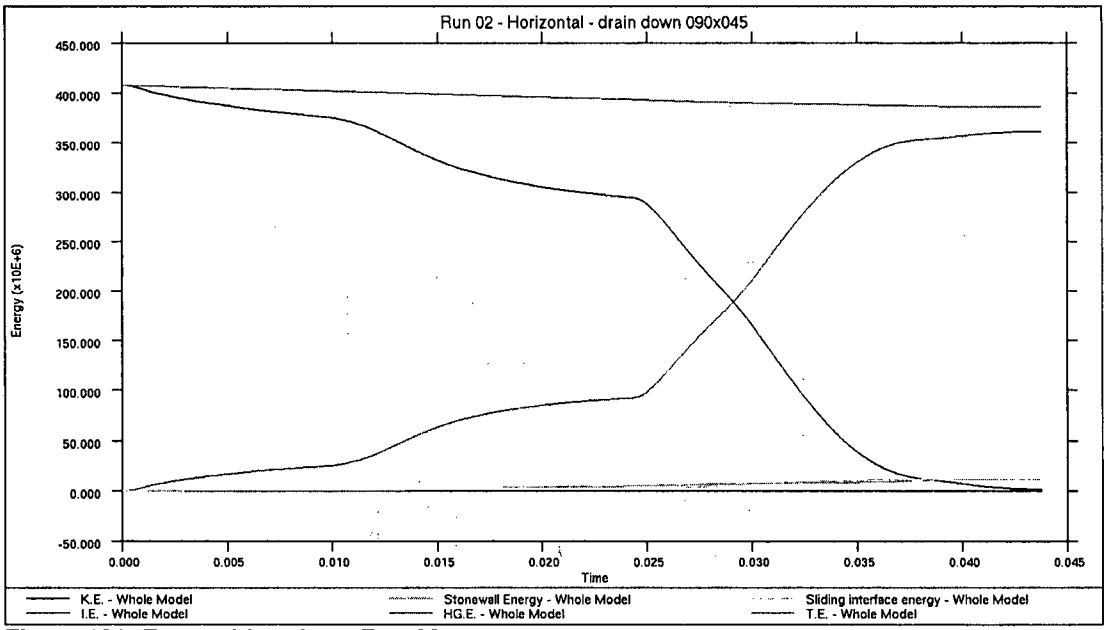

Figure 181: Energy histories – Run 02

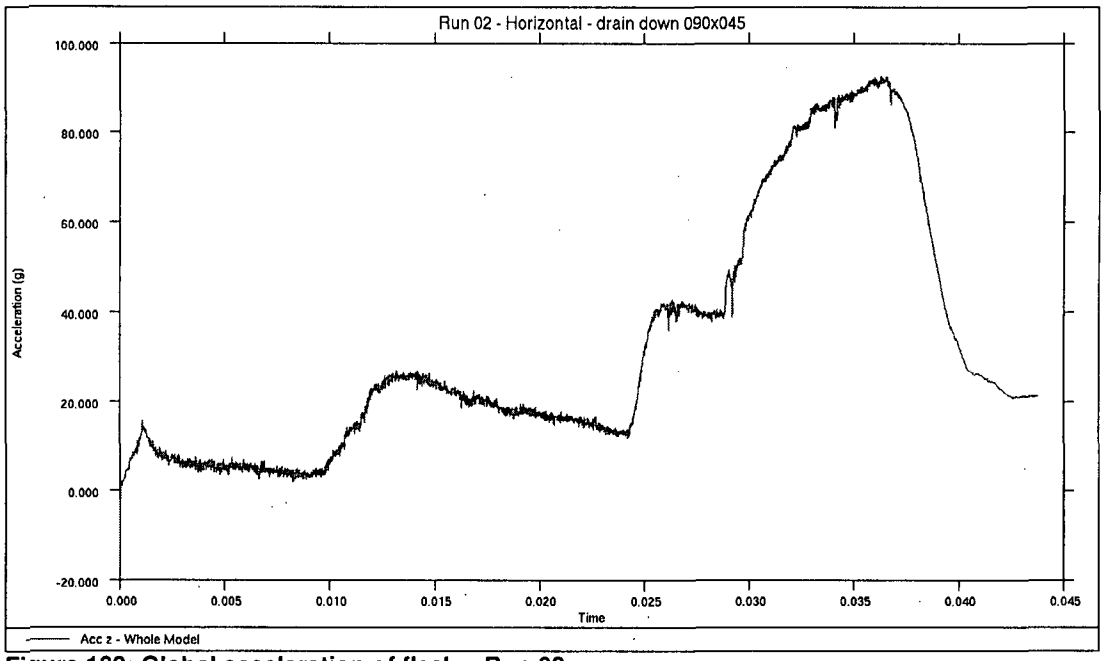

Figure 182: Global acceleration of flask – Run 02

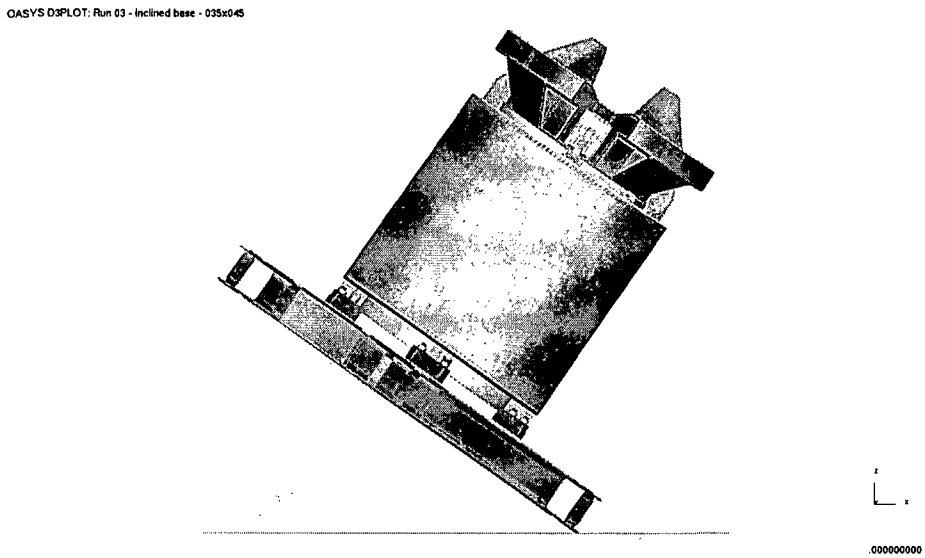

Figure 183: Initial impact orientation – Run 03

OASYS D3PLOT: Run 03 - inclined base - 035x045

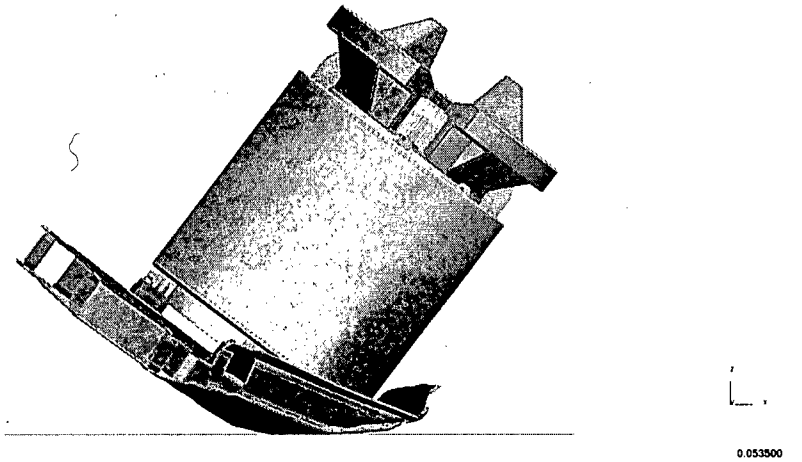

Figure 184: Final deformation – Run 03

OASYS D3PLOT: Run 03 - inclined base - 035x045

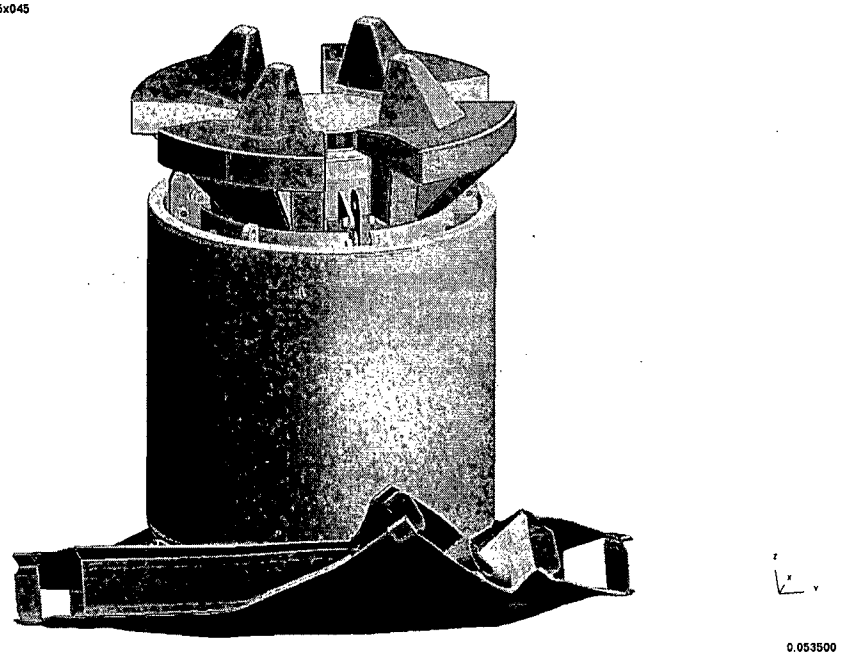

Figure 185: Deformation of flask – Run 03

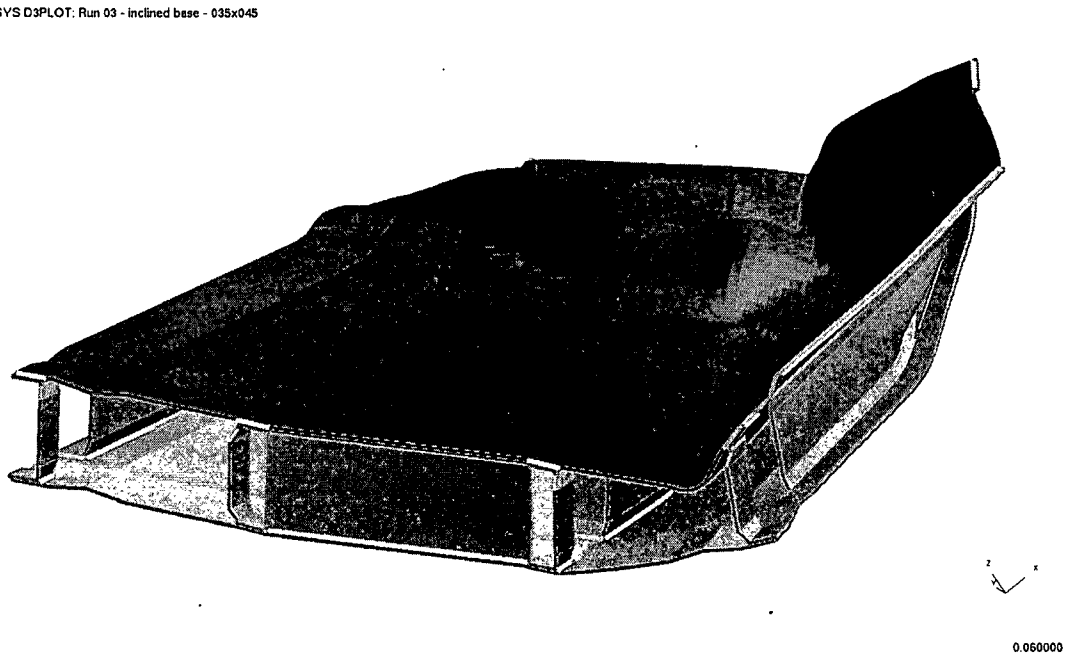

Figure 186: Deformation of pallet – Run 03

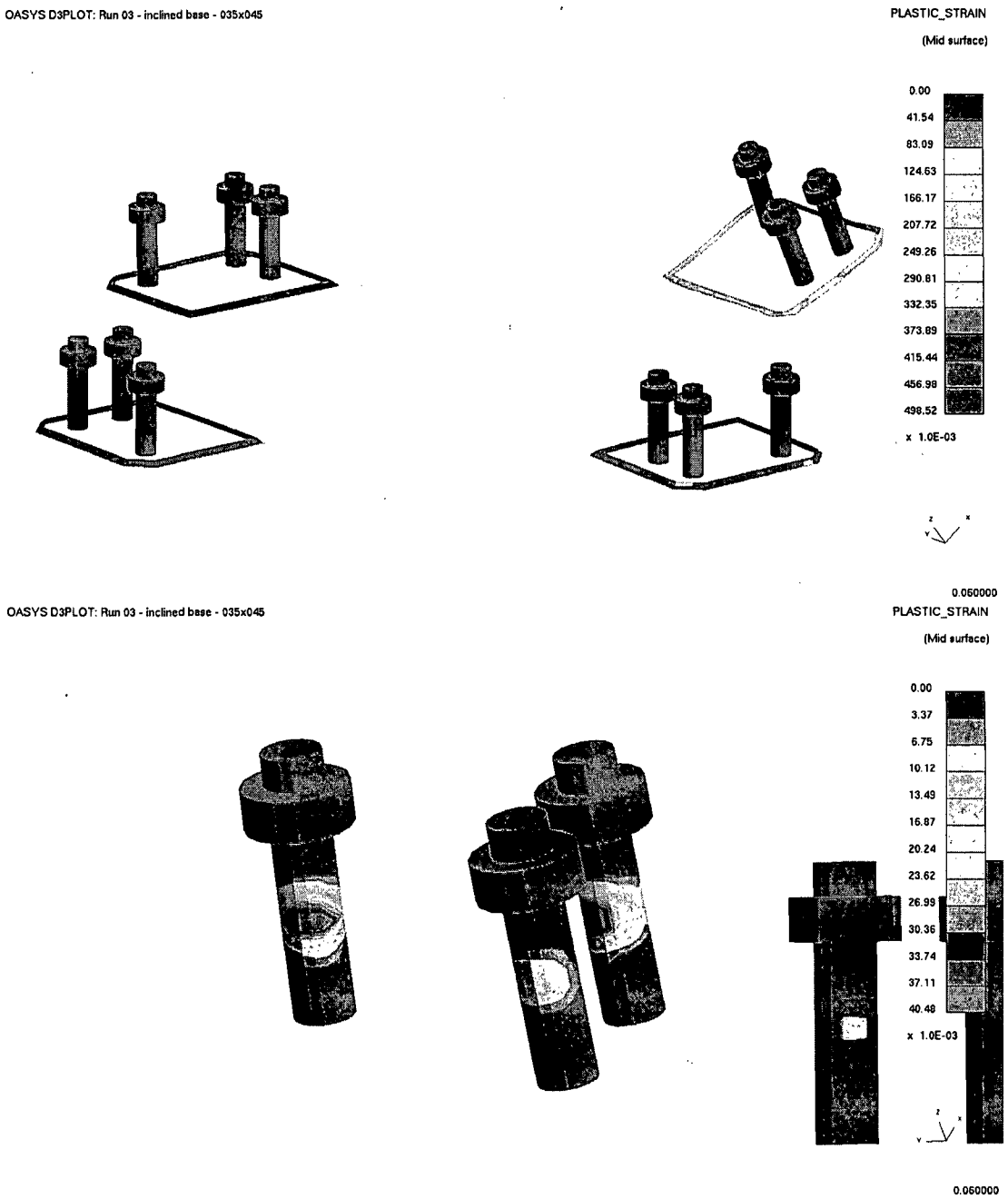

Figure 187: Effective plastic strain in pallet connections – Run 03

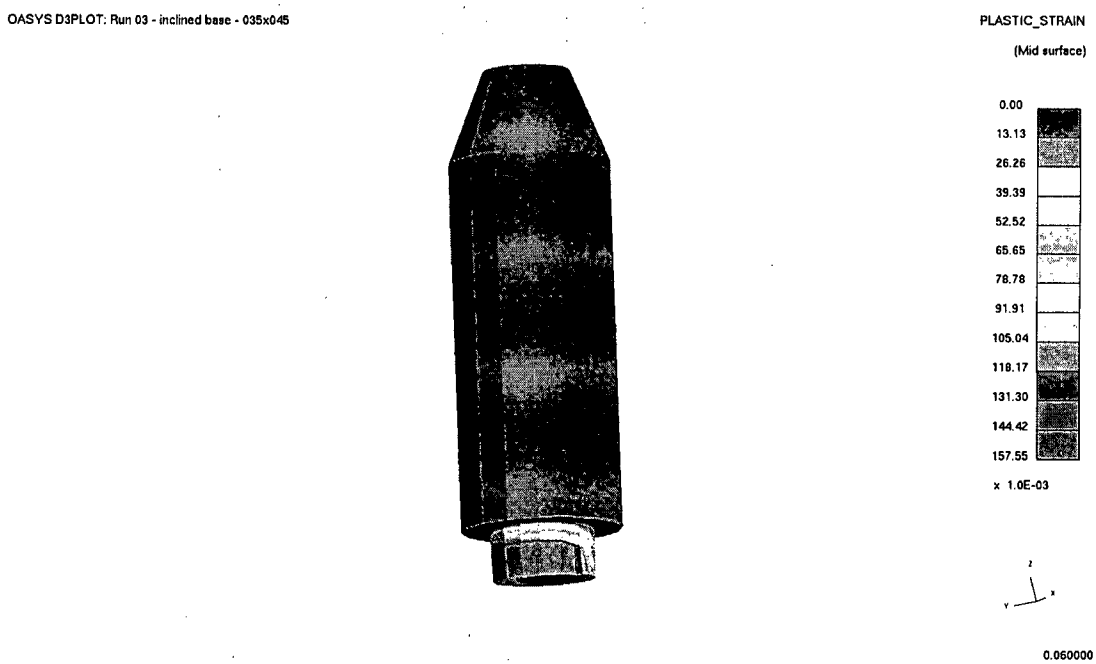

Figure 188: Effective plastic strain in dowels – Run 03

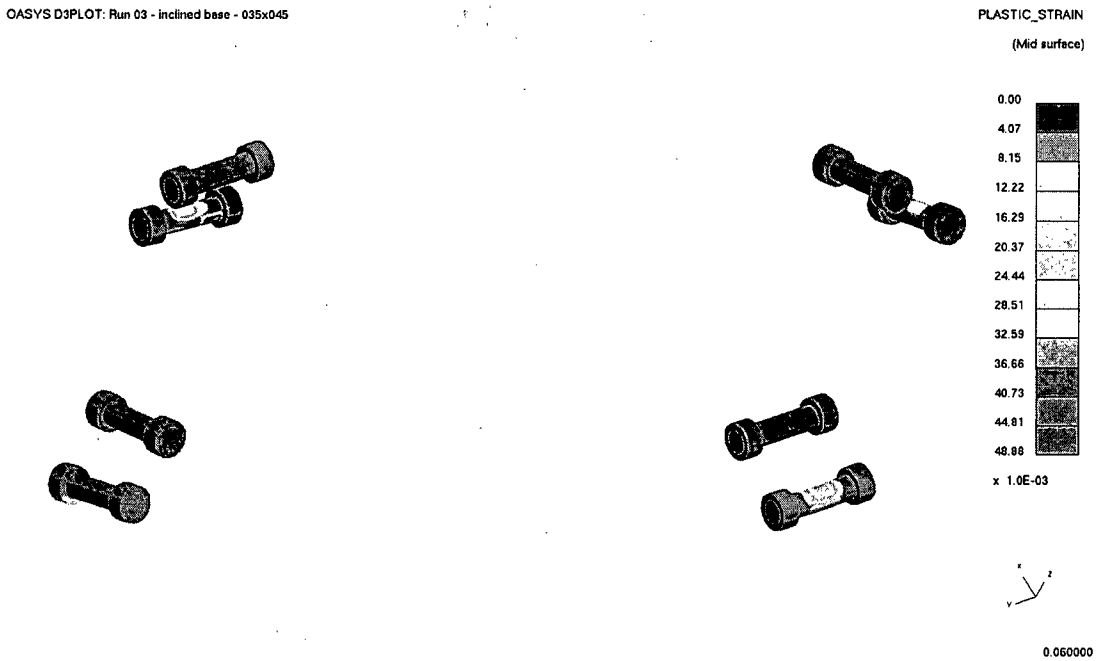

Figure 189: Effective plastic strain in shoulder bolts – Run 03.

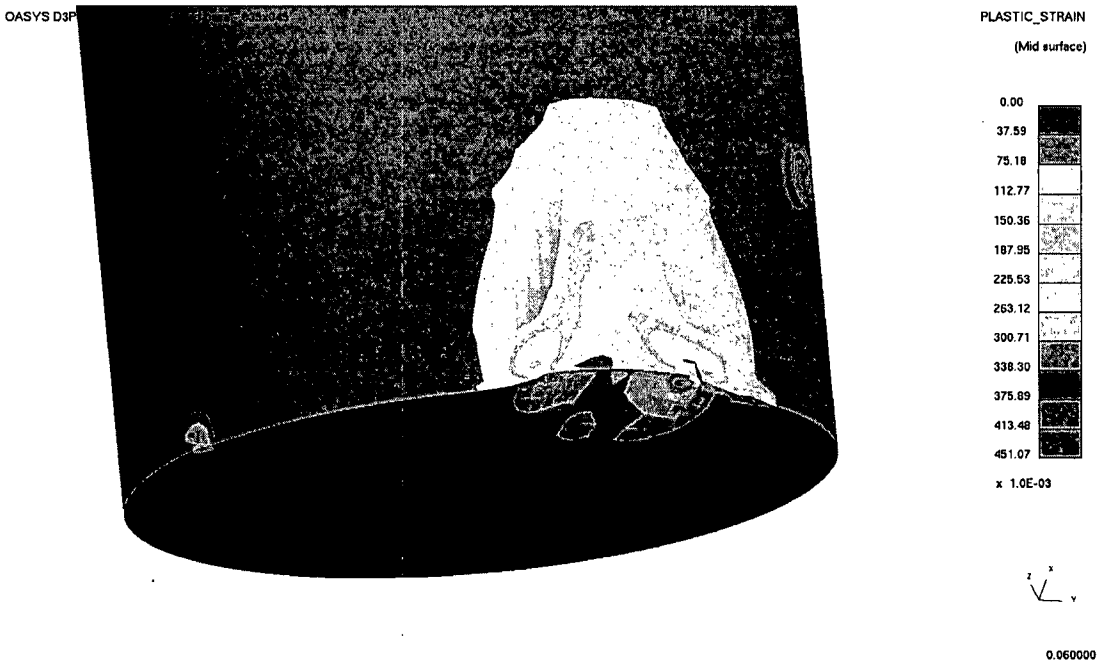

Figure 190: Effective plastic strain in flask wall – Run 03

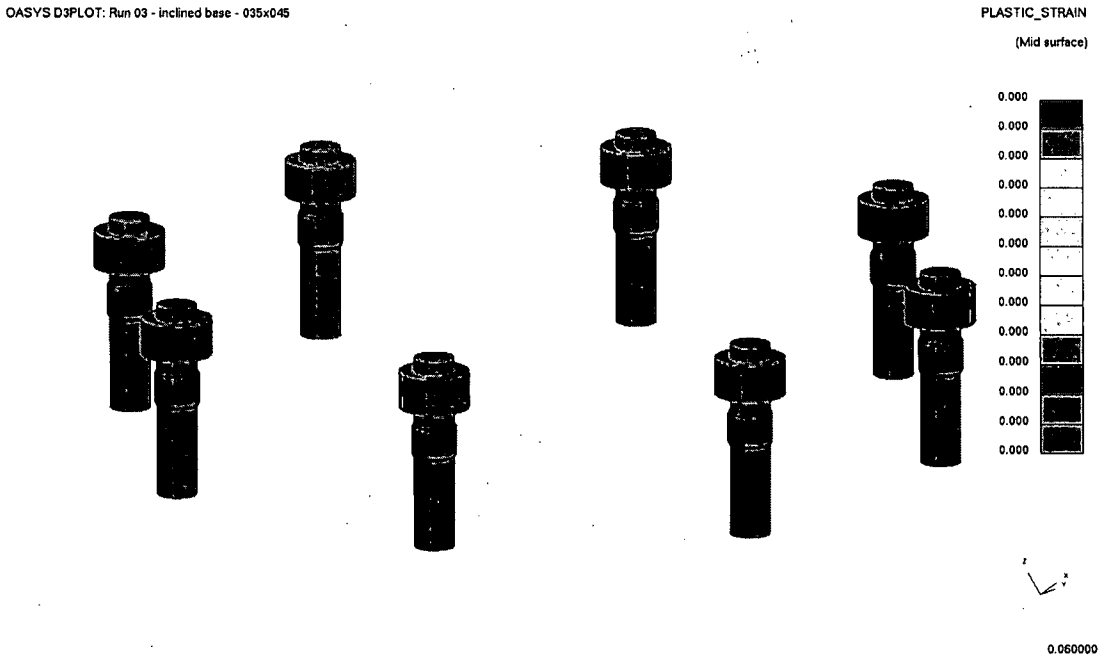

Figure 191: Effective plastic strain in closure studs – Run 03

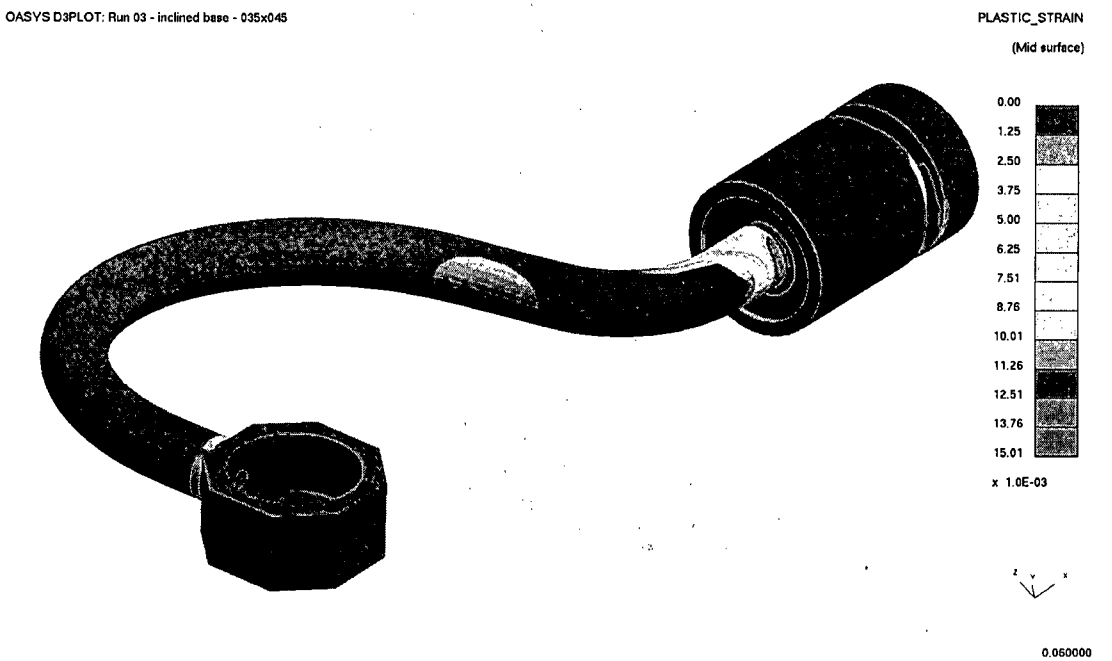

Figure 192: Effective plastic strain in outer tube – Run 03

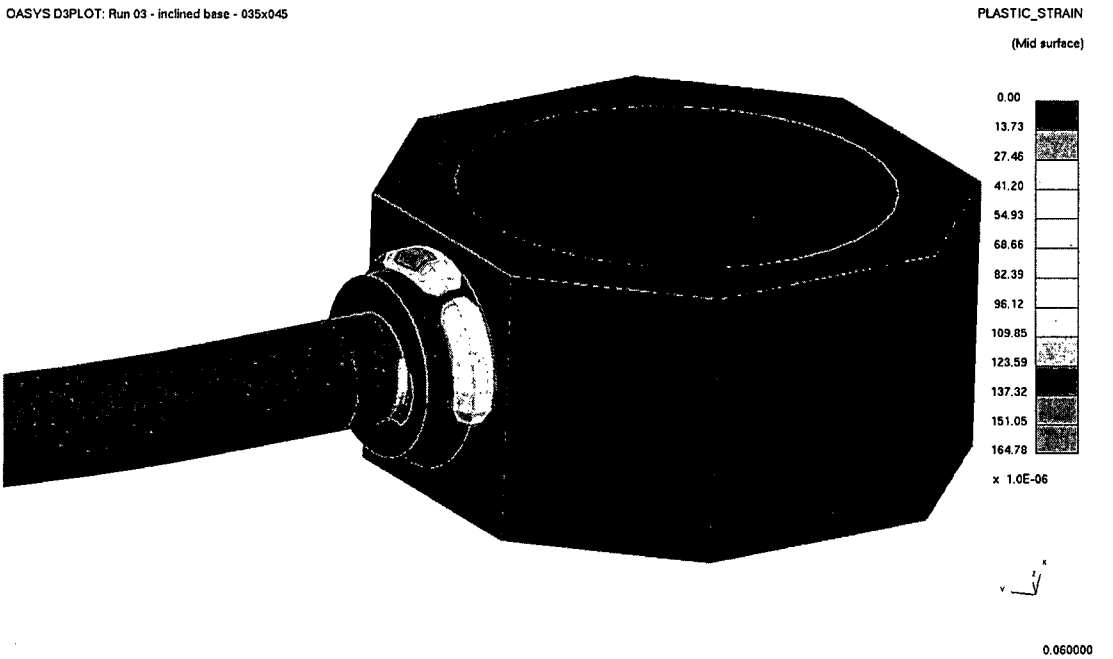

Figure 193: Effective plastic strain in drain tube – Run 03

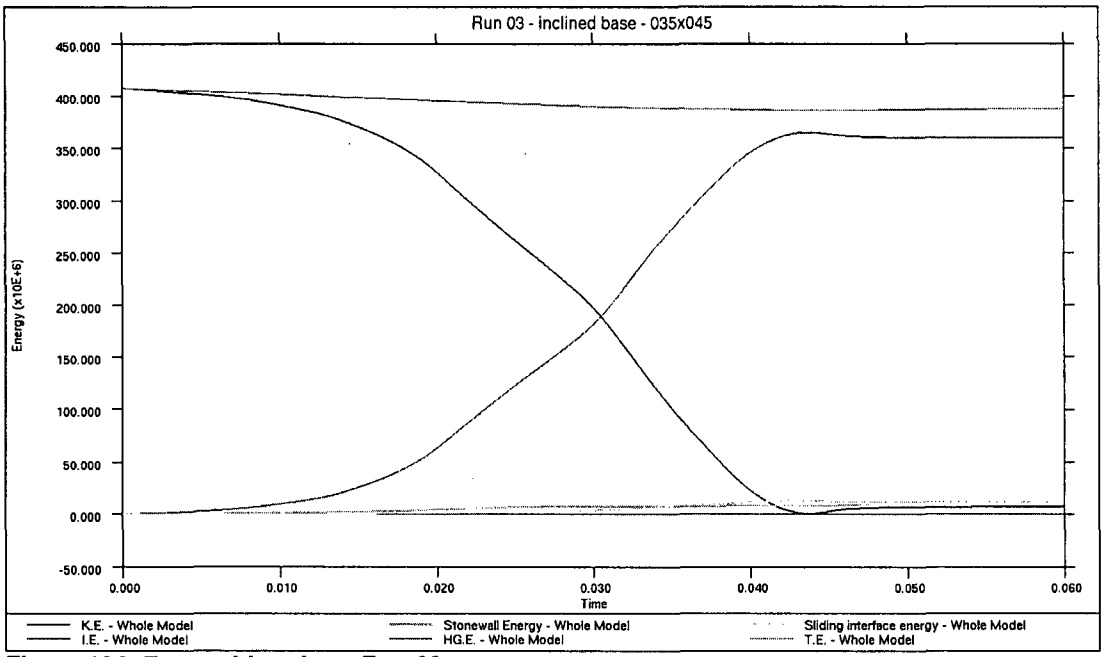

Figure 194: Energy histories – Run 03

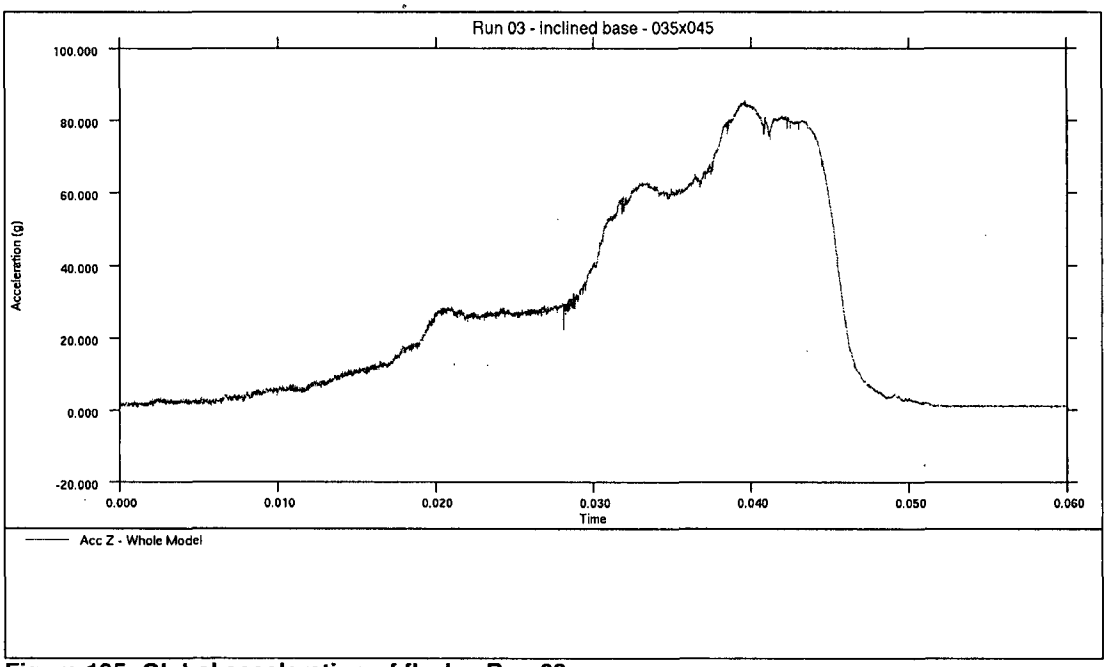

Figure 195: Global acceleration of flask – Run 03

OASYS D3PLOT: Run 04 - Vertical upright - 000x000 (Dr

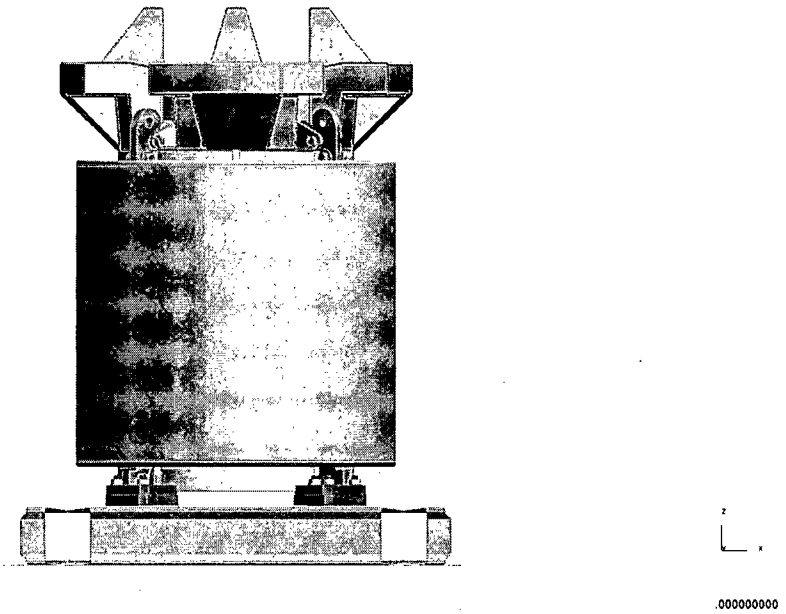

Figure 196: Initial impact orientation – Run 04

OASYS D3PLOT: Run 04 - Vertical upright - 000x000 (Dr

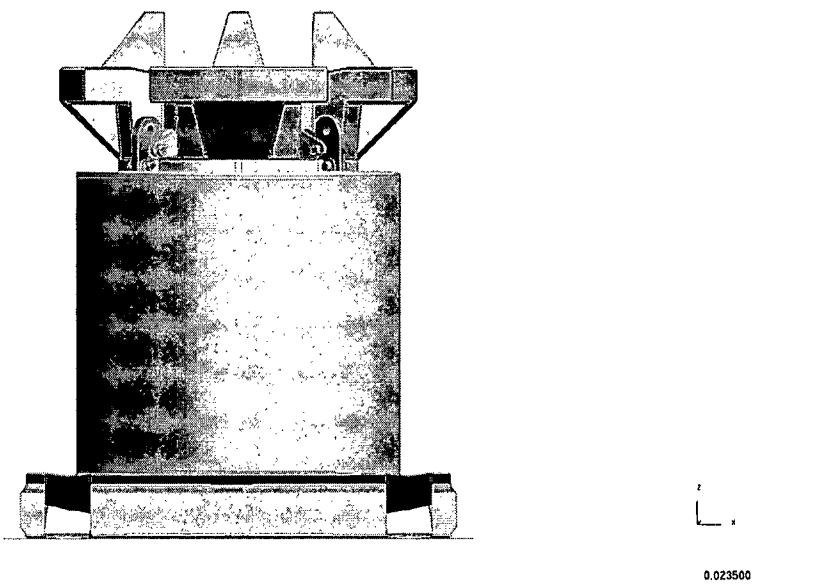

Figure 197: Final deformation – Run 04

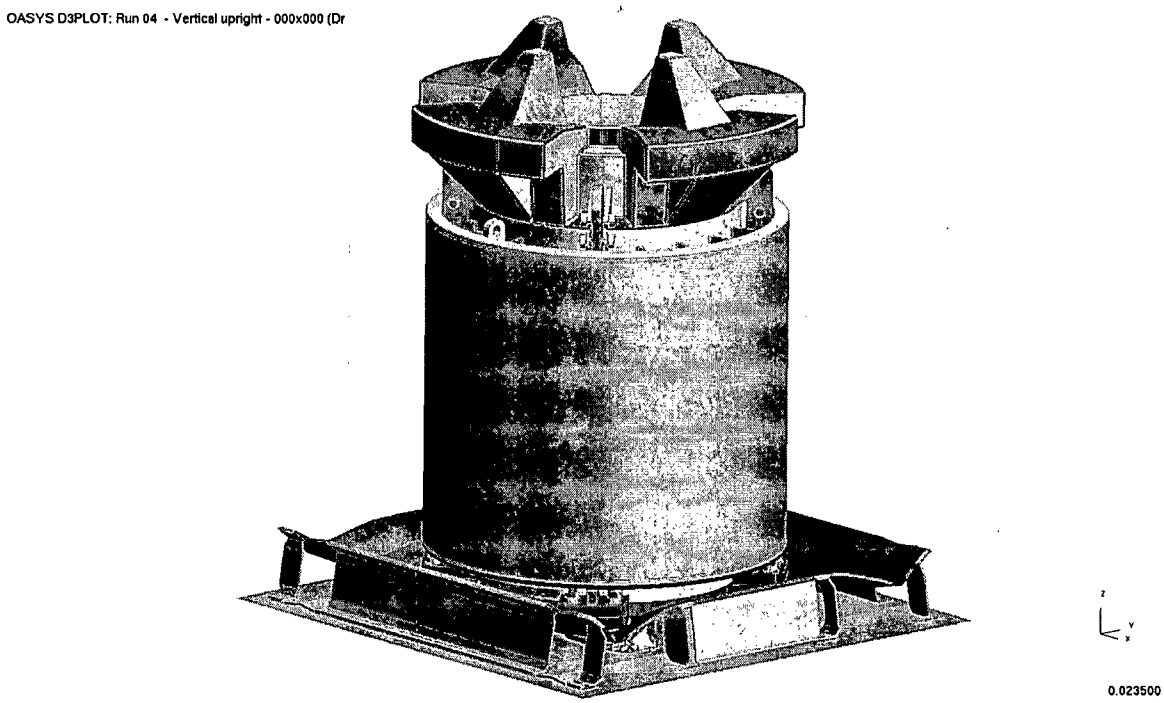

Figure 198: Deformation of flask – Run 04

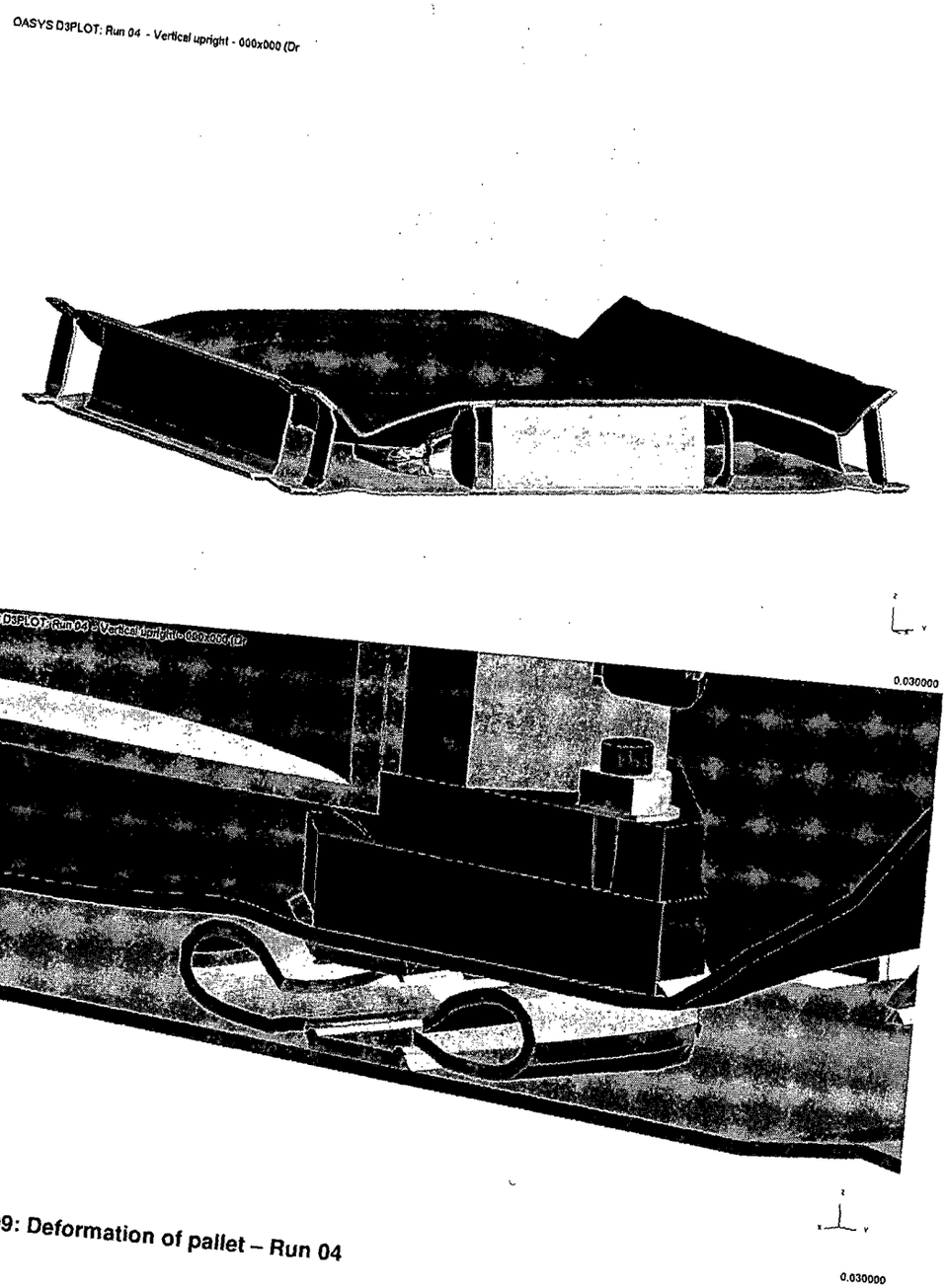

Figure 199: Deformation of pallet – Run 04

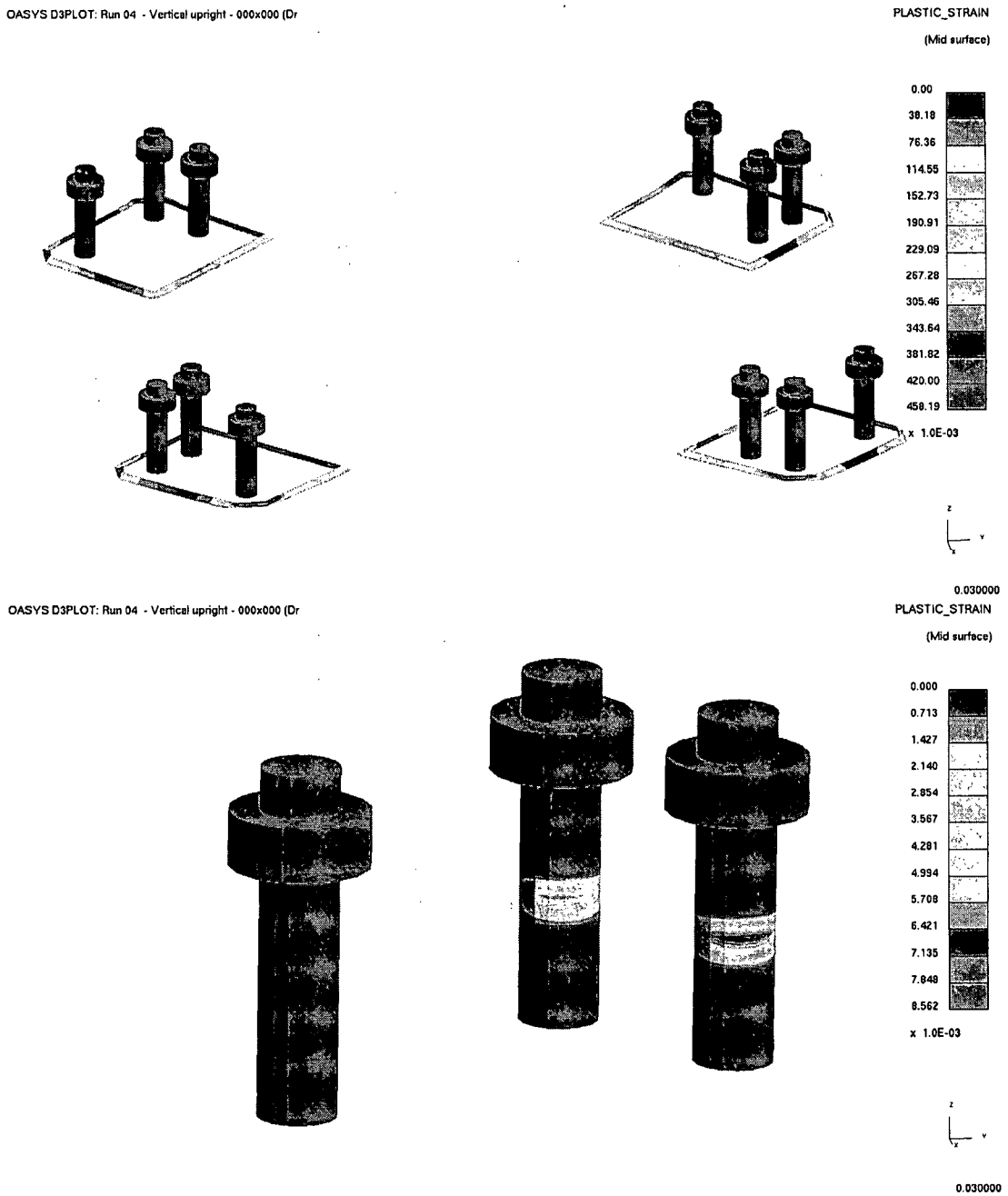

Figure 200: Effective plastic strain in pallet connections – Run 04

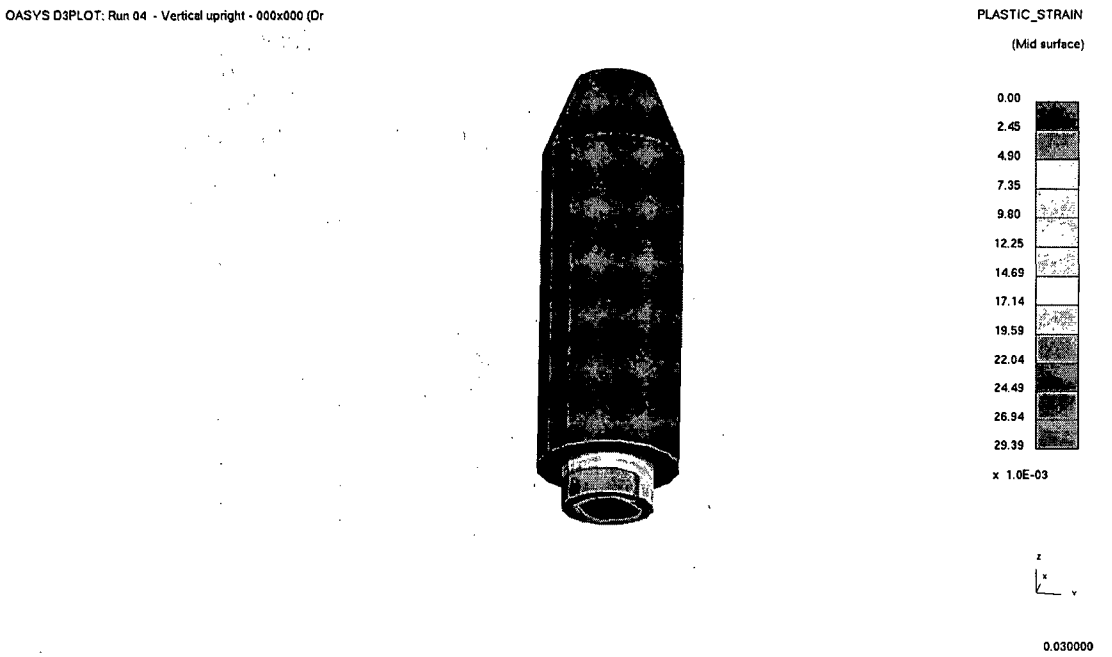

Figure 201: Effective plastic strain in dowels – Run 04

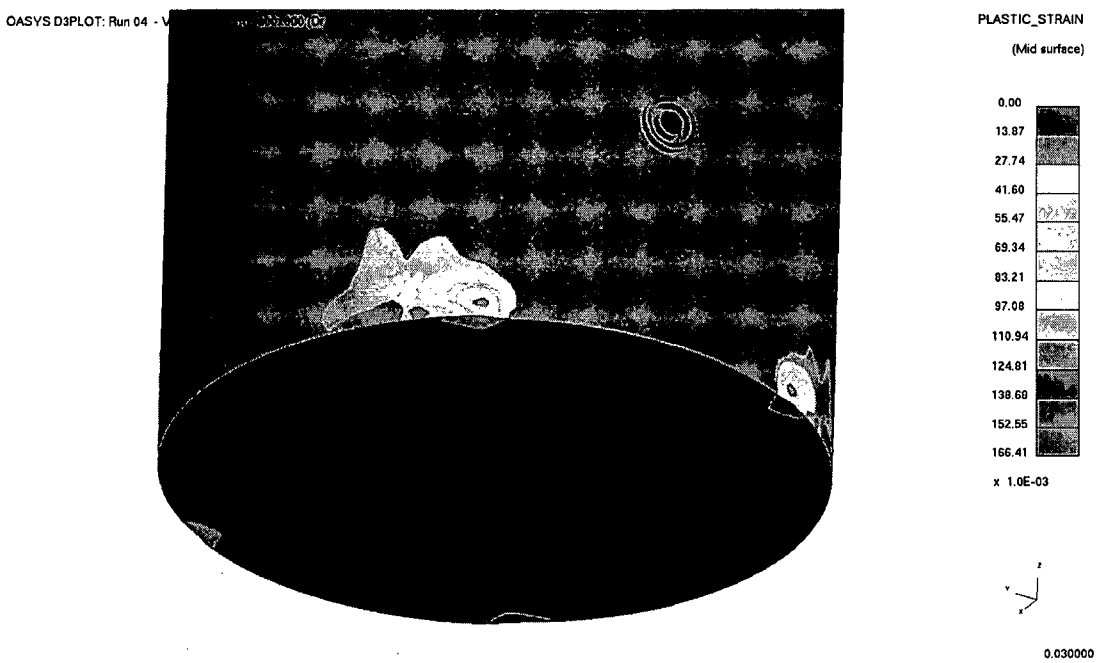

Figure 202: Effective plastic strain in flask wall – Run 04

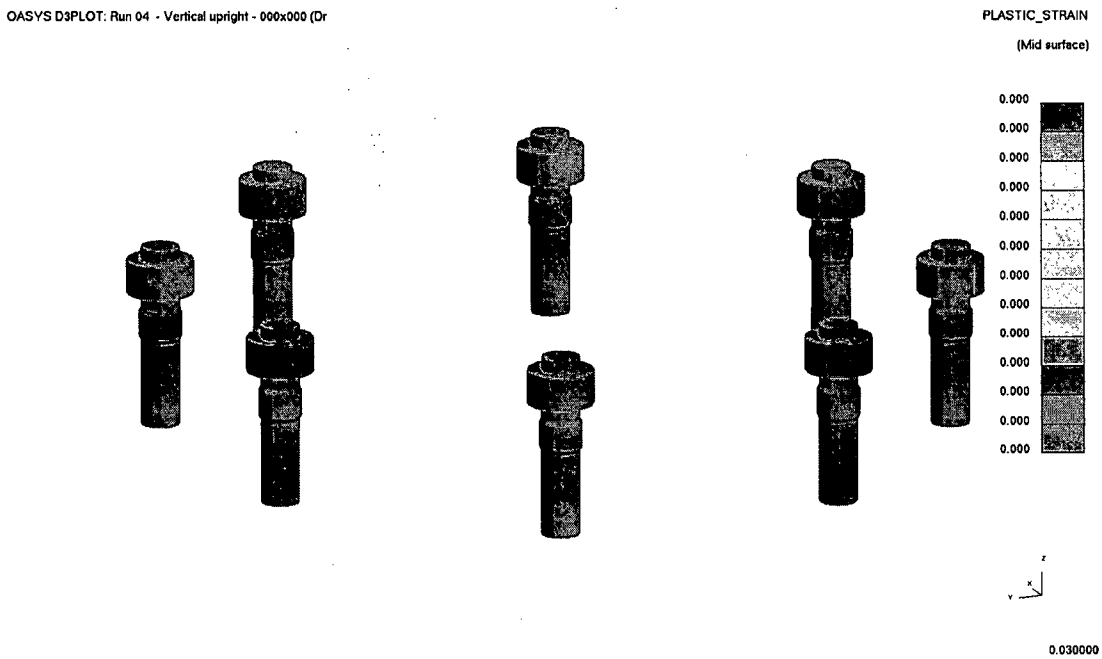

Figure 203: Effective plastic strain in closure studs – Run 04

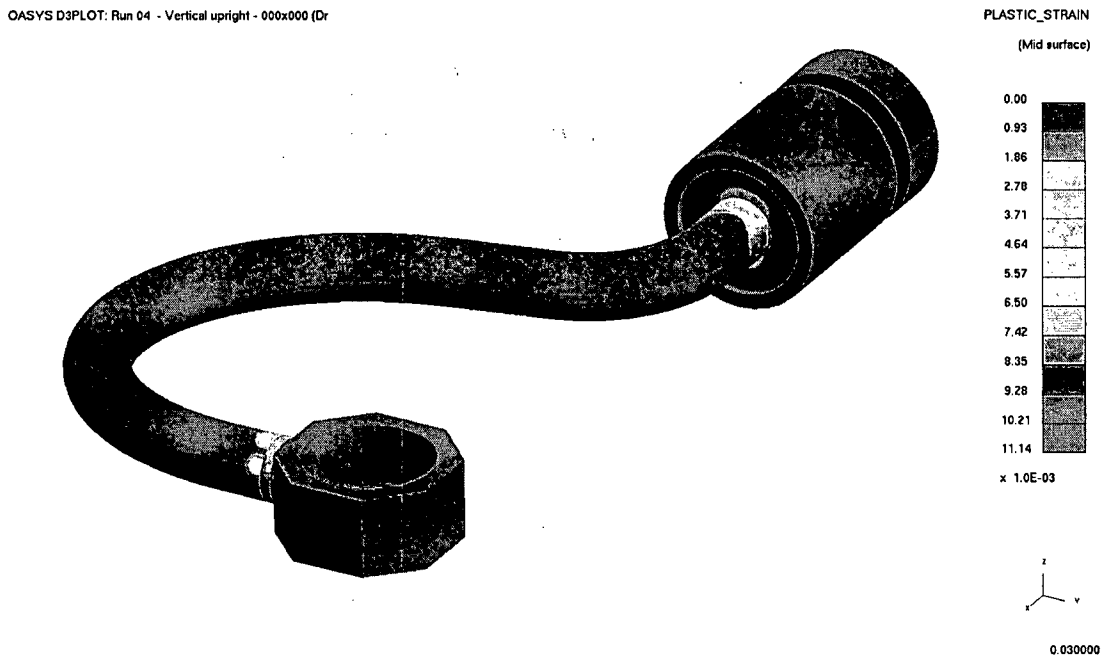

Figure 204: Effective plastic strain in outer tube – Run 04

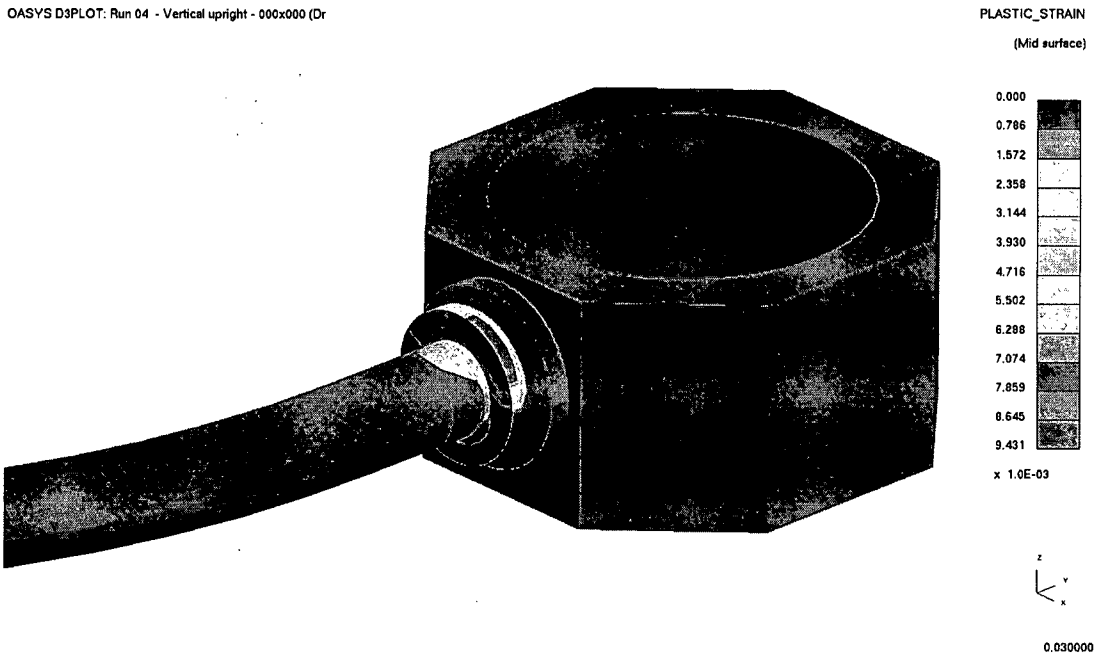

Figure 205: Effective plastic strain in drain tube – Run 04

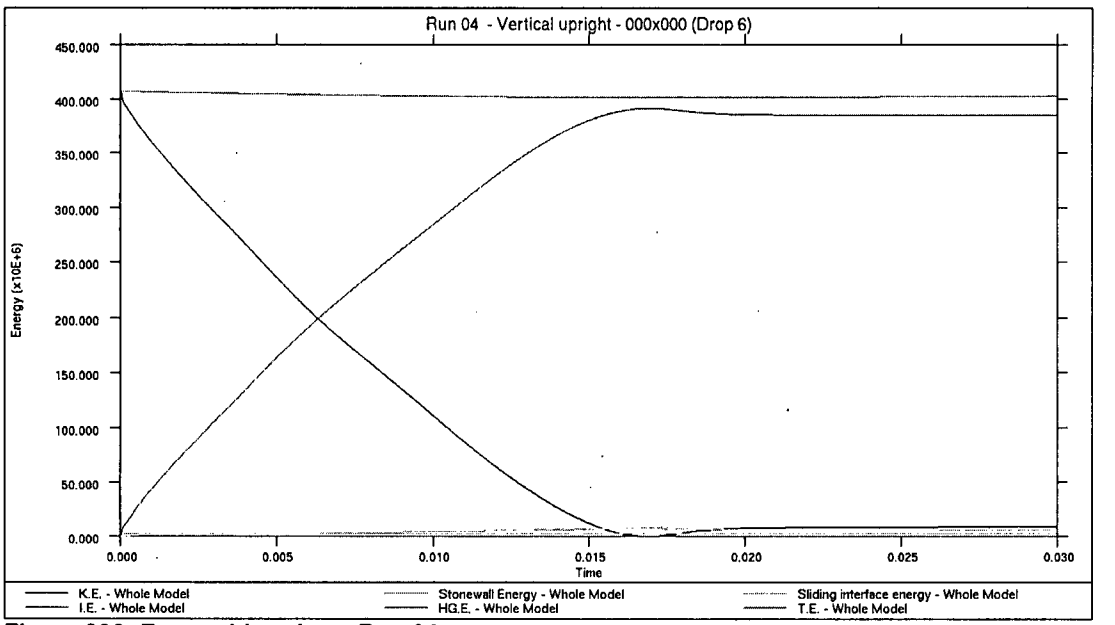

Figure 206: Energy histories – Run 04

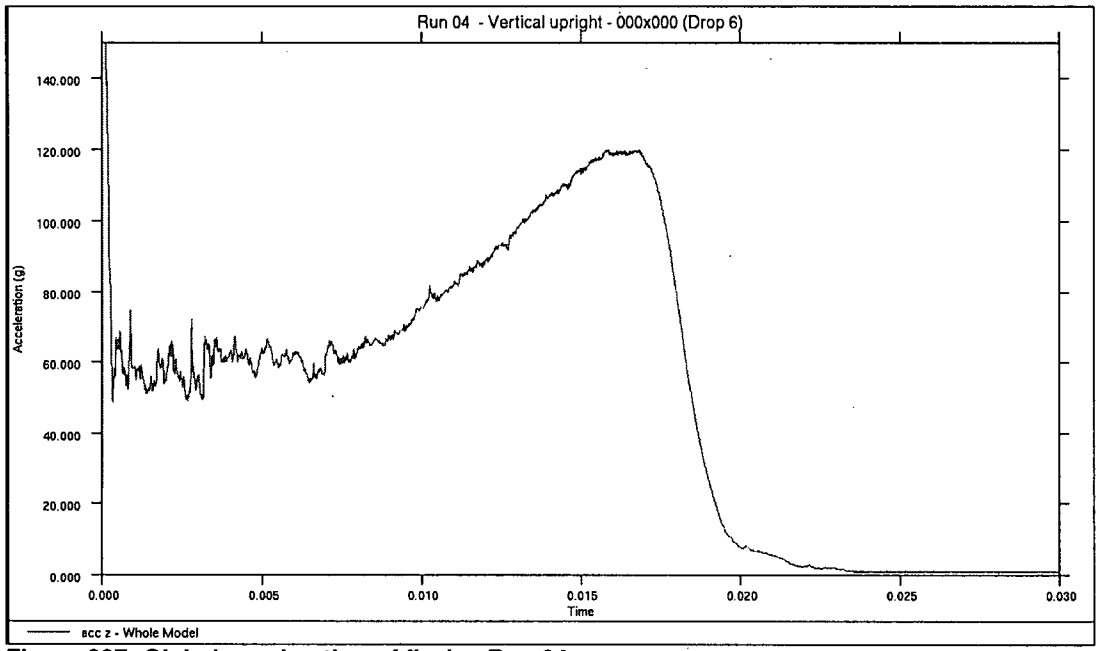

Figure 207: Global acceleration of flask – Run 04

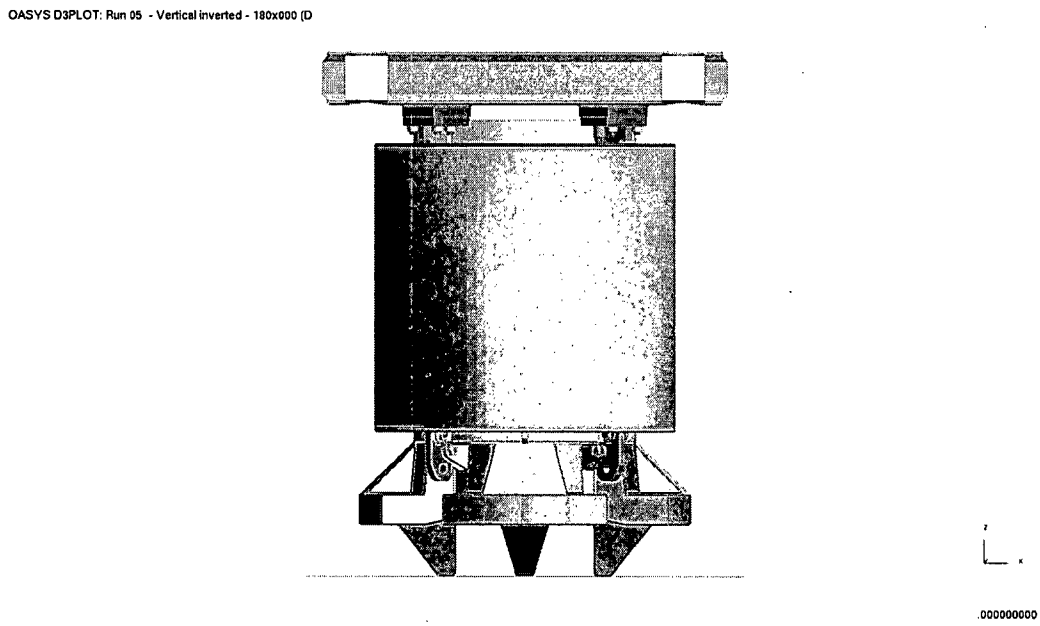

Figure 208: Initial impact orientation – Run 05

OASYS D3PLOT: Run 05 - Vertical inverted - 180x000 (D

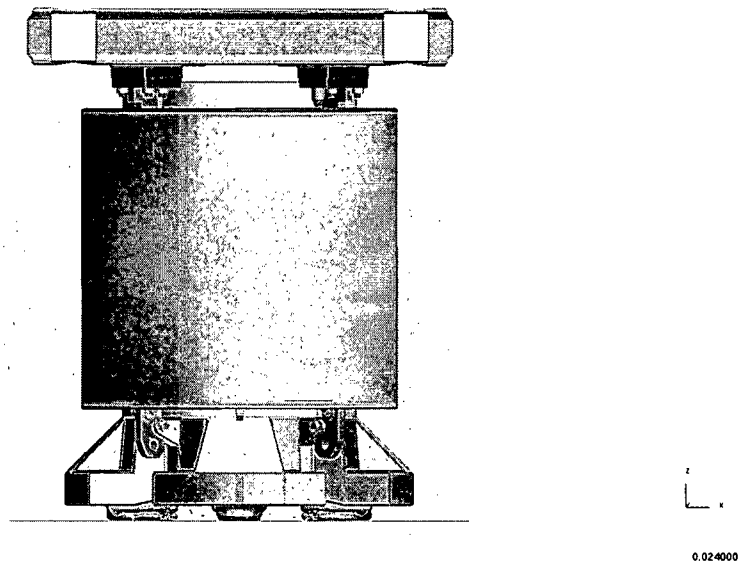

Figure 209: Final deformation – Run 05

OASYS D3PLOT: Run 05 - Vertical inverted - 180x000 (D

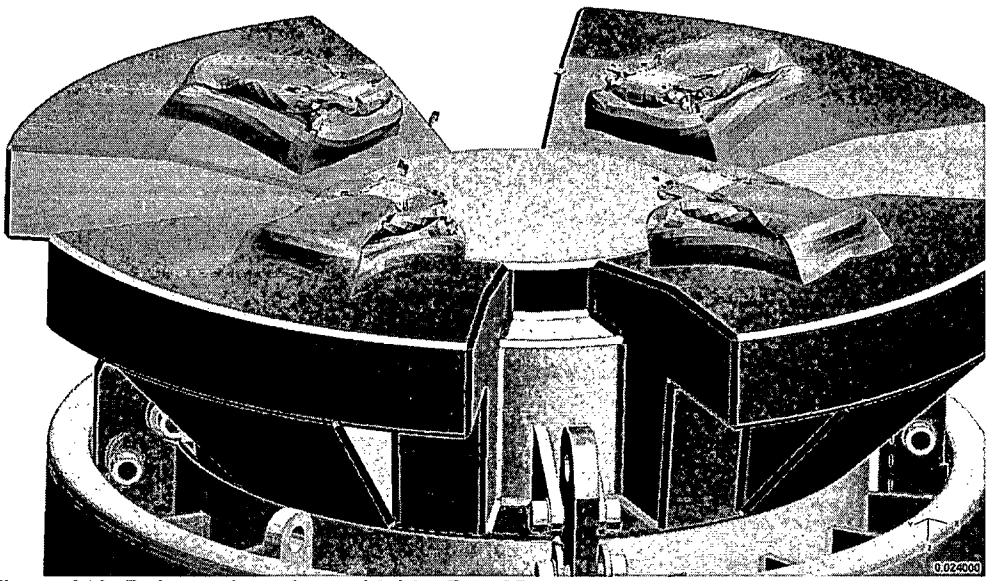

Figure 210: Deformation of top shield – Run 05

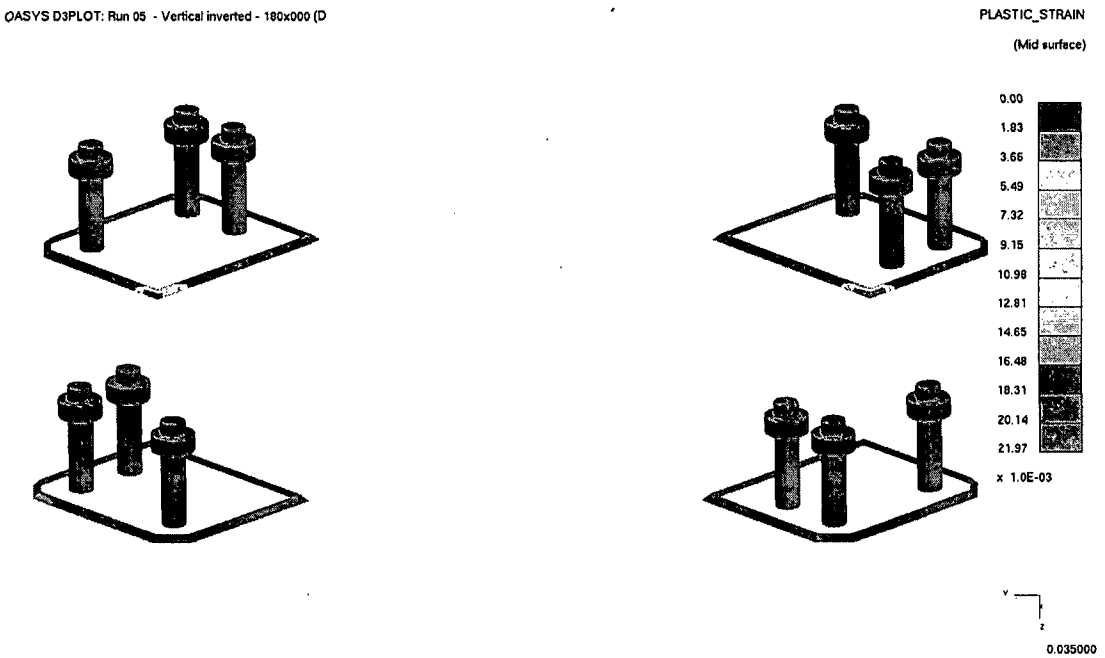

Figure 211: Effective plastic strain in pallet connections – Run 05

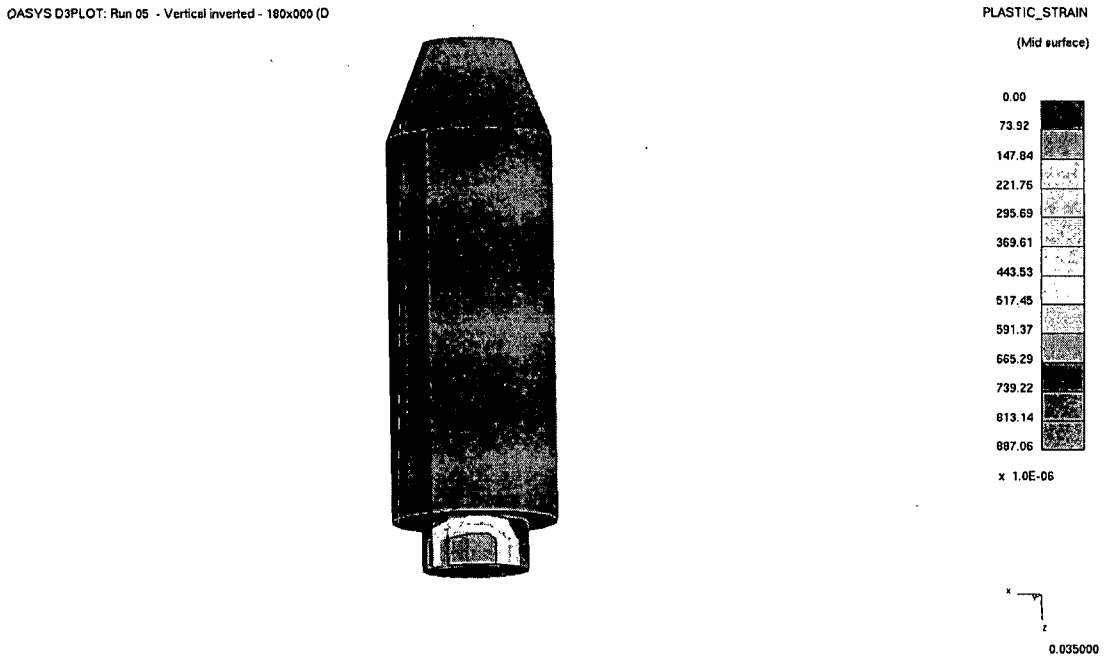

Figure 212: Effective plastic strain in dowels – Run 05

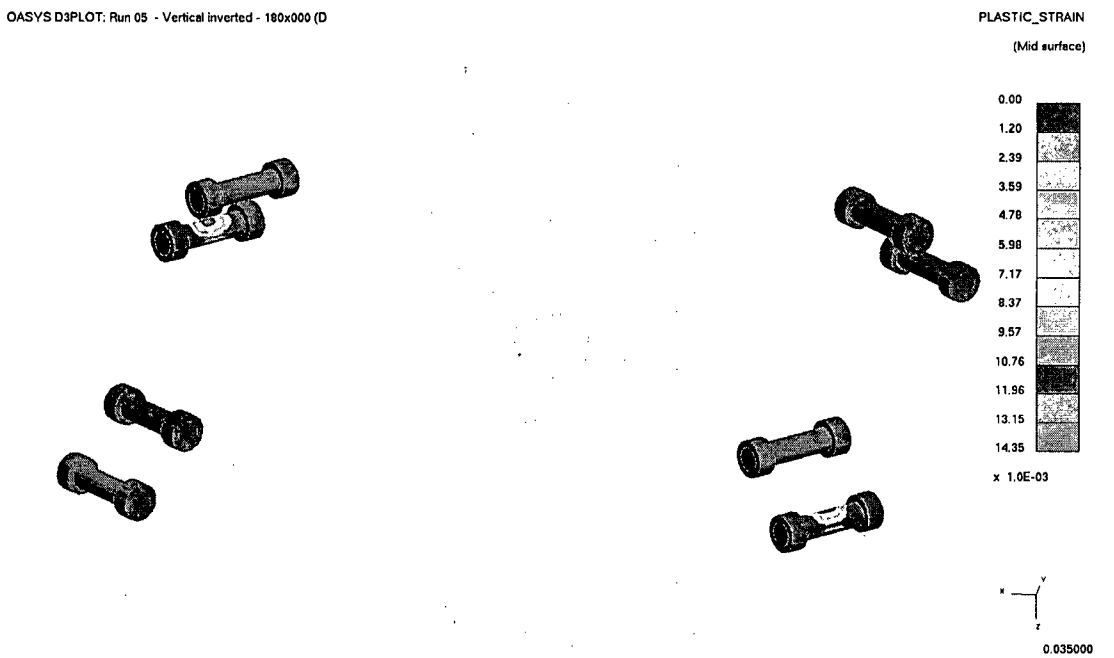

Figure 213: Effective plastic strain in shoulder bolts – Run 05

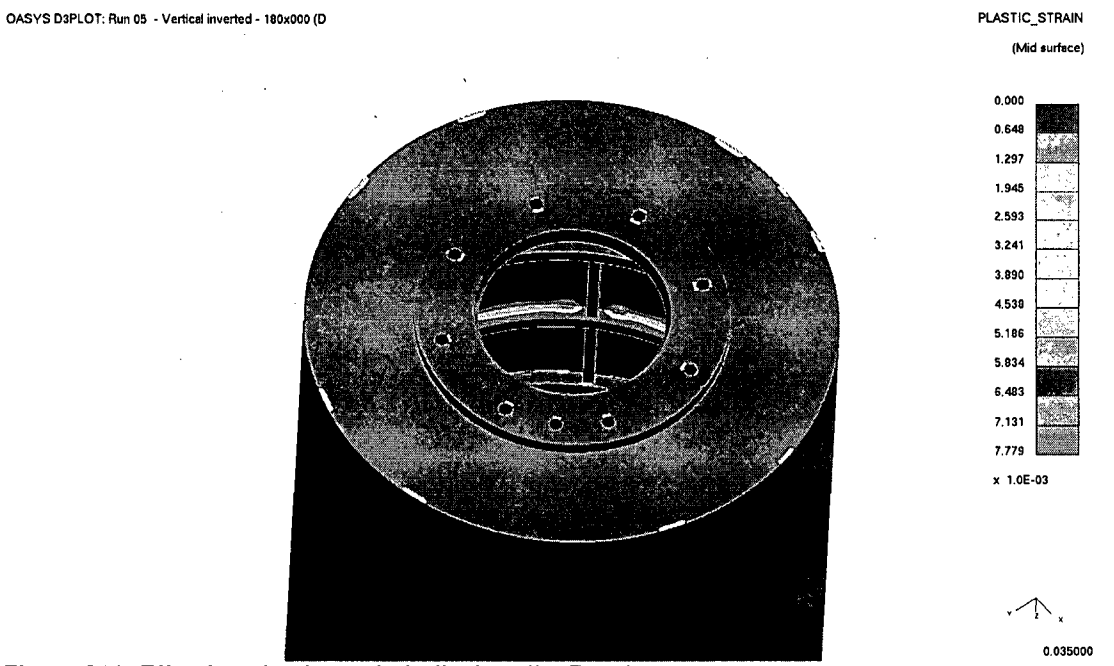

Figure 214: Effective plastic strain in flask wall – Run 05

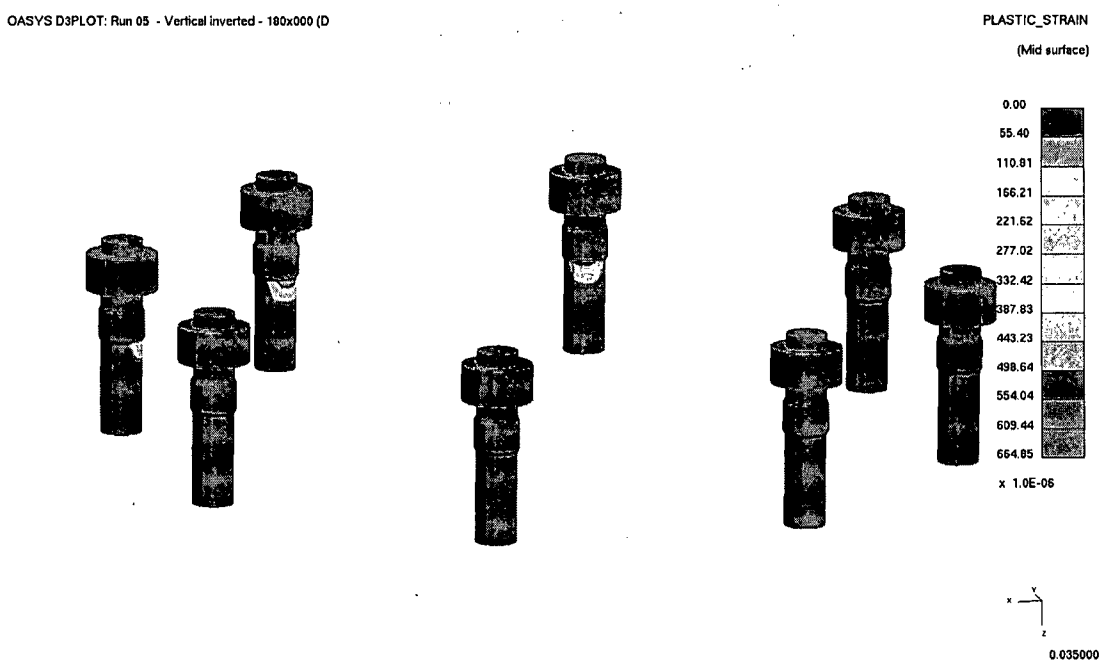

Figure 215: Effective plastic strain in closure studs – Run 05

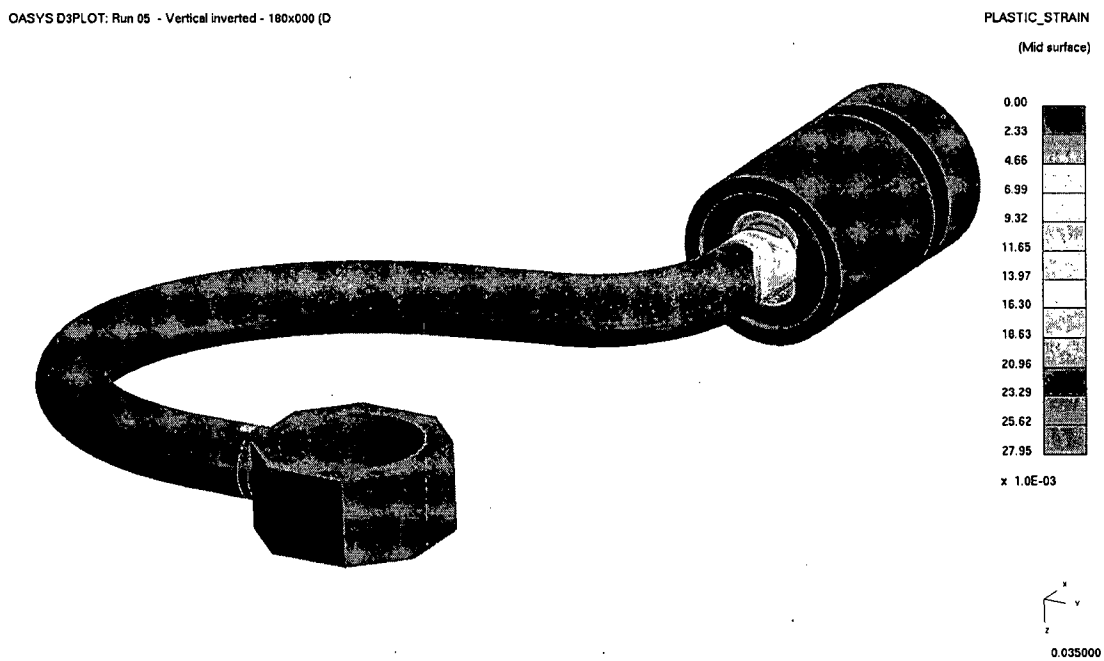

Figure 216: Effective plastic strain in outer tube – Run 05

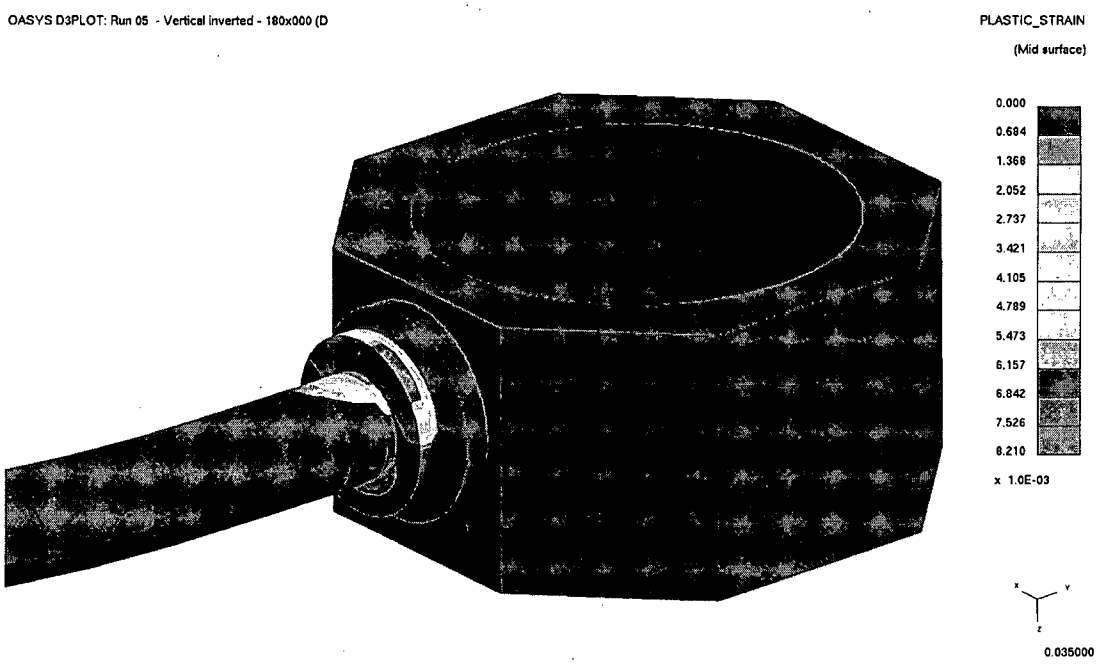

Figure 217: Effective plastic strain in drain tube – Run 05

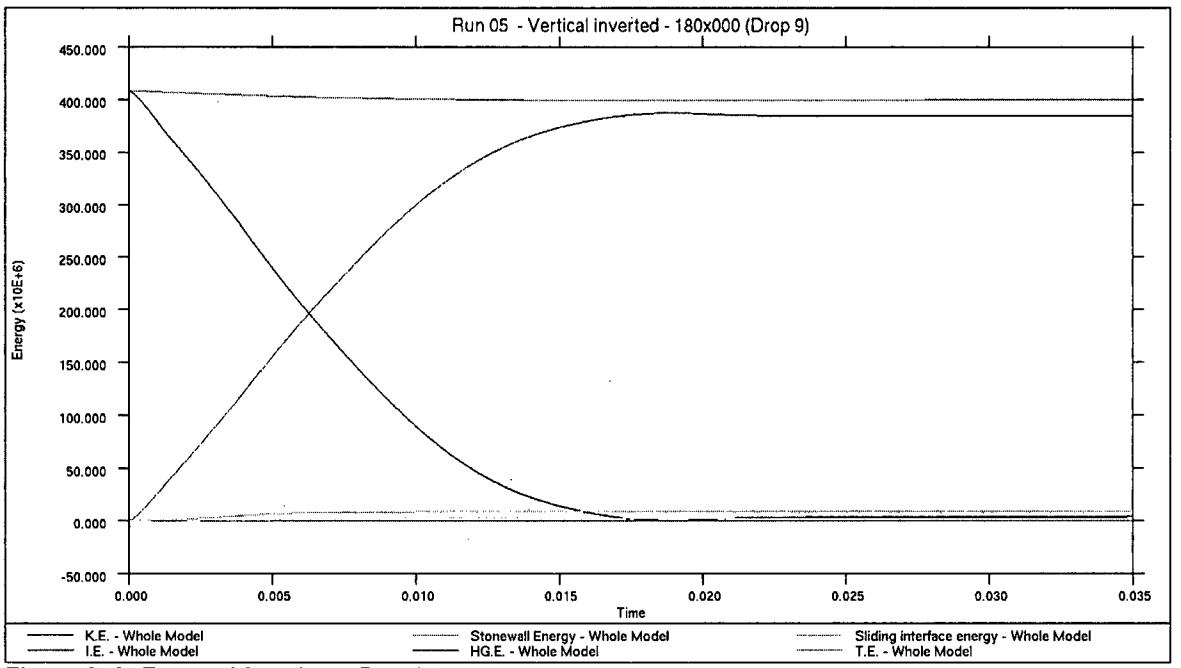

Figure 218: Energy histories – Run 05

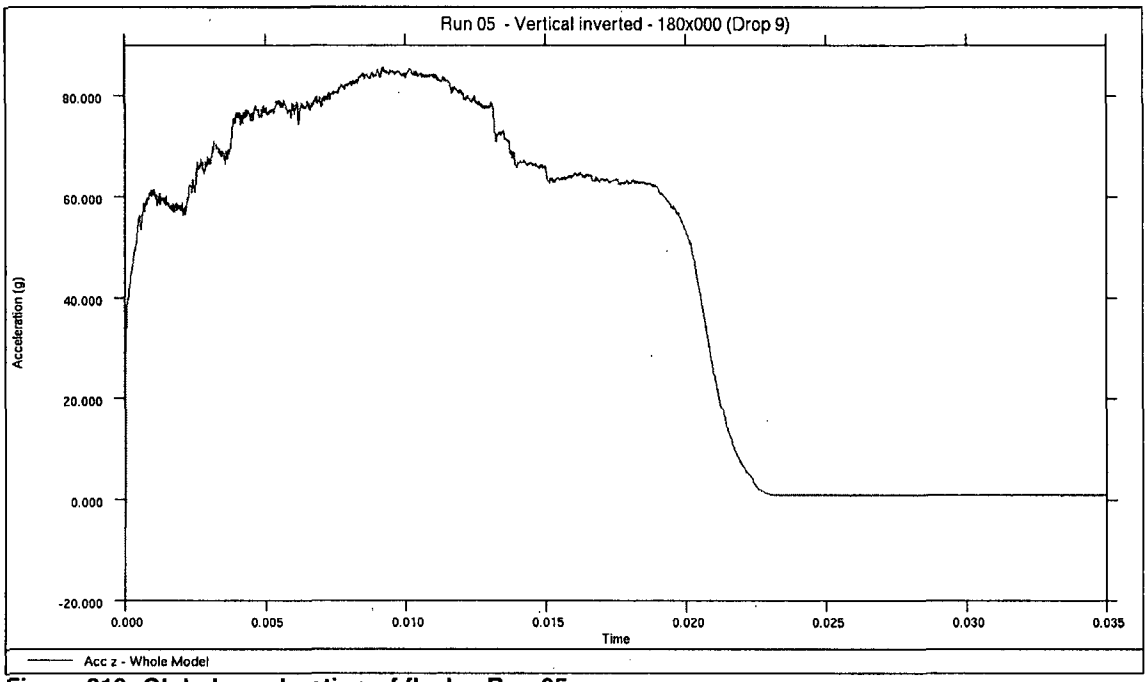

Figure 219: Global acceleration of flask – Run 05

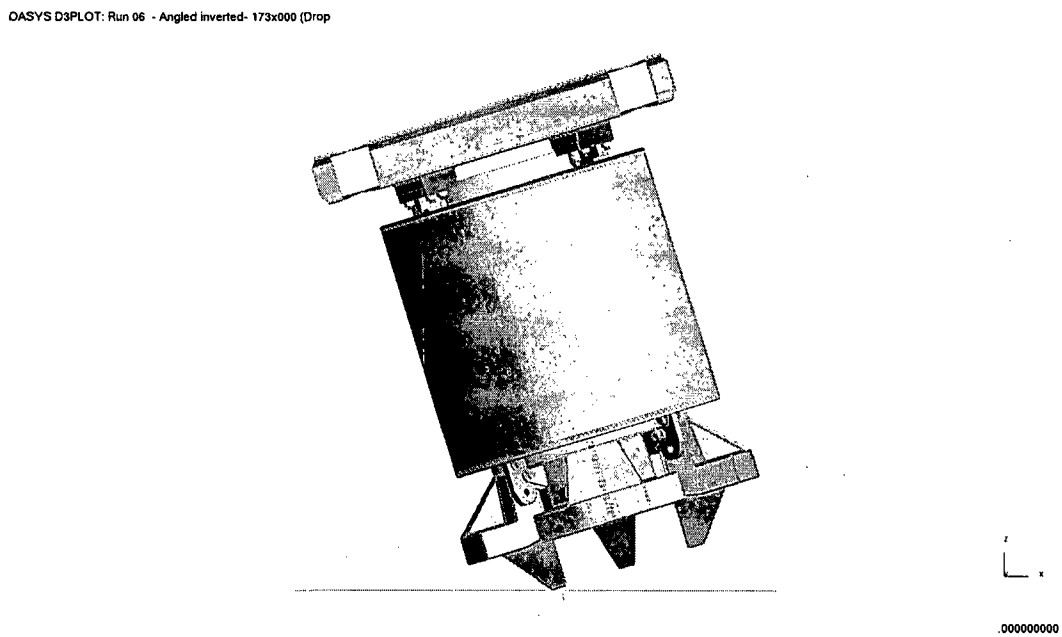

Figure 220: Initial impact orientation – Run 06

OASYS D3PLOT: Run 06 - Angled inverted- 173x000 (Drop

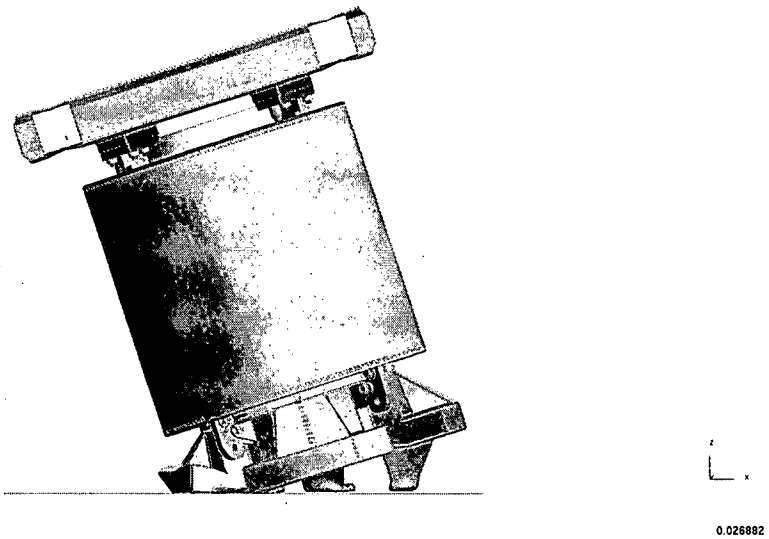

Figure 221: Final deformation – Run 06

OASYS D3PLOT: Run 06 - Angled inverted- 173x000 (Drop

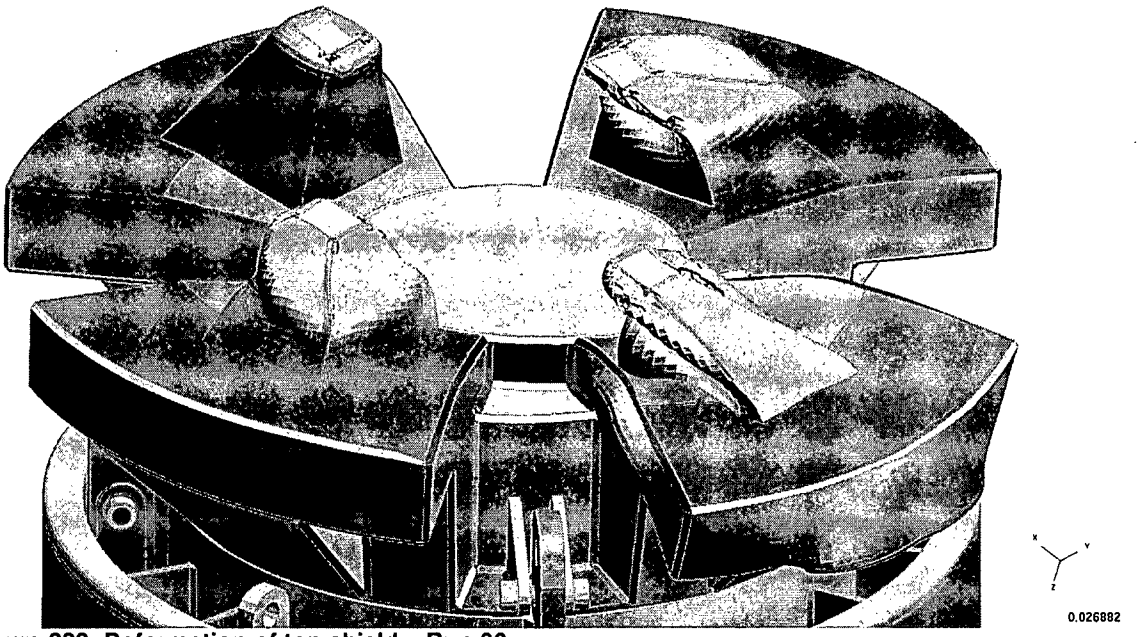

Figure 222: Deformation of top shield – Run 06

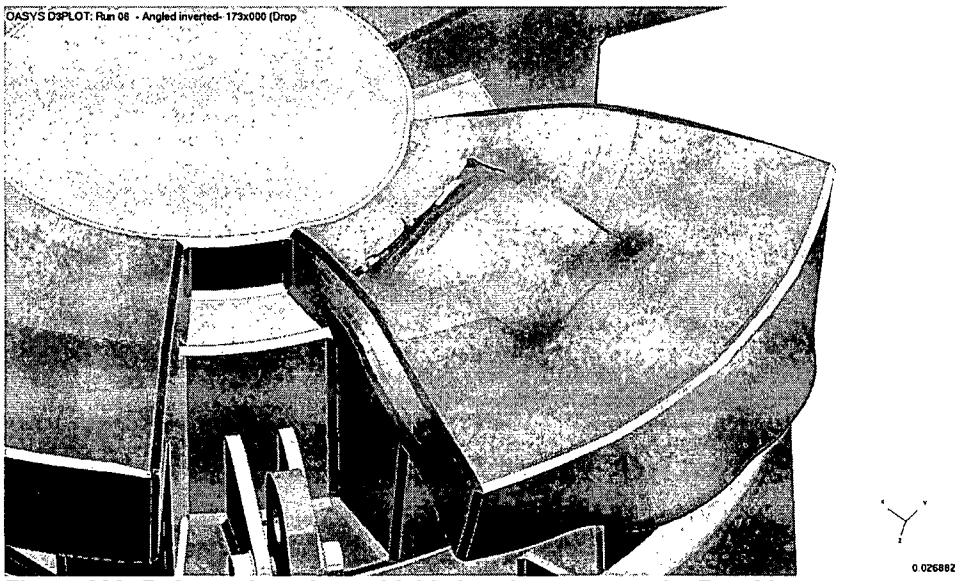

Figure 223: Deformation of top shield absorbers removed – Run 06

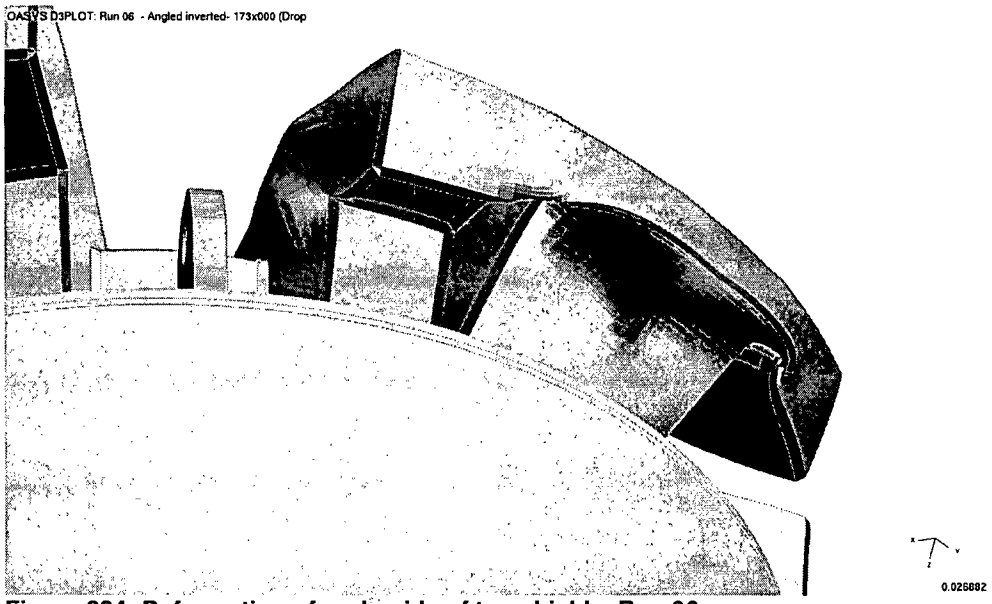

Figure 224: Deformation of underside of top shield – Run 06

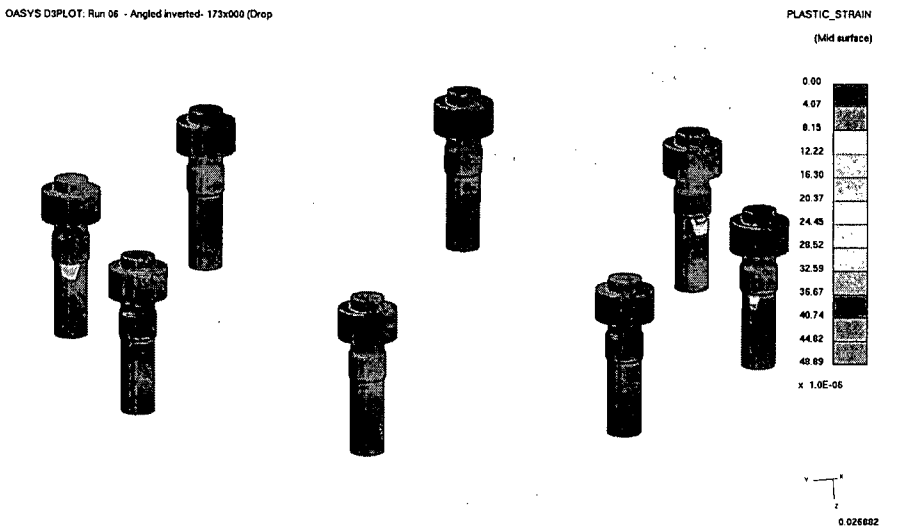

Figure 225: Effective plastic strain in closure studs – Run 06

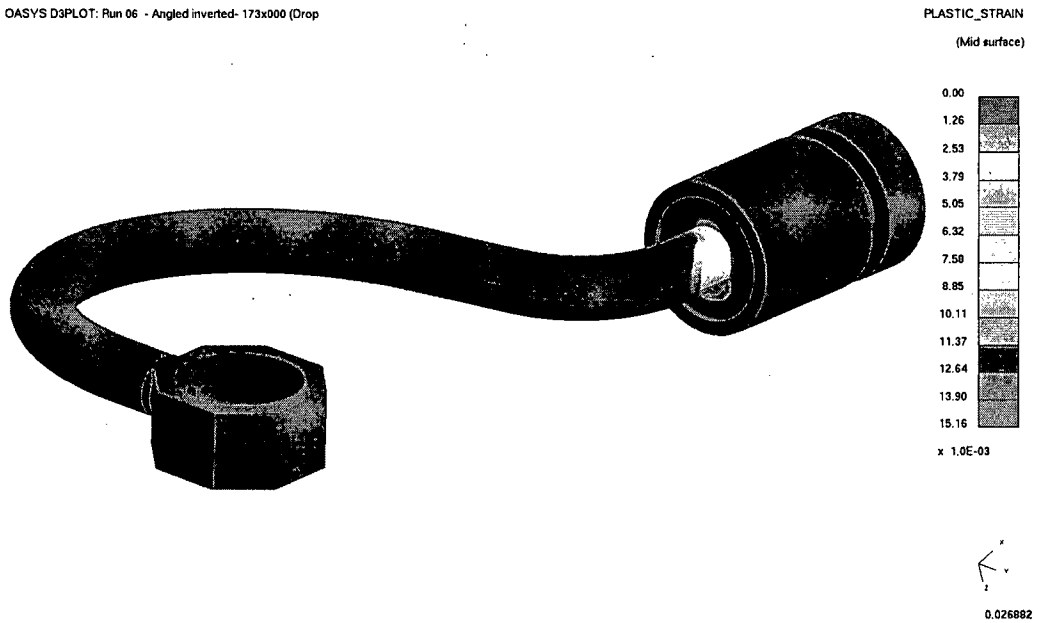

Figure 226: Effective plastic strain in outer tube – Run 06

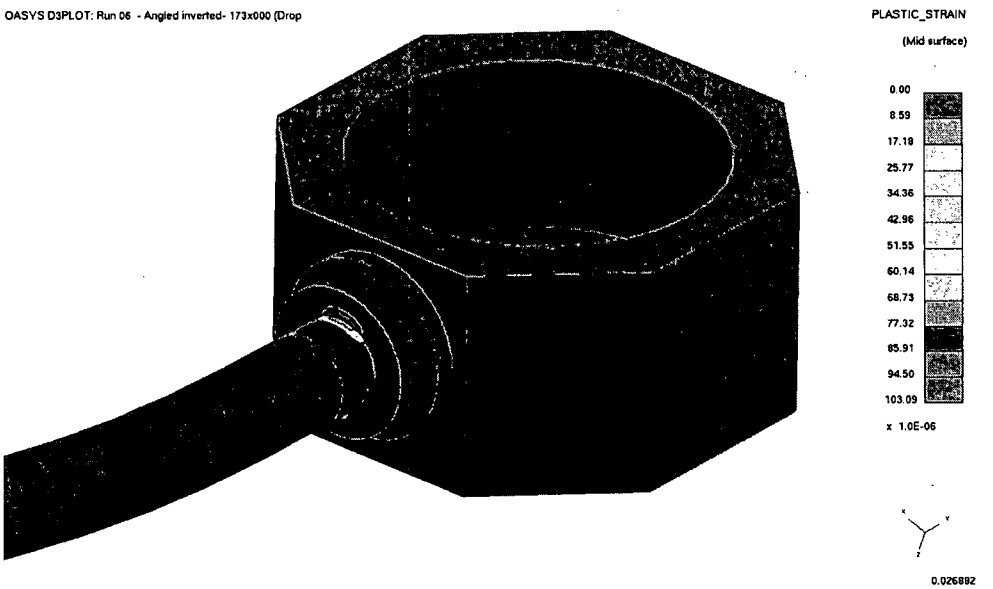

Figure 227: Effective plastic strain in drain tube – Run 06

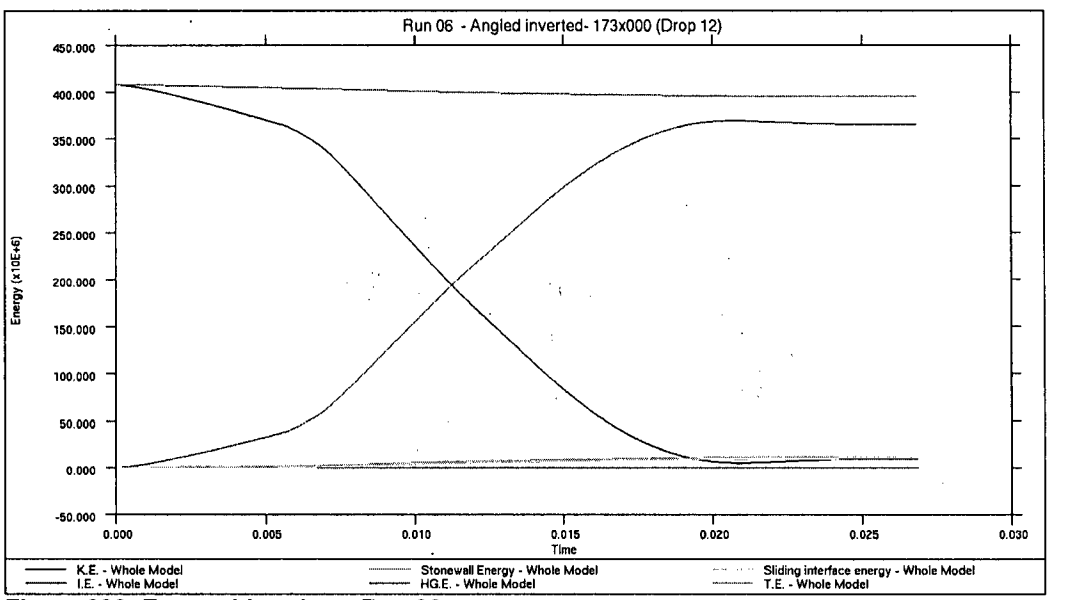

Figure 228: Energy histories – Run 06

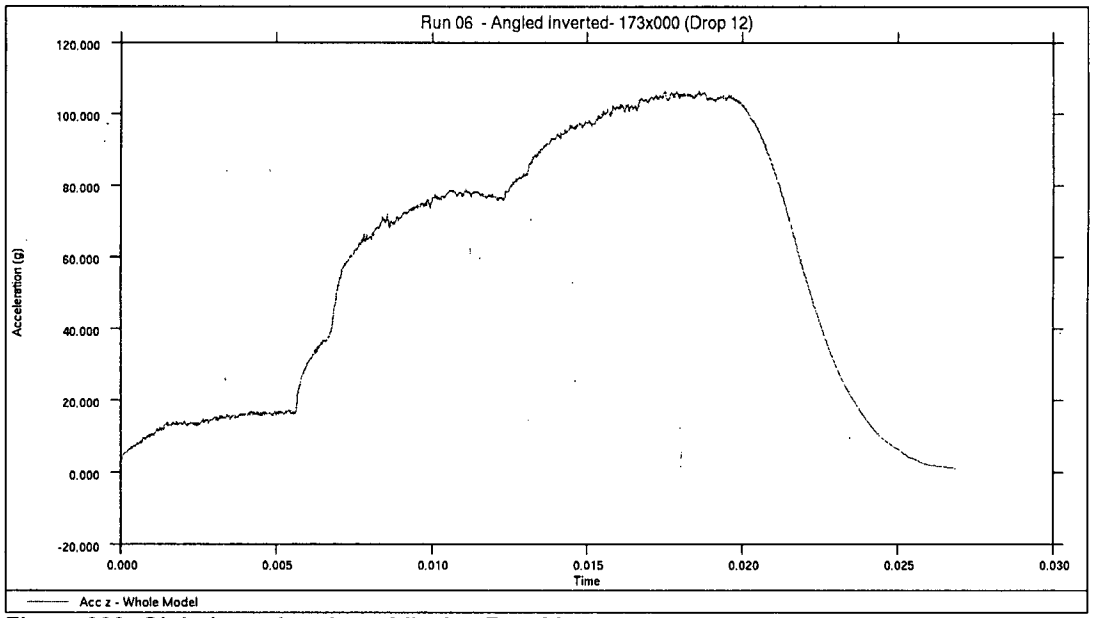

Figure 229: Global acceleration of flask – Run 06

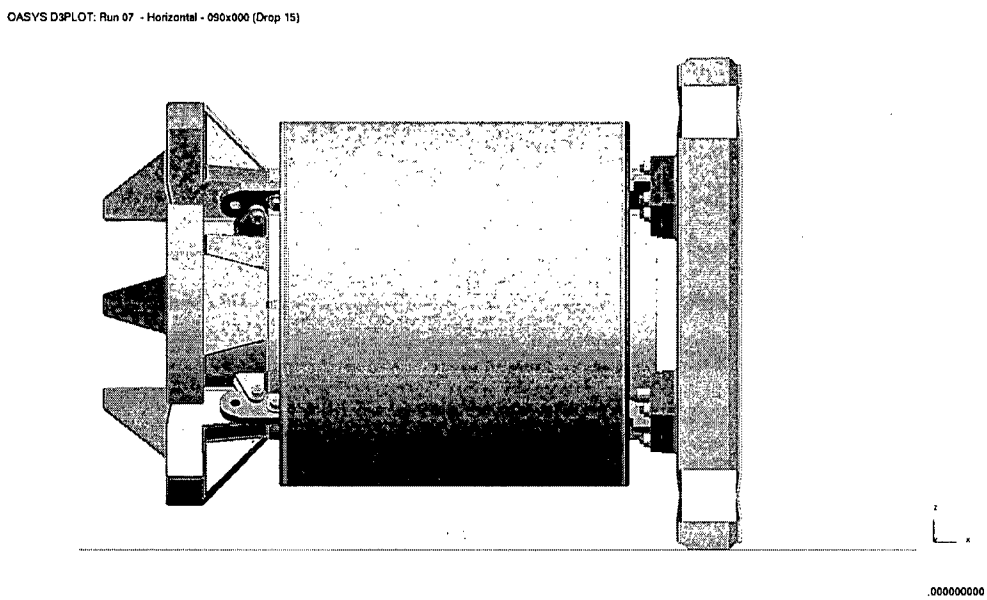

Figure 230: Initial impact orientation – Run 07

OASYS D3PLOT: Run 07 - Horizontal - 090x000 (Drop 15)

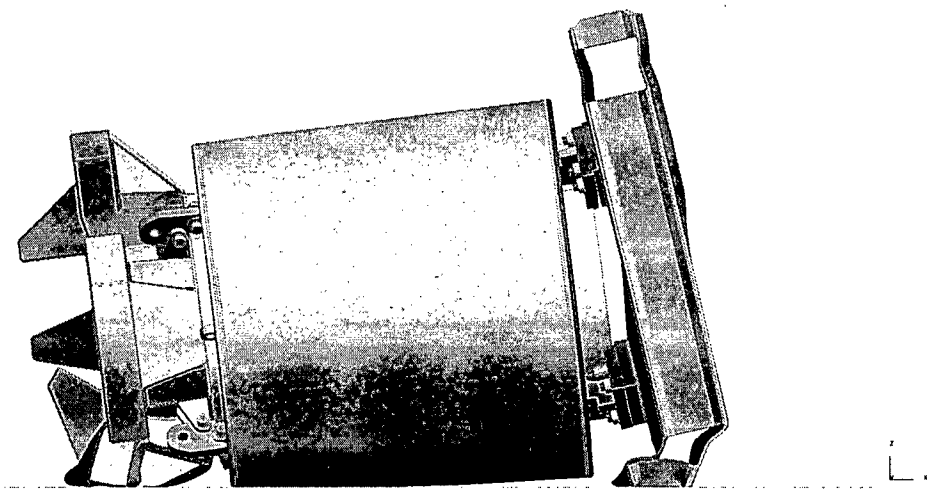

0.024275

Figure 231: Final deformation – Run 07

OASYS D3PLOT: Run 07 - Horizontal - 090x000 (Drop 15)

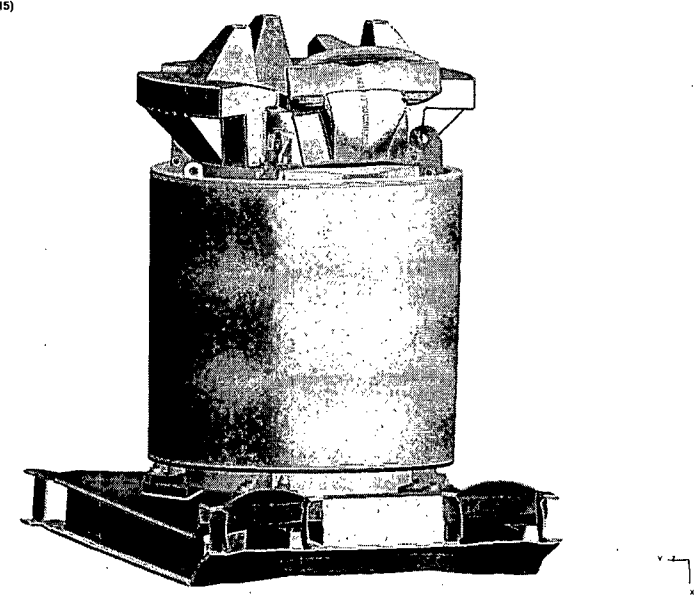

0.024275

Figure 232: Deformation of flask – Run 07

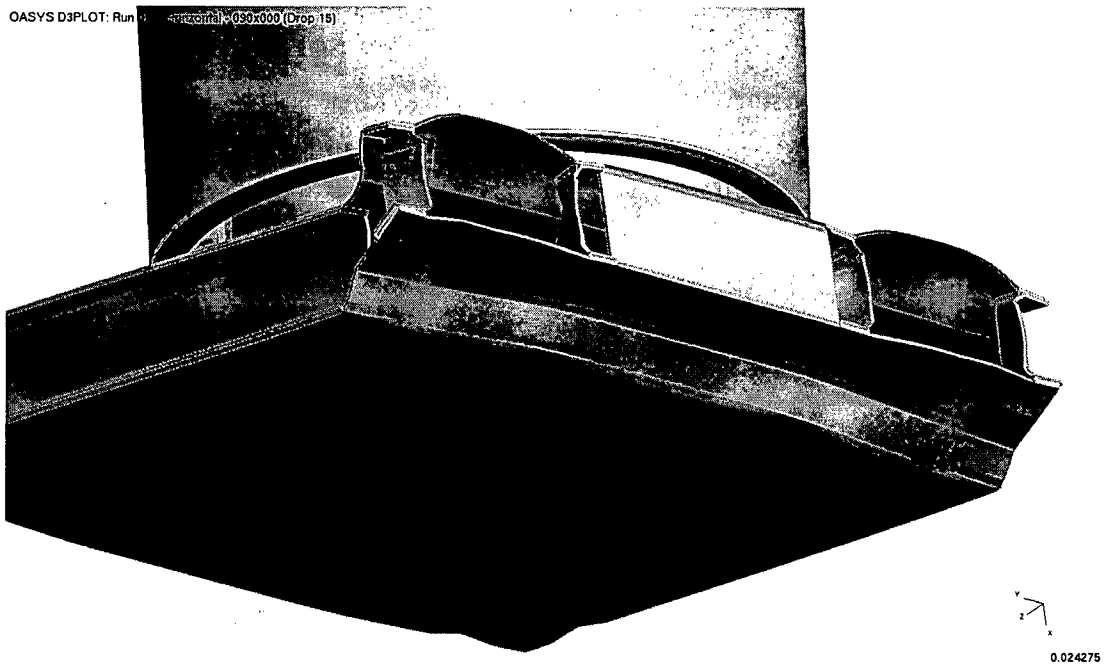

Figure 233: Deformation of pallet – Run 07

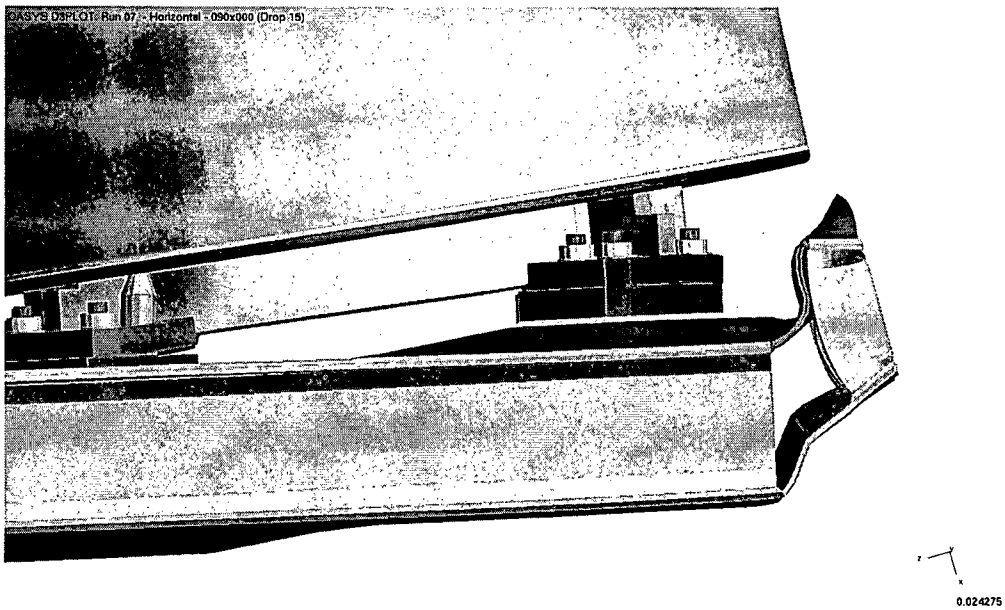

Figure 234: Deformation of pallet side view – Run 07

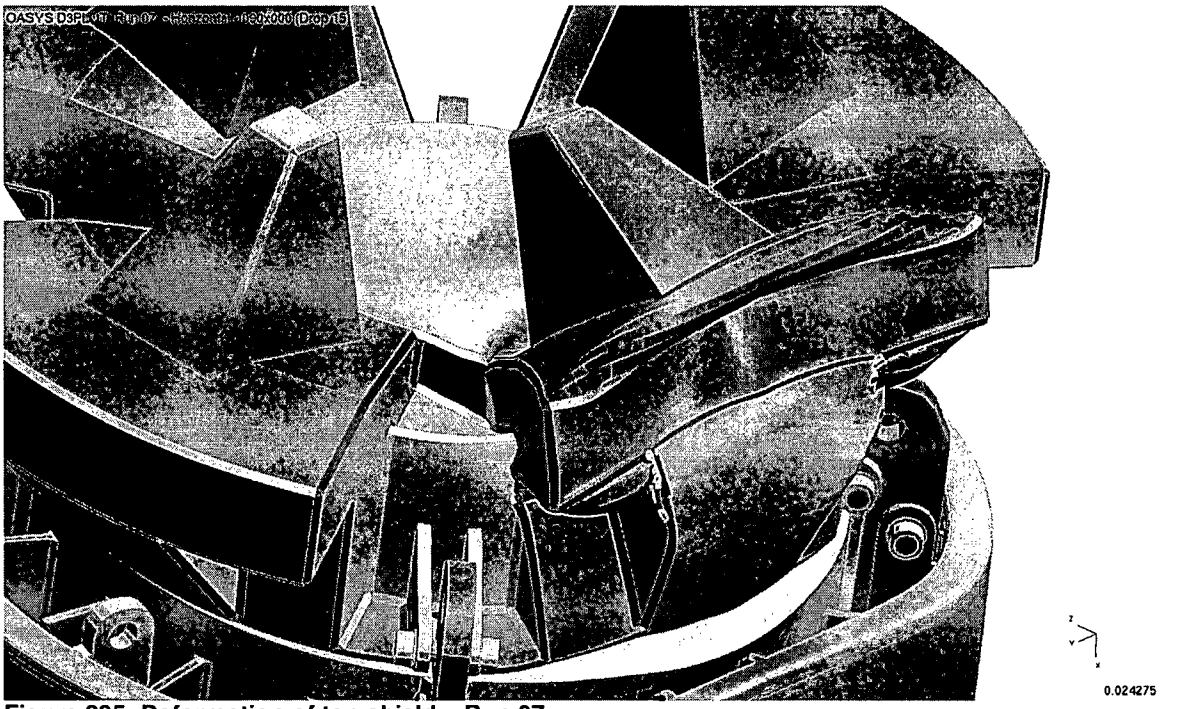

Figure 235: Deformation of top shield – Run 07

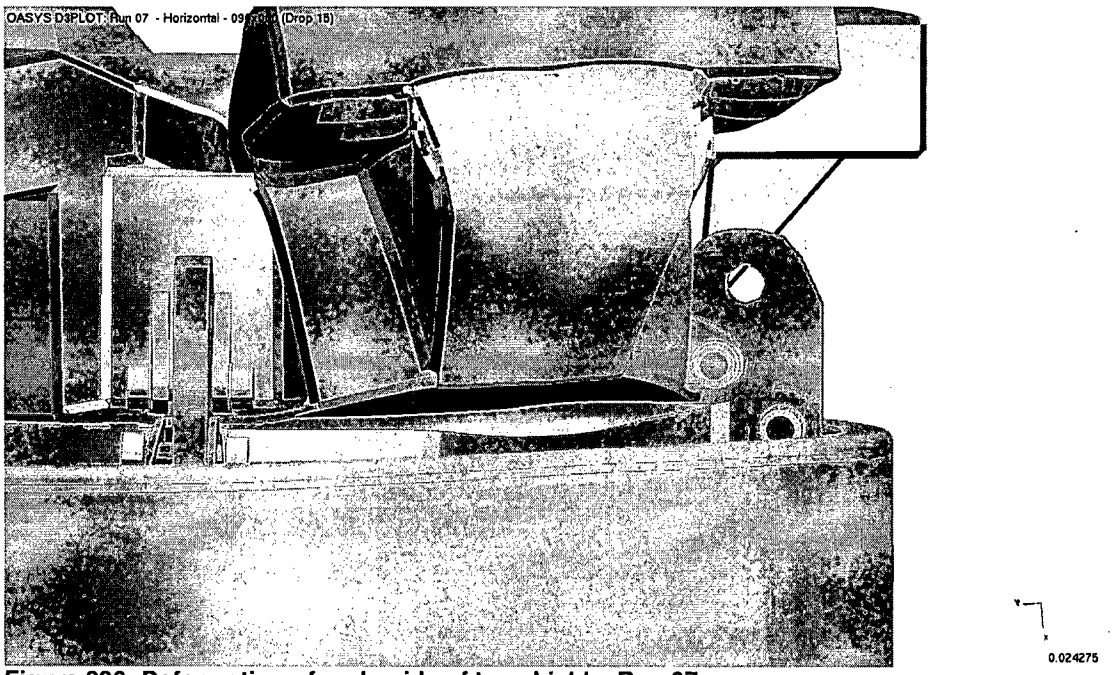

Figure 236: Deformation of underside of top shield – Run 07

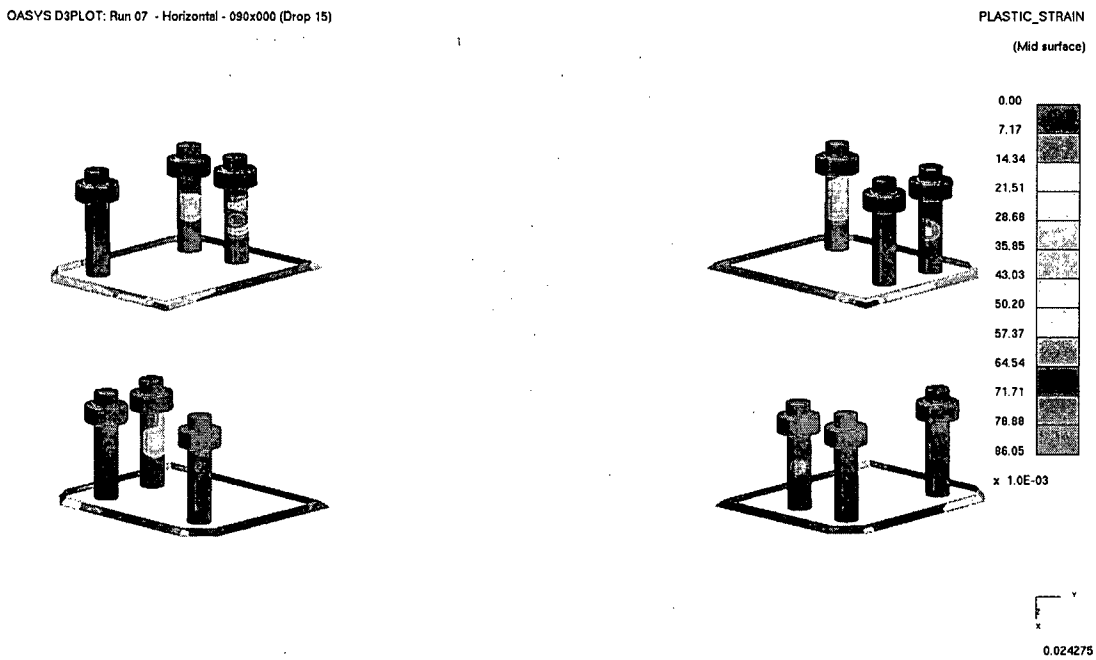

Figure 237: Effective plastic strain in pallet connections – Run 07

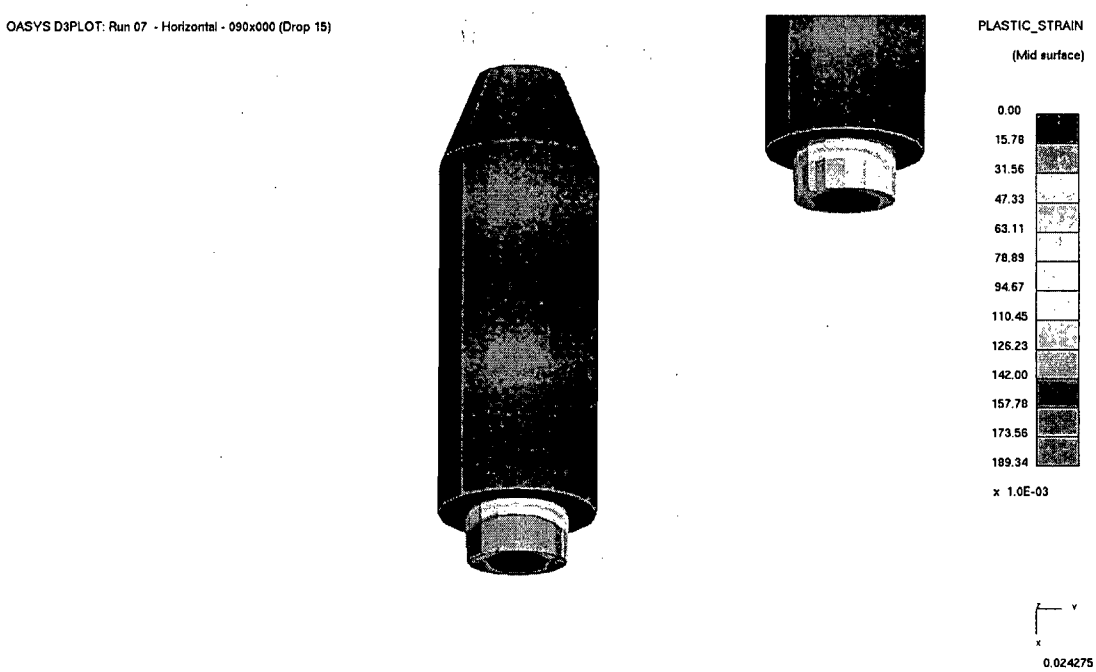

Figure 238: Effective plastic strain in dowels – Run 07

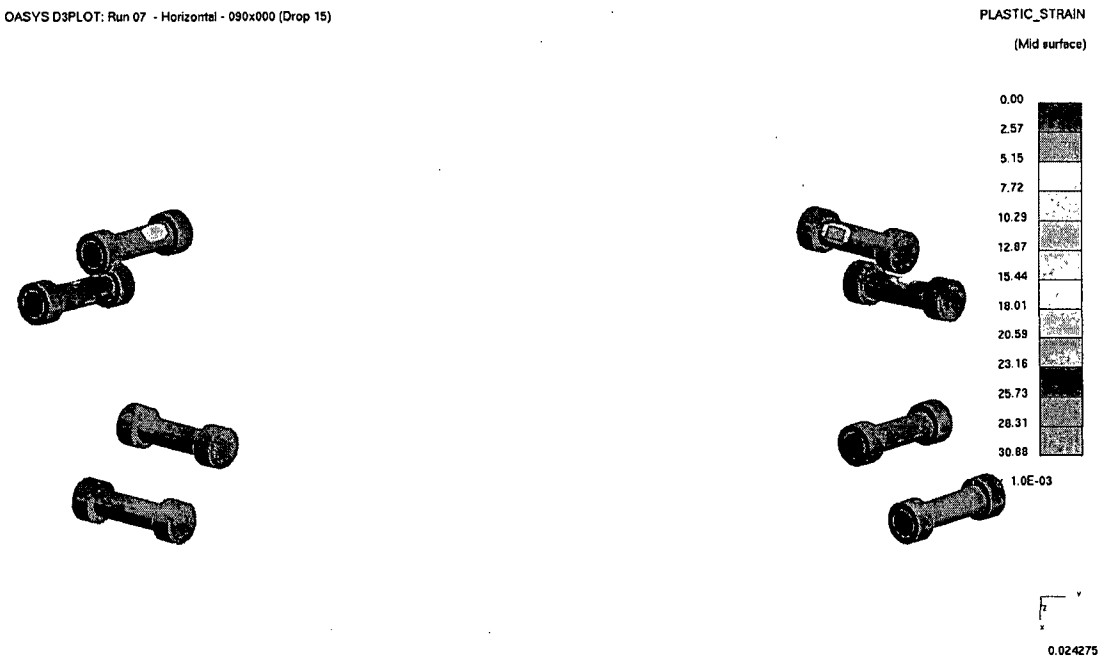

Figure 239: Effective plastic strain in shoulder bolts – Run 07

Figure 240: Effective plastic strain in flask wall – Run 07

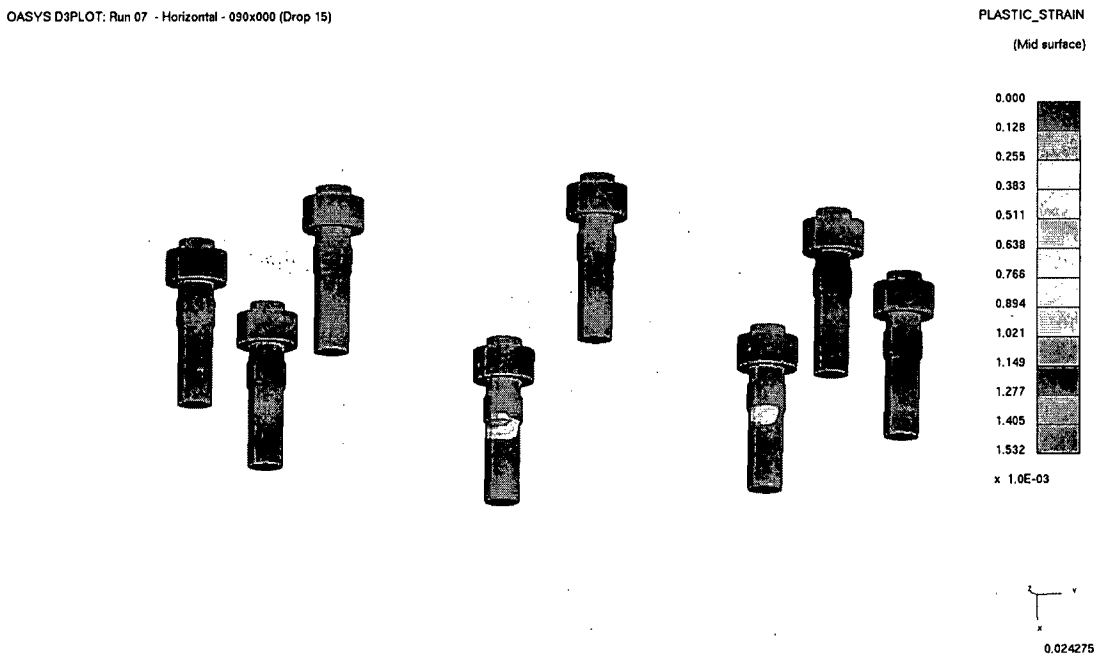

Figure 241: Effective plastic strain in closure studs – Run 07

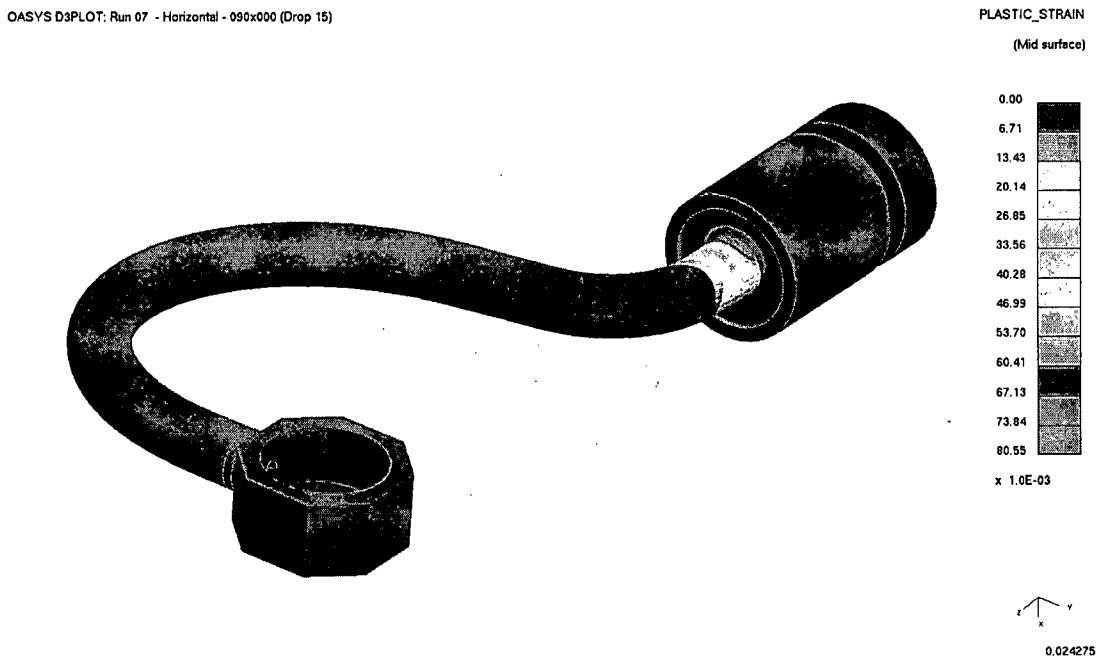

Figure 242: Effective plastic strain in outer tube – Run 07

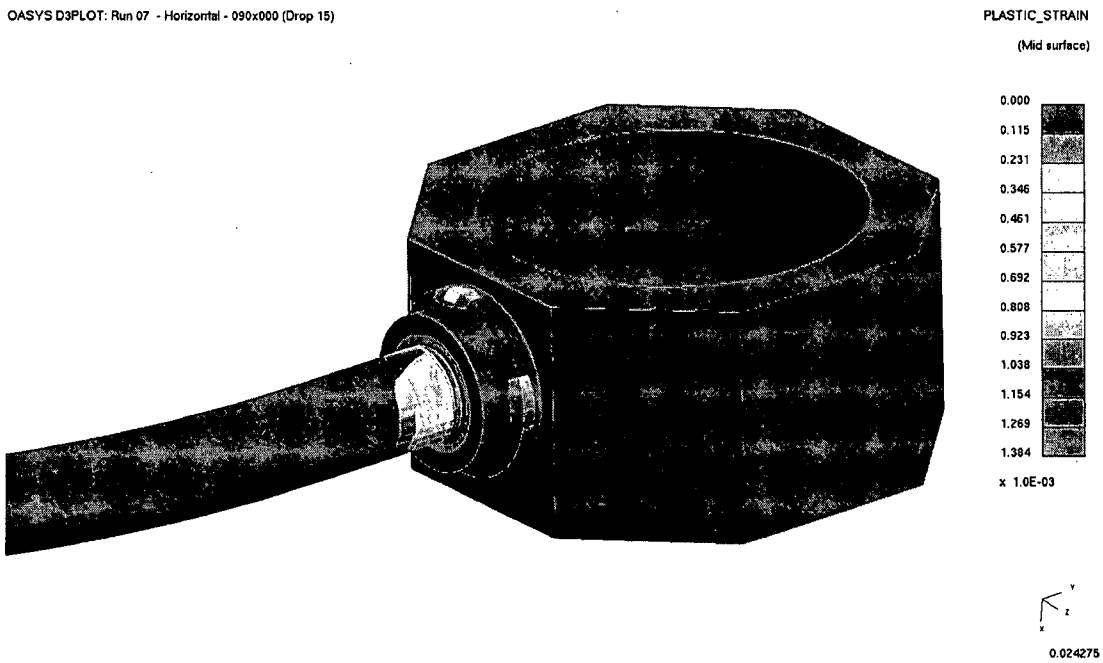

Figure 243: Effective plastic strain in drain tube – Run 07

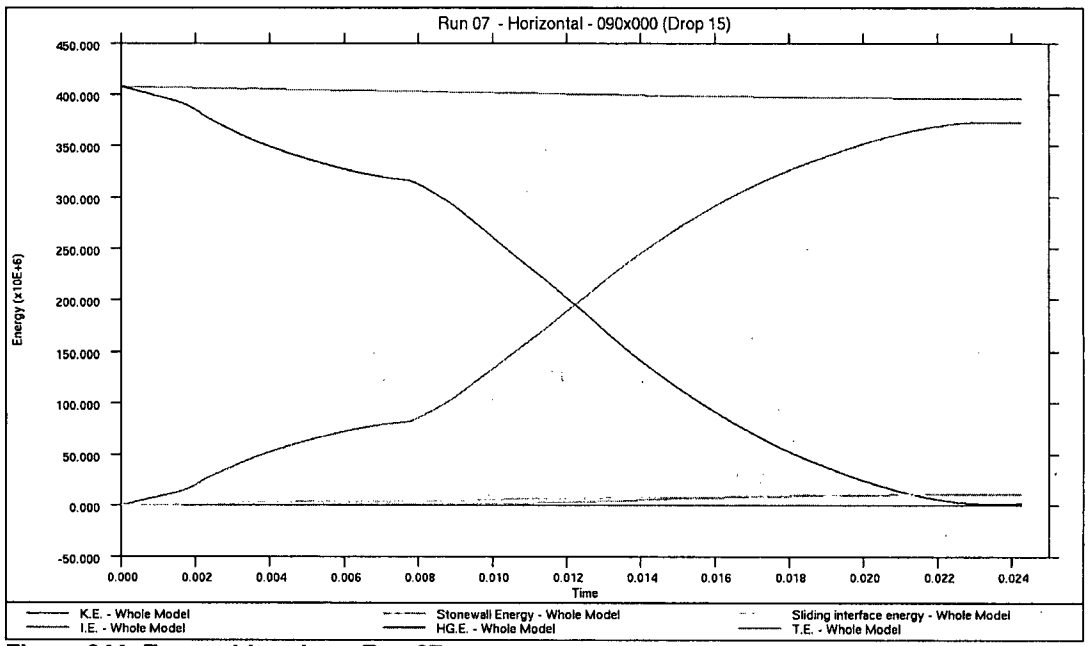

Figure 244: Energy histories – Run 07

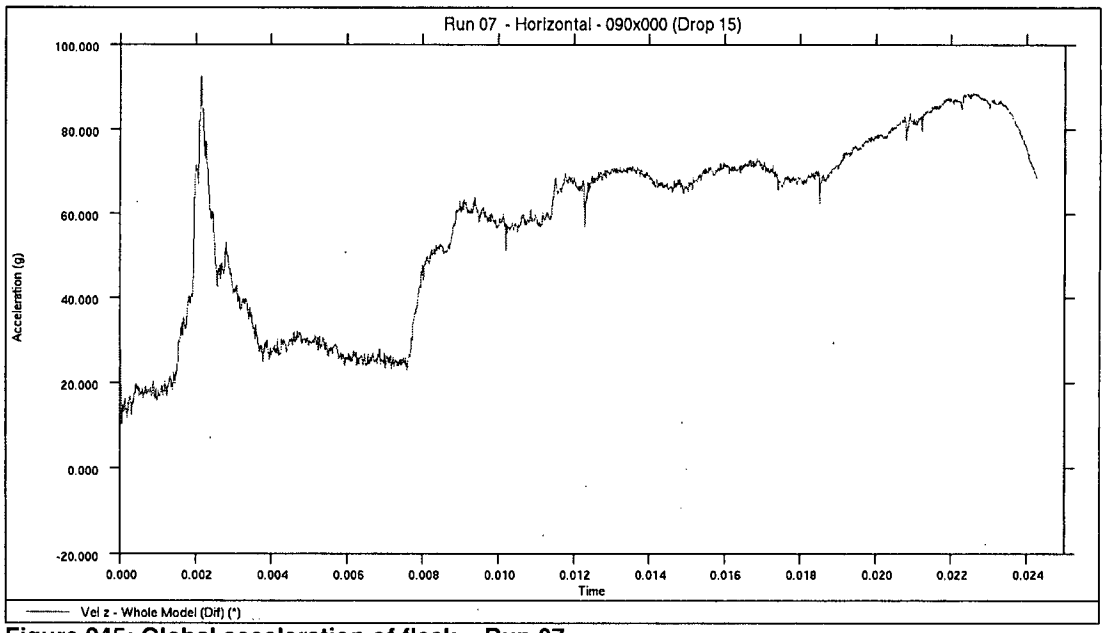

Figure 245: Global acceleration of flask – Run 07

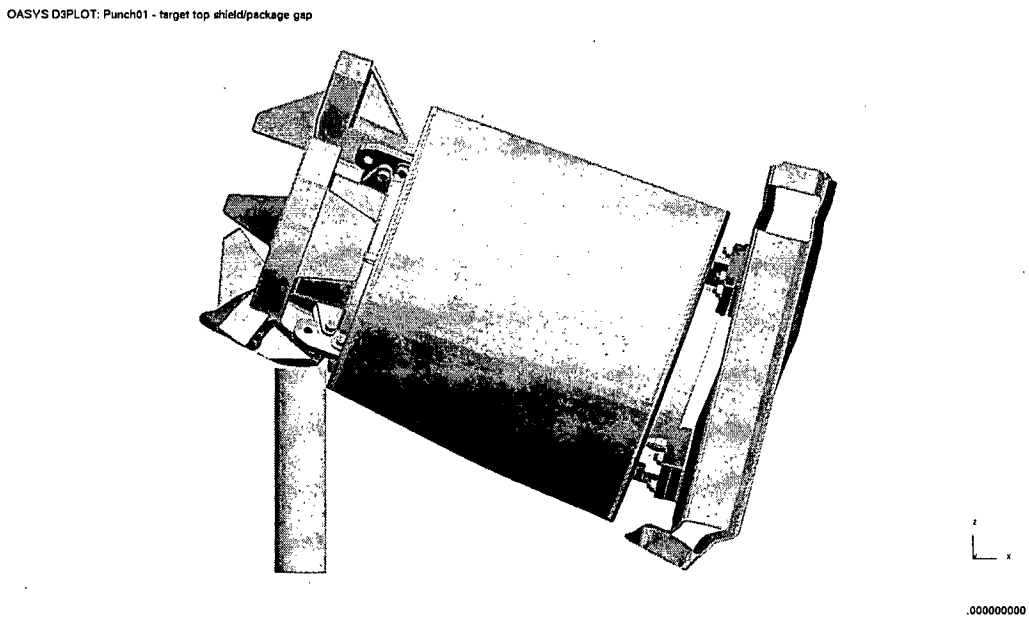

Figure 246: Initial impact orientation – Punch 01

OASYS D3PLOT: Punch01 - target top shield/package gap

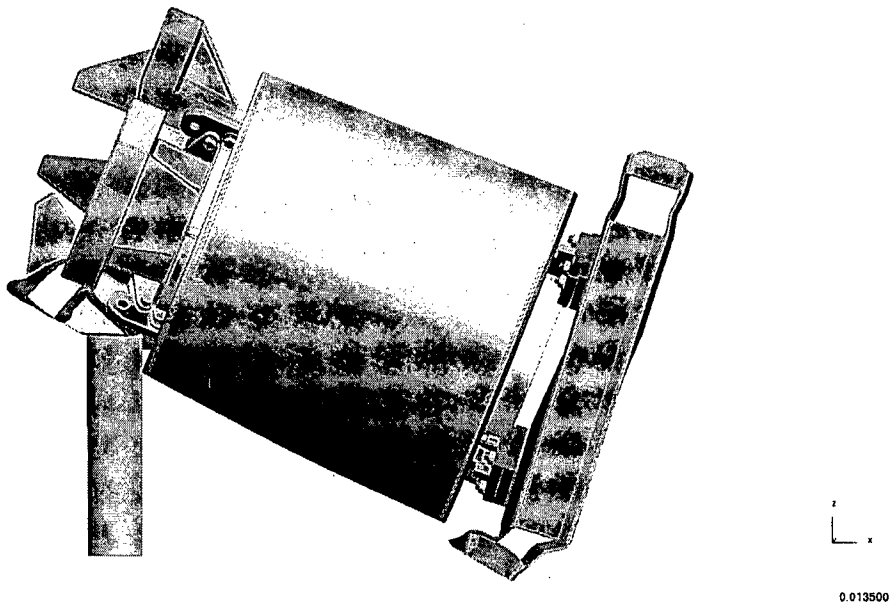

Figure 247: Final deformation – Punch 01

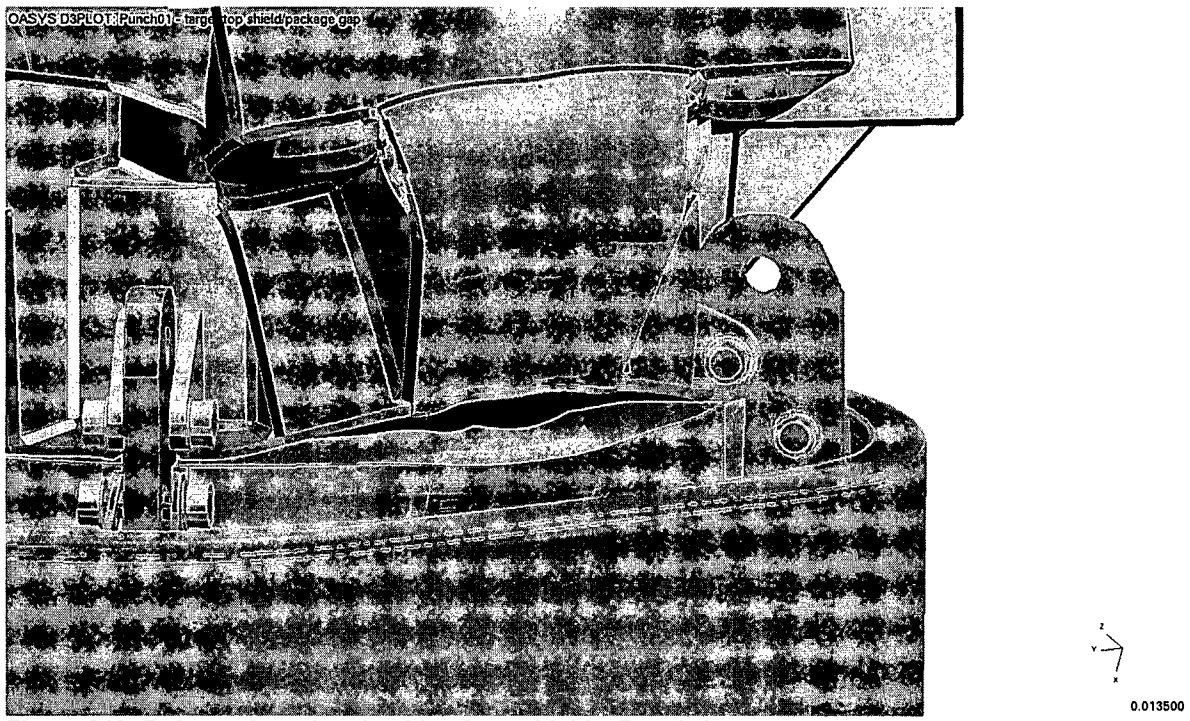

Figure 248: Deformation of underside of top shield – Punch 01

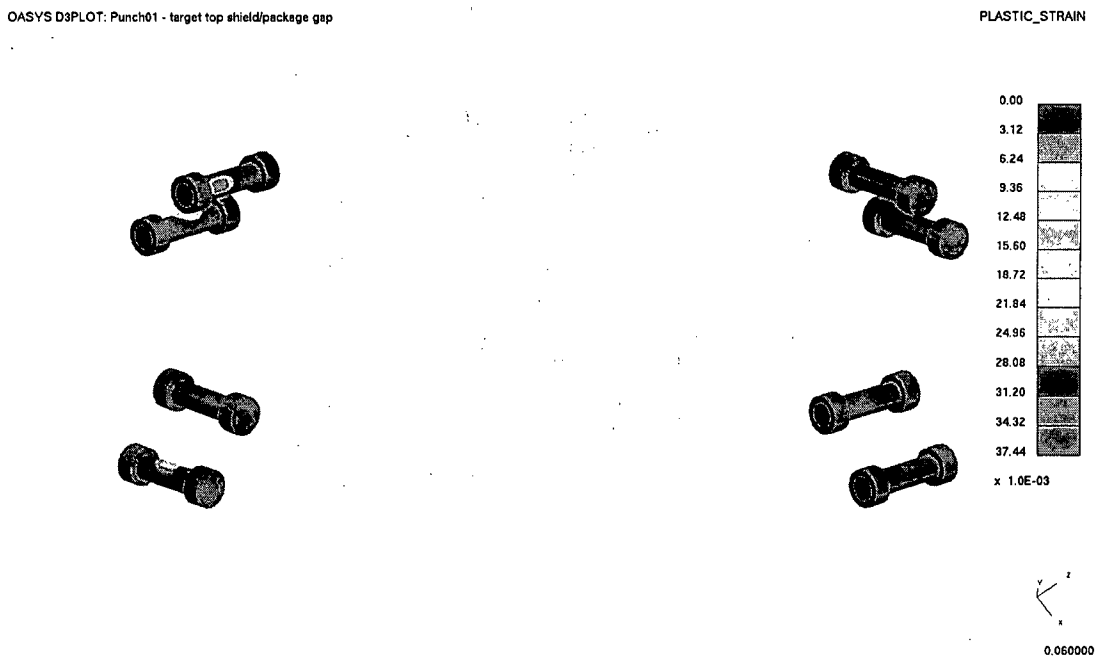

Figure 249: Effective plastic strain in shoulder bolts – Punch 01

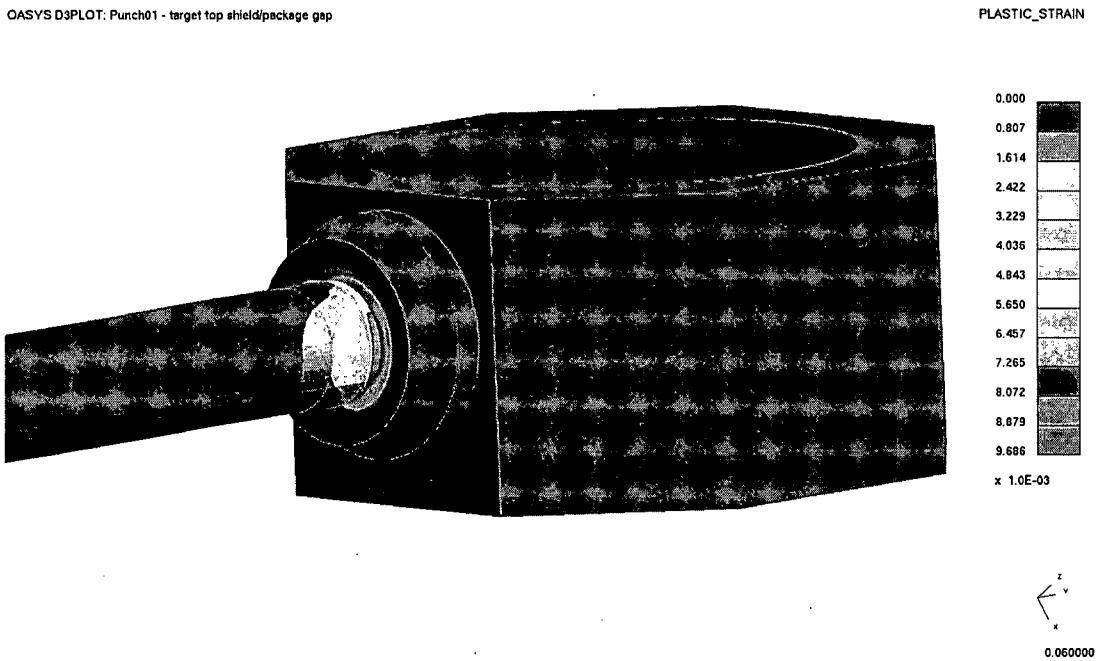

Figure 250: Effective plastic strain in drain tube – Punch 01

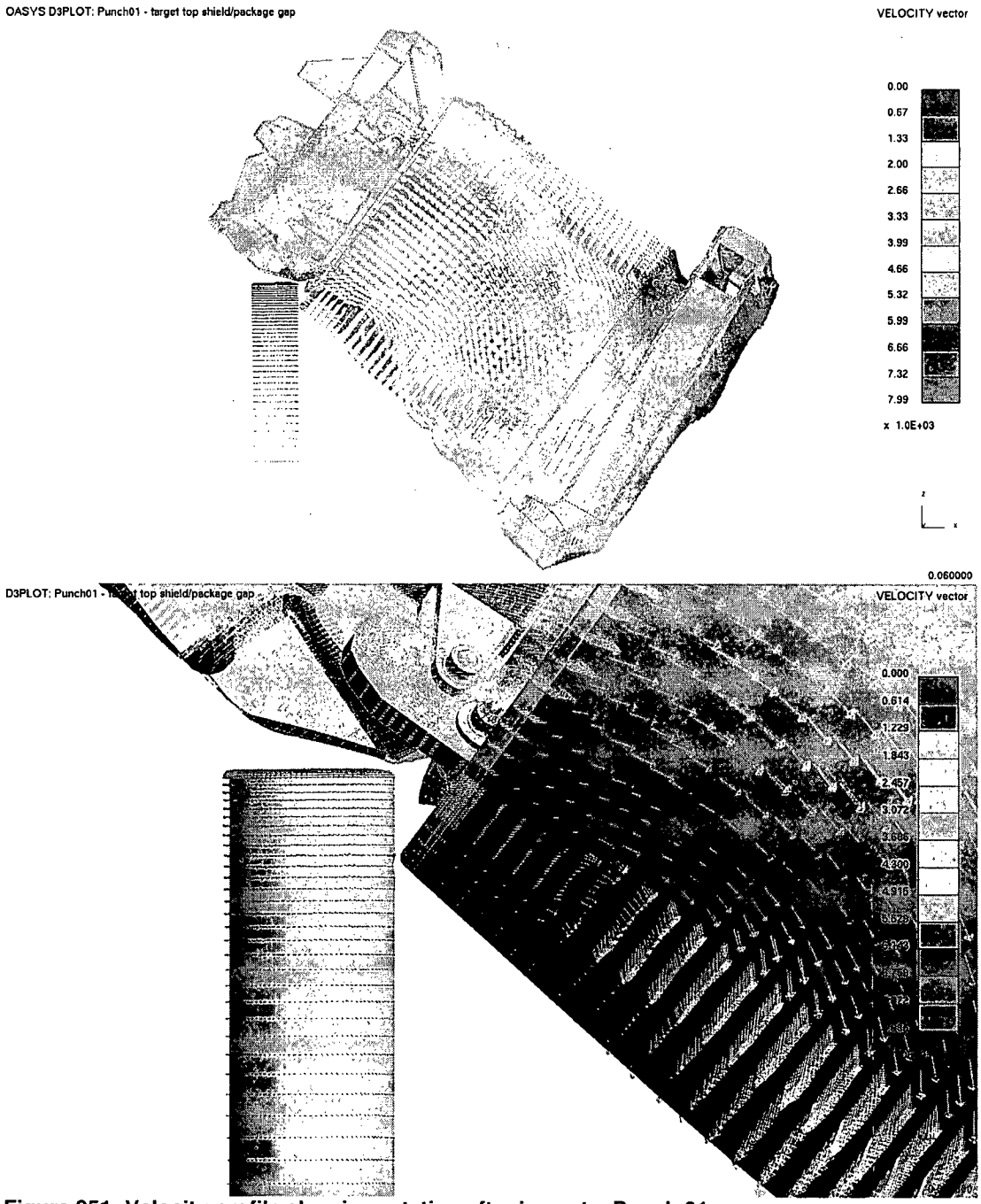

Figure 251: Velocity profile showing rotation after impact – Punch 01

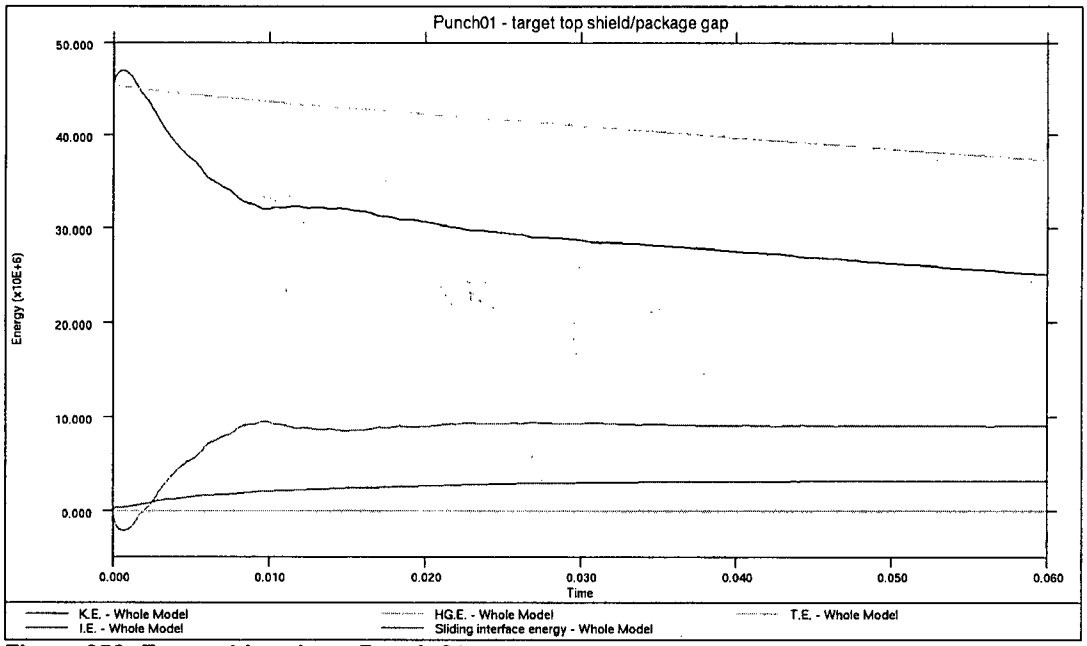

Figure 252: Energy histories – Punch 01

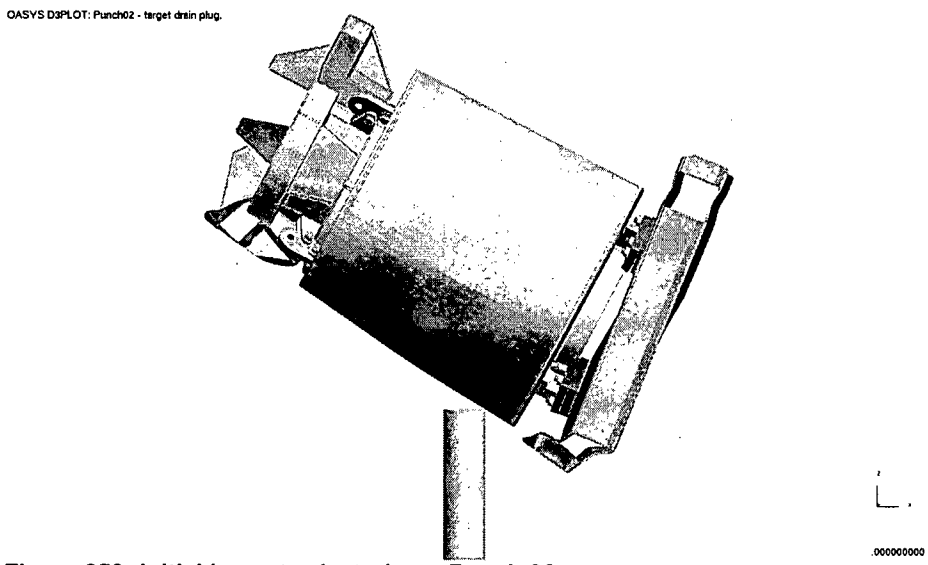

Figure 253: Initial impact orientation – Punch 02

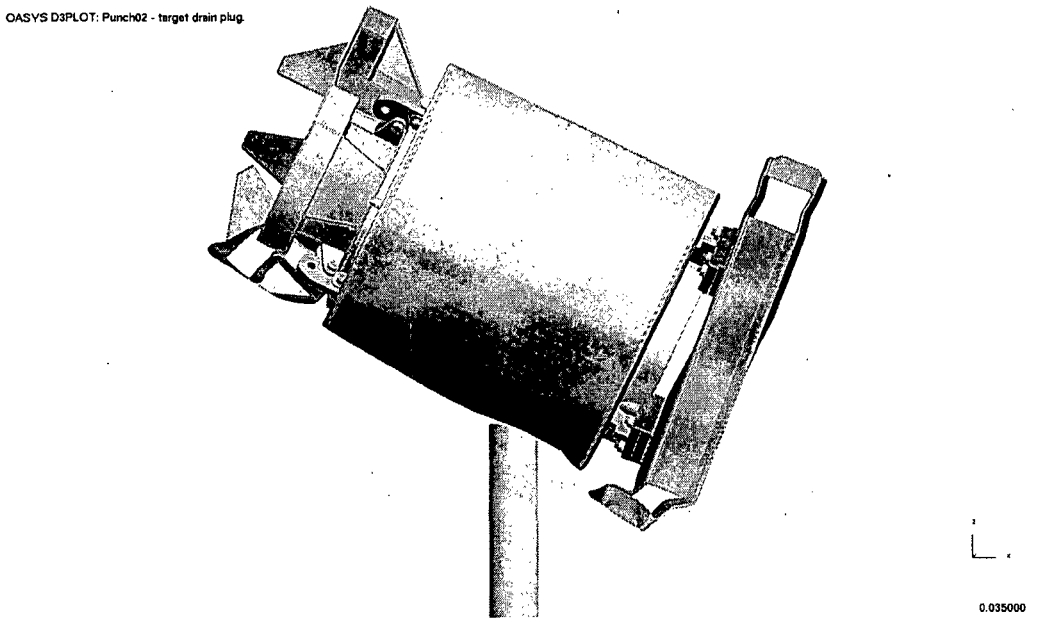

Figure 254: Final deformation – Punch 02

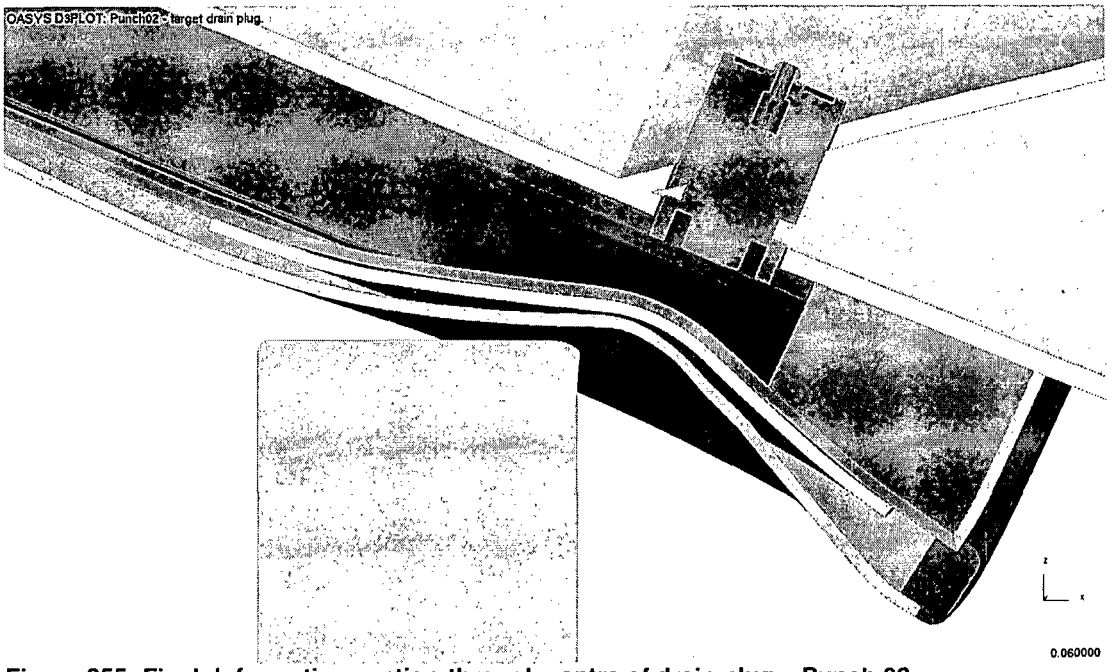

Figure 255: Final deformation section-through centre of drain plug – Punch 02

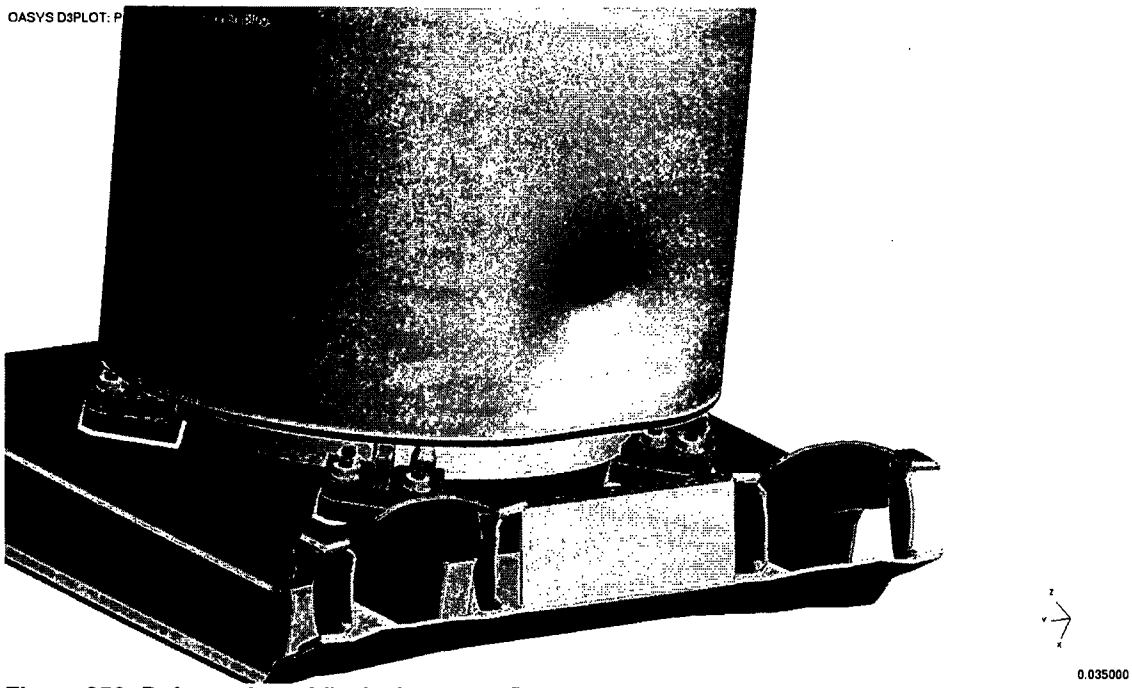

Figure 256: Deformation of flask close-up – Punch 02

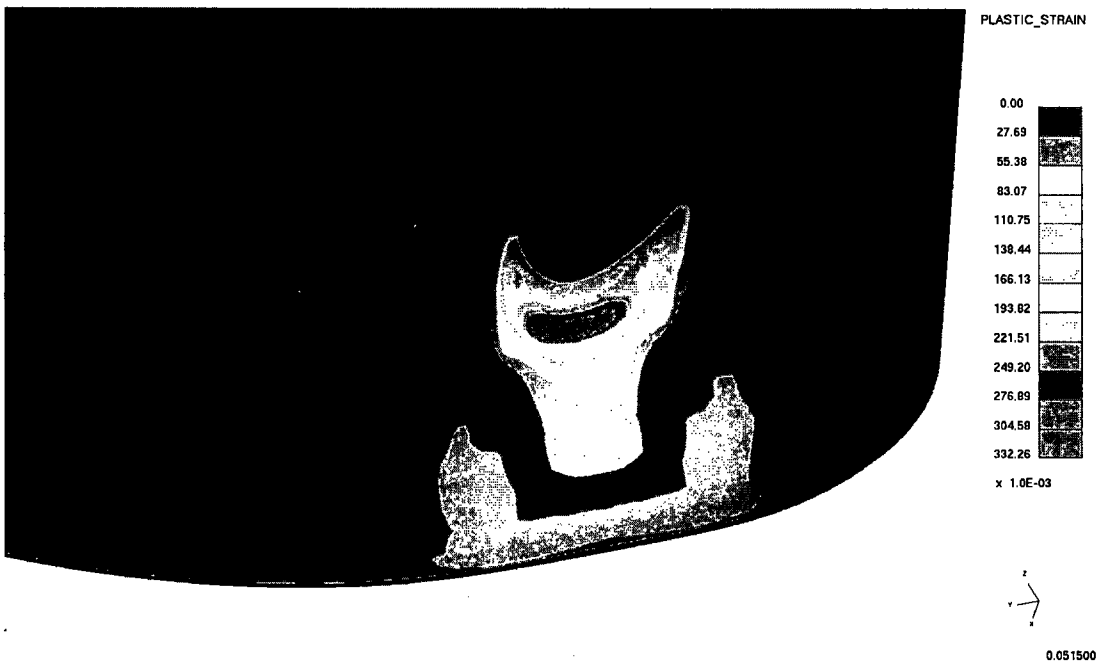

Figure 257: Effective plastic strain in jacket outer wall – Punch 02

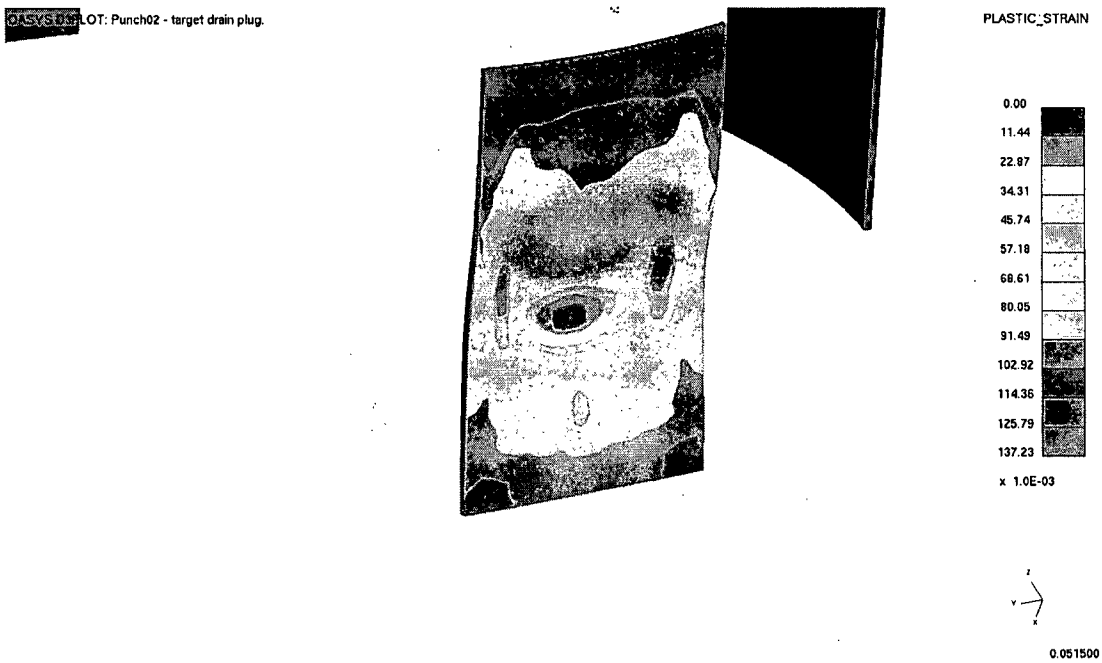

Figure 258: Effective plastic strain in jacket additional plate – Punch 02

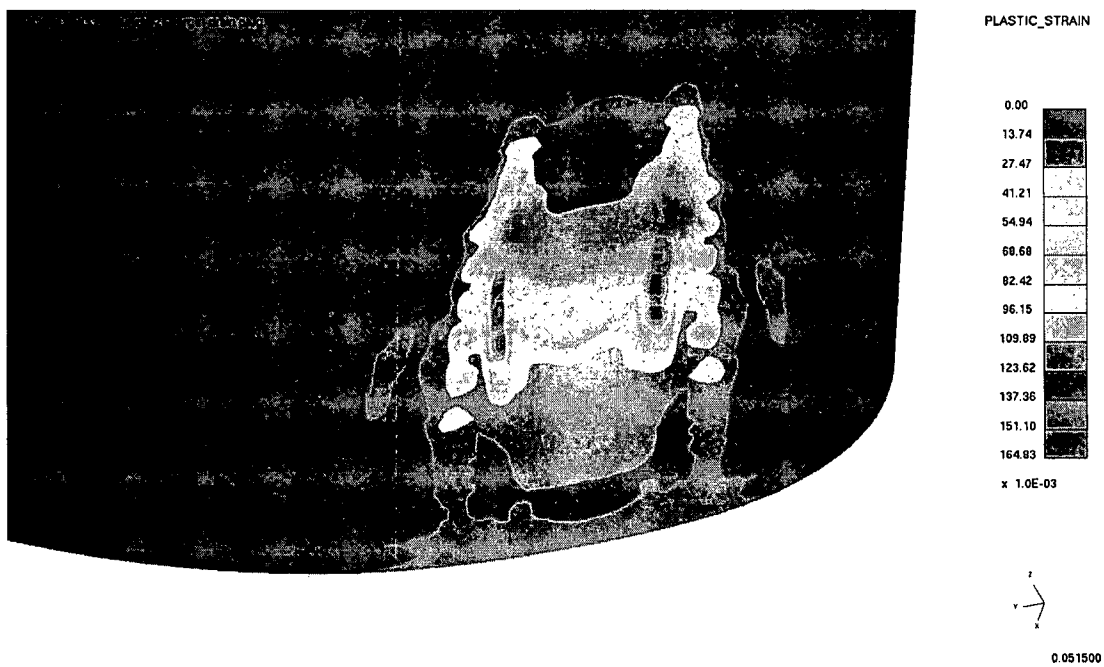

Figure 259: Effective plastic strain in jacket inner wall – Punch 02

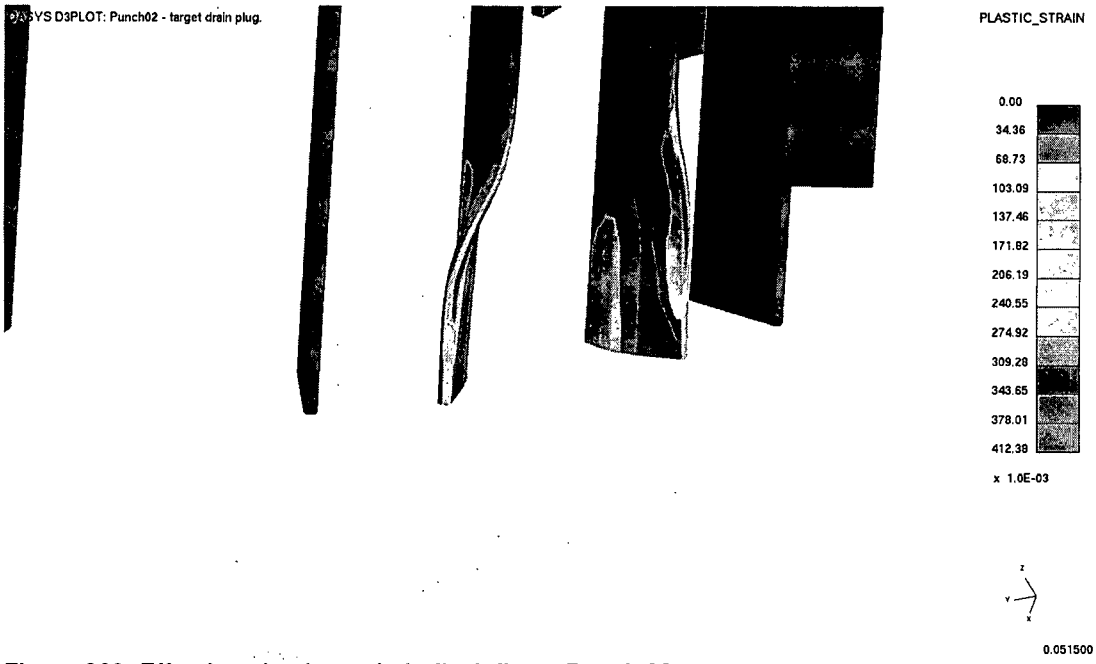

Figure 260: Effective plastic strain in flask fins – Punch 02

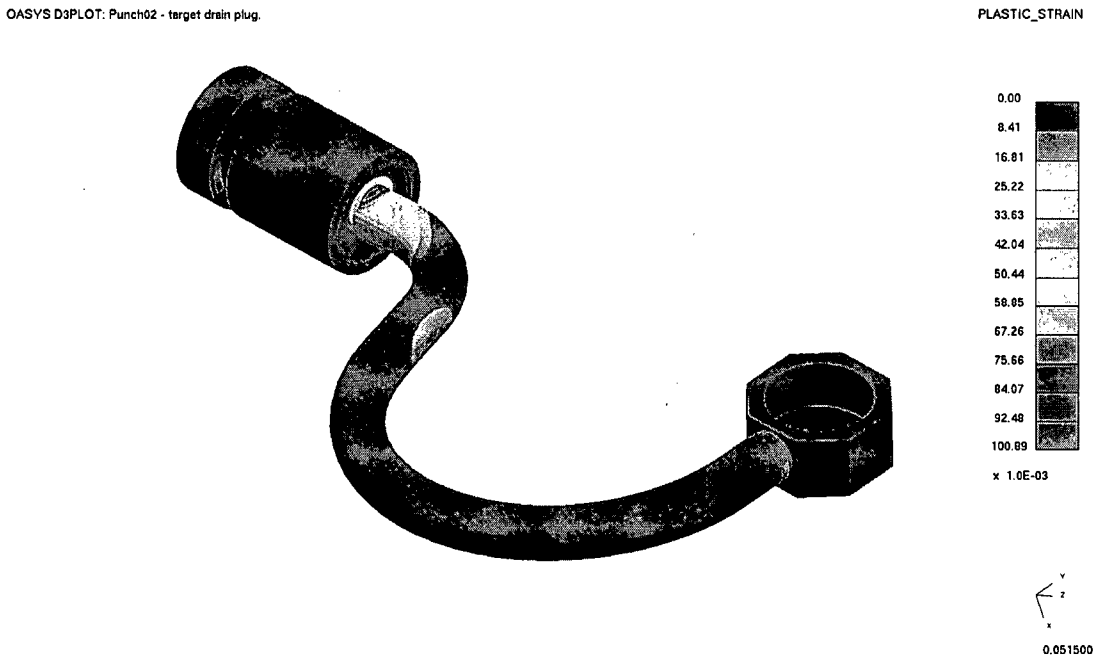

Figure 261: Effective plastic strain in outer tube – Punch 02

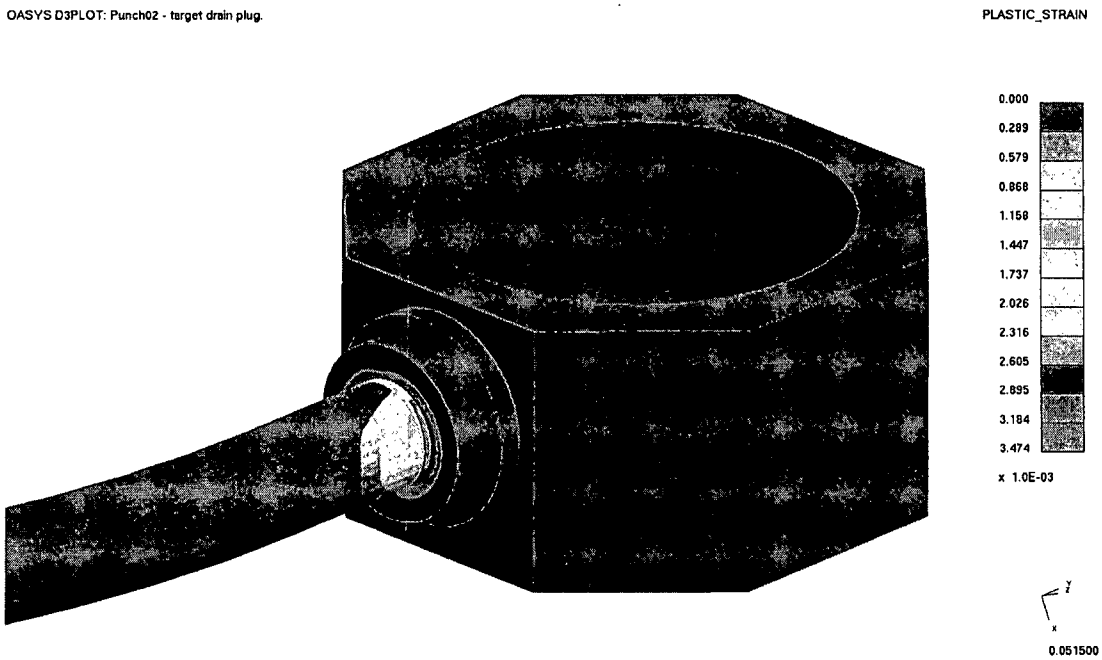

Figure 262: Effective plastic strain in drain tube – Punch 02

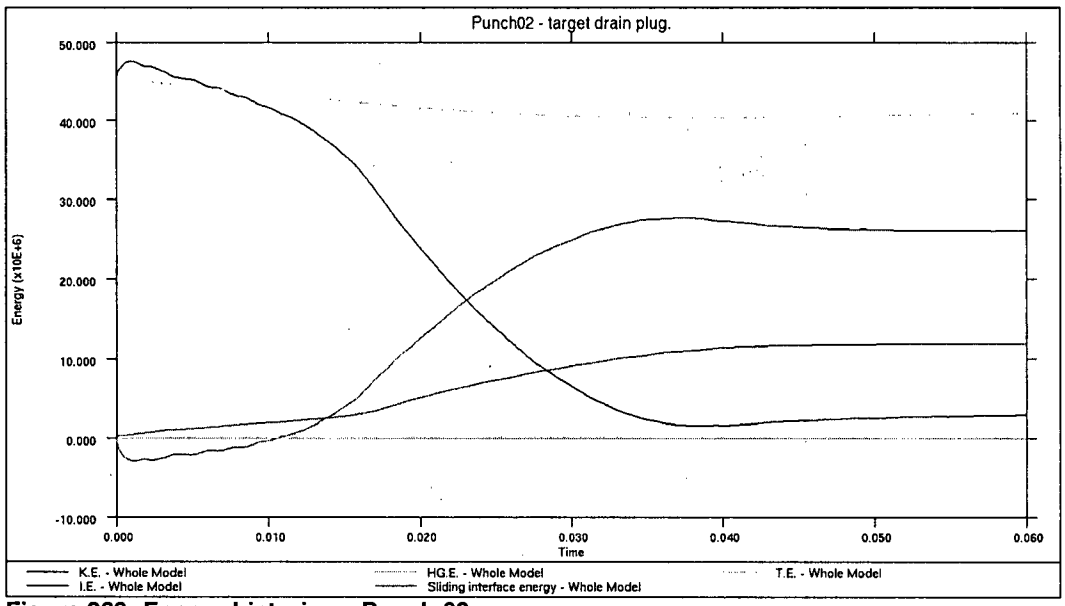

Figure 263: Energy histories – Punch 02

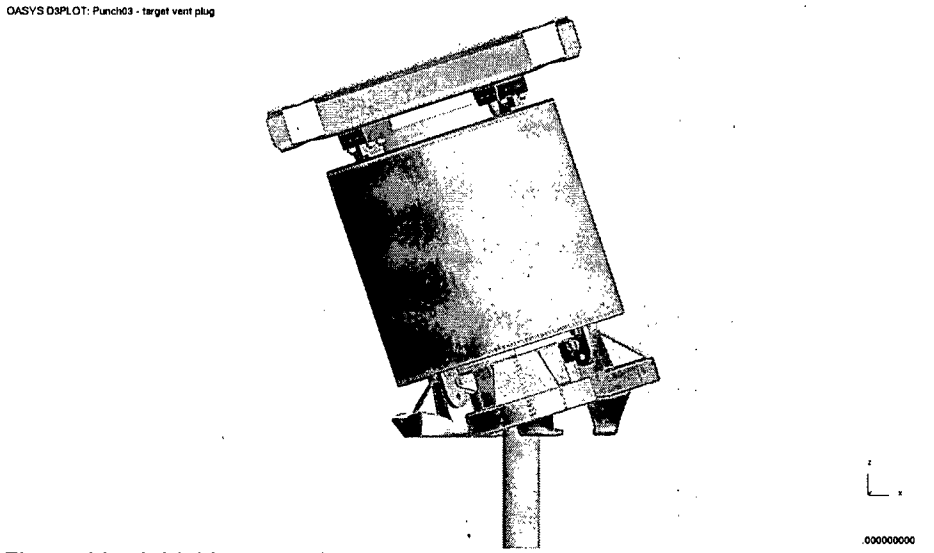

Figure 264: Initial impact orientation – Punch 03

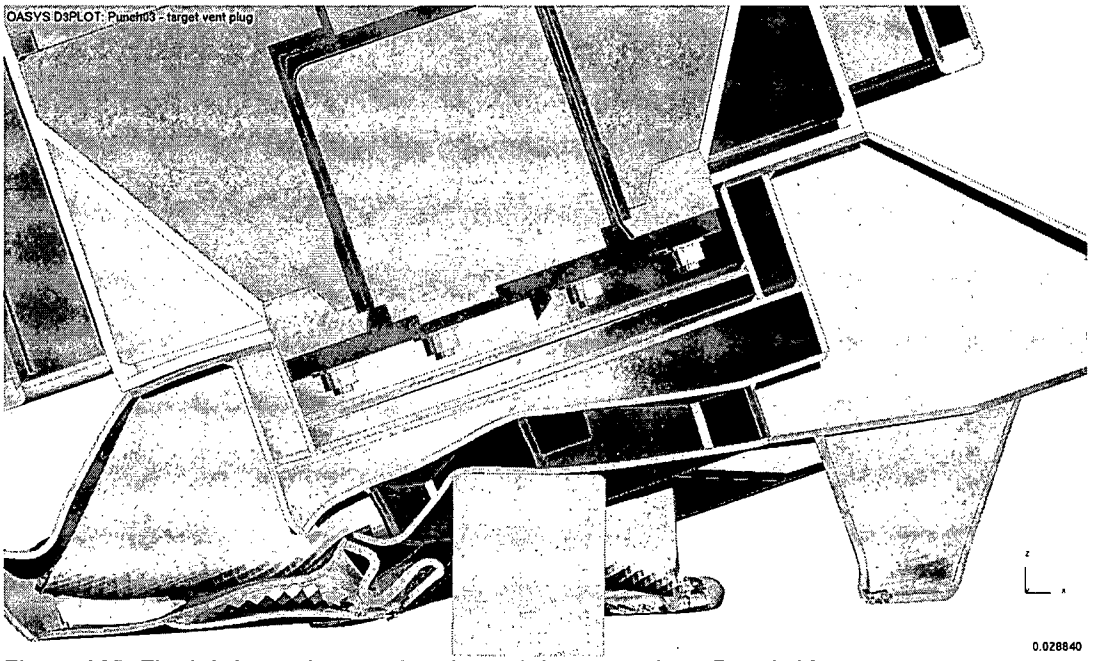

Figure 265: Final deformation section through impact point – Punch 03

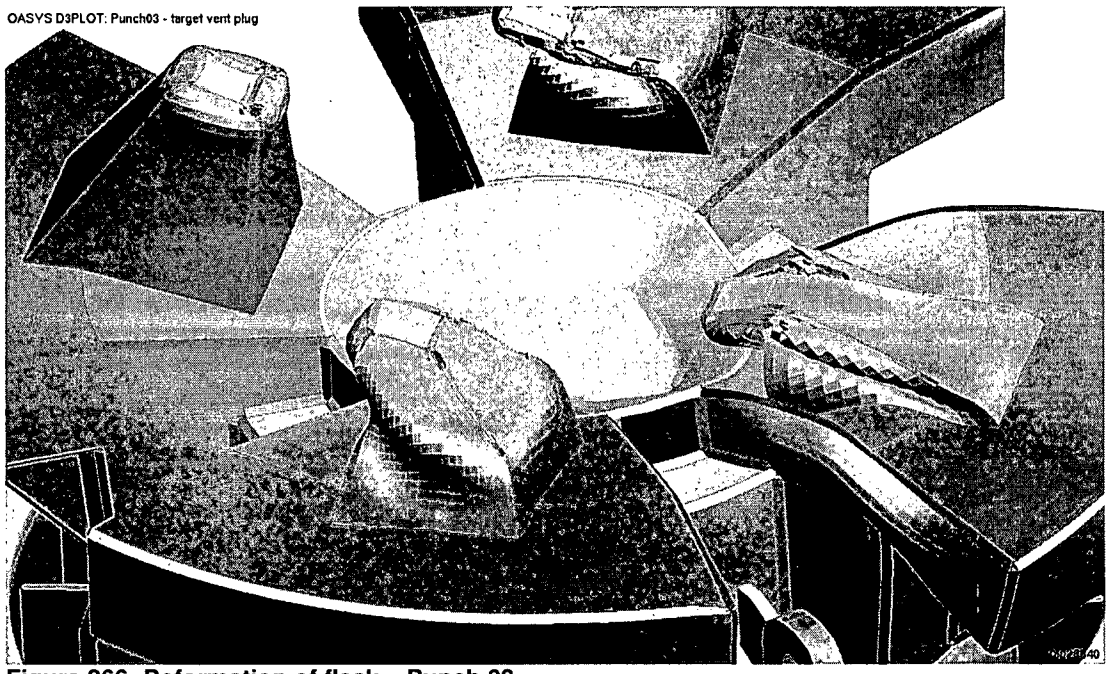

Figure 266: Deformation of flask – Punch 03

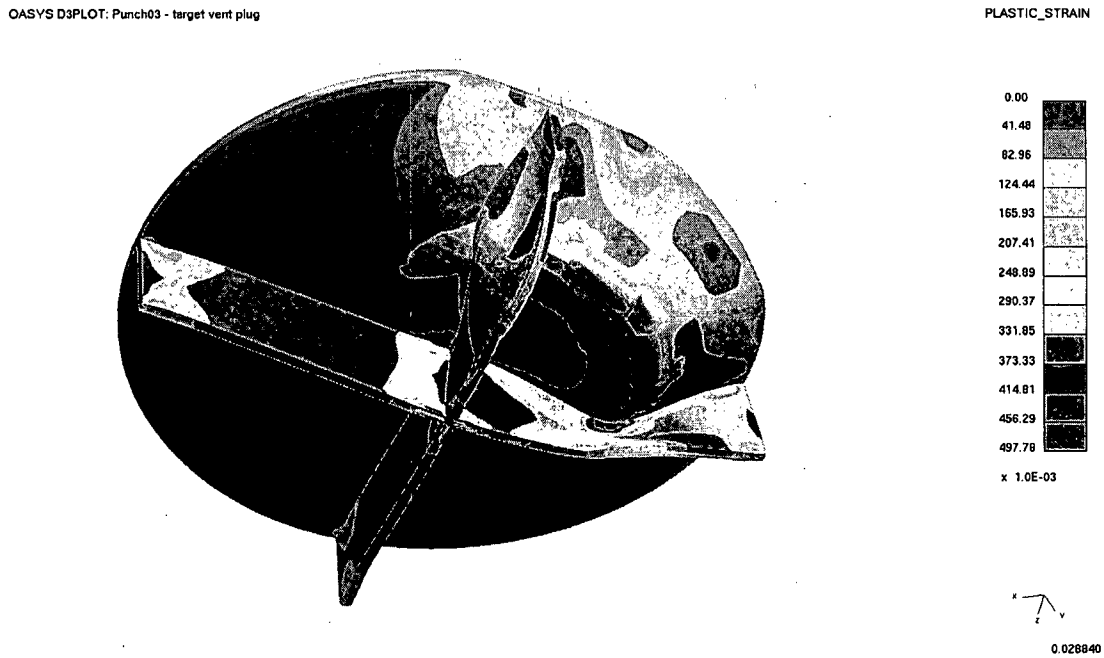

Figure 267: Effective plastic strain in top shield under punch– Punch 03

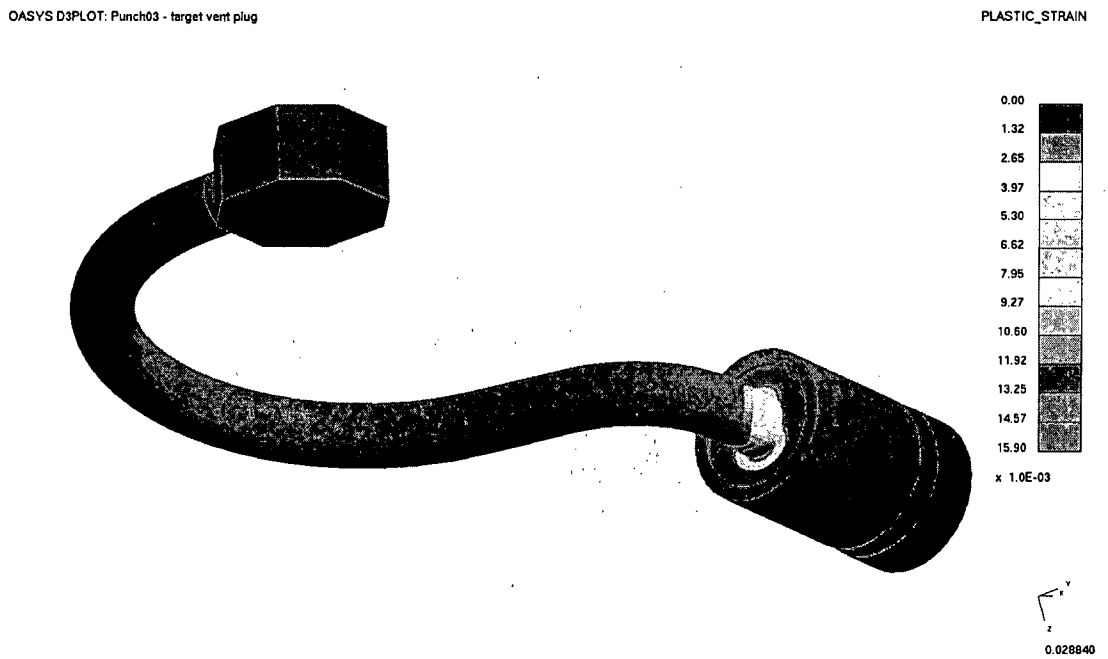

Figure 268: Effective plastic strain in outer tube – Punch 03

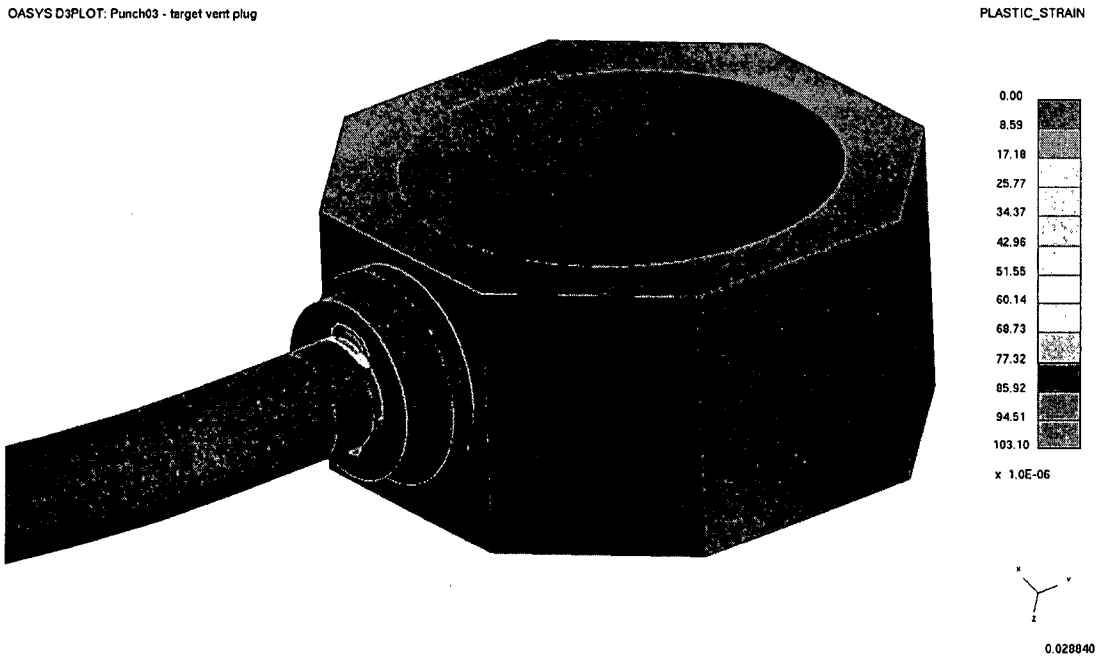

Figure 269: Effective plastic strain in drain tube – Punch 03

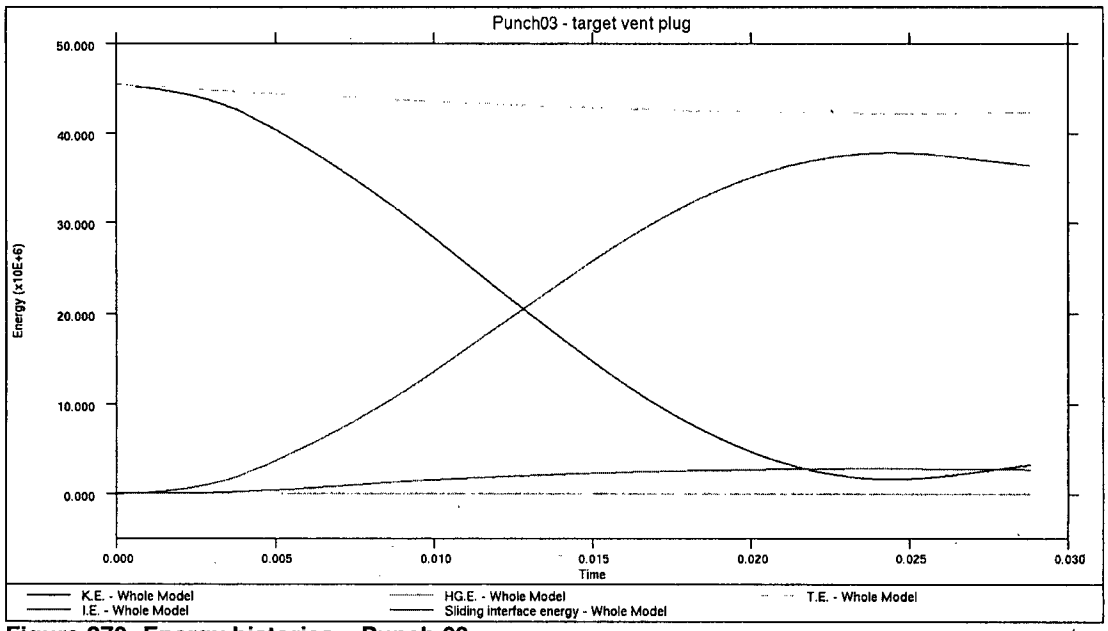

Figure 270: Energy histories – Punch 03

AMEC PLC
Booths Park
Chelford Road
Knutsford
Cheshire
WA16 8QZ
United Kingdom

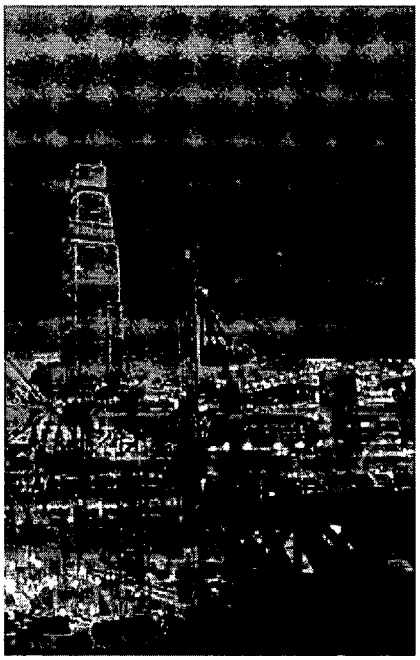

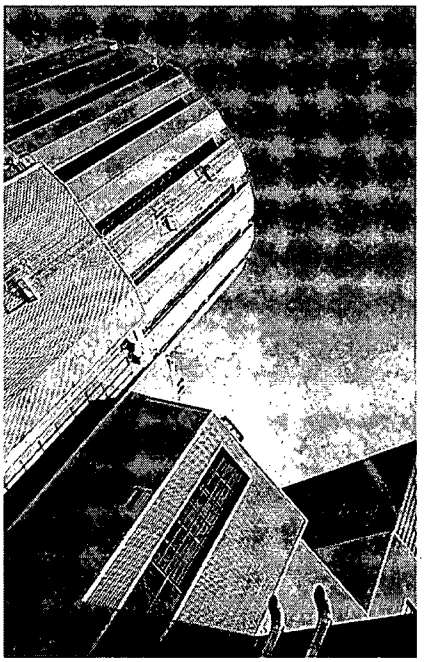

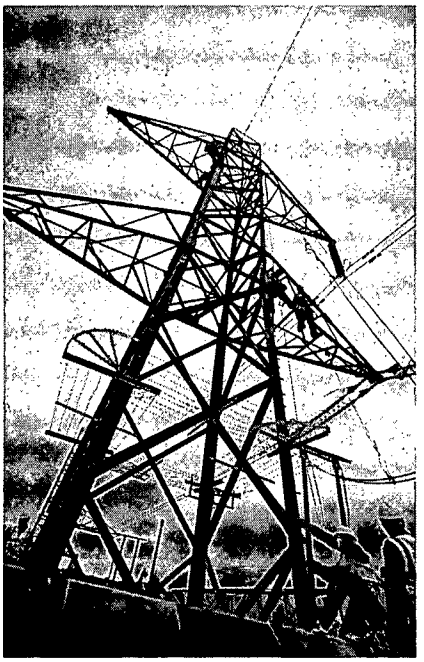

amec.com